DISS. ETH NO. 24262

COMPOSITE BAMBOO AND ITS APPLICATION AS REINFORCEMENT IN STRUCTURAL CONCRETE

A thesis submitted to attain the degree of

DOCTOR OF SCIENCES

of

ETH ZURICH

(Dr. sc. ETH Zurich)

presented by

ALIREZA JAVADIAN

Born May 28, 1985

Citizen of Tehran, IRAN

accepted on the recommendations of

Prof. Dirk E. Hebel (Supervisor)

Prof. Dr. Ian F.C. Smith (Co-Supervisor)

2017

Acknowledgements

In completing the PhD and writing the thesis, I am deeply indebted to a large number of colleagues, friends and family who have been essential throughout the past few years. This amazing journey would not have been possible without the support and encouragement of many people at ETH in Zürich, Singapore-ETH Centre and abroad.

First of all, I would like to thank ETH Global and Sawiris Foundation for Social Development for providing me with The Engineering for Development (E4D) doctoral fellowship award which helped me to work freely on the subject of my PhD. Secondly, I would like to acknowledge the funding provided jointly by the Singapore National Research Foundation (NRF) and ETH Zurich which made possible the extensive research over the past four years. I am also grateful to the company REHAU for believing in this research and providing the financial and technical support during the course of my PhD.

Accomplishing this PhD was a truly amazing experience for me and my greatest appreciation goes to my advisor Prof. Dirk Hebel at ETH Zürich for his trust and support for the past five years. I would like to thank him deeply for giving me the chance to work on an interesting and novel PhD topic with huge potential benefits for people in developing countries around the world. Since the first time I met Dirk in Singapore, he has been an inspiration to me in pursuing my PhD. He was the one who encouraged me to follow my dreams, to love what I do and do what I love. His determination, courage and enthusiasm to change the way we think about our future gave me the motivation to embark on the proposed research and to complete my PhD. I am thankful to him for advising me during all phases of my PhD, and also for giving me the opportunity to think out of the box, push the boundaries, and explore outside of my comfort zone.

Furthermore, I would like to express my sincere gratitude to my co-advisor Prof. Ian Smith at EPFL for his continuous support during the course of my PhD. Ian's patience, encouragement and immense knowledge of the field of study gave me the confidence to complete this PhD. His guidance during the research and writing of this thesis was exceptionally invaluable. The thesis could not have been successfully completed without Ian as my advisor and mentor.

Besides my advisors, I am especially grateful to the ETH Global committee members responsible for conferring the E4D doctoral fellowship: Dr. Barbara Becker and Patricia Heuberger-Meyer, who not only provided me with the funding opportunity, but also shared

Finally, I would like to thank my beautiful wife, Nazanin, for her outstanding support, encouragement, patience and love for the past couple of years, which gave me the confidence and motivation to pursue my dreams and complete this PhD thesis.

I dedicate this thesis to the many young, talented and brilliant students in Iran who are pursuing their dreams and making waves for a better future for Iran.

Abstract

The fast pace of development in many developing countries has led to an increased demand for building and construction materials for housing and infrastructure projects. Reinforced concrete is one of the most widely used building materials around the world. Unfortunately the majority of developing countries lack the resources to produce their own steel. Steel is not without alternatives. There is a material substitute that grows in the tropical zone of planet, an area that coincides closely with the developing world: bamboo. Research that has been conducted so far in the area of bamboo-reinforced structural concrete has demonstrated two things. First, replacing steel with bamboo as a reinforcement system is technically feasible. Second, up to now, no solution has been found for problems involving swelling, shrinking, chemical and biological decomposition and thermal expansion of raw bamboo in concrete.

The primary aim of this pioneering research is to evaluate the suitability of a newly developed bamboo-composite material for use as reinforcement for structural-concrete elements. This thesis also focuses on novel methods to fabricate a bamboo-composite material in an innovative way so that most of the inherent tensile capacity of the fibers is retained. Furthermore, durability aspects such as water absorption, swelling, shrinking, chemical resistance as well as challenges related to thermal expansion are studied and evaluated experimentally through an extensive series of tests.

Bamboo *Dendrocalamus asper* from Indonesia has mechanical properties that are suitable for composite fabrication. New relationships are proposed for estimation of mechanical properties of bamboo *Dendrocalamus asper* through measuring only the culm diameter and wall thickness after evaluating a total of 4,500 raw bamboo samples. These relationships are useful tools for on-site estimation of the properties of bamboo culms without the need for laboratory facilities. Of the two processing methods investigated in this research, the Bamboo Veneer Composite (BVC) fabrication technique which offers higher mechanical properties compared with the Bamboo Strand Composite (BSC) fabrication technique was chosen after evaluating the mechanical properties of nearly 5,000 bamboo composite samples. The ultimate tensile strength of longitudinal BVC reinforcement is found to be comparable to ASTM A615 grade 60 with a minimum tensile strength of 420MPa, while the BVC stirrup shows an average tensile strength comparable to ASTM A615 grade 40 reinforcing bar with a minimum tensile strength of 280MPa. These values are obtained after investigating tensile properties of close to 1,500 longitudinal and transverse BVC reinforcement samples.

Water-based epoxy coating and sand particles employed on the surface of around 500 BVC reinforcements proved to be useful firstly, by protecting the BVC reinforcement against potential chemical degradation in the alkaline environment of concrete and secondly, by maintaining the bonding strength with the concrete matrix that is necessary for stress transfer between the concrete matrix and the reinforcement. The longitudinal Coefficient of Thermal Expansion (CTE) of BVC reinforcement and concrete are similar and thus no significant longitudinal residual thermal stresses are developed within concrete beams during hardening. The differential transverse thermal expansion of BVC reinforcement in concrete has been mitigated by firstly providing a concrete cover of two times the thickness of BVC reinforcement and secondly, by ensuring a good bond between the BVC reinforcement and concrete. The transverse residual stresses developed at the interface of the concrete and reinforcement caused by transverse expansion and retraction of the BVC reinforcement during hardening do not result in observable tensile radial cracking around the reinforcement. Therefore, the variation of transverse CTE values has no significant effect on the bonding mechanism. Furthermore, exposures of nearly 500 BVC reinforcements to water and alkaline environments do not show a significant change in physical and mechanical properties.

A total of 110 concrete beams are reinforced with BVC material as longitudinal and transverse reinforcement. The BVC-reinforced concrete beams show ultimate failure loads that are comparable to that of reinforced concrete beams with ASTM graded steel-reinforcement bars. It is concluded that the newly developed BVC reinforcement system has much potential for low-cost and low-rise concrete infrastructure where loading and environmental conditions similar to those studied in this thesis are found.

Zusammenfassung

Das unglaublich hohe Entwicklungstempo in vielen Ländern des globalen Südens hat zu einer erhöhten Nachfrage nach Baustoffen für Wohnungs- und Infrastrukturprojekte geführt. Stahlbeton gilt als eines am weitesten verbreiteten Baumaterial der Welt. Den meisten Entwicklungsländern fehlen jedoch die notwendigen Ressourcen und Infrastrukturen, um ihren eigenen Stahl produzieren zu können. Stahl ist nicht alternativlos. Es gibt ein Material, das in den tropischen Zonen unseres Planeten wächst, eine Region, die deckungsgleich ist mit vielen Entwicklungsländern - Bambus. Bisherige Forschungen, die den Einsatz von rohen und unbehandelten Bambusteilen in Betonanwendungen angedacht haben, zeigen zwei Dinge. Erstens ist der Einsatz von Bambus als Armierungssystem in Betonanwendungen technisch möglich. Zweitens wurden bis dato keine Lösungen gefunden im Umgang mit Schwellen, Schrumpfen, chemischer und biologischer Zersetzung sowie der thermischen Ausdehnung von rohem und unbehandeltem Bambus in Beton.

Das Hauptaugenmerk der vorliegenden Forschung ist die Nutzbarkeit von neuartig entwickelten Bambus-Kompositmaterialien als Bewehrungssysteme in tragenden Betonteilen zu evaluieren. Die Arbeit beschäftigt sich ebenfalls mit Methoden der Herstellung eines neuartigen Bambus-Kompositwerkstoffs unter besonderer Beobachtung und Erhaltung der den Bambusfasern inherenten Materialeigenschaften, insbesondere der hohe Zugfestigkeit.. Desweiteren werden die Dauerhaftigkeit, insbesondere die Wasseraufnahme und das damit verbundene Quellen und Schwinden sowie die chemische Widerstandsfähigkeit und thermische Ausdehnungen untersucht und experimentell evaluiert.

Für die Herstellung des Komposits hat sich im Rahmen dieser Arbeit Bambus der Art *Dendrocalamus Asper* aufgrund der guten mechanischen Eigenschaften als geeignet erwiesen. Es werden neu entwickelte Zusammenhänge vorgestellt mit denen eine Abschätzung der mechanischen Eigenschaften von Bambushalmen der Art *Dendrocalamus Asper* durch Messen von Halmdurchmesser und Wandstärken ermöglicht wird. Damit könnendie Materialeigenschaften auf einfache Weise und ohne Zugang zu Prüflaboren in situ abgeschätzt werden. Im Hinblick auf die Kompositherstellung werden in dieser Arbeit zwei Methoden untersucht und vorgestellt. Zum einen die Bambusfurnierkomposite (BVC) und zum anderen Bambuskomposite aus gespaltenem Bambus (BSC), wobei die Furnierkomposite deutlich höhere mechanische Eigenschaften besitzen. Die Zugfestigkeit

von Lägsbewehrungsstäben aus BVC ist vergleichbar mit Bewehrungsstahl A615-60 gemäß ASTM mit einer Mindestzugfestigkeit von 420 N/mm^2 und die Mindestzugfestigkeit der aus BVC gefertigten Bügelbewehrung entspricht der von Bewehrungsstahl ASTM A615-40 und beträgt 280 N/mm^2. Als Beschichtung der Bewehrung hat sich Epoxidharz auf Wasserbasis in Kombination mit Sandpartikeln als geeignet erwiesen zum einen die Bewehrung vor chemischer Zersetzung im alkalischen Milieu des Betons zu schützen und zum anderen um einen dauerhaften Verbund zwischen Bewehrung und Beton sicher zu stellen. Weiterhin konnte festgestellt werden, dass die thermischen Dehnungen in Lägsrichtung der Bewehrungsstäbe identisch mit der des umgebenden Betons ist, wodurch beim Karbonisieren des Betons keine Zwangsspannungen bei Temperaturdifferenzen entstehen. Temperaturdehnungen quer zur Faserrichtung der Bewehrung wurden im Rahmen dieser Arbeit durch das Einhalten einer Mindestbetondeckung der Bewehrung von zwei Stabdurchmessern und durch Sicherstellung eines guten Haftverbundes zwischen Bewehrung und Beton eingeschränkt. Die aufgrund dieser Temperaturquerdehnungen vorhandenen Spannungen haben keinen signifikanten Einfluss auf das Verbundverhalten von Bewehrung und Beton während des Karbonisieren und es konnten keinerlei radial verlaufende Risse an entsprechenden Probekörpern festgestellt werden. Versuche zur Bestimmung des Einflusses von alkalischem Milieu und Wasserlagerung der Kompositbewehrung konnten zeigen, dass beides keinen Einfluss auf die mechanischen Eignschaften hat.

Die hier geprüften und mit Lägs- und Bügelbewehrung bewherten Betonbalken zeigten im Versuch eine deutlich höhere Steifigkeit und Tragfähigkeit als unbewehrte Betonbalken. Dabei konnte festgestellt werden, dass Bewehrung aus dem hier neu entwickelten Bambus-Kompositwerkstoff insbesondere für den Einsatz in kostengünstigen ein- bis zweigeschossigen Gebäuden, wo die Lastannahmen und äusseren Einflüsse ähnlich sind wie in der vorliegenden Arbeit beschrieben, den üblicherweise verwendeten Stahl als Bewehrung ersetzen kann.

Table of Contents

List of Figures

List of Tables

1. Introduction

Newly developed bamboo composite materials as reinforcement systems in structural concrete have the potential to revolutionize the concrete building sector, which has not changed significantly over the past 100 years. Steel reinforced concrete has become the most common construction material worldwide. This is because for decades, human beings have developed the technology to gain unrestricted access to a wide range of resources, including sand, limestone (cement), and iron ores. Today, we know that some of these resources are finite. In addition, very few developing countries have the ability or resources to produce the construction materials they need, forcing them into an exploitative import relationship with the developed world. For example, out of 54 African nations, only two produce steel in recognizable amounts (World Steel Association 2015). Most developing countries in the world compete in the global marketplace for this increasingly expensive and seemingly irreplaceable material.

Steel is not without alternatives. There is a substitute material that grows in the tropical zone of our planet, an area that coincides with location of many developing countries – bamboo. Bamboo belongs to the botanical family of grasses and is extremely resistant to tensile stress, and is therefore one of nature's most versatile plants. The research described in this thesis focuses on developing an alternative for steel reinforcement in concrete applications. This provides many advantages while addressing questions of social equity (value chains), affordability, weight, corrosion and strength.

1.1. Background

Between 1950 and 2016, the world population tripled and stands momentarily at 7.5 billion people. It is expected to increase further to 11 billion people by 2100, according to the United Nations Population Division ((UNDP) 2015). Much of this increase will occur in countries in the developing regions, mostly in Africa and Asia. According to the World Bank, developing countries are classified based on Gross National Income (GNI) per capita per year (World Bank 2016). Countries with a GNI of US$11,905 and less are defined as developing countries. These countries face many challenges in meeting the demands of their growing populations in the areas of housing, infrastructure, transportation and energy. Relying on finite non-renewable resources based on traditional technologies and without forward thinking do little to help governments tackle these challenges in the 21st century. To house such an increase in the world population, it is now already clear that non-regenerative

resources such as sand, gravel and metals cannot be the answer to address the challenge of finding appropriate building materials for the future.

Iron can be used as an exemplary case study. By the end of the 19th century and the beginning of the mass industrialization era in Europe and North America, iron became the most valuable resource; steel was used to make machinery and infrastructural elements such as rail systems, trains, ships, cars and housing (Offer 1993, Harrison 2005). Steel was produced from iron by removing impurities and adding carbon to make it stronger and more durable than cast iron (Zervas, McMullan et al. 1996). Steel replaced iron in almost all applications in the early 20th century due to its cheap production price, abundant resources and rapid development in a competitive global environment.

The fast pace of development during the industrial revolution led to excessive exploitation of natural resources which continued and further increased by the mid-20th century for the post World War II rebuilding of major cities worldwide. During this time, the demand for coal, iron ore and steel was very high. Most of the countries with ample natural resources had to increase supply to meet the booming demand.

Through technological innovations over the last decades, the production cost of steel has been dramatically reduced. By the end of the 20th century, steel became the most widely used metal on earth. It was extensively used in the construction of low- and high-rise buildings, harbors, airports and railways; in production of new cars, trucks, ships, trains and airplanes; and in the majority of household appliances such as fridges, washing machines, sinks and ovens (Liang, Dong et al. 2016).

The World Steel Association (WSA) expected global steel consumption to grow by 1.4% in 2016 (World Steel Association 2015). It also indicated that the world's steel consumption would increase to 2,500 million tons per year by 2050. Considering such demand, its environmental consequences and economic impact need to be evaluated.

In terms of environmental consequences, the high rate of exploitation of iron ore for steel production in the long term will lead to the depletion of a natural resource which is finite and limited in quantity. Furthermore, steel production is energy intensive and also responsible for the emission of large amounts of greenhouse gases. Producing a ton of finished steel products requires up to 16GJ energy, and the manufacturing process releases approximately 1.8 tons of

carbon dioxide into the atmosphere, according to the International Energy Agency (IEA) ((IEA) 2007).

Furthermore, mining the earth for large volumes of raw materials for the steel producing industry may potentially result in widespread deforestation and loss of top-soil, which is essential for agriculture and plant growth (Brown 1984). Deforestation and soil erosion severely affect the environment by destroying landscapes, forests and wildlife; eventually this changes the biodiversity of the surrounding flora and fauna (Kitula 2006, Sonter, Barrett et al. 2014).

The high demand for steel also poses short-term and long-term economic challenges for steel exporters and importers worldwide. Coal and gas resources are finite and non-renewable. Price fluctuations of steel and finished steel products affect major steel importers. For instance, in 2015, China's raw steel production slowed down for the first time in 35 years, falling 2.3% due to a slowdown in the Chinese economy. This ultimately had a major impact on global steel and iron ore prices (2016, Popescu, Nica et al. 2016).

Another example of economic challenges is the case of Anglo American, a multinational mining company based in the United Kingdom and South Africa, which had to downsize its business in 2015 by two-thirds and sell the majority of its assets due to the high cost of production and increased competition for iron ore worldwide, as reported by The Guardian (Farrell 2015).

The situation for most mining companies across the world is similar. They are exploring the earth for non-renewable resources such as iron ore, coal and gas for steel and similar metal production to meet the demand from the construction and manufacturing sectors.

Therefore, in the 21st century, there will be important changes in how construction materials are produced. While industrialization has resulted in a conversion from regenerative to non-regenerative material sources (from farming to mining), the next changes could involve the reverse: a shift towards cultivating, breeding, raising, farming or growing future resources as the mines are depleted. These renewable resources can be cultivated either within the conventional soil-based agricultural framework or in breeding farms, using microorganisms that so far have not been considered useful for the energy or building industries. A third option is the industrialization of natural and bio-chemical processes to rebuild bio-materials synthetically within a controlled environment.

When considering the use of natural and organic raw materials in the current framework of digitalization, prefabrication and mass production, the imperfections of living materials become a key aspect in material development. The underlying effort, alongside a continuous interest in advancing material properties, is in the standardization of natural processes in order to guarantee predictable and controllable properties (Hebel, Wisniewska et al. 2014). This thesis provides an example of a scientific approach and shows a way forward for new technologies to industrialize organic substances and ensure applications in the built environment to be regulated, safe and certified systems.

A paradigm shift in the construction industry

Among the alternative renewable natural resources which could potentially support the change described above are plant fibers. Many plants, including flax, cotton, jute, sisal, hemp and bamboo might be used to obtain fibers that possibly could be used as an alternative source for the production of sustainable construction materials, as well as becoming an alternative to some of the conventional building materials.

Plant fibers have largely unidentified physical and mechanical properties that could be used in the production of a new group of construction materials based on biologically activated processes. Among plant fibers, bamboo is shown to have properties that are suitable for the building and construction sector and thus for the development of a new class of sustainable construction materials.

Mike Woolridge, a BBC reporter from Nicaragua, recently said that bamboo could be the "super fiber of the 21st century". He stated that with the help of new technologies and industrial processing, bamboo has begun competing very effectively with building products in western markets (Wooldridge 2012).

The extremely widespread natural habitat of bamboo along the equator belt (Fig.1) supports the statement by Woolridge. The map in Fig. 1, showing the habitat of bamboo, aligns with the location of countries facing high population growth in Fig. 2. Most of these countries in Fig. 2 belong to the category of developing territories. According to the World Bank, countries are classified based on their Gross National Income (GNI) per capita per year, and those with a GNI of US$11,905 and less are defined as developing countries (World Bank 2016).

In these territories, the majority of the population usually has limited access to public services such as education, healthcare and public housing, as well as far less employment opportunities compared to developed and industrialized countries (Gylfason 2001). Most of the developing countries have a population growth rate of higher than 1% compared to the rest of the world, according to the data from the World Bank (World Bank 2015). The high rate of population growth in developing countries poses challenges in building sufficient housing, besides ensuring better infrastructure and improved living standards. Among the challenges is meeting the demand for construction materials for the upcoming expansion of housing and infrastructure, which will put tremendous pressure on local economies.
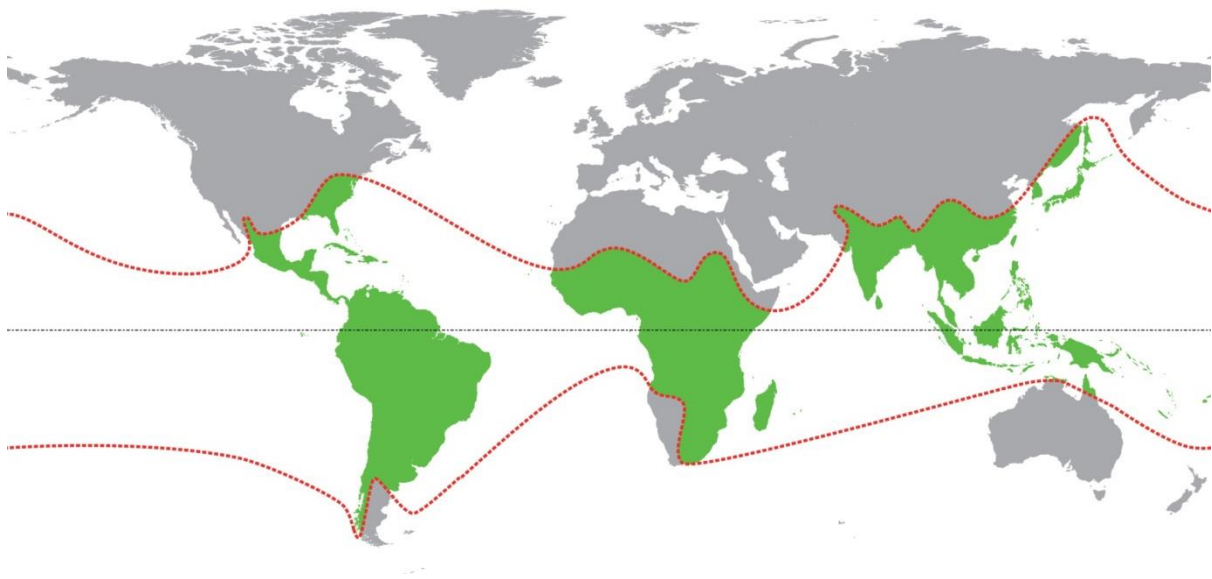
Fig. 1 Global natural habitat of bamboo
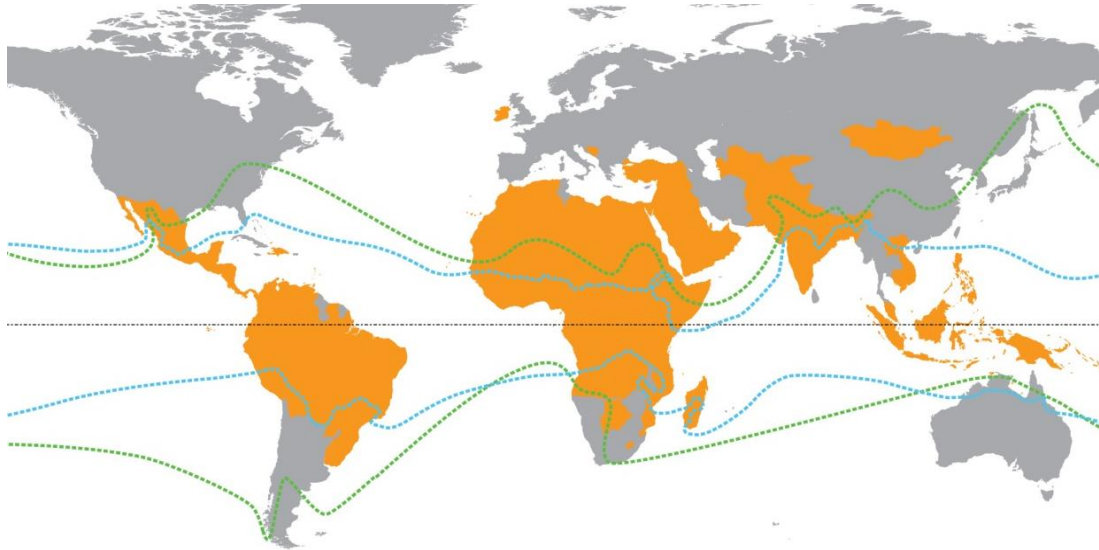
Fig. 2 Countries with population growth above 1%

Unfortunately, most of the developing countries mentioned above lack the resources to produce their own building materials. Therefore they need to import the majority of the construction materials they require from highly industrialized countries, following a traditional Western model for development, which forces them into exploitive relationships. For instance, the majority of African countries have to import steel reinforcements for their construction needs from developed nations. According to an International Monetary Fund (IMF) report in 2015, most African countries ran up trade deficits, including Ethiopia, where a US$11.7 billion deficit was recorded in 2015; it was primarily due to imports of construction materials to meet the demand for housing projects and to build new towns resulting from high population growth (International Monetary Fund 2015).

A similar situation exists in Southeast Asia where countries such as Myanmar, Thailand and Indonesia are facing high population growth and are meeting their construction demand by importing the majority of their construction steel from more developed countries such as Japan, South Korea and China. This situation pressurizes local governments to deal with the increasing demand for materials. As a result of rapidly rising imports, many Southeast Asian countries ran up trade deficits in recent years. According to IMF, Indonesia had a US$1.9 billion deficit in 2015 and Myanmar, US$752 million. These figures are expected to increase over the next 10 years as the urban population grows and the demand for materials and resources to support this growth continues to increase.

As described above, unfortunately, most countries in developing territories do not have the capability and necessary resources to produce their own steel. Due to the high population

growth rates expected over the coming decades, import surges are also expected which would result in trade deficits, economic slow-downs, loss of jobs, increased poverty, and lack of access to essential services such as healthcare and education. In view of this, local industries in developing countries should be proactive in preventing the crisis by helping the building sector meet the increasing demand for construction materials (Thompson 1938, Brennan 1993, Edwards 2016). One solution would be to provide the developing territories with novel technologies to produce new building materials from locally available natural resources. This would reduce their dependency on the world market and also confer socio-economic and environmental benefits.

Among natural resources, bamboo has shown great potential to be developed into an industrialized product by local industries in developing countries, and thus fulfill the demand for new construction materials through new technologies as developed in this research. Bamboo grows in the tropical zone of the planet, an area that largely coincides with the developing territories as shown in Fig. 1 and Fig. 2. Bamboo belongs to the botanical family of grasses and is extremely resistant to tensile stress; it is one of nature's most versatile plants. The ability of natural bamboo to withstand tensile forces makes it superior to timber and steel. This makes bamboo a feasible alternative to the increasing demand for steel reinforcement in the construction of reinforced-concrete buildings and infrastructure in developing countries. As such, bamboo has the potential to grow local industries by creating new jobs and by bringing new investments into developing countries in the research and development sector as well as in the educational system (Renard and GRET 2009). Local farmers could benefit from growing and harvesting bamboo; it is a good source of income, helps improve cultivation skills, and also empowers local communities in developing countries by enhancing their skills and knowledge in this field.

The ecological system may also benefit from the cultivation of bamboo plantations. They help reduce landslides and soil erosion, while unproductive land can be converted into productive land (Ben-Zhi, Mao-Yi et al. 2005). Degraded land and environments can be protected by cultivating bamboo. In addition, food security is improved by intercropping bamboo with other food plants and by using bamboo as an alternative biomass fuel for cooking (Scurlock, Dayton et al. 2000, Guta 2012).

Another advantage of bamboo cultivation is that it requires low investment for propagation, land and labor. The socio-economic benefits would be in the form of raw material cultivation

and product development, leading to the creation of long-lasting consumer goods and contributing to the economies of developing territories.

In this context, bamboo offers much potential for the development and production of new materials and technologies. These factors, together with its local availability, make bamboo an affordable resource as a raw material with outstanding properties.

From an engineering point of view, this research focuses primarily on the tensile capacities of bamboo. As mentioned earlier, bamboo is potentially superior to timber and construction steel in terms of its live-load capacity to self-weight ratio; the key challenge is to make these excellent mechanical properties available for the production of a new high-performance material. This is achieved by the appropriate cultivation and industrial processing of raw bamboo through the fabrication of a newly developed bamboo composite material.

Reinforced concrete is one of the most widely used building materials in the world; it constitutes cement, water, aggregates, sand and steel reinforcement. The steel reinforcement serves as an inseparable part of any reinforced concrete applications. It is estimated that over 10 billion tons of concrete are produced each year, and this is expected to double by 2050 (Meyer 2004). Moreover, the natural habitat of bamboo overlaps with the areas of high population growth rates in developing territories; this fact, together with the demand for reinforced concrete as a building material for housing and infrastructure, means there is much potential for a newly developed bamboo composite material to serve as a reinforcement in structural concrete.

This would help developing territories build up domestic supply channels and reduce dependency on imported building materials, especially steel reinforcement. In addition, new technologies for bamboo composite production have the potential to provide a new type of building materials with applications similar to timber and construction steel.

The idea of employing bamboo for concrete applications is not entirely new. It was first studied in 1914, when Chow, a PhD student from the Massachusetts Institute of Technology (MIT) in Boston, tested small diameter raw bamboo and raw bamboo splits as reinforcement materials for concrete beams and columns (Hidalgo-Lopez 2003). Following this early application, in 1935, Datta and Graf from Technische Hochschule of Stuttgart studied potential applications for raw bamboo, given the outstanding technical and mechanical

properties they found in raw bamboo samples from South America (Hidalgo-Lopez 2003). However, they were not successful in implementing their ideas.

In 1950, after World War II, Professor Glenn at the Clemson Agricultural College of South Carolina began extensive studies into the use of natural bamboo for reinforcement in concrete structures (Hidalgo-Lopez 2003). Using only small-diameter culms and bamboo splits, he demonstrated that the application was feasible in principle; however, regarding the module of elasticity, insect and fungus attacks, coefficients of thermal expansion, shrinkage and swelling, this natural bamboo reinforcement had major drawbacks. Glenn based additional research on minimising defects through, for example, coating the bamboo components with various materials before adding concrete. The results showed that the solutions were either so expensive that bamboo reinforcement could not compete with structural steel, or it was not a long-term solution due to durability issues occurring during the life span of the building. Unfortunately, most of the structures built during this period collapsed after being constructed. Due to such disappointing results, research in the area of bamboo reinforcement for structural concrete elements nearly came to an end.

Almost five decades later, in 1995, Professor Ghavami of the Pontificia Universidade Catolica in Brazil embarked on a study in the field of bamboo for concrete reinforcement (Khosrow 1995). He started a new series of mechanical tests on seven different species of bamboo from Brazil in order to find the most appropriate species to be used as reinforcement in lightweight concrete beams. The concrete beam with bamboo reinforcement displayed a remarkable load-bearing behaviour compared to the non-reinforced beam as well as concrete beam reinforced with steel reinforcement. This proved that in laboratory conditions, it is possible to activate the load-bearing capacity of bamboo in a concrete application.

However, the long-term behavior of bamboo in concrete structures remained a problem. Since bamboo is a natural material, its exposure to a concrete matrix can, through time, result in water absorption from the concrete. This may lead to a progressive de-bonding of the bamboo element from the concrete matrix due to the repetitive swelling and shrinking of the natural bamboo embedded in a concrete matrix. The expansion of the bamboo elements and the increase in its volume can create micro-cracks in the surrounding concrete matrix which, in the long term, may cause structural integrity loss due to excessive cracking, as shown in Fig. 3 by Ghavami (Ghavami 2005). The cracks would also be a source of moisture ingress,

which over the time allows for the biological degradation of the bamboo element (Kumar and Prasad 2003, Lima Jr, Willrich et al. 2008).
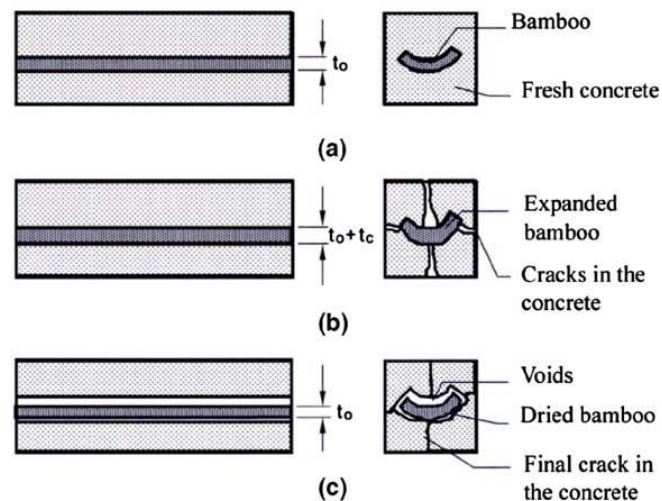
Therefore, so far it has been shown that it is generally possible to apply bamboo as a reinforcement system for concrete applications, but only if the problems with water absorption, swelling, shrinkage and thermal expansion can be solved and the inherent mechanical capacity of bamboo fibers maintained.

This PhD research focuses on developing a new methodology to use raw bamboo for the fabrication of a new bamboo-reinforced composite material, such that the cellulose structure of natural bamboo is retained and its mechanical properties are preserved. The methodology developed within this PhD research involves processing natural bamboo culms into a network of fibers. Together with an adhesive matrix, this network forms a water-resistant, non-swelling and high-strength composite material. Careful optimization of the processing of natural bamboo and the composite fabrication method comprise part of this research in developing a new bamboo-based high-performance composite material. The research also focuses on the application of the new bamboo composite material as reinforcement in structural concrete beams, while avoiding the negative side effects that were seen in previous work with raw bamboo in concrete.

1.2. Motivation

The motivation for this research relies on the observation that all related research conducted thus far in the area of bamboo-reinforced structural concrete applications shows two things.

First, replacing steel with bamboo as a reinforcement system has potential, given the superior mechanical properties of bamboo and its non-corrosive behavior compared to steel. Earlier research on some species of bamboo has shown that the tensile strength of the fiber bundle of some bamboo species is comparable to that of normal steel reinforcement with characteristic tensile strength of 400MPa. For some species of bamboo, the tensile strength of the single fiber reaches 1,500Mpa, which is close to that of carbon fiber, according to the literature (F. Ramirez 2011, Zhou, Huang et al. 2012). The application of high tensile strength bamboo elements in structural concrete can result in similar load-bearing behavior as that of structural concrete members reinforced with steel reinforcement (Khosrow 1995, Ghavami 2005). Besides the load-bearing behavior, bamboo has a big advantage over steel reinforcement. Unlike steel reinforcement, bamboo does not corrode. Corrosion of steel reinforcement is one of the major causes of deterioration of reinforced concrete structures worldwide; it was reported that in 2005 alone, in the US, the direct annual costs of corrosion of reinforced concrete structures were nearly $45 billion (Thompson, Dunmire et al. 2005).

Second, up till now, no solution has been found for problems with the swelling, shrinking, chemical and biological decomposition, and thermal expansion of raw bamboo. Also, durability and the methods required to ensure it has sufficient durability related properties over the long-term perspective are not addressed yet. Raw and untreated bamboo material has durability related challenges that must be addressed and controlled to prevent structural failure as explained.

Bamboo is a natural material. When it is used in concrete, it will draw moisture and water from the surrounding matrix and subsequently increases in volume and swells. Once the surrounding concrete matrix dries, the moisture absorbed by the bamboo element will dissipate and, consequently, the bamboo shrinks. Frequent shrinking and swelling of raw bamboo elements in concrete will result in loss of bonding with the concrete matrix as shown in Fig. 4.
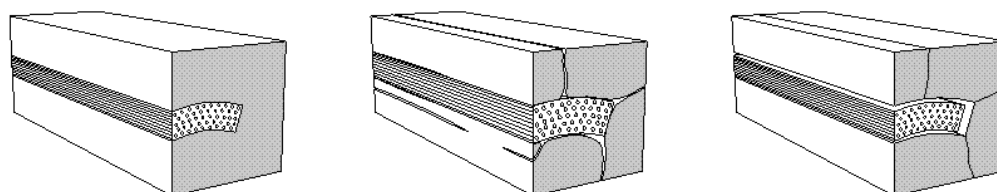
Fig. 4 Swelling, shrinking and volume change of raw bamboo elements in concrete (Heisel 2015)

11

In addition to the problems associated with the shrinking and swelling of raw bamboo, the alkaline environment of concrete can also adversely affect the integrity of natural bamboo and its tensile capacity, and may result in the loss of the load-bearing capacity of concrete reinforced with raw bamboo.

Therefore, this research focuses on the investigations of methods to employ bamboo in the fabrication of a new bamboo composite material in a way such that the inherent tensile capacity of the fibers are retained, and the durability issues, specifically water absorption, swelling, shrinking and chemical resistance, of the composite could be enhanced for application in structural concrete.

1.3. Goals

The goal of this research is to develop a new composite material made of natural bamboo fiber and an adhesive agent (epoxy-resin based) through a new technology to replace conventional steel reinforcement in structural concrete applications. The research includes improving the long-term durability of the bamboo composite materials while placed in the concrete matrix, and maintaining the superb mechanical properties of the bamboo fiber in a novel way without having adverse impacts on the structural performance of the newly developed bamboo composite reinforcement.

The main objectives that drive the research for this PhD work are listed here:

- The development of a new class of composite materials with natural bamboo fiber that possess the necessary mechanical and physical properties in terms of tension, compression and flexural capacity, thermal expansion, water absorption, and durability in order to be used for reinforcement in structural concrete applications.
- Provision of scientific knowledge to develop an alternative to steel reinforcement in structural concrete applications with a natural fiber-based composite material that adheres to international standards.

2. Research methodology

2.1. Summary

This chapter develops the research methodology, starting from the research hypothesis. The hypothesis of this research is that it is possible to develop a new bamboo composite material which can be employed as a reinforcement system in structural concrete applications. Seven research objectives are formulated to support this hypothesis. The seven objectives are related to the raw bamboo processing and properties, composite reinforcement production and its application in concrete beams. The chapter also discusses the methodology and tools employed within this thesis to evaluate the hypothesis and objectives of the research. Quantitative research methods used in this thesis, including sample collection techniques, design of the experiments and variables involved in sampling and testing, limitations and restrictions encountered during the experiments are described.

2.2. Primary research concept

There is a need for scientific research in the field of bamboo composite material and its application for structural concrete. The potential of using composite bamboo as a building material is often dismissed. The hypothesis of this research aims to address this issue through developing a novel bamboo composite material and exploring its potential through careful experiments in structural concrete.

2.3. Research hypothesis

The hypothesis of this research is:

It is possible to develop a new bamboo composite material designed to have the necessary mechanical and physical properties and which can be applied as a reinforcement system in structural concrete.

2.4. Research objectives

To support the research hypothesis of this research, the main objectives are set as follows:

- Determination of the physical and mechanical properties of raw bamboo
- Development of a standard procedure for the processing of raw bamboo into various shapes and thicknesses for composite production
- Optimization of the composite fabrication method using a range of epoxy-resin systems

- Enhancement of the physical and mechanical properties of bamboo composite materials through optimization of the composite fabrication technology for use in structural concrete

- Determination of the mechanical properties of structural concrete reinforced with bamboo composite reinforcement

- Investigation of the effects of water and alkaline environments on bamboo composite reinforcement for use in structural concrete

- Recommendation for the new designs for newly developed bamboo composite material as reinforcement in structural concrete

2.5. Research methodology and tools

To achieve the objectives of this research, a scientific quantitative research methodology is undertaken by dividing the research into three sections. The first section of the research is focused on a literature review of the studies carried out by various researchers on the development of common reinforcement systems for structural concrete applications, including steel and Fiber Reinforcement Polymer (FRP) materials as well as the use of natural bamboo in reinforced concrete buildings around the world. The literature review aims to provide sufficient evidence for the lack of scientific research in the field of bamboo composite material as reinforcement for structural concrete applications. The second phase of this research focuses on the characterization of raw bamboo culms, their physical and mechanical properties, as well as developing a processing technique to obtain bamboo fibers from the culms. The third phase of this research is concentrated largely on the development of a new bamboo composite material and optimizing its physical and mechanical properties. Finally, the fourth section of the research focuses on investigating the application of the newly developed bamboo composite material in concrete element as reinforcement, and studying the interaction between the concrete matrix and the bamboo composite material. The methods and tools applied to this research are discussed briefly in this section. Further details on literature review, testing methods and analytical tools used in this research are given in chapters 3, 4, 5 and 6.

2.5.1. Literature review

An extensive review of the literature on the development of different reinforcement systems for structural concrete applications was carried out. Reinforced concrete applications were reviewed as part of the literature survey as concrete is considered one of the most widely used

building materials in history. Steel reinforcement production, as the most common method of reinforcing materials in concrete construction since the beginning of the 18th century, was reviewed. The many theories of the design and computation of reinforced concrete members, including Koenen's theory of flexure, were described to cover the latest developments in the code of design for concrete structures. The limit state design, known as Load and Resistance Factor Design (LRFD), based on strength and serviceability design criteria was investigated. The pioneer works carried out by Professor Jain and Professor Punmia on various aspects of LRFD concepts were comprehensively investigated as part of the literature review. The American Concrete Institute (ACI) design code's strength and serviceability limit states were covered in the literature review process, as this design code was the basis for the analysis and design of newly developed bamboo composite reinforced concrete members in this thesis.

Corrosion of steel remained as the major challenge faced by the construction sector around the world for the wide application of steel reinforcement in concrete members. Therefore steel corrosion and the process involved were comprehensively reviewed in the literature review. Significant efforts have been made by researchers around the world to mitigate the problems associated with corrosion of steel in concrete, including the application of different types of coatings to prevent or delay the onset of corrosion. The works of Alberto Sagüés, Rodney Powers, Richard Kessler and several other pioneer researchers were thoroughly investigated, and the advantages and disadvantages of their applied methods were explained and a comparison was made with the properties of non-coated steel reinforcement bars.

Given the many disadvantages that steel reinforcement with and without coating had and as explained by many pioneer researchers in the literature, in the past 15 years, there was great interest in using alternative reinforcement, especially non-metallic reinforcement, for structural concrete to eliminate the corrosion problems. Many researchers started to work on new types of reinforcement consisting of two parts, a fiber and a resin, in which aligned continuous fibers were embedded in a resin matrix and then formed into a new class of composite materials called Fiber Reinforced Polymer (FRP) composites. Glass Fiber Reinforced Polymer (GFRP), Carbon Fiber Reinforced Polymer (CFRP), Basalt Fiber Reinforced Polymer (BFRP) composites and Aramid Fiber Reinforced Polymer (AFRP) are all described in the literature review chapter of this thesis, and their advantages and disadvantages in comparison with steel and natural fiber reinforced polymer composite reinforcement are comprehensively covered in the literature survey of this thesis. The works of Pankaj Mallick as well as Andrzej Bledzki and Jochen Gassan were among the pioneers

who investigated the various aspects of synthetic and natural fiber reinforced polymer composite reinforcement systems.

The literature review chapter aims to determine the originality of the objectives of this thesis based on the fact that, so far, no investigation has been carried out on utilizing bamboo for the fabrication of composites with applications in the construction and building sector as a structural and load-bearing element similar to what this thesis tries to explore and prove. Therefore, first of all, the state of art research on various aspects of bamboo as a plant, its taxonomy, ecology, mechanical and physical morphologies, the long- and short-term durability issues, application of bamboo in traditional ways, fabrication technology of modern materials from bamboo and bamboo construction technologies were investigated based on the pioneer works of Oscar Hidalgo-Lopez, a Colombian architect and one of the world's most knowledgeable bamboo experts, as well as Walter Liese, a German professor of forestry and wood biology. The most common bamboo species in Asia, Africa and America and their physical and mechanical properties are reviewed in the literature review chapter.

To further investigate the potential of using bamboo as reinforcement in concrete, the application of bamboo as reinforcing elements since it was first tested by Hou-kun Chow, a Bachelor of Science student at the department of Naval Architecture and Marine Engineering at the Massachusetts Institute of Technology (MIT) in 1914, is reviewed in detail. The pioneer works of Howard Glenn, Otto Graf, Kramadiswar Datta, Francis Brink, Paul Rush, Helmut Geymayer, David Cook and several other researchers are reviewed in the literature review chapter. The most recent comprehensive studies on the application of natural bamboo as reinforcement for concrete beams and columns were carried out by Professor Khosrow Ghavami at the Civil Engineering Department of Pontificia Universidade Católica do Rio de Janeiro between 1995 and 2005, which is covered in the literature review chapter. Several other studies on the investigation of employing natural bamboo as reinforcement in concrete members carried out in the early 21st century are investigated as part of the literature review process.

The literature review studies show that bond strength, water absorption, thermal expansion, as well as swelling and shrinking related issues concerning the use of natural bamboo reinforcement in concrete remain major barriers to bamboo's widespread application. Therefore new ideas and production methods which were not studied in the past need to be investigated to address these shortcomings to improve the durability related problems and to

control the swelling, shrinking and thermal expansion of the material. These findings are the main motivations for this PhD research thesis

2.5.2. Characterization and processing of raw bamboo

For the development of a new bamboo composite material, the mechanical and physical properties of raw bamboo must be investigated prior to any processing or fabrication. Therefore a detailed study of bamboo plants was carried out. Selected species of bamboo were investigated for their physical and mechanical properties, but only species from Indonesia were selected for the experimental part of the research. The reasons are: the widespread availability of this species (*Dendrocalamus asper*) in Southeast Asia, especially in Indonesia, and its easy accessibility due to its proximity to Singapore where this research was carried out.

Tensile, flexural and compressive strength as well as modulus of elasticity in tension and flexure of *Dendrocalamus asper* bamboo were evaluated according to the American Society for Testing and Materials (ASTM) standards and International Organization for Standardization (ISO) standards. However, when deemed necessary, adjustments were made to the sample sizes, shapes and numbers required for the tests. A Shimadzu 100kN Universal Testing Machine (UTM) was employed for the mechanical testing done at the Advanced Fiber Composite Laboratory (AFCL) in Singapore.

Among the physical properties, the moisture content, water absorption and density of raw bamboo samples were measured. The moisture content was measured with a Shimadzu moisture balance, while the geometrical properties, water absorption and density were evaluated according to methods specified by ASTM relevant standards. Further details of both physical and mechanical property tests of the raw bamboo are given in chapter 4.

A scientific statistical analysis was used by the PhD candidate to relate the physical and mechanical properties of the raw bamboo to its geometrical properties, e.g. culm diameter and wall thickness which could be helpful in estimating, for instance, the tensile and flexural strength of raw bamboo culms without the need for lab tests in nurseries and farms with limited access to testing facilities. The model and the respective analysis are discussed in chapter 4.

After the properties of the selected bamboo species were investigated, two methods of stranding and peeling were used to process the raw bamboo culms into suitable fibers with

specific size and shape for composite fabrication. Each method has its advantages and disadvantages, discussed in more detail in chapter 4. Once the necessary fibers were obtained from the processing methods, certain chemical and mechanical treatments were carried out on the raw bamboo fibers to improve their strength and enhance their quality, and to further improve the subsequent bonding with the epoxy-resin system in composite fabrication.

2.5.3. Development of bamboo composite material

First of all, a literature review on the state of the art of the current application of Fiber Reinforced Polymer (FRP) composite materials, such as Glass Fiber Reinforced Polymer composite materials as reinforcement systems in structural concrete applications, was carried out. The state of the art report helped the PhD candidate to evaluate the use of alternative FRP composite reinforcement in concrete and get to know their respective advantages and disadvantages concerning their applications in concrete.

A hand lay-up and hot-press compression molding technology were used throughout this research for the fabrication of the bamboo composite reinforcement. This method was chosen given the minimal investment required for the machineries, molds and other necessary equipment. Furthermore, the fibers obtained from the raw bamboo in the form of either strands or sheets could easily be compressed together with the epoxy-resin system under the pressure of the hot-press compression molding machine and quickly be cured with the help of hot-press molding machine used in the fabrication process at AFCL in Singapore.

The hand lay-up and hot-press compression molding method resulted in high-performance composite products specifically designed to have desirable shape, size, mechanical and physical properties. The hand lay-up process allowed the quality control of the whole composite manufacturing process to be carried out in a simple yet comprehensive manner without the need for high-tech machineries.

It should be emphasized here that a given epoxy-resin system for the bamboo composite material was used for this PhD thesis which proved to be the most adequate. This system was not an invention and the development of its composition was not part of the PhD thesis work. In the chemical realm, the PhD candidate worked closely with the industrial partner (Rehau) and senior chemists in the team to identify the most appropriate epoxy-resin system for the final production during the course of this research.

Once the final bamboo composite material came out of the hot-press compression molding machine, it went through comprehensive physical and mechanical properties tests to optimize the properties of the final reinforcement for application in concrete. The tests were carried out according to international standards approved by the American Society for Testing and Materials (ASTM) to make sure repeatable and comparable results could be obtained. Samples for each test were prepared according to the standard guidelines defined by ASTM and tested at the Advance Fiber Composite Laboratory (AFCL) in Singapore.

The mechanical property tests included tensile strength, flexural strength, modulus of elasticity in tension parallel to the fiber direction, and modulus of elasticity in flexure parallel to fiber direction, and finally compressive strength along the fiber direction. All the mechanical property tests were carried out with a Shimadzu 100kN Universal Testing Machine (UTM).

The physical property tests carried out in this research included moisture content, density, water absorption and coefficient of thermal expansion of final bamboo composite reinforcement. The moisture content was measured with a Shimadzu moisture balance, while the geometrical properties and density were evaluated according to methods mentioned in relevant ASTM standards. Further details of both physical and mechanical property tests of bamboo composite materials and bamboo reinforced concrete elements are given in chapters 4, 5 and 6 respectively.

The physical and mechanical properties tests are an essential part of this research, and designed to assess the quality of bamboo composite reinforcement produced as well as of the raw bamboo used to produce the bamboo composite reinforcement. The tensile capacity of any applied reinforcement system in concrete structures and its bond behavior are determining factors for the ultimate load-bearing behavior of the concrete element. As a result, testing the tensile properties of the new bamboo composite material before its use with concrete was one of the most crucial tests that had to be carried out during this research. Tensile strength tests carried out on raw bamboo were compared with those of the final bamboo composite material to understand the behavior of the bamboo fiber matrix before and after production into a composite form.

The modulus of elasticity of bamboo composite samples along the fiber direction gives an indication of the deflection behavior of the samples while under tensile or flexural loading. It is important in the design of structural reinforced concrete members to evaluate this property

using a scientific approach, since the modulus of elasticity could potentially affect the concrete member size, the number of reinforcement, as well as their arrangement to prevent excessive cracking and premature failure while in use.

Similar to tensile properties and their importance in the development of bamboo composite reinforcement in this research, the flexural strength and modulus of elasticity in flexure have essential importance and are a fundamental part of the research. The flexural strength and its respective modulus of elasticity will provide great insights into bamboo composite reinforcement behavior when it is used in a concrete beam application, specifically when the member is under flexural loading. For the purpose of flexural strength measurement, the four-point bending test was used according to ASTM standards throughout this research.

As mentioned earlier, among the physical properties that should be measured and controlled is the coefficient of thermal expansion. This property is of interest to the proposed research since the bamboo composite material will be used in concrete. Similar coefficients of thermal expansion between concrete and bamboo composites will help to prevent de-bonding of the reinforcement from the concrete mixture which is due to exposure to excessive heat or cold in different environmental conditions. To achieve a comparable coefficient of thermal expansion as concrete matrix, the epoxy-resin system and the bamboo fibers play important roles. Therefore, a series of tests was designed to investigate the effect of treatment with normal water and an alkaline solution on bamboo fiber adhesion to the epoxy-resin system as well as to the concrete matrix. In addition to thermal expansion tests, water absorption tests were carried out on the final bamboo composite reinforcement to investigate the materials' durability in the moist environment of the concrete matrix. A comparison between water absorption of raw bamboo and bamboo composite samples was carried out to prove the suitability of pre-treating the bamboo fibers and the epoxy-resin system used in the production of bamboo composite samples.

The series of tests and the results obtained helped to track the changes in the properties of the new bamboo composite material according to changes in the material and production variables; this would lead to regular improvements in the final bamboo composite reinforcement.

2.5.4. Bamboo composite reinforcement in concrete application

Besides developing the knowledge for the production of a new class of composite reinforcement, as part of this research, the properties of concrete reinforced with the new type

of bamboo composite reinforcement are investigated in the last section of this thesis. In order to understand the behavior of the new bamboo composite material when it is used in concrete, several physical and mechanical tests were conducted during the course of this research. Comparisons between steel reinforced concrete beams and bamboo-composite reinforced concrete beams were made according to several performance criteria.

A series of durability tests on bamboo composite reinforcement, such as water absorption and alkaline environment exposure tests was carried out to ensure that the new bamboo composite reinforcement was able to resist primary durability related issues when used in concrete. It should be mentioned here that there is no specific standard on testing bamboo composite reinforced concrete beams, although for the purpose of this research, the American Concrete Institute (ACI) standard "Building Code Requirements for Structural Concrete and Commentary" was used as the primary guide, besides the relevant ASTM standards for polymer composite materials. However the necessary changes were made to test set-ups and sample shape or size accordingly to suit the new bamboo composite reinforcement during the course of this research.

Normal-strength concrete mix design with compressive strength of 20MPa was employed in this work. Lab-scale beams and concrete cylinders were prepared with bamboo composite reinforcement. To investigate the bonding of the new bamboo composite reinforcement with concrete, a series of pull-out tests were designed with various types of coating and different embedment lengths. The coatings and embedment length were the main factors in improving the bonding between the concrete matrix and the bamboo composite reinforcement. The pull-out tests were carried out according to ASTM and ACI standards with some adjustments according to the sample properties used in this research. The coatings and their respective properties, together with the number of tests and details of test set-ups, are described in chapter 6.

The pull-out tests would identify the appropriate type of coating and treatment as well as the adequate embedment length for bamboo composite reinforcement. Following the results from the pull-out test series, lab-scale concrete beams were prepared with bamboo composite reinforcement. The bamboo composite reinforced concrete beams were tested under the four-point bending test with the UTM machine at AFCL in Singapore. Both the longitudinal and shear reinforcement were evaluated during the bending tests, and the results of the tests were

then compared with the results obtained through the methods described by the ACI 440.1R-15 guide for the design and construction of structural concrete reinforced with FRP bars.

ACI 440.1R was found to be the most relevant international standard for the application of bamboo FRP composite in structural concrete. Further details are given in chapter 6 on the design of the concrete beams and the analytical methods used in this research. The ultimate flexural strength of the beams, or the so-called ultimate load-bearing capacity of the beams with bamboo composite reinforcement, was evaluated according to ACI 440.1R-15, and the results were compared with non-reinforced concrete beams and steel reinforced concrete beams of similar sizes. All these tests helped the PhD candidate to fully understand the behavior of this newly developed bamboo composite reinforcement and to evaluate its capacity when used in structural concrete.

2.5.5. Data analysis

The analysis of the data obtained through this research was carried out with Microsoft Excel and IBM SPSS statistical software. The data series obtained in this PhD work was divided into three main categories;

- Data obtained from the investigation of the raw bamboo and the processing methods, including the physical and mechanical property tests that were conducted on raw bamboo samples to provide the PhD candidate with a better understanding of the behavior of bamboo fibers before composite manufacturing
- Data obtained from the evaluation of mechanical and physical properties of bamboo FRP composite reinforcement as well as the data obtained through optimization of manufacturing parameters, including the hot-press compression molding machine's temperature and pressure
- Data obtained from the assessment of concrete beams reinforced with bamboo composite reinforcement through four-point bending tests with varying numbers of longitudinal and shear reinforcement

Multiple regression analysis and t-test statistical analysis for evaluating the level of significance of the data and the respective confidence intervals, as well as variance analysis, were carried out as part of the data analysis to interpret the data obtained in each test series. These methods were used to predict and simulate the behavior of the raw bamboo samples with varying geometrical parameters under physical and mechanical tests. They were also used to evaluate the data with respect to the literature review. Further details are provided in

chapters 4, 5 and 6 following the presentation of the results of each series of experiments carried out in this work.

3. Literature review

3.1. Summary

This chapter contains the description of the extensive literature studies, the first of its kind with respect to the objectives of the thesis as described in chapter 2. Reinforced concrete applications are reviewed in this chapter since reinforced concrete remains one of the most widely used building materials in history. Steel reinforcement production processes have been the most common methods of reinforcing materials in concrete construction since the beginning of the 18th century. Significant efforts have been made by researchers around the world to replace steel with alternative reinforcing materials, including Fiber Reinforced Polymer (FRP) composites. The disadvantages of steel reinforcement are mainly related to the costs of the material, the amount of energy required by the production of steel, and the sensitivity of steel to corrosion, which, if not repaired, can lead to structural failure within the life span of the building. This chapter also contains comprehensive reviews of natural and synthetic materials used for reinforcing concrete structures. The chapter describes comprehensively the literature on relevant bamboo species found in bamboo resources of Latin America, Africa, and Asia, and explains, for the very first time within the scientific world, their respective physical and mechanical properties. No detailed study of the physical and mechanical properties of bamboo species with respect to culm geometry, including culm diameter, culm height and wall thickness, is available. Furthermore, the works carried out by Ghavami and Oscar Hidalgo-Lopez only show the suitability of bamboo as a natural material for replacing steel in structural concrete elements. However, the use of raw bamboo for reinforcing concrete members has disadvantages related to the durability of the material; this has not been addressed through systematic studies yet. So far, no studies related to the processing of the raw bamboo culms for fabrication of composite bamboo materials to obtain mechanical properties that are suitable for structural applications have been found. The chapter highlights the need for a comprehensive and unique study of bamboo composite fabrication and the enhancement of their main physical and mechanical properties to produce high-performance composite materials based on natural bamboo fibers. Other studies on alternative reinforcement materials, mainly Fiber Reinforced Polymer (FRP) composite reinforcement, are thoroughly reviewed in this chapter to show the originality of the objectives of this thesis related to the application of composite materials as reinforcement in concrete. Work on durability challenges, such as exposure to water and alkaline solutions, is included in this chapter. The advantages and drawbacks of the production processes of

common FRP reinforcement, including GFRP, CFRP, AFRP and BFRP, are discussed in detail in this chapter. This review provides all the necessary background for evaluating the objectives of this research related to the composite fabrication using epoxy and resin as matrix properties. At present, no other investigation has been carried out on the fabrication of bamboo composite reinforcement with high tensile and flexural strength. The literature in this chapter also indicates that, so far, no studies have investigated the process in which bamboo fibers in the form of thin veneer layers are used as the main fibers in an epoxy-resin system to create high-performance composite materials. Finally, this chapter includes a call for state-of-the-art designs to be developed for the new class of composite reinforcement systems.

3.2.   Common reinforcement systems for structural concrete

Pier Luigi Nervi, an engineer and contractor and one of the greatest 20th-century structural designers in reinforced concrete, described reinforced concrete as the "most fruitful and generous of all building materials" (Nervi 1956). Over the last century, reinforced concrete has changed the built environment greatly. It has a long history, beginning with the usage of mass concrete by adding sand, aggregate and a binder, and later, the addition of metal reinforcement.

Concrete is great in compression but weak in tension, which makes it relatively brittle when it is loaded under tension. Therefore reinforcement is added to concrete member to provide the necessary tensile capacity. The reinforcement element normally has superior tensile strength compared to concrete and can distribute the tensile forces in a way that the ultimate concrete cracking is delayed and the member reaches its maximum load-bearing capacity.

In 1848, in France, Joseph-Louis Lambot fabricated the first reinforced concrete application by building a boat out of iron rods and hydraulic cement (Kirby and Laurson 1932). Lambot exhibited his boat at the Paris Fair in 1855 and, in the same year, he applied for a patent in Brussels covering "iron cement as a substitute for timber" for application in structures exposed to moisture such as water tanks and boats. Unfortunately, his patents went no further and were superseded by patents of Joseph Monier (Collins 2004).

The first-ever patent for a system of reinforcing elements in a concrete application, where iron bars were used within the concrete, was made by William Boutland Wilkinson of Newcastle in England in 1854 (Wilkinson 1911). Wilkinson had a clear appreciation of the structural action of the reinforced concrete and used his idea in a small building in Newcastle in 1865, which had its structural elements designed based on his patent. The building, which

survived till 1955, had 6.5-inch-deep beams 26 inches apart and spanning 14 to 16 feet. But Wilkinson was not able to market this system successfully and the patent did not interest engineers and designers (Sutherland, Humm et al. 2001).

According to Frank Newby (Newby 2001), the first system of reinforced concrete to progress from a simple idea to a viable system of construction was developed by Joseph Monier. Monier, a French gardener, became famous in 1849 for using iron wire mesh and mortar to produce flower pots in a similar way to Lambot (Collins 2004). Monier patented this method in 1867 and, in the following year, he added reinforced concrete tanks to the patent. Monier's first patent for application of reinforced concrete in civil engineering came in 1873, which covered arched bridges and footbridges. Later in 1877, he took out another patent which covered concrete beams with iron bars, but it lacked the scientific background and necessary design concepts to go further (Langmead and Garnaut 2001).

The development of Monier's design into a successful building system only came in after 1884 when Conrad Freytag, a German contractor, bought the patent rights for South Germany. In 1887, Freytag, together with his partners Wayss and Heidschuch, carried out fire tests, pull-out tests and some bending tests to prove the feasibility of Monier's method to the authorities and to develop the idea for the building industry (Gössel and Leuthäuser 2001).

Almost during the same period, in 1879, a building contractor named Francois Hennebique used reinforced concrete for the first time for a private building in Brussels; instead of timber joist, he used precast concrete beams with round iron bars (Sozen, Ichinose et al. 2014). His main intention was to make the building fireproof. He continued his research on reinforced concrete design, and finally in 1892, patented his frame construction system consisting of concrete beams, columns and slabs. In his frame construction system, Hennebique provided a detailed design of stirrups and anchorage of longitudinal bars for the first time, showing he had a clear understanding of the practical problems and function of reinforcement (Slaton 2003, Collins 2004). Hennebique's design was essential in developing the conceptual framework for what is today called 'reinforced concrete design' and which has been widely used since the beginning of the 19th century.

The development of reinforced concrete concept was not limited only to Europe. In the USA, engineers and contractors were looking into concrete construction with iron bars at almost the same time (Collins 2004). In 1875, when Monier was developing his system of reinforced concrete in Europe, Thaddeus Hyatt, an American inventor, was promoting his new system of

construction blocks with iron bars in the USA. He carried out several tests to confirm the fact that iron, steel and concrete had compatible coefficient of expansion, so they would not disintegrate under heat and there would not be any de-bonding between the two elements in a reinforced concrete member (Newlon 1976, Slaton 2003).

The first major reinforced concrete builder in the USA was Ernest Ransome, according to Frank Newby. He patented the first-ever twisted square reinforcing bar in 1884, as shown in Fig. 5 (Newby 2001). Following Ransome's revolutionary work, by the early 19th century in the USA, reinforced concrete was well established as an architectural and industrial building material which was widely used for industrial and residential applications.

(No Model.)

E. L. RANSOME.

BUILDING CONSTRUCTION.

No. 305,226.   Patented Sept. 16, 1884.

FIG. 1.   FIG. 2.
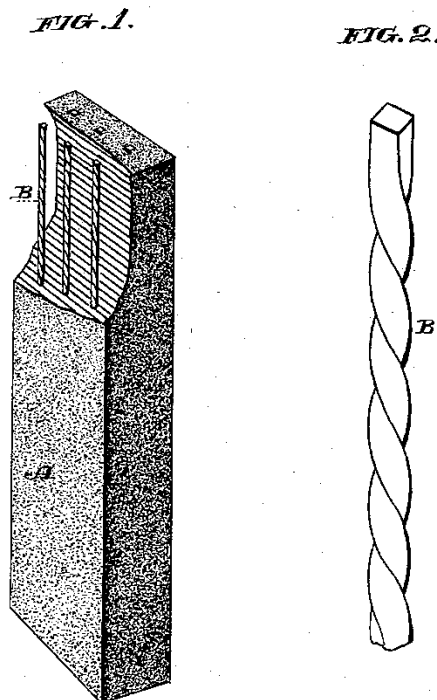
Fig. 5 Ransome's patented twisted bar used to reinforce concrete (Ransome 1884)

Wilkinson, Monier, Freytag, Hennebique and Ransome were all pioneers of reinforced concrete in their times. They showed that using iron bars in a concrete mix is practically possible. However, over the years, the major drawbacks of steel reinforcement became apparent to engineers and architects, and led to the development of alternative reinforcing

27

elements in concrete application, especially in the form of Fiber Reinforced Polymer (FRP) composites. Since the 18th century when the first patent for the design of concrete elements reinforced with steel reinforcement was published, the design concept of steel reinforced concrete has changed in many ways.

In the next section, the normal steel reinforcement system, its design concept, and the theories established to support the conceptual design for concrete beam applications are reviewed and discussed.

3.2.1. Normal steel reinforcement systems, theories, and designs

Much of the experimentation and use of reinforced concrete had been performed on a trial-and-error basis. Mathias Koenen, in Berlin, Germany, was the first experimenter to gather methods of computation for load tests, publishing his analysis of tests conducted in Germany in 1886 (Singer and Williams 1954, Gori 1999, Kurrer and Ramm 2012). Koenen's theory was based on deriving the neutral axis of the beam as a function of the height, and determining the internal stresses by assuming an elastic behavior for the concrete, and that plane sections remain plane. This theory was essential in developing design guides for reinforced concrete.

Koenen's theory of flexure is generally accepted today and is based on four assumptions:

1- Plane sections perpendicular to the neutral axis prior to bending remain so following bending;
2- Stress is proportional to strain;
3- There is a perfect bond between the concrete and steel;
4- Tension stresses in the concrete are not considered in the design.

Today's code of design for concrete structures is based on Limit State Design (LSD) known as Load and Resistance Factor Design (LRFD) which requires a structure to satisfy design requirements concerning both strength and serviceability.

The limit state method was originally developed in the Soviet Union in the period 1935 to 1955, and later was introduced in concrete codes in Eastern Europe in the 1950s (Jain 1993, Kotsovos and Pavlovic 1999, Varghese 2008).

According to LSD, a structure could become unfit for service in many ways, for instance, through complete or partial failure, or by excessive deflection, or even through large

cracking. When either of these failure modes happens, the structure enters into a limit state. Generally, there are two main categories, which correspond to the strength limit state and the serviceability limit state (Hughes 1976, Kotsovos and Pavlovic 1999, Varghese 2008).

In the strength limit state design, the ultimate strength of the structure or a member of the structure should allow an overload. Therefore, the structure should be designed via ultimate load theory to carry the required overload. The specific load could be the flexure, compression, shear, torsion or tension (Hughes 1976). Hence, strength limit state ensures that the structural elements of a building will neither become unstable nor collapse under any arrangement of overloads.

In the serviceability limit state, the structure should be fit for durability, deflection, cracking or overall stability (Punmia, Jain et al. 2007). In durability state, the structure should be fit for the environment, for instance, by achieving the minimum concrete cover for steel reinforcement in beams or columns to prevent any corrosion-induced failure or by following certain cement content in the concrete mix to satisfy the permeability limits specified in international code of practice (Varghese 2008).

As Ashok Jain, professor of civil engineering at the Indian Institute of Technology, described in his book titled "Reinforced Concrete: Limit State Design", in deflection limit state, the structure under service load conditions should not deflect more than the allowable limits set in international codes to prevent any unnecessary deflection that might significantly change the appearance of the structure or the finishes and partitions installed in the building. The deflection limit state could normally be reached by optimizing the size of any structural section or by adjusting the reinforcement ratio to prevent excessive deflection (Jain 1993).

Professor Punmia from MBM Engineering College in India explained, in his book on concrete limit state, that when cracking limit state design is practiced, the structure must not develop large cracks which are wider than the allowable crack width stated in international design codes. Similar to deflection, extreme cracking of concrete element can negatively affect the appearance or long-term durability of the structure (Punmia, Jain et al. 2007).

Finally, the overall stability should be achieved by following the specific design criteria set by international building codes for vertical, horizontal and internal ties in the structure to avoid or limit the effect of overturning or swaying of the substructure and foundation. Normally the tow limit states are considered in the design; that is, the strength limit state and

the serviceability limit state of deflection and cracking under service loads. Usually, the structure is designed for ultimate strength limit state, and then is checked for other limit state conditions such as deflection, cracking and stability limit state.

Limit state design philosophy uses the concept of probability and stochastic analysis. It is based on the fact that one cannot be certain about the strength of concrete or steel reinforcement due to manufacturing conditions or design limitations. Also, the loads applied to a structure might not be the precise values considered in the design due to errors in construction, or errors in calculations, or due to environmental effects. Therefore, the load might be greater than originally considered by the designer in designing the structure. To account for these limitations, in limit state design characteristic values are often used.

The maximum working load that any structural element of a building has to withstand and should be designed for is called characteristic load. The strength materials such as concrete and steel reinforcement are required to possess is called characteristic strength (Sinha 1996, Hartsuijker and Welleman 2007, Krishna 2007, Varghese 2008).

It is assumed by international standards in Europe and the USA that loads and strengths follow a normal distribution curve for the purpose of limit state design (Hughes 1976, Jain 1993, Kotsovos and Pavlovic 1999, Punmia, Jain et al. 2007, Varghese 2008). A normal distribution curve is shown in Fig. 6.
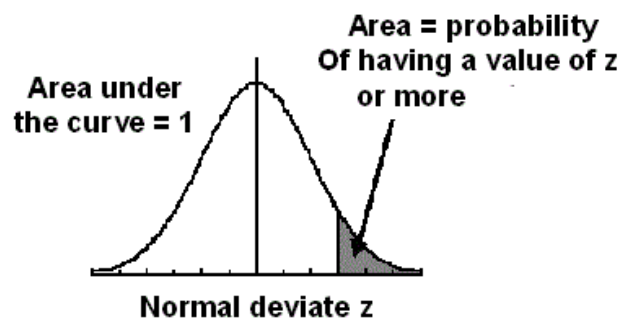
Fig. 6 Normal distribution curve for variations of load and strength (Punmia, Jain et al. 2007)

Fig. 7 shows a normal distribution curve that covers 95% reliability. From Fig.7, the value of K, which corresponds to 5% of the area of the curve, is 1.645. Fig. 8 shows the normal distribution curve for material strength where f_k is the characteristic strength and f_m is the mean strength of the material.

Characteristic strength is defined by Eq. 1:

$$f_k = f_m - K(S_d) \quad \text{(Eq. 1)}$$

where S_d is standard deviation for the series of test results.

Similar to characteristic strength, characteristic design load is defined as the value of load, which has a 95% probability of not being exceeded during the life span of the building. Fig. 9 shows the characteristic load distribution curve.
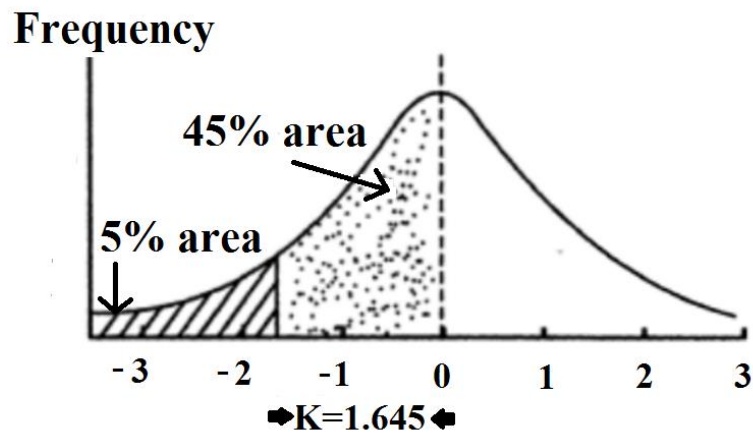
Fig. 7 Normal distribution curve for 95% reliability (Jain 1993)
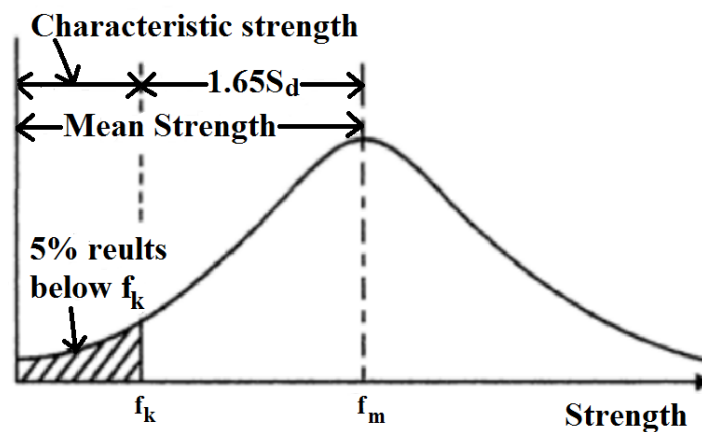
Fig. 8 Distribution curve for material strength (Jain 1993)
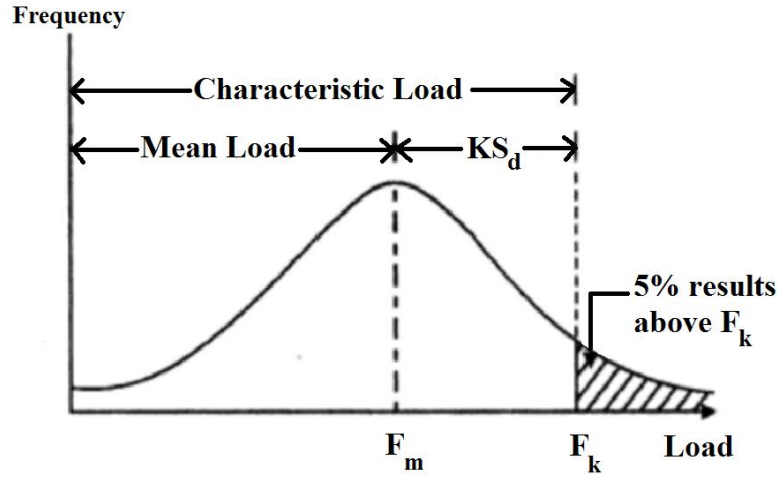
The characteristic load should be calculated from the mean and standard deviation with a statistical method similar to strength values, but since there is a lack of sufficient statistical data for loads applied to a structure, it is not possible to express loads in statistical forms. Therefore, international building codes come with specific values based on research and experiments for the characteristic loads. These characteristic loads are often defined as live load, dead load, wind load and some other partial loads.

Structures normally are designed according to international building codes where characteristic loads are multiplied with appropriate factors of safety based on the type of loads applied to them, and based on the limit state of design being considered. Therefore the so-called *design load* in limit state design concept is calculated by applying a safety factor to the characteristic load. Eq. 2 shows the design load calculation in the limit state design concept according to the American Concrete Institute (ACI) design guide (American Concrete Institute 2008).

Design load = $\gamma_f \times$ characteristic load   (Eq. 2)

In Eq. 2, γ_f is the load safety factor to cover the variation in loading, design and in construction as described earlier about the concept of limit state design. Similar to design load, *design strength* is also calculated by applying a strength safety factor according to the ACI design guide, which is shown in Eq. 3.

Design strength = $^1/\gamma_m \times$ characteristic strength   (Eq. 3)

32

In Eq. 3, γ_m is the strength safety factor which depends on the material strength and the limit state design being considered. In the ACI design guide, strength safety factor ($^1/\gamma_m$) is known as the *strength reduction factor* (Φ) (American Concrete Institute 2008). Therefore, the design strength can be calculated as shown in Eq. 4.

Design Strength = $\Phi \times$ characteristic strength   (Eq. 4)

With safety factors for loads and reduction factors for strength, the ACI design code has considered several load combinations to be used for limit state design calculations. In load combinations defined by the ACI design guide, there are two main categories of load which are applied to a structure: Dead Load (DL) and Live Load (LL).

Dead load usually refers to the weight of the elements of a building which are normally made of concrete or steel. In addition to the weight of the structure, there are permanent loads such as floor finishes, cladding and service equipment which are considered as dead loads in the structural design of the building elements.

Unlike dead loads, which are permanent in nature, live loads are of a transient nature. They may change during the life span of the structure, for instance by relocating the partitions over time in the buildings. Therefore, the majority of unfixed articles in a house – for example, people who are living in a building, or furniture which could be easily moved or relocated – will result in live load on the structure.

Besides dead load and live load, there are other types of loads, such as rain load, snow load, soil lateral load, flood load, wind load and earthquake load, which need to be considered in the design of reinforced concrete structures (Ambrose and Tripeny 2007). Each category of load mentioned have its own set of design guidelines which need careful planning and investigation during the early design stage of the structure.

According to the ACI design guide for reinforced concrete, the basic requirement for strength design is described in terms of design strength and required strength as shown in Eq. 5.

Design strength $\geq$ Required strength   (Eq. 5)

In this design approach which was described earlier, the ACI design guide recommends considering the strength reduction factor Φ and nominal strength, which is shown in Eq. 6.

Φ (nominal strength) ≥ U   (Eq. 6)

As can be seen from both Eq. 5 and Eq. 6, the design strength of a member that is equal to the applicable strength reduction factor Φ times the nominal strength of that member must be equal to or greater than the required strength U. The required strength U is calculated by multiplying load effects by load factors. The ACI design guide recommends different load combinations for strength design methods, which are based on three main parameters (American Concrete Institute 2008):

1- The level of accuracy in calculation:

   For instance, in the case of dead loads, there might be some variations arising from assumptions made in the design stage due to errors made at the construction site when casting concrete elements. The concrete member might not be accurately sized according to the specifications in the design stage, or its properties (such as density or weight) could differ from design requirements – these would affect the dead load calculations.

2- The variations during the life span of the structure:

   For example, in terms of live loads, they can vary in magnitude over time very frequently. The fixtures of the house can be relocated, or replaced with heavier or lighter materials, during the life span of the building.

3- The probability of the worst-case loading:

   For instance, the possibility of having all different load types applied simultaneously on the structure is relatively low.

Based on these factors, load combinations are designed by adding to the dead load, other loads such as live load, wind load, snow load or earthquake load with their respective load factors. The following equations are the most commonly used load combinations for the design of reinforced concrete structures according to ACI 318 section 9.2, which considers the most common type of loading on a building, including the dead load (DL) and live load (LL).

U = 1.4DL   (Eq. 7)

U = 1.2DL + 1.6LL   (Eq. 8)

To design a structural member, all of the load combinations must be checked, and the worst possible load combination should be used to determine the member size and required reinforcement in the reinforced concrete design.

As discussed earlier, the design strength of a member is calculated by multiplying the nominal strength by a strength reduction factor Φ according to Eq. 6. The Φ factors are determined based on the following criteria (Williams 2003, McCormac and Brown 2013):

- To allow for inaccuracies in design equations where assumptions are made for oversimplifications for material strengths or properties.
- To take into consideration the variations in material strengths, such as the concrete strength resulting from different type of cement or aggregates on site.
- To consider the importance of a member in which failure of that member in a structure is more crucial compared to other members. For instance, the failure of a column in a structure is more crucial than the failure of a beam.

The strength reduction factor Φ for a beam is 0.90 and for a column 0.75, according to the ACI design guide (American Concrete Institute 2008). The strength reduction factor Φ for columns is lower compared to that for beams; the reason is that column failures are more crucial compared to beam failures. A column supports a much greater area compared to a beam; therefore it should be designed with greater safety measures.

Once the load combinations are determined, the basic theories on the strength design of reinforced concrete elements will be used to evaluate the nominal strength of a section subjected to flexure, axial and shear forces, or a combination of all loads together.

As mentioned earlier in this chapter, many theories on the strength design of reinforced concrete structures emerged in the late 18th century and early 19th century. Much of the experimentation and use of reinforced concrete were on a trial-and-error basis. Mathias Koenen, in Berlin, Germany, was the first experimenter to deduce methods of computation for load tests, and published his analysis of tests conducted in 1886 in Germany. Koenen's theory of flexure for reinforced concrete beams was based on the following premises:

1- Plane sections perpendicular to the neutral axis prior to bending remain so following bending;
2- Stress is proportional to strain;
3- There is a perfect bond between the concrete and steel; and

4- Tension stresses in the concrete are not considered.

As the reinforced concrete element reaches its ultimate strength, both concrete and reinforcing steel behave rigidly. Therefore, the design theories should consider this behavior. Unlike steel, concrete is a strongly heterogeneous material which shows several inelastic behaviors such as shrinkage, creep and micro crack growth. As such, it is easier to analytically define the inelastic behavior of reinforcing steel than that of concrete. The strength design method is based on two important conditions:

1- Static equilibrium
2- Compatibility of strains

In static equilibrium, the compressive and tensile forces acting on any cross section of a member are in equilibrium. This condition is used in determining the nominal strengths of reinforced concrete elements.

In compatibility of strains condition, the strain in a reinforcing bar that is embedded in concrete is equal to the strain in concrete at that level. This condition is in line with Koenen's flexural theory that there is a perfect bond between the concrete and reinforcing steel bar, and both materials act together when undergoing any external loading (Williams 2003).

The ACI design guide recommends four major assumptions in the strength design method for members subjected to flexure or axial loads or both. These assumptions, which have developed over the years, are necessary to determine the nominal strength of a reinforced concrete member and are listed here (American Concrete Institute 2008):

1- Strains in the reinforcement bars and concrete are proportional to the distance from the neutral axis.

This is, in fact, one of the main assumptions in the strength design theory, and simply translates to the fact that plane sections perpendicular to the axis of bending prior to bending remain plane after bending. In other words, this assumption shows that reinforcing bars and concrete act together against any external force, as mentioned earlier in the compatibility of strains and in Koenen's theory of flexure. Therefore this assumption indicates that a perfect bonding between concrete and steel reinforcement exists.

Hognestad, Hanson, McHenry and Rusch have all shown that the distribution of strain is linear across a reinforced concrete element cross section (Hognestad, Hanson et al. 1955,

Rusch 1960, Mattock, Kriz et al. 1961). Fig. 10 shows the strain distribution over the depth (d) of a rectangular reinforced concrete element in the strength design method.

The depth of a concrete section (d) is measured from the extreme compressive fiber to the center of the steel reinforcement in the tension zone (Punmia, Jain et al. 2007). The strain in concrete (ε_c) and strain in reinforcing steel bar (ε_s) are directly proportional to the distance from the Neutral Axis (NA), which is located at distance c from the compression zone of the element. It is assumed in Fig. 10 that strains above the NA are compressive and strains below the NA are tensile. This assumption will help the engineers to determine the stress and strain in the reinforcement bars, and to estimate the required number of reinforcement bars to sustain the load and corresponding moment without premature failure.
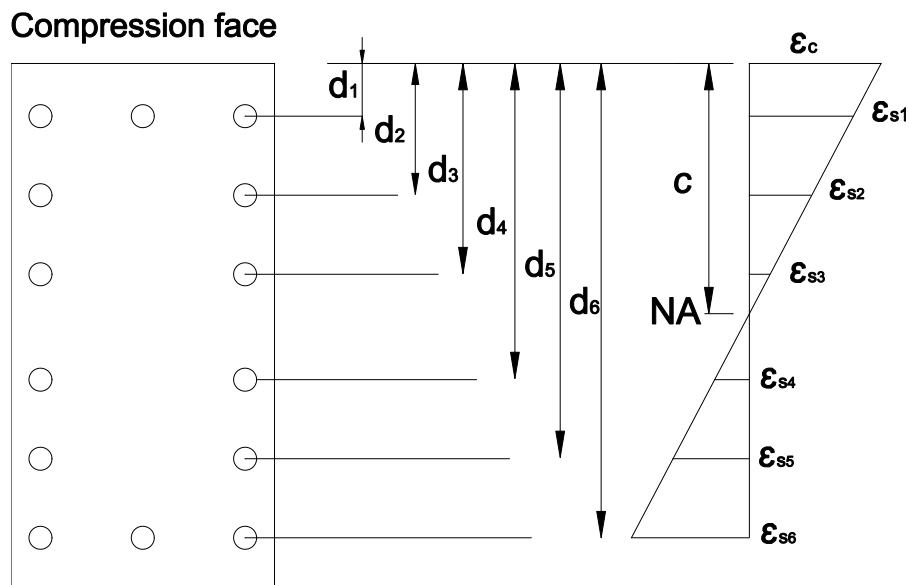
Fig. 10 Distribution of strain over the depth of a rectangular reinforced concrete beam section

2- The tensile strength of concrete is neglected in calculations for axial and flexural strength and in estimating the member size.

The tensile strength of concrete is generally between 10 to 15 percent of compressive strength (Krishna 2007). This assumption makes the flexural calculations of the beam simple and straightforward, since the contribution of tensile strength of the concrete to the ultimate flexural capacity of the beam is rather small and negligible. However for serviceability calculations, the tensile strength of concrete may be considered for crack and deflection control when necessary (American Concrete Institute 2008).

3- Maximum concrete working strain is assumed to be equal to 0.003.

In other words, this assumption indicates that the concrete member will fail if the maximum compressive strain in that member reaches 0.003, according to the ACI design guide. This value was obtained from tests of several concrete beams and columns over the past 50 years of research on reinforced concrete design (Rusch 1960, Desayi and Krishnan 1964, Popovics 1970, Wang, Shah et al. 1978, Nataraja, Dhang et al. 1999).

4- The compressive stress-strain distribution for concrete is assumed to be rectangular, trapezoidal, parabolic, or any shape that results in calculation of strength in substantial agreement with results from comprehensive laboratory tests.

This assumption implies simplicity in design computations of concrete stress-strain. The stress-strain relationship for concrete in compression is not a straight line but a curve similar to that shown in Fig. 11.
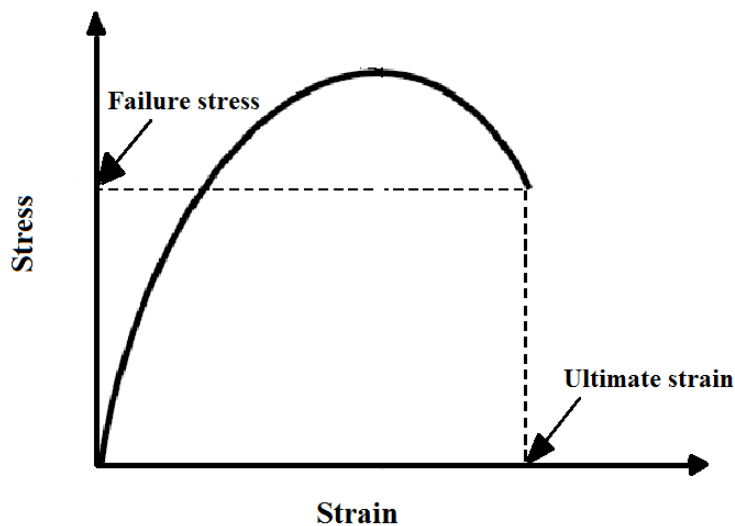
Fig. 11 Stress-strain curve for concrete in compression

The ACI design guide recommends using a comparable rectangular compressive stress distribution, or the so-called Whitney's stress block, to replace the stress-strain curve shown in Fig. 12 (Kong and Evans 2013). In the equivalent rectangular stress block, an average stress of 0.85$f'c$ is used where $f'c$ is the concrete compressive strength. The stress block has a depth of a, which is a function of the Neutral Axis depth, c and is measured from the edge of the concrete with the maximum compressive strain. The ACI design guide recommends that

β_1 shall be taken as 0.85 for concrete with compressive strength up to and including 30MPa and for concrete with $f'c > 30$MPa, Eq. 9 should be followed to calculate β_1.

$\beta_1 = 0.85 - 0.008 \, (f'c - 30\text{MPa}) \geq 0.65$ (Eq.9)

By assuming a rectangular stress block for the reinforced concrete section, the calculation of resultants forces becomes relatively simple. Fig. 12 demonstrates the compressive stress block together with the compressive force in concrete (C) and the ensile force (T) in steel reinforcement.
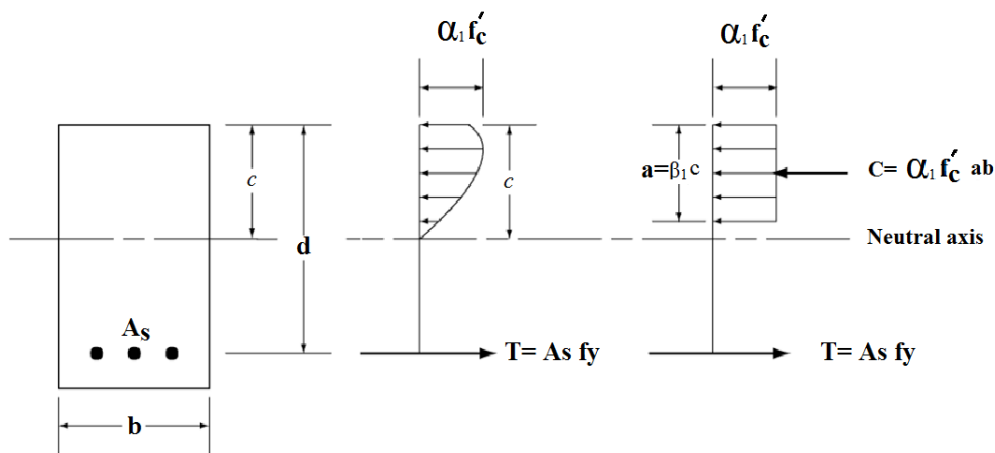
Fig. 12 Concrete stress block with compressive force in concrete (C) and tensile force (T) in steel reinforcement

The concrete compressive force as shown in Fig. 12 can be calculated using Eq. 10:

$C = \alpha_1 f'_c \, a \, b$ (Eq. 10)

Where a is the depth of compressive stress block, b is the width of the concrete section and α_1 is a load factor which takes into account variations in concrete compressive strength for which the ACI design guide suggests a value of 0.85 (American Concrete Institute 2008). Several laboratory tests carried out on beams under flexural load have shown comparable results with the analytical compressive stress block and the calculations of compressive and tensile forces based on the ACI stress block model (Popovics 1970, Kent and Park 1971, Mander, Priestley et al. 1988, Oztekin, Pul et al. 2003, Ozbakkaloglu and Saatcioglu 2004).

The tensile force in steel reinforcement in Fig. 12 can be calculated using Eq. 11:

$T = A_s f_y$ (Eq. 11)

Where A_s is the area of steel reinforcement in the tension zone of the concrete member and f_y is their yield strength. The ACI design guide assumes that the steel reinforcement in the tension zone of the concrete member yields before the concrete section crushes (American Concrete Institute 2008). Yield strength is defined as the strength of steel at a certain point where steel starts to have plastic deformation which is irreversible once the applied stress is released (Clifford, Simmons et al. 2012).

The nominal moment capacity (M_n) of any beam cross-section can be calculated from Fig. 13 by considering two requirements according to the ACI design guide (American Concrete Institute 2008):

1- Stress and strain compatibility, where stress at any section of a member should correspond to the strain at that section or, as stated earlier, strain in reinforcement and concrete is assumed to be proportional to the distance from the neutral axis.
2- Equilibrium, where there should be a balance between internal forces (Fig. 13) and the loadings applied to the member.

Eq. 12 shows the equilibrium condition and consequently the nominal moment capacity of the section can be calculated using Eq. 13.

$$T = C = \alpha_1 f'_c\, a\, b = A_s f_y \qquad \text{(Eq. 12)}$$

$$M_n = C\,(\,d - a/2\,) = T\,(\,d - a\,/2\,) \qquad \text{(Eq. 13)}$$

However, the assumption that was made regarding the yielding of steel reinforcement in Eq. 11 has to be checked and verified. To do so, the stress and strain compatibility condition should be applied to calculate the resulting strain in steel reinforcement (ε_s) and comparing that with the steel yield strain (ε_{sy}).

To control if the member size and amount of reinforcement for the applied load are adequate, the design equation for flexure has to be checked using Eq. 14.

$$\Phi\, Mn \geq Mu \qquad \text{(Eq. 14)}$$

Where Φ is the strength reduction factor and is defined by Eq. 4.

The ACI design guide defines four modes of failure for a beam under flexural load which include (American Concrete Institute 2008):

1- Balanced failure mode; where the strains in the concrete and steel reach their maximum limit. Concrete reaches the limiting strain of 0.003 and steel reinforcement in the tension zone of the member reaches its yield strain.

2- Tension-controlled failure mode; where the strain in the extreme layer of steel reinforcement in tension zone is equal to or greater than 0.005. This mode of failure is achieved by the yielding of steel reinforcement in the tension zone before the crushing of the concrete in the compression zone of the section.

3- Compression-controlled failure mode; where the crushing of the concrete in the compression zone of the section occurs before the yielding of the steel reinforcement. This is a brittle and sudden failure which the ACI design guide recommends to be avoided. This happens as a result of the application of too many steel reinforcement in the tension zone of the concrete member. Therefore the strain in the steel reinforcement is less than or equal to the compression-controlled strain limit set by the ACI design guide.

4- Transition-failure mode; which refers to a concrete section that is not either tension-controlled or compression-controlled.

The ACI design guide recommends a concrete beam which is designed for tension-controlled mode of failure, where the steel reinforcement in the tension zone yields before the crushing of the concrete in the compression zone. This failure mode ensures sufficient ductility and adequate warning before the final failure of the beam by displaying large deflections along the concrete beam length (Chen and Lui 2005).

In addition to the reinforcement used along the length of the concrete beam and in the tension zone of the section to resist the tensile stress developed by the external loading, there must be another group of reinforcement to resist the shear forces developed by the action of external loads. This group of reinforcement is called stirrup.

The shear stress is developed as a result of the internal actions of the concrete beam, and it affects the concrete member in both tension and compression; consequently it will be followed by diagonal tension and compression stresses. Fig. 13 shows the internal forces on a section of a concrete beam, and Fig. 14 displays the typical diagonal forces produced by the shear stress in the beam.
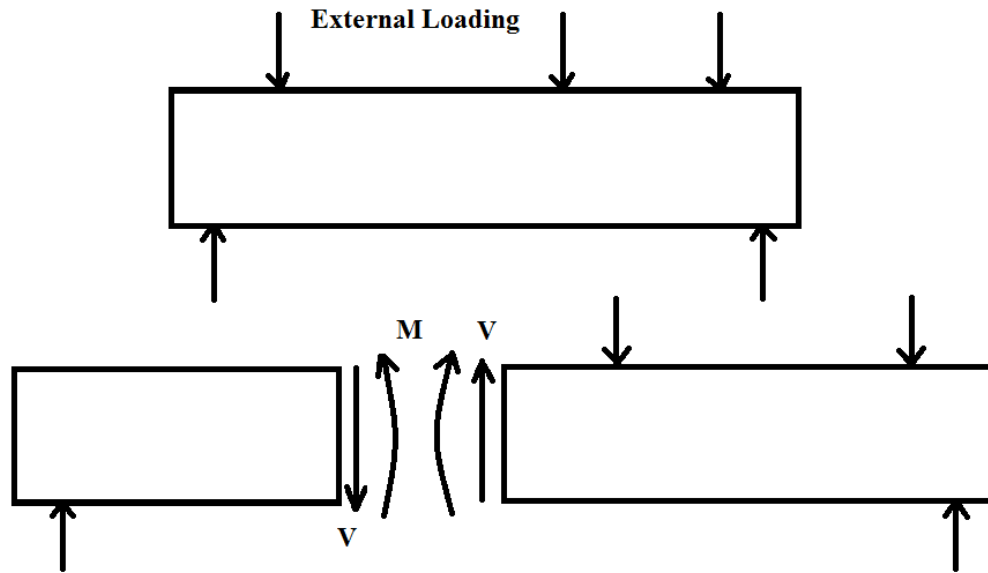
Fig. 13 Internal forces acting on a section of a concrete beam displaying the moment (M) and Shear force (V)

Tension   Compression   Tension in Beam
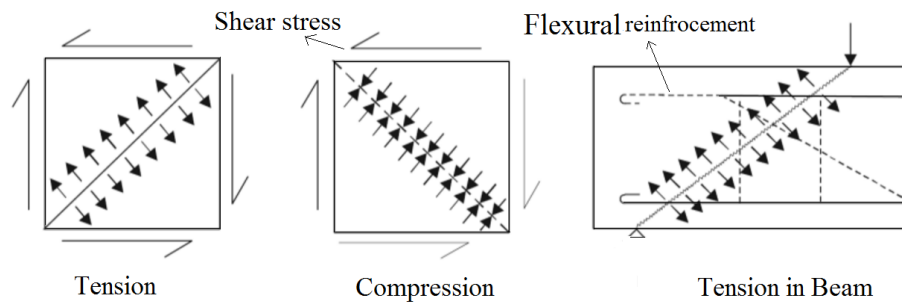
Fig. 14 Diagonal tension and compression stresses acting on a section of a beam as a result of internal shear stress (Varghese 2008)

The subsequent tension stresses developed by the shear stresses in the concrete beam can result in the cracking of the concrete beam, given the low tensile strength of concrete. Therefore vertical reinforcement or stirrups should be provided to resist the diagonal stresses and close any diagonal cracks which might occur during the life span of the beam. The diagonal shear cracks in a beam under external loads are displayed in Fig. 15.

The shear stress distribution for a concrete beam is shown in Fig. 16. In the calculations, the ACI design guide recommends an average shear stress across the cross section. The shear stress (υ) is obtained by dividing the shear force by the area of the cross section according to Eq. 15.

$\upsilon = V/bd$ (Eq. 15)
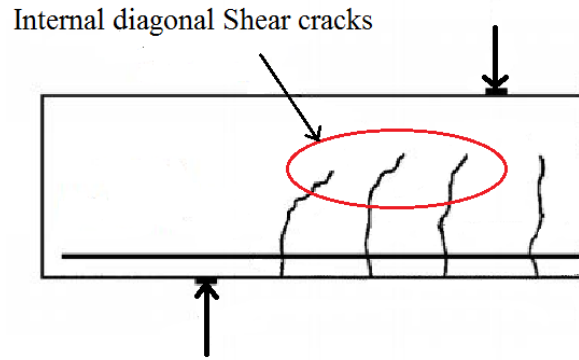
Fig. 15 The diagonal shear cracks in beam under external loads (Davies and Neal 2014)

Average Shear Stress
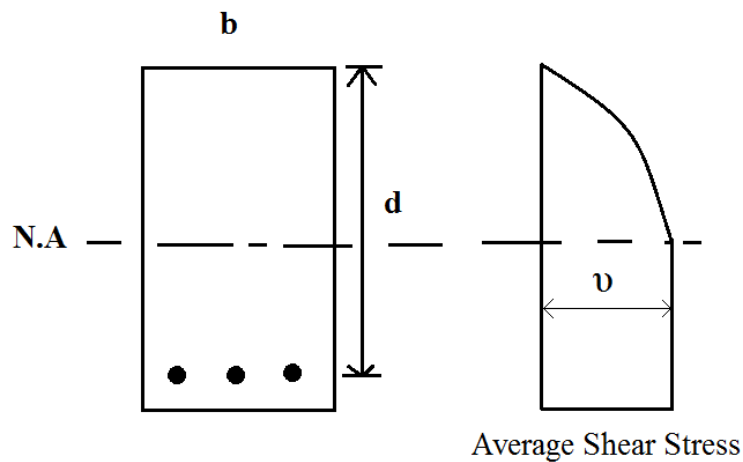
Fig. 16 Shear stress distribution in a concrete beam section

According to the ACI design guide, Eq. 16 is used to check the shear capacity of concrete beams. In this design equation, V_n is the nominal shear resistance of the concrete beam and V_u is the shear force from the loads acting on the beam. Unlike Eq. 14 for flexural capacity of the beam where Φ is equal to 0.90, in Eq. 16 for shear capacity control of the beam, Φ is taken as equal to 0.75 according to the ACI design guide and after numerous laboratory tests.

$\Phi V_n \geq V_u$ (Eq. 16)

The nominal shear resistance in a concrete beam is provided by the concrete and stirrups. Eq. 17 is used to calculate the nominal shear resistance of the reinforced concrete beam.

$V_n = V_c + V_s$ (Eq. 17)

In this equation, V_c is the shear strength provided by the concrete and V_s is the shear resistance developed by the stirrups. V_c for beams is calculated using Eq. 18 where several laboratory tests have shown that the concrete shear strength is in accordance with this

equation (Sarsam and Al-Musawi 1992, Tompos and Frosch 2002, American Concrete Institute 2008).

$$V_c = \frac{\sqrt{f_c}}{6} bd \quad \text{(Eq.18)}$$

The shear resistance of the stirrups can be calculated by the cross-sectional area of stirrups (A_v), the yield strength of the stirrups (f_y) and knowing the spacing between the stirrups (s), as shown in Fig. 17.

Eq. 19 is used to calculate the shear strength of the stirrups according to the ACI design guide (Angelakos, Bentz et al. 2001, Tompos and Frosch 2002, American Concrete Institute 2008).

$$V_s = \frac{A_v f_y d}{s} \quad \text{(Eq. 19)}$$
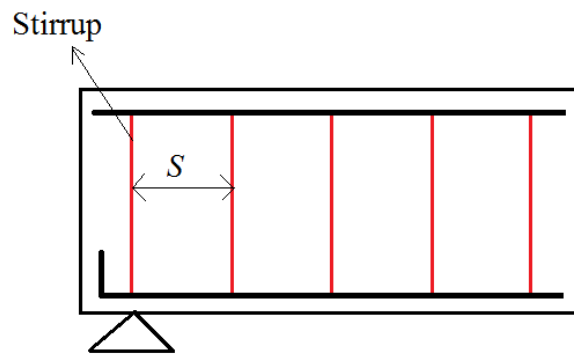
Fig. 17 Stirrups in a concrete beam section spaced regularly at intervals (s)

By combining Eq. 19 and Eq. 16, the spacing of the stirrups (s) can be estimated from Eq. 20.

$$S = \frac{A_v f_y d}{V_u/\Phi - V_c} \quad \text{(Eq. 20)}$$

Generally, in design calculations for the shear resistance of a concrete beam, the factored shear forces acting on the beam are computed according to the procedures for structural analysis stated in the design guides. Once the factored shear forces are known, Eq. 18 is used to calculate the concrete shear resistance, followed by Eq. 20 where the spacing of the stirrups can be estimated by assuming a nominal size for the stirrups. The whole procedure should be repeated till the optimal size and spacing of the stirrups are selected.

Once the axial and shear reinforcement are designed according to the limit state criteria, the ACI design guide recommends checking the serviceability limit states for deflection and

cracking. The limits are defined according to specific applications e.g. beams, columns or slabs in ACI 318-08.

3.3. Alternative reinforcement systems for structural concrete

Concrete is one of the most widely used building materials worldwide. As explained in the introduction, concrete has one major drawback; it has a very low tensile strength. Concrete performs well in compression but when is used in applications where it has to sustain tensile forces, for instance, in concrete beams, large cracks and premature failure are inevitable.

To overcome this problem and be able to use concrete widely for the construction sector in diverse applications, reinforcing bars with high tensile strength are used in structural concrete. The most common type of reinforcing bars is steel reinforcement. Steel reinforcement has been used in a variety of structural concrete buildings and infrastructure in the past decades. However, the major challenge of using steel reinforcement in concrete is the corrosion and the corrosion-induced problems.

Corrosion of the steel reinforcement in concrete is often initiated by either concrete carbonation or exposure of the concrete element to chloride ions as discussed in various works (Bentur, Berke et al. 1997, Broomfield 2002). Concrete itself provides a protection layer around the reinforcement bars. It provides an alkaline environment with a pH level of 12 to 13, where a thin oxide layer forms on the steel rebar and prevents iron atoms from dissolving; therefore steel reinforcement remains in a passive state and the corrosion is prevented or reduced (Bertolini, Elsener et al. 2013). However, the major challenge for steel reinforced concrete is when this protective layer around the steel reinforcement is damaged, which leads to the initiation of the corrosion process. The damage to the passive layer is caused by carbonation or exposure to chloride ions.

Carbonation is a process in which carbon dioxide (CO_2) from the air penetrates the concrete and reacts with hydroxides (OH^-), such as calcium hydroxide $Ca(OH)_2$, to form carbonates ($CaCO_3$) (Bertolini, Elsener et al. 2013). This reaction reduces the pH of the concrete pore solution to as low as 8.5, causing damage to the passive layer around the steel bars and initiating corrosion. Eq. 21 shows the carbonation process.

$$Ca(OH)_2 + CO_2 \rightarrow CaCO_3 + H_2O \quad (Eq.\ 21)$$

The carbonation process can only take place in the presence of water, in order for the CO_2 to dissolve. Therefore, if the concrete environment is dry, the CO_2 will not be able to react with

the hydroxides (OH$^-$) groups in the concrete matrix and carbonation will not occur (Broomfield 2002).

As explained by Professor Arnon Bentur from the Israel Institute of Technology, Neal Berke from Grace Construction Products in the USA and Professor Sidney Diamond from Purdue University in the USA in their book "Steel Corrosion in Concrete**:** Fundamentals and civil engineering practice", chloride-induced corrosion typically occurs when the reinforced concrete is exposed to de-icing salts, seawater or to the marine environment. Chloride ions penetrate through the concrete, reach the oxide film around the steel reinforcement bars and damage the protective layer around the bars (Bentur, Berke et al. 1997, Glass and Buenfeld 2000). Therefore, in the presence of oxygen and moisture, the corrosion of rebar can occur. With a continuous supply of oxygen and moisture, iron is dissolved in the form of ferrous hydroxide ($Fe(OH_2)$) and forms a layer of rust around the steel bars. The rust occupies a volume larger than the reinforcement bars, which induces extensive forces in the concrete in the form of tensile stress. Given the weak nature of concrete in tension, these forces initiate the cracking of the concrete layers around the steel reinforcement bars in the form of concrete delamination, or the debonding of the reinforcement bars from the concrete matrix (Bentur, Berke et al. 1997, Yoon, Wang et al. 2000).

Furthermore, these initial cracks will lead to more water and oxygen reaching the surface of the steel bars, increasing the corrosion rate, resulting in spalling of the concrete layer and ultimately exposing the reinforcement bars to severe corrosion as shown in Fig. 18 (Lee, Noguchi et al. 2002).

The corrosion will also lead to a reduction in the cross-sectional area of the reinforcement bars as a result of the dissolving of the iron from the reinforcement surface in the concrete matrix in the form of ferrous hydroxide, which reduces the load-bearing capacity of the reinforcement bars (Almusallam 2001). Fig. 19 displays the corroded reinforcement in a section of a reinforced concrete beam.
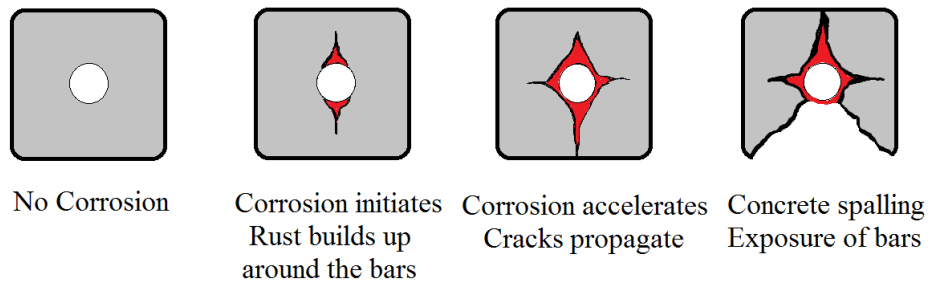
Fig. 19 Corroded reinforcements in a section of concrete beam
(Bertolini, Elsener et al. 2013)

As mentioned earlier, the major challenge in the use of steel reinforcement in structural concrete is corrosion and corrosion-related damages. To reduce the corrosion of the embedded steel reinforcement in concrete, different approaches can be undertaken:

1- Improving the quality of concrete:

By controlling the workmanship during the casting and placement of the concrete, or by adding admixtures which can improve the durability and reduce the porosity of concrete, and applying water repellent coating to the surface of the concrete, the ingress of chloride ions or diffusion of CO_2 into the concrete matrix can be prevented

or delayed substantially, as explained in various scientific research works carried out previously (Tripler and White 1966, Rasheeduzzafar, Al-Saadoun et al. 1992, Virmani and Clemena 1998).

2- Applying coating on reinforcement bars:

As described by Cheng, Huang, Wu, and Chen as well as Clifton, Beeghly and Mathey, the epoxy coating can be used to protect the reinforcement bar in a severely corrosive environment, especially for the concrete application in a marine environment or when the concrete member is exposed to de-icing salts. However, the quality of the coating applied on the surface of the reinforcement bars could affect the long-term resistance of the bars to corrosion (Clifton, Beeghly et al. 1974, Cheng, Huang et al. 2005). Therefore, it is necessary to take precautions in the handling and transportation of the bars or when placing the concrete to prevent any damage to the coated surface of the bar: if not, its corrosion rate will be similar to that of normal steel reinforcement bars (Venkatesan, Palaniswamy et al. 2006).

3- Application of a non-ferrous and non-metallic reinforcement material:

The problem of steel reinforcement corrosion has led many engineers and researchers to look for alternative reinforcement materials that do not corrode and have comparable mechanical properties to steel reinforcement, and which could potentially replace steel reinforcement in different applications. Among the alternative materials, Fiber Reinforced Polymer (FRP) materials have gained popularity in recent years due to the advantages they offer over metallic or ferrous reinforcement materials.

The first approach towards concrete quality control is not within the scope of this thesis and is covered extensively in the literature on concrete over the past fifty years. The second approach on coated reinforcement is reviewed briefly in this section. More emphasis has been given to the third approach on FRP reinforcement as it is more relevant to this research.

3.3.1. Coated reinforcement systems

Extensive research was carried out by James Clifton, Hugh Beeghly and Robert Mathey from the Materials and Composites Section Center for Building Technology of the National Bureau of Standards in Washington in 1974 to determine the feasibility of using organic coatings, especially epoxies, to protect the steel reinforcing bars embedded in concrete from accelerated corrosion at the Center for Building Technology in Washington. The findings of the research proved that coating of the reinforcement prevented corrosion beyond the concrete cover.

The coating could be a metallic or non-metallic material which acts as a protective layer around the steel bar. The coating provides an insulating layer around the steel reinforcement bar to prevent the ingress of CO_2 or chloride ions – the presence of which would cause corrosion to occur. The protection level is largely dependent on the type of coating, the adhesion between the coating and the steel bar, and also the type of environment to which it is exposed in the long term (Clifton, Beeghly et al. 1974, Lee, Krauss et al. 2004).

James Clifton, Hugh Beeghly and Robert Mathey further described that the common type of non-metallic coating could be the epoxy coating. Their study of more than 40 coatings indicated that Epoxy Coated Reinforcement (ECR) could provide improved corrosion resistance against carbonation and chloride ions (Clifton, Beeghly et al. 1974).

Kazusuke Kobayashi and Koji Takewaka at the Institute of Industrial Science, University of Tokyo, in 1984 showed that ECR could be produced via a continuous process in a plant where the steel bar was shot blasted to remove unnecessary particles and impurities and which also provided a surface finish required for the epoxy to bond. Subsequently, the bar was heated and passed through a spray area where the epoxy powder was sprayed onto the surface of the bar (Clifton, Beeghly et al. 1974, Kobayashi and Takewaka 1984). Fig. 20 shows steel reinforcement bars which have been coated with epoxy.

Epoxy coated reinforcing bars were used for the first time in the construction of a highway bridge over the Schuylkill River in Pennsylvania, USA, in 1973. Since then, it has become a predominant type of non-corrosive reinforcement in the USA and Canada, being mostly used in bridge deck construction (Erdogdu and Bremner 1993).

It was only in 1992 when several premature failures happened to a few bridges in Florida, USA, after being exposed to the severe marine environment, that the use of ECR was stopped by the authorities, according to several reports (Smith, Kessler et al. 1993, Manning 1996). A comprehensive investigation by Alberto Sagüés, Rodney Powers and Richard Kessler from the University of South Florida and the Florida Department of Transportation in 1994 showed that, within a few years, the epoxy coating started to de-bond from the steel reinforcement bar; due to the exposure to the marine environment, the corrosion process accelerated in the presence of chloride ions (Sagüés, Lee et al. 1994). The de-bonding process was likely initiated from damage to the surface of ECR during the handling or placing of the reinforcement in concrete.

Due to the vulnerable nature of epoxy coated reinforcement, researchers looked into alternative coating materials which could perform better than epoxy. Professor Stephen Yeomans from the University of New South Wales, Australia, explored alternative coatings for reinforcement, which were mainly metallic coatings due to their hardness and superior bonding to the base steel in reinforcement bar compared to epoxy coatings. Yeomans studied various metals for coatings for steel reinforcement bars, including zinc, copper and nickel. Among these, zinc coating in the form of galvanized coating was considered the most common type of metal coating which was effective in protecting the steel reinforcement from corrosion (Yeomans 2004).

In the process of galvanizing, the steel bar was cleaned to remove unnecessary particles or impurities, and then submerged into a bath of molten zinc at a temperature of around 450°C. This temperature was necessary in the process to ensure a chemical reaction between zinc and steel, and produced a coating on the surface of the steel bar (Clifton, Beeghly et al. 1974).

The main advantage of galvanized steel rebar over the ECR is that the coating in the former is chemically bonded to the steel bar. Therefore, a tough and abrasion resistant coating is produced with good strength and acceptable behavior for bending and formwork preparation. Unlike ECR where the epoxy coating does not allow for bending due to the weak nature of the epoxy, galvanized coated reinforcement can be bent on site before placement in concrete (Yeomans 2004, Bellezze, Malavolta et al. 2006).

Another advantage of galvanized steel reinforcement as shown by Montemor, Cabral, Zheludkevich, and Ferreira in 2006, Poursaee and Hansson in 2009, and Tan and Hansson in 2008, is that the galvanized coating increases the time required to initiate corrosion compared to conventional steel reinforcement without coating (Montemor, Cabral et al. 2006, Tan and Hansson 2008, Poursaee and Hansson 2009). The zinc layer, when it is in contact with concrete, starts to dissolve in the alkaline environment of concrete matrix and provides a protective atmosphere for the reinforcement bars. Furthermore, the corrosion products are in the form of powders: unlike uncoated steel reinforcement bars, they will not increase the volume of the steel reinforcement bars but will disperse consistently in concrete, and could help to fill in the porous area of the concrete matrix, as explained by Stephen Yeoman in his book "Galvanized Steel Reinforcement in Concrete" as well as in the research project carried out by a team of researchers from Marche Polytechnic University in Ancona, Italy (Yeomans 2004, Bellezze, Malavolta et al. 2006). This eventually could reduce the rate of chloride ion penetration by reducing the porosity of the concrete. Consequently, there will be no additional tensile stresses introduced into the concrete from the corrosion products, nor increase in the volume of the reinforcement bar which could potentially produce internal cracks.

However, a few cases of corrosion of galvanized steel reinforcement in severe marine environments were reported by Macias and Andrade in 1987, Saraswathy and Song in 2005, and Sistonen, Cwirzen, and Puttonen in 2008. When the pH level was as high as 13, the corrosion started a few years after placement of the reinforcement and continued until the protective layer of zinc was dissolved completely in concrete.

Hence, it is obvious that in poor quality concrete or in a concrete with a water-to-cement ratio (W/C) of higher than 0.50, porosity and permeability are greater than for high-performance concrete with a low water-to-cement ratio. Therefore, the rate of chloride ions or carbon dioxide ingress into the concrete will be much higher and as a result, corrosion can be initiated earlier and can damage the zinc and iron layers on the surface of the galvanized steel bar more rapidly (Macias and Andrade 1987, Saraswathy and Song 2005, Sistonen, Cwirzen et al. 2008).

When comparing the two common types of coatings for steel reinforcement, one has to consider not only the cons and pros in terms of corrosion, but also the cost of producing either type of coating and the long-term repair cost. The initial cost of epoxy coating on average can add up to 30% to the cost of the reinforcement, while in the galvanizing process, it can add up to 50% to the cost (El-Salakawy, Benmokrane et al. 2005, Berg, Bank et al. 2006).

Besides the initial investment required for the coating of the steel reinforcement, treatments are necessary over the lifetime of the coated reinforcement given the fact that in severe conditions, the coatings could also be damaged and corrosion might be initiated. Once corrosion occurs, the cost of repair and rehabilitation will be another major expense, which will be added to the initial cost; together, these can add up to more than 100% of the steel reinforcement cost and up to a 50% increase in the overall building cost (Slater 1983, Thompson, Yunovich et al. 2007).

All these problems rising from the corrosion of metallic reinforcement in concrete have put tremendous pressure on the building industry. As a result, in the past 15 years, there have been great interest in using alternative reinforcement, especially non-metallic reinforcement for structural concrete to eliminate the corrosion problems. Many researchers have started to work on new types of reinforcement consisting of two parts, a fiber and a resin, in which aligned continuous fibers are embedded in a resin matrix and then formed into different shapes.

There have been significant research on using aramid, glass, basalt and carbon fibers, and more recently, natural fibers to produce non-metallic composite reinforcement that is usually referred to as Fiber Reinforced Polymer (FRP) reinforcement. In the next section, some of the FRP reinforcement currently used in structural concrete applications are reviewed and discussed.

3.3.2. Fiber Reinforced Polymer (FRP) reinforcement systems

Fiber Reinforced Polymer (FRP) reinforcement made with synthetic or natural fibers have gained special interest in recent years given the superior properties they offer compared to conventional steel reinforcement. In general, they do not have the typical problems of corrosion of steel reinforcement, have high tensile strength and are non-magnetic. There are different types of fibers that can be used to produce FRP, including glass, carbon, basalt and aramid fibers. Recent advances in FRP technology have also allowed the use of some natural fibers such as cotton, kenaf, sisal and bamboo for production of FRP reinforcement.

Among the most common synthetic fibers used in FRP fabrications, Carbon Fiber (CF) and Glass Fiber (GF) are preferred by manufacturers and engineers, given their superior mechanical properties over traditional metals such as steel and aluminum. Carbon Fiber Reinforced Polymer (CFRP) composites and Glass Fiber Reinforced Polymer (GFRP) composites are the most popular FRP composites used as reinforcement.

CFRP composites have the highest mechanical properties, specifically tensile strength and elastic modulus, and are the lightest FRP composites used in construction. However, low-cost raw carbon fiber for the production of CFRP composites is hardly available globally. Therefore, the usage of CFRP composites is rather limited in structural concrete applications.

The Glass Fiber Reinforced Polymer (GFRP) composites are the most common type of reinforcement materials among all FRP composites and are used widely in concrete construction. GFRP composites have relatively lower cost compared to CFRP composites, and have shown fairly good performance in terms of strength and durability in applications where the use of steel reinforcement is prohibited.

Besides the CFRP and GFRP composites, Basalt Fiber Reinforced Polymer (BFRP) composites and Aramid Fiber Reinforced Polymer (AFRP) are the other types of FRP composites that are, in practice, seldom used for reinforcement application in structural concrete, even though they have shown relatively good mechanical properties compared to GFRP composites.

In this section, CFRP and GFRP composites, as the most common FRP composites reinforcement, are reviewed more in detail. In addition, reviews of the production and properties of BFRP and AFRP composites have been made.

Furthermore, in recent years, there has been tremendous interest in the application of natural fibers in the production of FRP composites to replace synthetic fibers such as glass, carbon, basalt and aramid fibers. Some natural fibers such as bamboo, flax and sisal have great mechanical properties comparable to glass or carbon fibers. They are renewable, widely available globally, and are several times cheaper than synthetic fibers. In this section, some of the most common types of natural fibers used in fabrication of FRP composites are reviewed.

Glass Fiber Reinforced Polymer (GFRP) reinforcement systems

Among the various types of synthetic fibers used to produce FRP materials, Glass Fibers (GF) are one of the most common and are widely used in the building and construction sector. The manufacturing process for GF has been explained by many researchers, among them Professor Pankaj Mallick at the University of Michigan in Dearborn who carried out one of the most comprehensive investigations with regard to the GF production process.

The process involves several steps. The various ingredients in glass formulation such as clay and silica are first dry mixed and then melted in a refractory furnace at about 1,370°C. The molten glass is extruded through a number of openings contained in a platinum bushing, with a large number of small nozzles or tips on their underside, and rapidly drawn into filaments of approximately 10μm in diameter. A protective coating is then applied on individual filaments before they are gathered together into strands. Finally a blend of lubricants will be added to the mixture to prevent abrasion between the filaments, alongside the antistatic agents which reduce static friction between the filaments, and a binder to pack the filaments together into a strand. Some GF may also contain small percentages of a coupling agent that promotes adhesion between the fibers and the specific matrix for which it is formulated (Mallick 2007).

There are several advantages of GF, including high mechanical properties, good chemical resistance, great thermal insulation, being corrosion-free, magnetic free, lighter than traditional steel bars and having lower carbon footprint compared to steel production (Kliger, Christian et al. 2012, Hensher 2013). E-glass and S-glass are the types of glass fibers more commonly used in the fiber-reinforced plastic industry. E-glass fibers have the lowest cost of all commercially available reinforcing GFs, which is the reason for their widespread use in the fiber-reinforced plastic industry. S-glass, originally developed for aircraft components and missile casings, has the highest tensile strength among all fibers in use (Mallick 2007). However, the compositional difference and higher manufacturing cost make it more

expensive than E-glass. The tensile strength of GF is in the range of 500MPa to 1,500MPa, and modulus of elasticity is in the range of 30GPa to 50GPa depending on the production process and additives used during manufacturing (Fu, Lauke et al. 2000, Kocaoz, Samaranayake et al. 2005).

There are two varieties of structural performance GFRP reinforcement for concrete applications, namely the short reinforcement and long reinforcement. Short glass fibers used in concrete applications are mostly for the prevention of shrinkage cracking and to improve the flexural failure behavior in concrete, rather than for improving the tensile or compressive strength of concrete, as explained in the work of Nayan Swamy and Harry Stavrides in 1979 (Swamy and Stavrides 1979).

As mentioned earlier, GF has high tensile strength which is higher than that of steel, but the modulus of elasticity is typically lower compared to steel reinforcement. Therefore, a low modulus of elasticity of dispersed short glass fibers in a concrete matrix allows the concrete to crack first. When the concrete cracks, the strong glass fibers do not allow the crack to propagate and lead to appearances of a new crack in a different position. This mechanism will help to minimize any failure due to premature shrinkage cracking, and postpone the onset of failure under different external loading patterns (Toutanji and Saafi 2000, Reis and Ferreira 2003).

However, recent advances in GF production technology have allowed companies to produce long GFRP bars similar to steel reinforcement bars for structural concrete applications (Kodur and Bisby 2005, Wambeke and Shield 2006, Lee, Kim et al. 2008). The long GFRP bars are widely used in applications in which the use of conventional steel reinforcement is prohibited or restricted. They are used in reinforced concrete bridge decks and roads where long-term exposure to de-icing salt can initiate the corrosion of steel reinforcement. GFRP reinforcement are currently being used as an alternative to steel reinforcement for structures built near sea water, such as offshore platforms and piers where corrosion of steel is the main cause of concrete degradation. Given their non-ferrous, non-magnetic properties, GFRP reinforcement are replacing steel reinforcement in structures exposed to high voltages and electromagnetic fields where metallic reinforcement cannot be used, such as in high voltage substations (Mallick 2007).

However, there are certain disadvantages associated with the application of GFRP in concrete structures as reinforcement. The initial cost is a major challenge in introducing the new

alternative reinforcement into the building and construction sector, as described by Halvard Nystrom, Steve Watkins, Antonio Nanni and Susan Murray in the case of FRP application in the USA. As a synthetic composite material, the initial cost of GFRP reinforcement could be three times that of steel reinforcement (Nystrom, Watkins et al. 2003). This cost ratio has limited the application of GFRP reinforcement only to specific cases where the use of steel reinforcement is not possible, as explained earlier. Nevertheless, if the initial cost of GFRP reinforcement is considered as a decisive factor for builders or contractors, choosing GFRP over steel would be an uneconomic and undesirable choice (Burgoyne and Balafas 2007).

Beside the high cost of GFRP reinforcement, lower elastic modulus compared to steel reinforcement is another challenge in using GFRP. The low elastic modulus could limit the application of GFRP reinforcement in cases where small deflections are essential in design, such as for long span bridges or tall buildings where large deflections should be prevented (Matos and COREA 2010).

Another challenge of using GFRP reinforcement is that it cannot be bent on site, or either cut or welded. All the necessary cutting or bending has to be done in the factory, as the exposed surface of the GFs can be degraded by the high pH level of the surrounding concrete matrix, which will negatively affect the mechanical properties of the GFRP reinforcement used in concrete in the long term (Chen, Davalos et al. 2007).

The difference between the Thermal Expansion Coefficient (CTE) of GFRP reinforcement and concrete, especially in transverse direction to fiber alignment, could be as high as 6. The higher CTE of GFRP has been reported by many researchers for the transverse direction, due to the presence of the epoxy-resin system used in the production of the polymer (Nanni 1993, Gentry and Husain 1999, Masmoudi, Zaidi et al. 2005). However, in the longitudinal direction to fiber alignment of GFRP material, the CTE of GFRP reinforcement remains relatively similar to the CTE of concrete matrix.

The difference in the CTE values of the concrete and GFRP reinforcement would result in differential tensile stresses in the concrete matrix around the reinforcement, which could result in tensile splitting cracks in the surrounding concrete matrix due to the lower tensile capacity of the concrete compared to the reinforcement.

A slight deterioration of the bond strength between the concrete and GFRP materials was reported during exposure to thermal cycles with a maximum temperature value of 70℃, due

to tensile splitting micro cracks in the concrete matrix surrounding the FRP reinforcement, as reported by Nestore Galatia, Antonio Nannia, Lokeswarappa Dharanib, Francesco Focaccic, and Maria Antonietta Aiello recently (Galati, Nanni et al. 2006). However, it was shown that the influence of the thermal treatment was more evident with the small values of the concrete cover. Such behavior was explained by the micro cracking of the concrete due to the tensile stresses developed during the thermal cycles as a result of thermal expansion of the FRP reinforcement in the transverse direction.

Few studies have been carried out to investigate the effect of thermal expansion of GFRP reinforcement on the strain distributions in concrete matrix. Extensive research was undertaken by Radhouane Masmoudi, Ali Zaidi, and Patrick Gérard at the University of Sherbrooke in Canada on the effect of differential thermal expansion coefficient of GFRP reinforcement and concrete on development of the tensile splitting cracks in surrounding concrete matrix (Masmoudi, Zaidi et al. 2005). Their studies included an experimental investigation for analyzing the influence of the ratio of concrete cover thickness to GFRP bar diameter on the strain distributions in concrete and FRP bars. They used concrete cylinders reinforced with GFRP bars and subjected to temperature rangeing from −30°C to +80°C.

The results of their tests demonstrated the higher transverse CTE values of the GFRP reinforcement compared to longitudinal CTE values. It was shown by their study that the ratio between the transverse and longitudinal CTE of GFRP reinforcement could be as high as 4. Their work also demonstrated that by adjusting the ratio of the concrete cover thickness to the diameter of the GFRP reinforcement, one could delay or prevent the onset of tensile splitting cracks in concrete matrix around the reinforcement. For instance, concrete samples with a ratio of concrete cover thickness to GFRP bar diameter of less than or equal to 1.5 showed signs of splitting diagonal cracks on the surface of concrete cylinders at a temperature range of between +50°C to +60°C (Masmoudi, Zaidi et al. 2005). A ratio of concrete cover thickness to GFRP bar diameter of greater than or equal to 2.0 was found to be sufficient to prevent tensile splitting cracking of concrete under high temperatures up to +80°C.

Similar to the studies carried out by Radhouane Masmoudi and his team, a series of concrete members subjected to high temperatures ranging from 20°C to 100°C and reinforced with different types of FRP reinforcement has been thoroughly investigated by Hany Abdalla from Cairo University in 2005.

Experimental and non-linear analysis of the thermal stresses was carried out in the study led by Hany Abdalla for concrete cylinders and concrete beams reinforced with FRP materials as reinforcement. It was shown that the tensile stress around the FRP bars would decrease at the outer face of the concrete beams away from the bar. However, it was demonstrated that the tensile stresses around the FRP reinforcement bars in concrete samples due to temperature increase were significantly reduced when the concrete cover thickness exceeded 1.5 times the diameter of the FRP bar. The results of the study suggested that concrete cover thicknesses in the range of 1.5 times the diameter of the FRP bar and 2 times the diameter of the FRP bar could safely prevent any tensile stresses developed as a result of differential thermal expansion coefficients between FRP bar and concrete. Furthermore, Hany Abdalla suggested the application of FRP reinforcement bars of less than 12mm in diameter for temperatures higher than 50°C, to avoid the development of tensile stresses near the FRP bars which could deteriorate the bond mechanism between the reinforcement and concrete (Abdalla 2006).

However, no detailed investigations have been carried out on the long-term bond performance of GFRP reinforcement systems in concrete application when exposed to various temperature cycles. Radhouane Masmoudi, Abdelmonem Masmoudi, Mongi Ben Ouezdou, and Atef Daoud have carried out one of the only available test series on the performance of the bond mechanism between GFRP bars and concrete matrix. The results of their study revealed no significant reduction of bond strength for temperatures up to 60°C. However, a maximum 14% reduction in the bond strength was observed for a temperature of 80°C after 8 months of thermal loading. Their study has further emphasized the effect of FRP bar diameter and concrete cover on the bond performance. It was found that the bond strength decreased when the diameter increased from 8mm to 16mm for the GFRP bars. Further research in this area is necessary to establish reliable results for the use within the building sector and to minimize the negative impacts of the difference between the CTE of concrete and FRP bars.

Given the high cost of GFRP reinforcement and certain technical deficiencies, the application of GFRP reinforcement has been limited to small bridges, piers and some other special structures where the use of steel reinforcement is not possible, and only in few places in Europe and America. Further research is necessary to improve the quality of GFRP reinforcement and lower the cost of production to broaden its applications and make GFRP reinforcement a feasible alternative to the conventional steel reinforcement system.

Carbon Fiber Reinforced Polymer (CFRP)

The other commonly used FRP in the construction sector is Carbon Fiber Reinforced Polymer (CFRP). CFRP is a category of FRP that uses Carbon Fiber (CF) as the primary structural component and epoxy resin as the binding matrix. CFs generally have excellent tensile properties, low densities, and high thermal and chemical stabilities in the absence of oxidizing agents, good thermal and electrical conductivities, and excellent creep resistance. CFs have been extensively used in composites in the form of woven textiles, continuous fibers and chopped fibers (Fu, Lauke et al. 2000).

A traditional GFRP composite using continuous fibers with a fiber percentage of 70% glass (weight of glass / total weight) normally has a density in the range of $1.80g/cm^3$ to $2.10g/cm^3$, while a CFRP composite, with the similar fiber percentage, has a density of $1.40g/cm^3$ to $1.60g/cm^3$. Not only are CFRP composites lighter, they also have higher tensile strength and better elastic modulus per unit of weight compared to GFRP composites, or even to steel reinforcement (Meier 1992). CFRP composite has tensile strength in the range of 600MPa to 3,700MPa and has modulus of elasticity in the range of 130GPa to 500GPa, depending on the type of production process (Fu, Lauke et al. 2000).

There are three types of CFs currently being used in the production of CFRP composites, which include Polyacrylonitrile (PAN), pitch and rayon carbon fibers as described by Professor Pankaj Mallick in his book on the state of the art of FRP manufacturing and design (Mallick 2007).

CFs are manufactured by a controlled pyrolysis of stabilized precursor fibers. Precursor fibers are first stabilized at about 200°C to 400°C in air by an oxidization process. The stabilized fibers are then subjected to high temperature treatment at around 1,000°C in an inert atmosphere to remove hydrogen, oxygen, nitrogen and other non-carbon elements. This step is often called carbonization. Carbonized fibers can be further graphitized at an even higher temperature up to around 3,000°C to achieve higher carbon content and higher elastic modulus in the fiber direction (Strong 2008). The high elastic modulus of CFs comes from the high crystallinity and the well alignment of crystals in the fiber direction, while the strength of carbon fibers is primarily affected by the defects and crystalline morphologies in fibers (Meier 1992).

Sandeep Pendhari, Tarun Kant and Yogesh Desai have reviewed different applications for fiber reinforced polymer composites. They showed that among various FRP composites, the

application of CFRP composites in structural concrete was mostly limited to the strengthening and retrofitting of existing structures such as bridges or historical monuments, where the performance of the structure in both load-bearing capacity and ductility could be enhanced. In this case, CFRP composites were used to repair or strengthen the existing structure and to bring its load-bearing capacity or its ductility back to its original values as first designed.

This situation could also happen during the life span of the building when the structure deteriorates due to age or environmental conditions, such as corrosion of steel which could lead to loss of structural performance (Pendhari, Kant et al. 2008).

The use of CFRP composites for structural retrofitting and strengthening was initiated in Europe, mainly in Switzerland in the late 1980s where CFRP composites replaced steel plates for strengthening existing railway bridges (Meier 1992, Ehsani and Saadatmanesh 1997). Since the 1980s, CFRP composites have been used in numerous projects around the world for the retrofitting and strengthening of existing structures, as they are lightweight, do not corrode or rust and have superior mechanical properties compared to steel. CFRP composites were used in many bridges in the US and Canada due to their light weight and high strength capacity either as a prefabricated reinforcement or for strengthening existing bridges (Brena, Benouaich et al. 2005, Zhang and Hsu 2005) .

In recent years, the CFRP composite rebar has gone from an experimental prototype to an effective replacement for steel in some projects. However, the replacement was partial due to the increase in the overall cost of the structure. As Chris Burgoyne and Ioannis Balafas described in their work on the financial success of the FRP composite, CFRP composites were cost prohibitive in many applications.

Depending on market conditions (supply and demand), the type of carbon fiber, and the fiber size, the price of CFRP composites can vary dramatically. CFRP composites can be between 3 to 5 times more expensive than GFRP composite, and 5 to 10 times more expensive than steel (Burgoyne and Balafas 2007, Kliger, Christian et al. 2012).

In addition to the initial cost of using CFRP composites in concrete applications, another significant barrier in using CFRP composites is the problem with recycling. As in case of CFRP composites, separating epoxy-resin matrix and carbon fiber is not straightforward. An extensive research led by Professor Robert Adams at the University of Bristol in UK in 2014

showed that, unlike steel which can be melted and re-used to manufacture new applications, CFRP composites cannot be melted down easily and be recycled. Recycling CFRP composites is rather difficult. The complex nature of epoxy-resin systems used in the fabrication of CFRP, the combination of CFRP with other materials (for instance in hybrid composites or with some metals) and finally the multiplex combination of fibers, fillers and matrix of CFRP composite, have made the recycling efforts pretty challenging and costly (Pickering 2006, Adams, Collins et al. 2014).

Similar work has been carried out at École Polytechnique Fédérale de Lausanne (EPFL) in 2013, which again proved that at the moment, most CFRP composites waste is land-filled and poses a threat to the environment and natural resources in the long term (Witik, Teuscher et al. 2013). Furthermore, if carbon fiber is recycled with all the difficulties involved, the recycled carbon fiber is normally weaker and shorter than the original fibers. Therefore carbon fiber recycled from a car is not suitable for structural applications or even for re-use in car body parts. It can only be used for applications in which the required physical and mechanical properties are less demanding (Witik, Teuscher et al. 2013).

Although CFRP composites exhibit better mechanical properties and notable performance in structural concrete applications, cost remains a major weakness, except for specific structures or historical monuments for which there is no alternative. Otherwise, the application of CFRP composites for structural concrete in typical housing and infrastructure projects is not economically feasible when there are alternative materials such as steel with acceptable mechanical properties and relatively lower cost.

Aramid Fiber Reinforced Polymer (AFRP)

In recent years, there have been huge interest in the application of Aramid Fibers (AF) for the production of FRP composites. Aramid fiber was first commercialized in the early 1960s; Stephanie Kwolek researched and developed these new synthetic fibers while working at chemical company DuPont in 1961 in the US. Since then DuPont has been a market leader in the production of aramid fibers worldwide (Stephanie, Wayne et al. 1962).

Aramid fibers are a type of nylon, but the molecular structure contains several linked benzene rings and amide bonds (Panar, Avakian et al. 1983). According to US Federal Trade Commission (FTC), the aramid fiber belongs to a group of synthetic fibers in which the fiber-forming ingredient is a long-chain synthetic polyamide in which at least 85% of the amide (-CO-NH-) linkages are attached directly between two aromatic rings (United States

International Trade commisson 1986, (FTC) 2015). The Amide groups (-CO-NH-) produce robust bonds that are resistant to heat. The aromatic rings are six-sided groups of carbon and hydrogen atoms that help to prevent polymer chains from spinning around the chemical bonds (United States International Trade commisson 1986).

There are many advantages to using aramid fibers in FRP composite fabrication. They exhibit superior resistance to impact loading and therefore can be used in areas likely to suffer damage due to impacts. AFRP composites have high tensile strength in the range of 2,500MPa to 4,100MPa and have high elastic modulus in the range of 69GPa to 179GPa (Young, Lu et al. 1992). These values are higher than for GFRP composites, which make aramid fibers a perfect alternative for steel reinforcement in concrete. AFRP composites are lightweight with a density of $1.30g/cm^3$ to $1.45g/cm^3$, which makes them lighter than normal GFRP composites. They show great thermal stability and have a relatively low thermal conductivity (Young, Lu et al. 1992, Mallick 2007). AFRP composites can be used as an electrical insulator in applications where steel cannot be used.

Applications of AFRP composites in structural concrete in recent years focused on the retrofitting and strengthening of existing buildings similar to CFRP composite applications. The high tensile strength and elastic modulus of AFRP composites are a great benefit in repairing and strengthening the existing buildings and infrastructure, as well as preventing additional damage (Demers, Hebert et al. 1996, Balaguru, Nanni et al. 2008). However, AFRP composite reinforcement has shown less potential to be used as an alternative to steel for flexural or shear reinforcement systems in structural concrete.

The main disadvantage of aramid fibers is their overall weakness to compressive forces and water absorption. Many researchers have reported that FRP composites made with aramid fibers can absorb up to 8% of their weight when in contact with water. Therefore, AFRP composites must be protected using additional coatings to prevent moisture ingress, especially when used in concrete as reinforcement (Verpoest and Springer 1988, Cervenka, Bannister et al. 1998).

Another disadvantage is the difficulty in bending the reinforcement. Special equipment is needed to cut or bend the reinforcement at the construction site, which makes on-site handling of the reinforcement bars challenging and laborious (Van Gemert, Brosens et al. 2002). AFRP composite use is also limited by its long-term strength degradation due to

moisture and water intake as well as UV radiation (Wilfong and Zimmerman 1977, Ceroni, Cosenza et al. 2006).

All these challenges have made the application of AFRP composites in structural concrete limited to strengthening and retrofitting, and only in cases where the high stiffness and low strains at failure of AFRP composites can help prevent unexpected failures of buildings or infrastructure subjected to impact loadings, for instance, as a result of an explosion or a fire. This is shown in various works, including the work carried out by Philip Buchan and Jian-Fei Chen at the Institute for Infrastructure and Environment of the University of Edinburgh on the blast resistance of FRP composites. Furthermore, the work led by John Crawford at Karagozian & Case, Inc., on the retrofitting of damaged reinforced concrete buildings with FRP composites sheets has shown the great benefits of retrofitting applications of FRP composites for the building sector (Crawford, Malvar et al. 1996, Buchan and Chen 2007, Malvar, Crawford et al. 2007).

Basalt Fiber Reinforced Polymer (BFRP)

Basalt fibers are produced from melting basalt rock at around 1,500°C. Basalt rock is one of the most common rock categories found in the earth's crust, and is composed mainly of silica (SiO_2), alumina (Al_2O_3), magnesium oxide (MgO) and ferric oxide (Fe_2O_3) (Czigány 2004, Singha 2012). The French scientist Paul Dhé was the first person to be granted a US patent in 1923 for his idea to extrude fibers from basalt rock.

By 1960, both the US and Soviet Union (USSR) began to investigate basalt fibers for applications in the field of military equipment, due to the high tensile strength and elastic modulus of the fibers and their great resistance to abrasion, vibration and temperature (Colombo, Vergani et al. 2012).

There are several advantages of using basalt fibers for the fabrication of FRP composites, as shown in the research carried out by Jongsung Sim and Cheolwoo Park at Hanyang University of South Korea in 2005. According to their study, basalt fibers have outstanding resistance to high temperatures and have high tensile strength capacity. They have relatively good durability, especially against acids, and demonstrate great electro-magnetic properties, resistance to corrosion, radiation, UV light and vibration (Sim and Park 2005). The tensile strength of BFRP composites is in the range of 2,500MPa to 4,800MPa and their elastic modulus can reach as high as 90GPa, as reported in different research works (Van de Velde, Kiekens et al. 2003, Quagliarini, Monni et al. 2012).

Tibor Czigany, professor of polymer engineering at Budapest University of Technology and Economics, summarized the main challenges preventing the wider application of BFRP composites. He emphasized that the downsides for the application of BFRP composites remained at the production stage, in which the high temperatures required during the production increased the energy consumption needed, and as a result, the cost of the final composite increased compared to GFRP composites.

However, further research is being carried out on reducing the cost of production of BFRP composites to make it a sustainable and more affordable alternative to GFRP and CFRP composites, given its superb mechanical properties and high resistance to environmental conditions such as moisture, acid and alkali (Czigány 2004).

Attempts to use BFRP composites as reinforcement to replace steel in concrete have been made since 1997, when Vladimir Brik conducted an extensive investigation into the use of BFRP composite reinforcement in concrete beams (Brik 1997). He showed it is possible to replace steel reinforcement with BFRP composites and BFRP composite rebars could potentially replace steel bars in reinforced concrete, by providing higher strength and durability in areas where corrosion is a major challenge. Since then, there have been various work on BFRP composites for reinforced concrete applications, but the majority of them have addressed the use of short basalt fibers for addressing the shrinkage cracking in concrete (Meng and Yan 2007, Li and Xu 2009, Palmieri, Matthys et al. 2009).

There have been a limited number of investigations emphasizing the application of BFRP composites as rebars in concrete. Due to lack of scientific research in this area thus far, the application of BFRP composite in concrete was mostly successful as an external reinforcing element in the repair and retrofitting of existing bridges and marine infrastructure in which high resistance to a marine environment is required (Chen and Teng 2003, Sim and Park 2005).

Natural Fiber Reinforced Polymer

Research on natural fiber composites was started since the early 1900s, but it was only by the late 1980s that natural fibers become an essential part of research and development of FRP composites (Wambua, Ivens et al. 2003). Most of the current research and development on the use of natural fibers in the fabrication of FRP composites are focused on plant fibers. However, there are non-plant based natural fibers available for composite fabrication, such as silk, which are not the focus of this PhD research and will not be discussed in this section.

The challenges with resource scarcity, the negative environmental impacts from synthetic fiber production, and the recent concerns about environmental sustainability have led many researchers to look for alternative green and eco-friendly sources of fibers for FRP composite fabrication. As alternatives, natural fibers could represent a sustainable source of raw materials from renewable resources for the production of FRP composites and potentially help to alleviate the need for synthetic fibers.

Eco-friendly composite reinforcement fabricated from plant-based fibers are innovative materials of the 21st century and could have a great impact on the building and construction industry, and could also be an answer to the growing environmental threats and address the resource scarcity issue.

Frederick Wallenberger and James Watson from Pittsburgh Plate Glass (PPG) Industries, Inc. have reviewed the latest applications of natural fibers in their book "Natural Fibers, Plastics and Composites". They summarized the properties of the various types of natural fibers, such as flax, kenaf, sisal, jute and bamboo used in production of FRP composites in recent years for several applications, including automobiles, boats, sport equipment, agricultural machineries and, more recently, in buildings. They concluded that these fibers are lighter and cheaper than synthetic fibers and have superior, if not comparable, physical and mechanical properties compared to synthetic fibers like glass, aramid and basalt (Wambua, Ivens et al. 2003, Wallenberger and Weston 2004).

Natural fibers are widely available in nature and therefore require relatively less energy in production. When natural fibers are used in FRP composite production, they can result in high-performance composite materials which could potentially replace all, if not many, of the synthetic composite materials at lower prices for applications in the building and construction sector, where weight savings have significant impact on the energy consumption and overall cost of the building or infrastructure.

Natural fibers consist mainly of cellulose, hemicelluloses, lignin, pectin, and waxy substances (Wallenberger and Weston 2004). Cellulose is a natural polymer containing long chains of connected glucose (sugar) molecules that gives the plant fiber its outstanding mechanical properties. Cellulose is the main constituent of the plant cell structure, and forms the main body of many plants and grasses (Biagiotti, Puglia et al. 2004, Rohit and Dixit 2016). Cellulose fibers are normally embedded in another complex matrix consisting of lignin and hemicellulose. Wolfgang Glasser and Simo Sarkanen from the American Chemical Society,

in their publication on lignin, explain extensively the lignin function and its properties in various plants. Lignin delivers the mechanical support for the fibers and provides the plant's stiffness. Lignin is the main element responsible for the strength required by large plants, such as wood and bamboo, to reach certain heights and grow skyward. Furthermore, lignin, together with other plant fiber constituents, provides resistance to fungi and insects (Glasser and Sarkanen 1989).

Lignin is interlinked with hemicellulose. Hemicellulose is comparable in structure to cellulose, the main difference being in the length of the connected chains. Chains of hemicellulose are normally shorter than those of cellulose, which makes them slightly weaker compare to cellulose's. Hemicellulose has an amorphous nature and so it is fairly soluble in water and in being degraded by alkaline solutions (Pérez, Munoz-Dorado et al. 2002). The percentages of cellulose, hemicellulose, lignin and other fiber constituents are different in various natural fibers, which affect the physical and mechanical properties of the natural fibers and the final FRP composites made with the various natural fibers (John and Anandjiwala 2008). Table 1 shows the major natural fibers produced for FRP composite fabrication throughout the world in 2012.

Table 1 Major natural fibers produced for FRP composite fabrication throughout the world (Faruk, Bledzki et al. 2012)

Fiber source	World production (x 10^3 ton)
Bamboo	30,000
Jute	2,300
Kenaf	970
Flax	830
Sisal	378
Hemp	214
Coir	100

Kiran Rohit and Savita Dixit have reviewed various aspects of natural fiber reinforced polymer composites. In their review article, they emphasize that the FRP composites made with natural fibers will have different performances, depending mostly on the mechanical properties of fiber, fiber orientation in composite, defects in fiber, fiber cell diameter, physical and chemical properties of the fiber, and the interaction of the fibers with the matrix used for the fabrication of the FRP composite (Rohit and Dixit 2016).

The matrix used in FRP composites will determine the overall durability and surface characteristics, while the fibers are responsible for the mechanical properties and overall stiffness and strength of the composite. As explained in the works of Pankaj Mallick as well as Andrzej Bledzki and Jochen Gassan, various types of matrices can be used to produce the natural FRP composites; these are divided into two main categories: thermosets, with cross-linked molecular chains; and thermoplastics, with linear molecular chains (Bledzki and Gassan 1999, Mallick 2007).

Brent Strong, a manufacturing engineering technology faculty member at the Fulton College of Engineering and Technology at Brigham Young University, USA, explained the basics of composites manufacturing in his book "Fundamentals of Composites Manufacturing: Materials, Methods and Applications". According to Strong, the thermoplastic polymer matrix becomes soft when it is heated to above the melting temperature and becomes hard when it is cooled down. In other words, the thermoplastic structure can be reversed through heating and cooling without negative impact on its mechanical properties. Unlike thermoplastics, thermoset polymers are not reversible through heating, and once it is heated above the melting temperature and cooled down subsequently, it becomes rigid and hard, due to the cross-linked molecular chains in their structure (Strong 2008).

The difference in structure between thermosets and thermoplastics results in variation of the mechanical properties between the two categories of polymers. The cross-linked molecular chains in thermosets will improve the overall stability against heat and result in better tensile and compressive strength compared to those of thermoplastics. Therefore thermosets are normally used for the fabrication of high-performance composite materials, specifically in load-bearing applications (McMullen 1984, Mallick 2007).

For the fabrication of natural FRP composites for load-bearing applications, thermoset polymers are normally chosen over thermoplastics due to the reasons explained here. There are various thermoset polymers available for FRP composite matrices, including polyester, epoxy and phenolic matrix. Among these matrices, epoxy has shown superior mechanical properties, better durability performance, better adhesion to the fibers and lower water absorption compared to the other thermosets. For the purpose of this research, an epoxy matrix was chosen to be used throughout the study (Puglia, Biagiotti et al. 2005, Holbery and Houston 2006).

As mentioned earlier, the fibers used in the FRP composite are responsible for the mechanical properties, overall stiffness and strength of the composite. Table 2 displays the density, tensile strength and elastic modulus of some of the common natural fibers used in FRP composite fabrication. As can be seen from Table 2, there are always variations in the properties of any kind of natural fibers. The reason for this variation is the fact that plants growing in a specific region differ from similar plants growing elsewhere, due to differences in temperature, soil properties, water availability and quality, or even in the air. These factors have an impact on the physical and mechanical properties of the plant fibers growing in different parts of the world.

Table 2 Density and tensile properties of some common natural fibers used in FRP composite fabrication (Food and Agriculture Organization of the United Nations 2003)

Property	Bamboo	Flax	Hemp	Jute	Sisal
Density (g/cm^3)	0.4 - 0.7	1.4 - 1.5	1.4 - 1.55	1.4 - 1.5	1.33 - 1.4
Tensile Strength (MPa)	300 - 800	800 – 1,500	550 - 900	400 - 800	600 - 700
Elastic Modulus (GPa)	30 - 70	60 - 80	70 - 80	10 - 30	30 - 40

The strength of FRP composites made with natural fibers is also dependent on the bonding between the matrix and fiber. The matrix transfers the stress to the fibers through interfacial bonding. A weak interfacial bonding of fiber and matrix will result in low strength composites even if the fibers have superior mechanical properties (John and Anandjiwala 2008). Natural fibers are hydrophilic substances, which means they can easily absorb moisture, unlike synthetic fibers in which better resistance to moisture is observed. Therefore the interfacial bonding between natural fibers and the matrix can be weakened with moisture uptake; to prevent this in natural FRP composites, chemical modification of the fibers must be carried out before placing them into the thermoset matrix (John and Anandjiwala 2008, Faruk, Bledzki et al. 2014).

Several treatment methods have been practiced by researchers around the world on different natural fibers. Among the various techniques, alkaline treatment (with NaOH) of the natural fibers have shown better results in terms of interfacial bonding between the fiber and matrix by improving the fiber wettability and removing the unnecessary chemical components of the fiber which are parts of the lignin structure (Wallenberger and Weston 2004, John and

Anandjiwala 2008, Faruk, Bledzki et al. 2012, Faruk, Bledzki et al. 2014, Rohit and Dixit 2016).

The application of natural fiber reinforced polymer composites in the building and construction industry has been successful in recent years, but mainly as non-structural elements applied as an insulation element for the structural members, for floor and wall covers, in door and window frames, for fitting elements such as door and window handles and for fencing. Among the various high-strength natural materials shown in Table 2, bamboo is considered one of the oldest natural construction materials used in buildings and bridges, particularly in tropical zones where it grows in abundance in South America, Africa and, in particular, in Southeast Asia (Ben-Zhi, Mao-Yi et al. 2005). However, the application of bamboo fibers for FRP composites fabrication has not been explored extensively, even though bamboo fiber production surpasses all other natural fibers worldwide (Table 1) and bamboo is one of the fastest growing plants on the earth. Besides its high production volume and fast growth, bamboo offers huge advantages in the form of FRP composites due to its high strength-to-weight ratio, stiffness, renewability, low cost and light weight compared to synthetic fibers.

Investigation on methods of extracting bamboo fibers have been carried out since the beginning of the 21st century when bamboo based FRP composites attracted interest as a replacement for synthetic FRP composites. A combination of chemical and mechanical treatments were first used by researchers in India to extract bamboo fibers from the bamboo culm, resulting in fiber bundles of 8cm to 20cm long for the fabrication of a polyester based FRP composite (Deshpande, Bhaskar Rao et al. 2000).

The flexural strength of the composites ranged from 30MPa to 175MPa and the flexural modulus was between 4GPa to 12GPa. Studies on the different extraction methods of bamboo fibers have shown varying results in terms of fiber length, fiber mechanical properties and quantity of fibers produced (Rao and Rao 2007, Defoirdt, Biswas et al. 2010, Phong, Fujii et al. 2012). The extracted fibers from different methods were used in the fabrication of various FRP composites for different applications.

Polyester, phenolic and epoxy based matrices have been used worldwide for this purpose and each matrix has shown specific physical and mechanical properties. Polyester based bamboo FRP composites have shown a tensile strength in the range of 60MPa to 175MPa with various chemical treatments such as alkali treatment, while the elastic modulus ranged from

2GPa to 12GPa (Jain, Jindal et al. 1993, Deshpande, Bhaskar Rao et al. 2000, Wong, Zahi et al. 2010, Prasad and Rao 2011). Unlike the polyester matrix, epoxy and resin based bamboo FRP composites have shown better performance in terms of physical and mechanical properties. Alkaline treated bamboo fibers together with phenolic resin and epoxy matrix have shown tensile strength in the range of 80MPa to 280MPa and an elastic modulus of 8GPa to 15GPa (Shin, Xian et al. 1989, Rajulu, Baksh et al. 1998, Kushwaha and Kumar 2009, Osorio, Trujillo et al. 2011).

The variation in the tensile properties of bamboo FRP composites fabricated by various research groups around the world is mainly associated with the type of epoxy/resin used, species of bamboo, length of bamboo fiber used in fabrication, fiber orientation and type of treatment carried out on raw bamboo fibers. From the literature survey, it is found that uni-directional oriented long bamboo fibers have shown better performance in terms of mechanical properties, more specifically, in the tensile strength and elastic modulus when they are pre-treated with alkaline solution (NaOH) and fabricated with an epoxy matrix (Khalil, Bhat et al. 2012).

So far, no investigation has been carried out on utilizing bamboo for the fabrication of FRP composites with applications in the construction and building sector as a structural and load-bearing element. Much of the literature on bamboo FRP composites is dedicated to non-load-bearing elements, e.g. fencing or flooring in buildings where the structural properties and mechanical capacities are far lower than for any structural member such as beams and columns. Therefore this PhD research aims to fill this gap via investigating various approaches to enhance the properties of bamboo FRP composites by developing a new processing and fabricating technique for bamboo FRP composites, and using the new material as a structural element for reinforcing conventional concrete buildings and infrastructure.

3.4. The bamboo plant

Bamboo is one of the oldest construction materials. Building with bamboo originates from ancient traditions in regions with domestic bamboo resources, such as Latin America, Africa, and Southeast Asia. In this section, the literature on bamboo species and their properties is examined.

In 1778, Carl von Linné, a Swedish botanist, physician, and zoologist and the father of modern taxonomy, introduced the word "bamboo" to science, based on the Indian word

"Mambu" or "Bambu". The family of the gramineae (grasses) also incorporates the subfamily of the bamboos (Hidalgo-Lopez 2003).

Oscar Hidalgo-Lopez, a Colombian architect and one of the world's most knowledgeable bamboo experts, published a comprehensive book "Bamboo – The Gift of the Gods" in 2003. In this book, Hidalgo-Lopez explains various aspects of bamboo; as a plant, its taxonomy, ecology, mechanical and physical morphologies, the long- and short-term durability issues, application of bamboo in traditional ways, fabrication technology of modern materials from bamboo and bamboo construction technologies. Hidalgo-Lopez also states that there are more than 90 genera and 1,400 different species of bamboo around the world (Hidalgo-Lopez 2003).

Walter Liese, a German professor of forestry and wood biology at the University of Hamburg, who is regarded as one of the world's bamboo pioneers, played an important role in the establishment of the International Network for Bamboo and Rattan (INBAR) as well as the World Bamboo Organization (WBO). Liese has described bamboo's morphology and anatomy in various technical reports and books. He uses the term 'bamboo' to cover all tree- or bush-like grasses having a durable woody or branched stem. The lignifying cell structure of the bamboo tissue and its technological properties are very similar to wood tissue as explained by Liese. Bamboo may therefore also be termed a wood. However, unlike wood, bamboo has a hard outer surface and is soft inside. In contrast to wood, bamboo is a hollow tube and could have varying wall thicknesses. Bamboo can be considered an ecological viable substitute for commonly used wood in many ways. Bamboo attains maturity in 4 to 5 years compared to wood which takes at least 20 years, depending on the species of wood (Liese 1985, Hidalgo-Lopez 2003).

Bamboo is a gigantic grass which belongs to the group *angiosperms* (seed-bearing vascular plants) and the subgroup of *monocotyledon* (flowering plants). The grass family of gramineae has one small subgroup called *Centothecoideae,* which are found in warm temperate tropical forests, and five large subgroups, *Arundinoideae, Pooideae, Chloridodeae, Panicoideae,* and *Bambusoideae*. Bamboo plants are categorized under the subgroup *Bambusoideae* (Liese 1998).

Walter Liese, in his book "Bamboos**:** Biology, Silvics, Properties, Utilization", further explains the morphology of the bamboo plant. According to Liese, bamboo is considered a natural composite which has a matrix and fibers. The physical and mechanical properties of

any bamboo culm are dependent on the anatomical structure of the culm. Bamboo culm is made of nodes and internodes. At the internodes, the bamboo fibers are axially oriented and provide the strength and stiffness of the bamboo. However, at the nodes, the bamboo cell structure provides interwoven layers that help to resist the transverse forces. Unlike wood, bamboo has no radial cell elements called rays (Liese and Jackson 1985, Liese 1998). The outermost layer of the culm, the skin layer, is made of epidermal cells that have a waxy cover. The innermost layer of bamboo culm section is wrapped by sclerenchyma cells. The main structure of the culm has parenchyma cells and vascular fiber bundles. Vascular bundles are a combination of vessels sieve tubes and fibers. In bamboo species investigated by Liese, the diameter of vascular bundles decreased from the bottom to the top of the culm; however, the extent of change varied from species to species (Liese 1998). Fig. 21 displays a typical vascular of fiber bundles of a culm section.
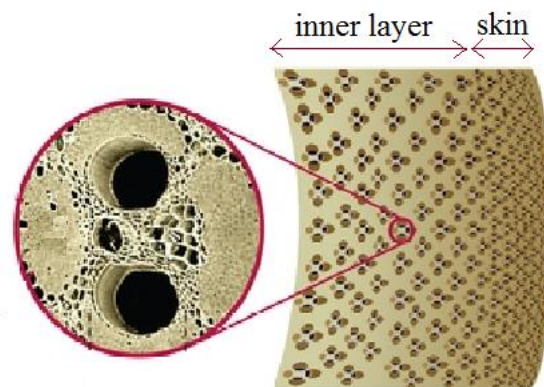
Fig. 21 Bamboo vascular fiber bundles (Liese 1998)

The main components of bamboo culms are cellulose, hemicellulose and lignin. The minor components consist of resins, tannins, waxes and mineral salts. However, the percentage of each component differs from species to species, and depends on the conditions of bamboo growth and the age of the bamboo, as well as the location of the section on the culm (Liese and Jackson 1985).

In general, cellulose in bamboo culms accounts for more than 50% of the bamboo chemical components. After cellulose, lignin has the highest percentage of chemical components in the bamboo, in which it normally accounts for more than 20% of the chemical constituents. Bamboo displays a round-shaped cell cross section as compared to the relatively larger cells in wood and timber species, which have nearly rectangular cell shapes. Furthermore, bamboo culms have a particular multi-layered cell wall structure with alternating thick and thin layers

of fibers, unlike the typical three-layered cell wall of wood or timber species which have a structure with a dominating middle layer (Liese and Jackson 1985, Liese 1998, Wang, Keplinger et al. 2014).

The growth behavior of bamboo culm and the extreme wind loads it has to sustain during its life cycle require a precise mechanical adaptation to the environment, and therefore material optimization has to be achieved effectively from the bamboo fibers and their cell structures. This results in an optimized microstructure with superior material performance as compared to various wood species.

Bamboo culms grow to their full height in less than a year. However, for the culm to reach its maximum growth and gain its mechanical strength, two to four years are normally required. Research has shown that the mechanical properties of mature bamboos are better than those of young bamboo. This finding is, in fact, in correlation with the increase in the specific gravity of bamboo culms, which changes by anatomical variations in the vascular fiber bundles through age (Latif 1993, Li, Shupe et al. 2007).

The variation in the specific gravity of bamboo could be in the range of $0.5g/cm^3$ to $0.9g/cm^3$, according to various studies on different bamboo species from around the world (Liese and Jackson 1985, Liese and Weiner 1996, Li, Shupe et al. 2007, Sen and Reddy 2011). It is reported that the outer section of the culm has a better specific gravity than the inner section, and the specific gravity increases along the culm height from the bottom part to the top part (Yu, Jiang et al. 2008).

The physical and mechanical properties of bamboo culms are correlated with the specific gravity and the fiber content, more specifically, with the vascular fiber bundles. Therefore the physical and mechanical properties of bamboo differ significantly from species to species and even within the same species or same culm, due to changes in chemical composition as well as specific gravity (Ray, Mondal et al. 2005).

Not all bamboo species have similar chemical compositions nor similar physical and mechanical properties. Therefore, to use any bamboo species, careful characterization is necessary before processing them into fibers for composite fabrication. However, not all species found around the world are easily accessible. In the next section, the bamboo species around the world and their availability are discussed.

3.4.1. Bamboo species worldwide

There are about 1,200 species of bamboo under some 90 genera. Bamboo is able to adapt to a wide variety of ecosystems and climatic conditions. Its diversity has been studied in many countries and regions. Taxonomists have developed an excellent and comprehensive knowledge of the variety of bamboo species worldwide. Bamboo's natural habitat is at the equator belt around the world, as seen in Fig. 1. Fig. 22 shows the share of world bamboo resources by continent.
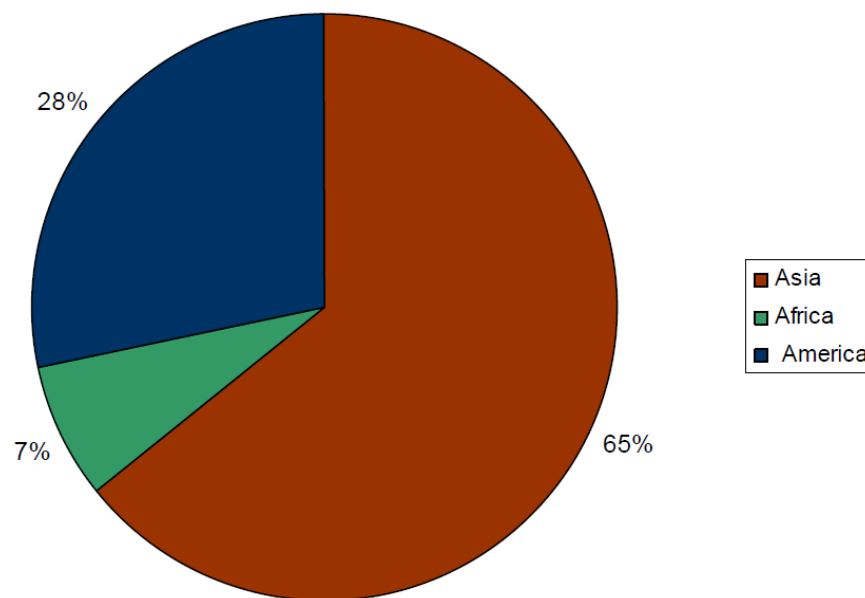
Fig. 22 Contribution of world bamboo resources by continent (Lobovikov, Paudel et al. 2009)

According to data released by United Nations Food and Agriculture Organization (FAO), Asia is the richest continent, with about 65% of total world bamboo resources (Lobovikov, Paudel et al. 2009). Although the information gathered from Africa is incomplete, a total of over 2.7 million hectares of bamboo forest was reported by six countries (Ethiopia, Kenya, Nigeria, Uganda, the United Republic of Tanzania and Zimbabwe). In Latin America, at least 10 countries have significant bamboo resources. Although precise assessments have yet to be carried out, over 10 million hectares is considered to be a realistic figure for this region where Brazil, Chile, Colombia, Ecuador and Mexico have the richest bamboo resources (Lobovikov, Paudel et al. 2009).

In Asia, the major bamboo producing countries are India (almost 11.4 million hectares), China (over 5.4 million hectares) and Indonesia (over 2 million hectares). In India, the major species are *Dendrocalamus strictus*, *Bambusa bambos*, *D. hamiltonii*, *B. tulda, B. pallida* and *Melocanna baccifera*, which account for 45%, 13%, 7%, 5%, 4% and 20% of the total

bamboo farms respectively (Bystriakova and Kapos 2006). Other species account for the remaining 6%. China has more than 600 species of bamboo. Moso bamboo, or *Phyllostachys heterocycla* var. *pubescens* or *Phyllostachys Edulis*, is the most common bamboo species in China, and the third most important plant species for timber production after *Pinus massoniana* and *Cunninghamia lanceolata* ("Chinese Fir").

Moso represents 70% of the bamboo resources in China. Nowadays, due to lack of timber, substituting *Moso* bamboo for conventional timber is of interest for many Chinese cities. Much progress has been made in the industrial usage of *Moso* bamboo. For instance, *Moso* bamboo plywood is used extensively for the flooring of trucks, trains, containers and housing units (Dajun and Shao-Jin 1987). Indonesia is home to nearly 35 bamboo species on almost every island from Java to Bali. The dominant bamboo species in Indonesia include *Dendrocalamus asper*, *Phyllostachys aurea*, *Schizostachyum blumei*, *Gigantochloa apus*, and 30 other species which have been cultivated over the decades by local farmers in smaller quantities (Lobovikov, Paudel et al. 2009).

Africa has about 43 species of bamboo growing on more than 1.5 million hectares of land. The Ethiopian natural bamboo forest is approximately 1 million hectares, which is 7% of the world total and 67% of the total African bamboo forest area. Two species are indigenous to Ethiopia: lowland bamboo or *oxytenanthera abyssinica*, which is found in altitudes of lower than 1,700m; and highland bamboo or *Arundinaria alpine*, which grows in altitudes of more than 2,200m (Lobovikov, Paudel et al. 2009).

South America is the richest region in the Americas in terms of the diversity and number of bamboo species. There is an estimated 9 million hectares of forest in the Amazon region which is dominated by bamboo. Brazil has the greatest bamboo diversity with 137 species followed by Colombia with more than 70 species. One of the most common species found in Latin America is *Guadua angustifolia*. Based on local people's experience passed from generation to generation, they have used it as a structural raw material, or for making furniture and household items (Lobovikov, Paudel et al. 2009).

Among all the species discussed in this section, only few species are commercially exploited for applications in the building and construction industry based on their availability in each country or region. To explore the idea of using bamboo fibers in composites production and as reinforcement in concrete application to replace conventional reinforcement elements, the

mechanical properties of the most common species of bamboo in each continent will be discussed and reviewed in the next section.

3.4.2. Mechanical and physical properties of selected bamboo species

To utilise bamboo and process it into industrialized fibers for the fabrication of FRP composite materials to be used as a structural element in the building and construction industry, its mechanical and physical properties need to be investigated. Although many studies have been carried out on various bamboo species and in measuring their properties, comparing the results from different studies is a complex task for several reasons.

Firstly, the same bamboo species but which grow in different regions do not necessarily have similar properties. They cannot be simply compared without evaluating their properties in the region where they grow. As mentioned earlier, the properties of bamboo are largely dependent on the climatic and soil conditions. Therefore, comparing the same species of bamboo growing in different Asian countries is not scientifically correct. Secondly, various research teams have applied different test methods and standards to evaluate the physical and mechanical properties of natural bamboo. As there is no specific international standard for testing the physical and mechanical properties of raw bamboo, comparing the results obtained via various national and local standards may not be justified.

There are over 1,400 species of bamboo worldwide, but only a few species are available or easily accessible for use in the FRP composite industry. In this PhD research, four widely available species of bamboo around the world have been chosen for their properties to be reviewed. Only one of these four species has been selected for the processing, testing and production of FRP composite reinforcement in the context of this PhD research, which is available in neighbouring countries and easy accessible for the period of the research.

The four selected species are *Dendrocalamus asper*, *Phyllostachys edulis*, *Oxytenanthera abyssinica* and *Guadua angustifolia*. In this section, their properties will be discussed and reviewed.

Dendrocalamus asper or Giant bamboo

Dendrocalamus asper is the most widely available bamboo species in Southeast Asia, particularly in Indonesia, Thailand and Malaysia. *Dendrocalamus asper* grows to 20m to 30m tall, depending on where it grows, and has a diameter of 8cm to 20 cm. It also has relatively thick wall thickness of up to 25mm at the bottom of the culm which becomes thinner at the

top. The relative density of *Dendrocalamus asper* is between 0.65 to 0.85 depending on the soil condition and climate.

The radial and tangential shrinkage ranges from 1.35% to 6.55% and 2.45% to 8.45% respectively. The mechanical properties of *Dendrocalamus asper* have been studied by many researchers, but the results show a wide range of values mainly due to the differences in culm properties from different regions. The flexural strength and modulus of elasticity range from 80MPa to 140MPa and 12GPa to 30GPa, respectively. The tensile and compression strength parallel to the grain of *Dendrocalamus asper* range from 250MPa to 330MPa and 30MPa to 60MPa respectively as shown in various works (Widjaja and Bogoriense 1998, Kamthai and Puthson 2005, Malanit, Barbu et al. 2009, Malanit, Barbu et al. 2011, Febrianto, Hidayat et al. 2012).

Sihati Suprapti from the Forest Product Research and Development Center of Indonesia has reviewed the application of various bamboo species from Indonesia, including *Dendrocalamus asper*. Sihati Suprapti explains in his work that *Dendrocalamus asper* bamboo has been in use in many Southeast Asian countries for decades, not only as scaffolding elements in construction, but also as a replacement for structural timber for constructing housing units in villages and small towns. Oscar Hidalgo-Lopez also notes in his book that *Dendrocalamus asper* has been used for creating handicrafts, furniture and household items in Asia for many decades, due to its wide availability and good performance in terms of physical and mechanical properties (Hidalgo-Lopez 2003, Suprapti 2010).

Phyllostachys edulis or Moso bamboo

Moso bamboo or *Phyllostachys edulis* is considered one of the most valuable bamboo species in Asia, especially China and Japan. For centuries, it has been used in a variety of applications in China to build houses and infrastructures or for making furniture and handicrafts. Although many researchers studied the properties of Moso bamboo, those from different regions, for instance, within China, will have varying properties (Fu 2001).

Researchers have shown that, on average, Moso bamboo culms grow up to 30m in height, with a culm diameter ranging from 6cm to 20cm; the internodes (distance between the knots) at mid-culm can reach a length of up to 40cm. The relative density of *Phyllostachys edulis* bamboo is reported to be between 0.55 and 1.05, and tangential shrinkage from green to oven-dry is in the range of 4.9% to 7.8%. It was found that the elastic modulus and tensile strength of *Phyllostachys edulis* bamboo is in the range of 8GPa to 20GPa and 150MPa to

300MPa respectively. The compressive and flexural strength of Moso bamboo have been reported by various researchers to be in the range of 65MPa to 90MPa and 100MPa to 200MPa, respectively (Obataya, Kitin et al. 2007, Yu, Jiang et al. 2008, Shao, Fang et al. 2010, Jiang, Wang et al. 2012, Berndsen, Klitzke et al. 2013).

Oxytenanthera abyssinica or Bindura bamboo

The *Oxytenanthera abyssinica* or low-land bamboo is a clump-forming type with solid culms that constitutes about 85% of the total bamboo forest in Ethiopia. *Oxytenanthera abyssinica* can also be found throughout west and east Africa in dry forests or near rivers. In Ethiopia, it grows on dry rocky hillsides of heights from 700m to 1,800m, where the annual mean temperature is around 30℃, as shown in the work of David Fanshawe at the beginning of the 1970s at the National Herbarium and Botanic Garden of Zimbabwe. A similar study was carried out by Yeshambel Mekuriaw, Mengistu Urge and Getachew Animut at Bahir Dar University in Ethiopia on the various geometrical properties of *Oxytenanthera abyssinica* (Fanshawe 1972, Mekuriaw, Mengistu et al. 2011). It has been shown in their work that the average length of the culms is 7m to 10m. The average diameter of the bottom part of the culms is 6cm to 8cm and the average thickness is 2cm to 3cm. The average diameter of the top part of the culms is 2cm to 4cm and the average thickness is 0.8cm to 1cm.

Information on the physical and mechanical properties of these species of bamboo in Ethiopia is very limited. One study led by Liese showed that the relative density is 0.8 for three-year-old bamboo and tangential shrinkage for the same sample was between 2.3% to 3.8%. It was also reported that the elastic modulus and flexural strength at the outer layer for the three-year-old bamboo *Oxytenanthera abyssinica* were 12GPa and 83MPa respectively. The compression and tensile strength parallel to grain were found to be 48MPa and 140MPa on average for samples without nodes, as reported by Kassahun Embaye in his work on the indigenous bamboo forests of Ethiopia, carried out at the Swedish University of Agricultural Sciences (Embaye 2000, Liese, Kumar et al. 2002, Embaye 2003, Kelemwork 2009). Though Ethiopia has the largest natural bamboo resources in Africa, most of these are underutilized. The local people have used the low-land bamboo mainly as a source of fuel and sometimes as a structural support system for scaffolding. But there is a great potential for the low-land bamboo resources to be used in large-scale industrial applications in the form of FRP composites for construction, which subsequently could benefit the local industry and improve the people's livelihood.

Guadua angustifolia

Bamboo *Guadua angustifolia* is considered one of the most common bamboo species in Central and South America, and is comparable with Moso bamboo of Asia in terms of availability and usage. *Guadua angustifolia* has been used as a construction material for building local housing units in these regions, especially in Colombia, Brazil and Ecuador, for many years due to its great strength and durability as described by Oscar Hidalgo-Lopez in his book "Bamboo – The Gift of The Gods". Besides construction and housing, *Guadua angustifolia* bamboo is used to make kitchen utensils, musical instruments and furniture in southern Mexico, Columbia, Argentina, Panama, Ecuador, Brazil and Paraguay (Riaño, Londoño et al. 2002, Cleuren and Henkemans 2003, Van Der Lugt, Van den Dobbelsteen et al. 2003).

Guadua angustifolia grows up to 30m high and 20cm in diameter. A few studies have shown that *Guadua angustifolia* has a relative density in the range of 0.6 to 0.7 and volumetric shrinkage in a range of 10% to 12%. It was found that the elastic modulus and flexural strength at the outer layer for the 5-year-old sample were 15GPa and 107MPa respectively. A few studies have been carried out on the compression and tensile strength parallel to grain of *Guadua angustifolia,* which have found its compression and tensile strength in the range of 39MPa to 50MPa and 90MPa to 300MPa for samples without nodes. However the tensile strength of the fiber bundles (single fiber bundles) of *Guadua angustifolia* has been recorded to be as high as 1,152MPa by professor Fernando Ramirez Rodriguez and his team at the University of Los Andes, Bogota in Colombia (Londoño, Camayo et al. 2002, Correal, Francisco et al. 2010, F. Ramirez 2011). However, extracting single fiber bundles for applications in composite fabrication for construction purposes is not feasible given the high cost of production involved, which makes the final product very expensive and not affordable for many developing countries.

Among these four species described here, bamboo *Dendrocalamus asper* or *Giant bamboo* from Indonesia has been selected to be used in this PhD research, and was brought to the newly-established Advance Fiber Composite Laboratory (AFCL) in Singapore for testing, investigation and processing into composite.

The reason for the selection is the availability and easy accessibility to this bamboo species in Southeast Asia, where Singapore is located and where the PhD research was being carried out, and the proximity of Singapore to Indonesia where this type of bamboo grows in

abundance. Since a constant supply of raw bamboo was necessary for the research, contacts were made with local bamboo farmers in several parts of Indonesia, including Java, Bandung and Bali, to arrange for the timely delivery of *Dendrocalamus asper* bamboo with specific requirements, such as age, height, and moisture condition, to the AFCL in Singapore.

In the next section, the literature on the application of bamboo as reinforcement elements in reinforced concrete will be reviewed.

3.5.   Bamboo as reinforcement for structural concrete

The application of bamboo as reinforcing elements first began in 1914, when Hou-kun Chow, a Bachelor of Science student at the department of Naval Architecture and Marine Engineering at the Massachusetts Institute of Technology (MIT), and one of the first Chinese students to come to the USA, tested small diameter raw bamboo culms and bamboo splits as reinforcement materials in concrete as part of his bachelor thesis (Chow 1914). Hou-kun Chow ordered bamboo species from Shanghai, China, to use as longitudinal reinforcement as well as the shear reinforcement (stirrups) in concrete beams. He tested the beams under the four-point flexural tests set-up at MIT in the USA in 1914. Fig. 23 shows the bamboo poles that Hou-kun Chow ordered from China and brought to the Applied Mechanics Laboratory of Naval Architecture and Marine Engineering department in 1914.

Fig. 23 Bamboo poles used by Hou-kun Chow at MIT in 1914 for reinforcing concrete beams (Chow 1914)

Fig. 24 displays the flexural test set-up at MIT for evaluating the concrete beams reinforced with bamboo.

The results from the tests showed that cracks in bamboo reinforced concrete beams developed at comparatively lower loads compared to steel reinforced concrete beams of the same size and property. This could be explained by the relatively lower modulus of elasticity of bamboo poles compared to that of steel reinforcement. Following this very first application, other researchers and research institutions around the world started experimenting with raw bamboo to replace steel reinforcement specifically for reinforced concrete beams and slabs. One of the pioneer research institutes in this field was the Technische Hochschule (TH) in Stuttgart. Professor Otto Graf, a German engineer and material scientist who headed the Institute for Building Materials Testing (MPA Stuttgart) at the University of Stuttgart (TH) during the two World Wars, and together with his student Kramadiswar Datta, carried out various investigations in 1935 on the application of raw bamboo poles and splints in reinforced concrete beams and columns by relying on the outstanding mechanical properties of bamboo.
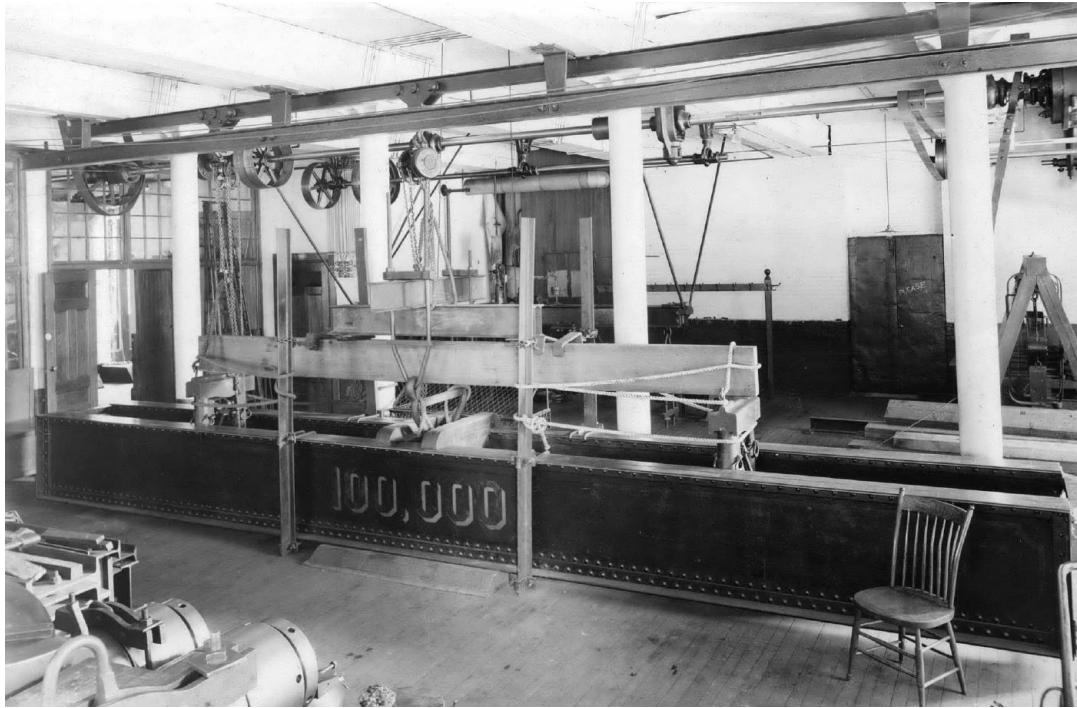
Professor Otto Graf, one of the founders of the Stuttgart school of structural engineering and considered one of the pioneers in the early concrete research in Germany, proposed numerous design concepts for the application of bamboo and steel reinforcement in concrete beams. As displayed in Fig. 25, Otto Graf and Kramadiswar Datta suggested various configurations for using bamboo as longitudinal reinforcement element and steel as stirrups. In their work, bamboo was used mainly in the tension side of the beams. However, no information was available on the performance of such beams over the time and in various locations (Hidalgo-Lopez 2003).

Professor Howard Emmitt Glenn from the Clemson Agricultural College in South Carolina conducted extensive research on the application of natural bamboo as reinforcement in structural concrete beams and slabs in 1950 (Glenn 1950). He tested bamboo reinforced concrete applications by building several full-scale buildings, and by referring to his experience from the previous work he undertook in 1944 on bamboo-reinforced concrete beams and evaluation of various bamboo species.
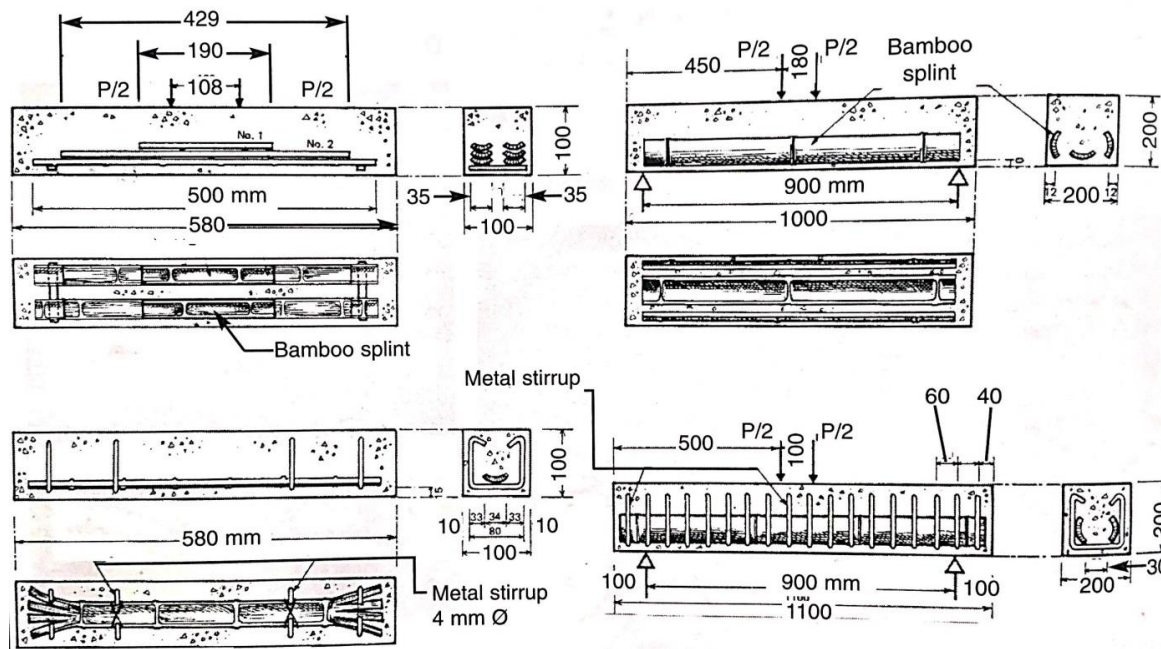
Fig. 25 Various types of concrete beams tested by Otto Graf and Kramadiswar Datta (Hidalgo-Lopez 2003)

Howard Glenn used only small diameter culms and bamboo splits, and demonstrated that though the application of bamboo as reinforcement is feasible in terms of load-bearing mechanisms, there were concerns regarding insect and fungus attacks, coefficient of thermal expansion, shrinking, swelling and, to some extent, the lower modulus of elasticity compared to steel.

Glenn applied various techniques to minimize the defects, but not all were successful except the application of coatings on the surface of bamboo splits. Covering the bamboo components with various coatings before placing them in the concrete mixture reduced exposure to moisture and alkaline environment of concrete. Therefore degradation due to fungus, shrinkage and swelling was reduced to some extent. However, the long-term suitability of such methods was not studied by Howard Glenn. The effect of temperature on the elongation of the natural bamboo reinforcement and bonding behaviour of bamboo splits to the concrete matrix were also not considered in the design of buildings by Howard Glenn (Glenn 1950).

Results showed that the solutions (coatings) applied were rather expensive and the natural bamboo reinforcement, with the addition of coatings, could not compete with steel reinforcement in terms of price in the long term (Glenn 1950). Fig. 26 shows the Press Box Building of the former memorial stadium in Clemson which was built by Glenn in 1950; bamboo was used as the reinforcement element for its concrete beams and columns. Fig. 27 displays the reinforcing details that Glenn designed for the Press Box Building. Several years

later (during the 1960s), when the building was completely demolished for the construction of a new stadium, it was found that the bamboo reinforcements were not in satisfactory condition.
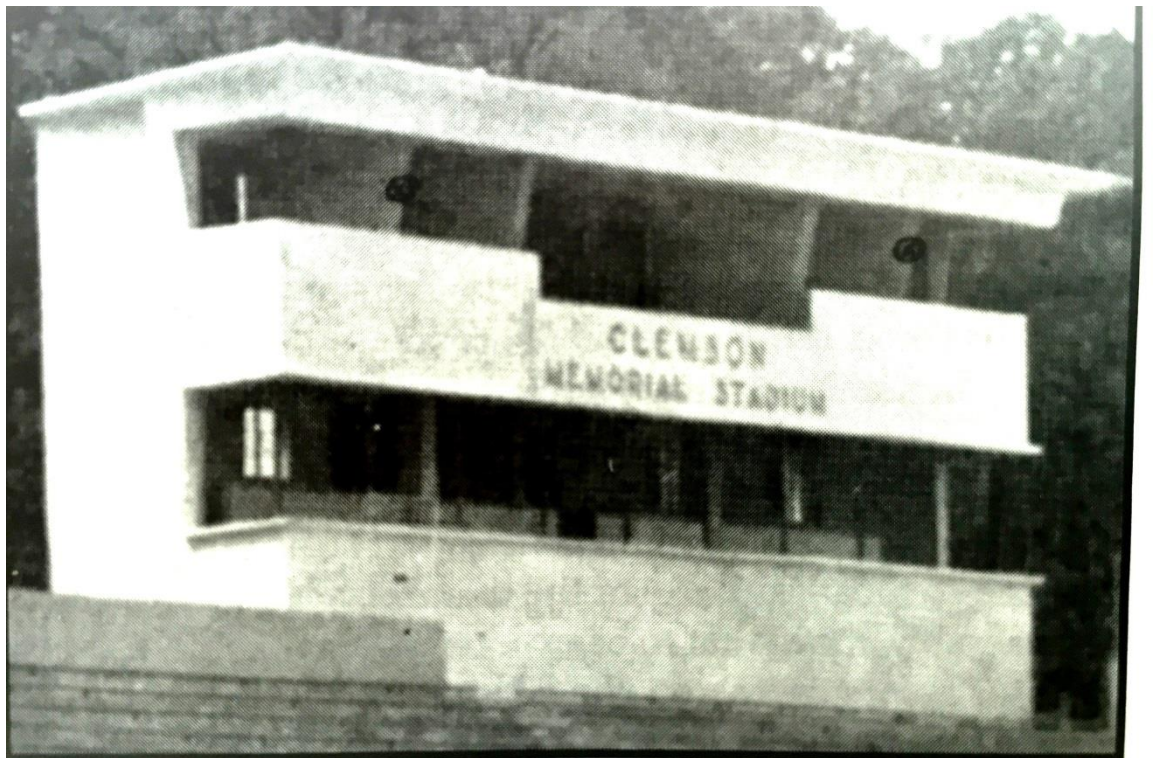
Fig. 26 Press Box Building of former memorial stadium in Clemson which was built by Glenn by using natural bamboo as the main reinforcement system (Hidalgo-Lopez 2003)

Fig. 28 shows the bamboo reinforced concrete girders and slab reinforced with small diameter bamboos in the Press Box Building designed and built by Howard Glenn in 1950.

Professor Howard Glenn's works on the various applications of natural bamboo as reinforcement in concrete elements were fundamental in military constructions during the Vietnam War at the beginning of the 1950s when several concrete vaults were built by the US armed forces using concrete and natural bamboo as reinforcement (Hidalgo-Lopez 2003). However, Professor Howard Glenn faced high costs for the natural bamboo application as reinforcement in concrete due to lack of design consideration and skilled workmanship required for constructing with natural bamboo. Furthermore the long-term behavior of bamboo reinforcement in concrete structures posed further challenges to the application of natural bamboo elements in structural concrete elements, including beams, columns and slabs.
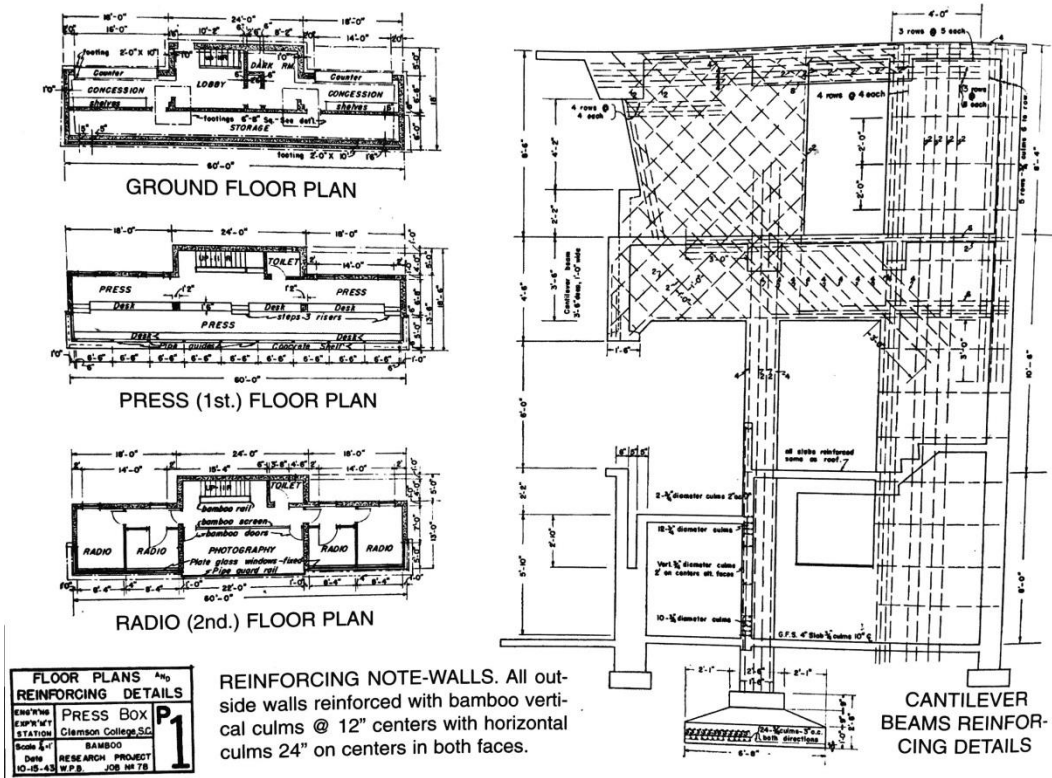
Fig. 27 Details of the bamboo reinforcement used for the Press Box Building by Glenn (Hidalgo-Lopez 2003)
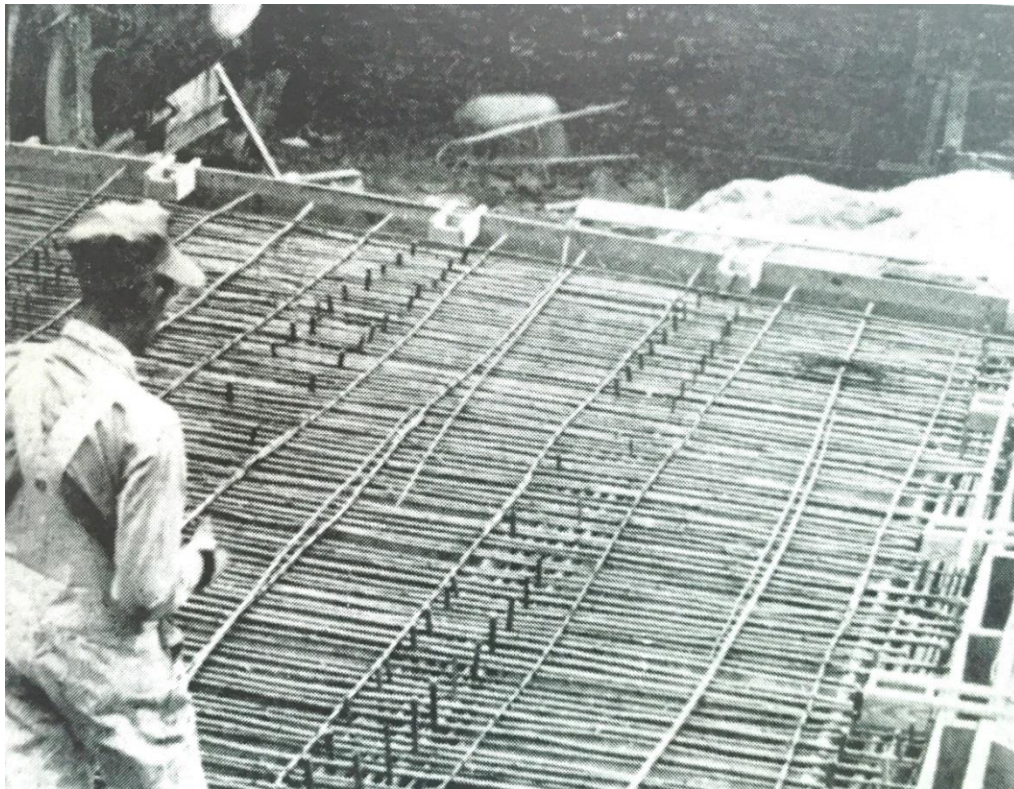
Fig. 28 Small diameter bamboos used for reinforcing concrete beams and slabs in the Press Box Building in Clemson (Hidalgo-Lopez 2003)

Bamboo is a natural material; when it is placed into a concrete matrix, it will absorb the water from the wet concrete matrix during the early stages of the concrete curing process. Due to the water absorption process, the natural bamboo element will swell and increase in volume. The increased volume of the natural bamboo reinforcement confined by concrete matrix will then put tremendous internal tensile stresses onto the concrete matrix, which can ultimately lead to micro and macro cracks within the cured concrete element.

The dimensional variation of the bamboo reinforcement sections in concrete is not only influenced by the water absorption, but also by the temperature variations. The temperature variation caused by external sources such as weather and from internal sources such as the heat produced during the hydration process of concrete could lead to thermal swelling or shrinking, similar to water absorption and evaporation.

Furthermore, the concrete matrix would also accelerate the development of cracks around the natural bamboo reinforcement through the process of shrinkage. Once the concrete hydration process is initiated through the chemical reactions between the cement and water, the volume of cured concrete is reduced, and as a result of the concrete contracting by volume due to water absorption by the natural bamboo, additional internal tensile stresses are built up within the concrete matrix. As a result, the micro and macro cracks developed by the dimensional changes of natural bamboo further expanded into more and larger cracks on the surface of the concrete member.

The cracks produced by the swelling and shrinking of natural bamboo reinforcement in concrete can reduce the bonding between the concrete and natural bamboo, which subsequently may result in a loss in the load-bearing capacity of the reinforced concrete elements, and ultimately results in the structure collapsing, as described by Oscar Hidalgo-Lopez.

The major factors that influence the bonding between the natural bamboo as reinforcement and the concrete matrix include (Sabnani, Latkar et al. 2013):

- Properties of the concrete matrix in terms of adhesion to reinforcement;
- The compression frictional forces developed on the surface of the reinforcement bar due to shrinkage of the concrete;
- The shear resistance of concrete which is mainly influenced by the surface roughness of the bamboo reinforcement.

The dimensional changes of natural bamboo due to water absorption and temperature changes influence all the three bond characteristics to a great extent. In addition, bamboo as a natural lignocellulosic material is prone to degradation due to attacks by termites and fungus, and also long-term exposure to the alkaline environment of concrete matrix; this imposes a major challenge for the long-term suitability of natural bamboo as reinforcement in concrete. The swelling and shrinking and degradation of natural bamboo in concrete are crucial limitation for its application as a reinforcement element in concrete.

The problems with excessive swelling and subsequent loss of bonding with concrete have led to various structural failures in the past, especially in the cases of military constructions built during the Vietnam War. Oscar Hidalgo-Lopez, in *"Bamboo – the Gift of the Gods",* reviewed some of major building collapses which occurred because of bamboo-concrete bond failure in concrete vaults and slabs in Vietnam. Fig. 29 shows a concrete vault reinforced with small bamboo poles and bamboo splits. As can be seen in Fig. 29, the bamboo reinforcement employed in the joint lost their bond to the concrete matrix due either to water absorption from external sources or moisture absorption from the wet concrete.
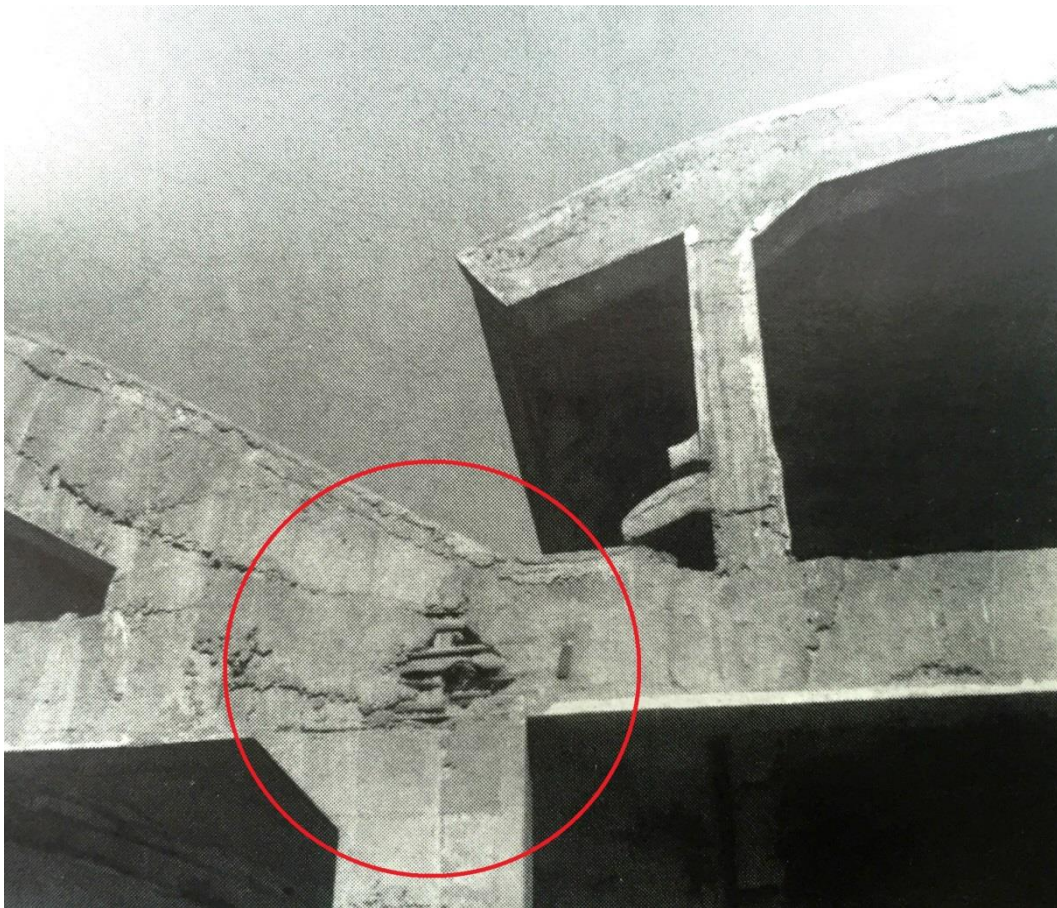
Fig. 29 Failure of concrete vaults reinforced with bamboo elements in Vietnam (Hidalgo-Lopez 2003)

The section of joints in structures built with concrete and reinforced with natural bamboo are highly prone to failures, due to a higher percentage of reinforcement normally allocated to the joints. The swelling and shrinking of natural bamboo reinforcement at joints due to repetitive water absorption and evaporation would ultimately result in micro and macro cracks in the concrete matrix. These cracks expand and develop into surface cracks at the joints, which subsequently result in loss of bonding strength between the concrete and bamboo reinforcement. Once the bond between the concrete and bamboo reinforcement is weakened, the regular stress transfer mechanism between the two materials will be disrupted, resulting in lower ultimate load-bearing capacity of the joint. In the presence of unexpected excessive loading patterns, the joints start to lose their integrity and thus the section fails ultimately. Fig. 30 shows another example of failure at the joints due to the loss of the bond between the concrete and bamboo reinforcement.
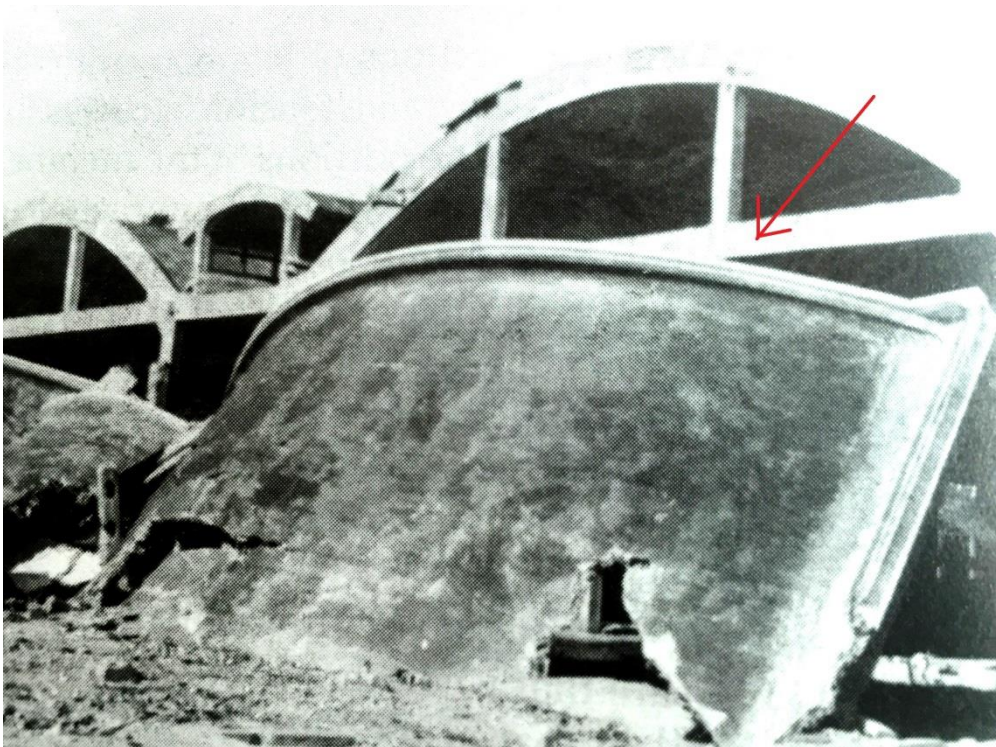
Fig. 30 The collapse of one section of the building was due to failure of the expansion joint, as a result of bond failure between the bamboo reinforcement and concrete. (Hidalgo-Lopez 2003)

The collapse of buildings reinforced with natural bamboo was not limited only to the joint sections; similar failure patterns were observed in columns reinforced with long natural bamboo poles. Fig. 31 shows the failure of a column section due to the premature rupture of the bamboo reinforcement.
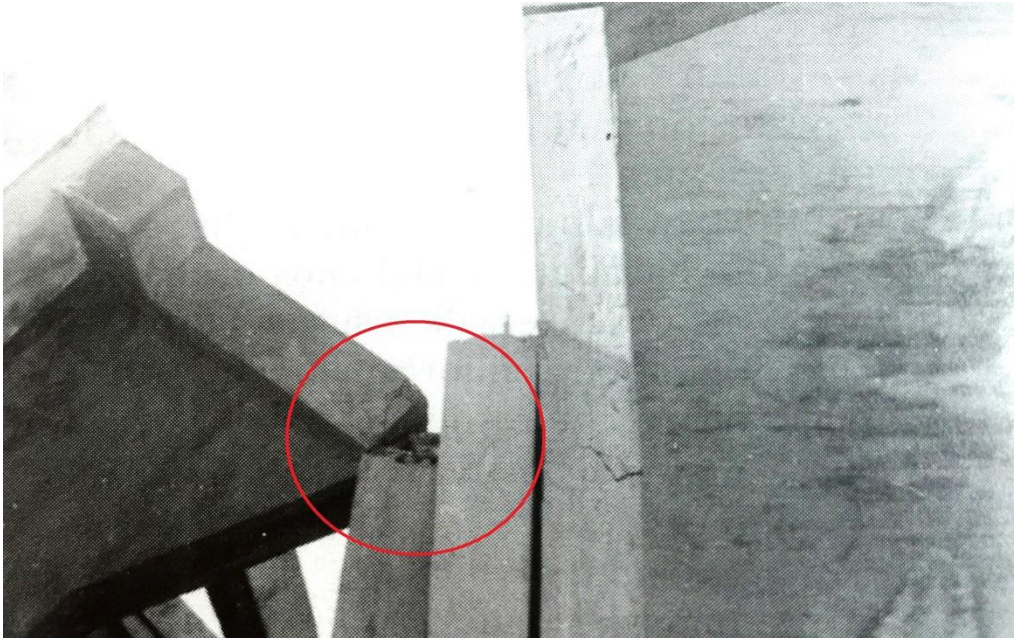
Fig. 31 Failure of concrete column due to premature rupture of bamboo reinforcement. (Hidalgo-Lopez 2003)

The loss of the bond between the natural bamboo reinforcement and concrete matrix was responsible for the collapse of the concrete walls shown in Fig. 32, which were reinforced with natural bamboo splits in vertical and horizontal directions.
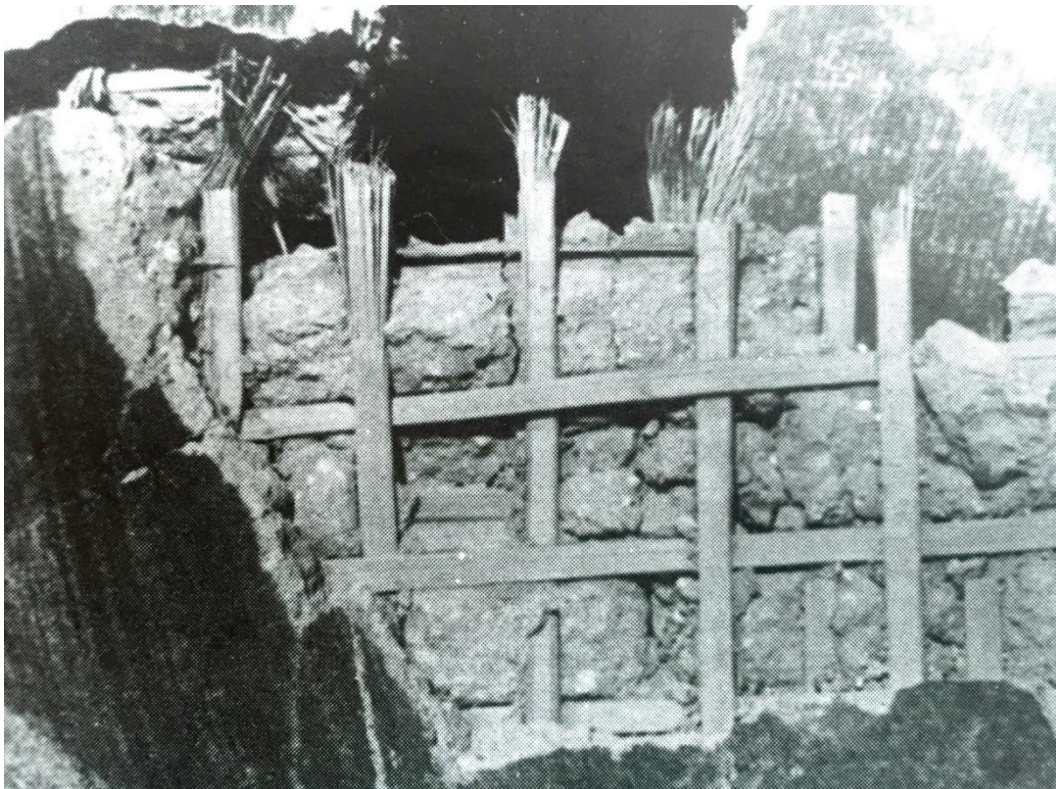
Fig. 32 Lack of adhesion between the concrete and bamboo reinforcement which resulted in the collapse of the concrete walls. (Hidalgo-Lopez 2003)

Professor Glenn's studies of using natural bamboo as reinforcement in concrete led to the development of valuable assumptions and facts for research on natural bamboo reinforced concrete. His works showed that (Hidalgo-Lopez 2003):

1- Employing bamboo reinforcement in concrete beam increases the ultimate failure load of the member by four to five times compared to non-reinforced concrete beam with similar cross-sectional dimensions.

2- The load-bearing capacity of concrete beams reinforced with natural bamboo increases by increasing the percentage of bamboo reinforcement, but only up to 4% of the cross-sectional area of concrete beam.

3- Coated bamboo reinforcements (with asphalt emulsion coating) show better performance in concrete beams in terms of load-bearing capacity compared to untreated bamboo reinforcement.

4- Loss of bond strength is the main cause of failure for concrete members reinforced with natural bamboo (Hidalgo-Lopez 2003).

Following the works of Howard Glenn, Francis Brink and Paul Rush from the Naval Civil Engineering Laboratory in the USA reviewed the design and construction details required for bamboo reinforced concrete applications in 1966 (Brink and Rush 1966). They recommended using bamboo splits which had been dried four weeks before employing them into the concrete matrix. In addition, to improve the performance of the concrete member and reduce the negative impacts of water and moisture ingress, waterproof coatings such as asphalt emulsion, latex, coal tar and paint should be used before placing the bamboo reinforcement in concrete. Francis Brink and Paul Rush assumed the mechanical properties of bamboo reinforcement follow the values displayed in Table 3, and therefore similar design principles to steel reinforced concrete members could be used for bamboo reinforced concrete elements.

Mechanical Property	Symbol	Value (psi)
Ultimate compressive strength		8,000
Allowable compressive stress	s	4,000
Ultimate tensile strength		18,000
Allowable tensile stress	s	4,000
Allowable bond stress	u	50
Modulus of elasticity	E	2.5×10^6

However, Brink and Rush did not elaborate further on the application of various bamboo species with properties different from the values presented in Table 1. As such, the design principles they came up with could only be used in circumstances in which the employed bamboo had similar properties to the bamboo species used by them.

Following the works of Howard Glenn, Francis Brink and Paul Rush, in 1970, Helmut Geymayer, a professor of civil engineering at the Technische Hochschule Graz in Austria, together with Frank Cox, a civil engineer at the Concrete Division of the US Army Engineer Waterways Experiment Station in Mississippi, studied the application of a local bamboo species from Mississippi called *Arundinaria tecta* for reinforcing concrete beams and concrete slabs (Geymayer and Cox 1970). Concrete beams with a three to four percent reinforcement ratio were prepared with bamboo splits that were coated with an epoxy or polyester resin before being placed into the concrete matrix. It was found that bamboo reinforced concrete beams could develop about three to four times the ultimate flexural strength of unreinforced beams with the same cross sections. Fig. 33 shows a typical cross section of the beam prepared by Geymayer and Cox for their experiments on using bamboo as reinforcement.
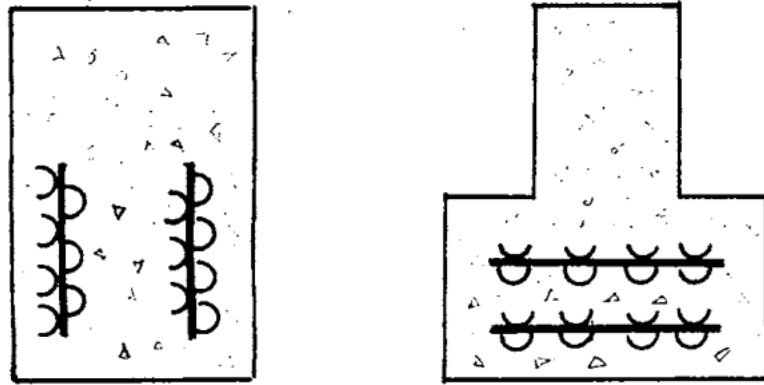
To limit the shrinkage process of bamboo splits in concrete, Geymayer and Cox relied on the assumptions that either a sufficiently thick, dense concrete cover could protect the bamboo splits from the environment, or that as long as the humidity of the environment around the splits remained above 80 percent, shrinkage would be controlled. But if the environment is always at a low humidity, shrinkage of the bamboo could be initiated and result in diagonal cracks in the surrounding concrete matrix. The results from their work conformed to the conclusion made by Howard Glenn on bamboo reinforced concrete beams bonding behavior described earlier.

However, Geymayer and Cox emphasized the fact that due to the differences in thermal expansion coefficients of bamboo and concrete, the cracking of the concrete cover due to differential thermal strains could not be prevented by either by presoaking for 72 hours or by any type of coatings (Geymayer and Cox 1970). In general, the coefficient of thermal expansion of bamboo could be as low as one-third that of concrete longitudinally, and as high as 10 times that of concrete diametrically, which can vary depending on the bamboo species. This difference would have negative impacts on the bond strength of bamboo splits in concrete matrix, especially if the concrete member is exposed to large temperature variations.

Cox and Geymayer also pointed out an important fact on using natural bamboo as reinforcement in concrete. They showed that even though bamboo has high tensile properties, the low bond strength between concrete and bamboo as a result of repeated swelling, shrinking and differential thermal strains, impedes the extensive application of bamboo as reinforcement for concrete elements.

Oscar Hidalgo-Lopez founded the Center for Bamboo Research at the National University of Colombia in 1974 and has carried out extensive research on application of natural bamboo as a reinforcement in concrete in Colombia and Ecuador. Hidalgo-Lopez developed a new technique to produce small diameter bamboo cables to reinforce concrete members (Hidalgo-Lopez 2003). Fig. 34 shows the techniques employed by Hidalgo-Lopez in 1974 to produce the bamboo braided cables. However, the manufacturing process of these cables required a longer time and higher cost compared to bamboo splits, which made the bamboo cables an undesirable choice for the building and construction industry. Hidalgo-Lopez applied these cables for bamboo housing projects in Guayaquil in Ecuador in the late 1970s. Fig. 35 shows the bamboo cables used for reinforcing floor slabs in Ecuador by Hidalgo-Lopez.

Hidalgo-Lopez in *"Bamboo – the Gift of the Gods"* reviewed various applications for bamboo culms and splits in Columbia in the 1970s, especially in reinforced concrete floors together with steel reinforcement. The bamboo culms would provide internal voids in the concrete floors to, firstly, reduce the weight of the floors and required steel reinforcement and, secondly, to lower the construction cost. Fig. 36 shows one of the design concepts proposed by Hidalgo-Lopez for the concrete floors shown in Fig. 37 and Fig. 38. Some of Hidalgo-Lopez's design concepts were used for housing projects in various cities in Colombia, including Bogota, Cali and Popayan, in the 1970s.

Following the works of Hidalgo-Lopez, Helmut Geymayer and Frank Cox, in 1978, Professor David Cook from the School of Civil Engineering, University of New South Wales, together with his partners at the Asian Institute of Technology in Thailand, studied the application of natural bamboo as reinforcement for concrete columns. Their work mainly focused on low-cost structures in military operations, mainly structures with life spans of less than five years and for structures subjected to low stress levels (Cook, Pama et al. 1978). Fig. 38 shows the details of the concrete columns designed by David Cook and reinforced with natural bamboo reinforcement.

D — Support of the free end of cable

Bamboo strips

A — Bamboo

B — Removing the soft part

C — Bamboo handle / Wood handle

E

The handles have to be turn around at the same time, in the same direction with the same speed

F — Wire

The bamboo cable can be made with three or more bamboo strips

Wire
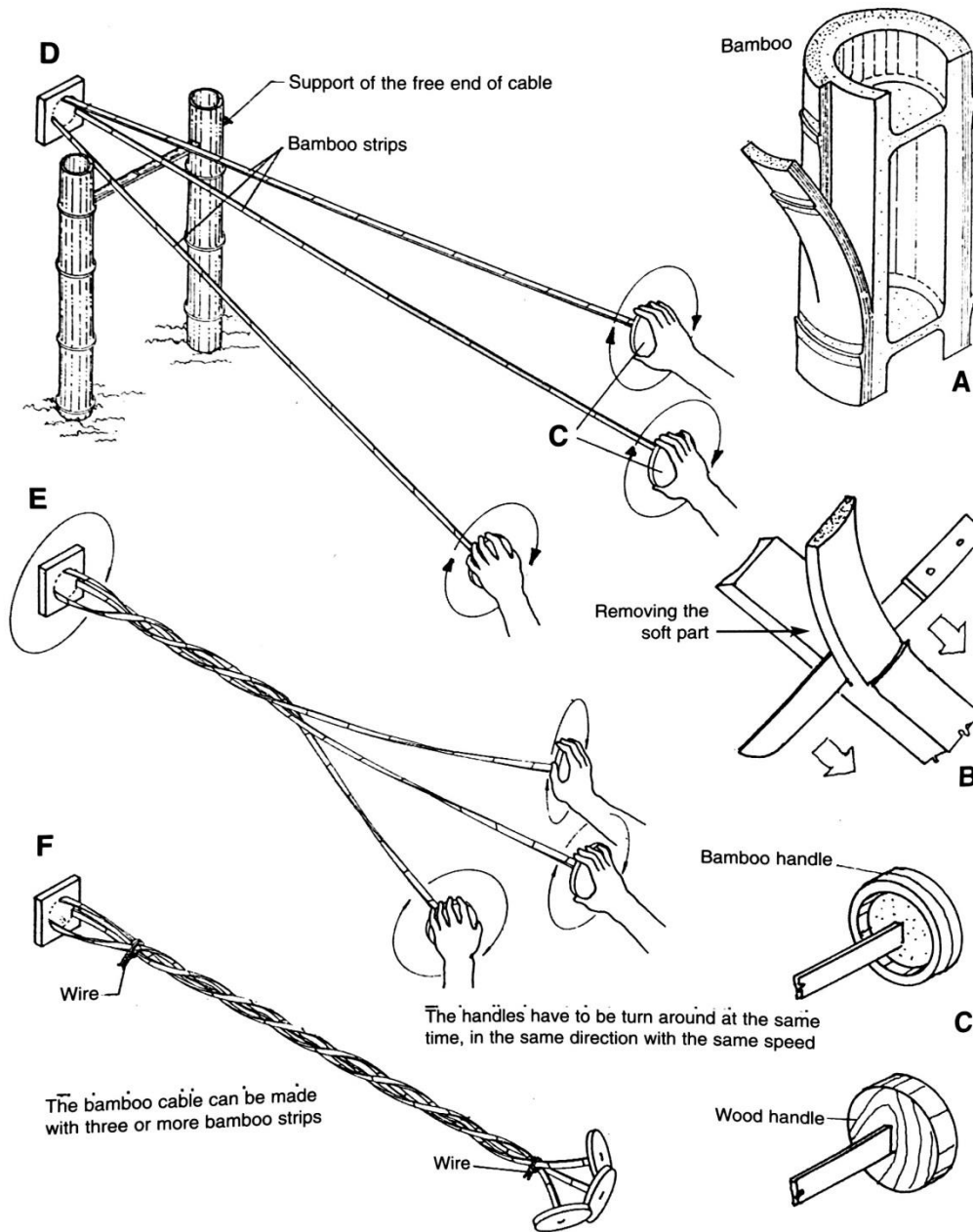
Fig. 34 Manufacturing techniques developed by Hidalgo-Lopez for the production of bamboo cables in the 1970s (Hidalgo-Lopez 2003)
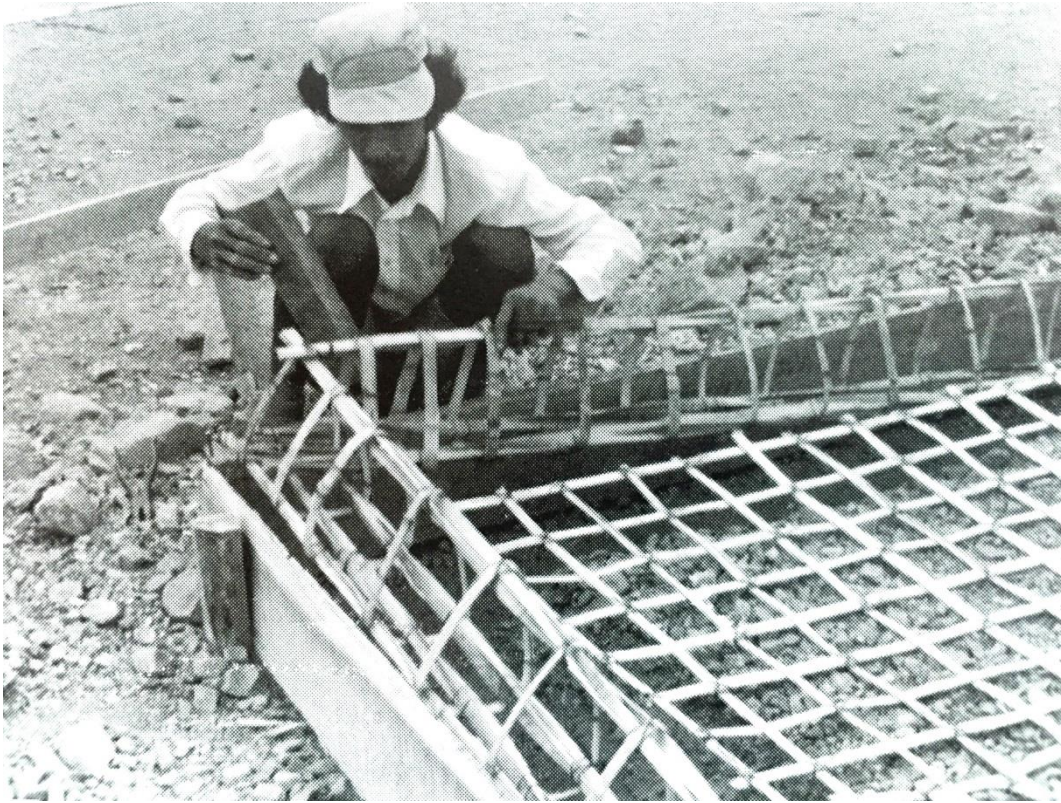
Fig. 35 Bamboo cables employed to reinforce concrete floor in Ecuador (Hidalgo-Lopez 2003)

Fig. 36 Bamboo culms used as reinforcement and providing voids for concrete floor in Colombia (Hidalgo-Lopez 2003)

Fig. 37 Bamboo reinforcement for concrete floors of housing projects in Colombia (Hidalgo-Lopez 2003)

The investigation showed that the ultimate load-bearing capacity of columns reinforced with natural bamboo splits increased up to three times compared to non-reinforced concrete columns. However, in comparison with steel reinforced columns of similar cross sections, the ultimate load-bearing capacity of bamboo reinforced columns was less than 50 percent of that of steel reinforced concrete columns. However, based on the cost of reinforcement, the comparison between natural bamboo and steel reinforcement in concrete columns with equal load-bearing capacity showed that natural bamboo reinforcement could be up to 49% cheaper than steel reinforcement, given their price and availability in the local market (Cook, Pama et al. 1978). However, no information on the durability of those columns were provided by David Cook and his partners, specifically on the shrinkage and swelling behavior of bamboo splits used as reinforcement in the concrete columns.

6·25 mm dia. steel ties at 50 mm centres

12·5 × 1·5 mm bamboo skin ties at 75 mm centres

12·5 × 1·5 mm bamboo skin ties at 175 mm centres

longitudinal bamboo

bamboo

150   125

125

150   125   875   125   150

A   A

150   125
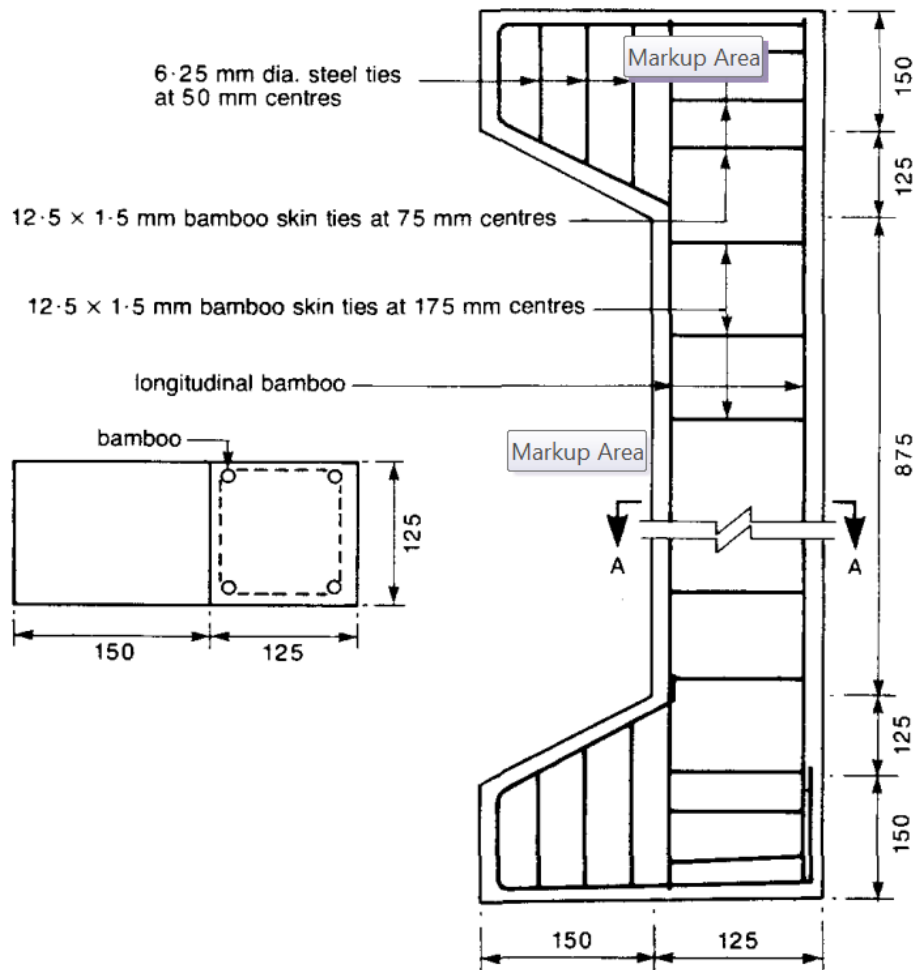
Fig. 38 Details of column test specimen in mm (Cook, Pama et al. 1978)

A more comprehensive study on the application of natural bamboo as reinforcement in concrete beams was undertaken by a group of researchers from the University of Science and Technology (UST) in Kumasi in Ghana and Trinity College, University of Dublin in the Republic of Ireland, in 1988. The research was carried out by Professor Joshua Ayarkwa Kankam and Professor Mike Ben George from the University of Science and Technology (UST) in Kumasi, School of Civil Engineering, together with Professor Simon Herbert Perry from Trinity College Dublin (Kankam, Ben-George et al. 1988). The most common African species of bamboo called *Oxytenanthera Abyssinica* was used in this study to replace steel for both the longitudinal and vertical (stirrup) reinforcement elements. A series of large-scale concrete beams with varying lengths from 1.8m to 3m were prepared with natural bamboo as reinforcement and tested until failure under the third-point loading test. Both coated and non-coated bamboo splits were used in this study. Fig. 39 shows a typical cross section of the beams tested in the work of Kankam, Ben-George and Perry.
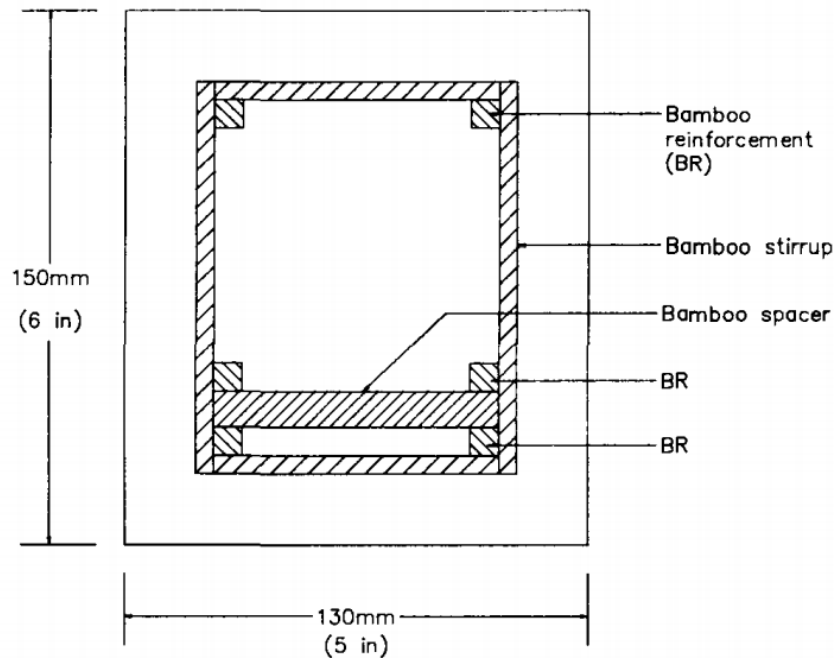
Fig. 39 Typical cross section of a beam with bamboo reinforcement and bamboo stirrup (Kankam, Ben-George et al. 1988)

The bamboo stirrups which were used in the investigation to resist the diagonal shear stress and activated during the loading are shown in Fig. 40. The stirrups consisted of two horizontal and two vertical bamboo splits with small notches made at the ends of the pieces and tied together using copper wire at the two ends. In most of the tests with bamboo stirrups, failure occurred through the diagonal shear failure of the concrete in the shear span, rather than flexural failure through the fracture of the longitudinal bamboo reinforcement.

Joshua Ayarkwa Kankam, Mike Ben George and Simon Herbert Perry related the shear failure of the bamboo reinforced concrete beams to the fact that the ties between the horizontal and vertical pieces of the bamboo stirrups were not as effective as the continuous corners of the steel stirrups. However, bamboo stirrups provided further stiffness, which resulted in deflections for beams with bamboo stirrups being smaller than beams without bamboo stirrups. Beams with bamboo reinforcement coated with a bituminous paint and covered with sand particles have shown better performance in bonding tests. On average, they led to a higher ultimate failure load in bending tests compared to non-coated bamboo reinforced beams.
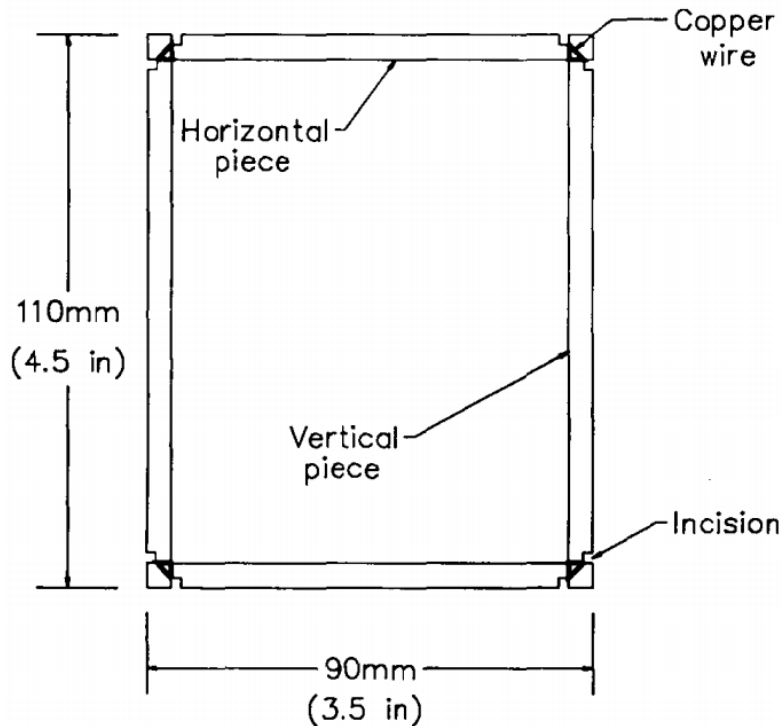
The research carried out by Professor Joshua Ayarkwa Kankam, Professor Mike Ben George and Professor Simon Herbert Perry revealed two interesting facts regarding the use of natural bamboo reinforcement in concrete. Firstly, the addition of a waterproof coating and sand particles to the surface of natural bamboo reinforcement could enhance the bonding between the reinforcement and concrete matrix. As a result, the ultimate load-bearing capacity of beams could be increased by up to 30%. Secondly, bamboo stirrups made with splits and tied with wire displayed partial contribution in preventing shear failure of the beams compared to steel stirrups, but helped to improve the stiffness of the beams by limiting the maximum deflections in third-point loading tests (Kankam, Ben-George et al. 1988).

The publications till the 1980s have mostly indicated the need for coatings for bamboo reinforcement for concrete. Bond strength remained one of the many disadvantages of using natural bamboo in its natural state in concrete, as discovered by researchers around the world. However, further research on the bond strength of bamboo reinforcement with concrete was carried out by Professor Joshua Ayarkwa Kankam and Professor Simon Herbert Perry in 1989, following their work on third-point loading tests of concrete beams reinforced with natural bamboo. They studied the effect of coating the bamboo reinforcement and various concrete strength on the bond mechanism between the reinforcement and concrete matrix

through a series of pull-out tests (Kankam and Perry 1989). Fig.41 displays the set-up for the pull-out test used in their investigation.
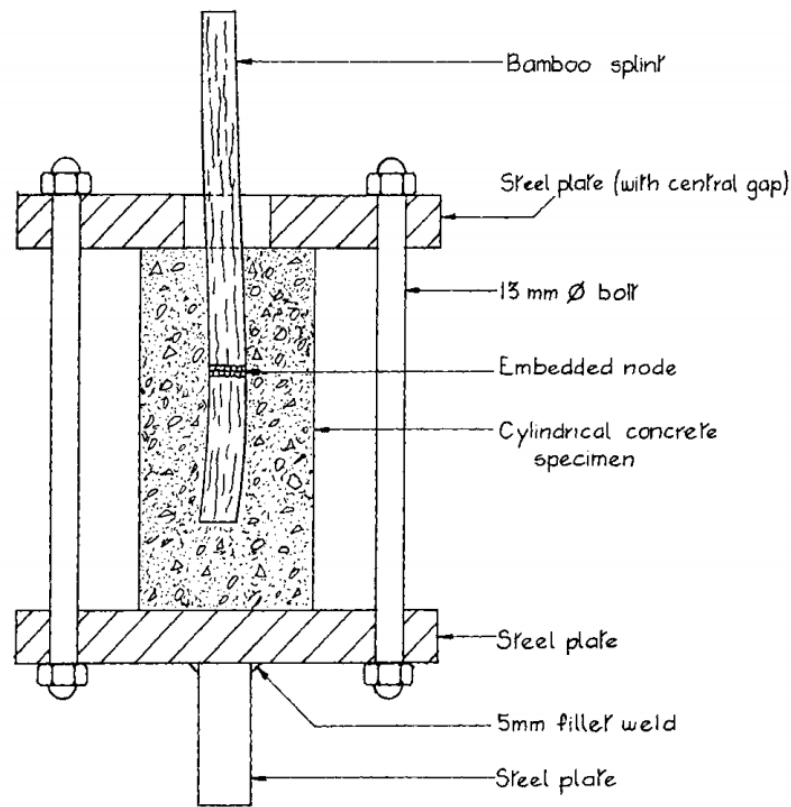
Fig. 41 Concrete cylinder with bamboo reinforcement used in the pull-out test (Kankam and Perry 1989)

The results of the pull-out tests indicated that bond strength could be improved both by having a higher strength concrete and through appropriate coating for the raw bamboo reinforcement. As a result of improved bond strength, the anchorage of bamboo reinforcement would be improved, which could lead to better performance and higher load-bearing capacity of the beams (Kankam and Perry 1989).

Similar studies on the application of bamboo as reinforcement in concrete were carried out in Indonesia on a local bamboo species called *Dendrocalamus asper* from Java by Professor Naresworo Nugroho and Professor Surjono Surjokusumo at the Department of Forest Product Technology, Faculty of Forestry, Bogor Agricultural University in Indonesia in 1995 (Surjokusumo and Nugroho 1995). Various sizes and profiles of bamboo were used together with three kinds of chemicals for protection and bonding enhancement. The results indicated that surface coating with varnish had the highest bond strength between the bamboo and the concrete matrix. Furthermore, the highest load-bearing capacity of the concrete with bamboo could be achieved by increasing the width of the rectangular bamboo profile by up to 30%.

100

Nevertheless, the study lacks scientific analysis regarding the optimum ratio of reinforcement that could be used in concrete beams. It also did not consider the long-term effect of the varnish coating on the bond strength between the bamboo and concrete. But the study showed that, in general, reinforcing concrete beams with coated bamboo could enhance the overall load-bearing capacity of the concrete element.

Comprehensive research on the application of bamboo species from Brazil to reinforce concrete beams was carried out by Professor Khosrow Ghavami at the Civil Engineering Department of Pontificia Universidade Católica do Rio de Janeiro in 1995 (Ghavami 1995). A series of large-scale concrete beams of 3.4m in length and reinforced with natural bamboo *Dendrucalamus giganteus* were tested under the four-point bending tests. Ghavami applied a water repellent coating, together with sand particles on the surface of bamboo reinforcement, and wrapped the reinforcement with 1.5mm-diameter wire around it to both protect the bamboo against water absorption and to enhance the bonding strength between the natural bamboo reinforcement and concrete matrix.

The bonding strength between the coated bamboo reinforcement and concrete matrix was enhanced up to 90% compared to the non-treated bamboo reinforcement. However, in comparison with steel reinforced concrete beams, the bamboo reinforced concrete showed larger deflections, mainly due to the lower modulus of elasticity compared to steel. Furthermore, it was shown in Ghavami's study that the ultimate applied load for the bamboo reinforced concrete beam increased up to 400% compared to the concrete beams without bamboo reinforcement (Ghavami 1995).

At almost the same time the studies by Ghavami in Brazil was done, Professor Bern Baier at the University of Duisburg-Essen in Germany experimented with natural bamboo as reinforcement for concrete beams in 1996 (Yu 2008). A series of tests was performed with various sizes of bamboo poles embedded in concrete beams and tested under the third-point bending tests. However, no information on the bond behavior of the bamboo reinforcement to concrete matrix was provided by the authors. Furthermore, no comparison with non-reinforced concrete beams was made in this study.

The results from various investigations on the application of natural treated or non-treated bamboo poles, culms or splits up to the beginning of the 21st century had showed that bamboo, in its natural state in the form of culm or splits, in general can be applied as a replacement for steel in reinforced concrete beams. However, further research is necessary to

find solutions to the durability issues, such as water absorption, effect of alkaline environment on concrete, the different thermal expansion coefficients of bamboo and concrete, as well as the bonding mechanism with concrete matrix. Furthermore, a system which is designed based on the physiognomy of the plant is always limited to the dimensions (length, width, density) according to the biological character of the plant. As this thesis tries to show, this limitation could be overcome by an industrialization of the production of a new material via using only the fibers of the plant, and not its physiognomy.

A detailed study of bamboo as a reinforcement for a wide range of applications, including concrete slabs, columns and beams, was carried out by Professor Khosrow Ghavami at the Civil Engineering Department of Pontificia Universidade Católica do Rio de Janeiro in 2005 in Brazil (Ghavami 2005). The bond behavior of the bamboo reinforcement to the concrete matrix was also studied through a series of pull-out tests. An epoxy-resin bonding agent called Sikadur-32 used in the study to treat the bamboo reinforcement. It showed an increased bonding strength for the bamboo reinforcement of 5.29 times, compared to that for untreated bamboo reinforcement. Similar to the previous study by Khosrow Ghavami in 1995 (Ghavami 1995), the bamboo reinforcement was wrapped with wires 1.5 mm in diameter before being placed into the concrete sample to further enhance the bonding.

Concrete slabs were prepared with half split treated bamboo culms, as both tensile reinforcement and also as permanent formwork. To improve the mechanical interlocking between the bamboo reinforcement and concrete and to create a composite action between the bamboo and concrete, sections of the entire bamboo culm were cut and installed in various segments of the formwork as shown in Fig. 42. However, the concrete slabs failed mainly due to de-bonding and crushing of the culm sections used as the composite interface, and eventually due to concrete compression failure. Therefore, in his work, Khosrow Ghavami emphasized the fact that further research must be carried out on enhancing the bonding and composite interface between the bamboo splits and concrete matrix.
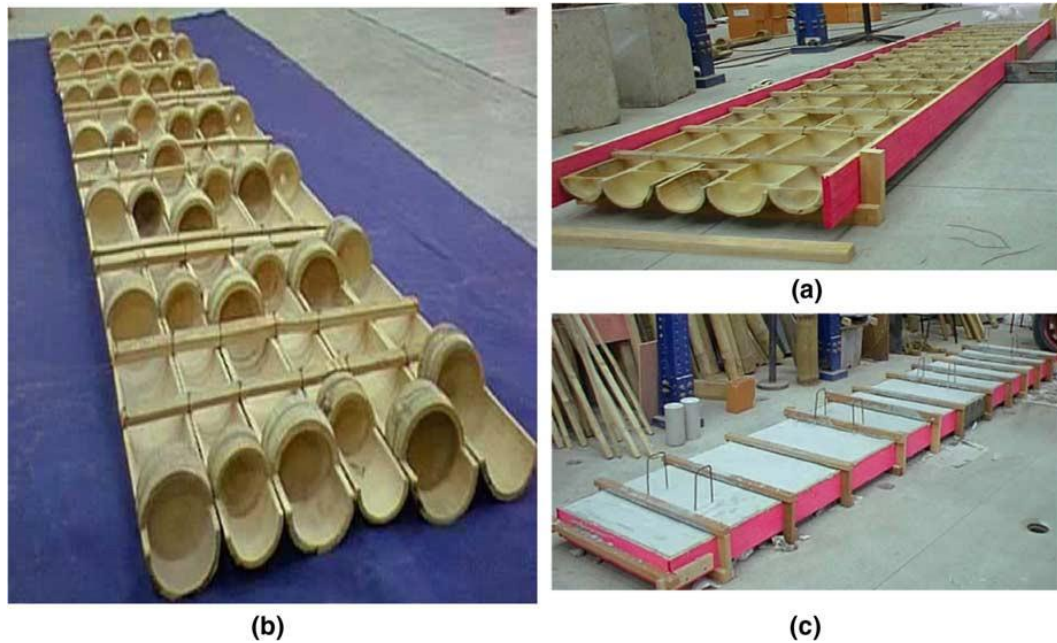
Fig. 42 Concrete slabs reinforced with bamboo permanent shutter forms. (a) Half bamboo diaphragm as connector. (b) Second type of connector. (c) Slab before testing. (Ghavami 2005)

As with the concrete slabs, a series of circular concrete columns was reinforced by treated bamboo splits and subjected to axial load tests in comparison to the concrete columns reinforced by steel reinforcement, as shown in Fig. 43. The bamboo reinforced columns showed relatively good performance by failing at nearly the same ultimate load as the steel reinforced concrete column, where the failure mainly occurred due to concrete crushing at the both ends of the column (Ghavami 2005).

Khosrow Ghavami's works from 1995 to 2005 on the application of natural bamboo in concrete showed that replacing steel reinforcement in concrete applications is possible in general terms, given the superior mechanical properties of natural bamboo. But the problems with bonding, shear strength, thermal expansion as well as durability of natural bamboo in concrete matrix remain as major barriers in the widespread application of bamboo as reinforcement in concrete. Nevertheless, the research by Khosrow Ghavami has paved the way for further investigations on the suitability of raw bamboo to replace steel reinforcement in various concrete applications around the world.
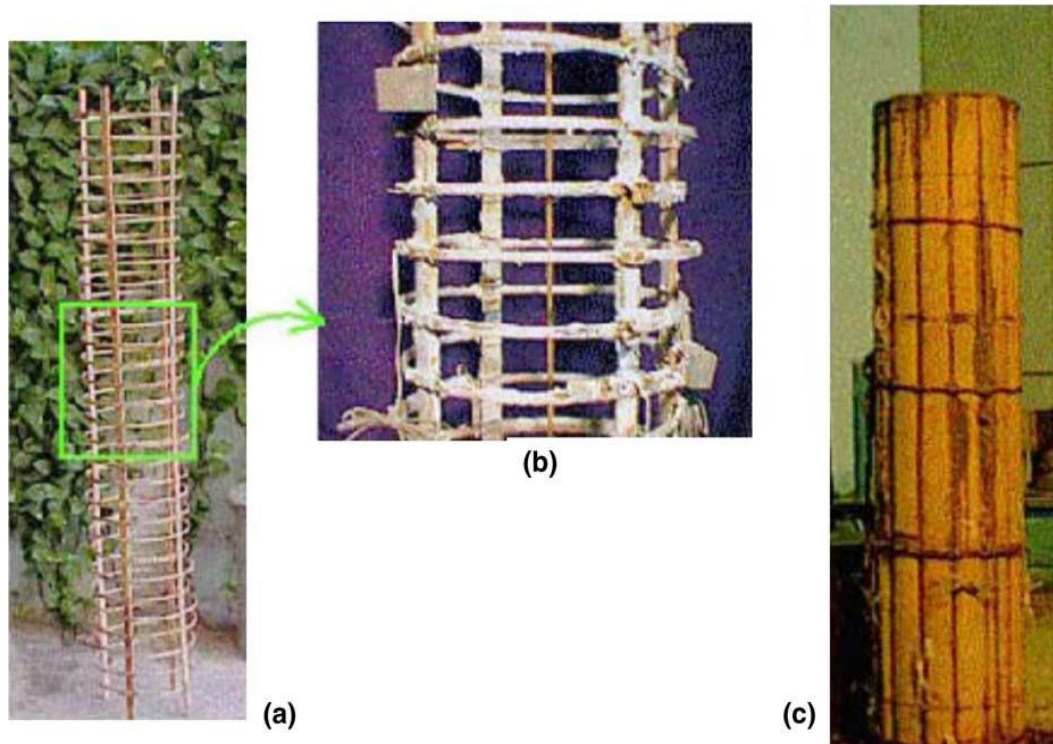
Fig. 43 Circular bamboo reinforced concrete column with permanent shutter: (a) column reinforcement, (b) details of reinforcement and (c) final product. (Ghavami 2005)

Leena Khare, a Master of Science student at the University of Texas at Arlington, undertook similar studies as Khosrow Ghavami by employing Moso and Tonkin bamboo from China to reinforce concrete beams of up to 2.5m in length as shown in Fig. 44 (Khare 2005). In this study, the bamboo stirrups were made of Tonkin bamboo due to its flexibility, and the main longitudinal reinforcements were made of Moso bamboo given its higher bending strength. All the bamboo reinforcement used in concrete beams were first coated with a waterproof coating to enhance the bonding with the concrete matrix and reduce water absorption. The results from the four-point bending tests showed that bamboo reinforcement improved the load-bearing capacity of concrete beam by up to 250% compared to the concrete beam without reinforcement. However, the results also showed that the ultimate load-bearing capacity of bamboo reinforced concrete beams on average was only 35% of the steel reinforced concrete beams with similar cross sections. The stirrups showed little resistance to shear forces; most of the beams failed due to diagonal shear stress in the concrete beams as a result of weak bonding between the reinforcement and concrete during the tests. Fig. 45 shows the shear failure of the bamboo reinforced concrete beams.

Fig. 44 Bamboo reinforcement and stirrups used to reinforce concrete beam of up to 2.5m in length (Khare 2005)
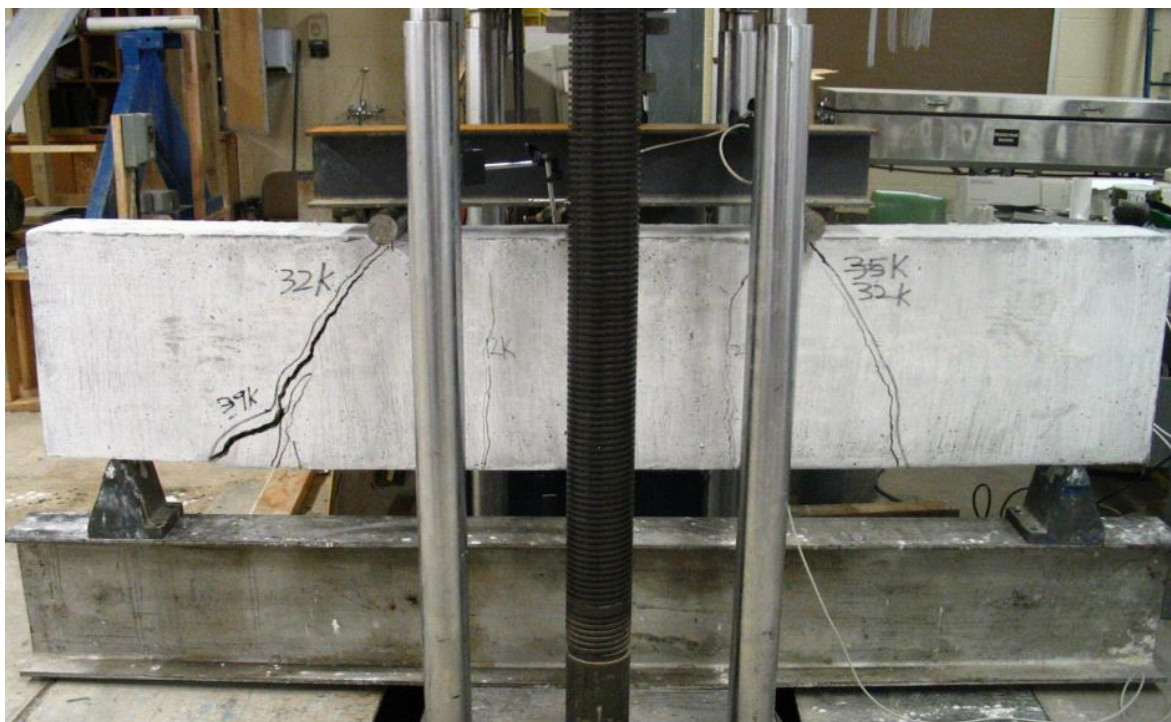
Fig. 45 Failure of bamboo reinforced concrete beam under four-point bending test due to shear (Khare 2005)

Similar to the studies carried out by Khosrow Ghavami and Ayarkwa Kankam, Leena Khare showed that natural bamboo has the potential to replace steel reinforcement but the problems with bonding and durability still exist.

A detailed investigation on the durability of bamboo as reinforcement in concrete was undertaken by Professor Humberto Correia Lima from the Federal University of Pernambuco in Brazil and his research team, including Fabio Willrich, Maxer Rosa and Bruna Cunha from the State University of Parana West in Brazil, and Normando Barbosa from the Federal University of Paraíba, in Brazil, in 2008 (Lima Jr, Willrich et al. 2008). A series of tensile

samples were prepared from bamboo *Dendrocalamus giganteus* of Brazil and subjected to 6-month wetting and drying cycles in normal tap water and alkaline solutions with similar pH as in concrete environments. The durability performance of the bamboo samples were discussed in relation to the tensile strength and modulus of elasticity of the samples before and after exposure to the 6-month wetting and drying cycles. The results showed that, in general, there was a decrease in both the tensile strength and modulus of the elasticity of the samples after the 6-month wetting and drying cycles, but the drop in these properties was not significant enough. The bamboo samples in this study were exposed only to a solution with a pH level of 7.5 and up to 6 months. But in reality, buildings are exposed to more severe conditions, such as the concrete matrix being attacked by acidic rain which would further reduce the pH level. Therefore, the results from the study by Professor Humberto Lima and his research team could only be valid for a common pH condition in concrete and only for a short exposure time. Further research on various pH levels and under different humidity and moisture conditions with varying exposure times is essential for a better understanding of the durability of natural bamboo reinforcement in concrete matrix.

Several other researchers have continued the investigation of using bamboo as reinforcement in concrete beams and columns applications in the early 21st century (Sethia and Baradiya , Leelatanon, Srivaro et al. 2010, Mahzuz, Ahmed et al. 2011, Rahman, Rashid et al. 2011, Salau, Adegbite et al. 2012). Similar to the earlier studies, these investigations proved that natural bamboo could potentially replace steel in concrete applications, though the ultimate load-bearing capacity of the concrete member reinforced with natural bamboo was less than 50% of the steel reinforced concrete member. Unfortunately, the investigations led by Satjapan Leelatanon at Walailak University in Thailand, HMA Mahzuz at the Shahjalal University of Science and Technology in Bangladesh, Mohammad Mansur Rahman at the University of Engineering & Technology in Bangladesh, Musbau Ajibade Salau at the University of Lagos in Nigeria and Arpit Sethia at the Institute of Engineering & Science IPS Academy in India, did not elaborate on the main problem of using natural bamboo in concrete: the bonding. The weak bonding between bamboo reinforcement and concrete due to water absorption, chemical decomposition in the alkaline concrete matrix, and different coefficients of thermal expansion between bamboo and concrete would result in a loss in the ultimate load-bearing capacity of reinforced concrete members.

Professor Damodar Maitya and Atul Agarwala from the Indian Institute of Technology of Kharagpur in India, together with Professor Bharadwaj Nandab from Veer Surendra Sai

University of Technology of Burla in India, carried out a series of pull-out tests in 2014 on treated bamboo bars with various coatings, including an epoxy-based thermosetting adhesive, acrylic based polymer modified cementitious coating, a two-component solvent free epoxy resin coating and a polyurethane based adhesive coating (Agarwal, Nanda et al. 2014).

The results of the investigation showed that the average bond strength between the bamboo and concrete is highest for a two-component solvent-free epoxy-resin coating (Sikadur-32 gel) and the rest of the samples coated with other types of coating failed due to slippage of the bamboo strips from the concrete cylinders. The concrete columns and beams reinforced with coated bamboo reinforcement showed better performance compared to non-treated bamboo in axial compression and four-point bending test respectively. The study also revealed that bamboo reinforced concrete members had higher capacity to absorb energy compared to steel reinforced concrete members, which could potentially be helpful in earthquake-prone areas.

In Japan, Professor Koichi Minami and Professor Masakazu Terai from Fukuyama University undertook a series of pull-out tests, followed by testing samples of bamboo reinforced concrete slabs, beams and columns (Terai and Minami 2011, Terai and Minami 2012). A synthetic resin coating was applied on the surface of the reinforcement which proved to enhance the bond strength. The reinforced concrete slabs showed signs of bond failure during the bending test, but the concrete beams and columns reinforced with treated bamboo reinforcement showed superior performance compared to non-reinforced concrete members. Koichi Minami and Masakazu Terai showed that the fracture behavior of bamboo reinforced concrete members could be evaluated by the existing formula of reinforced concrete members. However, the results also indicated that the bonding strength between bamboo reinforcement and concrete matrix was only half of that of deformed steel reinforcement and concrete (Terai and Minami 2012).

Following the work of Koichi Minami and Masakazu Terai on the theoretical calculations of the load displacement behavior of concrete beams reinforced with natural bamboo reinforcement, Professor Makoto Yamaguchi, together with Professor Kiyoshi Murakami and Professor Koji Takeda from Kumamoto University in Japan, carried out a series of four-point bending tests of concrete beams reinforced by Japanese Moso bamboo reinforcement and natural bamboo stirrups (Yamaguchi, Murakami et al. 2013). In this study, it was assumed that the Bernoulli-Euler beam theory or theory of elasticity (as explained in the literature

review) would be valid for bamboo reinforcement and the stress–strain relationship of bamboo was linear-elastic up to failure. The investigation showed that that the load-bearing capacity of the bamboo reinforced concrete beams could be predicted using section analysis based on the Bernoulli-Euler beam theory. However, the effect of the bamboo stirrups on shear failure and shear resistance capacity of the bamboo reinforced concrete beams was not investigated in this work.

Further research on the suitability of natural bamboo as a replacement for steel in concrete applications was carried out in recent years by various research groups around the world. These included the studies led by Dr. Adekunle Adewuyi at the Federal University of Agriculture of Abeokuta in Nigeria, the work of Ibrahim Khan at Aligarh Muslim University in India, the study led by Benitta Paulin Mary at Karunya University in India, and the studies of Professor Satish Pawar at the Shivajirao S. Jondhale College of Engineering & Technology in India (PaulinMary and Tensing 2013, Khan 2014, Pawar 2014, Adewuyi, Otukoya et al. 2015). In all these investigations, bamboo proved to be a suitable replacement for steel reinforcement due to its high tensile and flexural strength. Much effort was given to evaluate the mechanical advantages of bamboo as a reinforcement element rather than the durability properties and the bond strength of bamboo in concrete.

The research conducted so far in the field of bamboo reinforced structural concrete applications specified two major findings. Firstly, the possibility of replacing steel with bamboo material as a reinforcement system is feasible. Secondly, so far, no solution is available to improve the durability and measures to control the swelling, shrinking and thermal expansion of the material. Both findings were a motivation in this PhD research thesis.

3.6.   Conclusions

Steel reinforcement production requires much energy and, more importantly, steel comes from a non-renewable source. Its production is responsible for significant levels of greenhouse gas emissions. Reinforcement steel also suffers from corrosion which affects the long-term performance of many steel reinforced concrete members. In addition, steel is a product of the developed world; most countries in the developing world in Asia, Africa and in the Americas have little to no access to steel for construction purposes. Bamboo has many advantages, including high tensile strength, as well fast growth and availability in developing countries where steel reinforcement has to be imported at high cost. In comparison to

synthetic fibers, such as glass fibers which are currently being implemented in the building and construction sector, bamboo fibers have the advantages of low costs and high weight-to-strength ratios. The originality of the objectives is established by addressing the shortcomings with respect to each objective as found in the literature. No scientific studies have been carried out on the evaluation of the physical and mechanical properties of raw bamboo with respect to culm geometrical parameters, including diameter, thickness and height. Secondly, the studies on fabrication of composite materials based on natural fibers have generally been limited to non-structural and non-load-bearing applications. Furthermore, the earlier studies have not investigated the suitability of bamboo composite materials as reinforcement systems for structural concrete applications. Therefore, ideas and production methods which have not been studied in the past need to be investigated to address these shortcomings. Several attempts have been made by researchers to evaluate the suitability of natural bamboo as a reinforcement system in concrete applications. However, bond strength, water absorption, thermal expansion, as well as swelling and shrinking related issues concerning the use of natural bamboo reinforcement in concrete remain major barriers to bamboo's widespread application. There is a need for a systematic study on enhancing the properties of composite bamboo materials and evaluating the performance of bamboo composite materials within the concrete matrix. Finally, state-of-the-art designs for the newly developed bamboo composite reinforcement systems need to be investigated as part of this research.

4. Raw bamboo selection and evaluation of properties

4.1. Summary

In this chapter, the bamboo species used in this study are identified. The selection process of the raw bamboo is important to the production of newly developed bamboo composite reinforcement systems. Detailed descriptions and comprehensive information related to the harvesting, transportation, curing and storage of the selected bamboo culms for this pioneer research are explained. This is followed by comprehensive and meticulous investigations of the physical and mechanical properties of more than 4,500 samples of bamboo, *Dendrocalamus asper* from Indonesia, the selected bamboo species. For the very first time, novel statistical models are established between the modulus of elasticity in flexure, modulus of rupture, modulus of elasticity in tension, compressive strength, and tensile strength of *Dendrocalamus asper* bamboo with its geometry, including culm diameter, wall thickness, specific density and moisture content. The pioneer models are useful tools for quick estimation of the mechanical properties of raw bamboo culms by measuring only the culm diameter and wall thickness. The chapter establishes the necessary mechanical properties of the raw bamboo samples, including tensile strength, flexural strength, modulus of elasticity in tension, modulus of elasticity in flexure and compressive strength according to the relevant international standards for testing timber, in the absence of pre-existing international standards for testing raw bamboo samples. Therefore new designs of samples with appropriate shapes suitable for evaluating the raw bamboo's physical and mechanical properties are proposed and have been successfully tested. The bamboo culms are cut into sections and classified into seven groups with culm diameters ranging from 80mm to 150mm, and wall thicknesses ranging from 6mm to 20mm covering all the 4,500 raw bamboo samples. Unlike the culm diameter, the wall thickness has an obvious effect on reaching a certain MC by the specific time under certain RH conditions. Similarly, a complex behavior is found for the first time with respect to the specific density and its variation with the change in culm diameter and wall thickness. By increasing the culm diameter for culms with diameters from 120mm to 150mm, the specific density decreases for wall thickness of less than 13mm. The highest average tensile strength of 323MPa and modulus of elasticity of 28,230MPa are found in samples of bamboo *Dendrocalamus asper* with culm diameters from 110mm to 120mm and with wall thicknesses of 6mm to 10mm. The highest average modulus of rupture of 205MPa is found in bamboo samples with culm diameters from 80mm to 90mm and with wall thicknesses of 6mm to 9mm, while the highest average modulus of elasticity in

flexure of 12,851MPa is measured within samples of *Dendrocalamus asper* with culm diameters in the range of 90mm to 100mm and wall thicknesses from 6mm to 10mm. The highest compressive strength of 66MPa can be found within bamboo samples with culm diameters of 80mm to 90mm and with wall thicknesses from 6mm to 9mm. A statistical analysis confirms the correlations between specific density and the mechanical properties by showing that bamboo sections with larger culm diameters and thicker wall cross sections have lower specific density, resulting in lower mechanical properties. No strong correlation is found between moisture content and mechanical properties except for the modulus of rupture.

4.2. Raw bamboo selection

As mentioned in section 3.4, there are more than 1,200 species of bamboo globally, but only a few of these are suitable for the purpose of manufacturing bamboo composite materials. As described earlier, in this PhD thesis, four widely available species of bamboo were chosen for the review of their properties in section 3.4.2. The four species selected are *Dendrocalamus asper*, *Phyllostachys edulis*, *Oxytenanthera abyssinica* and *Guadua angustifolia*. Their physical and mechanical properties were discussed in section 3.4.2 in detail. Bamboo **Dendrocalamus asper** or **Giant bamboo** from Indonesia was selected for the purpose of this PhD research, and further evaluations and investigations were carried out on this bamboo species.

The reason for this selection pertains to two main aspects:

1- **Dendrocalamus asper,** which is known locally as *Petung* bamboo, in Indonesia is the most widely available bamboo species in Southeast Asia, particularly in Indonesia, Thailand and Malaysia. It is widely used in the construction sector as a natural building material. By exploring the most common species of bamboo used for construction in the region, where Singapore is located and where this PhD research is being carried out, other bamboo species in this region or around the world could subsequently be used in the processing technology developed in this thesis and be applied in bamboo composite fabrication and manufacturing. This would eliminate the dependency of the processing technology or composite fabrication on specific species of bamboo.

2- During this research, a constant supply of raw bamboos was necessary. Access to one of the most common bamboo species in the world in the vicinity of Singapore, where

the research was conducted, would ensure on-time delivery of raw bamboo and smooth continuation of the research.

Therefore contacts were made with local bamboo farmers in Indonesia, mainly in Java, Bandung and Bali where bamboo grows in abundance, to arrange for the delivery of *Dendrocalamus asper* bamboo to the AFCL in Singapore. The bamboo used had to meet specific requirements including age, height, wall thickness and moisture condition.

The suitability of *Dendrocalamus asper* bamboo for the production of bamboo composite materials is largely dependent on its mechanical and physical properties. *Dendrocalamus asper* culms are normally 20m to 30m in height and their diameters range from 80mm to 220mm. *Dendrocalamus asper* bamboo has relatively large wall thickness in the range of 10mm to 20mm. However, these numbers could differ depending on the ecological conditions where the bamboo grew. The mechanical and physical properties of the culms are largely dependent on the culm density and moisture content, which change along the culm wall thickness, height and diameter.

Presently, there is no standardized system for harvesting bamboo from either bamboo forests or nurseries. Therefore, a set of guidelines was prepared by the PhD candidate for the farmers prior to the harvesting season. These guidelines help them to obtain decent quality bamboo culms with almost no defects or a minimum number of flaws for the course of this research. The following guidelines were used for harvesting and preparing the raw bamboo culm before shipment to Singapore:

1- Harvesting: It was demanded from the farmers to harvest the necessary bamboo culms at the end of the rainy season and right at the beginning of the dry season. This is because of the low content of starch and sugar in bamboo culms at the end of the rainy season, which reduces the chances of fungi and insect attack. Since bamboo matures within 3 to 4 years and has optimum mechanical properties by that age, only bamboo culms of that age range were used in this research. Each bamboo culm was marked accordingly after cutting and labeled.

2- Post-harvesting: It was demanded from the farmers to steam each culm and pump the water through the bamboo culms for 4 weeks; this was to reduce the amount of starch and sugar content to the lowest possible in order to limit insect attacks during transportation to Singapore. It is common for the industry to use borax (sodium borate), a salt-based chemical substance to treat the cut bamboo culms and prevent

insect attacks, but studies have shown the environmental and human health hazards associated with the long-term usage of borax (Bakirdere, Orenay et al. 2010). For the purpose of this thesis, the bamboo culms were not pre-treated with any chemical substances (such as borax) before shipment to Singapore, to prevent any unknown chemical reactions with the epoxy-resin matrix during the production of the bamboo composite reinforcement.

3- Post curing: To prevent any cracks while the bamboo was being dried after harvesting, it was demanded from the farmers to season the bamboo within 3 to 4 weeks of gentle drying under the shades; this was to prevent abrupt moisture content changes which could result in repeated swelling and shrinking of the bamboo culm. The seasoned bamboo culms should have a uniform yellowish color and be free of any cracks.

4- Transportation: Culms were cut into sections of 2m length for easy handling and transportation to AFCL in Singapore. To prevent any moisture ingress and water absorption due to rain, all cut culms were packaged in proper waterproof packaging materials. This process is essential in protecting the bamboo culms from any degradation during shipment which could result in loss of mechanical properties.

5- Storage: Once the culms arrived in AFCL in Singapore, they were first checked for cracks, diseases, insect infestation and small holes (a sign of insect infestation). Bamboo culms with any of these signs were discarded. The cut culms were then stored at a room temperature of 27℃ and a controlled humidity of 65% for the duration of testing and processing. Fig. 46 shows the cut bamboo culms stored at AFCL in Singapore.

4.3. Evaluating the physical and mechanical properties of *Dendrocalamus asper*

The suitability of any raw bamboo for production of bamboo composite materials is largely dependent on its mechanical and physical properties. It is essential to fully investigate all the necessary properties of raw bamboo before processing the bamboo into fibers and subsequent composite fabrication. Since the physical and mechanical properties of raw bamboo have a major influence on the properties of the final bamboo composite material, a series of experiments was designed to evaluate these properties and correlate them using a mathematical model for future reference. A total of 4,500 samples of bamboo *Dendrocalamus asper* from Indonesia were prepared for the physical and mechanical evaluation in this section.

It should be emphasized here that, for the composite fabrication, not every single section of bamboo *Dendrocalamus asper* at AFCL could be evaluated due to time and cost constraints; as such, the suggested novel statistical models presented in this chapter could help in selecting the right section of the culm for the processing and production of the bamboo composite samples without the need for destructive testing. This model also saved time and cost during the course of this PhD research by reducing the number of mechanical tests

required for raw bamboo before processing into fibers or strands, as a means of quality control using only physical measurements of the culms.

Dendrocalamus asper culms used in this study ranged from 20m to 30m in height and with diameters in the range from 80mm to 150mm. The wall thicknesses of bamboo used in this study ranged from 6mm to 20mm. The mechanical and physical properties of raw bamboo culms are largely dependent on the density of the culm and, to some extent, on the moisture content, which normally could vary across the wall thickness, diameter and height of the culms. In this section, investigations of Moisture Content (MC), Specific Density (SD), Compressive Strength (CS) along the fiber direction, Tensile Strength (TS) along the fiber direction, modulus of Elasticity in tension (E_t), flexural strength or Modulus of Rupture (MOR) and modulus of Elasticity in flexure (E_f) were carried out. These properties were subsequently correlated with the culm geometry of bamboo *Dendrocalamus asper,* mainly its height, wall thickness and diameter.

As mentioned earlier, during the harvesting duration, each bamboo culm was labeled so as to be distinguishable from other culms. Subsequently, the culms were cut into three sections which were labeled as the top, middle and bottom sections. The criteria for the labeling of top, middle or bottom section was based on the length of each subsection cut from the main culm. Each subsection was 5m in length. Fig. 47 shows the top, middle and bottom sections of the culms used in this research. Samples for physical and mechanical tests were prepared from the top, middle and bottom sections of the culms.

To prepare the necessary samples for each physical and mechanical test, the 5m subsections were cut into shorter pieces of 1m in length which were subsequently split along the fiber direction lengthwise. For the thick culms, the wall section was divided into two equivalent subsections and samples were prepared from each subsection. The reason for that division is the constraint of the available testing machines. The average values from the test result of the two sections were then used for evaluation. The samples for this study were classified into seven groups according to the culm diameter and wall thickness of the bamboo culms of the *Dendrocalamus asper* of Indonesia delivered to AFCL in Singapore. Fig. 48 shows the splitting of bamboo culms, and Fig. 49 shows the thick sections of the culms which were divided into two equivalent sections for testing.

Fig. 47 Top, middle and bottom section definitions of a typical bamboo culm used in this research

Fig. 48 Splitting the bamboo culms into sections for testing

Fig. 49 Thick split culm sections were further split into two equivalent pieces for testing

Table 4 summarizes the various diameters and wall thicknesses of the bamboo culms tested in this research. As can be seen in Table 4, not all the categories of culms had similar wall thicknesses. Usually, sections from bottom of the culm had thinner wall thicknesses and the wall thickness tended to decrease from the bottom to the top section of the bamboo culm. The culm diameter also decreased from the bottom to the top part. In fact, this is the case for any bamboo species. The categories shown in Table 4 were only meant as a guide for arranging the different sections of bamboo culms in this research according to the geometrical properties of the culm. This helped to alleviate the need to test every single bamboo sections before processing them into fibers or strands and using them in bamboo composite fabrication. Therefore, when selecting the bamboo section for processing, one only needs to measure the culm geometrical properties and find the relevant category the specific section would fit into according to Table 4.

For classes 6 and 7, the samples with diameters of more than 130mm, larger wall thicknesses were observed up to 20mm. Since in classes 1 to 5, the wall thickness of the culms could only reach the maximum of 12mm, to evaluate the effect of thicker wall sections on culm properties, samples from classes 6 and 7 with wall thicknesses of up to 20mm were also tested. Another note to Table 4 was the fact that not all classes of bamboo sections had common wall thicknesses. For instance, wall thicknesses of 6 mm to 7 mm were not present

117

in classes 5 to 7, due to culm geometry whereby larger culms normally have thicker wall sections. The range of wall thicknesses and culm diameters investigated in this research validated the literature regarding the size and geometry of bamboo *Dendrocalamus asper*.

Table 4 Labeling of the samples used in this study according to culm diameter and wall thickness

Class	Culm diameter (mm)	Wall thickness (mm)
Class 1	80 to 90	6-7 7-8 8-9
Class 2	90 to 100	6-7 7-8 8-9 9-10 10-11
Class 3	100 to 110	6-7 7-8 8-9 9-10 10-11
Class 4	110 to 120	6-7 7-8 9-10
Class 5	120 to 130	8-9 9-10 10-11 11-12
Class 6	130 to 140	10-11 11-12 12-13 14-15
Class 7	140 to 150	11-12 12-13 16-17 19-20

As mentioned earlier, for thick wall sections of more than 16mm in thickness, the samples were split into half (Fig. 49), and each subsequent section was tested, and the average of the tests results were used for comparison and explanation. In the next section, the main properties evaluated in this research and specific international standards and methods used for the evaluations are discussed in detail.

4.3.1. Moisture Content (MC)

Moisture content (MC) is an important property of raw bamboo, especially in building and construction applications and for bamboo composite fabrication. MC may adversely affect the bonding strength of bamboo fibers in composite bamboo materials, as shown in previous studies (Okubo, Fujii et al. 2004, Chen, Miao et al. 2009). Therefore, MC is a crucial physical property with a major influence on the performance and service life of the bamboo composite materials developed in this research.

In addition to its influence on mechanical properties, such as tensile strength and flexural strength of raw bamboo, MC also affects geometrical properties such as dimensional stability of the both the raw bamboo and final bamboo composite materials. Therefore, it is important to determine the MC of the various sections of raw bamboo, and classify the MC according to the location within the culm length before processing the fibers into composites or laminates. This helped the PhD candidate to carefully select appropriate section of bamboo culms with MC values suitable for fabrication of bamboo composite materials, which would ultimately be used as reinforcement elements in concrete.

The MC was measured for samples taken from the 1m subsections prepared from the bottom, middle and top portions of the culms. From each subsection, ten samples were prepared. The ASTM D4442-07 standard test method for direct moisture content determination of wood and wood-based materials was followed for measuring the MC of raw bamboo samples in this research (ASTM International 2015).

The samples size chosen for the MC measurement according to the standard were (10) mm × (10) mm × (thickness of the section) in size. Once the samples were cut from the culms, they were weighed using a Shimadzu BL320H balance with an accuracy of 0.001g. The samples were then dried using a convection oven that could maintain a temperature of 103^0C for 24 hours. MC can be calculated from Eq. 22:

$$MC, \% = \frac{A-B}{B} \times 100 \quad \text{(Eq. 22)}$$

where A is the original weight in grams and B is the dried weight in grams.

4.3.2. Specific Density (SD)

The specific density (SD) is another important physical property that should be monitored before processing the bamboo culms into bamboo composite materials. SD is the oven-dry

weight of a given volume of raw bamboo divided by the weight of an equal volume of water. SD is correlated with the mechanical properties of raw bamboo culms (see results and discussion).

A standard method of measuring SD was implemented in this study together with a statistical model which was developed from the data obtained. The SD of raw bamboo could be used as a potential indicator for the mechanical properties of raw bamboo culms, and subsequently for bamboo-based products in the form of bamboo composite materials. Therefore, it is essential to measure SD values in relation to the mechanical properties of raw bamboo.

SD values will differ from the outer to inner section of the wall cross section as the fiber density changes over the wall thickness of the bamboo culms. Therefore, for any application of raw bamboo, it is important to know which part of the wall cross section is processed and what the corresponding SD values of that part are. Measuring SD values and correlating them with wall thickness, culm diameter and mechanical properties provide an affordable and valuable method for selecting the appropriate bamboo segments for the production of bamboo composite materials with the required properties for application as reinforcement in concrete.

The samples for SD measurement were prepared according to the ASTM D2395-14 standard test method for density and specific gravity of wood and wood-based materials (ASTM International 2014). The samples were prepared from 1m subsections of the bottom, middle and top portions of the bamboo culms. From each subsection, ten samples were prepared randomly. For each sample, the width, the length and the thickness were determined for the volume (*V*) calculation. The initial mass (*m*) of each sample was measured with the use of a Shimadzu BL320H balance with an accuracy of 0.001g. The samples for the determination of SD were dried in a convection oven at 103^0C for 24 hours to reach equilibrium conditions. ASTM D2395-14 recommends at least a 24-hour duration drying at 103^0C for wood and wood-based materials to reach a practical equilibrium in which the change in mass is not more than 0.2%. The density (ρ) and SD were calculated using the Eq. 23 and Eq. 24 as follow:

$$\rho = \frac{m}{V} \text{ (Eq. 23)}$$

$$SD = K.\rho \text{ (Eq. 24)}$$

where $K = 1{,}000$ mm^3/g and (*m*) is in gram and (*V*) is in mm^3

4.3.3. Tensile strength along the fibers (TS)

The suitability of any bamboo species for the production of bamboo composite materials is largely dependent on their mechanical properties. Among various mechanical properties, the tensile strength is of great importance to this study, because the final bamboo composite material would be used as reinforcement elements in structural concrete applications in which they would need to withstand tensile stresses. Since the tensile capacity of the final bamboo composite reinforcement is largely dependent on the tensile strength of the bamboo fibers, investigation of the tensile properties of bamboo *Dendrocalamus asper* was an essential part of this research for evaluating the mechanical potential of raw bamboo culms before processing them into fibers for composite fabrication.

The tensile strength of the samples was measured with reference to the ASTM D143-14 standard test method for small clear specimens of timber (ASTM International 2014). This standard was chosen in view of the lack of reputable international standards for measuring properties of bamboo materials. Samples were cut from the 1m sections of bamboo culms and chosen from different radial locations along the sections and then formed into dog-bone shapes. Fig. 50 shows tensile test samples prepared from the raw bamboo sections.

Fig. 50 Tensile test samples from raw bamboo sections

The average width and length of the sample grips were 25mm and 50mm respectively. The average gauge length was 130mm. However, the gauge length was adjusted according to the internode distance of each culm. The samples prepared from the thick culms were first split into sections with the similar thicknesses along the length of the culms. Consequently, each section was prepared according to ASTM D143-14 into dog-bone shapes and tested using a Shimadzu AG-IC 100kN machine at AFCL Singapore, as shown in Fig. 51. The average

values from the tensile tests of the two sections were then used for analysis and evaluation. Five samples were taken from the internodes of 1m subsections. The loading rate was set to 1 mm/min. All tests were performed at room temperature with 65% relative humidity.

Fig. 51 Bamboo tensile samples under UTM machine for testing

The tensile strength (σ_t) was calculated by measuring the ultimate load at failure of the test (F_{ult}) and then dividing it by the cross section of the sample across the gauge length (A). The following formula was used to determine the tensile strength.

$$\sigma_t = \frac{F_{ult}}{A} \text{ (Eq. 25)}$$

4.3.4. Modulus of elasticity in tension (E_t)

The tensile strength measurement gives information about the capacity of raw bamboo culms in sustaining tensile loading and the ultimate load-bearing capacity of fibers before processing them into composite. However, to understand the deformation behavior of bamboo fibers under certain load condition, the modulus of elasticity in tension (E_t) should be measured. This is of high importance when the fibers are processed into composite form and

used as reinforcement in concrete. The high modulus of elasticity of steel reinforcement makes steel reinforcement a suitable material for applications in reinforced concrete beams to reduce deformation and large deflections. Furthermore, steel reinforcement exhibits a ductile behavior compared to the brittle behavior of bamboo fibers. In designing structural concrete beams, it is necessary to have an adequate warning period before the final failure occurs. Concrete without reinforcement is considered a brittle material which cannot provide sufficient warning before collapse, but the ductile properties of steel reinforcement could contribute to the design. However, bamboo as a natural material is known as a brittle material and showed lesser E_t compared to steel, which could potentially influence the load-deflection behavior of concrete beams reinforced with the new bamboo composite reinforcement.

Therefore, measuring E_t of raw bamboo fibers is as important part of this study; it could possibly help the PhD candidate to better understand the stiffness of raw bamboo fibers and their deformation behavior under tension loading before fabricating the composite reinforcement. The modulus of elasticity in tension (E_t) was measured with a Shimadzu AG-IC 100kN machine according to the ASTM D143-14 standard test method for small clear specimens of timber (ASTM International 2014). Dog-bone shape samples were prepared for this test. An Epsilon axial extensometer with a gauge length of 20mm was used to measure the sample deformation along the fibers direction during the test, as shown in Fig. 52.

Fig. 52 Modulus of elasticity measurement with extensometer attached to the gauge length of dog-bone samples

The gauge length was adjusted for modulus of elasticity test to 20mm and the grip width and length remained similar to those for tensile tests. The loading rate was set to 1mm/min. Load-deformation curves were obtained from each test to measure the modulus of elasticity in tension. The modulus of elasticity had been calculated by measuring the slope of the initial linear portion of the stress-strain curves obtained from the tests results according to ASTM D143-14.

4.3.5. Modulus of Rupture (MOR) or Flexural strength

Modulus of Rupture (MOR), or simply the flexural strength of raw bamboo sections, is another important mechanical property that must be addressed and measured prior to composite production as part of this research. Modulus of rupture in flexure is simply the maximum stress at failure of bamboo fibers under the flexural test set-up shown in Fig. 53. In this study, flexural concrete members reinforced with bamboo composite reinforcement were the main subject of evaluation and testing; understanding the flexural behavior of raw

bamboo fibers in bending would be beneficial for the fabrication of bamboo composite reinforcement and subsequently for the design of structural concrete beams in this study.
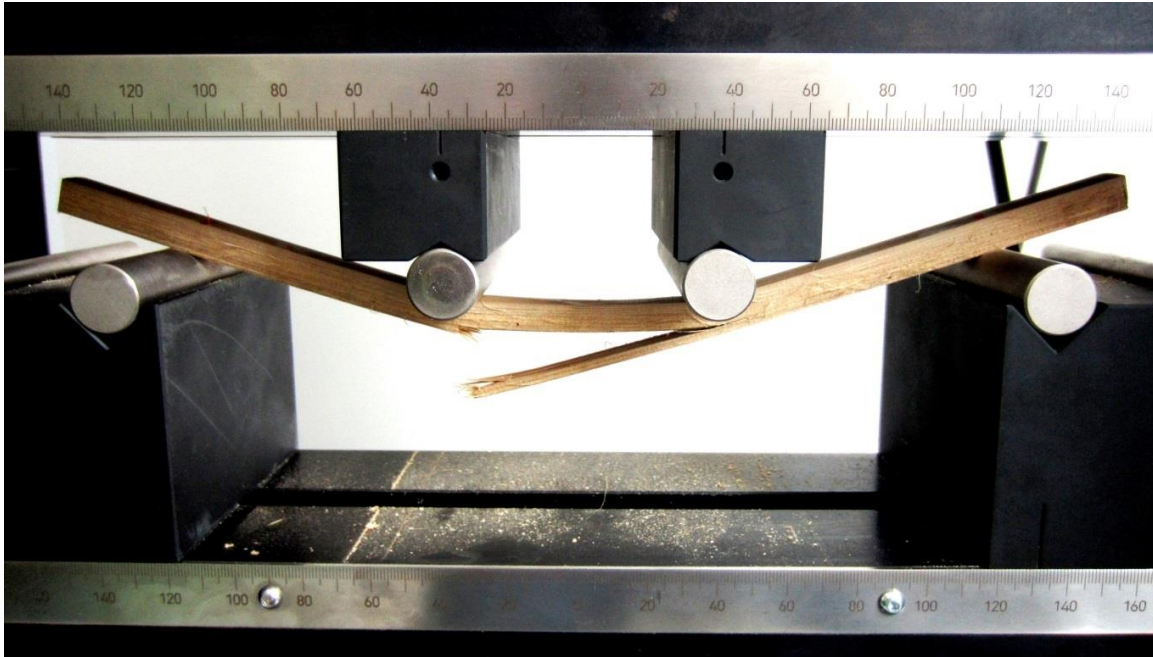
Fig. 53 Raw bamboo failure under MOR testing

MOR or flexural strength was measured according to the ASTM D3043-00 (2011) standard test method for structural panels in flexure (ASTM International 2011). This standard was chosen as there was no available international standard for testing the flexural property of raw bamboo sections which could be acknowledged worldwide at the time of this research.

A four-point loading flexural test was carried out in this study as shown in Fig. 53. The advantage of a four-point loading flexural test over a center-point flexural test is the fact that during the four-point loading test, a larger area of the sample is subjected to peak stress, unlike the center-point flexure test, where the ultimate stress is applied to an isolated location. Therefore, the possibility that any crack or flaw exists between the two loading supports will be higher, which results in a more reliable test.

Five samples without nodes and five samples with nodes were prepared from 1m subsections of each culm. Each MOR sample had a length which varied according to the thickness of the bamboo section, following the ASTM standard. In general, for each bamboo section, the length of the sample prepared for flexural tests varied from 24 to 48 times the thicknesses of the section. The Shimadzu AG-IC 100kN machine was used for this test. All tests were carried out at room temperature with 65% relative humidity. The loading rate was calculated

according to ASTM D3043 with respect to sample thickness and width. Fig. 54 shows the schematic test set-up.
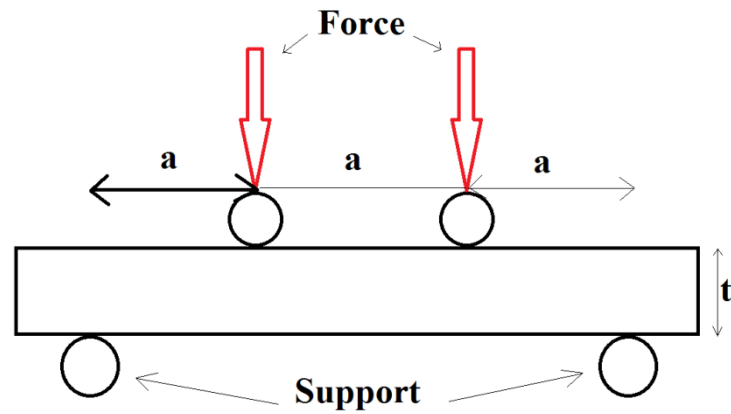
Fig. 54 Four-point loading test of MOR

The following formula was used to determine MOR of each sample.

$$MOR = \frac{3Fa}{bt^2} \quad \text{(Eq. 26)}$$

Where F is the total force applied to the sample with the help of two loading rollers measured in Newton (Fig. 53), a is the distance between the loading point and support in mm (Fig. 54), b is the width of the sample and t is the corresponding thickness, both measured in mm.

4.3.6. Modulus of elasticity in flexure (E_f)

Modulus of elasticity in flexure (E_f) is simply the resistance of the material to deformation during bending. Bamboo is a natural material and, unlike metals which are homogenous and isotropic in composition, bamboo's properties vary across cross sections. Therefore modulus of elasticity in tension (E_t) and flexure (E_f) have different values. The modulus of elasticity in flexure (E_f) would be a useful parameter when considering properties of raw bamboo across culm wall thickness, given the heterogeneous nature of bamboo with varying properties from outer to inner sections of the wall cross-section as explained earlier in the literature.

The modulus of elasticity in flexure was measured by obtaining the load-deflection and stress-strain curves during the flexural strength test. E_f is the ratio of the stress to strain or simply the slope of the stress-strain curves. An Epsilon extensometer with a maximum gauge length of 25mm was used to measure the mid-span deflection of the samples during the flexural strength test. The measurement and calculation of the modulus of elasticity were carried out according to ASTM D3043-00 (2011) (ASTM International 2011) at room temperature with 65% relative humidity. Various sections of bamboo culms with different wall thicknesses and culm diameters were tested in this research to find any significant correlation between E_f and other mechanical properties of *Dendrocalamus asper* bamboo.

4.3.7. Compressive strength

Compressive strength is the ability of the material to resist compression forces in the opposite direction of tension. The compressive strength of raw bamboo sections can be measured by either testing the whole section of the culm or by preparing small specimens from the culm cross-section. In this study, the compressive strength of the whole culms cut from the bottom, middle and top section of the bamboo was investigated. Fig. 55 shows a section of culm under a Shimadzu AG-IC 100kN Universal Testing Machine (UTM) for compression test. Unfortunately, the only available standard for such tests is not available within ASTM, but from The International Organization for Standardization (ISO) which is not widely accepted by all countries. But for the purpose of this research and due to the lack of reputable international standards for compression tests of raw bamboo, ISO22157-2004 was adopted (The International Organization for Standardization (ISO) 2004). A loading rate of 0.5mm/s was used for all the tests. Only samples of culm without nodes were tested in this study as the presence of the nodes would complicate the evaluation of the test results (Liese 1985).
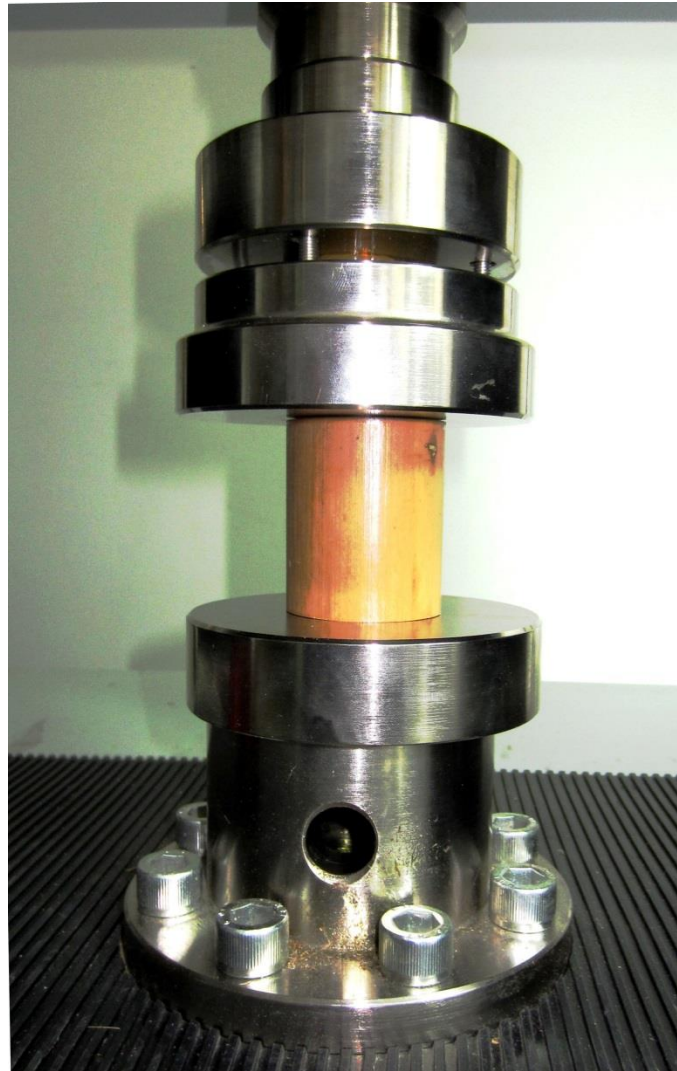
The ultimate compressive strength (σ_c) can be calculated by measuring the ultimate load at failure of the test (F_{ult}) and then dividing it by the cross-section of the culm (A_c). The following formula has been used to determine the compressive strength.

$$\sigma_c = \frac{F_{ult}}{A_c} \quad \text{(Eq. 27)}$$

Where A_c can be calculated by the following formula:

$$A_c = \frac{\pi}{4}\lfloor D^2 - (D - 2t)^2 \rfloor \quad \text{(Eq. 28)}$$

Where D and t are the outer diameter and the wall thickness of the bamboo culm respectively, used for compressive strength.

4.3.8. Statistical analysis

Statistical analysis was carried out on the data after performing the relevant test. SPSS version 22 statistical software was employed in this research for the analysis of the results obtained (SPSS Inc., Chicago, IL). To establish if there was a relationship between the culm diameter, wall thickness, SD, MC and the mechanical properties of bamboo, Pearson's correlation coefficients (r) were calculated. Pearson's correlation coefficient (r) is a statistical means to measure the strength of any relationship between two sets of data and ranges between -1 and 1. Therefore a correlation could be a positive or negative one depending on the value of (r). The correlation is stronger when the value of (r) is closer to 1 in case of positive correlation, and -1 in case of a negative correlation. Different levels of correlation were defined in this research for the data analysis section (i.e., strong, $r > 0.5$; moderately strong, $0.3 < r < 0.5$; and weak, $r < 0.3$). The basic assumption for Pearson's correlation coefficient (r) is that the variables are normally distributed. The normality test of the data was carried out with SPSS software prior to establishing the Pearson's correlation coefficients between the variables.

To further examine the relationships between the physical and mechanical properties of bamboo, stepwise multiple linear regressions were also performed on the data sets. Beside the correlation analysis (r factor), which helps to measure the strength of the relationship between the physical and mechanical properties, multiple linear regression analysis assumes that there is a dependency or relationship between one or more of the independent properties of bamboo and one dependent property.

The models from multiple linear regressions can be used to forecast the mechanical properties (dependent variables) with the change in physical properties (independent variables) without the need for destructive tests in the lab or at bamboo forests when collecting bamboo culms. This could be a useful method for estimating the mechanical properties of bamboo culms without the need to test the sections, and which can be employed when working with bamboo farmers without the required testing facilities. The models performance was evaluated with an adjusted r^2 value, which represented the percentage of the variation that each model's independent variables could describe. The r^2 in general is a statistical parameter to demonstrate that the results of the study are close to the model obtained through multiple regression analysis. The values of r^2 are normally between 0 and 1; however, if the values of r^2 are closer to 1, it indicates that the model obtained can represent more of the data points.

4.4. Results and discussion

4.4.1. Moisture content (MC)

The Moisture Content (MC) was measured at two relative humidity conditions: one at 20$^\text{o}$C and 65% relative humidity (RH) and one at 45$^\text{o}$C with 80% relative humidity (RH). The two conditions were set according to ASTM D4442-07. The results for the samples from various categories of bamboo *Dendrocalamus asper* are shown in Table 5.

Table 5 Moisture content measurement results at two relative humidity conditions

Class	Wall thickness (mm)	MC(%) at 20$^\text{o}$C with 65% RH	Average MC(%) 20^{0}C with 65% RH	MC(%) at 45$^\text{o}$C with 80% RH	Average MC(%) at 45$^\text{o}$C with 80% RH
Class 1	6 to 7	9.8		13.2	
	7 to 8	9.0	9.2	11.7	12.2
	8 to 9	8.7		11.5	
Class 2	6 to 7	10.7		13.6	
	7 to 8	10.6		13.7	
	8 to 9	10.7	10.3	13.4	13.3
	9 to 10	8.4		11.5	
	10 to 11	10.9		14.2	
Class 3	6 to 7	10.0		13.5	
	7 to 8	10.7		14.2	
	8 to 9	10.7	10.4	14.1	13.8
	9 to 10	11.2		15.0	
	10 to 11	9.2		12.2	
Class 4	6 to 7	9.8		12.9	
	7 to 8	9.6	9.9	13.0	13.2
	9 to 10	10.4		13.7	
Class 5	8 to 9	9.5		12.7	
	9 to 10	9.8	9.9	12.7	13.3
	10 to 11	9.7		13.0	
	11 to 12	10.8		14.6	
Class 6	10 to 11	9.4		12.8	
	11 to 12	10.3	9.9	14.0	13.4
	12 to 13	10.0		13.6	
	14 to 15	9.9		13.3	
Class 7	11 to 12	9.6		13.1	
	12 to 13	10.1	10.1	13.6	13.5
	16 to 17	10.1		13.8	
	19 to 20	10.5		13.8	

The culm diameter did not display any significant influence on the necessary time for achieving a certain equilibrium MC. Unlike culm diameter, wall thickness appeared to have an obvious effect on reaching a certain MC by a specific time under certain RH conditions. At a relative humidity of 80%, the MC increased for all classes of bamboo *Dendrocalamus asper* compared to those at a relative humidity of 20%. The 80% RH condition was achieved after 6 days in a moisture conditioning oven for wall thicknesses greater than 13mm while it only took 3 days for wall thickness less than 13mm to achieve the same RH condition. The increase in MC of various wall thicknesses tested in this study was in the range of 25% to 35%. However, the change in MC for classes 4 to 7 with varying wall thicknesses was not significant at 80% RH condition.

The average MC under both relative humidity conditions was also shown in Table 5. The average MC for classes 4 to 7 did not show any considerable change with culm diameter, but for classes 1 to 3, it increased with an increase in the culm diameter. This behavior could be explained by the fact that culms with 100mm or less in diameter in general had wall sections that were thinner compared to larger culms. Therefore they had less amount of lignin matrix and higher percentage of cellulose fibers compared to culms larger than 100mm in diameter, as shown in the literature (Alvin and Murphy 1988, Murphy and Alvin 1992, Latif 1993).

The lignin matrix is responsible for creating hydrogen links with water molecules, therefore culms with higher lignin content are more stable when exposed to various relative humidity conditions compared to smaller culms with thinner wall sections and less lignin content. Usually, thinner wall sections in smaller culms have a higher fiber density and lower percentage of lignin matrix compared to larger culms with thicker wall cross sections (Zou, Jin et al. 2009). As a result, the relative humidity conditions have more impact on MC of smaller culms with thinner wall cross sections.

For processing the raw bamboo culms into sections suitable for composite fabrication in this study, it is essential to carefully analyze the change in MC with various culm diameters and wall thicknesses. The average MC of the raw bamboo culms selected for processing should fall in a range which helps to reduce the effect of excessive delamination or long-term environmental impact through the degradation of the final composite product. High MC of raw bamboo fibers used in the fabrication of bamboo composite reinforcement could result in weak chemical bonds between bamboo fibers and the glue matrix, which in the long term could negatively affect the mechanical and physical properties of the composite

reinforcement. By measuring the moisture content of chosen bamboo culms for composite production, a preliminary estimation of the required time to achieve a certain MC percentage suitable for processing of the raw bamboo and fabrication of composite becomes possible.

4.4.2. Specific density (SD)

The oven-dry Specific Density (SD) of bamboo *Dendrocalamus asper* was measured according to ASTM D2395-14. The results of SD measurement are presented in Table 6 for various classes of bamboo culms.

Table 6 Oven-dry SD of various classes of bamboo *Dendrocalamus asper*

Class	Wall thickness (mm)	Specific Density	Average Specific Density
Class 1	6 to 7	0.878	0.872
	7 to 8	0.842	
	8 to 9	0.896	
Class 2	6 to 7	0.837	0.826
	7 to 8	0.782	
	8 to 9	0.794	
	9 to 10	0.882	
	10 to 11	0.837	
Class 3	6 to 7	0.889	0.864
	7 to 8	0.848	
	8 to 9	0.858	
	9 to 10	0.869	
	10 to 11	0.856	
Class 4	6 to 7	0.940	0.907
	7 to 8	0.860	
	9 to 10	0.920	
Class 5	8 to 9	0.789	0.764
	9 to 10	0.772	
	10 to 11	0.754	
	11 to 12	0.741	
Class 6	10 to 11	0.749	0.733
	11 to 12	0.738	
	12 to 13	0.724	
	14 to 15	0.720	
Class 7	11 to 12	0.735	0.721
	12 to 13	0.720	
	16 to 17	0.717	
	19 to 20	0.711	

The one-way ANOVA (Analysis of variance) test showed that there was no significant difference between SD values of various wall thicknesses within class 1 to class 3. However SD for classes 4 to 7 decreased when increasing the culm diameter. The only common wall thickness group between classes 5 to 7 was 11mm to 12mm. The SD for wall thicknesses between 11mm to 12mm for classes 5, 6 and 7 was 0.741, 0.738 and 0.735 respectively. The results proved that by increasing the culm diameter for culms with diameters of 120mm to 150mm, the SD decreased for similar wall thickness categories. Bamboo samples from classes 5 to 7 showed a drop in SD when the wall thickness increased. Bamboo sections from class 7 had the largest wall thicknesses among the various classes, and showed the lowest SD among all the wall thickness categories.

Class 7 showed the lowest average SD of 0.721, while class 4 had the highest average SD of 0.907. The reduction in SD of larger culms can be explained by the fiber density characteristics of bamboo. Culms with larger diameters and thicker wall cross-sections were normally found at the bottom of the culm where the fiber density was lower.

Generally, bamboo culms have higher fiber density at the top parts where the fibers are closely packed, as proved by other studies on the microstructure of bamboo culms of different species (Alvin and Murphy 1988, Ray, Das et al. 2004). As a result, the SD will be lower in the bottom parts where the culm diameter and wall thickness are much larger as compared to the middle and top sections.

4.4.3. Tensile strength along the fiber (TS)

The tensile strength of the bamboo *Dendrocalamus asper* from Indonesia along the fiber direction was measured according to ASTM D143-14 by preparing dog-bone shape samples as explained in methodology. Table 7 summarizes the results of the tensile tests.

The maximum tensile strength within class 1 samples was 295MPa for wall thickness category of 7mm to 8mm. Wall thickness categories of 6mm to 7mm and 8mm to 9mm in class 1 had almost similar tensile strength values. In class 2, the samples with a wall thickness of 7mm to 8mm had the highest tensile strength of 298MPa. Other categories of wall thickness in class 2 showed similar tensile strength while one-way ANOVA test showed that there was no significant difference between various thicknesses in this class of bamboo samples.

In class 3, samples with wall thicknesses of 10mm to 11mm had the highest tensile strength of 301MPa. In class 4 samples, the difference between various wall thicknesses was less significant compared to class 3 samples. The highest tensile strength measured in class 4 was 326MPa, an increase of less than 10% compared to the maximum value of 301MPa for class 3 samples.

Table 7 Tensile strength results of bamboo *Dendrocalamus asper* along the fiber direction

Class	Wall thickness (mm)	Tensile strength (MPa)	Average Tensile strength (MPa)
Class 1	6 to 7	281	287
	7 to 8	295	
	8 to 9	285	
Class 2	6 to 7	260	285
	7 to 8	298	
	8 to 9	292	
	9 to 10	280	
	10 to 11	294	
Class 3	6 to 7	288	290
	7 to 8	290	
	8 to 9	285	
	9 to 10	287	
	10 to 11	301	
Class 4	6 to 7	324	323
	7 to 8	320	
	9 to 10	326	
Class 5	8 to 9	340	307
	9 to 10	318	
	10 to 11	303	
	11 to 12	268	
Class 6	10 to 11	310	276
	11 to 12	282	
	12 to 13	263	
	14 to 15	247	
Class 7	11 to 12	244	216
	12 to 13	224	
	16 to 17	203	
	19 to 20	193	

The highest tensile strength measured within the samples from various classes belonged to class 5 samples with wall thicknesses between 8mm to 9mm. The lowest tensile strength belonged to class 7 samples with 19mm to 20mm wall thickness.

The one-way ANOVA test revealed no significant differences between class 1 to class 3 samples as shown in Table 7. Classes 1 to 3 samples had similar values for average tensile strength. However, the average tensile strength for classes 4 to 7 decreased with an increase in culm diameter.

When culm diameter, specific density and tensile strength were compared, a correlation between the results presented in Table 7 and Table 5 can be found. The results indicated that there was no significant change in SD and tensile strength while increasing the culm diameter for class 1 to class 3 samples. Although for samples in class 4 to class 7, by increasing the culm diameter, both tensile strength and SD were reduced. This suggested that for culms with diameters larger than 110 mm, the tensile strength could be governed by the fiber density of bamboo. Larger culms were expected to have lesser cellulose fibers and higher lignin content. Therefore, the tensile strength of the large diameter bamboo culm, which was mainly influenced by the tensile capacity of the cellulose fibers, was mostly reduced.

This outcome is in accordance with the trend found for the SD of bamboo *Dendrocalamus asper*. As stated previously, SD is largely governed by the fiber density, therefore by decreasing the fiber density, SD will also decrease, as also showed in studies carried out by Ray et al, (Ray, Das et al. 2004).

The correlation between SD, tensile strength and fiber density is important in selecting the bamboo culms for bamboo composite fabrication. The correlation could lead to easy and fast selection of bamboo culms with varied tensile strengths by only needing to measure the respective SD and estimating their tensile capacity. This could lead to a valuable method in choosing suitable culms for bamboo composite materials fabrication and processing. Further statistical analysis were carried out in the following sections for the correlation values.

4.4.4. Modulus of elasticity in tension (E_t)

The modulus of elasticity in tension for bamboo *Dendrocalamus asper* was measured for 7 classes with various culm diameters and wall thicknesses according to ASTM D143-14. Table 8 summarizes the results of the modulus of elasticity measurement. The modulus of

elasticity of any bamboo section is a measure of the stiffness of the bamboo matrix and its resistance to elastic deformation.

The highest modulus of elasticity in tension of 28,230MPa belonged to class 4 samples with 9mm to 10mm wall thickness. The lowest modulus of elasticity in tension of 18,140MPa belonged to class 7 samples with wall thicknesses of 19mm to 20mm.

Table 8 Modulus of elasticity in tension results of bamboo *Dendrocalamus asper*

Class	Wall thickness (mm)	Modulus of elasticity (MPa)	Average Modulus of elasticity (E_t) (MPa)
Class 1	6 to 7	21570	
	7 to 8	22780	21863
	8 to 9	21240	
Class 2	6 to 7	19360	
	7 to 8	20180	
	8 to 9	20340	20422
	9 to 10	21670	
	10 to 11	20560	
Class 3	6 to 7	23970	
	7 to 8	23380	
	8 to 9	22370	22750
	9 to 10	22280	
	10 to 11	21750	
Class 4	6 to 7	24460	
	7 to 8	25660	26117
	9 to 10	28230	
Class 5	8 to 9	23890	
	9 to 10	22820	22130
	10 to 11	21510	
	11 to 12	20300	
Class 6	10 to 11	22150	
	11 to 12	21540	21270
	12 to 13	21920	
	14 to 15	19470	
Class 7	11 to 12	20710	
	12 to 13	20330	19658
	16 to 17	19450	
	19 to 20	18140	

The one-way ANOVA test showed no significant difference between modulus of elasticity of various wall thicknesses within class 1 samples. The relative standard deviation was less than 4.0% for class 1 samples with wall thicknesses between 6mm to 9mm. A similar trend was observed for classes 2 and 3 samples with wall thicknesses ranging from 6mm to 11mm.

The relative standard deviations for classes 2 and 3 samples were 4.0% and 3.9% respectively. Unlike classes 1, 2 and 3, the modulus of elasticity of the samples in class 4 increased with increasing the wall thickness. By increasing the wall thickness from 6mm to 11mm, the modulus of elasticity increased from 24,460MPa to 28,230MPa, an increase of 15.4%.

Furthermore, among the 7 classes of bamboo Petung, class 4 displayed the highest average modulus of elasticity of 26,117MPa. Samples from classes 5 to 7 displayed a reduction in values of the modulus of elasticity with increasing wall thickness. The reduction in modulus of elasticity values for class 5 samples was 15% when the wall thickness increased from 8mm to 12mm. Class 6 samples showed a reduction of 12% when the wall thickness increased from 10mm to 15mm. A similar reduction factor was observed for class 7 samples when the wall thickness increased from 11mm to 20mm.

These results were well in accordance with the results obtained from the tensile strength tests of the samples from classes 5 to 7, in which an increasing wall thickness lowered the tensile strength. By comparing Table 6 to Table 4, one could observe that in classes 5, 6 and 7, the values of both tensile strength and modulus of elasticity in tension decreased with an increase in wall thickness.

As described in the literature and introductory sections, the high tensile capacity of any bamboo species depends largely on the tensile capacity of its cellulose fibers. This is true for the modulus of elasticity in tension of the bamboo. The modulus of elasticity in tension is simply the sum of the modulus of the cellulose fibers and the modulus of the lignin matrix weighted by their volumetric fractions. Bamboo culms with diameters of less than 110mm have nearly similar volumetric ratios of cellulose fibers and lignin, therefore they display similar modulus of elasticity when various wall thicknesses are tested.

Culms with larger diameter display larger wall thickness compared to smaller diameter culms where thinner wall sections are observed. With increasing wall thickness in larger culms, the volumetric ratio of cellulose fibers to lignin is also reduced, as shown in other studies on the

microstructure of bamboo (Alvin and Murphy 1988, Murphy and Alvin 1992). As a result, a higher percentage of lignin as compared with the cellulose fibers is expected in thicker wall sections. This leads to lower modulus of elasticity of larger bamboo culms compared to smaller culms in which the volumetric ratio of cellulose fibers to lignin is higher.

4.4.5. Modulus of rupture (MOR)

The Modulus of Rupture (MOR) was measured by applying the load against the inner section of bamboo and placing the skin section at the bottom layer during the four-point bending test according to ASTM D3043-00(2011). Table 9 summarizes the results of the MOR tests.

Table 9 MOR results of bamboo *Dendrocalamus asper*

Class	Wall thickness (mm)	MOR (MPa)	Average MOR (MPa)
Class 1	6 to 7	209	205
	7 to 8	207	
	8 to 9	198	
Class 2	6 to 7	172	173
	7 to 8	180	
	8 to 9	162	
	9 to 10	190	
	10 to 11	161	
Class 3	6 to 7	172	165
	7 to 8	168	
	8 to 9	158	
	9 to 10	160	
	10 to 11	168	
Class 4	6 to 7	166	160
	7 to 8	159	
	9 to 10	155	
Class 5	8 to 9	159	153
	9 to 10	153	
	10 to 11	149	
	11 to 12	150	
Class 6	10 to 11	165	160
	11 to 12	162	
	12 to 13	160	
	14 to 15	151	
Class 7	11 to 12	138	128
	12 to 13	127	
	16 to 17	125	
	19 to 20	121	

Class 1 samples had the highest range of MOR values while class 7 samples showed the lowest average MOR values. Within samples of class 1, by increasing the wall thickness from 6mm to 9mm, MOR decreased from 209MPa to 198MPa. For classes 2 and 3 samples, no significant relationship was found between the wall thickness and the MOR values. Class 4 samples displayed a similar trend as classes 1 and 2 samples, whereby an increase in the wall thickness from 6mm to 10mm resulted in a reduction in the MOR values from 166MPa to 155MPa, which corresponded to a reduction of 6.7%.

For class 5, the MOR for wall thickness of 10mm to 11mm was the lowest with 149MPa. The MOR in class 5 decreased from 159MPa to 149MPa. The MOR values in class 5 displayed a standard deviation of less than 5%. Similar to class 5 samples, class 6 samples displayed a decreasing trend for MOR with an increase in wall thickness of bamboo *Dendrocalamus asper*. The standard deviation of samples in class 6 was less than 4%. The MOR for class 7 samples was also reduced with an increase in wall thickness from 138MPa to 121MPa. The highest MOR belonged to class 1 samples with 6mm to 7mm wall thickness, while the lowest measured MOR belonged to class 7 samples with 19mm to 20mm wall thickness.

Culms with larger diameters had thicker walls, particularly at the bottom sections. The thicker wall thickness led to a higher percentage of lignin and a lower proportion of cellulose fibers. As observed earlier regarding the tensile capacity and its relationship with the fiber density, similar conclusions can be made concerning MOR.

The cellulose fibers were densely packed at the top sections of the bamboo culms where a smaller diameter prevailed. The MOR increased with decreasing culm diameter. Except for class 2 samples, the MOR decreased with increasing wall thickness within a class.

This result underlines the importance of the fiber density on the mechanical properties of raw bamboo. Cellulose fibers contribute to the high mechanical capacities of bamboo. The cellulose fiber density is higher at the outer layer of the wall sections and at the top portions of the culms. Therefore, the MOR increases with increasing fiber content and decreasing lignin content at the surroundings of the fibers.

4.4.6. Modulus of elasticity in flexure (E_f)

The modulus of elasticity in flexure was measured according to ASTM D3043-00(2011), through a four-point bending test with the use of an extensometer in the mid-span of the

samples to capture the load deflection curve. The effect of various wall thicknesses and culm diameters on the modulus of elasticity in flexure of bamboo *Dendrocalamus asper* was studied for the 7 classes and the results are shown in Table 10. The highest modulus of elasticity of 14,279MPa was observed for class 2 samples with a wall thickness in the range of 9mm to 10mm. The lowest modulus of elasticity of 9,375MPa was observed in samples of class 7 with wall thicknesses between 19mm to 20mm. This finding was comparable with the results of MOR tests where class 7 samples showed the lowest MOR of all samples.

Table 10 Modulus of elasticity in flexure (E$_f$) results for bamboo *Dendrocalamus asper*

Class	Wall thickness (mm)	Modulus of Elasticity (Ef) (MPa)	Average Modulus of Elasticity (E$_f$) (MPa)
Class 1	6 to 7	11,517	
	7 to 8	12,892	12,500
	8 to 9	13,091	
Class 2	6 to 7	12,247	
	7 to 8	12,463	
	8 to 9	12,756	12,851
	9 to 10	14,279	
	10 to 11	12,509	
Class 3	6 to 7	11,951	
	7 to 8	12,588	
	8 to 9	13,267	12,492
	9 to 10	12,776	
	10 to 11	11,878	
Class 4	6 to 7	12,217	
	7 to 8	12,903	12,636
	9 to 10	12,787	
Class 5	8 to 9	11,695	
	9 to 10	11,574	
	10 to 11	12,752	12,236
	11 to 12	12,922	
Class 6	10 to 11	12,517	
	11 to 12	11,520	
	12 to 13	11,842	11,718
	14 to 15	10,993	
Class 7	11 to 12	10,427	
	12 to 13	10,255	
	16 to 17	10,103	10,040
	19 to 20	9375	

When the results of various wall thicknesses were compared, a decrease in modulus of elasticity in flexure of samples was found when wall thickness was increased for class 4 to class 7 samples. However, for all other classes of bamboo *Dendrocalamus asper*, random variations in modulus of elasticity with increasing the wall thickness were observed.

As shown in Table 10, bamboo Petung showed a decrease in modulus of elasticity with increasing culm diameter from 80mm to 150mm. Samples with culm diameters of less than 110mm showed less significant changes in the modulus of elasticity with the change in culm diameters. Nevertheless, for samples with culm diameters of 110mm and larger, the modulus of elasticity significantly dropped with increasing the culm diameter as shown in Table 10.

The effect of culm diameter on modulus of elasticity in flexure was similar to MOR where an increase in culm diameter resulted in a reduction of the modulus of elasticity in flexure. This observation can be explained by the culm microstructure. The bottom and middle sections of bamboo culm normally have larger diameters and therefore higher lignin content is expected compared to cellulose fiber content. As a result, the fiber density decreases for larger diameter culms. As explained earlier regarding the fiber density variation along the height of the culm, the top sections of a culm exhibit higher fiber densities compared to the bottom sections. The higher fiber density is therefore responsible for the high mechanical properties of the bamboo culm, including the modulus of elasticity in flexure.

For some classes of bamboo *Dendrocalamus asper*, the change in modulus of elasticity in flexure with varying wall thicknesses was not linear. This could be explained by spatially varying microstructure of the bamboo culm wall cross sections. Samples tested in this study for measurement of modulus of elasticity in flexure were collected randomly at different cross sections and varying height locations. Therefore, the variations in modulus of elasticity with wall thickness were expected from culm to culm.

Furthermore, the modulus of elasticity of bamboo *Dendrocalamus asper* measured from tensile strength test contrasted with the modulus of elasticity measured from the flexural strength test. The highest modulus of elasticity measured in tensile test was 28,230MPa while the highest modulus of elasticity in flexure was 14,279MPa – which was only 50.5% of the modulus of elasticity in tension. This difference could be explained by, firstly, the localized deformation under the bottom roller supports and top roller load introduction points during the four-point flexural test and, secondly, by the heterogeneous properties of bamboo samples across the wall cross section.

In the tensile test, samples are under uniaxial stress-strain conditions, while in a flexural test, a combination of compression, tension and shear forces act on the samples cross section which results in multidirectional stress-strain situations in the mid-span. Therefore the mid-span section of the sample does not carry only pure tensile or pure bending stress, but rather a combination of compressive, tensile and shear stresses. This combination results in deformations not only along the load introduction points, but also along the direction of induced shear and compressive stresses along the cross section. Therefore the analysis of modulus of elasticity in flexure becomes rather complicated for a natural material like bamboo, as it has different properties across thickness and along the height. However, for homogenous materials like most of metals, there is not a significant difference between the two modulus of elasticity.

Furthermore, in this study, the flexural strength samples were tested against both the inner layer of bamboo and with the skin layer at the bottom and against the skin layer with the inner layer at the bottom of the samples during the test. The results displayed in Table 10 are the average of the two tests. The inner section of bamboo is known to have lower fiber density and therefore possesses a higher flexibility as compared to the skin section. In the skin layer, the cellulose fibers are densely distributed and, as a result, a lower ductility is expected. Therefore, the inner layers of bamboo cross sections experience larger deformation compared to the skin layer; early failure usually initiates from the inner side of bamboo which could result in lower modulus of elasticity during the flexural test as compared to tensile modulus of elasticity.

4.4.7. Compressive strength

The compressive strength of bamboo culms along the fiber direction in various classes was measured according to ISO22157-2004. The results are displayed in Table 11. Class 1 samples with 6mm to 7mm wall thickness displayed the highest compressive strength of 68.4MPa, while class 7 samples with 19mm to 20mm wall thickness had the lowest compressive strength of 43.2MPa. This corresponded to a drop of 36% in compressive strength values. All 7 classes of bamboo samples tested in this study showed a reduction in compressive strength by increasing the wall thickness and culm diameter.

The difference in the average compressive strength between class 1 to class 4 samples was not very significant when compared to the average values of compressive strength obtained from samples belonging to class 5 to class 7. The results of the compressive strength tests

were in accordance with the results obtained from MOR tests, in which the increase in culm diameter and wall thickness had a negative effect on the mechanical properties. The majority of the samples tested under compression failed due to buckling of fibers followed by a longitudinal crack along the height of the culm section, except for culms larger than 130 mm in diameter in which the samples were compressed under the test set-up without any longitudinal cracks being observed during the test.

Table 11 Compressive strength results of bamboo *Dendrocalamus asper*

Class	Wall thickness (mm)	Compressive strength (MPa)	Average Compressive strength (MPa)
Class 1	6 to 7	68.4	
	7 to 8	66	66
	8 to 9	62.6	
Class 2	6 to 7	66	
	7 to 8	63.6	
	8 to 9	62.4	62
	9 to 10	61.2	
	10 to 11	58.8	
Class 3	6 to 7	67.2	
	7 to 8	62.4	
	8 to 9	61.4	62
	9 to 10	60	
	10 to 11	57.6	
Class 4	6 to 7	64.8	
	7 to 8	60	60
	9 to 10	56.4	
Class 5	8 to 9	60	
	9 to 10	54	
	10 to 11	52.8	54
	11 to 12	49.2	
Class 6	10 to 11	50.4	
	11 to 12	48	
	12 to 13	46.8	47
	14 to 15	44	
Class 7	11 to 12	46.8	
	12 to 13	44.4	
	16 to 17	43.8	45
	19 to 20	43.2	

The reduction of compressive strength by increasing the culm diameter could be explained by the change in fiber density along the culm height and wall cross section. Larger diameter culm in classes 5 to 7 had thicker wall cross sections which resulted in a higher percentage of lignin and lower percentage of cellulose fibers. As described earlier regarding the MOR results and their relationship with the fiber density, similar conclusions could be made here with regard to compressive strength. Cellulose fibers are responsible for the high mechanical capacities of bamboo. The compressive strength of bamboo culm increases by increasing the cellulose fiber percentage from the bottom to the top of the culm and by decreasing the wall thickness of the culm.

4.4.8. Statistical modeling

To measure the strength of any possible relationship between mechanical properties, culm diameter, wall thickness, specific density and moisture content, Pearson's correlation coefficients (r) are calculated. Table 12 summarizes the correlation coefficients for only statistically significant correlations with a p-value of less than 0.05 by a two-tailed t-test between mechanical and physical properties measured in this study.

Table 12 Pearson correlation between mechanical and physical properties of bamboo *Dendrocalamus asper*

Parameters	Correlations (r) *			
	Culm diameter (mm)	Wall Thickness (mm)	MC	SD
Modulus of elasticity in flexure (MPa)	-0.689	-0.668		0.614
MOR (MPa)	-0.721	-0.615	-0.427	0.430
Modulus of elasticity in tension (MPa)		-0.530		0.620
Compressive Strength (MPa)	-0.904	-0.893		0.832
Tensile strength (MPa)	-0.451	-0.742		0.573

The correlations are judged according to value of (r) in Table 12. When (r) is closer to 1 in case of positive correlation and -1 in case of a negative correlation, the correlation is

considered stronger. As described in chapter 3, different levels of correlation are defined in this study for the data analysis (i.e., strong, $r > 0.5$; moderately strong, $0.3 < r < 0.5$; and weak, $r < 0.3$).

Modulus of elasticity showed strong correlations with culm diameter, wall thickness and specific density. The (r) values indicated that, by increasing the culm diameter or wall thickness, modulus of elasticity in flexure decreased, while an increase in specific density would have a positive effect. This is in accordance with the results obtained from the measurement of modulus of elasticity in flexure and their variation with culm geometry or specific density. However, moisture content did not show any significant correlation with modulus of elasticity in flexure. This result indicated that moisture content could not be an indicator of modulus of elasticity in flexure, unlike culm geometry.

MOR displayed moderate to strong correlations with culm diameter, wall thickness, specific density and moisture content. When either the culm diameter, wall thickness or moisture content increased, the MOR decreased. However, similar to modulus of elasticity in flexure, specific density had a positive correlation with MOR. The higher the specific density, the higher the MOR as a result of greater fiber density.

Modulus of elasticity in tension had moderate and strong correlation with only wall thickness and specific density respectively. Among all the mechanical properties measured in this research, only modulus of elasticity in tension did not show any significant correlation with culm diameter. As the results of the test from Table 8 suggested, only random variations were observed between culm diameter and modulus of elasticity in tension compared to other mechanical properties.

Tensile strength showed moderate correlation with culm diameter and strong correlations with wall thickness and specific density. However no significant correlation was found between tensile strength and moisture content. By increasing the culm diameter and wall thickness, tensile strength decreased while an increase in specific density of bamboo section resulted in higher tensile capacities. However, the variation between moisture content and tensile strength was not statistically significant.

Compressive strength had the highest correlation factors with culm geometry and specific density among all the mechanical properties. However no significant correlation was found between moisture content and compressive strength similar to tensile strength and modulus of

elasticity. The correlation coefficient between culm diameter and compressive strength was the highest (r = -0.904) among all the properties measured in this research.

Mechanical properties had strong correlation with wall thickness and specific density of bamboo culms, which indicated the importance of culm geometry and fiber density in enhancing the quality of bamboo. Specific density itself showed strong correlations with both culm diameter and wall thickness. Table 13 displays the correlation coefficients (r) between specific density, culm diameter, wall thickness and moisture content.

Table 13 Pearson correlation coefficients between specific density, culm geometry and moisture content

Parameter	Correlations (r) *		
	Culm diameter (mm)	Wall Thickness (mm)	MC
SD	-0.728	-0.753	-

As discussed earlier regarding specific density and the relation with culm geometry, Table 13 confirmed the discussed relation and showed that bamboo sections with larger culm diameter and thicker wall cross section would have lower specific density. Consequently, the lower specific density would result in lower mechanical properties as shown in Table 12. To better understand the specific type of relationship between the physical and mechanical properties, multiple linear regression models were used. Furthermore, mathematical models and equations were suggested for estimating the mechanical properties of bamboo *Dendrocalamus asper* by only measuring the culm diameter and wall thickness. Table 14 displays linear-model parameter values created with the data obtained in this study. In Table 14, all mechanical properties have units of MPa while D and t are in mm and MC is in percentage.

Two linear models were created for MOR, one with only diameter (D) and one with diameter (D) and moisture content (MC). Both models were statistically significant with P-value of less than 0.001. Modulus of elasticity in flexure (E_f) had only one significant model with only D, while modulus of elasticity in tension (E_t) had four linear models which were statistically significant. Among the four models, the model with SD, D and wall thickness (t) showed the highest r^2 (coefficient of determination) value of 0.65, which demonstrated the fact that 65% of the data variation could be explained by the three variables (SD, D, t) in this model.

In case of compressive strength (CS), three significant models were established as shown in Table 14. These models displayed the largest r^2 value among all the models established with linear regression. This indicated that a large proportion of the variance in compressive strength variable was predictable from the three independent variables of D, t and SD. Tensile strength (TS) showed one significant model with only wall thickness (t) as a variable and with r^2 value of 0.53.

Table 14 linear regression models for mechanical properties of bamboo *Dendrocalamus asper*

Model	r^2	Model significance	Parameter	Coefficient	Significance	Constant
MOR						
1	0.50	<0.001	D	-0.78	<0.001	250.40
2	0.63	<0.001	D	-0.75	<0.001	363.56
			MC	-11.70	0.004	
E_f						
1	0.46	<0.001	D	-33.15	<0.001	14375.91
E_t						
1	0.36	<0.001	SD	18550.28	<0.001	6874.06
2	0.25	0.004	t	-362.70	0.004	25303.91
3	0.54	<0.001	SD	33593.88	<0.001	13074.99
			D	70.44	0.002	
4	0.65	<0.001	SD	27236.26	<0.001	-7178.92
			D	95.10	<0.001	
			t	-364.57	0.008	
CS						
1	0.81	<0.001	D	-0.36	<0.001	96.69
2	0.92	<0.001	D	-0.22	<0.001	92.78
			t	-1.30	<0.001	
3	0.93	<0.001	D	-0.18	<0.001	70.68
			t	-1.12	<0.001	
			SD	20.56	<0.005	
TS						
1	0.53	<0.001	t	-8.46	<0.001	362.56

The empirical relations between MOR, E_f, E_t, CS, TS and culm physical properties are developed and summarized here. These equations should be considered to provide only preliminary estimation of the mechanical properties for bamboo *Dendrocalamus asper*. For other species of bamboo and bamboo from other regions around the world, the model coefficients and constants could differ. All the equations have standard error of estimates of less than 8%.

$$MOR = -0.78D + 250 \qquad \text{(Eq. 29)}$$

$$E_f = -33D + 14300 \qquad \text{(Eq. 30)}$$

$$E_t = -3620t + 25300 \qquad \text{(Eq. 31a)}$$

$$E_t = 18550SD + 6874 \qquad \text{(Eq. 31b)}$$

$$E_t = 33600SD + 70.4D + 13075 \qquad \text{(Eq. 31c)}$$

$$E_t = 27200SD + 95.1D - 364.6t - 7180 \qquad \text{(Eq. 31d)}$$

$$CS = -0.36D + 96.7 \qquad \text{(Eq. 32a)}$$

$$CS = -0.22D - 1.30t + 92.8 \qquad \text{(Eq. 32b)}$$

$$CS = -0.18D - 1.12t + 21SD + 71 \qquad \text{(Eq. 32c)}$$

$$TS = -8.5t + 363 \qquad \text{(Eq. 33)}$$

Furthermore, the SD of the bamboo culms could also be estimated by measuring only the culm diameter and wall thickness using Eq. 34.

$$SD = -0.002D - 0.009t + 1.075 \qquad \text{(Eq. 34)}$$

For estimating E_t, four equations are suggested. Each equation can be used when a specific type of culm geometry is available. For instance, when only wall thickness measurement is possible, then Eq. 31a can be used to estimate E_t. Similarly, Eq. 31d is used when both culm diameter and wall thickness can be measured. In case of compressive strength (CS), three equations are established. Eq. 32a is used when only culm diameter measurement is available, while Eq. 32b can be used when both culm diameter and wall thickness can be measured.

4.5. Conclusions

After considering various aspects of the bamboo selection process, bamboo *Dendrocalamus asper* from Indonesia is chosen for this research on bamboo composite material fabrication and its application in concrete. The results of the tests carried out in this chapter show that culm diameter and wall thickness have important impacts on the mechanical properties of raw bamboo. Culms with larger dimeters or thicker wall cross sections display lower mechanical properties as a result of lower specific density and lesser cellulose fiber content. Although moisture content does not show a significant effect on the mechanical properties, it plays an important role in the composite fabrication in which the interaction with the epoxy-resin system can be affected with variations in moisture content. Among all the mechanical

properties measured in this section, only modulus of rupture shows a correlation with moisture content in which lower moisture content results in higher modulus of rupture. Specific density shows a strong correlation with both culm diameter and wall thickness but not with the moisture content. For the first time, several linear statistical models are established to support quick selection of the raw bamboo sections in contexts such as nurseries where no laboratory testing facilities are available. Finally, the results of the mechanical evaluation of nearly 4,500 bamboo samples in this chapter show that the bamboo sections from the top part of the culms have better mechanical properties compared with the middle and bottom parts. The highest average tensile strength and modulus of elasticity of bamboo samples of *Dendrocalamus asper* are 323MPa and 28,230MPa respectively. In terms of flexural properties measured in this chapter, the highest average MOR and modules of elasticity in flexure are found to be 205MPa and 12,851MPa respectively. The maximum compressive strength measured for bamboo samples of *Dendrocalamus asper* in this chapter is 66MPa. These values reveal much potential for structural engineering applications of bamboo.

5. Fabrication process of bamboo composite material and evaluation of properties

5.1. Summary

The production process of bamboo composite materials is explained here. Two novel methods are investigated for processing the bamboo culms: bamboo veneer and bamboo strand. Each method has advantages and disadvantages in terms of the production and quality of the final composite. A comparison between the two methods is carried out through evaluating the mechanical properties of nearly 5,000 bamboo composite sample and bamboo veneer is selected for this research due to the higher mechanical properties. Advanced chemical and mechanical treatments, including the alkaline treatments of the veneer layers and creating perforations or linear cracks along the fiber direction of the veneer layers, are carried out to further enhance the properties of the final bamboo composite materials. Tensile strength and modulus of rupture, compressive strength, modulus of elasticity in tension and flexure of bamboo composite materials are obtained for each of the 5,000 bamboo composite samples produced within this thesis. In addition to the physical and mechanical properties of the bamboo composite materials, the microstructure of each sample produced in this research is also examined to understand the chemical reaction between bamboo fibers and the epoxy-resin matrix used in this study. The results show that longitudinal bamboo composite reinforcement produced with the novel fabrication method developed within this research, which includes the application of NaOH treated veneer layers with a series of perforations along the fiber direction and mixed with the INF/CLR epoxy-resin systems under a pressure of 20MPa and a temperature of 100°C of the hot-press machine, have the highest average tensile strength of 408MPa and flexural strength of 327MPa. Even though the final bamboo composite stirrups display slightly lower mechanical properties compared to longitudinal reinforcements caused by the limitations of the fabrication process, their average tensile strength are comparable to ASTM A615 grade 40 reinforcing bar with a minimum tensile strength of 280MPa. Around 1,500 samples of longitudinal and transverse BVC reinforcements are produced and evaluated in this research before their final application within the concrete beams to ensure of the consistency of the composite fabrication process.

5.2. Raw Bamboo processing techniques

To produce the bamboo composite materials, the bamboo culms must be processed into bamboo sections with the desired width, length and thickness. Two novel methods are investigated in this research: bamboo stranding and bamboo veneering. In this section, both methods are described, and the advantages and disadvantages of each method are explained. From the bamboo with various culm diameters and wall thicknesses classified in this research, only classes 3, 4 and 5 were used for composite fabrication in which a minimum average tensile strength of 290MPa could be obtained.

5.2.1. Bamboo stranding method

In this method, bamboo fiber bundles are obtained through a series of mechanical processing with the use of several machines at AFCL. As described earlier, bamboo culms of *Dendrocalamus asper* are between 20m to 30m in height. Therefore bamboo culms were first cut into sections of 5m in length before shipment to Singapore. Once in the laboratory, the 5m section was cut lengthwise into shorter sections of 1.6m to 1.8m. This length was chosen given the maximum length of the molding press employed for the production of bamboo composite materials. A bamboo splitting machine was employed in this research to split the shorter bamboo sections lengthwise along the fiber direction into planks of similar width and thickness as shown in Fig. 56 and Fig. 57.

Fig. 56 Bamboo splitting machine at AFCL
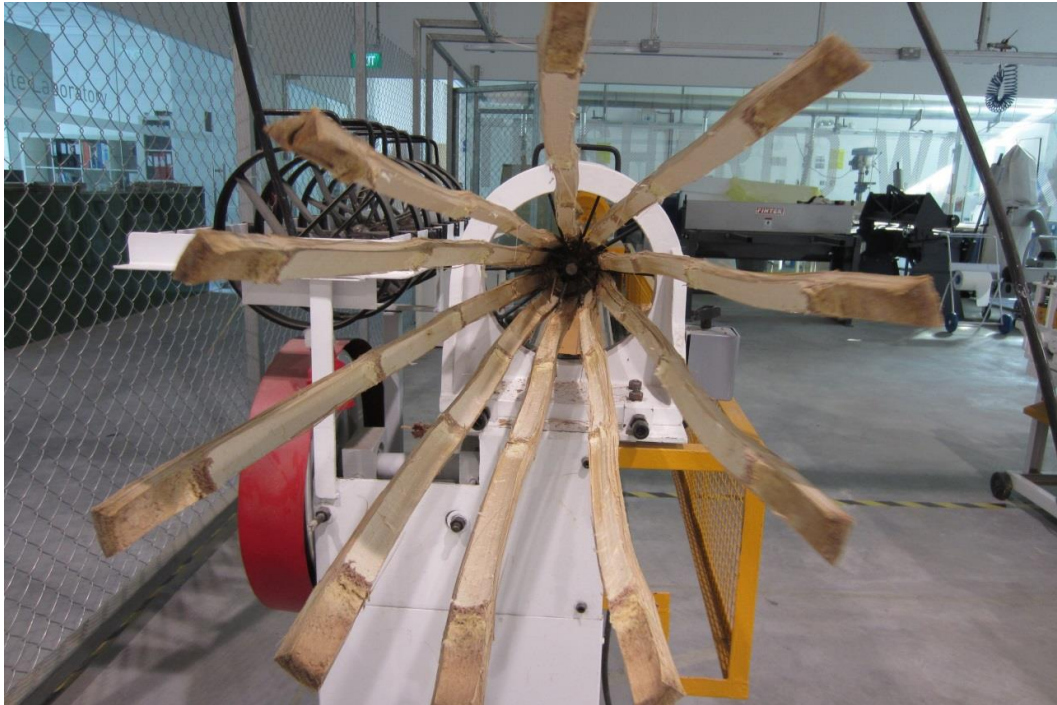
Fig. 57 Bamboo planks produced by bamboo splitting machine

To improve the surface area of the bamboo planks and enhance the bonding between bamboo fibers and epoxy-resin matrix in composite fabrication, the bamboo planks were passed through a delamination process in which the inner nodes and waxy skins were removed. The waxy part of the skin layer of the bamboo sections has a high content of silica acid, which makes the exposed layer of bamboo highly resistant against chemical and animal exposure during its growth in nature (Ray, Mondal et al. 2005). However, this hard and waxy layer is not bonded chemically to the epoxy-resin matrix and must be removed to improve the chemical bond between bamboo fibers and the epoxy-resin matrix for producing high-performance bamboo composite materials.

The inner nodes are only removed to produce a flat and smooth surface which is easily stacked and wetted with epoxy-resin matrix. However, the knots are not totally removed and the outermost layers of the bamboo sections are kept for the composite fabrication, given their proven high fiber density as described earlier in chapter 4 and widely explained in the literature (Wang, Ren et al. 2011). The high fiber density of the outer layers of the bamboo cell wall structure, due to presence of a higher amount of vascular bundles, is a perfect structural adaptation towards a high stiffness and strength of the bamboo culm; therefore, the cellulose fibers of the bamboo culms remain the main components of the microstructure of the bamboo culms responsible for the high mechanical properties of bamboo. For the fabrication of bamboo composite reinforcement, it is crucial to keep the outer layers that

possess higher fiber density and superior mechanical properties to obtain higher mechanical properties of final bamboo composite samples, by incorporating more of the cellulose fibers which contribute to the strength and elastic modulus of the composite.

Fig. 58 shows a flat plank section of bamboo after being passed through the delamination machine and removal of the waxy layer of skin and inner nodes. The average thickness of the bamboo plank sections after running though the delamination machine was between 6mm to 15mm, depending on the wall thickness of the available bamboo culms.

Fig. 58 Bamboo slats after removal of waxy skin and inner nodes

The mechanical and physical properties of the bamboo composite materials are influenced by the interaction between the natural bamboo fibers and the polymer matrix (e.g. epoxy system). The interface between the fibers and polymer matrix of any composite material determines the effectiveness of the stress transfer at the interface between the two main components of composites. It has been proven in previous studies that the adhesion of the fibers to the polymer matrix at their interface plays a critical role in the overall integrity and performance of composite materials (Madhukar and Drzal 1991). As described by Laurent Matuana, Raymond Woodhams, John Balatinecz and Chul Park, the surface properties at the interface between the polymer matrix and cellulosic fibers (e.g. bamboo fibers) strongly influence the mechanical properties of the final composite samples (Matuana, Woodhams et al. 1998). Among the surface parameters that could enhance the interaction between the fibers and polymer matrix and improve the adhesion of the fibers to the polymer matrix in a composite material are the fiber specific surface area and the fiber aspect ratio (Valadez-Gonzalez, Cervantes-Uc et al. 1999).

The specific fiber surface area is simply the total surface area of available fiber bundles per unit of mass, and the fiber aspect ratio is the ratio of the fiber length to the fiber diameter.

The fiber aspect ratio has been shown to have a close relationship to the mechanical properties of the composite, as well as the interfacial shear strength between the fibers and polymer matrix within the composite sample. Professor Hayley Cox in 1952 showed that by increasing the fiber length and reducing the fiber diameter, and therefore increasing the fiber aspect ratio, the ultimate tensile strength of the composite increases through the improvement of the interfacial shear strength which is responsible for the stress transfer between the fibers and polymer matrix (Cox 1952).

The surface area and aspect ratio of the fiber bundles are the key surface characteristics that determine the wetting behavior of the epoxy-resin matrix to the bamboo fibers as explained in detail by Omar Faruk, Andrzej Bledzki, Hans-Peter Fink and Mohini Sain (Faruk, Bledzki et al. 2012). However, measuring the surface characteristics or wetting properties of the fibers require special equipment which were not available at AFCL during this PhD work. Therefore, to evaluate the incorporation of the effect of the surface area and fiber aspect ratio, the bamboo slats were cut across their thickness into thinner sections, with various thicknesses, with the use of a flaking machine; a study was then carried out on the effect of the various thicknesses of bamboo slats on the mechanical properties of the final bamboo composite samples, which is explained further in detail in section 5.3.

The thinner sections with similar width had higher fiber aspect ratios given their lesser thicknesses. Besides the effect of thickness on the aspect ratio, reducing the slat thickness increases its surface area to volume ratio, which subsequently results in better interaction of the fibers with the polymer matrix through the wetting process as explained in this section. Therefore, this single study could guide the PhD candidate in choosing the right thickness of slats which could result in higher mechanical properties of the composite. Fig. 59 shows the flaking process of the bamboo slats across their thickness into thinner slats.

Unlike some common bamboo reinforced composite materials discussed in the literature which are produced only with short and dispersed bamboo fibers, in this research, a novel approach was undertaken via employing unidirectional long bamboo fiber bundles for the fabrication of bamboo fiber reinforced polymer composite. Furthermore, through bamboo processing tools employed in this research, for the first time the long fiber bundles and their inherent high tensile capacity remained intact.

Unlike the common bamboo reinforced composite materials produced elsewhere (e.g. in China) where most of the fiber bundles are damaged through the process and thus the tensile capacity of the processed fibers are reduced by a large extent, in the new processing method developed in this research, it is possible to protect the fiber bundles throughout the process. Knowing that the final bamboo composite reinforcement would need to resist tension forces, for the purpose of this research, the composite samples were fabricated in unidirectional shapes to ensure that the highest tensile capacity could be achieved through activating the bamboo fiber's inherent tensile strength along the fiber direction.

The advantage of long bamboo fibers over short bamboo fiber composites is their higher aspect ratio and increased specific surface area, as explained earlier, contributing to a higher interfacial shear strength between the bamboo fiber bundles and the polymer matrix which is responsible for the stress transfer between the two within the composite material's microstructure.

Furthermore in comparison with the common methods used to produce most of the natural fibers (e.g. kenaf, bamboo and sisal) employed in production of natural fiber reinforced polymer composites as discussed in section 3.3.2 where hi-tech machineries and sophisticated chemical and mechanical processes are used, in the bamboo stranding method employed in this research, simple and straightforward techniques and processes are developed. The stranding method allows for the production of long fiber bundles without harming the fibers by slicing the bamboo slats along the fiber direction. Additionally the simplicity of the developed tools and techniques for bamboo stranding can benefit many of the developing countries through establishing low-tech yet high performance bamboo processing machineries.

In comparison with glass fiber production process, the new methods developed within this research for processing the bamboo fibers are far more efficient in terms of energy consumption and cost. The glass fiber production is a highly energy intensive process involving various steps in which large furnaces with high temperatures of up to 1,400°C are employed for the melting of the glass mixture. Furthermore glass fiber formation, or fiberization, involves a combination of extrusion and attenuation process which require expensive and high-tech tools and techniques.
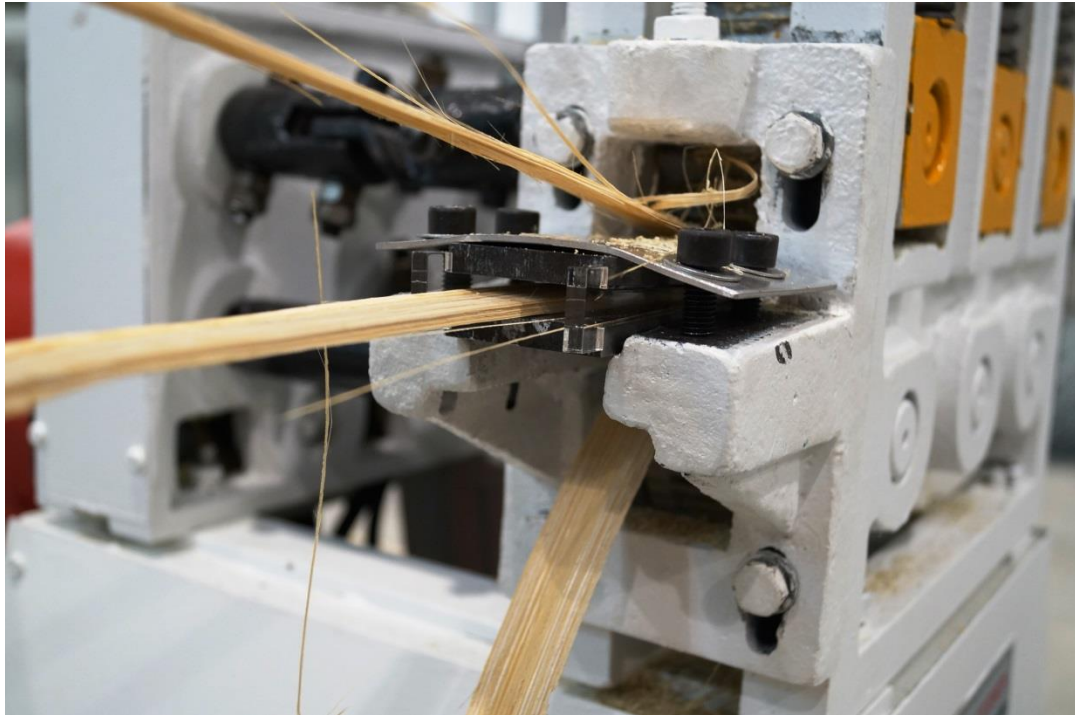
The mechanical properties are discussed in section 5.3. The thicker bamboo slats were passed through the bamboo flaker machine several times until the thickness of the processed sections could not be further reduced. The final bamboo slats had thicknesses in the range of 1mm to 3mm. The thicker sections (>3mm) were not used for the fabrication of the composite samples after careful investigation of the results from the mechanical properties presented in section 5.3. Furthermore, for the epoxy-resin matrix to penetrate through the layers of the bamboo flakes, a second-step mechanical processing technique was used to increase the pore size and improve the surface area of the bamboo fiber bundles. As explained earlier in this section, the improved surface area of the fibers could help to enhance the fiber-matrix interfacial strength through the fiber wetting process and increase the ultimate mechanical properties of the final bamboo composite samples. The bamboo flakes were passed through a unique strip stranding machine in which a series of dotted and/or linear cracks were produced along the fiber direction of the bamboo slats. Fig. 60 shows the stranding machine in which a series of wheels were used to push the bamboo flakes through the designated discs where the linear cracks along the fiber direction were produced. The final bamboo strands were pieces of 1.6m to 1.8m-long fiber bundles connected together with linear grooves along the fiber direction, which could increase the fiber surface area and enhance the interfacial strength between the fiber and resin matrix during the composite fabrication. To evaluate the effect of linear cracks on the fiber-matrix interaction, a series of bamboo strand composite samples

156

were prepared with and without the grooves and their tensile properties measured accordingly. These tests and their results are discussed in detail in section 5.3. Fig. 61 shows a bamboo strand strip before and after final stranding.
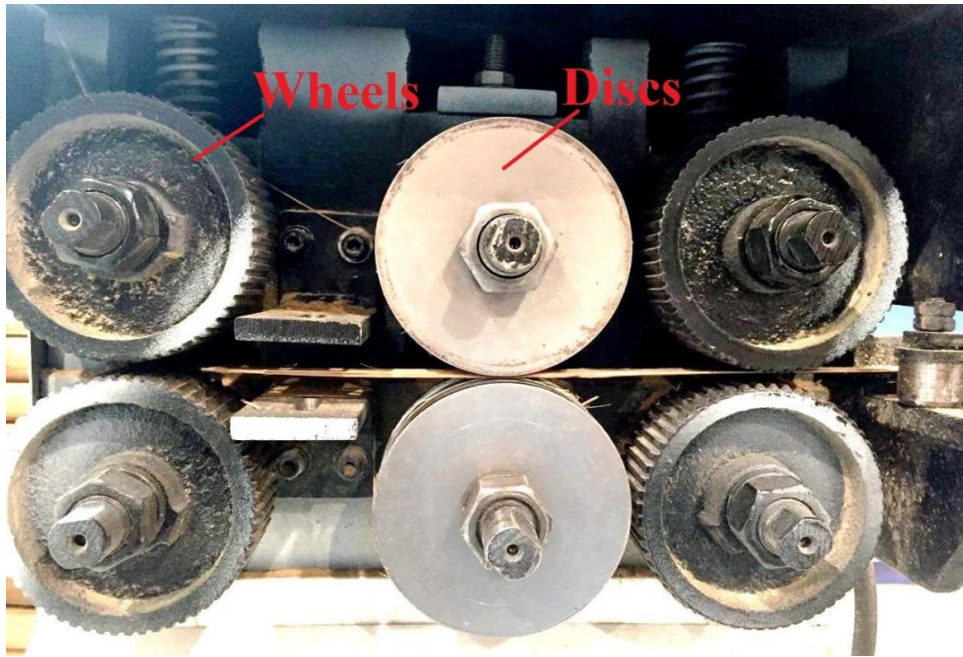
Fig. 60 Bamboo stranding machine, including the metal discs and wheels

Fig. 61 Bamboo strips before (top) and after (bottom) stranding process

The strips of bamboo strands were subsequently dried in an air-circulated oven at various temperatures to evaluate the effect of drying at different moisture content on the tensile properties of the raw bamboo strips, and to find the optimum temperature for drying the raw bamboo strips for bamboo composite fabrication. Table 15 shows the various temperatures

applied for drying the bamboo strips and with the moisture contents measured, according to ASTM D4442-07 which was discussed in detail in section 4.3.1.

Table 15 Moisture content of bamboo strips at various temperatures according to ASTM D4442-07

Class	Wall thickness (mm)	Average MC(%) at 60°C with 65% RH	Average MC(%) at 80°C with 65% RH	Average MC(%) at 100°C with 65% RH
Class 1	6 to 7	9.6	9.5	9.0
	7 to 8	9.1	9.1	8.8
	8 to 9	9.3	9.2	8.9
Class 2	6 to 7	9.9	9.8	9.1
	7 to 8	9.8	9.8	9.2
	8 to 9	9.9	9.8	9.1
	9 to 10	8.9	8.8	8.6
	10 to 11	10.1	10.0	9.5
Class 3	6 to 7	9.4	9.4	9.0
	7 to 8	9.9	9.8	9.3
	8 to 9	9.8	9.8	9.1
	9 to 10	10.4	10.3	9.6
	10 to 11	9.1	9.1	8.5
Class 4	6 to 7	9.3	9.3	8.9
	7 to 8	9.0	8.9	8.7
	9 to 10	9.6	9.6	9.0
Class 5	8 to 9	9.0	8.9	8.4
	9 to 10	9.1	9.1	8.6
	10 to 11	9.6	9.5	8.9
	11 to 12	10.1	10.0	9.2
Class 6	10 to 11	9.0	8.9	8.0
	11 to 12	9.6	9.5	8.8
	12 to 13	9.5	9.4	8.7
	14 to 15	9.7	9.5	8.6
Class 7	11 to 12	9.4	9.1	8.7
	12 to 13	9.2	9.0	8.5
	16 to 17	8.9	8.8	8.1
	19 to 20	10.0	9.9	9.0

The relative standard deviations of the samples' moisture content dried at 60℃, 80℃ and 100℃ were less than 11%, 8% and 18% respectively. Only one relative humidly condition was chosen for this preliminary study to reduce the impact of higher humidity conditions (80%) on water uptake and drying behavior, which would make the study rather complex.

Furthermore, as explained by Amandine Célino, Sylvain Fréour, Frédéric Jacquemin and Pascal Casari in their work on "The hygroscopic behavior of plant fibers and their applications for composite manufacturing", the most relevant difference between synthetic fibers (such as glass fibers) and natural fibers (such as bamboo) is their response to humidity (Célino, Fréour et al. 2013). Unlike glass fibers which are considered hydrophobic materials, bamboo fibers exhibit a hydrophilic behavior and could attract water molecules to their surface and ultimately into their microstructure. Therefore, at higher humidity conditions, strong hydrophilic behavior of bamboo fibers leads to higher level of moisture absorption. Furthermore, as described widely in the literature, high content of water in the form of inherent moisture in natural fiber could adversely affect the fiber-matrix interaction and further reduce the interfacial bond between the fiber and polymer matrix during composite fabrication (Wallenberger and Weston 2004, Rao and Rao 2007).

Currently, no systematic study is available regarding the optimum moisture content of bamboo fibers suitable for composite fabrication. However, studies on the water absorption behavior of bamboo-glass fiber reinforced polymers have shown that reducing the water content of fibers prior to composite fabrication can improve the fiber-matrix interfacial bond strength, and further reduce water accumulation in the available interfacial voids of the composite matrix and prevents excess water from entering the composite structure (Thwe and Liao 2002).

As shown in Table 15, at 60°C, the Moisture Content (MC) of the samples was reduced compared to the MC measured in section 4.3.1 at 65% RH. By increasing the temperature to 80°C and 100°C, a further drop in MC measurement was observed. However, as the results suggested, at 100°C, traces of fluctuation in the values of MC measured were observed, unlike the MC measured at 80°C for which the majority of the samples within the seven classes of bamboo Petung a state of balance and moderation is recognizable among the three levels of temperatures chosen for drying the samples. This observation was further verified by the higher standard deviations of the samples dried at 100°C (less than 18%) compared to 11% and 8% for the 60°C and 80°C drying temperatures. To further evaluate the impact of drying on fiber properties, the tensile strength of the dried samples were measured extensively according to ASTM D143-14, according to section 4.2.3. Table 16 shows the results of the tensile tests for the various drying temperatures.

Table 16 Tensile strength test results for various drying temperatures

Class	Wall thickness (mm)	Average tensile strength after drying at 60°C (MPa)	Average tensile strength after drying at 80°C (MPa)	Average tensile strength after drying at 100°C (MPa)
Class 1	6 to 7	278	280	265
	7 to 8	293	294	260
	8 to 9	286	288	255
Class 2	6 to 7	257	260	253
	7 to 8	295	294	258
	8 to 9	289	290	270
	9 to 10	281	282	266
	10 to 11	292	295	274
Class 3	6 to 7	291	294	275
	7 to 8	293	296	270
	8 to 9	288	286	266
	9 to 10	286	290	260
	10 to 11	299	304	259
Class 4	6 to 7	322	325	281
	7 to 8	321	322	277
	9 to 10	325	327	275
Class 5	8 to 9	338	341	302
	9 to 10	317	312	295
	10 to 11	300	305	291
	11 to 12	270	272	263
Class 6	10 to 11	311	317	294
	11 to 12	283	281	272
	12 to 13	260	255	255
	14 to 15	246	252	231
Class 7	11 to 12	246	240	230
	12 to 13	226	231	209
	16 to 17	201	208	197
	19 to 20	192	189	181

The relative standard deviations of the samples' tensile strength dried at 60°C, 80°C and 100°C were less than 14%, 6% and 21% respectively. The one-way Anova test of variances showed there was no significant difference between the means of the tensile strength of the samples dried at 60°C and 80°C. Even though the bamboo strips from some classes of bamboo Petung showed a slight decrease or increase in the average tensile strength, the variations were not of high significance. However, the pairwise comparison showed a

significant difference between the mean tensile strength of the samples dried at 80℃ and 100℃. The mean tensile strength of the samples dried at 100℃ showed relatively high variations in the results compared to the other two temperatures chosen for drying the samples. Furthermore, when the mean tensile strength of the samples dried at 100℃ for various classes were compared to the mean tensile strength of the samples dried at 80℃, a reduction in the values of tensile strength ranging from 7% to 14% was observed from the results presented in Table 16.

Therefore, to have reliable and consistent values for the tensile strength of the raw bamboo fibers for composite fabrication and to further eliminate variations due to drying temperatures, all raw bamboo fibers were dried in an air-circulated oven at 80℃ to reach an equilibrium MC of less than 10% prior to composite fabrication. Once dried, the stacks of bamboo strands were used for manual lay-up to produce bamboo composite samples as described in section 5.3.2.

5.2.2. Bamboo veneering method

The bamboo veneer was obtained with a uniquely designed bamboo peeling machine as shown in Fig. 63. The 5m bamboo culm is cut into sections of maximum 90cm length. This length was the maximum possible length that the available peeling machine at AFCL could process. Due to the relatively high hardness of raw bamboo, it is not easy to peel bamboo culms while they are dry. Therefore the bamboo sections were first boiled at 90℃ in normal water in a closed container for 24 hours to soften the microstructure through weakening the lignin interface's adhesion with the cellulose fibers. During the course of this research, this method showed higher efficiency compared to peeling the dry bamboo.

However, to ensure that boiling the raw bamboo did not negatively affect the mechanical properties of the bamboo fiber bundles, an investigation of the tensile strength of the raw bamboo sections after boiling for 24 hours at 90℃ was carried out prior to the peeling process. The tensile strength of the samples was measured according to ASTM D143-14 following the methods described in section 4.3.3. Table 17 summarizes the results of the tensile strength tests of the bamboo samples after boiling for 24 hours in comparison with the results of the tensile tests presented in Table 7 for non-boiled bamboo samples. For each class of bamboo *Dendrocalamus asper,* at least five samples were boiled at 90℃ for 24 hours and the results shown for each class were the average values of those samples. The boiled

samples were first dried at 80°C in the air-circulated oven to reach the equilibrium MC values of less than 10% before the tensile strength test.

Table 17 The effect of boiling on the tensile strength of bamboo *Dendrocalamus asper* along the fiber direction

Class	Wall thickness (mm)	Tensile strength before boiling (MPa)	Tensile strength after boiling (MPa)
Class 1	6 to 7	281	283
	7 to 8	295	293
	8 to 9	285	289
Class 2	6 to 7	260	262
	7 to 8	298	296
	8 to 9	292	291
	9 to 10	280	284
	10 to 11	294	298
Class 3	6 to 7	288	291
	7 to 8	290	290
	8 to 9	285	288
	9 to 10	287	291
	10 to 11	301	305
Class 4	6 to 7	324	321
	7 to 8	320	324
	9 to 10	326	329
Class 5	8 to 9	340	338
	9 to 10	318	320
	10 to 11	303	301
	11 to 12	268	274
Class 6	10 to 11	310	314
	11 to 12	282	279
	12 to 13	263	270
	14 to 15	247	243
Class 7	11 to 12	244	241
	12 to 13	224	229
	16 to 17	203	210
	19 to 20	193	201

The relative standard deviations of the samples' tensile strength measured after boiling for the various classes of bamboo *Dendrocalamus asper* were in the range of 7% to 10%. Furthermore, a one-way Anova test of variances showed there was no significant difference between the means of tensile strength of the samples before boiling and after boiling. This

proved that boiling for 24 hours at a temperature of 90°C to soften the bamboo culms for the peeling process did not negatively affect the mechanical properties, primarily the tensile strength. Fig 62 shows the comparison between the tensile strength of the raw bamboo samples before and after boiling.
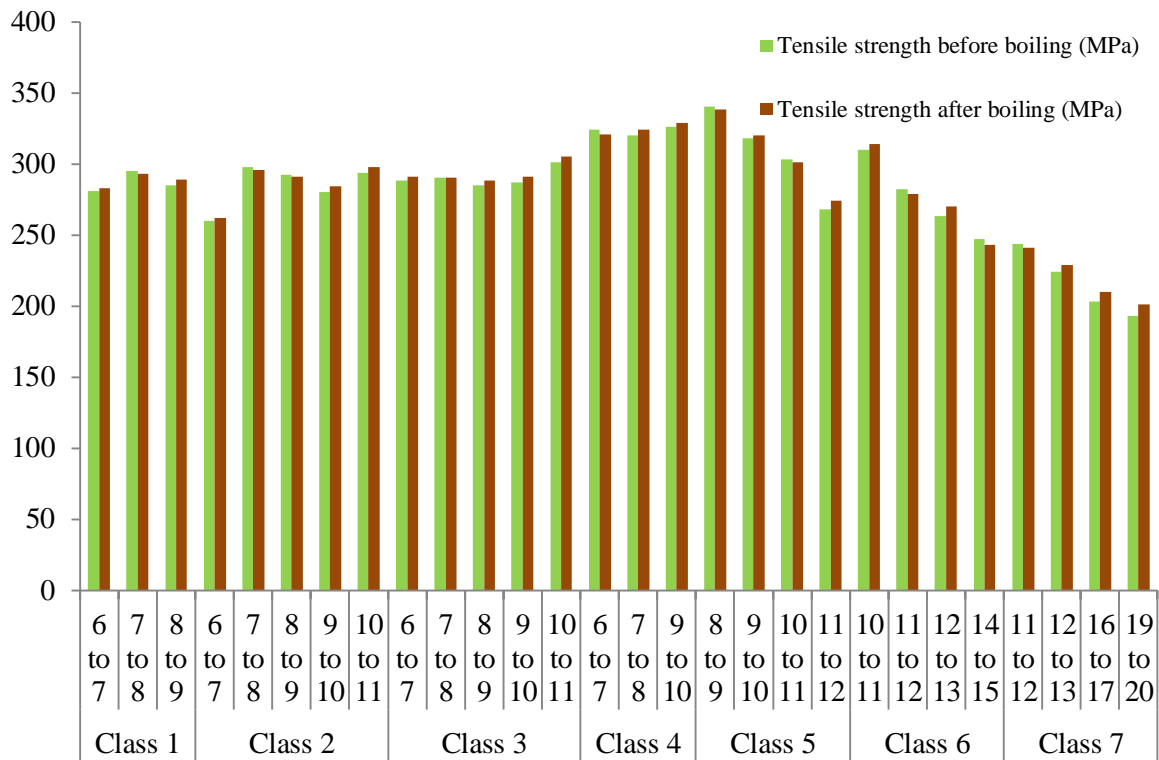
Fig. 62 Comparison between tensile strength of the raw bamboo samples before and after boiling

Fig. 63 Bamboo section fixed to the set-up of a peeling machine

The boiled bamboo was taken out of the container and fixed to the two rotary grips on the sides of the peeling machine by applying bearing pressure. Once fixed, the rotary grips started to rotate at a speed of 30 to 50 rounds per minute (rpm). Depending on the quality of the bamboo and its wall thickness, the rotation speed was adjusted accordingly. The thicker wall cross sections worked efficiently with higher rotation speeds while thinner wall cross sections worked better with lower rotation speeds.

Once the rotary grips started to rotate, a sharp long blade peeled the veneer off the surface of the bamboo section. The blade cross section is shown in Fig. 64. The space between the edge of the blade and the top steel block determined the thickness of the veneer. The thickness of the veneer was also influenced by the quality of the bamboo, mainly the presence of invisible cracks, the wall thickness of the bamboo and the distance between the knots.
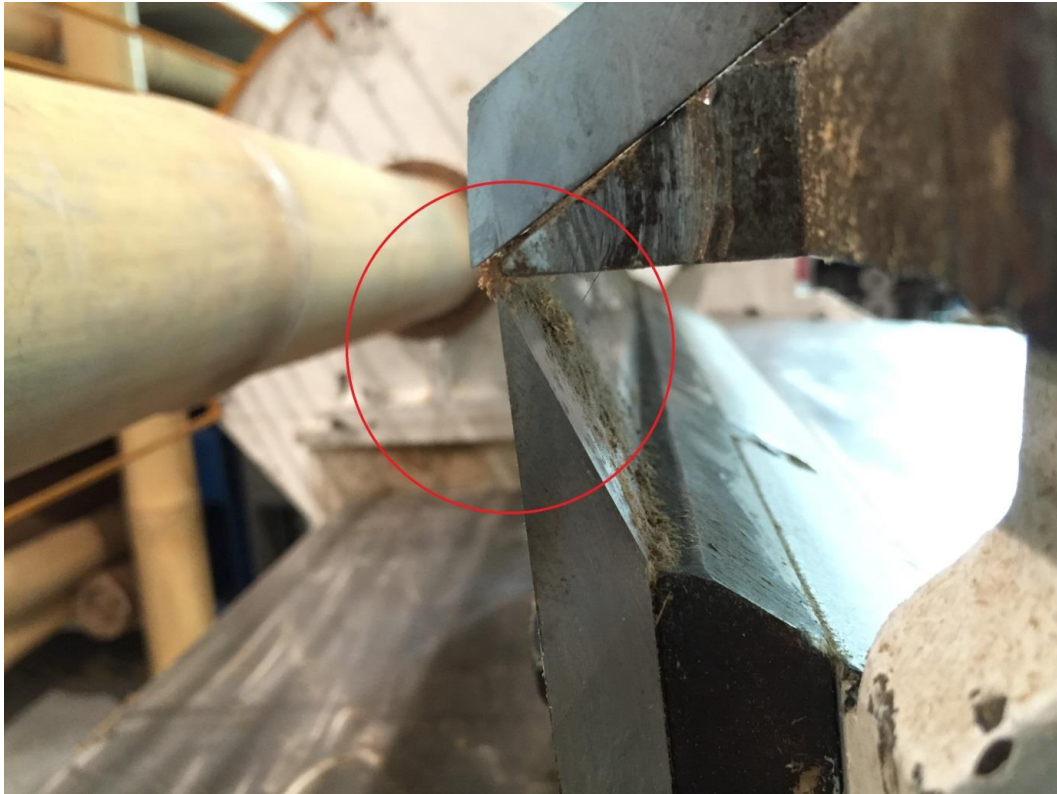
Fig. 64 The edge of the blade used in the peeling machine to produce the veneer layer from the bamboo culm

The presence of longitudinal cracks along the fiber direction in some of the available bamboo culms made the peeling process challenging and less efficient compared to culms without any cracks. The longitudinal cracks were further widened as a result of the high contact pressure applied on the surface of the culm in the peeling process. Once the cracks were enlarged, the bamboo culms were split apart into pieces and the peeling process was stopped. The output from cracked bamboo culms was much lower compared to intact culms. The cracks could have been formed during harvesting, shipping or while being stored at AFCL. Therefore, to increase the yield of the veneer production and improve the efficiency of the peeling process, all the available bamboo culms with visible cracks were marked before boiling and peeled separately even though the yield was not significant.

Another important detail that had to be taken care of during the peeling process was the wall thickness of the raw bamboo. As described earlier, bamboo culms with thicker wall thicknesses require a higher rotation speed of the machine during the peeling process. Furthermore, due to the microstructural characteristics of the bamboo culms in which a higher percentage of lignin and lower fiber density are observed with the bottom sections of bamboo culms, the thicker bamboo culms showed higher efficiency and better yield in terms of veneer layers produced. Lower fiber density as a result of a higher lignin content of thicker

culms, mainly found at the bottom of the culms, created a softer tissue which could be peeled off smoothly compared to thinner culms with higher fiber density and superior hardness. However, to better understand the peeling process of various classes of bamboo *Dendrocalamus asper* before moving to the fabrication of bamboo composite samples, for the first time a series of experiments were designed carefully to evaluate the influence of culm wall thickness on the efficiency and output of veneer production in this research. For each class of bamboo culms and for each series of wall thickness, 500 sections of bamboo culms were randomly chosen and boiled at 90°C for 24 hours prior to the peeling process. The efficiency of the peeling process can be measured by the following formulae.

$$\eta = \frac{W_v}{W_b} \times 100 \quad \text{(Eq. 35)}$$

Where:

W_v: is the dry weight of the veneer layers with an equilibrium MC of less than 10% in kg,

W_b: is the weight of the raw bamboo sections before boiling with an equilibrium MC of less than 10% in kg.

Table 18 shows the efficiency (η %) of veneer production for various classes of bamboo *Dendrocalamus asper* measured in this study.

As Table 18 shows, the efficiency of the peeling process increased for the thicker walls of bamboo culms. The highest efficiency rate was achieved for class 7 samples with wall thickness of 19mm to 20mm. However, in general, the efficiency of the peeling process was not very significant. This could be attributed to the limitations of the newly designed peeling machine. For instance, as described earlier, only certain lengths of bamboo sections could be peeled (maximum length of 90cm) compared to the stranding process where any bamboo length could be processed by the splitting, stranding or flaking machine.

Table 18 Efficiency of peeling process for various classes of bamboo *Dendrocalamus asper*

Class	Wall thickness (mm)	η (%)
Class 1	6 to 7	12
	7 to 8	14
	8 to 9	13
Class 2	6 to 7	10
	7 to 8	12
	8 to 9	11
	9 to 10	14
	10 to 11	16
Class 3	6 to 7	11
	7 to 8	10
	8 to 9	14
	9 to 10	12
	10 to 11	15
Class 4	6 to 7	12
	7 to 8	11
	9 to 10	14
Class 5	8 to 9	13
	9 to 10	16
	10 to 11	15
	11 to 12	18
Class 6	10 to 11	15
	11 to 12	17
	12 to 13	18
	14 to 15	18
Class 7	11 to 12	16
	12 to 13	18
	16 to 17	19
	19 to 20	21

Furthermore, though boiling the bamboo sections prior to peeling process helped to soften the bamboo tissue and improve the peeling process, the inherent hardness of bamboo, especially at the outer layers, resulted in sudden splitting and/or breaking of the sections during the process before the whole bamboo section could be peeled completely. On the other hand, it was observed that for bamboo sections that had slight off-axis deformations, the sudden splitting/breaking occurrence was notable. This could be explained by the development of

abrupt stress concentrations at the point of local contacts with the blade of the machine, where the off-axis deformations prevented the blade from entirely touching the full length of the bamboo section being peeled. Fig. 65 shows the mechanism involved in the splitting behavior of the curved bamboo sections during the peeling process.
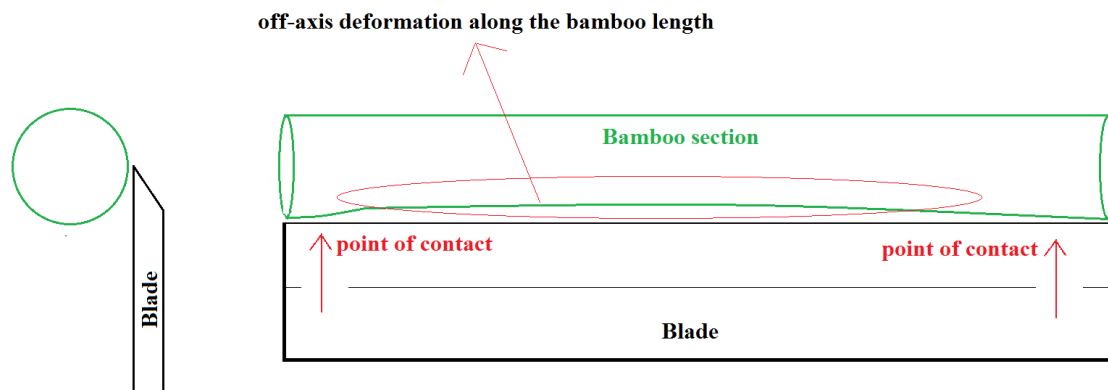
Fig. 65 Off-axis deformations observed within some of the available bamboo sections during peeling process

Though the veneer production efficiency of some classes of bamboo *Dendrocalamus asper* was low given the limitations of the available peeling machine at AFCL, for the purpose of this research, all of the bamboo sections with various culm diameters and wall thicknesses were used in different proportions for the composite fabrication described in section 5.3.

The peeling process resulted in veneers of various thicknesses. Several attempts were made to optimize the thickness of the veneer layers by processing more than 500 bamboo sections of various thicknesses. However, the minimum thickness that could be achieved for a boiled bamboo section with a length of 90cm, and with internodes and wall thickness of 6mm to 19mm, was 0.40mm. In general, the thickness of the veneer layers produced by the peeling process was in the range of 0.40mm to 1mm after adjusting the blade. Therefore, to investigate the optimum thickness of the veneer layers for the composite fabrication in terms of interaction between the fibers and matrix which could ultimately enhance the composite's mechanical properties, a series of bamboo composite samples produced with various veneer thicknesses from 0.4mm to 1mm and their tensile strengths were measured. These tests and their results are discussed in detail in section 5.3. The optimum thickness was maintained throughout this research specifically for the fabrication of the final bamboo composite reinforcement in section 5.5.

Depending on the distance between the knots of the bamboo sections used for peeling, some veneers showed vertical lines, indicating the presence of knots, and some veneers were free of any knots and no lines were observed. The internode distance varied for various bamboo sections and ranged from 40cm to 80cm. Fig. 66 and Fig. 67 show some of the veneers with and without knots obtained in this research. The average width (along the fiber direction) of the veneer layers were between 75cm to 85cm and the average length (perpendicular to fiber direction) of the veneer layers ranged from 40cm to 120cm. The width and length of the veneer layers were largely dependent on the quality of the bamboo pieces used for peeling, mainly on the presence of any internal/external cracks.

For the production of composite samples, only bamboo sections with a minimum average tensile strength of 290MPa were used for veneer production. The veneer layers were kept in an air-circulated oven at 80°C until the moisture content reached not more than 10%, which had been discussed in section 5.2.1.as the optimum MC of the fiber bundles for fabricating the composite samples. To improve the active surface area of the veneer layers for composite fabrication, the layers were hand-pressed to create cracks/perforations along the fiber direction similar to the stranding methods employed for bamboo strip strands. However, due to lower thickness of veneer layers (0.40mm to 1mm) compared to strands (1mm to 3mm), the manual pressing was deemed sufficient to create the perforations along the fiber direction.

To evaluate the effect of cracks/perforations in the veneer layers on the mechanical properties of the composite samples, a series of experiments were designed in which bamboo veneer composite samples fabricated with and without cracks/perforations were evaluated for their tensile properties. The tests and their results are discussed in section 5.2. For bamboo composite fabrication, comparable amounts of veneer layers from classes 3, 4 and 5 samples with a minimum tensile strength of 290MPa were used.

The production of veneer layer in this research relies on a novel and inexpensive peeling machine developed mainly for this research which requires least amount of energy and maintenance in comparison with carbon fiber or glass fiber production where high-tech machineries and energy-intensive mechanical and chemical processes are involved.

Furthermore, the peeling machine is designed to process the bamboo culms via an innovative approach where the bamboo fibers remained intact and thus the inherent tensile properties of

the bamboo fiber bundles are protected throughout the whole process.

Fig. 66 Bamboo veneers without any knots in between

Fig. 67 Bamboo veneers with horizontal lines due to presence of knots

The peeling process has the advantage of producing thinner fiber bundles in comparison with stranding method, which can be useful when bamboo composite samples of thinner cross sections are required.

5.3. Bamboo composite materials fabrication

In this section, the methods and materials employed for the fabrication of bamboo fiber reinforced polymer composites are discussed. The epoxy-resin system and the two types of raw bamboo fiber bundles mentioned in sections 5.2.1 and 5.2.2 produced in this study are discussed. The results from mechanical testing of nearly 5,000 samples of bamboo composites fabricated with the two types of raw materials were compared in order to select the most efficient type of raw material for the production of high-performance bamboo composite reinforcement. The comparison study aimed to investigate only the tensile and flexural properties of bamboo composite samples made from bamboo strands and bamboo veneers. Therefore, only strands and veneers with lengths of 50cm and without knots between the fibers were used for this purpose. Following the test series, conclusions were made with regard to the advantages and disadvantages of each method, and the method which resulted in higher mechanical properties was chosen for the production of the bamboo composite reinforcement.

5.3.1. Epoxy-resin matrix

The composite material consisted of two parts: fiber and matrix, as discussed in the introduction. There are various types of matrix that can be used for composite fabrication. Polyester, vinyl ester, epoxy, phenolic, polyimide, polyamide, polypropylene and polyether ether ketone are some of the well-known matrices used in fiber reinforced polymer composites. The ratio of the matrix to fiber is an influential factor in the strength of the final composite. The lower the ratio of the matrix to fiber, the better the mechanical properties of the composite due to higher presence of fibers. The role of the matrix is to hold the dispersed fibers together and transfer the load to the fibers. The matrix phase of any fiber reinforced polymer composite can be classified as either thermoset or thermoplastic.

Thermosetting matrices, which include polyesters, vinyl esters, epoxies and polyamides, are commonly used in many types of fiber reinforced polymer composites. Among the various thermosetting matrices, the epoxy system is considered one of the high-performance systems used mostly for advanced composites with high qualities. The viscosity of the epoxy-resin system is low before being mixed with the fibers. Once the curing process takes place, the matrix turns into a stable structure. The curing process requires certain temperatures for it to be initiated. Once the curing process is initiated, the chemical reactions that take place in the matrix will crosslink the polymer chains of the thermoset system. Therefore, the entire matrix

links together in a three-dimensional complex system. This three-dimensional crosslinked network is responsible for the stability, high temperature resistance and higher performance of the thermoset matrices compare to thermoplastics. Thermoplastic matrices include some polyesters, polyphenylene sulfide and polyether ether ketone. Thermoplastic matrices consist of long molecule chains that normally melt at temperatures of around 200℃ to 350℃, depending on the length of molecular chains. Once the matrix is cooled down, it forms an unstructured, semi crystalline, or crystalline solid. The final matrix properties depend largely on the level of crystallinity of the structure. The major difference between thermoset and thermoplastic matrices is the curing process. Thermoplastic resins do not cure but rather undergo a reversible process in which reheating the structure allows the resin to be reshaped and deformed.

Thermoplastics, due to their temperature-sensitive characteristics and lower chemical stability compared with thermosets, are attractive to the automotive industries in which high volume manufacturing is important. Furthermore, thermoplastics are used commonly with short fiber reinforcement in composites where short natural or synthetic fibers are used mainly in applications, in which the strength and chemical resistance are not the main concerns, but rather the shape, form and manufacturing techniques. Therefore, for high-performance applications such as reinforcement in structural concrete where high strength and high resistance to chemicals are required, thermoset resins provide a better solution.

For the purpose of this research, a series of two-part epoxy resin systems were selected based on three main criteria. The selection process of the matrix was carried out in collaboration with the industrial partner (REHAU), given their expertise in polymer chemistry. The criteria for the selection of epoxy resin systems are as follow:

- Low Volatile Organic Compounds (VOCs) content

Volatile Organic Compounds (VOCs) include a variety of chemicals such as formaldehyde, benzene, ethylene glycol, methylene chloride, tetrachloroethylene, toluene and xylene; these are used in a variety of building materials such as paints, adhesives as well as home products such as cleaning agents and air fresheners. VOCs are normally released into the air as toxic gases which could have short- and long-term harmful health effects for people in close contact with sources of VOCs. The majority of wood-based building materials such as particleboards and plywood are produced by formaldehyde resins which have high VOCs content. Formaldehyde resins are one of the most common types of resins employed for the

production of molded and laminated materials in various industries. However, in 1987, the US Environmental Protection Agency (EPA) classified formaldehyde as a probable human carcinogen under conditions of high or prolonged exposure (Albert 1994). Therefore, for the purpose of this research, an epoxy-resin system free of formaldehyde resin and with low level of VOCs was chosen.

- Acceptable mechanical properties

In general, an epoxy-resin system shows superior performance over thermoplastic matrix as discussed earlier, but among the various available epoxy-resin systems not all have similar properties. Furthermore, among the mechanical properties, the tensile strength and modulus are crucial properties for the fabrication of bamboo composite materials employed as tensile reinforcement in concrete applications. The tensile strength and modulus of elasticity in tension of the epoxy-resin system can affect the overall load-bearing capacity of the bamboo composite reinforcement, and are therefore considered the most relevant mechanical criteria in choosing the right epoxy-resin system for the purpose of this PhD research.

- Sustainable epoxy resin systems

Most of the available epoxy-resin systems in the market contain petrochemical-based raw materials, including Bisphenol A and Epichlorohydrin. Therefore, a fully bio-based epoxy-resin system requires replacement of Bisphenol A and Epichlorohydrin with a bio-based element. Currently, there is no completely bio-based epoxy-resin system available in the market; however, research in this area is being carried out at a fast pace compared to the past decades, given the high emphasis on the application of raw materials from renewable recourses or from waste by-products in creating epoxy-resin systems. Therefore it is of great interest to the PhD candidate to look for epoxy resin-systems that could contribute to sustainable development and construction. Currently, only a few epoxy-resin systems are available in in the market which incorporate non-fossil bio-based raw materials as their chemical components. In search of a suitable epoxy-resin system, the PhD candidate considered these criteria and narrowed down the choice to four types of epoxy-resin matrices available in the market which could potentially be used for fabrication of the newly developed bamboo composite materials. The four epoxy-resin systems were:

- SUPER SAP® INF epoxy system
- SUPER SAP® CPM epoxy system

- SUPER SAP® 100/1000 System
- ARALDITE® AW 106 Resin and HV 953U Hardener epoxy system

SUPER SAP® epoxy systems, including the INF, CPM and 100/1000, are produced by Entropy Resins Inc. in the US. According to the manufacturer, these contain up to 40% bio-based and renewable contents sourced from waste materials such as wood pulp and bio-fuels production (Entropyresins 2012, Entropyresins 2013). The SUPER SAP® INF epoxy system is composed of Super Sap® CLR epoxy, a modified clear liquid epoxy resin, with Super Sap® INF as a hardener and, once cured, creates a clear, UV stabilized and low-viscosity system. The SUPER SAP® CPM system consists of Super Sap® CPM as epoxy, a modified, liquid epoxy resin and Super Sap® CPL as hardener. According to Entropy Resin Inc., the SUPER SAP® CPM system is a versatile epoxy system designed specifically for the compression molding fabrication of composite parts and therefore suitable for this PhD research. The SUPER SAP® 100/1000 system is composed of Super Sap® 100 as epoxy, a modified liquid epoxy resin and with Super Sap® 1000 as hardener. According to the technical data sheet of SUPER SAP® 100/1000, it has high bio-content and can cure at room temperature quickly. Furthermore, due to its medium viscosity and great adhesion to all substrates, it can be applied together with various type of fibers used in composite fabrication, including natural fibers (Entropyresins 2012, Entropyresins 2012, Entropyresins 2013).

The fourth type of epoxy-resin system investigated in this PhD research is the Araldite AW 106 as the epoxy resin and HV 953U as hardener. The Araldite epoxy adhesive is produced by Huntsman International Inc. and is a multi-purpose, viscous material. According to the manufacturer, it is suitable for bonding to a variety of materials, including metal, ceramic, and wood and therefore has the potential to be employed for the bamboo composite fabrication. It is claimed by the manufacturer that Araldite epoxy adhesive system is produced by using renewable raw materials, especially those derived from the waste products of other industries such as the paper and food industries (Huntsman International LLC 2011).

Table 19 shows selected properties of the described epoxy-resin systems investigated in this research, according to their respective data sheets. The Pot life in Table 19 is a standard term that refers to a defined time during which the viscosity of the mixed resin and hardener system doubles. In other words, it suggests the required time for the epoxy system to start curing and turns from the liquid phase to a gel-like phase. The bio-based content in Table 19 refers to the amount of bio-based carbon in the material as a percent of weight (mass) of the

total organic carbon in the material. ASTM has developed a standard approach to calculate the level of bio-based or renewable material included in a resin which is labeled "ASTM D6866 – Standard Test Methods for Determining the Bio-based Content of Solid, Liquid, and Gaseous Samples Using Radiocarbon Analysis". Although the Araldite® system is claimed to be produced by some content of renewable raw materials, the bio-based content of the system was not available from the manufacturer.

Table 19 Selected properties of epoxy-resin systems investigated in this research

	SUPER SAP® INF/CLR	SUPER SAP® CPM/CPL	SUPER SAP® 100/1000	AW 106 Resin HV 953U Hardener
Tensile Strength (MPa)	73	62	57	33
Modulus of elasticity in Tension (MPa)	4067	3006	2620	1880 - 2050
Modulus of rupture (MPa)	125	93	77	66 - 75
Modulus of elasticity in flexure (MPa)	3624	2845	2276	1810 - 2120
Compressive strength (MPa)	117	79	72	55 - 70
Mix ratio (by weight)	100 to 33	100 to 40	100 to 48	100 to 80
Mixed Specific Density	1.105	1.107	1.109	1.005
Pot Life at room temperature (minutes)	30	50	25	120
Min curing time @ 80℃ (minutes)	20	25	25	30
Required total curing time @ 25℃	7 days	7 days	7 days	6 days
Bio-based Content	19%	31%	37%	NA

In terms of tensile properties, the Super Sap® INF/CLR system stays at the top of the list due to its tensile strength of 73MPa and a tensile modulus of elasticity of 4,067MPa. It also has the highest flexural and compressive properties among the four types of epoxy systems shown in table 19. However, among the Super Sap® epoxy systems, the Super Sap® 100/1000 has the highest bio-based content of 37%, but at the same time, it shows the least mechanical properties among the three Super Sap® systems. The Araldite® system has the longest Pot life which could be an advantage in terms of production time over the Super Sap® systems during the bamboo composite fabrication where the hand-layup method is being used, by providing the PhD candidate with sufficient time to process and prepare the raw bamboo materials and mix them with the epoxy-resin system. Though the Araldite® system has lower performance indexes in terms of mechanical properties, it is considered one of the most widely used epoxy adhesive systems for applications with glass and carbon fibers, and therefore could potentially be used with bamboo fibers given its claimed bio-based contents.

To evaluate the performance of these four groups of epoxy adhesive systems together with bamboo fibers and subsequently employ the most suitable one for the fabrication of the bamboo composite reinforcement in this research, a preliminary study was carried out before moving towards the final bamboo composite optimization methods. In section 5.3.2, bamboo strips (before making the perforations) were used together with these four epoxy adhesive systems and their tensile properties evaluated according to ASTM standard test methods. The tests and their results are presented in the next section.

The next section explains two methods for the fabrication of bamboo composite materials – one with bamboo strands and one with bamboo veneers. A comparison of the most important mechanical properties, including tensile and flexural properties, was carried out. The method which achieved higher mechanical properties of bamboo composite was used for the production of bamboo composite reinforcement for structural concrete beam design and testing. The two methods are referred to as bamboo strand composite and bamboo veneer composite.

5.3.2. Bamboo Strand Composite (BSC)

In this section, the methods employed for the fabrication of the composite samples from the bamboo strands are explained. The effects of the various thicknesses of the bamboo slats and the presence of grooves/linear cracks, through the stranding method as discussed in section 5.2.1, on the tensile properties of the Bamboo Strand Composite (BSC) samples are investigated in this section. Furthermore, the four types of the epoxy adhesive systems discussed in section 5.3.1 were used together with the bamboo strands, and the tensile properties of the composites were investigated to find the most suitable epoxy-resin system for the fabrication of the bamboo composite reinforcement. For the bamboo composite fabrication, comparable amounts of strands from classes 3, 4 and 5 samples with a minimum average tensile strength of 290MPa were used, as discussed earlier in section 5.2. Tensile properties including tensile strength and modulus of elasticity in tension were measured according to ASTM D3039-08, "Standard Test Method for Tensile Properties of Polymer Matrix Composite Materials" (ASTM International 2014). This standard was chosen due to the lack of specific international standards for the measurement of tensile properties of newly developed bamboo composite materials. Furthermore, this standard is the most relevant available scientific standard for the evaluation of tensile properties of composite samples.

Investigating the type of epoxy resin systems

In this section, the four types of epoxy-resin systems mentioned in section 5.3.1 are used together with the bamboo slats to investigate the tensile properties of the composites produced. To minimize the other parameters contributing to the tensile parameters, such as the presence of grooves or varying thicknesses, only bamboo slats with the minimum achievable thickness of 1mm and without any grooves or preformation were used. The effects from grooves and varying thicknesses had been investigated in separate studies discussed in this section.

The bamboo slats produced in section 5.2.1 were first dried in an air-circulated oven at 80°C until the moisture content was less than 10%, as explained in section 5.2.1. The moisture content was measured according to the ASTM D4442-07 standard test and by using Eq. 22. The slates were then passed through the flaking machine to produce bamboo strips with a thickness of 1mm ± 0.1mm. The epoxy resin and the hardener of each type of the four systems described in section 5.3.1 were mixed by the ratios recommended by the manufacturers showed in Table 19. For the investigation of the epoxy systems, 2,000gr of bamboo strips were mixed with sufficient amounts of each epoxy system. Once the epoxy matrix mix was prepared using the required ratio of resin and hardener, the bamboo strips were first impregnated by the mix. Every single strip was checked thoroughly for dry surfaces and necessary wetting with epoxy mix was further carried out to ensure that a homogenous layer of epoxy system had covered all the bamboo strips. The presence of dry surface is a sign of insufficient wetting or inadequate impregnation of the strips which could result in weak interface bond between the bamboo fiber bundles and epoxy system during composite fabrication. A weak interface bond, as explained in section 5.3.1, translates into a weaker interfacial shear strength; this is responsible for transferring the loads from the matrix to the fibers and vice versa. Therefore, careful impregnation and wetting process of the strips were carried out to ensure a better interface bond between the bamboo fiber bundles and epoxy system, as it ultimately contributed to the overall mechanical strength of the bamboo composite sample. The required amount of the epoxy resin system was measured only after applying adequate amounts of the epoxy system to the bamboo strips during the impregnation process to ensure sufficient wetting of the strips and further control of the impregnation process of the bamboo strips during production. Subsequently, after the composite fabrication, the actual amount of epoxy used was calculated by measuring the density of the final composite sample. It was observed that the epoxy-resin system in general made up 15%

to 18% by weight of the final bamboo composite sample, while the bamboo strips made up the other 82% to 85%. The explicit ratio (mass) of the bamboo strips to the epoxy-resin system is presented for each type of epoxy system in Table 20.

The epoxy-impregnated bamboo strips were then aligned along the fiber direction and assembled layer by layer on top of each other through a hand lay-up technique for the fabrication of bamboo composite sample. For the purpose of this research, only continuous unidirectional bamboo composite samples were prepared by aligning the strips along the fiber direction. The bamboo fiber orientation impacts the mechanical properties, especially the tensile strength and tensile modulus of elasticity, which are of the great interest to this research given the final application of bamboo composite materials as reinforcement systems in structural concrete. The longitudinal reinforcement bars in a concrete beam are effective when they are loaded along the main load-carrying axis which would be the fiber direction. Therefore, when a unidirectional continuous bamboo fiber composite material is loaded in a direction parallel to its fibers, the maximum strength and stiffness (modulus) can be obtained, as explained in various composite manufacturing textbooks and references (Strong 2008, Rohit and Dixit 2016). Unlike short bamboo fiber reinforced composites in which randomly oriented bamboo fibers are mixed with an adhesive (e.g. epoxy) to form a composite sample, the unidirectional continuous bamboo fiber composites are produced by carefully orienting the fiber bundles along their longitudinal axis to take advantage of the axial stiffness and strength provided by the bamboo fibers, as explained earlier in section 3.3.2.

A simple yet effective semi-automatic hot-press compression molding machine was employed for this research; it had a maximum pressure of 25MPa supported by three hydraulic cylinders and a maximum temperature of 140°C as shown in Fig. 68. The U-shaped mold designed in this study had a dimension of 150mm (width) by 1,800mm (length) and was made of heat-treated stainless steel for better hardness and lower deformation over time.

A hand lay-up technique was used for producing the composite sample as shown in Fig. 69. For this purpose, the bamboo strips were firstly impregnated with the desired type of the epoxy resin matrix, and secondly the layered impregnated bamboo strips (or veneers) were placed into the mold of the hot-press machine. To minimize the effect of inner nodes on the strength of final bamboo composite samples, only strips without knots in between were selected for the comparison study. The hot-press compression molding machine operated at various combinations of temperature, pressure and time. A detailed study of these parameters

and their influence on the mechanical properties of the bamboo composite materials developed in this research was carried out in a separate study discussed in section 5.4. The temperature required for the epoxy systems to cure and form the necessary crystalline structures within the composite sample were recommended by the manufacturers. However, according to the data sheets of each type of epoxy system and as recommended by the manufacturers, a minimum temperature and least amount of time were required for the chemical reactions contributing to the curing process to be initiated. Therefore, the combination of time and temperature could be fine-tuned to achieve the optimum properties of the final composite sample as discussed in section 5.4. Besides the temperature and time, the applied pressure has considerable effects on the mechanical properties of the bamboo composite sample via improving the fiber density of the composite through introducing homogenous forces along the surface of the strips and binding the fiber bundles together with the epoxy system. By increasing the number of bamboo fibers in a specific surface cross section of the composite sample, and therefore improving the fiber density, there would be more unidirectional fibers to withstand the applied loads and therefore enhancing the ultimate mechanical properties of the bamboo composite sample. As such, the applied pressure from the hot-press compression molding machine is beneficial in increasing both the fiber density and mechanical properties of the final bamboo composite sample.

Furthermore, the applied pressure facilitated the penetration of the epoxy system through the layers of the bamboo strips to ensure that all the fiber bundles were fully covered by the epoxy matrix. The epoxy matrix contributed to the overall integrity of the composite material by holding the bamboo fibers in place and ensuring a smooth load transfer between the matrix and fibers. Therefore, it is crucial to have the epoxy system interact perfectly with the bamboo fibers within the composite microstructure as discussed in this section as well as section 5.4.

However, for the preliminary studies in this section, only one combination of temperature, time and pressure was chosen to minimize any coupling effects of pressure and temperature as well as duration of pressing on the results of this preliminary investigation. The chosen temperature for the preliminary investigation was 80°C, which was the minimum applied temperature as discussed in detail in section 5.4. Temperatures lower than 80°C (e.g. 70°C) were insufficient for the curing process of the epoxy matrix to be initiated within the timeframe of the specified Pot life for each type of epoxy systems as shown in Table 19. Therefore temperatures lower than 80°C were not investigated further in this thesis. The

pressure applied was set to 12MPa for the preliminary study. The aim of the study was to find the suitable epoxy systems among the four types, therefore only one pressure parameter was chosen. Pressures lower than 11MPa were not sufficient to bind the bamboo strips with epoxy systems and the composite samples produced disintegrated due to lack of adequate adhesion between the layers of the bamboo fiber bundles. Therefore pressures lower than 11MPa were not further investigated in this research as explained in section 5.2.1. On the other hand, the higher pressures would enhance the mechanical properties of the composite samples through the mechanisms explained earlier. Therefore, to achieve a high-performance bamboo composite reinforcement which retains the maximal obtainable mechanical properties, higher pressures are favorable.

Another important factor in achieving a high-performance polymer composite is the time required for curing and post-curing as explained in section 5.3.1. The time required for pressing the epoxy-impregnated bamboo strips was selected in combination with the applied temperature, the Pot life of each epoxy system, employed pressure and by considering the manufacturers' recommendations for curing the epoxy systems. The total time required for pressing the impregnated bamboo strips with the hot-press compression molding machine was divided into two distinct time periods for curing and post-curing.

Fig. 68 Hot-press compression molding machine at AFCL Singapore

Fig. 69 Hand lay-up process for composite fabrication

During the first curing timeframe, the epoxy system could be cured primarily by providing the required heat for initiating and maintaining the chemical reactions in which the epoxy

resin and the hardener could react, and necessary modifications into the molecular structure could occur. The combination of applied pressure and temperature further stimulated the two parts of the epoxy system, mainly the hardener and the resin, to start to react and form the crystalline networks within the composite microstructure. The second curing timeframe, which is called post-curing, together with the applied pressure provided the necessary force required to further compact and compress the bamboo strips and also remove the entrapped bubbles of air and voids to ensure the final composite had the least amount of voids. The presence of voids or bubbles might ultimately cause a reduction in the overall performance of the final composite sample by weakening the interface bond between the epoxy matrix and bamboo fibers which, as explained earlier, is responsible for the continuous load transfer between the matrix and fibers. Furthermore, the post-curing time frame supported the continuation of the chemical reactions between the hardener and resin to ensure that the crosslinks between the bamboo fibers and the epoxy molecular system form uniformly and completely. The first curing timeframe was set to 15min and the pressure was maintained at 12MPa. The second timeframe, for post-curing, was set similarly to 15min but with lower pressure of 5MPa. The lower pressure in the second step was chosen according to the hot-press manufacturer's recommendation to maintain the minimum operating pressure at 5MPa to prevent potential damage to the hydraulic pump of the machine while pressing the samples for the specific duration. Otherwise lower pressure could be used since the post-curing pressure functioned mainly as degasification of the final bamboo composite sample.

Fig. 69 shows the final bamboo composite board produced with the strips after pressing with the hot-press machine. The final board had a dimension of 150mm (w) $\times$ 1500mm (l) $\times$ 10mm (t). Table 20 shows the density of the final bamboo composite samples and the content of each type of the applied epoxy-resin systems.

Table 20 Specific density and epoxy content of bamboo strip composite samples

	Type of epoxy system used for bamboo strip composite sample			
	SUPER SAP® INF/CLR	SUPER SAP® CPM/CPL	SUPER SAP® 100/1000	AW 106 Resin HV 953U Hardener
Bamboo composite specific density	1.42	1.44	1.47	1.36
Epoxy content (% of composite mass)	16.8	16.3	15.8	17.7

Before preparing the bamboo composite samples into suitable shapes to measure the tensile properties, a second post-curing process was carried out for 48 hours at 55°C at an air-circulated curing oven. The curing oven works by circulating the heated air through a heating compartment, where air is heated and the heated air is circulated inside the oven through circular fans. The humidity is controlled by means of humidity sensors to limit the ingress of moisture into the composite samples during the curing process. This additional post-curing process was performed to fulfill the total curing time recommended by the manufacturers of the epoxy systems as shown in Table 19. The recommended total curing time was to ensure that the optimal cross-link networks were fully developed at the recommended temperature by providing the essential energy to give the epoxy molecules the flexibility needed to move, and to fully form the networks within the microstructural cross sections of the epoxy matrix (Vyazovkin and Sbirrazzuoli 1996).

Fig. 70 shows the final bamboo composite board after pressing with the hot-press machine.

Fig. 70 Bamboo strand composite board after pressing

The curing and post-curing process would ensure that the final composite board could reach its full mechanical capacities by maintaining its high crosslink networks. Once the curing process was over, the bamboo strand board composite board was cut into various shapes according to ASTM standards for measuring its tensile properties as well as density. Table 21 shows the results of the tensile properties for various types of epoxy matrix used in this investigation together with their respective standard deviations. For each test and for each type of epoxy system used during production, at least 5 samples were prepared into

appropriate shapes, and the results shown in Table 21 are the average properties of those samples.

Table 21 Tensile properties of the bamboo composite sample produced by various types of epoxy systems

Type of Epoxy used	Tensile Strength (MPa)	Modulus of elasticity in Tension (MPa)
SUPER SAP® INF/CLR	302±18	28443±1665
SUPER SAP® CPM/CPL	289±21	27102±2168
SUPER SAP® 100/1000	291±26	27001±2412
AW 106 Resin HV 953U Hardener	295±23	28024±2588

As shown in Table 21, the bamboo composite boards produced with Super Sap® INF/CLR epoxy system showed the highest tensile strength of 302MPa and highest modulus of elasticity in tension of 28,443MPa. Furthermore, the one-way Anova test of variances showed there was no significant difference between the means of tensile strength and means of modulus of elasticity in tension of the samples fabricated with the Super Sap® CPM/CPL and Super Sap®100/1000 epoxy systems. The Araldite epoxy system showed the second highest tensile properties of the bamboo composite samples within the four selected epoxy systems. However, when it comes to selecting the right epoxy systems for the rest of the research, Super Sap® INF/CLR epoxy system was chosen for two reasons:

1- It showed the highest tensile properties, including tensile strength and modulus of elasticity. Tensile properties, as explained earlier in this chapter as well as in chapter 3, are crucial for the development of bamboo composite reinforcement systems for structural concrete. Furthermore, the tensile properties results showed an improvement of around 10% in both tensile strength and modulus of elasticity of the composite samples compared to the raw bamboo properties. This proved that the chosen epoxy system, and the methods of processing of the raw bamboo and fabrication techniques used in the production of the bamboo composite sample were able to maintain or further enhance the properties of the bamboo fiber bundles through the newly developed bamboo composite.

2- The Super Sap® INF/CLR epoxy system has 19% of mass bio-based contents which makes it a suitable choice of epoxy systems over traditional petrochemical-based epoxy systems for the production of the newly developed bamboo composite material.

Therefore, over the next sections, only the Super Sap® INF/CLR epoxy system was used for the production of newly developed bamboo composite materials in this research.

Investigating the effect of bamboo strip thickness

The bamboo slats produced in section 5.2.1 showed thicknesses in the range from 1mm to 3mm as the range achievable by the flaking machine. To investigate the suitable thickness to attain the optimum mechanical properties from the final bamboo composite sample, the obtained strips were divided into three thickness groups covering the whole range of obtainable thickness by the available machine at AFCL. The three groups were:

- Strips with thickness of 1mm ± 0.1
- Strips with thickness of 2mm ± 0.2
- Strips with thickness of 3mm ± 0.3

As explained in the previous section on the production method of the composite sample, first of all, the strips were dried in an air-circulated oven to reach an equilibrium MC of less than 10%. The strips were then aligned along the fiber direction for the production of the uni-directional bamboo composite sample. The Super Sap® INF/CLR epoxy system was used as the matrix. Once the hardener and resin were mixed according to the ratio given in Table 19, they were used to impregnate the strips. The layered impregnated bamboo strips were placed into the mold of the hot-press machine as shown in Fig. 68 and Fig. 69. The bamboo strips were pressed at a temperature of 80°C by maintaining a pressure of 12MPa for the first 15min, followed by a pressure of 5MPa for an additional 15min, as described in detail in the previous section. Once the pressing was completed, the boards were post-cured for 48 hours at a temperature of 55°C and subsequently prepared into suitable shapes to measure their tensile properties. For each thickness of bamboo trips, 2,000gr of strips were used for the fabrication of the bamboo composite boards. Three boards were produced per thickness level. Furthermore for each test, at least 5 samples were prepared from each and tested according to the ASTM standard. Table 22 summarizes the properties of the final composite boards after measuring their tensile properties, density and epoxy content.

Table 22 Properties of the final bamboo composite boards produced with different strip thicknesses

	Thickness of bamboo strip (mm)		
	1	2	3
Tensile Strength (MPa)	304 ± 15	289 ± 21	272 ± 29
Modulus of elasticity in tension (MPa)	28851 ± 1804	25540 ± 2155	24188 ± 2581
Specific density	1.41	1.42	1.41
Epoxy content (% of composite mass)	17.1	16.2	15.3

As shown in Table 22, the bamboo composite samples produced with 1mm thick strips showed the highest tensile strength of 304MPa and the highest modulus of elasticity of 28,851MPa. Strips with thickness of 3mm had the lowest tensile properties. Furthermore, table 22 suggested that by increasing the strips thickness from 1mm to 3mm, the standard deviations of the results for both tensile strength and modulus of elasticity in tension of the bamboo composite boards tended to increase. By increasing the thickness of strips used during the composite fabrication, the amount of epoxy system applied for impregnation was also reduced from 17.1% to 15.3% of the composite mass. The reduction in tensile properties of the bamboo composite sample via using thicker strips could be explained by the lower fiber specific surface area and the lower fiber aspect ratio both contributing to the loss of tensile properties.

The lower content of the epoxy matrix used with thicker bamboo strips could also be explained by the fact that 2,000gr of bamboo strips with thinner sections resulted in more strips, given the similar specific density of the raw bamboo samples used within this investigation. Therefore, to impregnate thicker strips in which fewer numbers of strips were available, a lower content of epoxy matrix was required.

Thus to continue with the research and to further enhance the mechanical properties of the final bamboo composite samples, strips with an average thickness of 1mm ± 0.1mm were used. All the thicker strips produced in section 5.2.1 were passed through the flaking machine several times till the required thickness was obtained.

Investigation of the effect of strips with grooves on tensile properties

As discussed earlier in section 5.1.1, following the flaking process, the bamboo strips went through a mechanical process called stranding which was shown in Fig. 60 and Fig. 61. The

stranding process aims to improve the surface characteristics of the strips by creating linear cracks/grooves along the fiber direction. These linear cracks/grooves could improve the specific surface area of the bamboo strips and interact better with the epoxy matrix during the composite fabrication as explained in sections 5.2.1 and 5.3.1.

For this investigation, only bamboo strips with thickness of 1mm ± 0.1mm were used, since they displayed better tensile properties compared to thicker strips, as shown in the previous section. Both sides of the strips were passed through the stranding machines to ensure grooves were created on both sides of the raw bamboo strips. Subsequently, the bamboo strips with grooves, or so-called bamboo strands, were further dried to reach an equilibrium MC of less than 10%. Once dried, 2,000gr of bamboo strands were impregnated with the Super Sap® INF/CLR epoxy system. The impregnated bamboo strands were pressed at a temperature of 80°C by maintaining a pressure of 12MPa for the first 15min, followed by a pressure of 5MPa for an additional 15min. Once the pressing was completed, the bamboo strand composite boards were post-cured for 48 hours at a temperature of 55°C as described earlier. The final composite board after post-curing was prepared into the shapes required by the ASTM standard for measuring its tensile properties. For each tensile property, at least 5 samples were tested and the average results displayed in Table 23.

Table 23 Tensile properties of bamboo composite samples produced with strands

	Type of bamboo strips used	
	No grooves	With Grooves
Tensile Strength (MPa)	304 ± 15	317 ± 11
Modulus of elasticity in tension (MPa)	28,851 ± 1804	29,705 ± 1812
Specific density	1.41	1.40
Epoxy content (% of composite mass)	17.1	17.9

As shown in table 23, both the tensile strength and tensile modulus of elasticity of the composite samples were increased by employing the strands where grooves were created through the stranding machine on the surface of the strips. The increase in tensile properties could have been the result of the enhanced specific surface area of the bamboo strips through stranding, as well as improved interaction between the fiber bundles and epoxy matrix. The pressure applied via the hot-press compression molding machine further forced the epoxy matrix to go through the perforations and grooves and penetrate deeper into the strand layers,

thus creating a strong interface. Therefore, in this case, the strong interface resulted in better mechanical properties compared to composite samples produced via only using the bamboo strips without grooves. The better interface layer also translated to a smooth and continuous load transfer between the fiber bundles and the epoxy matrix, which is crucial for the performance of the composite in any load-bearing applications in long-term. As shown in this section, the improvements in both tensile strength and modulus of elasticity of the bamboo strand composite samples were made through incorporating the right type of epoxy system, employing the suitable thickness for the raw bamboo strips, and finally by enhancing the surface characteristics of the raw bamboo fiber bundles through stranding the bamboo split. Fig. 71 and Fig. 72 show the tensile strength and modulus of elasticity of the bamboo strand composite samples and the improvements made through the investigations in this section.
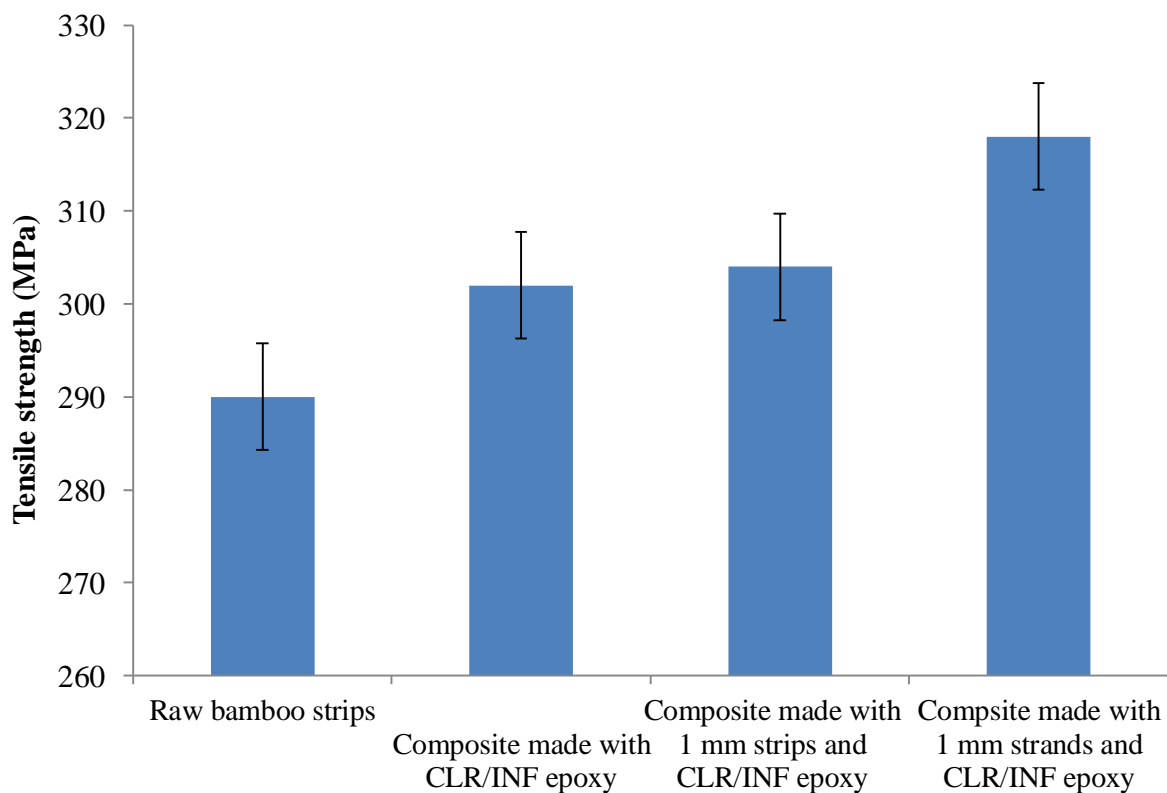
Fig. 71 Improvement in tensile strength of bamboo strand composite samples
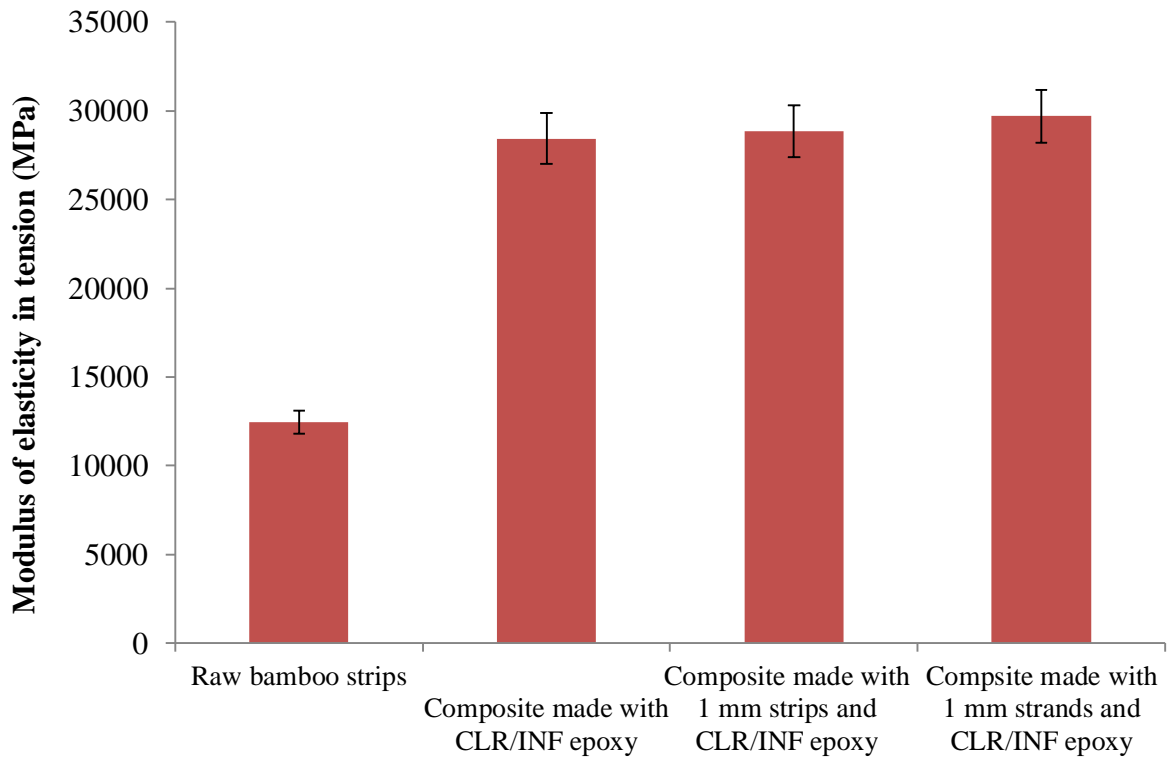
Fig. 72 Improvement in tensile modulus of elasticity of bamboo strand composite samples

5.3.3. Bamboo Veneer Composite (BVC)

In this section, the methods employed for the fabrication of unidirectional bamboo composite samples with bamboo veneer layers are explained. In addition, the effects of various thicknesses of the veneer sheets and the presence of grooves/linear cracks, as discussed in section 5.2.2 on the tensile properties of the Bamboo Veneer Composite (BSC) samples, are investigated in this section. For bamboo composite fabrication, comparable amounts of veneer sheets from classes 3, 4 and 5 bamboo samples with a minimum average tensile strength of 290MPa are used, as discussed earlier in section 5.1. Tensile properties, including tensile strength and modulus of elasticity in tension, were measured according to the ASTM D3039-08, Standard Test Method for Tensile Properties of Polymer Matrix Composite Materials (ASTM International 2014), as also discussed in the previous section on the BSC sample production and evaluation.

Investigating the effect of veneer thickness

As described in section 5.2.2, bamboo veneer layers produced within this study with the available peeling machine (Fig. 63 and Fig. 64) had thicknesses in the range of 0.40mm to 1mm. Therefore, to evaluate the effect of various thicknesses of the veneer sheets on the

189

mechanical properties of the final bamboo veneer composite sample, the obtained veneer layers were divided into four thickness groups, similar those of the bamboo strip samples studied in the previous section, covering the whole range of obtainable thickness. The four groups are as follow:

- Veneer layers with thickness of 0.40 ± 0.04mm
- Veneer layers with thickness of 0.60 ± 0.06mm
- Veneer layers with thickness of 0.80 ± 0.08mm
- Veneer layers with thickness of 1.00 ± 0.10mm

The veneer layers were first dried, similar to what the bamboo strands underwent, in an air-circulated oven at 80°C until the moisture content was less than 10%. The moisture content was measured according to the ASTM D4442-07 standard test and by using Eq. 22, and with some modifications according to the thickness of the layers compared to the bamboo strands. The bamboo veneers were then sorted according to their thickness. Fig. 73 shows some of the veneer layers obtained during the peeling process, sorted according to their thicknesses. The veneers with inner nodes were separated from the rest of veneer layers, and only veneer layers without knots were used for the composite fabrication to minimize the effect of knots on the final mechanical properties for the comparison with the bamboo strand composite samples. The effect of knots on the tensile properties of final bamboo veneer composite sample was studied separately in section 5.5.

For each group of veneer thickness, the veneer layers were first prepared into rectangular sheets with an average length (perpendicular to fiber direction) of 150mm and an average width (along the fiber direction) of 750mm. The selected length of 150mm fitted perfectly into the steel mold of the hot-press that had a width of 150mm. The width of 750mm was also chosen given the range of the available widths of the veneer layers as discussed in section 5.2.2. The Super Sap® INF/CLR epoxy system was used as the matrix as it showed better performance in the previous section when used with bamboo strands. In this section, only veneer layers without perforations and cracks were used for the fabrication of the BVC sample. Once the resin and hardener of the Super Sap® INF/CLR epoxy system were mixed in the ratios given in Table 19, each veneer layer was impregnated with the epoxy matrix and aligned along the fiber direction. The impregnated veneer layers were stacked on one another to form a layered structure similar to the bamboo strand composite production. For each thickness group, 5 boards were produced. For each board, 2,000gr of bamboo veneer layers were mixed with a sufficient amount of epoxy system to ensure comparable results within the boards with various veneer thickness could be obtained, and so that further comparisons with bamboo strand composite samples could be made. A roller was used to further spread the epoxy system on the surface of each veneer layer and to ensure all the layers were sufficiently wetted by the epoxy system before stacking the other layers. The explicit amount of the

191

epoxy system used was obtained after final bamboo composite samples were produced by measuring their final density.

The layered impregnated bamboo veneers were placed into the mold of the hot-press compression molding machine along the fiber direction and pressed at a temperature of 80°C by maintaining a pressure of 12MPa for the first 15min followed by a pressure of 5MPa for an additional 15min, as described in detail in section 5.2.2. The boards were finally post-cured for another 48 hours at a temperature of 55°C and then prepared into the suitable shapes to measure their tensile properties. Fig. 74 shows one of the unidirectional bamboo veneer composite boards after it was removed from the hot-press mold.

Fig. 74 Bamboo veneer composite board

Table 24 shows the results of the tensile properties for the four groups of thickness of veneer layer types used in this investigation, together with their respective standard deviations. For each thickness group, 5 boards were produced and from each board, at least 5 samples were prepared into appropriate shapes; the results shown in Table 24 are the average properties of those samples.

Table 24 Properties of the Bamboo Veneer Composite boards

	Thickness of bamboo veneer (mm)			
	0.40	0.60	0.80	1
Tensile Strength (MPa)	335 ± 25	326 ± 28	322 ± 31	320 ± 24
Modulus of elasticity in tension (MPa)	33155 ± 2149	32448 ± 2288	31885 ± 2157	31447 ± 2581
Specific density	1.34	1.36	1.37	1.41
Epoxy content (% of composite mass)	16.4	16.1	16.7	16.5

As shown in Table 24, the tensile strength of the bamboo veneer composite samples was the highest when veneer layers with an average thickness of 0.40mm were used during production. Similarly, the modulus of elasticity of the samples produced by the veneers layers having an average thickness of 0.40mm was the highest among the various thicknesses of veneer employed for the fabrication of BVC boards. By reducing the veneer thickness from 1mm to 0.40mm, an increase of more than 5% in both tensile strength and tensile modulus of elasticity of the BVC samples was observed. BVC samples produced with 1mm-thick veneer layers displayed similar tensile strength to BSC samples produced with 1mm-thick strands, as shown in Table 23. However, BVC samples fabricated with 1mm-thick veneer layers showed an increase of 7% in the modulus of elasticity compared to BSC samples with similar thickness of strands. There was no significant change in the epoxy content used during the fabrication of the BVC samples with various thicknesses. The specific density of the samples did not show any significant change along with the increase in the thickness of the veneer layers.

The increase in tensile properties by incorporating thinner veneer sheets can be explained by the higher fiber density of the BVC samples produced. The thinner sections have lower lignin content compared to thicker sections, as discussed in the literature as well as in section 5.2 in detail. Through the peeling process in section 5.2.2, the lignin matrix, which is considered the weakest part of the bamboo microstructure, was further broken and destabilized through the peeling process. Subsequently, some of the lignin networks fell apart, but not the cellulose fibers due to their higher stiffness and strength compared to lignin matrices. Therefore by employing the thinner veneer layers which contained higher cellulose fiber content and less lignin matrix for the fabrication of BVC samples though the compression molding technique, samples with higher fiber density could be produced. Higher fiber density, as explained in

section 5.2, contributed to the higher mechanical properties, especially in the tensile strength and tensile modulus of elasticity as shown in Table 24.

Investigation of the effect of perforation/linear cracks on tensile properties

As discussed in section 5.2.2, the surface characteristics of the veneer layers could be improved through the peeling process, by reducing the thickness as shown in the previous section, as well as through creating linear cracks and perforations similar to the stranding method. Therefore, in this section, veneer layers with an average thickness of 0.40mm were further manually pressed to create the perforations and linear cracks.

To fabricate the BVC samples, the perforated veneer layers were firstly dried in the oven to reach an equilibrium MC of less than 10%. Once dried, to obtain comparable results with the previous sections, 2,000gr of perforated veneer layers were prepared. Subsequently the layers were impregnated with the Super Sap® INF/CLR epoxy system, as this epoxy system exhibited the highest tensile properties in the previous sections. The impregnated veneer layers were ultimately pressed at a temperature of 80°C by maintaining a pressure of 12MPa for the first 15min followed by a pressure of 5MPa for an additional 15min with the hot-press compression molding machine. Once the pressing was completed, the bamboo veneer composite boards were post-cured for an additional 48 hours at a temperature of 55°C. The final composite board after post-curing was cut into the shapes required by the ASTM standard for measuring the tensile properties. The tensile strength and tensile modulus of elasticity, together with density and epoxy content of BVC samples with and without perforations, are displayed in Table 25. At least 5 samples were tested for the tensile properties, and the results shown in Table 25 are the average values together with their respective standard deviations.

Table 25 Properties of the BVC samples produced with perforated veneer layers

	Type of veneer layer used	
	No perforations	With perforations
Tensile Strength (MPa)	335 ± 25	347 ± 31
Modulus of elasticity in tension (MPa)	33155 ± 2149	35214 ± 1812
Specific density	1.34	1.35
Epoxy content (% of composite mass)	16.4	16.9

As shown in Table 25, the tensile strength of the BVC samples was enhanced by more than 4% and the modulus of elasticity increased by more than 6% when perforated veneer sheets were used for the fabrication of the BVC samples. No significant change in specific density or epoxy content used for the production was observed compared to non-perforated veneer composite samples. The results obtained in this investigation further validated the discussions in section 5.2 and 5.3.2 regarding the relationship between the surface characteristics of the raw bamboo fiber bundles and the optimum mechanical properties of the bamboo composite sample. The cracks/perforations function in two ways:

- Increasing the specific surface area and the surface roughness of the veneer sheets
- Providing pathways for the epoxy system to penetrate deeper into the inner layers of the stacked veneer sheets through applied pressure

In both ways, the interfacial bond between the bamboo fiber bundles and the epoxy matrix is enhanced, which results in better load transfer between the matrix and the fibers. Therefore higher mechanical properties of the composite can be achieved through continuous transfer of stress in the microstructural level of the bamboo veneer composite samples. This smooth load transfer ensures that the bamboo fibers used in the composite are fully activated to their maximum tensile capacities without any disruptions arising from weak interfacial bonds.

Therefore, for the comparison of the BVC and BSC samples in the next section, veneer layers with average thickness of 0.40mm and with perforations were used to achieve high-strength BVC samples.

5.3.4. Comparison study of bamboo veneer and bamboo strand composite

In previous sections, novel techniques were employed to enhance the mechanical properties of both BVC and BSC samples. The methods employed included the reduction of the thickness of the strands and veneer layers, creating perforations and linear cracks in both the strands and veneer layer, and finally in choosing the right epoxy matrix. All these novel methods and new materials resulted in improved mechanical properties for both the BVC and BSC samples. In this section, the optimum conditions previously discussed had been employed to produce comparable bamboo composite samples from veneer layers and strands. The goal of this comparison study is to evaluate the performance of bamboo composite samples produced with strands in comparison with samples produced with veneer layers. The comparison of the two different fabrication methods (veneer vs. strand) were carried out through investigating the tensile and flexural properties of composite samples produced with

comparable conditions, as discussed in the previous sections. The method with superior mechanical properties was chosen for the production of the final bamboo composite materials to be used as reinforcement for structural concrete beams in chapter 6. For the comparison study in this section, 5 BVC boards and 5 BSC boards were produced. For the production of the composite boards, 2,000gr of perforated dried veneer layers (for the BVC board) and 2,000gr of bamboo strands (for the BSC board) with an average MC of less than 10% and with no knots were mixed with Super Sap® INF/CLR epoxy systems and pressed with the hot-press compression molding machine at a temperature of 80°C, by maintaining a pressure of 12MPa for the first 15min followed by a pressure of 5MPa for an additional 15min, as described in detail in the previous sections. After post-curing for an additional 48 hours at a temperature of 55°C, the boards were processed into appropriate shapes according to the ASTM standards for tensile and flexural property tests discussed in the following sections. In this comparison study, 5 BVC and BSC boards were produced, and at least 5 samples were tested from each board for each tensile or flexural property.

Tensile properties

Tensile properties, including tensile strength and modulus of elasticity in tension, were measured according to ASTM D3039-08, "Standard Test Method for Tensile Properties of Polymer Matrix Composite Materials" (ASTM International 2014). This standard has been chosen due to the lack of a specific international standard for the measurement of tensile properties of newly developed bamboo composite materials. This standard is also considered the most relevant available scientific standard for the evaluation of tensile properties of composite samples. The tensile strength test sample was prepared from the composite boards by cutting rectangles of 280mm × 15mm × 10mm, as shown in Fig. 75.

Fig. 75 Samples for tensile properties measurement

The two ends of the tensile sample were glued to fiberglass sheets to enhance the friction between the grips of the Universal Testing Machine (UTM) and the composite sample. This method ensured that failure would only occur in the middle third section of the samples and no failure would occur in the grips of the samples, as recommended by the ASTM standard as an acceptable mode of failure. The additional fiberglass sheets simply provided necessary protection against the pressure applied by the metal bites of the UTM grips during the tensile test. The Shimadzu AG-IC 100kN UTM was employed with a loading rate of 1mm/min. The loading rate was in compliance with the ASTM standard. The tensile strength was calculated by recoding the ultimate load at failure and measuring the cross-sectional area of the test sample according to Eq. 25.

The modulus of elasticity in tension along the fiber direction was measured using an axial extensometer with a gauge length of 100mm, to determine the strain and obtain stress-strain curves as shown in Fig. 76. The gauge length is simply the length of the section of sample measured for its strains by the available extensometer. From each composite board, 5 specimens were tested for their tensile properties and results exceeding a 10% standard deviation range, which has been statistically set as the confidence interval, have been discarded.
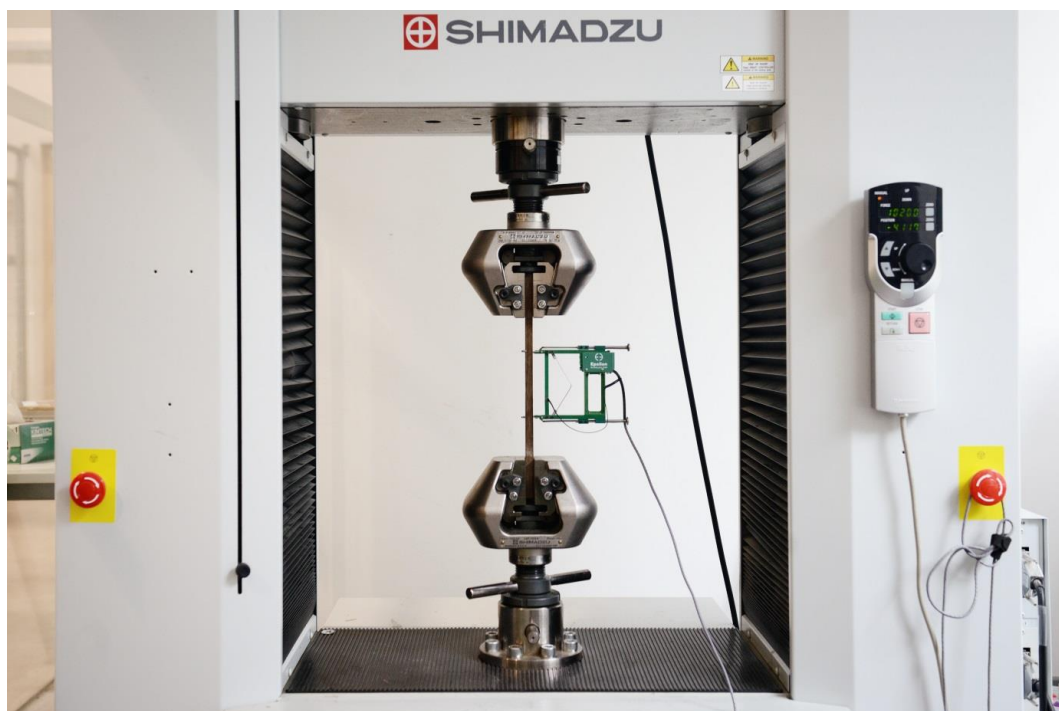
Fig. 76 Tensile strength and modulus of elasticity measurements of composite boards

Table 26 summarizes the results of the tensile properties of the bamboo veneer composite and bamboo strand composite samples. The comparison of the properties is also depicted graphically in Fig.77 and Fig.78.

Table 26 Tensile properties of bamboo composite boards produced with veneer and strand

Board	Modulus of elasticity in Tension (MPa)		Tensile strength (MPa)	
	BVC	BSC	BVC	BSC
1	34,230	29,340	344	298
2	35,051	28,451	349	320
3	34,404	28,740	340	315
4	35,301	28,852	341	322
5	35,890	29,903	345	311
Average	34,975	29,057	344	313
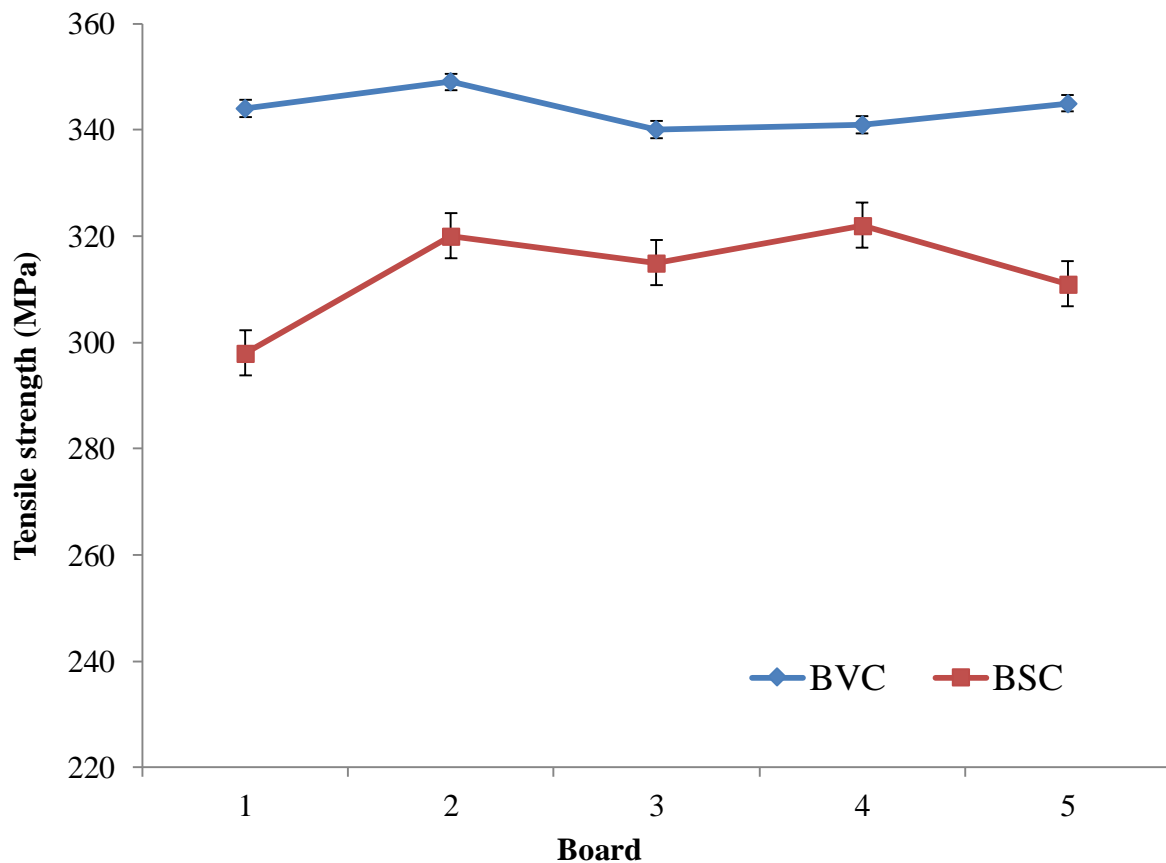
Fig. 77 Tensile strength comparison between bamboo veneer composite (BVC) and bamboo strand composite (BSC)

The tensile strength of the bamboo veneer composite samples (BVC) was higher compared to bamboo strand composite samples (BSC). The increase in tensile strength from BSC to BVC

198

was almost 10% on average. Similarly, the modulus of elasticity in tension of the BVC samples was higher compared to the BSC samples. The modulus of elasticity in tension of BVC increased by more than 20% compared to that of BSC on average, almost double the difference between the two composite boards in tensile strength.
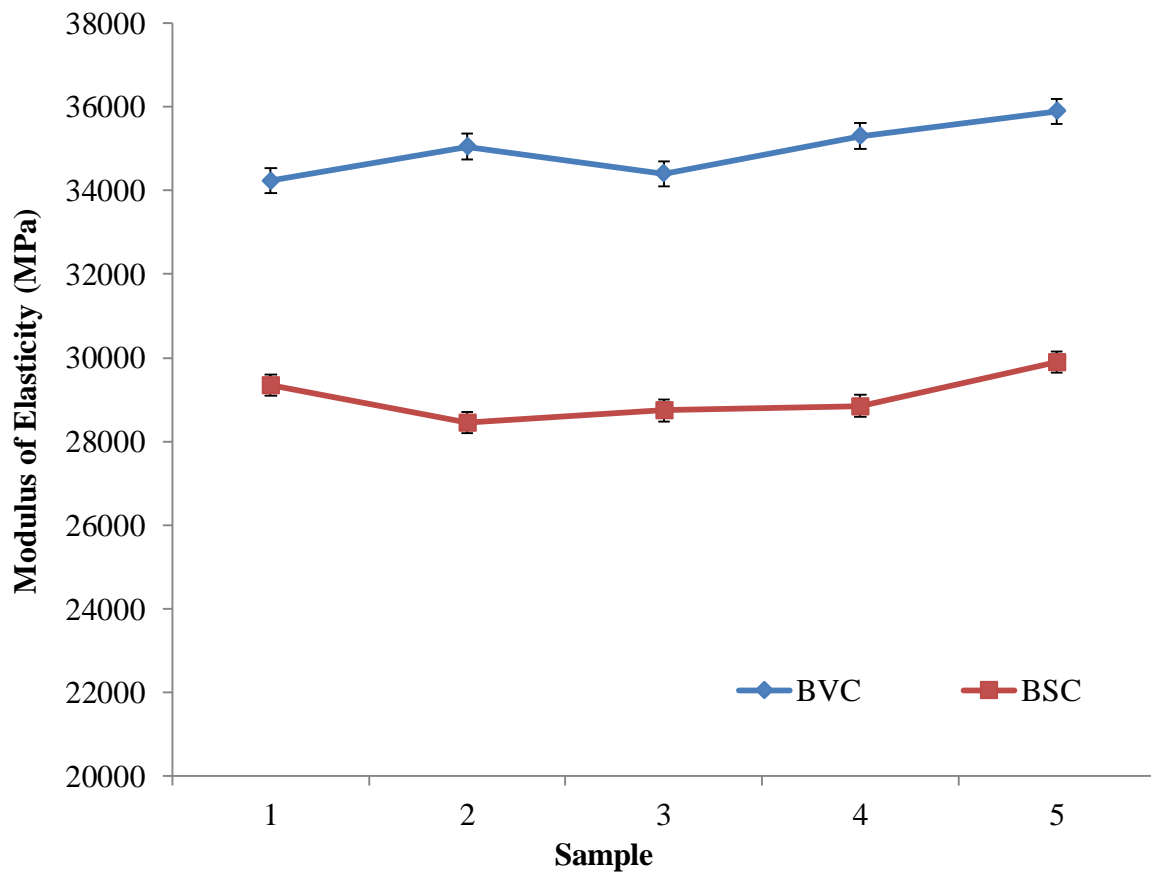
Fig. 78 Comparison of tensile modulus of elasticity between bamboo veneer composite (BVC) and bamboo strand composite (BSC)

Furthermore, the bamboo strand composite samples displayed a larger standard deviation in both tensile strength and modulus of elasticity. For both types of bamboo composite boards, only bamboo sections from classes 3, 4 and 5 with a minimum average tensile strength of 290MPa and minimum average modulus of elasticity of 22,130MPa were used for the fabrication.

The tensile strength of the BVC was improved through the processing and fabrication techniques used in this research. When the raw bamboo tensile strength was compared with BVC tensile strength, an increase of 19% on average was observed, while the BSC samples showed an increase in the tensile strength of less than 8% on average compared to the raw

bamboo tensile strength. The improvement in the modulus of elasticity of BVC samples compared with raw bamboo modulus of elasticity was even higher compared to the tensile strength. The modulus of elasticity of BVC samples increased by more than 58% while the increase for BSC was around 31% compared to the raw bamboo properties. Overall, bamboo veneer composite boards showed better performance in tensile properties compared to bamboo strand composite boards. The mechanisms involved for the better performance of BVC samples over BSC samples are discussed in the following sections. The next section evaluates the flexural properties of the BVC and BSC boards.

Flexural properties

Flexural properties, including Modulus of Rupture (MOR) and modulus of elasticity in flexure, were measured according to ASTM D7264, "Standard Test Method for Flexural Properties of Polymer Matrix Composite Materials through a four-point bending test" (ASTM International 2015). This standard was chosen due to the lack of international standards for bamboo composite materials. ASTM D7264 was the most relevant available international standard which could be followed for this research. Five rectangular-shaped samples with a span-to-thickness ratio of 32:1 were prepared from each of the BVC and BSC boards. The span-to-thickness ratio recommended by the ASTM standard ensured that the final failure was dominated by the tensile stress developed on the bottom outer side of the specimens rather than by the shear stress developed along the middle line. In other words, by increasing the sample's span long enough compared to the sample's thickness, the shear stress component could be minimized since the shear stress was not directly affected by sample's length, unlike the flexural stress which was directly proportional to sample's span or length. To measure the modulus of elasticity in flexure, an extensometer was attached to the center of the loading span of each sample to measure the deflection and obtain the load deflection curves. The modulus of elasticity in tension was calculated by obtaining the linear portion of the load deflection curves. Subsequently, the UTM TRAPEZIUM X software was used to draw the stress-strain curves and calculate the modulus of elasticity of the samples.

The loading was applied perpendicular to the fiber direction. Fig.79 and Fig 80 display one of the samples being tested with the UTM machine with a loading rate of 1mm/min according to the ASTM standard. The final flexural properties test sample was prepared from each composite board and had dimensions of 360mm × 25mm × 10mm.
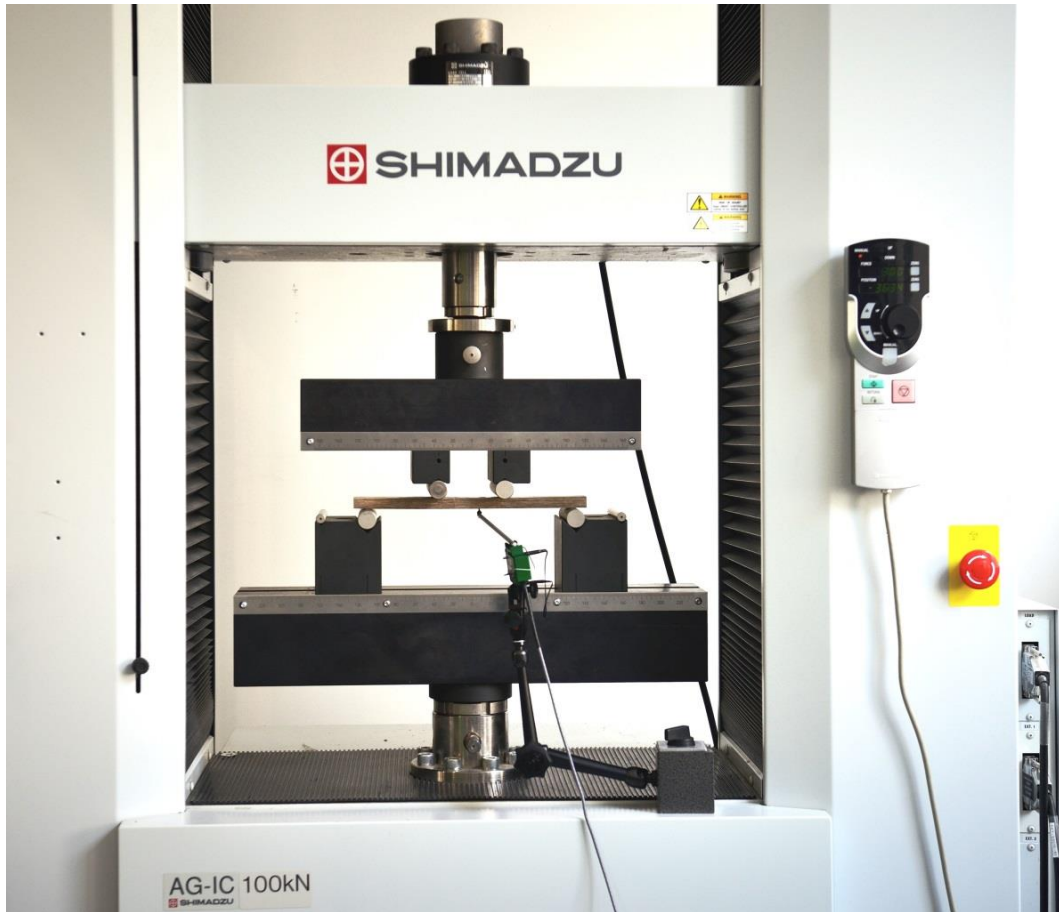
Fig. 79 Flexural sample with extensometer under UTM machine
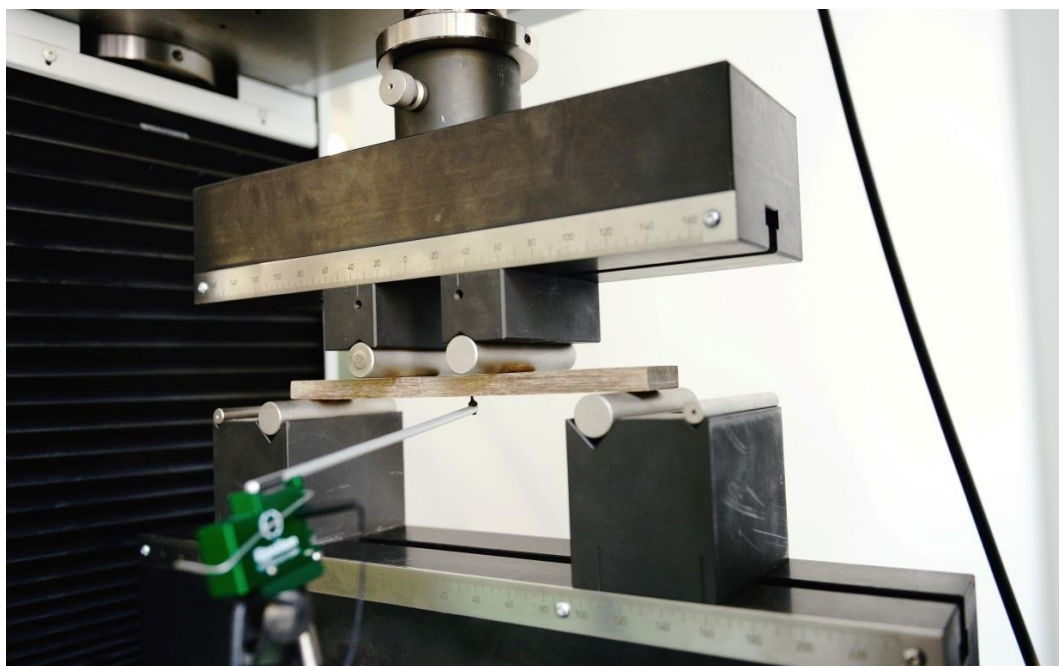
Fig. 80 The composite sample being tested under flexural test setup with the use of extensometer

The results of the tests are displayed in Table 17. Results exceeding a 10% standard deviation range, which had been statistically set as the confidence interval according to the ASTM standard, were discarded. Fig.81 and Fig.82 display the variation of the results graphically.

Table 27 Flexural properties of bamboo composite boards produced with veneer and strand

Sample	Modulus of elasticity in flexure (MPa)		MOR (MPa)	
	BVC	BSC	BVC	BSC
1	30,342	23,900	309	231
2	33,010	22,561	288	217
3	29,810	24,040	295	255
4	30,203	22,901	316	219
5	31,411	26,041	320	210
Average	30,955	23,888	305	226
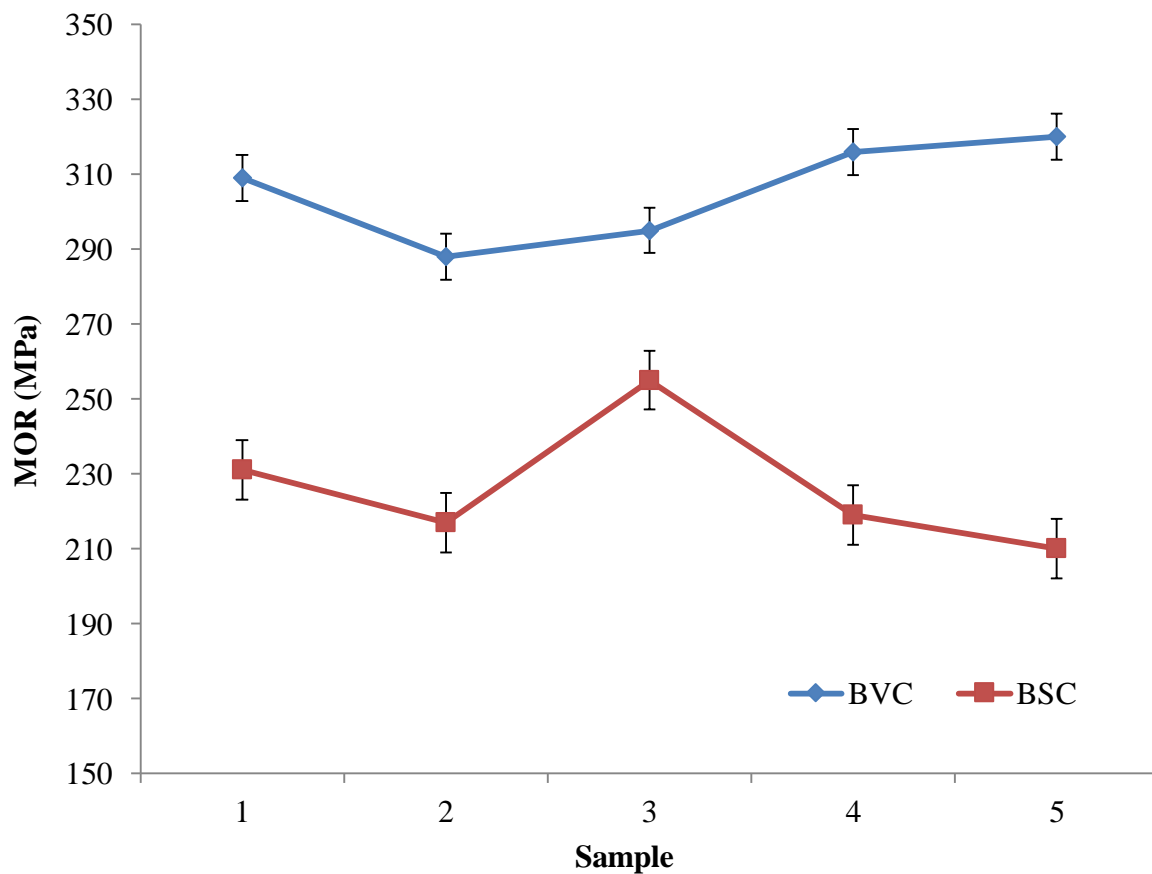
Fig. 81 MOR comparison between bamboo veneer composite (BVC) and bamboo strand composite (BSC)
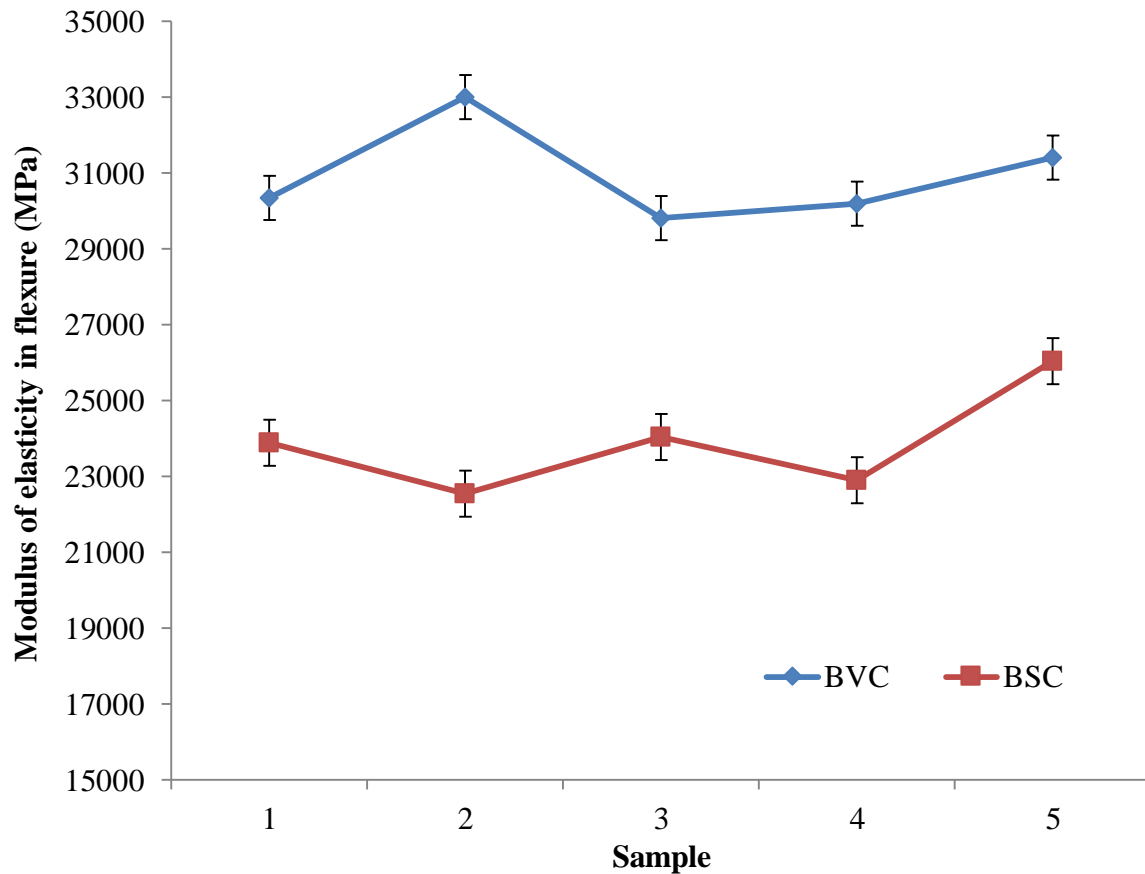
The average MOR for BVC samples was 305MPa, while for BSC samples, the average MOR was only 226MPa, a difference of 35%. When the MOR of BVC boards was compared to the average MOR of raw bamboo sections from classes 3,4 and 5, an improvement of up to 88% was observed. This result clearly showed that the production methods used together with the veneer layers as raw bamboo elements improved the flexural strength of the final bamboo composite board.

The BVC board showed higher modulus of elasticity in flexure compared to the BSC board. The average modulus of elasticity of the BVC samples was almost 30% higher than the BSC samples. When the modulus of elasticity of the BVC board was compared to the raw bamboo sections, an improvement of up to 1.5 times the raw bamboo modulus of elasticity in flexure was observed. The following section elaborates more on the various mechanisms involved in the overall performance of the BVC and BSC boards, and suggests the more suitable types of composite board based on the results obtained in the investigations.

Remarks and conclusions

Using bamboo veneer layers for the fabrication of bamboo composite boards show better performance in terms of tensile and flexural properties as shown in Table 26 and Table 27. The difference in the performance of bamboo veneer composite and bamboo strand composite samples could be explained in two main aspects:

- Microstructure of the composite
- Fabrication techniques

As explained in in detail in the previous sections, the interface bond between the bamboo fiber bundles and the epoxy matrix determines the overall performance of either of the BVC or BSC board. If the interfacial bond between the bamboo fibers and the epoxy system could be perfectly maintained while testing the sample, the ultimate mechanical properties, including tensile and flexural properties, would be higher as long as the ultimate applied load did not exceed the load-bearing capacity of the bamboo fibers in tension or flexure. A good interfacial bond contributes to enhanced stress transfer from the matrix to the fibers and vice versa during the tests, and therefore results in higher ultimate tensile and flexural properties. The interfacial bond, as mentioned in the previous sections, is affected by the surface characteristics of the bamboo fiber bundles as well as the epoxy system. The same epoxy system was used during the comparison study of the veneer layers and strands as raw fiber bundles for composite fabrication. Therefore, only the surface characteristics remain the most influential factor in determining the superior performance of the BVC compared to the BSC samples. The surface characteristics, including the specific surface area and the surface roughness of the raw bamboo fiber bundles as described in section 5.1.1, could influence the interfacial bond. The surface roughness of both veneer layers and strands were improved by creating the perforations and linear cracks along the fiber direction, as also shown by the results of the tensile tests of the composites produced by the veneer and strands with and without perforations. Furthermore, the surface area of the fiber bundles was improved by employing thinner veneer layers and thinner strands. Higher improvements in both tensile and flexural properties of the BVC samples compared to BSC samples were observed, which could indicate the improved interfacial strength within the BVC boards. Therefore, to investigate the interfacial microstructure between the bamboo fibers and epoxy matrix, visual microscopic analysis of both BVC and BSC sections were carried out with a Carl Zeiss Axio Zoom Microscope at AFCL. Fig. 83 and Fig 84 show the visual microscopic analysis of the cross-section of the BVC and BSC samples respectively.
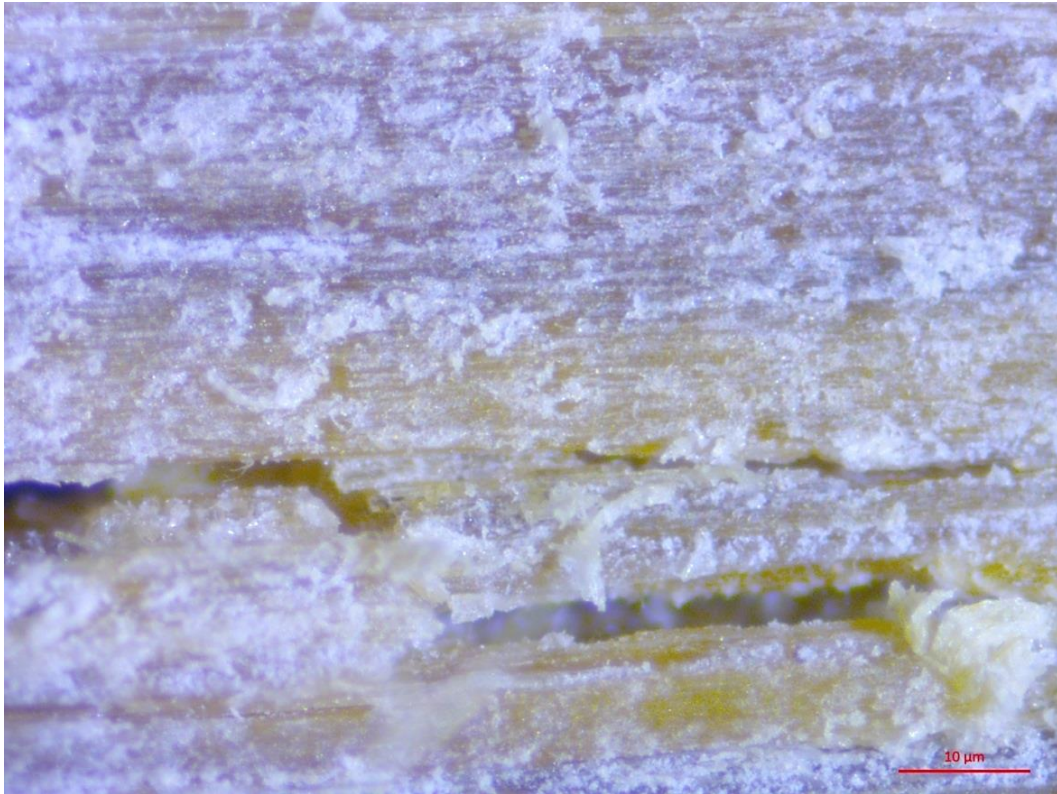
The BVC samples displayed a rather homogenous white crystalline layer of epoxy matrix according to Fig. 83, which demonstrated the fact that the polymer networks of the epoxy matrix were well developed at the microstructural level of the bamboo veneer composite sample. This observation further affirmed that the combination of the temperature and pressure parameters chosen for the hot-press compression molding machine as well as the post-curing process were effective in activating the polymer networks of the epoxy matrix and creating the crystalline microstructure. As a result of the development of this crystalline layer of thin epoxy system on the veneer layers, the interface between the bamboo veneer fiber bundles and the epoxy matrix could have been improved and thus improved the stress transfer between the matrix and the bamboo fibers. Hence, the bamboo veneer composite samples showed relatively higher mechanical properties compared to bamboo strand composite samples.

Fig. 84 shows the micrograph of the BSC cross-section under the microscope. As Fig. 84 shows, the polymer networks of the epoxy system did not cover fully the strand fibers, unlike for the BVC sample. Only some of the bamboo strand fibers were covered with epoxy matrix and the white crystalline layers of the polymer network were not fully developed across the microstructure of the composite sample. The lack of homogenous coverage of the bamboo

strands fibers by the epoxy polymer networks, as described earlier, could adversely affect the interfacial bond between the bamboo fibers and the epoxy matrix, and would weaken the interface networks between epoxy and bamboo fibers. The weak interfacial bond subsequently could result in the lower tensile and flexural properties of bamboo strand composite samples compared to the bamboo veneer composite samples.
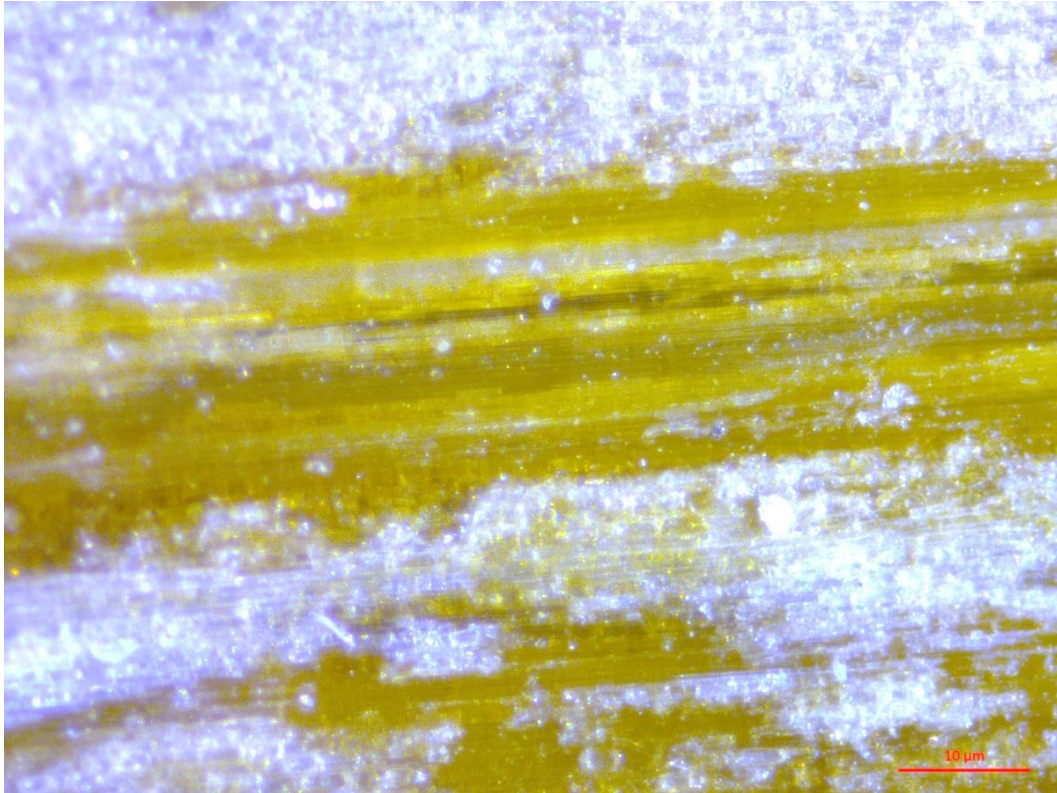
Fig. 84 Micrograph of BSC cross-section

This conclusion was further strengthened through microscopic investigation of both BVC and BSC samples after their failure in tension. Fig. 85 shows a cross-section of the BVC sample after breaking at its ultimate tensile strength, while Fig. 86 shows the BSC sample after its final tensile failure. As Fig. 85 shows, the crystalline layer of epoxy system covered the broken pieces of the BVC sample almost consistently after tensile failure. While in the case of the BSC as shown in Fig. 86, the broken pieces were not entirely covered by the crystalline layer of epoxy matrix. The samples of both BVC and BSC were prepared under similar conditions, therefore the surface characteristics would be the main factors affecting the interfacial microstructure and subsequently the ultimate mechanical properties. From Fig. 84 and Fig. 86, a preliminary conclusion could be made regarding the lower ultimate mechanical properties of BSC compared to BVC samples based on two facts:

- The epoxy matrix did not react completely with the raw strand fiber bundles during the BSC fabrication, or

- The epoxy matrix did not pass through some of the cracked/perforated strand layers and therefore the crystalline networks could not consistently cover the entire microstructure of the BSC samples.

The two factors mentioned above could have created an uneven distribution of stresses within the microstructure of the BSC samples when they were loaded in tension or flexure due to the irregular stress transfer within the interfaces of the bamboo fibers and epoxy matrix. Therefore, some areas of the BSC microstructure would be able to resist higher tensile or flexural stresses compared to other sections where the epoxy matrix did not fully react with the bamboo fibers or did not consistently cover some of the bamboo fibers. The lack of a smooth and continuous stress transfer between the epoxy matrix and bamboo strand fibers could cause premature failure in the BSC samples compared to the BVC samples.
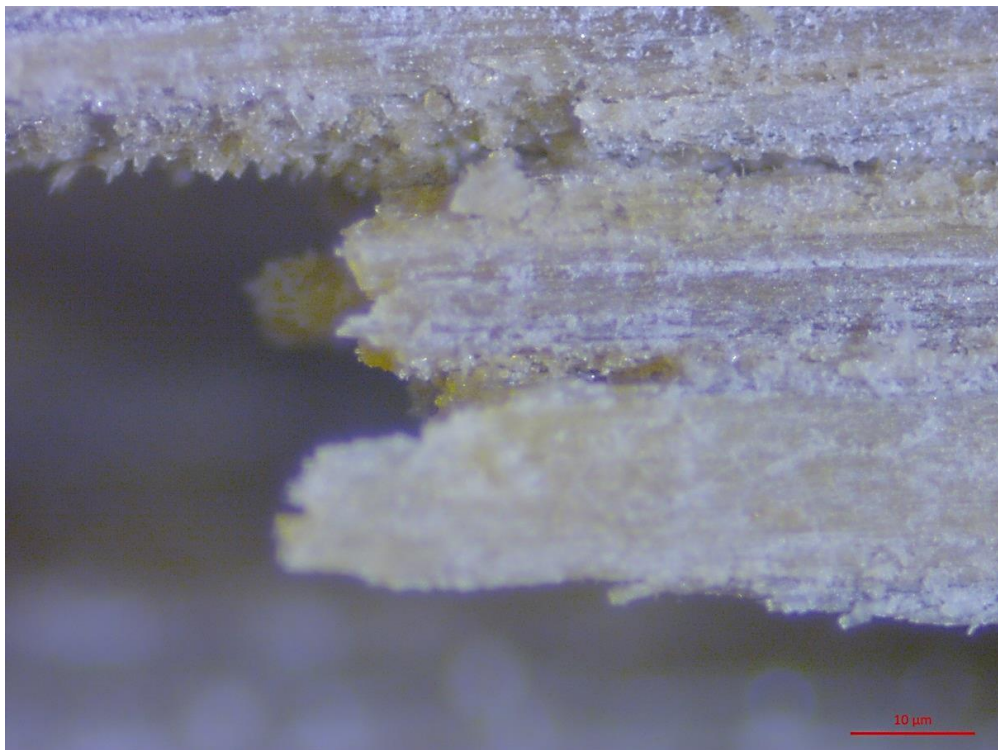
Fig. 85 Micrograph of BVC cross-section after final tensile failure
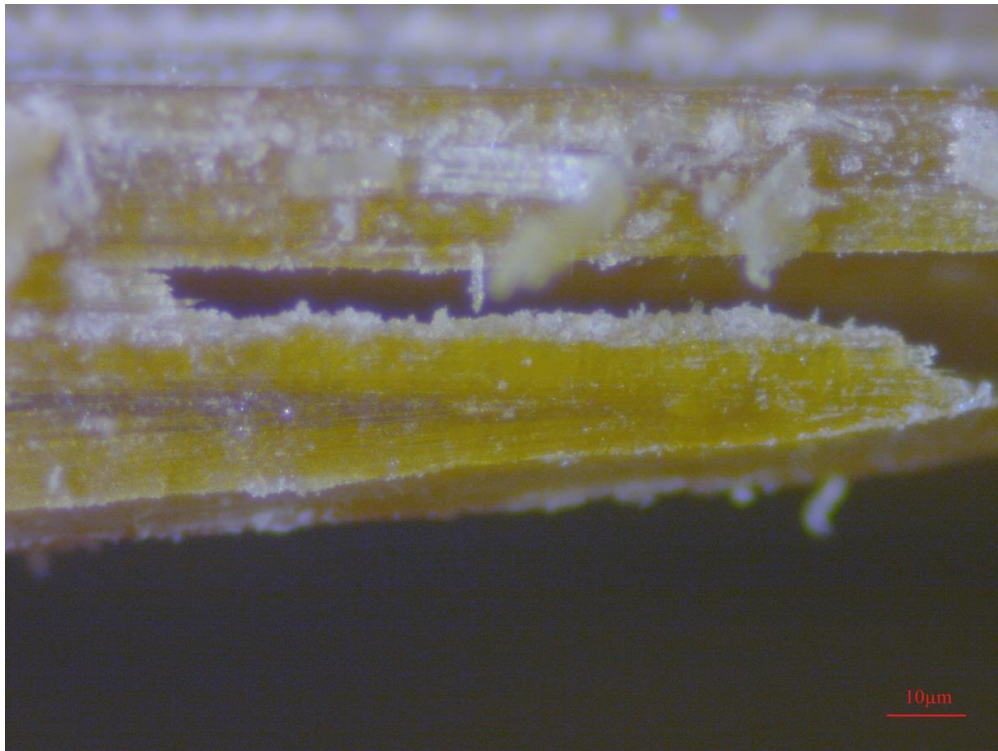
Fig. 86 Micrograph of BSC cross-section after final tensile failure

Beside the microstructural differences between the BSC and BVC samples, the fabrication and processing techniques employed in this research could also be responsible for the better performance of the BVC compared to the BSC samples. When the fiber bundles of the two fabrication methods were compared, the veneer layers showed homogenously connected long pieces of fiber bundles, while the bamboo strands showed rather heterogeneous pieces of fiber bundles with regard to fiber orientation and length. The veneer layers were produced in larger widths and lengths compared to strands in which the width of the strips was limited by the available width of processing machine. This could have made a huge difference in terms of the properties of the final unidirectional composite samples during the production of the composite boards, when various layers of impregnated fiber bundles were stacked on one another. In the case of strands with smaller width, it was rather challenging to maintain the unidirectional fiber orientation when more layers were added to the stack of stands. For some middle layers, there could have been misalignments due to movements during production or pressing which would have not been identified or avoided during the fabrication. The misalignment, even the small ones, would create completely different pathways for the stress transfer between the strand fibers and the epoxy matrix, which could then contribute to lower ultimate tensile or flexural properties of unidirectional BSC samples. Unlike the strands, the veneer layers had larger width and length which made the fabrication of unidirectional BSC

samples rather manageable in terms of maintaining the fiber direction during the production of the composite boards. The larger width allowed the impregnated layers to be stacked on one another with the same width as of the mold of the hot-press machine width. Therefore the similarity in the widths of the mold and the veneer layers eliminated the need for overlaying the processed bamboo bundles along the width of the mold, as shown in Fig. 69 in the case of bamboo strand composite fabrication. As shown in Fig. 69, the smaller width of the bamboo strands required the overlaying technique to be used to fill the available width of the steel mold and therefore maintaining the fibers orientation in each layer was rather challenging as discussed earlier.

Besides the fabrication technique influencing the composite properties, the production process used for the veneer layers and strands could also have affected the fiber properties. Therefore the fiber bundles of the two production processes were investigated under the microscope to search for potential defects created during the processing of the raw bamboo. Fig. 87 and Fig. 88 show the micrographs of the bamboo strands under the microscope. As can be seen from both figures, the fiber bundles of the bamboo sections of the strands were not entirely intact as a result of the processing methods used. Some of the long fiber bundles of the strand sections were damaged along their length during the production as shown in Fig. 88. Some of the fiber bundles were cut in directions perpendicular to the fiber orientation and some disintegrated by the processing machines, as shown in the microscopic images. It was necessary to trace the origin of these defects. The structure of the defects present in Fig. 87 and Fig. 88 were carefully studied, especially the dimensions, the depth as well as the patterns. Among the various machines used during the strand production, it was found that both flaking and stranding machines could be sources of the damage to the fiber bundles.

Both machines have metal wheels with various sizes of ribs. The ribs are created to physically engage the bamboo strips and move them towards the end of the machine in each process. As shown in Fig. 89, the metal ribs of the wheels would press the bamboo strips while pushing them to run through the machine and complete the process. However, due to softness of some of the available bamboo sections, the pressure applied by the wheels could have penetrated deeply into the fiber bundles and created the defects by cutting through the fiber bundles and disintegrating the matrix holding the fibers in their place. Given the large number of strips used for the production of the BSC samples, it was not feasible to ensure quality control every single strip and every section of the strip through the use of the visual

micrograph. Therefore, some strips with defects could have been used during the composite fabrication.
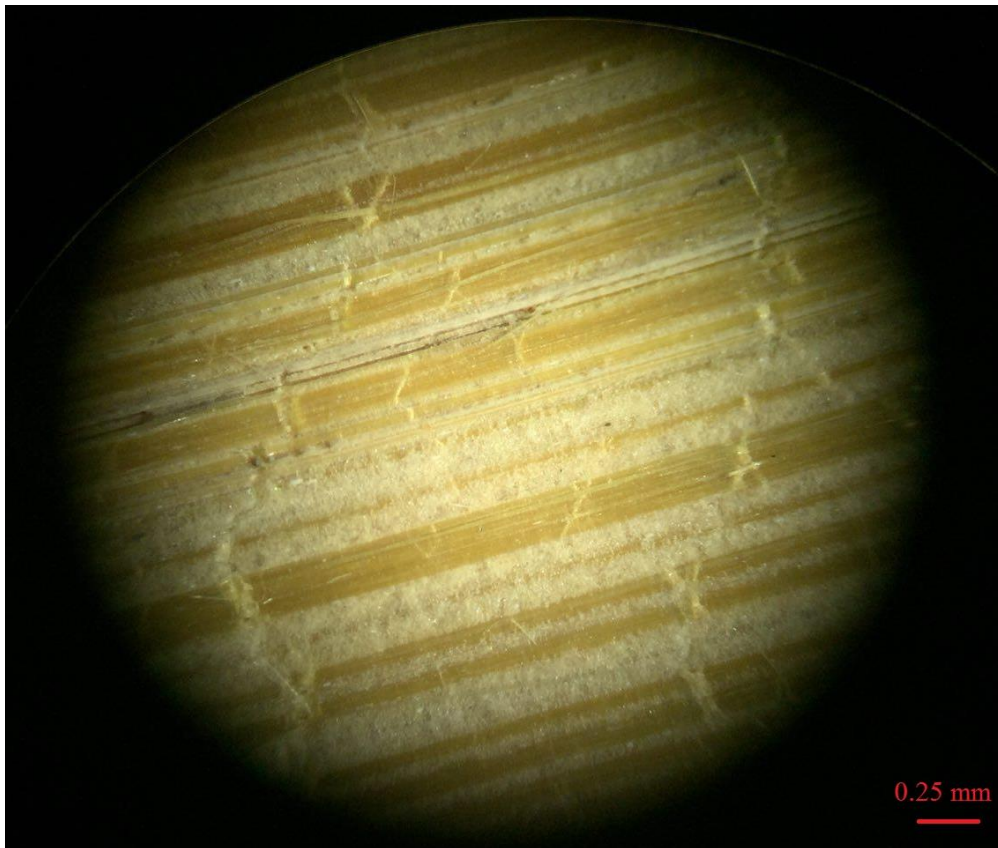
Fig. 87 Micrograph of the surface of the bamboo strands

The presence of such defects could have negatively affected the interfacial strength between the fiber and epoxy system during the composite production as a result of lower specific surface area. Furthermore, the presence of discontinuous fiber bundles could have introduced localized stress concentration points into the composite microstructure which would contribute to the lower load-bearing capacity of the BSC samples through premature failure of composites initiating from those points.

However, the defects were not observed in all the available bamboo strips and only some of the processed strips showed signs of defects. Furthermore, as mentioned earlier, it was not feasible to monitor every single strip. In the case of the veneer layers, the preliminary microscopic investigations did not reveal any damaged fiber bundles in the microstructure.
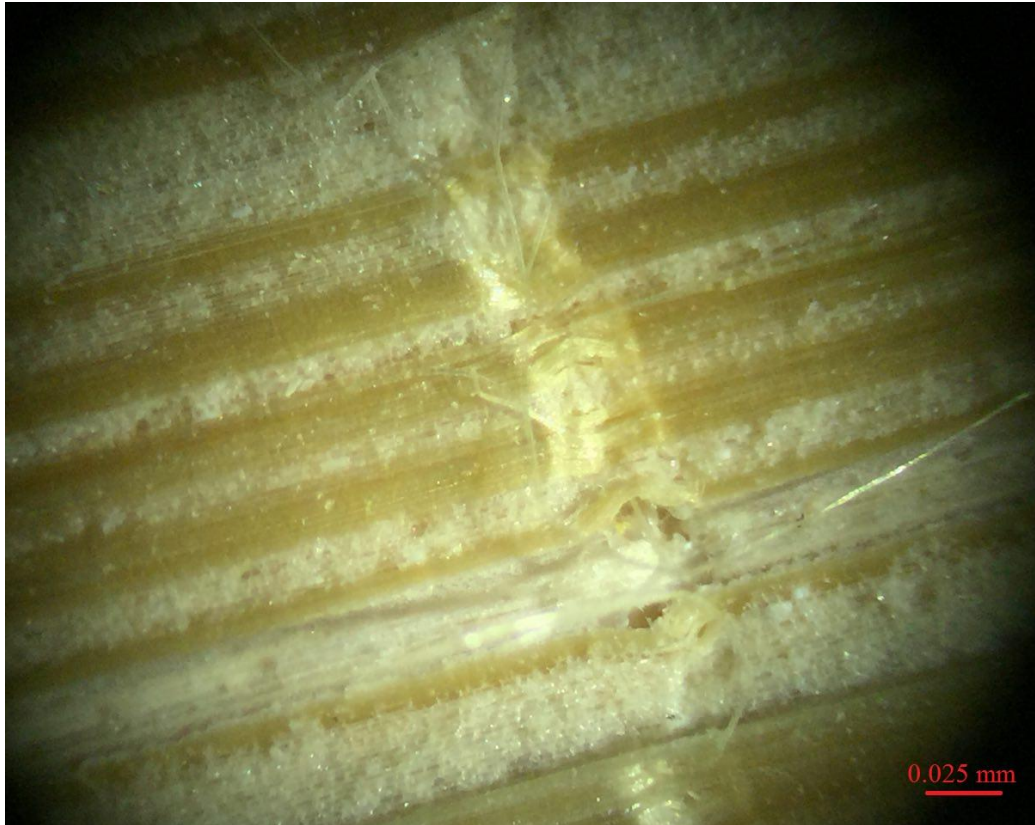
Fig. 88 Presence of defects on the surface of the bamboo strands

Fig. 89 The metal wheels with ribs used during the bamboo strand processing

Given the different mechanisms of the operations of the processing machines for veneer layers and strands, no such defects in the fiber bundles should have been expected. Based on

the results obtained in this chapter, though the bamboo strand composite fabrication method showed improved mechanical properties compared to raw bamboo samples, in general, the bamboo veneer composite samples exhibited superior performance in terms of mechanical properties compared to strand composite samples. The novel fabrication methods and new techniques employed in this research through employing the right veneer layer, suitable hot-press compression molding parameters and the choice of epoxy system, taken together, showed substantial improvements in the mechanical properties of the final bamboo veneer composite material as compared to the properties of the raw bamboo sections.

Furthermore, when these techniques and fabrication processes for the newly developed bamboo veneer composite materials are compared with the production methods of synthetic FRP composite materials such as GFRP or CFRP as discussed in section 3.3.2, significant advantages in terms of energy and cost required for production are observed. Two of the most common manufacturing processes for FRP composites are the pultrusion and vacuum infusion methods. In both methods, higher temperatures and more sophisticated machineries are employed compared to the peeling machine and the hot press compression molding machine used in this research. The processes developed within this research require lower temperatures and lesser pressures in comparison with pultrusion and vacuum infusion process. The hand lay-up manufacturing process combined with hot press compression molding machine have resulted in production of high performance bamboo veneer composite samples without the need for high-tech, costly and energy-intensive machineries extensively employed by FRP composite manufacturing industry worldwide.

The results obtained in this chapter further supported the hypothesis of this PhD research that "in general, it is possible to maintain and/or improve the mechanical properties of raw bamboo fibers through the fabrication methods and techniques" developed in this research. As explained in section 3.3.2, so far no other investigation has been carried out on developing methods similar to that undertaken in this research for extracting the bamboo veneer in a simple yet efficient process without the need for energy-intensive machineries. The production of the high performance bamboo veneer composite samples with the use of hot press compression molding machine and through hand lay-up process has been shown to be suitable in achieving the required properties of the final bamboo composite material without the need for complex and intricate manufacturing processes as explained earlier in the case of FRP composite materials.

Therefore, the bamboo veneer composite production method is preferred over the bamboo strand composite production for the fabrication of final bamboo composite reinforcement to achieve a high-performance composite material that could be used for structural concrete applications.

The parameters used in this chapter for the hot-press compression molding machine in the comparison study of veneer and strand composite production methods, including pressing time, temperature and pressure, were set to values acceptable for the comparison purpose of the mechanical properties of the BSC and BVC samples. To further enhance the production methods of the bamboo veneer composite material and improve its mechanical properties that could be comparable with conventional steel reinforcement materials, fine-tuning of the parameters were required. Beside the enhancement of the hot-press compression machine parameters, improvement of the bamboo fiber and epoxy matrix interaction, and thus strengthening the interface bond through chemical treatment of the veneer fiber bundles, was also investigated as part of the research at the Future Cities Laboratory and in collaboration with industrial partner Rehau. These improvement techniques are briefly discussed in the following sections.

5.4. Methods for optimizing the properties of bamboo veneer composite

To further improve the tensile characteristics of the bamboo veneer composite material, two approaches were employed as explained in this section. These two approaches were undertaken in cooperation with the industrial (chemical) partner Rehau and carried out through detailed investigations over two years of extensive research via a joint project collaboration between ETH in Zurich, the Future Cities Laboratory in Singapore, Empa in Dübendorf and Rehau in Zurich, funded by the Commission for Technology and Innovation (CTI/KTI) of Switzerland (Wielopolski, Aigner et al. 2016). The results of the CTI R&D project were acknowledged and taken into account in this PhD research. However, the detailed description and analysis of the results can be found in the CTI final project report, since they were beyond the scope of this PhD thesis.

The first approach was to fine-tune the hot-press compression molding machine parameters (time, pressure and temperature) to increase the chemical bonding capacities of the used adhesive system with the bamboo fibers such that it resulted in improved mechanical properties of the BVC boards. Therefore, a vast series of BVC samples were prepared with

various combinations of these parameters and were subsequently investigated for their mechanical properties, mainly the tensile strength and modulus of elasticity in tension.

The second approach used in this research was to improve the chemical fiber-matrix interaction through a pre-treatment of the bamboo veneer layers with an alkaline solution. Alkaline treatment is generally known to reduce the fiber diameter and roughen the surface structure of the natural fibers. As discussed in chapter 4, by improving the surface characteristics of the bamboo fibers, the fiber-matrix interface bonding can be improved and therefore higher mechanical properties are expected, as discussed in the literature (Valadez-Gonzalez, Cervantes-Uc et al. 1999, Li, Tabil et al. 2007). Therefore, a vast series of BVC samples were prepared with pre-treated veneer layers and their mechanical properties evaluated to study the effect of alkaline pre-treatment. In the following sections, these two approaches are summarized and the results of the investigations carried out during the two-year CTI funded project are presented for the use within this PhD research.

5.4.1. Optimizing hot-press compression molding parameters

Perforated bamboo veneer layers without internodes and with an average moisture content of less than 10% were used to prepare the composite samples in this study, as explained in detail in section 5.2.3. The composite samples were prepared at various pressures, temperatures and times to find the optimum combination of the parameters which could result in higher tensile properties. Only tensile strength and modulus of elasticity in tension of the samples were measured in this study, given the importance of tensile properties for the application of BVC samples as reinforcement in concrete beams tested in chapter 6.

The temperatures investigated for this study were 80°C, 100°C, 120°C and 140°C. The pressures chosen for this optimization study were set to 12MPa, 15MPa, 20MPa and 25MPa. The initial pressing time and the post-curing time for the hot-press were set to 15/15 min, 30/30 min and 45/45 min.

The results from testing various samples from each BVC board are shown in Table 28 and Table 29. A total of 1,325 samples were tested to evaluate their tensile properties for the optimization of the hot-press compression molding parameters in this section.

Table 28 Tensile strength of bamboo veneer composite boards at various temperatures, pressures and pressing times

Pressure (MPa)	Time (min)	Temperature (°C)			
		80	100	120	140
12	15/15	313	332	301	289
	30/30	329	347	310	280
	45/45	331	344	314	271
15	15/15	337	369	312	267
	30/30	348	387	319	251
	45/45	346	383	311	NA
20	15/15	369	391	307	189
	30/30	382	432	300	151
	45/45	384	421	308	NA
25	15/15	397	374	174	NA
	30/30	418	356	167	NA
	45/45	410	359	NA	NA

The highest average tensile strength of 432MPa within all samples tested in this section was observed when a pressure of 20MPa and a temperature of 100°C were applied at a press/post-curing time of 30/30min. Similarly, the highest average modulus of elasticity in tension of 42,060MPa was observed for the same combination of pressure, temperature and pressing/post-curing time.

Table 29 Modulus of elasticity in tension of bamboo veneer composite boards at various temperatures, pressures and pressing times

Pressure (MPa)	Time (min)	Temperature (°C)			
		80	100	120	140
12	15/15	32,920	32,872	33,109	30,221
	30/30	32,105	33,348	33,390	31,039
	45/45	32,181	33,420	33,310	30,311
15	15/15	34,405	36,601	33,401	30,190
	30/30	34,904	37,192	33,049	30,406
	45/45	35,206	37,547	33,502	NA
20	15/15	36,820	39,721	33,183	28,031
	30/30	37,287	42,060	33,021	27,395
	45/45	37,239	41,907	32,991	NA
25	15/15	38,910	37,092	32,010	NA
	30/30	40,131	35,340	31,101	NA
	45/45	41,090	35,101	NA	NA

At a pressure of 25MPa and for temperatures beyond 100˚C, carbonization (blackening) of the bamboo veneer layers and disintegration of the boards were observed. The combination of temperatures beyond 100˚C with pressure of 25MPa resulted in decomposition of the raw bamboo fiber bundles in the veneer layers employed in the composite sample.

Fig. 90 and Fig. 91 show the results of the tensile strength and modulus of elasticity in tension of BVC samples with various combinations of time, temperature and pressure. Further information can be found in the CTI project report.

From the results of both tensile strength and modulus of elasticity in tension tests obtained during the two-year CTI funded project, it can be concluded that the optimum temperature range to achieve a high-strength BVC specimen is from 80˚C to 100˚C, while the pressure applied should be in the range of 20MPa to 25MPa. The press/post-curing time of 30/30min showed higher values for the optimum range of temperature and pressure applied by the hot-press compression molding machine. Therefore, for the fabrication of the final BVC reinforcement for concrete tests, a temperature of 100˚C and a pressure of 20MPa with a press/post-curing time of 30/30min were used as these resulted in the highest tensile properties according to Table 28 and Table 29.
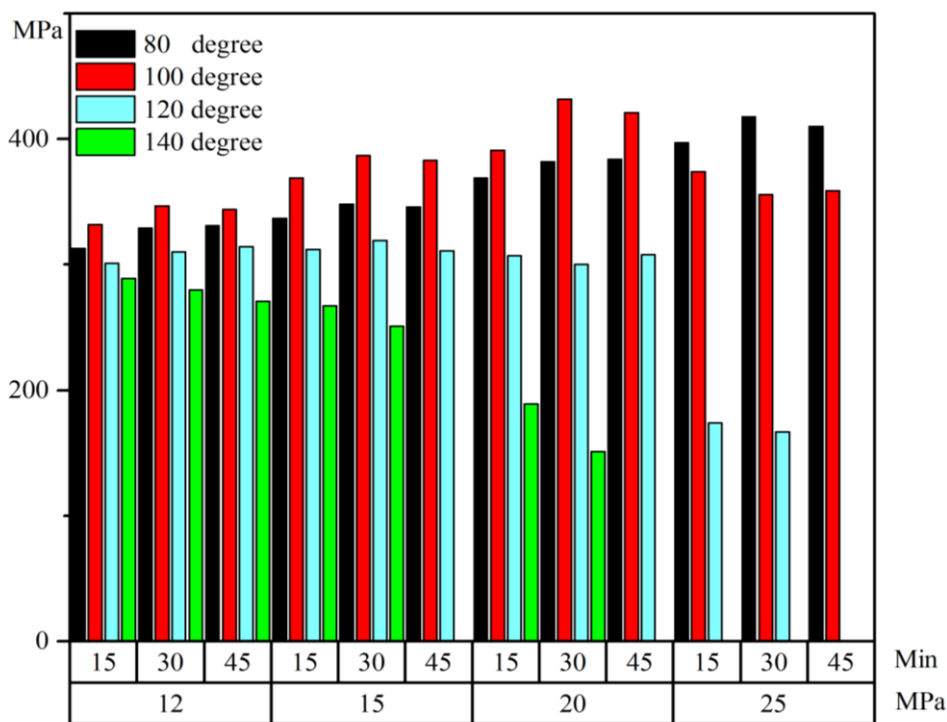
Fig.90 Tensile strength of BVC samples under various hot-press compression molding parameters
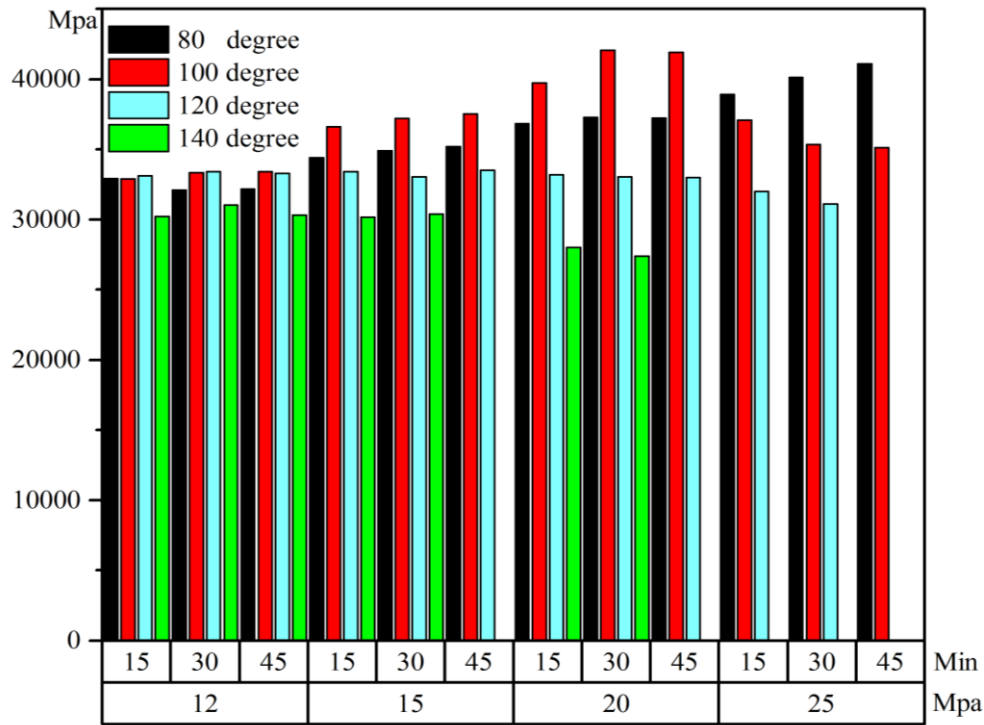
Fig.91 Modulus of elasticity in tension of BVC samples under various hot-press compression molding parameters

5.4.2. Alkaline treatment of raw bamboo veneer layers

To evaluate the effects of alkaline treatments on the mechanical properties of the BVC samples, the raw perforated bamboo veneer layers were first soaked in sodium hydroxide (NaOH) solutions of varying concentrations by weight percentage of 1wt%, 2wt%, and 5wt% for 12, 24 and 48 hours as well as distilled water, as a reference for comparison during the CTI project collaboration between ETH, Empa and the Future Cities Laboratory led by the chemists in the team (Wielopolski, Aigner et al. 2016). The knots were not included in this study to, firstly, eliminate any unknown effects that knots might have on the final composite properties and, secondly, to have comparable results with the samples tested in the previous sections. The layered impregnated treated bamboo veneers were pressed with the hot-press compression molding machine at a temperature of 100°C and pressure of 20MPa for a press/post-curing time of 30/30 minutes. The hot-press compression molding parameters were chosen in accordance with the previous section where a temperature of 100°C and pressure of 20MPa for a press/post-curing time of 30/30 minutes exhibited the highest average tensile properties of the BVC samples. Table 30 shows the results of the tensile strength measurement of the BVC boards with various alkaline concentrations and distilled water. Table 31 shows the results from the measurement of the modulus of elasticity in

tension BVC boards with various alkaline concentrations and distilled water and with varying exposure times. The standard deviations of all the results obtained in this study were less than 8%.

Table 30 Tensile strength of BVC samples after NaOH treatment with varying concentrations

Time (hr)	Treatment type			
	Distilled water	1% NaOH	2% NaOH	5% NaOH
12	433	434	433	428
24	421	452	448	441
48	429	440	430	431

Table 31 Modulus of elasticity of BVC samples after NaOH treatment with varying concentrations

Time (hr)	Treatment type			
	Distilled water	1% NaOH	2% NaOH	5% NaOH
12	41,235	43,981	43,880	42,445
24	41,855	44,880	44,021	43,110
48	40,401	44,014	43,125	42,601

As both Table 30 and Table 31 show, the alkaline treatment of bamboo veneer layers led to higher tensile properties of the composite samples as compared to distilled water treatment. In all three different concentration levels, the tensile strength was improved. However, the highest average tensile strength of 452MPa was achieved only with 1wt% NaOH treated veneer layers. Similarly, the highest average modulus of elasticity of 44,880 was observed in bamboo composite samples in which the veneer layers were treated with 1wt% NaOH solution.

Since the highest average tensile properties were observed for BVC samples produced with veneer layers treated for 24 hours with 1wt% NaOH concentrated solutions, for the production of the final BVC reinforcement samples in the following sections, the same conditions were used to achieve high tensile and high-performance BVC reinforcement.

The optimization study showed noticeable enhancement in the tensile properties of the BVC samples during the CTI funded project. Further analysis and discussion of the results are provided in CTI project report published jointly with industrial partner Rehau, the Empa's

Applied Wood Materials research group and the Chair of Architecture and Construction Prof. Dirk E. Hebel at ETH in Zurich (Wielopolski, Aigner et al. 2016).

5.5. Final BVC reinforcement: production and properties

The series of tests carried out in sections 5.2 and 5.3 displayed the superior mechanical properties that could be achieved through the fabrication methods and techniques employed for the production of BVC samples to be used as reinforcement in structural concrete. The optimization techniques employed in this research and as largely discussed in section 5.4 had further enhanced the BVC samples' mechanical features through fine-tuning the hot-press compression molding parameters and alkaline treatment of raw bamboo veneer layers. In sections 5.3 and 5.4, to minimize the size impact on the evaluation of the test results and to eliminate any unknown effects arising from the inclusion of various parameters, only pieces of bamboo veneer layers without any knots in between the fibers and with certain lengths were used for all the studies on the effects of fabrication techniques, optimization of hot-press molding parameters and NaOH treatment of veneer layers. This approach was necessary to achieve comparable results as in previous sections and to ensure the studies were focused only on the designated parameters. In this section, the production of the BVC reinforcement for reinforcing the concrete beams of up to 1,200mm in length is explained. There were two types of reinforcement used in chapter 6 for reinforcing the concrete beams: longitudinal and transverse (shear) reinforcement. The longitudinal reinforcements were placed parallel to the long axis of the beam to provide the required tensile and flexural capacity, while transverse reinforcements were employed to provide sufficient shear strength perpendicular to the long axis of the concrete beam. The production process and the properties of the final reinforcements to be used in chapter 6 in concrete beams are explained in this section.

5.5.1. Production of longitudinal BVC reinforcement

The longitudinal BVC reinforcement were produced by employing perforated/cracked veneer layers with and without knots between the fibers. In this section, the knots were also included in the production of the composite samples to ensure that the whole length of the culms was used for the processing of the veneer layers. The veneer layers were first treated with 1wt% NaOH solutions for 24 hours, which was explained in the previous section to have significant effects in enhancing the properties of the BVC samples. The treated veneer layers were then washed with water to remove the alkali solution, followed by neutralization with HCl acid to ensure there was no sign of alkalinity left on the raw bamboo veneer layers before the

composite fabrication. The veneer layers were subsequently dried at 80°C for 48 hours to reach an equilibrium moisture content of less than 10% suitable for the fabrication of the composite samples. For each composite board, 2,000gr of the dried veneer layers were first prepared into rectangular sheets with an average length (perpendicular to fiber direction) of 150mm and an average width (along the fiber direction) of maximum 750mm. The selected length of 150mm fitted perfectly into the steel mold of the hot-press that had a width of 150mm. However, the average width of the veneer layers produced ranged from 500mm to 750mm, due to the limitations imposed by the available peeling machine at ACFL. Subsequently, the dried treated veneer layers were impregnated with Super Sap® INF/CLR epoxy as the matrix. The length of reinforced concrete beams in chapter 6 was set to 1,300mm as the UTM machine at AFCL had limited capacity in handling longer beam sizes for the purpose of this research. The length of 1,300mm was the maximum length that could be handled by the available UTM machine which had a loading capacity of 100kN. Therefore BVC reinforcement with length of 1,200mm was chosen to reinforce the proposed concrete beams. The additional 100mm was designed as the cover of the reinforcements on the both ends of the reinforced concrete beams. However, to obtain continuous unidirectional bamboo veneer composite samples of 1,200mm, several layers were manually overlaid and overlapped to adopt a pre-defined lamination structure and maintain a smooth load transfer between the non-continues layers. Sometimes, only two impregnated veneer layers of 700mm in width were sufficient for the overlay, and sometimes more than three or four layers of impregnated veneer sheets were necessary to create the overlaid structure, depending on the available width of the veneer sheets produced from raw bamboo culms during the peeling process. The schematic of overlaying and overlapping techniques developed in this research for various widths of veneer layers is shown in Fig. 92.
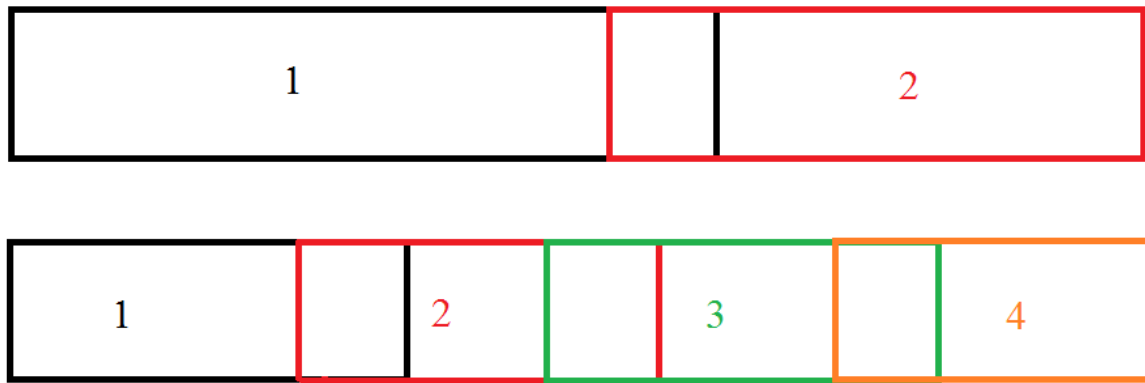
Fig. 92 Overlaid and overlapped techniques used for different width of veneer layers

Fig. 93 shows the simple yet novel hand lay-up technique used to overlay and overlap the impregnated veneer layers into the required width of 150mm and length of 1,200mm for the composite fabrication.

The epoxy-resin matrix was further applied with the help of a brush on the overlapping impregnated veneer layers to uniformly spread the epoxy matrix along the overlapping areas. To ensure the sections with overlaid veneer layers were uniformly structured along the bamboo fiber direction, the hand-layup process was employed to control each and every veneer layer in overlaid sections and to maintain the unidirectional properties of the final composite. Once all the veneer layers were stacked on top of each other, a roller was moved along the full length of the impregnated layers, which applied pressure on the layered structure to remove any trapped air as well as the excess epoxy resin matrix within the layers.

Before placing the layered impregnated stack of bamboo veneers into the mold of hot-press, a release gel was sprayed on the mold surface to avoid the sticking of the composite sample to the surface. Furthermore, thin non-stick Teflon sheets were used to cover the top and bottom of the mold steel plates to achieve a smooth surface finish on the final BVC reinforcement. The stacked bamboo veneer layers were placed into the mold of hot-press and pressed at a temperature of 100°C and a pressure of 20MPa for 30/30 min of curing/post-curing duration. The settings were chosen according to the optimization study carried out in section 5.3.1.

The final composite board was cured for 48 hours in a curing oven at a temperature of 55°C, as explained in section 5.2.3, before being cut into suitable shapes for mechanical testing. The final board had a length of 1,200mm, a width of 150mm and a thickness of 10mm. Fig. 94 shows the densely pressed cross-section of the final BVC board.
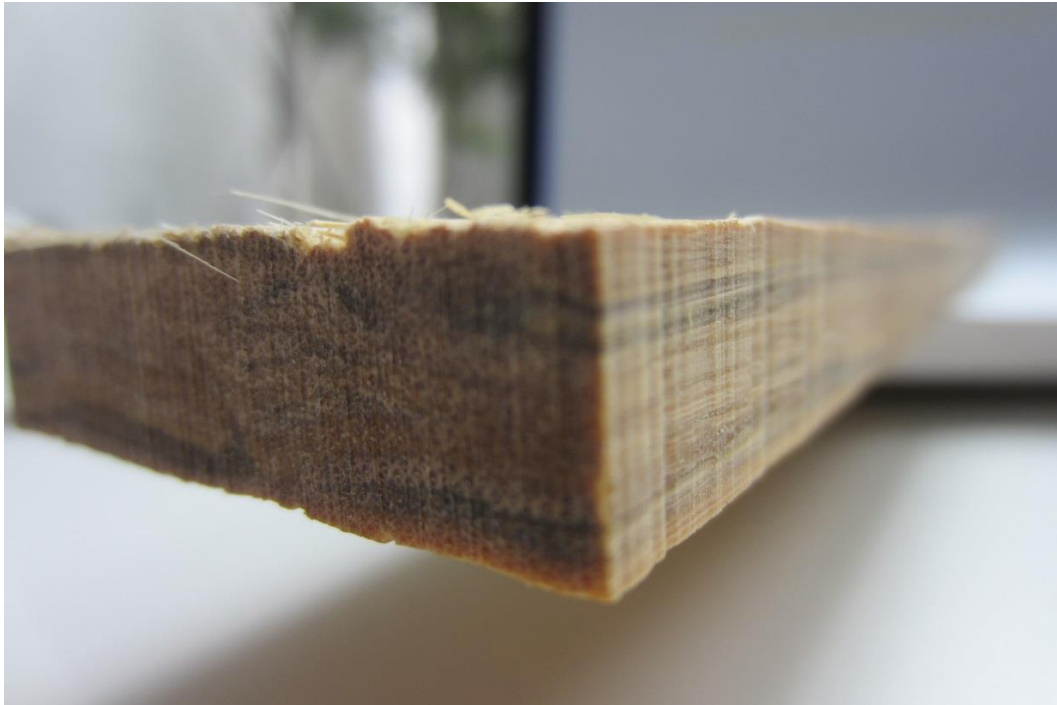
Once fully cured, the BVC boards were cut into appropriate samples sizes to measure their tensile, flexural and compressive properties. Furthermore, the density and Coefficient of Thermal Expansion (CTE) of the final reinforcement samples were also measured as part of this study as explained in the following sections. The final BVC boards were then cut into reinforcement of size 10×10×1200mm for reinforcing the concrete beams in chapter 6.

All the BVC reinforcement produced in this study had square cross sections of 10×10 mm. The square cross section was the result of the production process of the BVC materials as explained in section 5.3.3. The common reinforcement materials currently being used for reinforcing structural concrete members have round cross sections with and without ribs on the surface, including steel and GFRP reinforcement systems. However, for the production of the BVC reinforcement in this study, only square cross sections were considered, as a result of the production process in which flat and U-shape steel molds were used with the hot-press compression molding machine.

The shape of the BVC reinforcement cross section could have various impacts on the performance of the final BVC reinforced concrete beams. The round shape of the reinforcement cross section, which has been used over the past decades as the most common shape for steel reinforcement used in concrete members, could provide the most optimum surface area which binds with the concrete matrix efficiently, and at the same time would

contribute to the balanced distribution of forces, and thus resulting in uniform distribution of the stresses within the concrete matrix around the reinforcement. This uniform distribution of the internal stresses ensures that the concentration of stresses at a specific location around the reinforcement element can be prevented or minimized. However, a square cross section could increase the possibility of stress concentration at the corners of the reinforcement cross section at the interface with concrete matrix.

The coatings used on the surface of the BVC reinforcement in chapter 6 for the enhancement of the bond strength between concrete and reinforcement could be helpful in creating a smooth surface area around the square section of the BVC reinforcement; this smooth surface area could minimize undesirable impacts of potential stress concentrations at the corners. It should also be emphasized that the production of round cross sections of the BVC reinforcement in this study was not feasible due to the limitations of the available hot-press compression molding machine at AFCL, in which only flat steel mild could be employed and the required pressure could only be applied from the bottom hydraulic cylinders. Therefore, for the purpose of this study, only square cross sections were produced and employed as the primary shape for the cross sections of the BVC reinforcement systems. Further investigations on the impact of various shapes of the cross sections of BVC reinforcement are beyond the scope of the present study; it has been proposed in the future works section of this thesis that such impacts be investigated in a separate study.

5.5.2. Production of transverse BVC reinforcement

The production of transverse reinforcement or stirrups requires careful and novel design of the hot-press mold and optimization of the veneer width and length. The stirrups are placed perpendicular to the long axis of the beam to resist the shear forces and provide sufficient anchorage to the longitudinal reinforcements, as explained in section 3.2.1. Therefore, the load transfer within the veneer layers in the BVC samples for stirrup production should be directed in a continuous loop, unlike in longitudinal reinforcement in which only a unidirectional load transfer in one axis is required. To do so, a U-shape mold was fabricated from heat-treated steel for the production of the BVC stirrups in this study. Fig. 95 shows the mold and its cross section before it was placed into the hot-press machine. The U-shape mold had a length of 1,800mm. The cross-sectional size was designed according to the preliminary reinforced concrete beam design before the casting and production of the concrete samples by considering the shear design concept of reinforced concrete member. Furthermore, the wide-angle corners of the cross sections gave the corners and sides of the stirrups sufficient

pressure from the hot-press compression molding machine during production. This design ensured sufficient epoxy penetration into the veneer layers at the corners and along the sides of the composite samples. A U-shape mold with parallel sides would not have received sufficient pressure, given the fact that hydraulic cylinders applied pressure only from the bottom side of the hot-press machine and no pressure was directly applied to the side legs of the stirrup mold.

Therefore, to optimize the side pressure and ensure the infusion of epoxy matrix within the cross section of the stirrup legs, the final angle chosen for the sides of the steel mold was designed after careful calculation of the side pressure through consultation with the hot-press compression molding manufacturer and its engineering design team. Computer simulations of the pressing process with various angles of the U-shaped steel mold were carried out by the hot-press machine manufacturer, in order to provide adequate feedback to the PhD candidate regarding the side pressures applied to the legs of the stirrups before the final design was chosen. The final design shown in Fig. 95 was chosen for the fabrication of the BVC stirrups in this study.
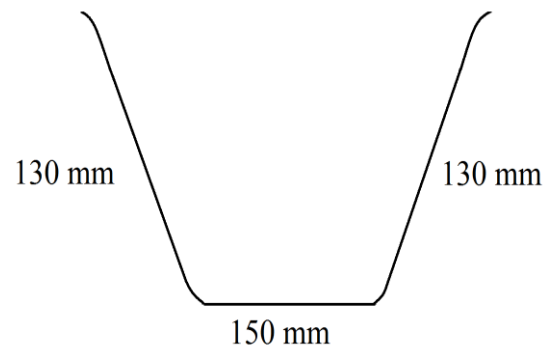
Fig. 95 U-shape steel mold for fabrication of stirrups

1,300gr of veneer layers were formed into pieces with dimensions of minimum 500mm (along fiber direction) and 1,000mm (perpendicular to fiber direction). The veneer layers with and without knots were used in this section to produce the BVC stirrups. The veneer layers were first treated with 1wt% NaOH solution for 24 hours, followed by rinsing with normal water to remove the alkali solution and finally neutralized with HCl acid. The wet veneer

layers were then dried at 80°C for 48 hours to reach an equilibrium moisture content of less than 10%.

Once dried, the veneer layers were impregnated with the Super Sap® INF/CLR epoxy resin system. The Super Sap® INF/CLR epoxy resin system comprised up to 17% of the final composite sample. The BVC stirrups were prepared by aligning the shorter side (along the fiber direction) of impregnated veneer layers along the short axis of the U-shape mold covering the two sides and bottom section of the mold. The fiber direction of the veneer layers was maintained along the sides of the steel mold as shown in Fig. 96. This arrangement was made possible after an intensive period of three months of fabricating various samples of BVC stirrups with different veneer alignments to find the most optimum fiber directions which would result in high mechanical properties of the final stirrups.
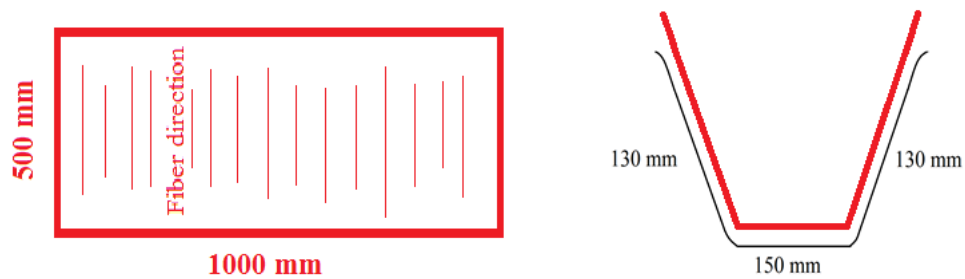
Fig. 96 The schematic of veneer layers placement into U-shaped mold

Maintaining the fiber direction along the shorter axis of the steel mold had the advantage of achieving the highest axial strength (e.g. tensile, shear or compressive) of the BVC stirrups along the fiber direction by utilizing the bamboo fibers' unidirectional properties which gave the stirrups their maximum mechanical capacities. This process would ensure sufficient shear resistance from the BVC stirrups and thus smooth shear transfer from the concrete matrix to the stirrups perpendicular to the longitudinal axis of the beam during the tests described in chapter 6.

The overlaying technique developed for the production of longitudinal reinforcement was avoided in this section by fabricating BVC samples with maximum length of 1,000mm which was the available size of the veneer layers used during the fabrication process. Therefore, the continuous impregnated veneer layers with length of 1,000mm were stacked and made into a layered structured for fabricating the stirrups with the required thicknesses. Mild pressure

was applied on the stack of impregnated veneer layers through a metal roller to remove trapped air and excess epoxy-resin matrix between the layers. The stack of impregnated veneer layers was then placed into the U-shape mold of the hot-press compression molding machine and pressed at a temperature of 100°C and a pressure of 20MPa for 30/30min of press/post-curing. The final BVC stirrup sample was cured for 48 hours in a curing oven at a temperature of 55°C to achieve its full strength. Fig. 97 and Fig 98 show the BVC stirrups with their full length after the curing process was completed, before being cut into the required width and length. The final sample had a length of 1,000mm and a thickness of 8mm ± 0.2mm. As seen from both Fig. 97 and Fig. 98, the fiber direction of veneer layers was maintained along the shorter axis of the samples.

Fig. 97 BVC stirrup samples after removal from the curing oven before cutting into required width

As explained earlier, the fiber directions had to be maintained along the shorter axis of the sample, given the resistance required by the stirrups to the shear forces that would act perpendicular to the long axis of the concrete beam. The BVC samples shown in Fig. 97 and Fig. 98 were then cut along the fiber direction into stirrups with cross sections of 15mm in width and 6mm in thickness. This width and thickness were chosen after preliminary calculations of the shear capacity of stirrups with various sizes for reinforcing the concrete beams in chapter 6 and with regard to the loading capacity of the available UTM machine at AFCL.
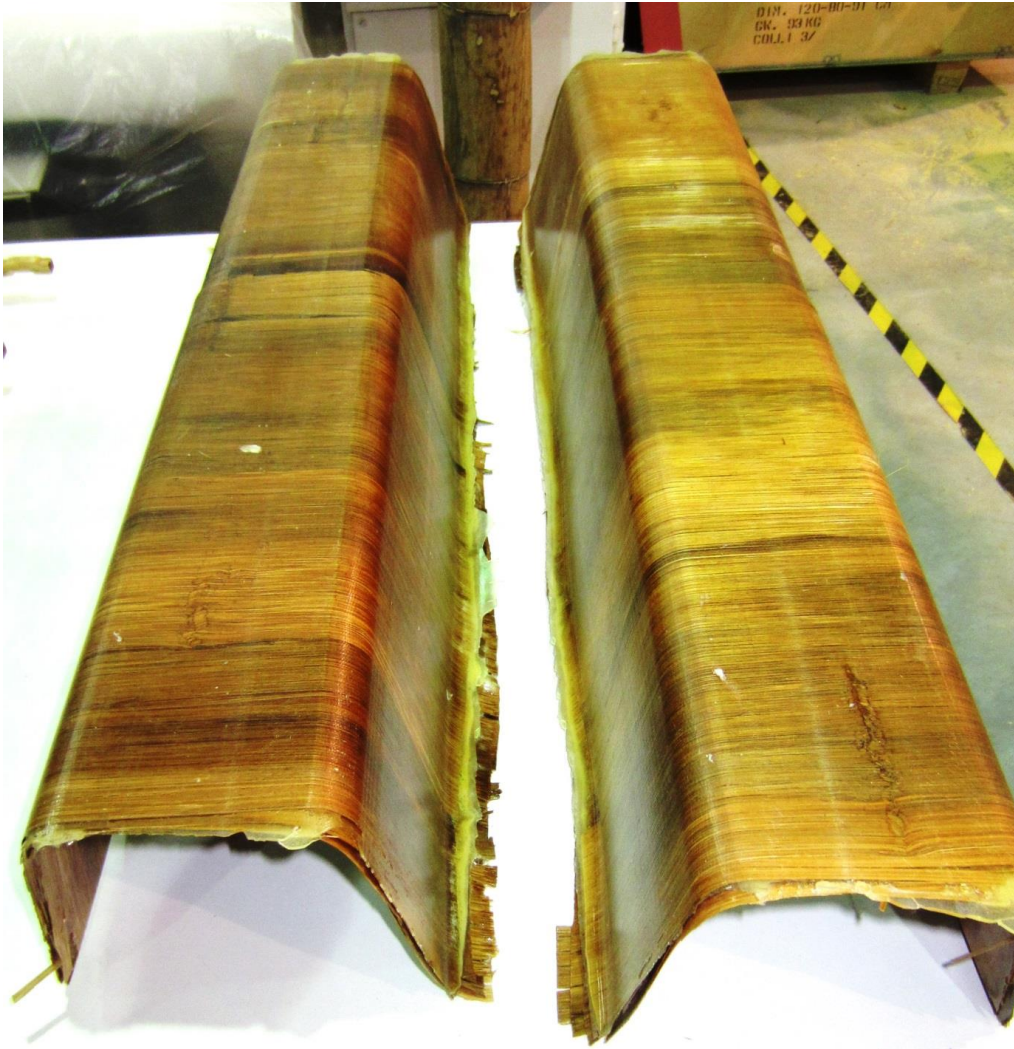
The detailed discussion and calculation were provided in chapter 6. Fig. 99 shows the stirrups after the larger BVC samples had been cut to the desired width and thickness. However, according to ACI 318 "Building Code Requirements for Structural Concrete and Commentary", to provide sufficient confinement to the longitudinal reinforcement in both compression and tension zone of the beam, the stirrups should have a closed loop shape in which they could stay intact before the failure was initiated from the longitudinal tension reinforcement. Furthermore, the closed loop stirrups could resist the torsion force, if any, during the loading and testing of the concrete beam. In simple terms, the failure of the concrete beam should not be introduced by the failure of the stirrups, but rather the longitudinal reinforcement.
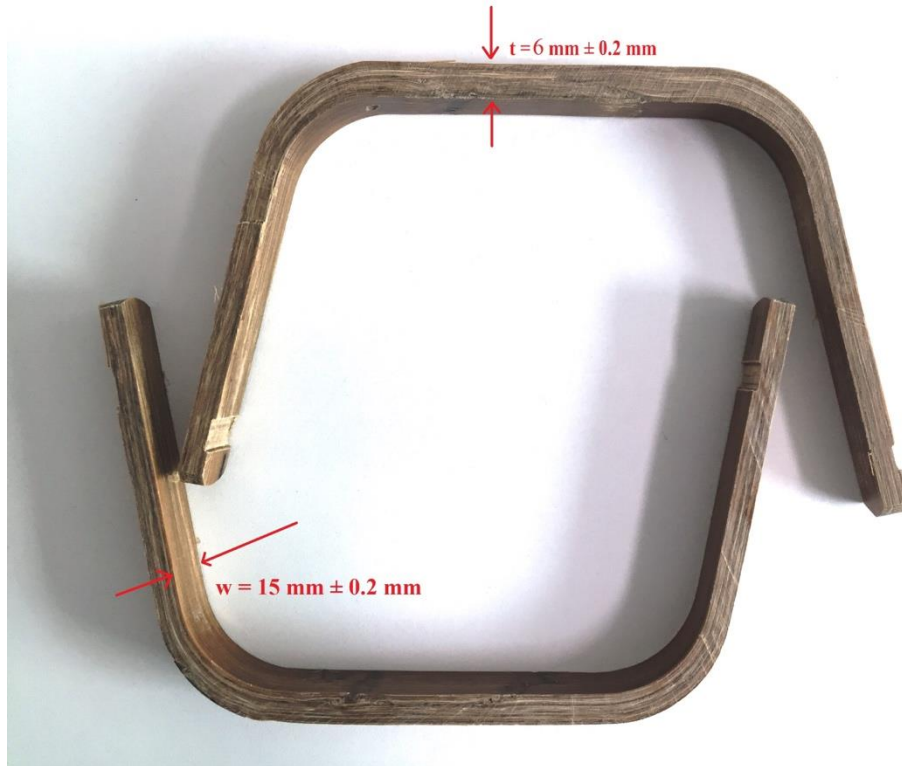
Furthermore, as ACI 318 recommends, the closed loop shape would provide sufficient development length along both vertical (parallel) sides of the stirrups. This development length ensures that sufficient bonding between concrete and stirrups is developed and that smooth stress transfer at the interface between the concrete matrix and stirrups are carried out which could resist diagonal cracking. Diagonal cracking is generally induced by shear forces along the various cross sections of any concrete beam. Without the shear reinforcement (stirrups), the concrete beam would fail due to diagonal tension cracks, as shown in Fig. 14, before the flexural failure of the longitudinal reinforcement could be initiated, as explained in detail in section 3.2.

To prevent such undesirable failure modes, sufficient shear resistance must be provided by the stirrups. To do so, preliminary investigation and calculation of the BVC stirrups according to the ACI design guidelines were carried out to find the suitable width and thickness of the stirrups, as explained in chapter 6. To follow the ACI recommendations and to provide sufficient development length and anchorage, the closed loop stirrups were prepared in this study which had the advantage of accommodating the BVC reinforcing bars at each corner. To prepare the closed loop stirrups, the two wide-angled single stirrups shown in Fig. 99 were bent slightly so that the two legs of the stirrups could stay parallel and side by

side. Since the curing process led to hardening of the fiber-epoxy matrix, a certain amount of pressure was necessary to form the parallel legs. To do so, a unique approach was undertaken in this research in which a mechanical clamp was employed to bend the stirrups through applying side pressure on the vertical legs. Once each single stirrup was bent to form the vertical legs, a high modulus stainless steel cable tie system was employed to hold the two stirrups together in a close loop shape, side by side, as shown in Fig. 100.

The final stirrups shown in Fig. 100 had dimensions of 130mm × 130mm. The squared shape of the stirrups would lead to a square cross section for the final concrete beams in chapter 6. This could contribute to the rather straightforward design and calculation of the final BVC reinforced concrete beams compared to rectangular cross sections in which the moment of inertia of the section can vary according to the axis of the cross section.

The selection of stainless steel cable tie, and not the nylon or bamboo based ties, was based solely on the high modulus of elasticity of steel which could provide sufficient stiffness to the closed loop system and prevent the single stirrups from detaching from one another once placed into concrete beam. Furthermore, the application of nylon or bamboo based ties with much lower stiffness would have increased the complexity in designing the beams and interpreting the results as they would have added unknown deformation patterns during the tests. Therefore, throughout this thesis, only high-performance stainless steel cable ties were used to tie the single stirrups and provide sufficient anchorage to the overlapped vertical legs.

The bent portion of the stirrups would have lower mechanical properties compared to the straight parts of the stirrups. Earlier studies on the different types of Fiber Reinforced Polymer (FRP) stirrups, including Glass Fiber Reinforced Polymer (GFRP) stirrups, had shown a tensile strength reduction of up to 45% of the strength parallel to the fibers' direction for the bent sections, due to the localized stress concentration as a result of the curvature which introduced radial stresses within the bent portions (Ishihara, Obara et al. 1997, Ahmed, El-Sayed et al. 2009).

However, in this work, the bent portions were not tested for their mechanical properties, especially the tensile strength, due to the complexity of the test set-up and unavailability of required machines and necessary testing facilities for the evaluation of the bent portions at AFCL in Singapore.
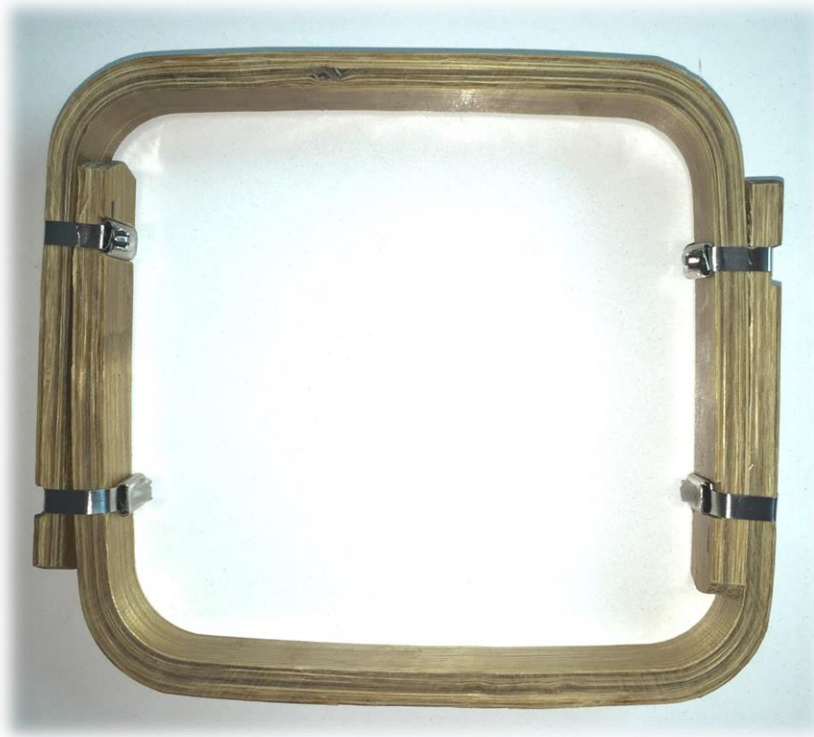
A strength reduction factor was applied according to ACI 440.1R-15 for the bent portions during the design process of the reinforced concrete beams with bamboo composite reinforcement. The argument for choosing this approach is that the recommended safety factors or reduction factors by the ACI design guide are largely over conservative, and therefore an additional margin of safety is normally considered when such factors are suggested. However, the tensile, flexural and compressive strength of the straight sections were measured. Further discussions on the design and calculation of the BVC reinforced concrete beams reinforced for shear and flexure were provided in chapter 6.

5.5.3. Properties of BVC reinforcement

Longitudinal reinforcement

Before preparing the reinforcement bars from the final BVC boards, the tensile and flexural properties, including strength and modulus of elasticity, were measured according to ASTM D3039-08 and ASTM D7264 respectively. The compressive strength of the boards was obtained according to ASTM D6641, "Standard Test Method for Compressive Properties of Polymer Matrix Composite Materials", along the fiber direction. For each series of tests, 5 samples were prepared from each 1,200mm-long board. A total of 10 boards were prepared for the longitudinal reinforcement and at least 50 samples were tested for each property.

Samples were taken from various locations along the boards to obtain average values which represented the composite properties along the full length and width of the boards. The Coefficient of Thermal Expansion (CTE) of BVC boards was also measured in this study with a Shimadzu TMA-60 Thermomechanical Analyzer for a temperature range of -20℃ to 50℃ along the fiber direction and perpendicular to the fiber direction. A total of 10 samples for each direction were tested for the Coefficient of Thermal Expansion (CTE) from each board. Table 32 shows the average mechanical properties and standard deviations of the boards fabricated for preparing the final longitudinal BVC reinforcement.

Table 32 Mechanical properties of longitudinal BVC reinforcement

Tensile Strength (MPa)	408±48
Modulus of elasticity in tension (MPa)	41,350±3,553
Modulus of rupture (MPa)	327±31
Modulus of elasticity in flexure (MPa)	33,835±3,460
Compressive strength along the fiber (MPa)	183±15
CTE along the fiber (µm/(m·℃))	7.35±0.45
CTE perpendicular to fiber (µm/(m·℃))	45.15±0.95

The final BVC boards fabricated for the reinforcement's preparation had an average specific density of 1.35. As shown in Table 32, the average tensile strength for the boards fabricated with NaOH treated perforated veneer layers, with knots between the fibers, and applying the optimized hot-press compression molding parameters, was 408MPa. This value corresponded to a 10% reduction in the average tensile strength of the BVC boards as shown in Table 30 where no knots were present in the treated veneer layers used for the fabrication of the BVC samples. Similarly, modulus of elasticity in tension was also reduced from 44,880MPa (Table 31) to 41,350MPa for veneer layers with knots in between the fibers in which overlaying and overlapping techniques were used. A reduction of almost 8% was observed in the modulus of elasticity of the samples tested in this section compared to samples shown in Table 31. Two factors contributed to the reduction of the tensile properties of the final BVC reinforcement boards:

- Overlaying technique used for the fabrication of the BVC sample
- Presence of knots between the fibers along the veneer section

As explained earlier, to produce the long composite boards to prepare for the BVC reinforcement in this section, the shorter pieces of the veneer layers were joined through the overlaying methods shown in Fig. 92 and Fig. 93. To fabricate the required length of 1,200mm for the reinforcement boards, a minimum of two layers with varying widths of up to 700mm and, in some cases, more than two layers with shorter widths, had to be connected to create the continuous layers of veneer. In this case, the load transfer between the two/three non-continuous veneer layers would only be carried out continuously if the fiber directions could have been maintained along the main axis of the composite between the layers at the overlaid areas not only in one section, but also throughout the entire impregnated stacks of veneer layers that were overlaid. Furthermore, the strong interfacial bond between the bamboo fiber and the epoxy matrix at the overlaid sections would also contribute to the smooth stress transfer between the non-continuous layers of veneer sheets.

However, maintaining the uniaxial fiber direction in all the layers of the impregnated stack of veneer sheets through hand-layup processing technique was not efficiently workable. Given the nature of bamboo as a heterogeneous material with varying fiber properties and surface characteristics even along the same section of veneer, the uniaxial stress transfer between overlaid veneer layers could be easily interrupted between the two overlaid sections in various layers when there were misalignments in the direction of the veneer layers. Even slight misalignments could negatively affect the overall axial properties of the BVC samples by disrupting the uniaxial path for the stress transfer between the two adjacent overlaid fiber bundles. As bamboo fibers have good uniaxial properties, any interruption to the axial transfer of stress could result in a reduction in uniaxial mechanical properties of the final BVC sample.

Beside the overlaying techniques affecting the tensile properties, the presence of knots between the fibers could also negatively affect the stress transfer between the fibers and matrix. This effect is mainly due to the irregularity of the bamboo microstructure at the knots. At the nodes (knots) of the bamboo culm, the arrangement of the cellulose fibers is distorted, unlike at the internodes where the fibers are axially oriented. The fibers at the nodes run transversely through the cross section and create an interwoven microstructure to provide the necessary stiffness for the bamboo culm when it grows vertically against lateral loads such as wind. Therefore, the transfer of uniaxial loads in the fibers is interrupted at the nodes' locations. This would then result in the reduction of uniaxial properties of raw bamboo veneer layers.

By employing the veneer layers with nodes between the fibers in the fabrication of the BVC samples, due to reduced uniaxial properties of the fiber bundles, the average uniaxial properties of the final BVC sample would decline subsequently, as proven by the results obtained in this section and shown in Table 32. If the nodes were not meant to be used for the fabrication of the composite reinforcement, the efficiency of the raw bamboo processing in this study would have deteriorated since all the veneer layers had to be processed once again after peeling and the nodes must be removed manually using scissors or a saw. This would have further increased the waste by-products of the whole process, and thus could have negatively affected the efficiency of the fabrication process, in which employing all parts from the bamboo culms for the composite fabrication and reducing the waste were integral aspects of this PhD research.

Nonetheless, the average tensile strength of the final BVC samples fabricated for the longitudinal reinforcement was above 400MPa. At this strength, the BVC reinforcement could stand at a higher tensile level compared to ASTM grade A615-40 reinforcing steel bars, and would be comparable to ASTM grade A615-60 reinforcing steel bars in terms of tensile strength. This result was achieved through processing the raw bamboo into the right veneer size and by optimizing the hot-press compression molding parameters, and with the selection of a suitable epoxy system. Furthermore, including the nodes in the veneer layers had inconsiderable effects on the tensile strength of the BVC reinforcement. However, unlike tensile strength, the modulus of elasticity of the BVC reinforcement was only one-fifth that of the ASTM A615 reinforcing steel bars. This low modulus of elasticity could pose a challenge in the design of the concrete beams reinforced with BVC reinforcement, especially when deformation and deflection govern the design of reinforced concrete beams. However, ACI 440.1R-15 has a set of designated safety factors to be used during the design stage to minimize the negative impacts of the brittle behavior of fiber reinforced polymer reinforcement compared to steel. This is discussed in the next chapter on reinforced concrete beam design and testing.

The average modulus of rupture (flexural strength) and modulus of elasticity in flexure of final BVC reinforcement were 327MPa and 33,835MPa respectively. The modulus of rupture and modulus of elasticity in flexure did not show significant changes compared to the values presented in Table 27 for the flexural properties of the BVC samples produced with veneer layers that contained no nodes. Though the veneer layers used in the production of the BVC reinforcement in this section had nodes in between the fibers and the overlay method was

used to produce the boards for reinforcement, the average flexural properties did not decrease in comparison with the BVC samples produced with veneers that had no nodes in between the fibers. This result clearly indicated that, unlike the negative effects that overlaying techniques and presence of nodes in veneer layers had on tensile properties of BVC samples, the flexural properties were not affected by these factors, as shown in this section via the test results in Table 32.

The likely reason for this performance could be the different behaviors that the BVC samples exhibited during the tensile and flexural tests. In the tension tests, all fibers of the composite sample were loaded by nearly the same uniaxial stresses; during a flexural test, most of the external fibers resisted the maximum stress and therefore the stress distribution varies across sample's thickness. Therefore, the thickness of the composite sample plays an important role in determining the sample's stiffness as well as moment of inertia which contributes to the ultimate flexural properties of the composite.

In the case of metals, the difference between flexure and tension is not significant, given the homogenous nature of the material, but in the case of non-homogenous brittle bamboo composite materials, the difference between tension and flexure seems to be more significant. In the case of bamboo composite materials, while in pure tension the load distribution along the thickness remains relatively unchanged, during the flexural test, due to the presence of various unknown defects, the stress distribution could potentially vary across the thickness.

In simple terms, during the flexural test, the probability of having overlapping veneer layers or nodes in the specific volume of the sample being tested is lower compared to that in the tensile test. Therefore, the negative side effects on flexural properties would be lesser compared to tensile properties of the BVC samples. However, this argument needs further evaluation and investigation in future works through a combination of laboratory experiments and statistical methods, such as Weibull statistics.

Transverse reinforcement (stirrup)

The stirrups from various BVC samples were selected randomly to evaluate their mechanical properties. As mentioned earlier in section 5.4.2, the bent portions of the stirrups were not tested; instead, the recommendations from ACI 440.1R-15, "Guide for the Design and Construction of Structural Concrete Reinforced with Fiber-Reinforced Polymer Bars", were followed by applying strength reduction factors to the mechanical properties of the straight (vertical and flat) sections of the stirrups. The design guide is discussed in chapter 6.

The tensile and flexural properties, including strength and modulus of elasticity, were measured according to ASTM D3039-08 and ASTM D7264 respectively. The compressive strength of the boards was obtained according to ASTM D6641. The straight sections of the stirrups, including the vertical legs and the flat bottom parts, were prepared for testing by cutting away the bent portions. For each test, at least 5 samples from the vertical sections and 5 samples from the flat bottom sections were prepared randomly and tested accordingly. Table 33 shows the properties and standard deviations of the straight sections of stirrups fabricated from the larger BVC samples.

Table 33 Mechanical properties of the straight and flat sections of the transverse BVC reinforcement (stirrups)

Tensile Strength (MPa)	371 ± 49
Modulus of elasticity in tension (MPa)	$38,101 \pm 3,023$
Modulus of rupture (MPa)	315 ± 28
Modulus of elasticity in flexure (MPa)	$30,401 \pm 3,911$
Compressive strength along the fiber (MPa)	161 ± 19
CTE along the fiber ($\mu m/(m \cdot °C)$)	7.15 ± 0.85
CTE perpendicular to fiber ($\mu m/(m \cdot °C)$)	52.43 ± 0.76

The average specific density of stirrups was 1.33, similar to the longitudinal reinforcement's specific density. All the mechanical properties measured were lower in comparison with longitudinal reinforcement's mechanical properties. The average tensile strength dropped by 9% whereas the average modulus of elasticity in tension decreased by 8%. Similarly, average modulus of rupture decreased from 327MPa for longitudinal reinforcement to 315MPa, a reduction of almost 4%. The average modulus of elasticity in flexure and the average compressive strength also decreased by 10% and 12% respectively.

The reduction of mechanical properties could be explained by the production process of the stirrups in comparison to the production of longitudinal reinforcements. As explained in detail in section 5.5.2 on the fabrication of the stirrups, due to the complexity of the shape required for the steel mold during the hot-press compression molding process, the inclined side legs of the BVC stirrups received less pressure compared to the bottom flat sections laid on the bottom side of the steel mold due to the wide angle chosen for the mold on the two sides.

The reduced pressure on the inclined sides of the steel mold would subsequently lead to lesser penetration and infusion of the epoxy matrix into the veneer layers, as explained in sections 5.4.1 and 5.5.2. Therefore, when the epoxy matrix was cured without interacting with all the fiber bundles due to the lack of complete infusion into the various layers of veneer, the interface between the epoxy and fibers could not be completely developed to its full strength. Thus the weak interfacial bond strength between bamboo fibers and epoxy system would subsequently result in lower mechanical properties.

Nevertheless, the angle of the side portions of the mold was designed after careful calculation of the optimum side pressure applied to the veneer layers through consultation with the hot-press compression molding manufacturer. Angles wider than the chosen one could have given the side legs higher pressure and better mechanical properties, but re-bending the cured composite samples into vertical shapes as shown in Fig. 106 would have been almost impossible nor feasible with the available facilities at AFCL in Singapore used for this PhD research. Therefore, in this work, the optimum angle was chosen according to preliminary calculations done together with the manufacturer for designing the appropriate steel mold to produce the necessary stirrups with the maximum possible mechanical properties. Other sizes of stirrups or different side angles of the steel mold could be the subject of future studies.

The Coefficient of Thermal Expansion (CTE)

The average CTE of the longitudinal BVC reinforcement along the fiber direction which is dominantly controlled by the bamboo fibers was 7.35×10^{-6} m/(m·°C). This CTE value is very close to the linear CTE values of concrete which varies between 7×10^{-6} m/(m·°C) to 12×10^{-6} m/(m·°C), depending on the concrete grade and cement type used in production. However, the CTE in perpendicular to fiber direction, which is controlled by the epoxy matrix, was higher than the average CTE of BVC reinforcement along the fiber direction. The CTE values of the stirrups along the fiber direction and perpendicular to the fiber direction were comparable to the CTE values of longitudinal reinforcement. However, the relative standard deviations of the BVC stirrups during the CTE measurements in this section ranged from 8% to 14%, which were slightly larger than the standard deviations obtained for the BVC longitudinal reinforcement samples.

In steel reinforced concrete members, the CTE values of the steel reinforcement and concrete are similar, so no significant difference between the thermal expansion values of concrete and steel reinforcement is observed. Therefore, under thermal loading, both steel and concrete in

steel reinforced concrete member would expand and shrink in all directions similarly. However, in the case of FRP reinforcement materials including GFRP and CFRP reinforcement, the CTE values are higher compared to steel and concrete, especially in the direction perpendicular to the fiber orientations (Nanni 1993, Gentry and Husain 1999). Concrete has CTE values in the range of 7×10^{-6} m/(m·°C) to 12×10^{-6} m/(m·°C). Depending on the type of cement, aggregate and the ratio of the ingredients, the values of the CTE of concrete could vary. ASTM graded steel reinforcement has a CTE of 8×10^{-6} m/(m·°C) to 12×10^{-6} m/(m·°C), which is in the same range as of that concrete mix.

In the case of BVC reinforcement, the longitudinal CTE controlled by bamboo fibers is similar to the CTE of concrete matrix with a range of 6×10^{-6} m/(m·°C) to 10×10^{-6} m/(m·°C), while the transverse CTE of BVC reinforcement is 4 to 5 times the average CTE value of concrete matrix. The CTE values of BVC materials depend largely on the type of epoxy-resin matrix used and also the ratio of fiber to epoxy resin matrix. The transverse CTE of BVC reinforcement is controlled mainly by the epoxy-resin matrix which has relatively high CTE values compared to the fibers.

Therefore, in the longitudinal direction, both BVC reinforcement and concrete expand similarly, which ensures sufficient bond between the concrete and BVC reinforcement is provided when the two materials undergo thermal cycles. In the transverse direction, due to the difference between the CTE of BVC reinforcement and concrete, thermal stresses are developed within the concrete sample around the reinforcement element, as explained in the literature in section 3.3.2. The thermal stresses developed within the concrete should be controlled to prevent internal tensile cracks which might affect the bond.

Two approaches are employed in this thesis to control the thermal stress induced by the transverse thermal expansion of the BVC reinforcement. The first approach, which extends the work carried out by Masmoudi, Zaidi and Gérard in 2005, considers a suitable ratio of concrete cover thickness to BVC reinforcement thickness to prevent or delay tensile cracking. The second approach, which builds on the work of Hany Abdalla in 2006, compares the thermal stresses developed within the concrete matrix at various temperatures with the tensile strength of the concrete to predict any potential thermal cracking that can occur. This approach allows for the preliminary evaluation of possible bond failure that can be initiated at the interface of the concrete and reinforcement. These two methods are found to be suitable for limiting and preventing the development of internal thermal stresses caused by the

transverse thermal expansion of the BVC reinforcement. More details are provided in chapter 6 where these two approaches and the experiments carried out are explained.

5.6. Conclusions

Based on the two methods studied on processing raw bamboo culms, bamboo composite samples produced with bamboo veneer layers and with a bisphenol-A-based resin and a diamine-based hardener composed of Super Sap® CLR epoxy and Super Sap® INF hardener have the best mechanical properties. Therefore, Bamboo Veneer Composite (BVC) materials produced with this epoxy system are chosen for the rest of the research. Pressing the epoxy impregnated perforated bamboo veneer layers pre-treated by 1wt% NaOH solution at a temperature of 100°C and a pressure of 20MPa for 30/30 minutes of curing/post-curing time, followed by a second post-curing step at a temperature of 55°C for 48 hours lead to the highest mechanical properties for the BVC samples. Two series of reinforcement designs are presented: one for longitudinal reinforcement which resists the axial and flexural loads, and one for transverse reinforcement to resist the shear forces. The longitudinal reinforcement have an average tensile strength of more than 400MPa, which is comparable to some commercial steel reinforcing bars available in the market, mainly the ASTM A16 series of reinforcing bars of grades 40 and 60. The transverse reinforcements show slightly lower values for the mechanical properties compared to the longitudinal reinforcements due to the limitations imposed by the fabrication process. The average Coefficient of Thermal Expansion (CTE) of BVC reinforcement along the fiber direction dominantly controlled by the bamboo fibers is comparable to the linear CTE values of concrete, while the transverse CTE range from 4 to 5 times the CTE values of concrete, as it is largely affected by the high thermal expansion coefficient of the epoxy resin. In spite of such differences, the newly developed composite bamboo material has much potential for use as reinforcement in concrete elements.

6. Bamboo Veneer Composite (BVC) reinforced concrete

6.1. Summary

The production of the concrete beams reinforced with Bamboo Veneer Composite (BVC) reinforcement is examined in this chapter. Pull-out experiments are designed to evaluate the bonding mechanism between the concrete and the newly developed BVC reinforcement. Different types of coatings and admixtures are investigated to evaluate their impact on the bond strength between the BVC reinforcement and concrete matrix. The bond strengths of treated and non-treated BVC reinforcement are subsequently evaluated through the pull-out tests of 150 concrete cylinders reinforced with BVC reinforcement. The influence of different CTEs of concrete and BVC reinforcement is investigated through monitoring the internal and external temperatures of the concrete pull-out cylinder samples. The results from the pull-out tests provide information regarding the type of treatment to be applied to enhance the bonding between reinforcement and concrete matrix for BVC reinforced concrete beam tests. The effect of water absorption and alkaline environment of concrete on performance of BVC reinforcement is also investigated by evaluating the tensile properties of 350 BVC reinforcements after exposure to various environments. The average tensile properties of coated BVC samples are reduced by less than 10% after 3 months' exposure to an alkaline environment. The coated BVC samples do not show a significant water uptake. BVC bars coated with water-based epoxy coating and sand particles and with an embedment length of 200mm show the highest average bond strength. The temperature difference between the internal and external concrete surfaces recorded during the concrete curing and before the pull-outs is shown to be between 0°C to 28°C; this is not enough to develop internal tensile cracks due to tangential stresses around the BVC bars, and thus the bond mechanism between the BVC reinforcement and concrete is not affected. The results of the flexural tests of 110 BVC reinforced concrete beams reveal the advantages of using BVC reinforcement in enhancing the load-bearing capacity of the concrete beams in comparison with non-reinforced concrete beams of similar cross sections. Furthermore, the results indicate that steel reinforced concrete beams of similar characteristics show comparable ultimate loads. However, their initial cracking loads are higher compared to BVC reinforced concrete beams. The design guidelines stated in ACI 440.1R-15 for FRP reinforcement bars are also compared to the experimental results obtained in this study, which indicate the suitability of the ACI design guidelines for the preliminary design and construction of BVC reinforced concrete members.

6.2. Bond strength evaluation of BVC reinforcement with concrete

The key factor for employing the newly developed BVC reinforcement in concrete is the bonding mechanism of BVC reinforcement bars to the surrounding concrete matrix at an acceptable temperature range. Sufficient bonding between BVC reinforcement and the concrete matrix ensures a smooth stress transfer between the two materials, and therefore contributes to the overall performance of the BVC reinforced concrete member. If sufficient bonding strength between the two materials is not developed, the stress transfer between reinforcement and concrete matrix will be constantly disrupted by the discontinuous interfacial microstructure at the concrete-reinforcement interface, and thus premature failure of the reinforced concrete member will follow due to the lack of continuous tensile stress transfer from the weak concrete matrix to high-performance BVC reinforcement, especially in the tension zone of the member. However, a perfect bond between concrete and BVC reinforcement would contribute to higher ultimate load-bearing capacity of the reinforced concrete member by activating the maximum mechanical capacities of the BVC reinforcement through providing an interfacial microstructure which would guarantee smooth tensile stress transfer between the two materials.

To understand the bonding mechanism between the newly developed BVC reinforcement and concrete, a series of pull-out tests were designed to find a suitable technique which could enhance the bonding between the two materials. The pull-out tests are widely accepted for steel reinforcement and some FRP materials as means of evaluating their bond mechanism with concrete matrix. Furthermore, the pull-out tests were selected for this study due to the absence of suitable techniques to investigate the bond mechanism of newly developed BVC reinforcement with concrete.

To enhance the bond mechanism between the BVC reinforcement and concrete matrix, 4 types of coatings have been investigated in this research. The coatings were applied on the surface of the reinforcements before being placed into the concrete cylinders to investigate the bonding behavior with concrete matrix. The coatings and their chemical composition are discussed in this chapter. Normal strength concrete with an average compressive strength of 20MPa was used to prepare the concrete cylinders for the pull-out tests. The low strength concrete grade was chosen primarily to eliminate any complex behavior that could rise due to the combination of high compressive strength concrete and BVC bars during the pull-out tests. Higher strength concrete could further enhance the pull-out strength and the bonding

between concrete and BVC bars by developing higher compressive stresses at the interface of the BVC bar and concrete. Therefore, to ensure that only the bonding performance of the BVC bars were investigated through the pull-out tests and that the concrete strength would not play a significant role, only the lowest available concrete grade was chosen for this study.

6.2.1. Pull-out sample preparation

The BVC samples were prepared from the composite boards produced in section 5.5 into half dog-bone shaped bars with a cross section size of 10mm × 10mm. The dog-bone shape for the grip of the UTM machine was chosen to ensure that the risk of slippage during the tests could be minimized, based on the preliminary tests carried out in the laboratory on the grip size, shape and pull-out test setups. Fig. 101 displays the BVC samples prepared for the pull-out test.

Fig. 101 BVC pull-out samples with dog-bone shaped grip

In addition to the samples that were coated on the surface and placed into the normal concrete mix, a series of concrete samples were prepared by adding an adhesive system directly into the normal concrete mix to study the bonding enhancement through increasing the viscosity of the concrete without adding any coating on the surface of the bamboo composite samples. Two bonding lengths of 200mm (20 × thickness) and 100mm (10 × thickness) were considered in this study.

The chosen lengths were in accordance with the ACI design guide of 440.1R-15 for the application of FRP reinforcement in concrete in which similar bond lengths in ratio of reinforcement thickness are recommended to enhance the bonding mechanism. Furthermore, in steel reinforced concrete design guides published by the ACI, similar ratios are also recommended for steel reinforcement in concrete to ensure adequate bonding strength between concrete and steel was provided. The chemicals and coatings used in this study are explained here.

- Moisture Seal: a two part water-based epoxy coating (Bostik 2015)

Moisture Seal is a two-component, water-based epoxy system which was chosen for this study based on its waterproof vapor barrier membrane system. The waterproof system could impede the flow of any moisture or water backlog from the microstructural interface of the concrete and BVC reinforcement, thus creating a prefect interfacial environment for the stress transfer between concrete and reinforcement. Furthermore, due to its water-based formulation, it contained less harmful petrochemical based ingredients, according to its manufacturer. However, the exact formulation was not available from the manufacturer. The two parts of the Moisture Seal, namely the hardener and resin, were mixed in a 1:1 ratio. The coating was applied on the reinforcement bars with the help of a brush one day before concrete casting in order for the curing process of the coating to be completed. Once curing was completed (after 24 hours), the coated BVC bars were placed into the concrete matrix of the pull-out cylinders.

- ExaPhen coating; a bio-based epoxy resin system (Composite Technical Services 2012)

ExaPhen coating is a two-part epoxy resin formulation system which was chosen for this research since it offers high moisture and chemical resistance. Furthermore, as claimed by the manufacturer, the ExaPhen system is based on the well-known structure of cardanol, which is obtained by vacuum distillation of "cashew nut shell liquid" (CNSL) and thus is a byproduct of cashew nut processing. Therefore the ExaPhen system used in this study had a high bio-content of up to 75% by its weight. The ExaPhen system, when used as a coating for BVC reinforcement, could protect the reinforcement not only against water and moisture, but also against temperature fluctuations by creating a high thermal insulation layer around the reinforcement. This could be helpful in preventing any bond failure due to the inherent differences between the CTEs of BVC reinforcement and concrete as explained earlier. After

mixing the resin with the hardener, the coating was applied on the surface of the reinforcement bars with this help of a brush. The coating was cured for two days in a curing oven at a temperature of $45\,^0$C and relative humidity of 80%, as advised by the manufacturer of the ExaPhen system.

- Enamel Coating; a two-part epoxy resin coating (Conren Limited 2015)

Enamel Coating is a two-part epoxy coating system. It is resistant to a wide range of chemicals, which makes it an attractive coating for protecting the BVC reinforcement from the alkaline environment of concrete over a longer exposure time. Furthermore, as explained by the manufacturer, it has good abrasion resistance which could be beneficial in concrete applications as the surface layer of the BVC reinforcement could be damaged during the concrete casting process, due to contacts with the various aggregate sizes present in the mix. Damaged BVC reinforcement would be susceptible to faster degradation if any were due to exposure to the thermal cycles or alkaline environment of the concrete. The coating was applied on the surface of the reinforcement bars 2 days before the concrete casting, and the curing process was completed in a curing oven at a temperature of $45\,^0$C and relative humidity of 80%.

- TrueGrip BT; a two-part epoxy resin based surfacing system (Conren Limited 2015)

TrueGrip BT is a two-part epoxy resin based surfacing systems that can be used together with any concrete matrix. TrueGrip BT is a high-friction surfacing system which is mainly used on urban roads to minimize the risk of skidding of the vehicles on areas such as sharp bends, major junctions, gradients, roundabouts, traffic signals, pedestrian crossings and railway level crossings. Therefore it might be able to provide resistance to de-bonding forces between concrete and BVC reinforcement through its anti-skid formulations. Furthermore TrueGrip BT shows good resistance to variety of chemicals including petrol, diesel and salt according to the manufacturer's data sheet, and thus could provide a good protection for the BVC reinforcement in concrete against alkaline environment while maintaining the bond between concrete and reinforcement. The coating was applied on the surface of the BVC reinforcement two days prior to casting of the concrete samples to give the epoxy system sufficient time for the curing process to complete. The coated samples were kept in a curing oven at a temperature of $45\,^0$C and relative humidity of 80% for 48 hours before being placed into the concrete cylinders.

To further investigate the bonding mechanism between the concrete and BVC reinforcement, the addition of sand particles to the coating was also studied in this research. Two particle sizes for the sand coating were used; fine silica sand with particle sizes between 0.20mm and 0.30mm, and coarse silica sand with particle sizes of 0.70mm to 1mm. Silica sand was applied in this study together with various types of coatings. All the coatings were applied with and without sand particles to compare the effect of sand coating on the bonding mechanism between the BVC samples and concrete matrix. Fig. 102, Fig. 103, Fig. 104 and Fig. 105 show the pull-out samples prepared with moisture seal, ExaPhen coatings, Enamel and TrueGrip BT coatings respectively.

The sand particles are known to improve the surface roughness of reinforcements, therefore they could improve the bonding with the concrete matrix through creating physical and mechanical interlocking systems with the aggregates of the existing concrete matrix (Baena, Torres et al. 2009). Furthermore, the sand particles used on the coatings could develop chemical bonds through the hydration process with the cement particles and water within the concrete matrix, and thus might further improve the bond strength of the BVC reinforcement to concrete matrix.
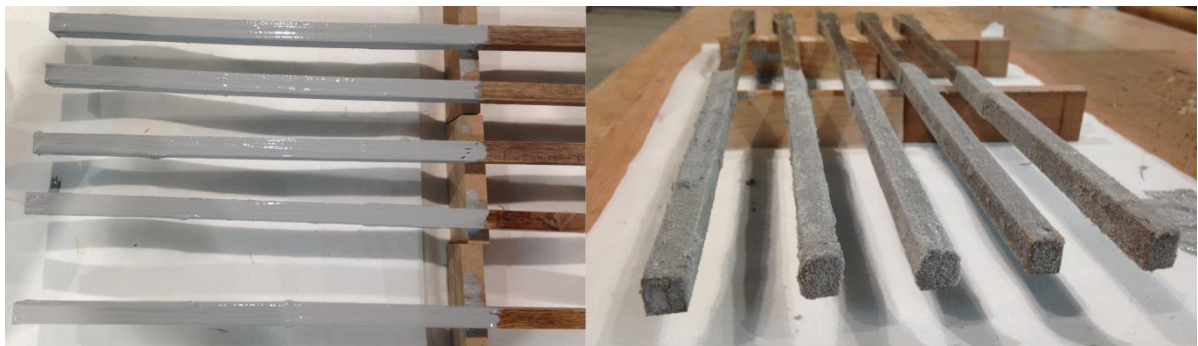
Fig. 102 Moisture seal water-based coating applied on the surface of reinforcement;
Left: Without sand particles   Right: With sand particles
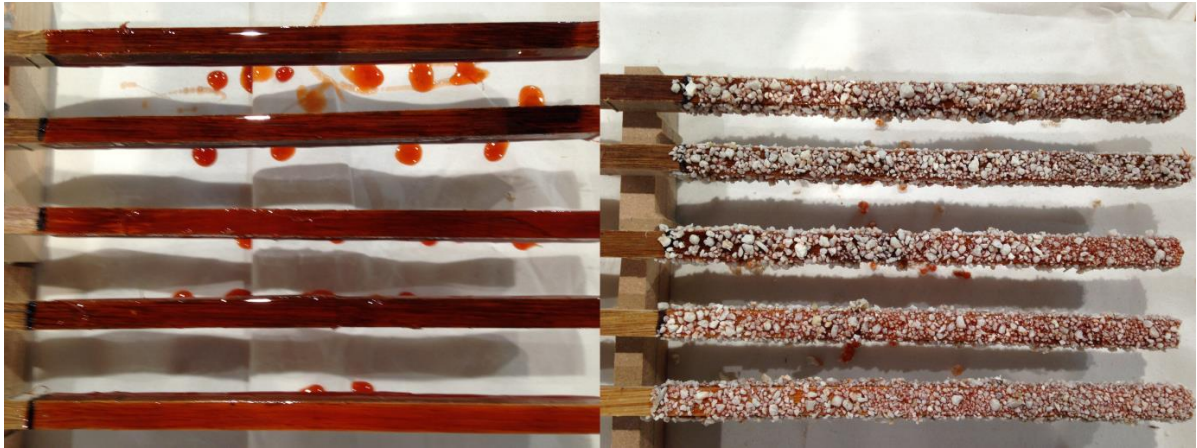
Fig. 103 ExaPhen coating applied on the surface of reinforcements;
Left: Without sand particles   Right: With sand particles

Fig. 104 Enamel coating as applied on the surface of reinforcements 30min before casting the concrete
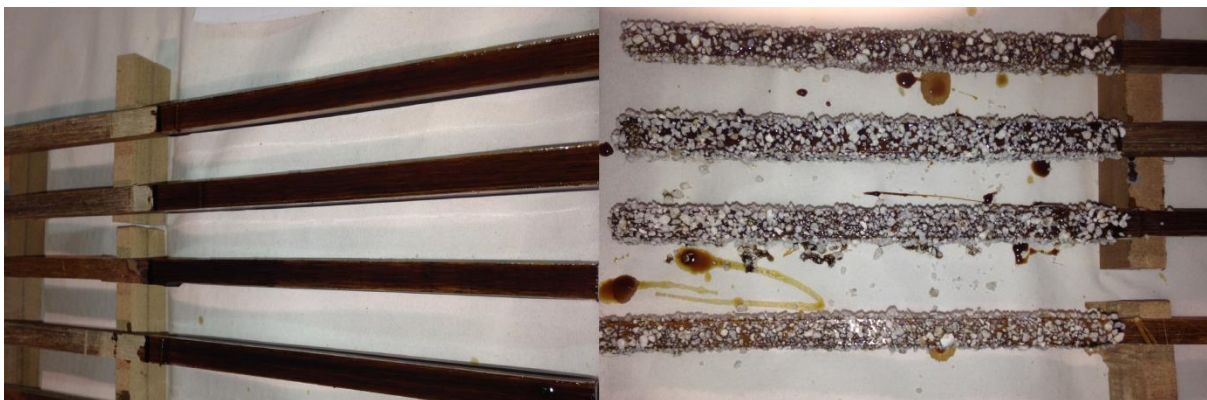
Fig. 105 TrueGrip BT coating applied on the surface of reinforcements;
Left: Without sand particles; Right: With coarse sand particles

246

Normal strength concrete of grade 20MPa prepared with Ordinary Portland Cement (OPC) was used for this study. The concrete mix for a volume of $1m^3$ concrete is shown in Table 34.

Table 34 Concrete mix proportions used to prepare pull-out samples

Water (kg/m^3)	182
Cement (kg/m^3)	280
Sand (kg/m^3)	850
20 mm Aggregates (kg/m^3)	1050
Water/Cement	0.65
Density (kg/m^3)	2362
Slump (mm)	100

The concrete grade of 20MPa was chosen due to its wide range of applications in many countries, including developing countries in Asia, Africa, and South and Latin America. Cylinders of 300mm in height and 150mm in diameter were used to prepare the concrete pull-out specimens. The recommendations of ASTM C900-15 standard titled "Standard Test Method for Pull-out Strength of Hardened Concrete" were largely followed, except in some cases where the sample size and shape had to be modified in order to be compatible with the available testing machine at AFCL in Singapore. For each batch of casting, a slump test was performed according to ASTM C143 titled "Standard Test Method for Slump of Hydraulic-Cement Concrete" to control the quality and consistency of the concrete mix for each batch, and to ensure similar physical and mechanical properties between the various batches of concrete mix could be obtained during the casting of the various concrete cylinders (ASTM International 2015). The slump value for all the batches was between 110mm and 95mm. Fig. 106 shows a typical slump test at the laboratory.

Concrete mixes with slump values of more than 110 or lower than 95 were not used to prepare the concrete cylinders, in order to maintain the consistency and workability of all the samples in this research. The slump test functioned as a time- and cost-saving method in this study to prevent the creation of unfavorable results with large standard deviations from the pull-out tests after the 28-day curing of the concrete cylinders. Without the slump test, an unknown number of samples of pull-out tests with potential scattered results and large deviations would have to be prepared and cured for 28 days before the new series of tests could be carried out to repeat the whole process which would have required extra effort.

BVC bars with and without coating were placed at the center of the concrete cylinders during the casting process according to the ASTM guidelines, and at the specified embedment length of 200mm and 100mm as shown in Fig. 107 and Fig. 108. The concrete samples were cured in a curing room at 65% relative humidity and a temperature of 45°C for 28 days before

testing to ensure cement hydration process could take place in an environment with adequate moisture and temperature.

To further monitor the strength development of the concrete samples, 7-day and 28-day compressive strength tests were performed by casting concrete cylinders of 150mm in diameter and 300mm in height according to ASTM C39-16b titled "Standard Test Method for Compressive Strength of Cylindrical Concrete Specimens" (ASTM International 2016). The 7-day and 28-day compressive strength tests helped to evaluate closely the properties of the concrete mix for each batch of pull-out test samples before the final pull-out test was carried out.

Therefore in the case of large deviations from the average compressive strength obtained during the 7-day or 28-day compression test, the respective batch of concrete pull-out samples would not be used any further. Furthermore, when large variations in concrete compressive strength were observed during the 28-day curing process through compression tests, certain batches of concrete pull-out samples were cast again to ensure comparable quality and consistency within all the pull-out tests were maintained throughout the experiments in this study.

Furthermore, the tensile strength of the cylinders was also measured according to ASTM C496-11 titled "Standard Test Method for Splitting Tensile Strength of Cylindrical Concrete Specimens" (ASTM International 2011). The splitting tensile strength is normally used in the design of structural concrete members to investigate the shear strength provided by the concrete matrix and also to analyze the required development length of the reinforcement in concrete. Therefore, the results of the tensile tests of concrete cylinders in this section could be used further in section 6.3 for the design of BVC reinforced concrete beams.

Beside the compressive and tensile strength, the modulus of elasticity in compression was also measured in this section, according to ASTM C469-14 titled "Standard Test Method for Static Modulus of Elasticity and Poisson's Ratio of Concrete in Compression" (ASTM International 2014).
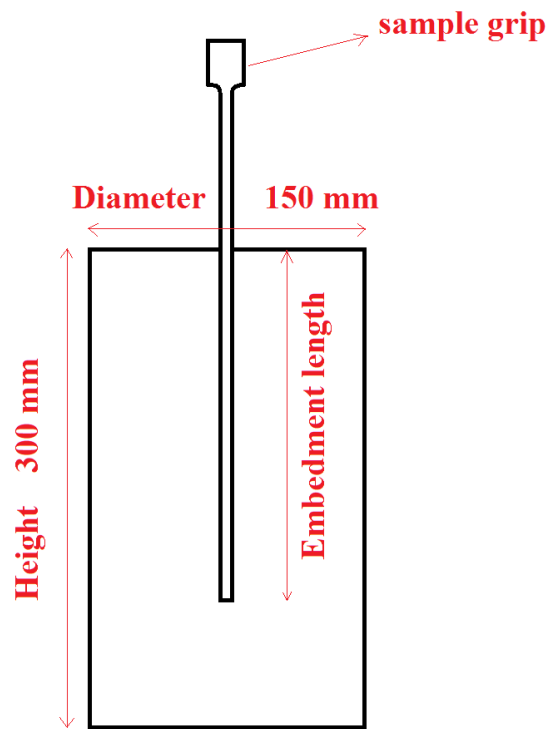
Fig. 107 Details of the pull-out concrete sample with embedment BVC bar

Fig. 108 Concrete pull-put samples with embedded BVC bars

The modulus of elasticity of concrete sample plays an essential role in the design of reinforced and non-reinforced structural concrete members, especially for evaluating the required number of reinforcements and computing the primary size of the concrete member. The results of the concrete mechanical properties are presented in Table 35.

Table 35 Mechanical properties of concrete cylinders used for the pull-out tests

	7-day	28-day
Compressive strength (MPa)	17±1.5	20±1.8
Tensile strength (MPa)	3.9±.4	6.2±.6
Elastic modulus in compression (MPa)	19,255±2,411	25,410±1,822

As Table 35 shows, the average 28-day properties of the concrete cylinders had improved compared to the 7-day properties. The enhancement of the mechanical properties over time was the result of the cement hydration process in which, through the various chemical reactions occurring between water and cement molecules over time, the products of the cement hydration process slowly bonded the individual sand particles and various aggregates used in the mix together to form the hardened concrete matrix with the required mechanical properties.

6.2.2. Test preparation and evaluation of the bond strength

Pull-out tests were carried out by fabricating a custom-made insert for the Shimadzu UTM machine at AFCL in Singapore. The insert was made from hardened steel and secured the position of the concrete cylinder during the test in which the bar was pulled out by the machine. The standard tensile grip could be used for this test due to the half-dog-bone shape chosen for the pull-out BVC bars. The loading rate was set to 2mm/min, similar to the tensile tests of the BVC samples. Tests were performed at a temperature of 23°C and a relative humidity of 65%. Fig. 109 shows the specimen and the test set-up at AFCL in Singapore.

Fig. 109 Pull-out test set-up

Before the test, a strain gauge was also attached to the exposed section of the BVC bar to measure the strains outside the concrete matrix as well as modulus of elasticity as shown in Fig. 110. This measurement was helpful in identifying any potential bond slippage due to the pull-out forces, rather than the tensile failure of BVC bar, during the test.

Table 36 summarizes the characteristics of the BVC bars employed in the pull-out tests in this thesis. As mentioned earlier, besides the coating treatments, two series of concrete mix were prepared with the addition of Moisture Seal water-based epoxy as an additive into the mix to investigate the effect of enhancing the concrete viscosity on the bond performance of BVC bars to the concrete. For these two concrete mix designs, only embedment lengths of 200mm were used to compare the results with the BVC bars without coatings embedded in normal concrete mix as shown in Table 36.

A schematic representation of the forces associated with the bond strength between the concrete and the BVC reinforcement is shown in Fig. 111. P is the pull-out force applied through the UTM machine in kN, l_a is the embedment length in mm, τ is the bond strength in MPa, a and b are the cross-sectional dimensions of the composite bar in mm.
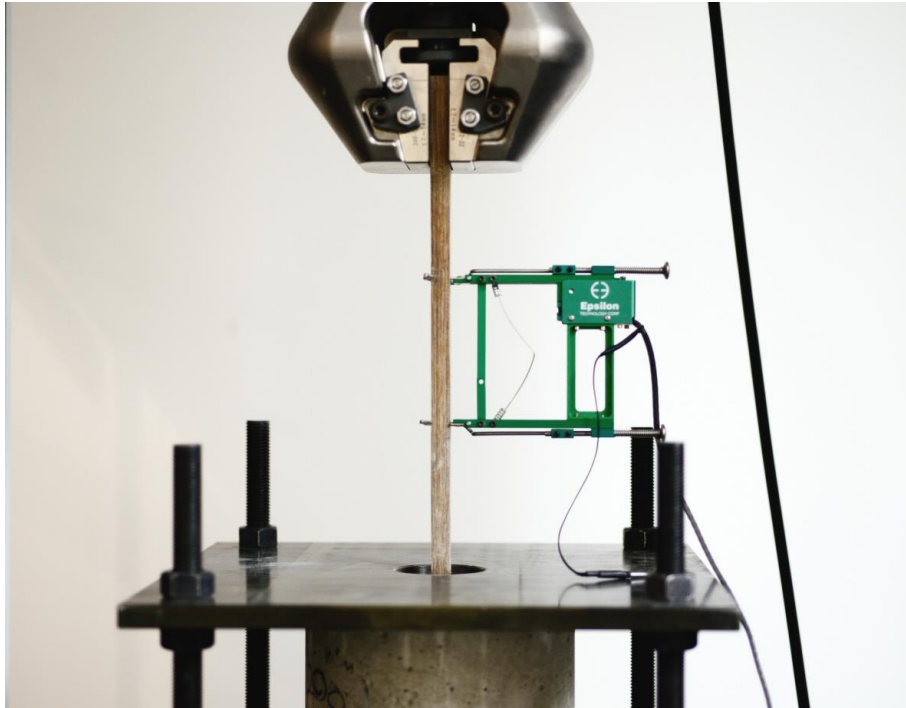
Fig. 110 Strain gauge attached to the free end of BVC bar during pull-out test
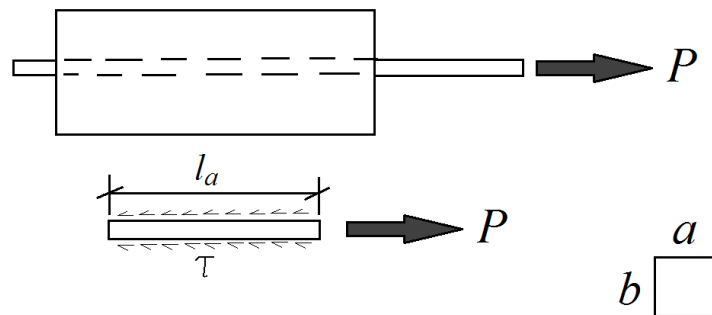
Fig. 111 Equilibrium of forces in bond strength evaluation of BVC bar and concrete during the pull-out test (Javadian, Wielopolski et al. 2016)

Equilibrium between the pull-out force and the shear force leads to the following equation:

$$\tau.(2a + 2b).l_a = P \quad \text{(Eq. 36)}$$

From Eq.36, the bond strength is determined using Eq. 37:

$$\tau = \frac{P}{(2a+2b).l_a} \quad \text{(Eq. 37)}$$

Table 36 Pull-out samples general properties

Batch	Type of treatment	Embedment length (mm)
1	No coating	100
2	No coating	200
3	Water-based epoxy coating	100
4	Water-based epoxy coating	200
5	Water-based epoxy coating + fine sand	100
6	Water-based epoxy coating + fine sand	200
7	Water-based epoxy coating + coarse Sand	100
8	Water-based epoxy coating + coarse Sand	200
9	Exaphen coating	100
10	Exaphen coating	200
11	Exaphen coating + fine Sand	100
12	Exaphen coating + fine Sand	200
13	Exaphen coating + coarse Sand	100
14	Exaphen coating + coarse Sand	200
15	Enamel coating	100
16	Enamel coating	200
17	Enamel coating + fine Sand	100
18	Enamel coating + fine Sand	200
19	Enamel coating + coarse Sand	100
20	Enamel coating + coarse Sand	200
21	TrueGrip BT coating	100
22	TrueGrip BT coating	200
23	TrueGrip BT coating + fine Sand	100
24	TrueGrip BT coating + fine Sand	20
25	TrueGrip BT coating + coarse Sand	100
26	TrueGrip BT coating + coarse Sand	200
27	Cement Epoxy in concrete mix by 25% weight of cement	200
28	Cement Epoxy in concrete mix by 10% weight of cement	200

The bond strength was measured for all the series of pull-out samples displayed in table 36. For each series of pull-out test, five specimens were prepared and tested till failure. Two modes of failure were observed during the tests: bamboo tensile failure and bond failure.

Fig. 112 shows the typical load-displacement curve for pull-out samples with bamboo tensile mode of failure, in which the BVC bar breaks before any slippage occurs due to bond failure. As the curve in Fig. 112 shows, the BVC bar has a linear elastic behavior until it fails due to the tensile rupture mode of failure. This mode of failure indicates that there is sufficient

bonding between BVC bar and concrete which prevents the slippage of the bar due to bond failure. Furthermore, it shows that the bonding strength exceeds the tensile capacity of the BVC bar.

Fig. 113 shows the load-displacement curve when the failure is due to bond failure between the BVC bar and concrete matrix. As Fig. 113 indicates, the pull-out sample exhibited a linear elastic behavior before it slipped due to bond failure, and the curve developed into a plateau. Eventually, the BVC bar pulled out of the concrete cylinder due to complete bond failure, which could be seen from the load-displacement curve when the curve was descending. There was no concrete splitting failure mode observed for the samples during the testing.

Fig. 114 and Fig. 115 show the BVC pull-out sample with 100mm embedment length which slipped due to insufficient bond strength with the surrounding concrete matrix. The applied stress exceeded the bond strength of the bar and eventually overcame the frictional forces between the concrete matrix and the BVC bar. Fig. 114 and Fig. 115 correlated with the load displacement curve shown in Fig. 113 in which, after a linear elastic behavior, a plateau was observed and subsequently the bond strength between BVC bar and concrete was overcome by the pull-out force employed by the UTM machine where the bar completely slipped out from the concrete cylinder. The tensile mode of failure is shown in Fig.116, Fig. 117 and Fig. 118. In all the figures, the tensile mode of failure was clear and there were no signs of bond failure or slippage during the test.
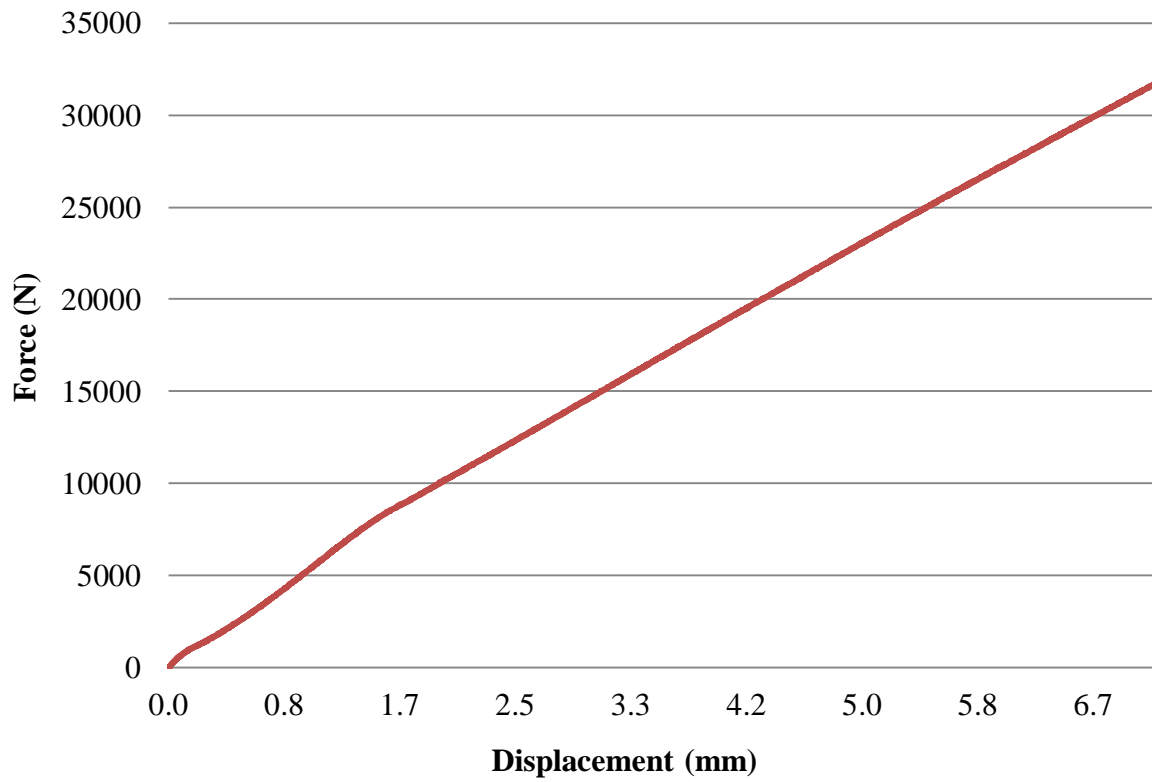
Fig. 112 Typical load-displacement curve for a tensile failure mode of pull-out samples
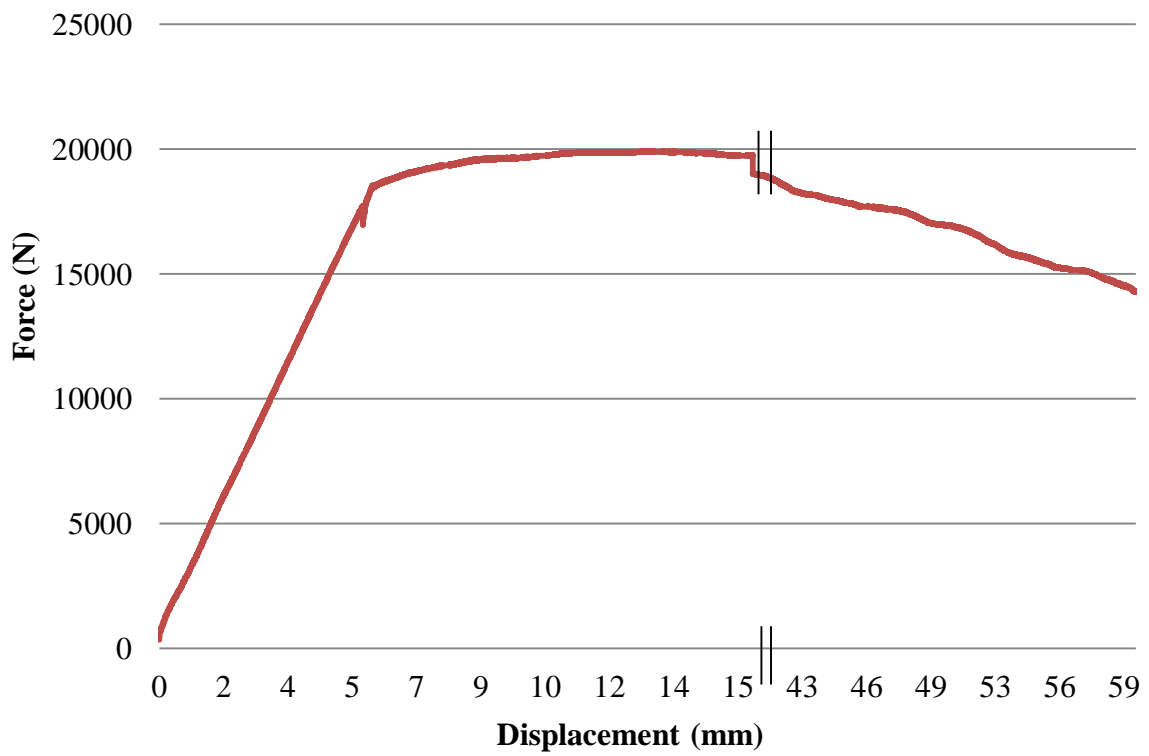
Fig. 113 Typical load-displacement curve for the bond failure mode of pull-out samples

256

Fig. 114 Bond failure and slippage of BVC bar from the concrete matrix

Fig. 115 Complete pull-out of BVC bar from the concrete cylinder sue to bond failure

257

Fig. 116 Tensile rupture of the BVC bar during the pull-out test

Fig. 117 Tensile failure of the BVC bar tested under the UTM machine

Fig. 118 Tensile failure of the BVC bar

Table 37 summarizes the results of the pull-out tests with the average bond strength and mode of failure, either tensile or bond failure, obtained for each batch of specimens. The standard deviations for each batch of specimen are also shown in Table 37. The sand coating was used with all type of coatings to compare its effect in improving the bond mechanism between the concrete and BVC bar.

As seen from Table 37, the difference in bonding strength of 100mm and 200mm embedment lengths was noteworthy for all types of coating employed in this study. Samples with 100mm embedment length did not show any tensile failure mode, except for samples of water-based epoxy coating, and sand particles where the tensile failure modes were observed with bond strength of 3.05MPa and 3.10MPa for fine sand and coarse sand respectively.

All samples with 200mm embedment length showed better performance in terms of bond strength between the concrete and BVC bar, even for reference samples where no coating was applied. Samples coated with water-based epoxy and fine sand had the highest average bond strength of 3.65MPa for 200mm embedment length, while the lowest average bond strength of 2.44MPa was observed for samples coated with TrueGrip BT coating without any sand particles while the embedment length was only 100mm.

Table 37 Pull-out test results for BVC bars

Batch	Type of treatment	Embedment length (mm)	Bond Strength (MPa)	Failure Mode
1	No coating	100	2.88±0.15	Bond failure
2	No coating	200	3.61±0.23	Tensile failure
3	Water-based epoxy coating	100	2.91±0.11	Bond failure
4	Water-based epoxy coating	200	3.47±0.16	Tensile failure
5	Water-based epoxy coating + fine sand	100	3.05±0.21	Tensile failure
6	Water-based epoxy coating + fine sand	200	3.65±0.10	Tensile failure
7	Water-based epoxy coating + coarse Sand	100	3.10±0.30	Tensile failure
8	Water-based epoxy coating + coarse Sand	200	3.61±0.18	Tensile failure
9	Exaphen coating	100	2.77±0.18	Bond failure
10	Exaphen coating	200	3.36±0.27	Tensile failure
11	Exaphen coating + fine Sand	100	3.16±0.21	Tensile failure
12	Exaphen coating + fine Sand	200	3.46±0.30	Tensile failure
13	Exaphen coating + coarse Sand	100	3.36±0.27	Tensile failure
14	Exaphen coating + coarse Sand	200	3.53±0.19	Tensile failure
15	Enamel coating	100	2.85±0.24	Bond failure
16	Enamel coating	200	3.10±0.19	Tensile failure
17	Enamel coating + fine Sand	100	3.16±0.21	Tensile failure
18	Enamel coating + fine Sand	200	3.47±0.12	Tensile failure
19	Enamel coating + coarse Sand	100	3.29±0.18	Tensile failure
20	Enamel coating + coarse Sand	200	3.52±0.20	Tensile failure
21	TrueGrip BT coating	100	2.44±0.24	Bond failure
22	TrueGrip BT coating	200	2.67±0.31	Bond failure
23	TrueGrip BT coating + fine Sand	100	2.57±0.31	Bond failure
24	TrueGrip BT coating + fine Sand	200	2.79±0.31	Bond failure
25	TrueGrip BT coating + coarse Sand	100	2.60±0.29	Bond failure
26	TrueGrip BT coating + coarse Sand	200	2.85±0.22	Bond failure
27	Cement Epoxy in concrete mix by 25% weight of cement	200	3.52±0.28	Tensile failure
28	Cement Epoxy in concrete mix by 10% weight of cement	200	2.75±0.11	Bond failure

The samples coated with Enamel and ExaPhen coatings showed comparable results for various combinations of embedment lengths and sand particles. Overall, they showed lower bond strength values compared to Moisture Seal water-based coatings. An addition of 10% wt. water-based epoxy to the concrete mix resulted in bond strength of 2.75MPa while adding 25% wt. water-based epoxy to the concrete mix resulted in a bond strength of 3.52MPa, an increase of almost 28%. The bond strength values of the BVC samples tested in concrete cylinders with an addition of 25% wt. water-based epoxy were comparable to the bond

strength values obtained from samples coated with ExaPhen and Enamel coating sand particles with an embedment length of 200mm. This observation suggested that the viscosity of the concrete mix was modified by the addition of the water-based Moisture Seal coating to the concrete matrix; therefore a higher degree of adhesion was achieved between the concrete and BVC bars though no coating was directly applied on their surfaces.

The increase in embedment length from 100mm to 20mm resulted in an increase of 19% to 25% in bond strength values for all samples. It showed that the shorter embedment length was not sufficient to provide adequate shear resistance to the external pull-out force. No bond mode of failure was observed for the 200mm embedment length which was in accordance with this finding. All the samples with bond strength values of less than 3MPa reached their failure limits following a bond mode of failure as shown in Table 37. This result could be useful in establishing the development length of the BVC reinforcement with various cross sections and with different concrete grades. The bond strength of 3MPa could function as a threshold limit for the failure mechanisms moving from bond mode of failure to bamboo tensile mode of failure.

Beside the embedment length, the addition of sand particles also improved the bonding strength by up to 26% compared to non-sand coated samples. The general aim of the application of sand coatings was to determine whether the sand particles could help to increase the bond strength between the BVC bars, the coating and the concrete. It was observed that by adding sand, either fine or coarse silica sand particles, to the coatings, the bonding between the concrete and the BVC bars was improved. However, no significant differences were observed between the results of the pull-out tests when fine or coarse sand particles were added to coatings. Both fine and coarse sand particles generally improved the bond strength between the BVC bar and concrete as shown in Table 37.

The sand particles increased the bonding between the BVC bars and the concrete aggregates by enhancing the frictional forces between the sand particles and the rough cured concrete surface surrounding the composite bars. When the BVC bar was pulled out of the concrete cylinder, frictional forces developed due to the interlocking mechanism between the sand particles and concrete aggregates; especially fine and large aggregates prevented the slippage of the BVC bar by overcoming the pulling forces applied by the UTM machine. When the pull-out force could overcome this friction force, then the tensile capacity of the BVC bar could be activated. With further increases in the pull-out force, tensile failure of the BVC bar

would occur as shown in Fig. 116, Fig. 117 and Fig. 118. However, if the pull-out force exceeded the frictional forces but not the tensile capacity of the BVC bar, then the BVC bar would slip entirely from the concrete cylinder as shown in Fig.114 and Fig. 115.

The BVC bar could develop a strong bond with concrete when the concrete was completely cured after the 28-day curing process as shown by the results of the pull-out tests in this section. However, as shown in Table 37, the average bond strength of BVC bars without any coating and in normal concrete mix with an embedment length of 200mm was as good as BVC bars coated with Moisture Seal water-based epoxy coating and sand while the embedment length was 200mm. Thus to maintain the bond in the long term, the addition of a coating and sand could provide many advantages.

Firstly, the coatings applied on the surface of BVC reinforcement have long-term resistance to the alkaline environment as shown by their respective manufacturers and the data sheets of the testing results. Therefore, in concrete with an alkaline environment, the addition of coating on the surface of BVC bars could be helpful in further protecting the BVC reinforcement against potential long-term degradation and therefore maintaining the required bonding with the concrete matrix. Secondly, addition of sand particles to the coating would enhance the bonding by increasing the mechanical interlocking between the concrete matrix and BVC reinforcement. The bond strengths of the BVC bars with and without coating were similar to the bond strength of the plain Glass Fiber Reinforced Polymer (GFRP) reinforcement in normal strength concrete, as shown in the work of Brad Wambeke and Carol Shield from the American Concrete Institute (ACI) in 2006, as well as in the study carried out by Omar Chaallal and Brahim Benmokrane in Canada in 1993 (Chaallal and Benmokrane 1993, Wambeke and Shield 2006).

Therefore, in preparing the concrete beams reinforced with BVC reinforcement, two factors were taken into consideration: application of Moisture Seal water-based epoxy coating with sand and embedment length of 200mm (20 times the thickness of the BVC reinforcement). The Moisture Seal water-based coating and sand showed the highest bond strength between the BVC bars and concrete, while the 200mm embedment length contributed to higher bond strength values in comparison with shorter embedment length of 100mm. These two considerations could ensure sufficient bonding between the BVC reinforcement and concrete matrix during the tests and guarantee that external factors, such as temperature fluctuations

and difference in CTE between BVC bar and concrete, would have minimum impact on the performance of the BVC reinforced concrete beams.

6.3. Monitoring the transverse thermal expansion

As shown in section 5.5.3, the CTE of the BVC reinforcement in longitudinal direction was similar to the CTE of the concrete matrix. Both BVC reinforcement and concrete would expand or shrink similarly in the longitudinal direction. Therefore, according to investigations carried out in the literature, no significant thermal stresses around the reinforcement would develop along the length of the concrete element parallel to the reinforcement alignment when the reinforced concrete element undergoes different temperature cycles. However, in the direction perpendicular to the reinforcement alignment, the effect of higher transverse CTE of BVC reinforcement compared to concrete matrix on the bond performance of BVC reinforcement should be investigated.

As explained in chapter 5, two approaches were employed in this thesis to control the thermal stresses caused by the transverse thermal expansion of the BVC reinforcement. The first approach was the extension of the work by Masmoudi, Zaidi and Gérard in 2005. In this approach, a suitable ratio of concrete cover thickness to BVC reinforcement thickness was considered to prevent or delay tensile cracking. The second approach, which was built upon the work of Hany Abdalla in 2006, compared the thermal stresses developed within the concrete matrix to the tensile strength of the concrete at different temperatures to predict the possible thermal cracking that could occur within the concrete matrix.

6.3.1. Effect of concrete cover thickness

As explained in the literature review chapter regarding the effect of transverse thermal expansion of the GFRP reinforcement on the strain distributions in concrete matrix, the extensive work carried out by Radhouane Masmoudi, Ali Zaidi, and Patrick Gérard at the University of Sherbrooke in Canada showed that concrete cover thicknesses which were 1.5 to 2 times the diameter of the GFRP bar could safely prevent any tensile stresses developed as a result of the differential thermal expansion coefficient between the GFRP bar and concrete. To extend the work of Masmoudi, and to monitor possible cracking due to internal thermal stresses within the concrete matrix during the concrete curing and before the beam tests, a series of experiments, which included concrete cylinders and beams with concrete cover thickness in the range of 1.5 to 2 times the thickness of BVC reinforcement, were designed.

The concrete beams had a concrete cover of 21mm (2 times the thickness of the BVC bar), similar to the BVC reinforced concrete beams tested in section 6.5, while the concrete cylinders were prepared similarly to the concrete pull-out tests with concrete cover of more than 2 times the thickness of BVC bars. Each sample of the concrete cylinder and concrete beam was also equipped with a series of thermocouples embedded within the concrete matrix and near the surface of the BVC reinforcement to monitor the temperature variations during the 40-day monitoring process. The room temperature was also monitored with a series of thermocouples attached to the external surface of the concrete samples.

During the first 7 days of concrete curing process, an exothermic chemical reaction between cement and water called hydration took place when the cement was mixed together with water and sand, releasing energy in the form of heat. This heat could increase the internal temperature of the concrete matrix up to 70°C (Sozen, Ichinose et al. 2014). However, the hydration process would continue up to 28 days when the hydration products were developed to give the concrete matrix the maximum strength that needed for load-bearing applications. The heat of hydration would slowly decrease over the 28-day curing process with the peak temperature within the first 7 days.

The curing process of concrete cylinders and beams was carried out at a relative humidity of 65% and a temperature of 40°C for 28 days inside a curing oven. However, after 28 days of curing, all the samples were kept in the laboratory at a temperature of 23°C, therefore there was a temperature difference between the embedded and exposed sections of the bamboo composite bars used for the pull-out tests. To monitor the differential temperature, the thermocouples were employed to record the temperature variations. A total of five concrete cylinders and five concrete beams were prepared with the thermocouples attached inside and outside the cylinders.

Only BVC bars with Moisture Seal water-based epoxy coating and sand particles were used for the temperature monitoring tests of the concrete samples to ensure comparable results with the concrete beam tests in chapter 6, in which water-based epoxy coated BVC reinforcement were employed throughout the tests, could be achieved. Table 38, Table 39 and Table 40 show the internal temperature, external temperature and temperature differences measured during the 40-day monitoring period respectively.

Table 38 Internal temperature of the concrete samples (°C)

	Sample	1 day	7 days	14 days	21 days	28 days	35 days	40 days
Cylinder	1	62	45	42	41	41	24	24
	2	68	42	44	42	41	24	24
	3	65	45	41	41	40	25	24
	4	64	43	40	41	41	24	24
	5	66	44	42	42	41	23	24
Beam	6	64	47	41	40	41	24	24
	7	65	45	40	41	40	25	23
	8	68	42	43	40	41	24	23
	9	64	42	41	42	40	24	24
	10	62	44	42	41	41	25	23

Table 39 External temperature of the concrete samples (°C)

	Sample	1 day	7 days	14 days	21 days	28 days	35 days	40 days
Cylinder	1	40	40	39	40	40	23	24
	2	41	40	40	41	41	21	22
	3	39	40	40	39	40	23	22
	4	40	39	41	40	41	23	23
	5	40	40	40	39	40	24	23
Beam	6	39	41	40	40	39	23	22
	7	40	41	40	41	40	22	23
	8	40	40	39	40	42	23	21
	9	41	39	40	40	40	22	22
	10	40	41	40	40	41	21	23

Table 40 Temperature differences measured between the inside and outside of the concrete samples (°C)

	Sample	1 day	7 days	14 days	21 days	28 days	35 days	40 days
Cylinder	1	22	5	3	1	1	1	0
	2	27	2	4	1	0	3	2
	3	26	5	1	2	0	2	2
	4	24	4	1	1	0	1	1
	5	26	4	2	3	1	1	1
Beam	6	25	6	1	0	2	1	2
	7	25	4	0	0	0	3	0
	8	28	2	4	0	1	1	2
	9	23	3	1	2	0	2	2
	10	22	3	2	1	0	4	0

As shown in Table 38, the highest temperature rise was observed within the first day of the concrete curing when the hydration of cement took place. After 7 days of curing, the internal temperature dropped to the ambient temperature of the curing oven. Once the pull-out samples were taken out of the curing oven, the internal temperature measured for all the concrete samples was comparable to the external recorded temperature. Therefore, except for the first day of curing when a temperature difference in the range of 22℃ to 28℃ was observed, no significant temperature difference was recorded for the concrete samples during this study. Furthermore, no significant difference in temperature variations of the concrete cylinders and concrete beams was observed, as seen in Table 38. The temperature differences between the internal and external surface of the concrete beams and cylinders were similar.

The results of the temperature measurement were further compared with the visual inspection of all the concrete samples monitored during the 40-day evaluation period. No significant cracking patterns were observed on the surface of the concrete cylinders and concrete beams. Hairline cracks observed on the surface of the concrete beam samples were linked to the concrete shrinkage, but not the BVC reinforcement expansion or de-bonding, since the cracking followed a unique pattern in which discontinuous fine cracks developed only randomly along the surface of the concrete beam without following the alignment of the reinforcement in the beam.

This type of shrinkage cracking has been well explored by concrete experts in the past decades and is often explained as being due to the change in the moisture condition of the concrete samples during the 28-day curing process. When the surface of the concrete dries due to evaporation of the surface water, the concrete shrinks, which results in fine, discontinuous hairline cracks on the surface. However, shrinkage cracks will not cause any possible structural failure due to loss of bonding between reinforcement and concrete, and often are repaired with recommended chemicals, including concrete repair epoxies.

No de-bonding crack was observed within the beam and cylinder samples along the length of the embedded BVC reinforcement. The results showed the effectiveness of the concrete cover with a thickness of 2 times the BVC reinforcement thickness in preventing the tensile cracks that could develop via thermal stresses within the concrete samples around the reinforcement in the transverse direction. The observation showed that the bond between the concrete matrix and BVC reinforcement was sufficient to overcome any potential residual stresses that occurred during the temperature variations as a result of the transverse thermal expansion of

the BVC material. The next section evaluates the transverse thermal stress developed within the concrete samples through an analytical approach.

6.3.2. Evaluation of the thermal stress development in concrete

To investigate the effect of temperature differences on the interface of the concrete and BVC reinforcement in concrete samples, an analytical evaluation of the onset of tensile splitting cracking of concrete matrix surrounding the BVC bar was carried out, based on the works of Radhouane Masmoudi, Ali Zaidi and Patrick Gerard in 2005 followed by Hany Abdalla in 2006 (Abdalla 2006). Analytical models developed in this section for the thermal stress calculation of FRP reinforcement in concrete could support the temperature monitoring of the concrete cylinders and beams in the previous sections, in which no de-bonding was caused by the temperature variations during and after curing concrete specimens.

Longitudinal and transverse thermal stresses could normally be developed within the concrete matrix due to the difference between the CTE of concrete and the longitudinal and transverse coefficients of the BVC/FRP bars. As shown earlier, the longitudinal CTE of the BVC reinforcement and concrete were similar, thus the longitudinal thermal stresses developed within the concrete cylinders at the interface between the BVC bar and concrete were not significant in this study. The difference in the transverse CTE of the BVC bar and concrete thermal stresses could result in radial cracking in the concrete matrix, thus affecting the bond between the reinforcement and concrete as well the effectiveness of the concrete cover in the long term.

The tangential stresses that might cause the radial cracks could be computed by considering a ring of concrete surrounding the round FRP bar, as shown in Fig. 119 similar to studies carried out by Radhouane Masmoudi, Ali Zaidi and Patrick Gerard in 2005. For simplicity, it was assumed that the BVC reinforcement had round cross sections and the effect of the stress concentration near the corners of BVC reinforcement embedded in concrete cylinder was neglected.

When the temperature was raised, the FRP bar expanded in the transverse direction larger than the surrounding concrete matrix, and subsequently created radial pressure on the concrete. A small element from the concrete ring was considered for calculating the radial and tangential stress and strain as shown in Fig. 119. The element was defined at radius r by an angle increment dt and a radial increment dr. By circular symmetry, the stresses σ_t and σ_r

were functions of r only. Furthermore, the shear stress on the element must be zero based on radial force equilibrium according to the following expression and for a unit thickness.

$$(\sigma_r + d\sigma_r)(r + d_r)d_t = \sigma_r \, r \, d_t + \sigma_t \, d_t \, d_r \qquad \text{(Eq. 38)}$$
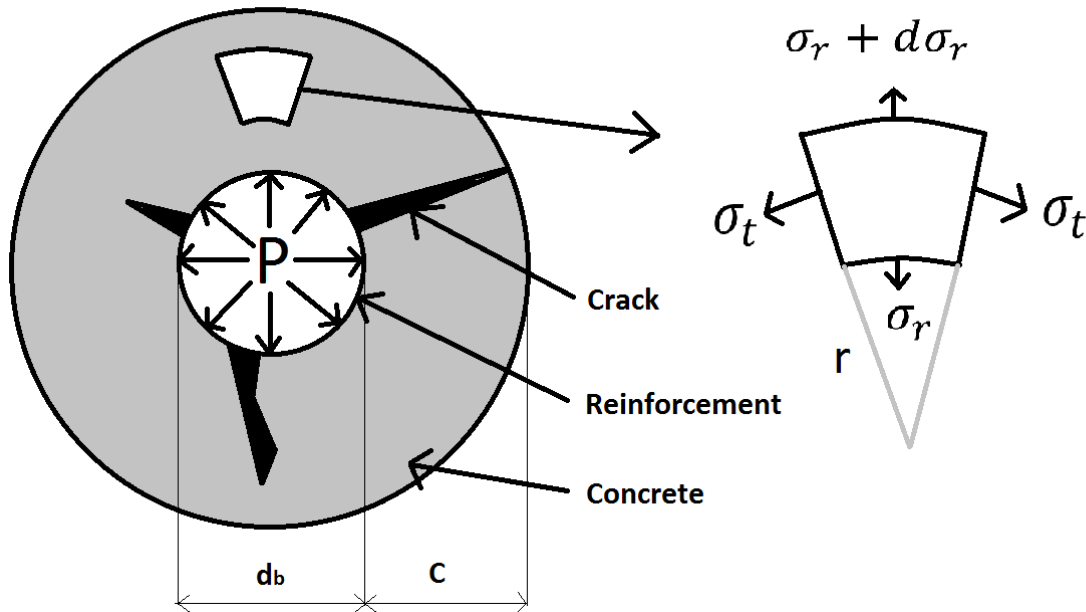
Fig. 119 Cracking due to transverse thermal expansion of FRP bar embedded in concrete

Ignoring second order terms, the following expression could be obtained:

$$\frac{d\sigma_r}{d_r} + \frac{\sigma_r + \sigma_t}{r} = 0 \qquad \text{(Eq. 39)}$$

It was assumed that no body forces existed for the element shown in Fig. 119 and u was the radial displacement. Therefore, a displacement of ($u + du$) over the element length of dr would result in a radial strain of:

$$\varepsilon_r = \frac{u + du - u}{dr} = \frac{du}{dr} \qquad \text{(Eq. 40)}$$

Similarly, the tangential strain was calculated for an angle increment of dt where the length of element was increased from rdt to ($r + u$)dt. The following expression shows the tangential strain;

$$\varepsilon_t = \frac{(r + u)d_t - rd_t}{rd_t} = \frac{u}{r} \qquad \text{(Eq. 41)}$$

By considering plane stress conditions and according to Hooke's law, the relationship between the strain and stress was found accordingly.

$$\varepsilon_r == \frac{du}{dr} = \frac{1}{E}(\sigma_r - v\sigma_t) \quad \text{(Eq. 42)}$$

$$\varepsilon_t = \frac{u}{r} = \frac{1}{E}(\sigma_t - v\sigma_r) \quad \text{(Eq. 43)}$$

Where v is the Poisson's ratio.

The tangential and radial stress were found by solving Eq. 42 and Eq. 43 which resulted in the following expressions;

$$\sigma_r = \frac{E}{1-v^2}\left[\frac{du}{dr} + v\frac{u}{r}\right] \quad \text{(Eq. 44)}$$

$$\sigma_t = \frac{E}{1-v^2}\left[\frac{u}{r} + v\frac{du}{dr}\right] \quad \text{(Eq. 45)}$$

By substituting the above equations into Eq. 39, the following expression was found;

$$\frac{d^2u}{dr^2} + \frac{1}{r}\frac{du}{dr} - \frac{u}{r^2} = 0 \quad \text{(Eq. 46)}$$

The general solution for the above expression could be found as:

$$u = A.r + \frac{B}{r} \quad \text{(Eq. 47)}$$

Where A and B are variables calculated according to the boundary conditions of the element shown in Fig. 119. Therefore, the radial and tangential stresses could be found as per below formula.

$$\sigma_r = \frac{E}{1-v^2}\left[A(1 + v) - B(\frac{1-v}{r^2})\right] \quad \text{(Eq. 48)}$$

$$\sigma_t = \frac{E}{1-v^2}\left[A(1 + v) + B(\frac{1-v}{r^2})\right] \quad \text{(Eq. 49)}$$

When the boundary condition was set to the following:

$$\sigma_r\left(r = \frac{d_b}{2}\right) = -P \text{ and } \sigma_r\left(r = \frac{d_b}{2} + c\right) = 0$$

Where d_b is the reinforcement diameter and c is the concrete cover.

Subsequently the terms A and B could be found by the following expressions:

$$A = \frac{1-v}{E}\left[\frac{\left(\frac{db}{2}\right)^2 P}{\left(\frac{db}{2}+c\right)^2 - \left(\frac{db}{2}\right)^2}\right] \quad \text{(Eq. 50)}$$

$$B = \frac{1-v}{E} \left[\frac{\left(\frac{db}{2}\right)^2 \left(\frac{db}{2}+c\right)^2 P}{\left(\frac{db}{2}+c\right)^2 - \left(\frac{db}{2}\right)^2} \right] \qquad \text{(Eq. 51)}$$

Therefore, the radial and tangential stresses were found as functions of the reinforcement diameter (d_b) and the concrete cover (c) as shown in Fig. 119 and by the expressions below:

$$\sigma_r = \frac{P\left(\frac{db}{2}\right)^2}{\left(\frac{db}{2}+c\right)^2 - \left(\frac{db}{2}\right)^2} \left[1 - \frac{\left(\frac{db}{2}+c\right)^2}{r^2} \right] \qquad \text{(Eq. 52)}$$

$$\sigma_t = \frac{P\left(\frac{db}{2}\right)^2}{\left(\frac{db}{2}+c\right)^2 - \left(\frac{db}{2}\right)^2} \left[1 + \frac{\left(\frac{db}{2}+c\right)^2}{r^2} \right] \qquad \text{(Eq. 53)}$$

At the interface of the reinforcement and concrete where $r = \frac{db}{2}$ the maximum stresses were found:

$$\sigma_t = P \left[\frac{\left(\frac{db}{2}+c\right)^2 + \left(\frac{db}{2}\right)^2}{\left(\frac{db}{2}+c\right)^2 - \left(\frac{db}{2}\right)^2} \right] \qquad \text{(Eq. 54)}$$

$$\sigma_r = -P \qquad \text{(Eq. 55)}$$

The radial deformation in concrete around the reinforcement due to radial pressure P at a distance r could be found by Eq. 56:

$$\varepsilon_{cr}(r) = \frac{du}{dr}$$

$$= \frac{1}{E_c} (\sigma_r - v_c \sigma_t)$$

$$= \frac{P}{E_c \left[\left(\frac{\frac{db}{2}+c}{\frac{db}{2}}\right)^2 - 1 \right]} \left[\left(1 - \frac{\left(\frac{db}{2}+c\right)^2}{r^2} \right) - v_c \left(1 + \frac{\left(\frac{db}{2}+c\right)^2}{r^2} \right) \right] \qquad \text{(Eq. 56)}$$

Where v_c and E_c are Poisson's ratio and modulus of elasticity of concrete. Similarly, the tangential deformation in concrete due to the radial pressure P was found by using Eq. 57:

$$\varepsilon_{ct}(r) = \frac{u}{r} \frac{1}{E_c} (\sigma_t - v_c \sigma_r)$$

$$= \frac{P}{E_c \left[\left(\frac{\frac{db}{2}+c}{\frac{db}{2}}\right)^2 - 1 \right]} \left[\left(1 + \frac{\left(\frac{db}{2}+c\right)^2}{r^2} \right) - v_c \left(1 - \frac{\left(\frac{db}{2}+c\right)^2}{r^2} \right) \right] \qquad \text{(Eq. 57)}$$

The tangential deformation in concrete, at the interface of the reinforcement and concrete where $r = \frac{db}{2}$ and due to the radial pressure P and a temperature variation of ΔT could be expressed by the following formulae:

$$\varepsilon_{ct} = \frac{P}{E_c}\left(\frac{(\frac{\frac{db}{2}+c}{\frac{db}{2}})^2+1}{(\frac{\frac{db}{2}+c}{\frac{db}{2}})^2-1} + v_c\right) + \alpha_c \Delta T \qquad \text{(Eq. 58)}$$

where α_c is the coefficient of thermal expansion of concrete.

The radial displacement u at any point of the reinforcement bar was calculated similarly by considering the external pressure P applied by the concrete matrix on the reinforcement bar according to Eq. 59.

$$u(r) = -\frac{(1-v_{ft})P}{E_{ft}}r \qquad \text{(Eq. 59)}$$

Where v_{ft} and E_{ft} are Poisson's ratio and modulus of elasticity of reinforcement bar in transverse direction.

The tangential deformation of the reinforcement bar, at the concrete interface due to the effect of the radial pressure P and the temperature variation ΔT, could be found by the following expression:

$$\varepsilon_{ft} = \alpha_{ft}\Delta T - \frac{(1-v_{ft})P}{E_{ft}} \qquad \text{(Eq. 60)}$$

Where α_{ft} is the transverse coefficient of thermal expansion of reinforcement.

The radial pressure P employed by the reinforcement bar on the concrete matrix due to temperature variation ΔT was calculated according to the compatibility of transverse strains at the concrete and reinforcement bar interface. The following expression shows the compatibility of transverse strains between concrete matrix and reinforcement bar according to Eq. 58 and Eq. 60.

$$\alpha_{ft}\Delta T - \frac{(1-v_{ft})P}{E_{ft}} = \frac{P}{E_c}\left(\frac{(\frac{\frac{db}{2}+c}{\frac{db}{2}})^2+1}{(\frac{\frac{db}{2}+c}{\frac{db}{2}})^2-1} + v_c\right) + \alpha_c \Delta T \qquad \text{(Eq. 61)}$$

From Eq. 61, the radial pressure P was found accordingly:

$$P = \frac{(\alpha_{ft}-\alpha_c)\Delta T}{\frac{1}{E_c}\left(\frac{(\frac{\frac{db}{2}+c}{\frac{db}{2}})^2+1}{(\frac{\frac{db}{2}+c}{\frac{db}{2}})^2-1}+v_c\right)+\frac{1}{E_{ft}}(1-v_{ft})} \qquad \text{(Eq. 62)}$$

The maximum tangential stress will occur at the interface between the concrete and the FRP bar, at $r = \frac{db}{2}$, thus Eq. 54 can be used to find the maximum tangential stress.

However, when above equations were used for the BVC reinforcement in this study, several factors needed to be considered and adjustments made to the calculations of the tangential stresses.

Firstly, the BVC reinforcement had a rectangular cross section of 10×10mm, but Eq. 38 to Eq. 62 were developed for FRP bars of circular cross sections with a diameter of d_b. Therefore, to estimate the radial pressure and subsequently the stress at the concrete and reinforcement interface, it was assumed that the BVC reinforcement in this study had a diameter of 10mm, thus ignoring the effect of sharp corners on stress distribution around the BVC reinforcement. Further details of future studies on the effect of stress concentration at the sharp corners and shape of BVC reinforcement on maximum tangential stress are discussed in chapter 8 as part of future work.

Furthermore, all the mechanical proprieties of the BVC materials in this study were measured along the fiber direction but not perpendicular to the fiber direction; therefore, to use the above equations, the transverse modulus of elasticity and the Poisson's ratio had to be calculated. These parameters were measured in cooperation with Empa in Switzerland through the joint project collaboration between ETH in Zurich, the Future Cities Laboratory in Singapore, Empa in Dübendorf and the industrial partner Rehau in Zurich, as the necessary facilities to do the tests were not available at AFCL. The detailed results and evaluation of the tests could be found in the final project report of CTI (Wielopolski, Aigner et al. 2016).

The BVC materials had an average Poisson's ratio of $v_{fT} = 0.347$ and an average transverse modulus of elasticity of $E_{fT} = 4,300$MPa. The Poisson's ratio of the concrete matrix was found to be 0.17 for grade 20MPa concrete strength. The coefficient of thermal expansion of concrete matrix used in this study was found to be 10.15×10⁻⁶ m/(m·°C). By substituting the necessary parameters into Eq. 54, Eq. 58 and Eq. 62, the maximum stress at the interface of

the concrete and BVC bars was estimated. The results of the radial pressure and the tangential stresses are shown in Table 41 for all the 10 concrete cylinders and beams prepared in the previous section. The maximum tangential stress of 5.27MPa was recorded for samples with a maximum temperature difference of 28°C. The maximum tangential stress of 5.27MPa was slightly lower than the measured tensile strength of concrete samples (6.2MPa) shown in Table 35, indicating that radial cracks did not occur by the transverse thermal expansion of BVC reinforcement. The maximum temperature difference that could be investigated in this study was only 28°C caused by the difference between the temperature of the curing oven and the internal temperature of the concrete matrix measured by the thermocouples. Furthermore, assumptions were made regarding the cross section of the BVC reinforcement which could potentially affect the maximum tangential stresses. Fig. 120 and Fig. 121 display the impact of reinforcement size and concrete cover on the tangential stresses at the interface between the concrete and the reinforcement respectively. As can be seen in both Fig. 120 and Fig. 121, increasing either of the reinforcement size or concrete cover could reduce the tangential stress. In the case of reinforcement size, increasing the diameter from 10mm to 22mm resulted in a reduction of around 4% in tangential stress. The concrete cover thickness had a greater impact on the tangential stress developed due to transverse thermal expansion of reinforcement.

Table 41 The radial pressure and the tangential stresses developed at the interface of the concrete and BVC bar

	Sample	Maximum temperature difference	Radial pressure	Maximum tangential stress
		(T), °C	(P), MPa	(σ_t), MPa
Cylinder	1	22	3.90	3.94
	2	27	4.79	4.83
	3	26	4.61	4.65
	4	24	4.25	4.29
	5	26	4.61	4.65
Beam	6	25	4.37	4.71
	7	25	4.37	4.71
	8	28	4.90	5.27
	9	23	4.02	4.33
	10	22	3.85	4.14
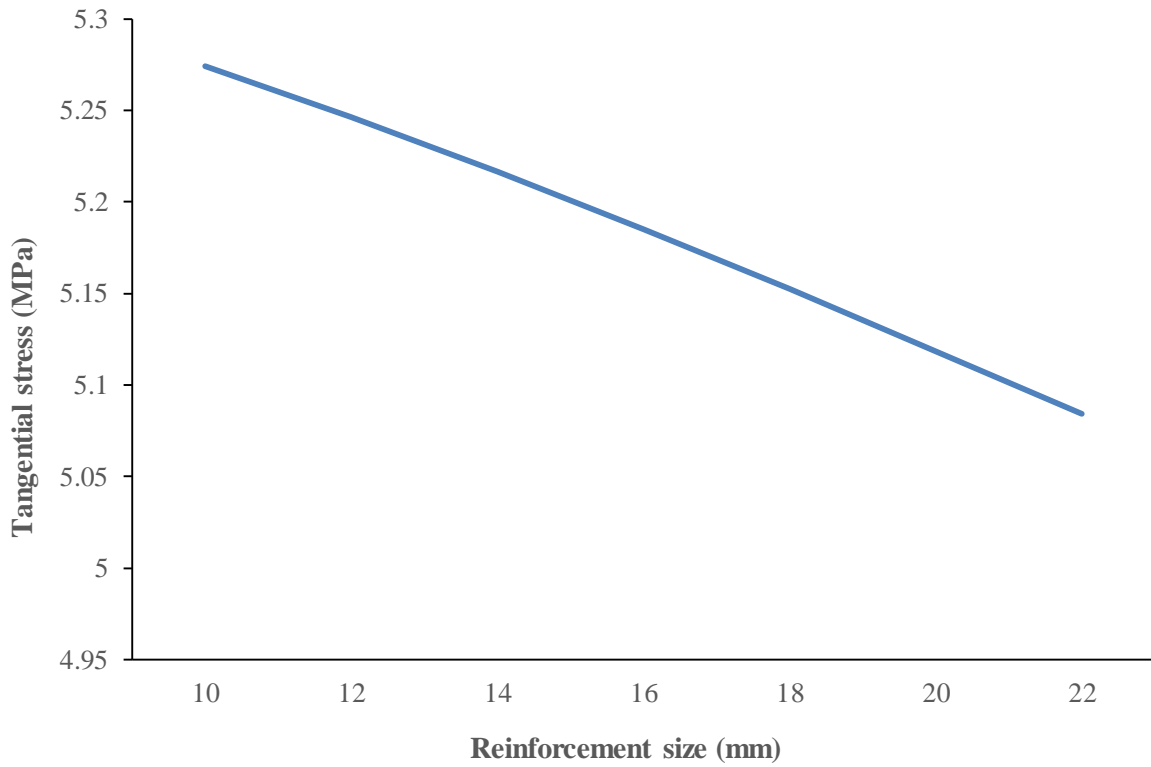
Fig. 120 Effect of reinforcement size on tangential stress

By increasing the concrete cover thickness from 10mm to 40mm the tangential stress decreased by up to 14%. The results from the developed models showed the great impacts that both concrete cover thickness and reinforcement size had on tangential stress.
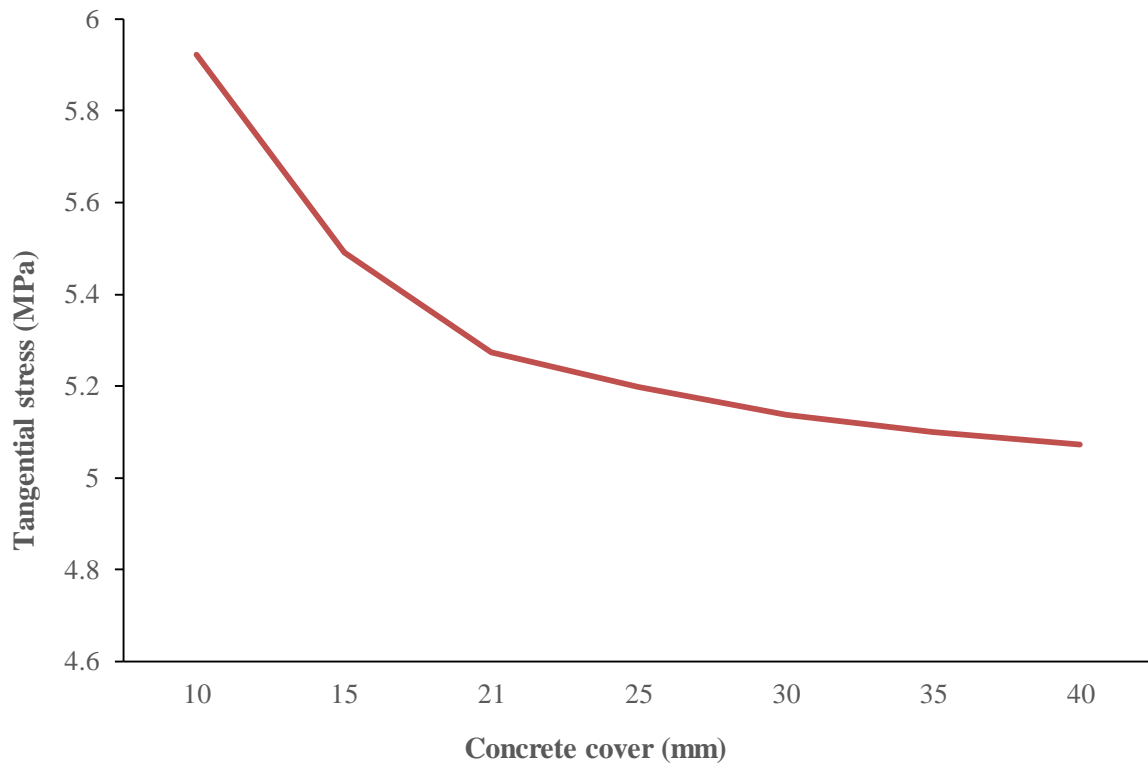
The BVC reinforcement employed in this study had a square cross section with a higher surface area in comparison to a similar circular cross section. Therefore, there could be advantages and disadvantages when using the suggested analytical models for thermal stress evaluations of the BVC reinforcement with square shapes. The better surface area provided by the square cross section would help in developing a better bond with the concrete matrix compared to the round cross section of the common FRP reinforcement, which would allow smooth stress transfer at the interface of concrete and BVC bar. The residual stresses developed at the interface of the concrete and reinforcement caused by the expansion or compression of the BVC reinforcement did not show a significant effect on the bonding mechanism. This could be explained by the results of the pull-out tests in which the water-based epoxy coating and sand particles developed perfect bonds between the BVC reinforcement and concrete. The bond strength was shown to be sufficient to prevent the tangential stresses and residual stresses which would result in tensile cracks that could propagate around the reinforcement and thus affect the bonding mechanism.

The proposed models could be used primarily as an estimate of the onset of cracking due to the transverse CTE of the BVC reinforcement when used in concrete samples of various cover thicknesses. Furthermore, the analytical model could give a relatively good estimate of

the maximum temperature at which the first radial cracking, due to difference between the transverse CTE of BVC reinforcement and concrete matrix, could occur.

The maximum tangential stress developed due to the transverse thermal stresses within the BVC reinforced concrete beam being slightly lower than the tensile strength of the concrete mix. This result indicated that internal radial cracks did not take place due to transverse thermal expansion of BVC reinforcement within the concrete beams. Furthermore, maintaining a temperature difference of less than 28°C between the internal and external concrete beams during the first day of concrete curing could also prevent any potential internal radial cracking.

Furthermore, the presence of transverse reinforcements (BVC stirrups) around the longitudinal BVC reinforcement could limit the transverse expansion of the longitudinal reinforcement due to a temperature rise. The onset of radial cracking due to transverse thermal stress could be further prevented by employing a concrete mix with higher tensile strength.

No significant difference between the temperature of the internal concrete matrix and the surrounding environment was recorded after 7 days of concrete curing, thus no internal radial cracking could have been developed at the interface of the concrete matrix and BVC reinforcement of the concrete beams.

Further investigation is needed to quantify the relationship between the temperature cycles, the transverse thermal expansion of the BVC reinforcement, the bonding between the BVC reinforcement and concrete, the effect of reinforcement shape and size as well as the residual stresses developed within the matrix. The proposed models could further be developed to include these parameters in future studies. The effect of transverse reinforcement (stirrup) on controlling the transverse thermal expansion of the longitudinal BVC reinforcement should also be evaluated and quantified in future studies.

Future research could be carried out on the type of the epoxy-resin matrix used for the production of the BVC materials within this study to control the transverse CTE values, through either chemical modification of the current matrix or by developing new types of epoxy-resin systems with lower transverse CTE values compared to the current type of epoxy-resin matrix. Such investigations are beyond the scope of the present study and could be the subject of future studies.

Visual and microscopic investigation methods would be useful techniques to evaluate the concrete and BVC reinforcement interface before and after the temperature variations. Techniques such as Fourier Transform Infrared Spectroscopy (FTIR) and Acoustic-Emission monitoring (AE) systems could be used in future studies.

When the ACI 440.1R-15 code's recommendations for FRP reinforcement in concrete were reviewed, a minimum concrete cover around the FRP bars in concrete, similar to the suggestions made by Masmoudi, was found. The minimum concrete cover thickness, which also depended on the size of the reinforcement, would help to reduce the direct exposure of the fiber reinforced polymer materials used in concrete as reinforcement to fluctuating weather conditions and environmental heating and cooling cycles; this could help to reduce the negative impacts of the higher transverse CTE of the FRP/BVC reinforcement compared to the concrete matrix. The results of the tests carried out in this section supported the recommendations given by the ACI 440.1R-15 code regarding the concrete cover thickness of 2 times the reinforcement thickness (20mm for BVC reinforcement).

6.4.   Durability evaluation of BVC reinforcement in concrete

Reinforcement in concrete structures would deteriorate over time due to various issues, as explained in detail in chapter 3. Exposure of concrete to an alkaline environment is one of the key factors that could potentially affect the integrity of Fiber reinforced Polymer (FRP), such as Glass Fiber Reinforced Polymer (GFRP), used as reinforcement in concrete, as discussed in detail by Francesca Ceronia, Edoardo Cosenzab, Manfredi Gaetanob and Marisa Peccea in their work "Durability issues of FRP rebars in reinforced concrete members" (Ceroni, Cosenza et al. 2006). Given the similarity of the newly developed Bamboo Veneer Composite (BVC) reinforcement with some existing FRP reinforcement such as GFRP in terms of production process, properties and characteristics, it would be crucial to investigate the durability related issues, primarily the effect of an alkaline environment of concrete and water absorption behavior on the performance of the BVC reinforcement.

There are several external factors which might potentially affect the physical and mechanical properties of the BVC reinforcement in a concrete application in an adverse way. Water ingress through micro cracks in concrete matrix over time, from various sources such as air humidity or rain, is an important factor that needs to be properly evaluated and considered in the design of structural concrete elements with BVC as reinforcement. In this section, the

effect of water ingress and exposure to an alkaline environment on the mechanical properties of BVC reinforcement is investigated.

In this section, a series of tests were carried out to evaluate the effect of water absorption both at room temperature (23°C) and elevated temperature (60°C) on the tensile properties of BVC samples. The higher temperature was chosen to further investigate the influence of the combined effect of temperature and water ingress on the tensile properties of the BVC reinforcement compared to room temperature water ingress. In this section, only tensile properties of BVC reinforcement were evaluated given their importance in the design of reinforced concrete beams compared to other mechanical properties such as compressive or flexural strength.

Alkaline environments were also designed by simulating the pH level of normal concrete matrix to investigate the effect of exposure to alkaline solutions on the tensile properties of the BVC samples. Samples of the BVC bars were exposed to water absorption and an alkaline environment for up to three months and the tensile properties were measured at different phases of the exposure. The 3-month time period was chosen based on the duration of this PhD thesis to allow sufficient time for the repetition of the whole process of production and testing of the samples, if there was a need, in case of unacceptable and scattered results with large variations occurring which would have made the analysis impossible.

6.4.1. Water uptake behavior of BVC samples

Most polymer composites are known to absorb a certain amount of water, which is largely dependent on their chemical composition. The percentage of water uptake and the change in dimensional properties of the composites are of high importance, given their potential impact on both their physical and mechanical properties as well as viscoelastic behavior of composites which could have negative impact on the overall load-bearing capacities of the structural composites. In this section, samples were prepared from the final BVC reinforcement boards produced in section 5.4 into cubes of $10 \times 10 \times 10$mm and immersed in distilled water with a temperature of 23°C (normal room temperature) and 60°C (extreme condition). The sample sizes and the range of temperatures were chosen in accordance with ASTM D5229M-14 titled "Standard Test Method for Moisture Absorption Properties and Equilibrium Conditioning of Polymer Matrix Composite Materials" (ASTM International 2014).

However, some modifications to sample size and duration of the tests were made in addition to the ASTM D5229M-14 standard to adapt the tests for the newly developed BVC samples. It is important to add that the majority of the available ASTM standards and guides do not cover bamboo based composite materials, thus such modifications and revisions of the current standards are necessary to adapt the testing conditions to the newly developed BVC samples. The sample thickness of 10mm was chosen to allow for a direct comparison with actual BVC reinforcement in which a similar thickness of 10mm was used to reinforce the concrete beams in section 6.3.

Weight and dimensional changes were measured every 2 hours during the first week of the experiment when the water uptake rate was relatively high; subsequently, measurements were carried out only once per day for up to three months' immersion in water (2,160 hours) when the rate of water absorption was reduced. Fig. 122 shows the water uptake in percentage by mass for the 3-month measurement period. Fig. 123 and Fig. 124 show the dimensional changes of the BVC samples due to water absorption along the fiber and perpendicular to fiber direction at 23°C and 60°C respectively. The standard deviation of all the samples measured for water absorption and dimensional change were below 6%.

It should be emphasized here that all the samples for dimensional and water uptake measurements were first coated with water-based epoxy coating, similar to the pull-out test samples, to ensure comparable results could be obtained for the usage of the coated BVC reinforcement in concrete beams.
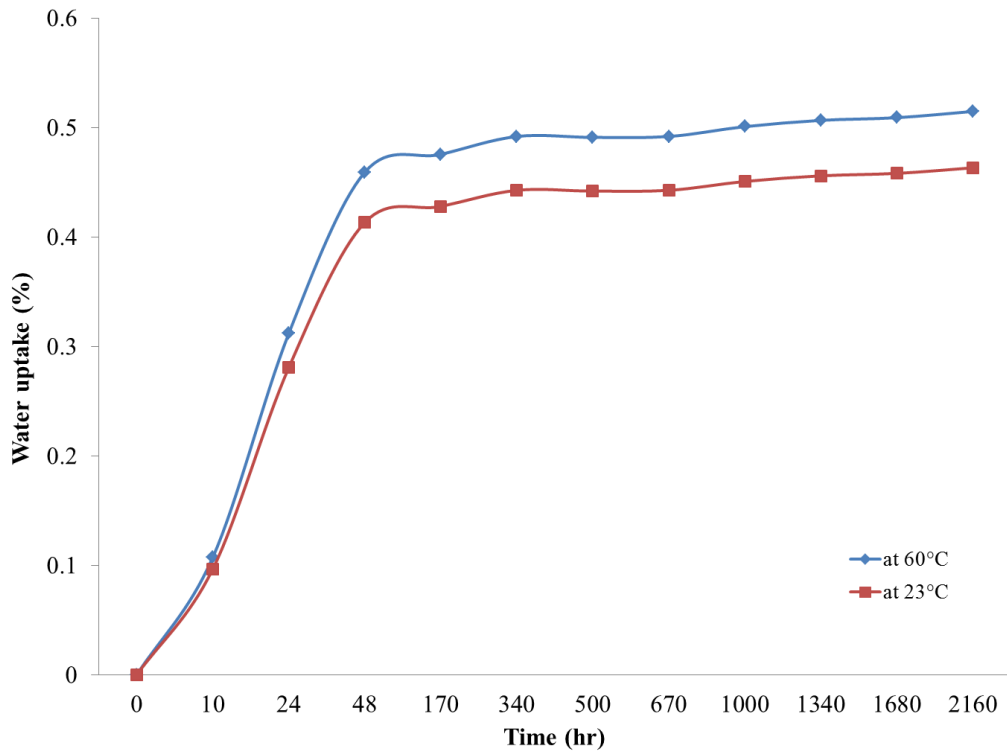
Fig. 122 Measurement of water uptake of BVC samples for three months
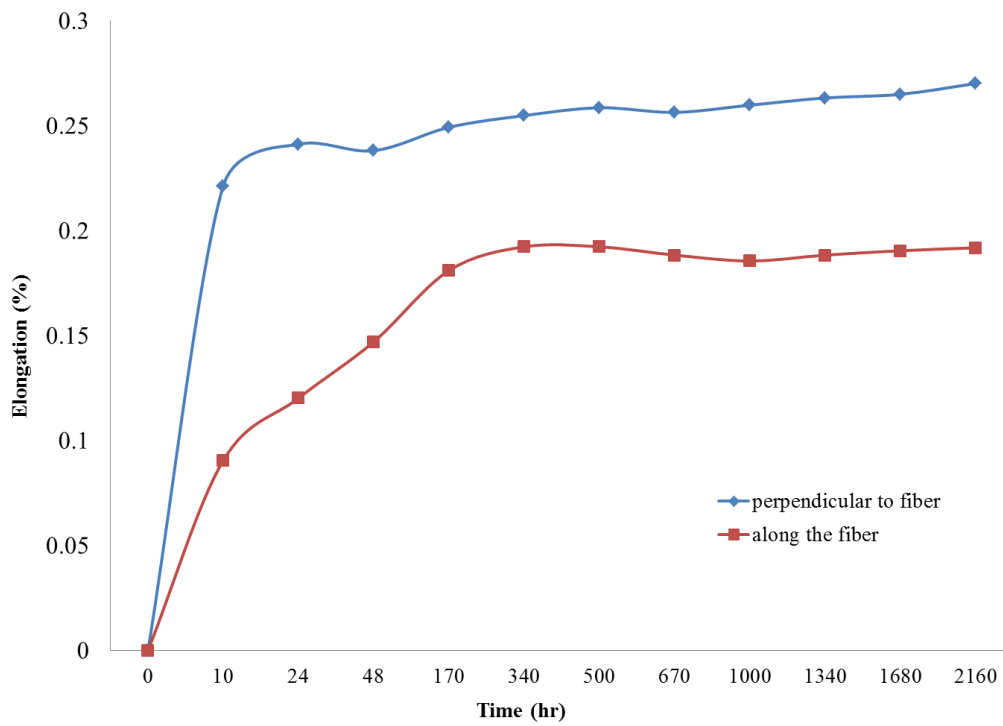
Fig. 123 Elongation of BVC samples after exposure to room temperature (23°C) water for up to three months

At different time periods, the percentage of the weight gain was calculated by measuring the difference in weight between the BVC sample in dry conditions and the weight after water immersion at various soaking times according to Eq. 63 below:

$$W_t(\%) = \frac{m_t - m_0}{m_0} \times 100 \quad \text{(Eq. 63)}$$

Where m_t is the weight of the sample at time t when is immersed in water and m_0 is the initial weight of the dry sample before any immersion occurs. A similar equation was employed to monitor the elongation behavior of the BVC samples at various times. Eq. 64 was used to calculate the elongation in percentage by measuring the length of the sample (along the fiber or perpendicular to fiber direction) at specific times (t) during the immersion process, by taking out the sample from water and leaving it to dry at room temperature to reach a surface-dry condition.
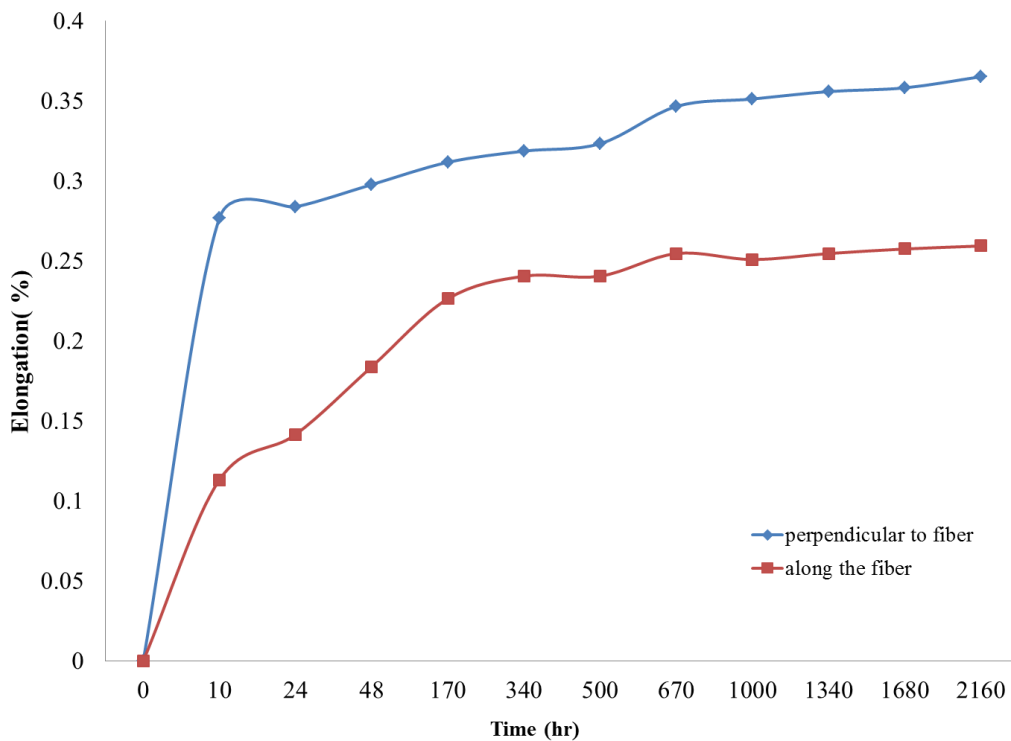
Fig. 124 Elongation of BVC samples after exposure to 60°C water for up to three months

$$E_t(\%) = \frac{L_t - L_0}{L_0} \times 100 \quad \text{(Eq. 64)}$$

Where L_t is the length of the sample at time t when it is immersed in water and L_0 is the initial length of the dry sample before immersion in the water.

281

As shown in Fig. 122, a quasi-equilibrium state was achieved in both 23℃ and 60℃ temperatures after 170 hours of immersion in water. However, the water absorption values for samples immersed in water at a temperature of 60℃ were relatively higher than samples immersed in room temperature water for a similar period of time. Though the difference observed between absorption values of samples immersed in 23℃ and 60℃ water was not significant, it could potentially point to a risk of polymer network breakdown of the water-based epoxy coating at higher temperatures, as was discovered by various researchers in the field of fiber reinforced polymer composites (Soles and Yee 2000, Nogueira, Ramirez et al. 2001, Abdel-Magid, Ziaee et al. 2005).

During the exposure of BVC samples to water, damage may occur in the form of interfacial micro-cracks between the water-based epoxy coating and BVC sample's surface. These interfacial micro-cracks might only lead to water absorption by the water-based epoxy coating applied on the BVC surface rather than having a direct effect on the BVC sample. Therefore, the water absorption could also be affected by the type of the coating, thickness of the coating applied, the presence of voids in the interface between the coating layer and BVC surface, and the quality of the water used for absorption tests. To minimize the impact of all these factors, firstly, only distilled water which had no impurities was used throughout the tests and, secondly, only one type of coating was employed for all the samples tested for the water uptake behavior. Furthermore, to coat the BVC samples, similar weights of water-based epoxy coating were used to ensure that all the BVC samples tested in this section were coated identically. To minimize the possibility of having voids at the interface of the BVC surface and the coating, each BVC sample was thoroughly cleaned on the surface by the use of Acetone, a water soluble and inexpensive solvent. The application of Acetone before coating helped to remove dust or other impurities on the surface of which had no impurities BVC sample, which could otherwise have intervened in the process of adhesion between the water-based coating and the BVC sample's surface. Similar water absorption behavior was observed for other polymer composite samples, such as GFRP or CFRP samples as shown in a detailed study carried out by Professor George Papanicolaou at the University of Patras in Greece (Papanicolaou, Kosmidou et al. 2006). Overall, the coated BVC samples did not show a significant water uptake value, with the highest abortion value being less than 0.55% observed after three months of exposure.

A noticeable difference was observed when the dimensional changes were measured along the fiber direction versus the perpendicular-to-fiber direction for both the 23℃ and 60℃

water temperatures. As shown in Fig. 123, at a temperature of 23℃, the highest average elongation value along the fiber direction of BVC samples was less than 0.20%, while the maximum elongation perpendicular to fiber direction was slightly higher than 0.27%. At 60℃, the highest average elongation measured was 0.25% and 0.36% along the fiber direction and perpendicular to fiber direction respectively.

As the results suggested, temperature played a significant part in elongation and changing the dimensions of the samples both along the fiber and perpendicular-to-fiber directions. When the maximum elongation of samples along the fiber direction was compared, an increase of 25% could be observed when the temperature was raised from 23℃ to 60℃. For elongations perpendicular to the fiber direction, an increase of 33% in elongations was observed when the temperature was raised from 23℃ to 60℃. The effect of temperature on water uptake behavior could be explained by diffusion theory, whereby the moisture diffusion into the composites and polymers are largely influenced by the temperature. Diffusion is simply the movement of individual molecules of a material through a fluid substance as a result of random movements of those molecules (Vrentas and Duda 1977). At higher temperatures, the diffusion rate tends to be influenced by the quicker movement of the individual molecules compared to lower temperatures; therefore the moisture or water uptake would increase as a result of a higher diffusion rate. However, it should be emphasized that the relationship between diffusion rate and temperature could be very complex at higher temperatures, and therefore a systematic study would be required; it is beyond the scope of this PhD thesis. The diffusion of water molecules into the micro voids between the water-based coating layers and the surface of the BVC samples could be advanced by increasing the temperature to 60℃. Besides the diffusion mechanism, the capillary transport of the water into the voids of the water-based coating itself, as well as the micro cavities at the interface of coating and BVC sample's surface, could have further contributed to the water uptake of the samples tested in this section.

Besides the water uptake behavior of the BVC samples, elongation of the samples was investigated similarly. It was observed that along the fiber direction, the elongation proved to be less significant as compared to the elongation perpendicular to the fiber direction. This could be explained by the stability of the fibers in one direction in the unidirectional polymer composites and the dominancy of the epoxy-resin system in directions perpendicular to the fiber direction, as discussed in detail by Xiaodong Tang, John Whitcomb, Yanmei Lib and

Hung-Jue Sue from the Texas A&M university in their work titled "Micromechanics modeling of moisture diffusion in woven composites" (Tang, Whitcomb et al. 2005).

Similar trends were observed earlier in section 5.5.3 when the CTE of the BVC samples was measured along the fiber and opposite to the fiber direction. However, the elongation reached a steady state of equilibrium after 340 hours of immersion for 23°C, and after 500 hours of immersion in the case of the 60°C water temperature. The results clearly showed that, unlike water absorption where saturation point could be reached within 170 hours of immersion, the elongation continued for a longer period of time before it reached a steady state of equilibrium. This observation has significant implications for the design and application of BVC materials as reinforcement for structural concrete applications, as large elongations could negatively influence the bonding mechanism between the concrete matrix and BVC reinforcement, and thus interrupt the smooth stress transfer between the two materials.

Therefore, the values obtained in this study played important roles in the design of concrete elements reinforced with BVC reinforcement. For this reason, the ACI 440.1R standard guide for the application of FRP materials as reinforcement in concrete has established various safety factors pertaining to the external load as well as strength reduction factors pertaining to the strength of the FRP materials, which take into account the variations in CTE, the moisture content, water uptake as well as dimensional stability changes which could occur with the fluctuations of both time and temperature over the life span of the structure. However, most of these factors described by ACI 440.1R-15 are for FRP composites produced with glass, carbon or aramid fibers rather than natural fibers such as bamboo. Therefore, in most cases, the safety factors advised by the ACI 440.1R lead to overestimated design elements if used for natural fiber reinforced polymers, which indicate the possibility that these safety factors could be safely employed for the newly developed bamboo-based composite reinforcement in concrete. However, further research in this area is needed to establish the relevant safety factors or strength reduction factors suitable for the newly developed BVC reinforcement for structural concrete applications, which is beyond the scope of this PhD thesis.

The results obtained for both water absorption and dimensional changes of the BVC samples indicated that water and moisture ingress in severe conditions (higher temperature) could have adverse effects on the stability of the BVC samples. Nevertheless the presence of water-based coating played an important role in impeding the water uptake into the voids and cavities of the BVC sample, if there are any, and it further prevented polymer degradation of

the BVC reinforcement when used in concrete elements and subjected to various cycles of temperature and moisture fluctuations.

6.4.2. Alkali resistance of BVC reinforcement

To investigate the effect of a concrete alkaline environment on the performance of the BVC reinforcement, the alkaline resistance of BVC bars used as reinforcing elements in concrete were evaluated according to ASTM D7705-12 "Standard Test Method for Alkali Resistance of Fiber Reinforced Polymer (FRP) Matrix Composite Bars used in Concrete Construction". ASTM D7705-12 recommends measuring the alkali resistance by subjecting the BVC bars to an alkaline environment with a similar pH level as the concrete matrix, and subsequently testing them under tension with the UTM machine at different periods of time (ASTM International 2012). Therefore, tensile test samples from the final BVC boards were prepared according to ASTM D3039-08 as shown in Fig. 75. The samples were then coated with a water-based epoxy coating (Moisture Seal) before being subjected to an alkaline solution consisting of 118.5g of $Ca(OH)_2$, 0.90g of NaOH and 4.2g of KOH in 1 liter of tap water with an initial pH value of 12.6 to 13.0, similar to the pH value of the pore water inside the concrete matrix. The coated BVC samples were immersed in the alkaline solution at 60°C for a period of up to 3 months (2,160 hours). At different periods of time, the samples were removed from the alkaline solution and carefully washed with tap water to remove the excess alkaline solution from their surface. Subsequently, the samples were subjected to a tensile test and tested until failure with the UTM machine to measure both tensile strength and modulus of elasticity. To maintain the pH within the range of 12.6 to 13.0 during the immersion period, an Eutech® PC2700 digital pH meter was used and, when necessary, NaOH solution or water was added to solution to increase or decrease the pH value accordingly. The tensile capacity retention was calculated according to Eq. 65.

$$R_{et}(\%) = \frac{F_{tu1}}{F_{tu0}} \times 100 \qquad \text{(Eq. 65)}$$

Where:

R_{et} = tensile capacity retention (%)

F_{tu0} = initial tensile capacity before immersion, in Newton

F_{tu1} = tensile capacity after immersion, in Newton

Fig. 125 and Fig. 126 show the results of the tensile strength and elastic modulus respectively after various exposure times to the alkaline solution. The ultimate tensile strength of the samples subjected to alkaline solution dropped from 371MPa to almost 340MPa after 3 months, a reduction of around 8%. A similar trend was observed for modulus of elasticity where the values dropped from 38,000MPa to 34,000MPa after 3 months' exposure to the alkaline solution, a drop of about 10%. Fig. 127 shows the tensile capacity retention (R_{et}) for tensile strength and modulus of elasticity of the samples. As the Fig. 127 suggested, the reduction in both tensile properties followed a similar trend; however, the modulus of elasticity tended to be more affected by the immersion of the sample in alkaline solution over time.
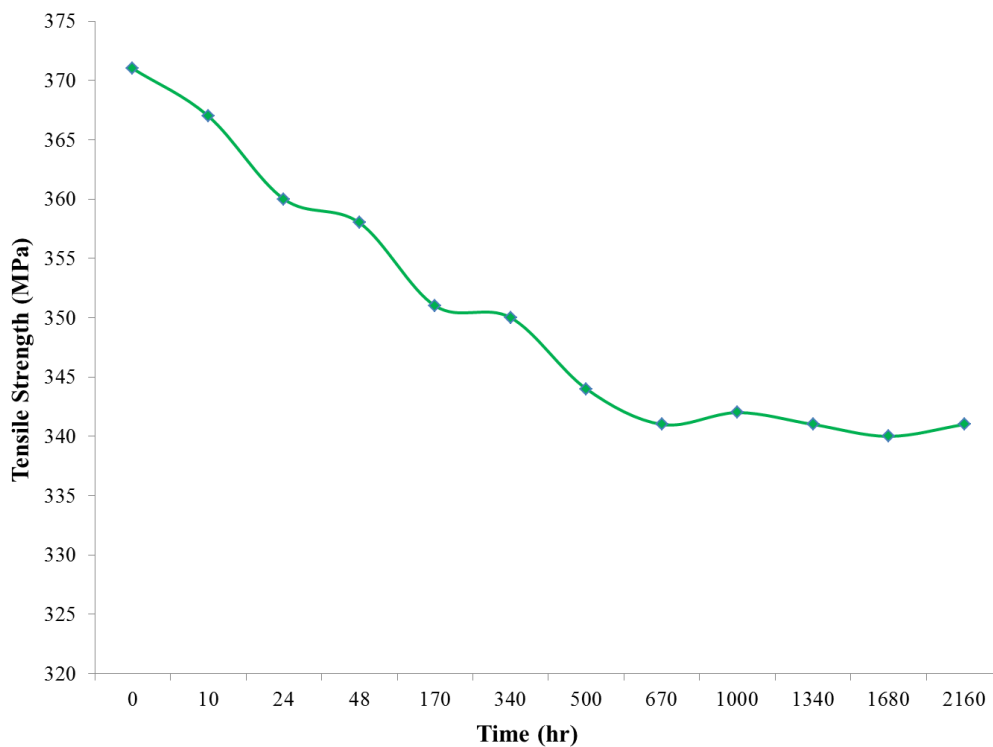
Fig. 125 Tensile strength measurements after exposure to the alkaline solution

286

Furthermore, both tensile strength and modulus of elasticity reached a steady state after one month's immersion in the alkaline solution. The results suggested that the ultimate tensile properties were expected to drop within the first month of placing the BVC reinforcement into the alkaline environment of concrete. In addition, during the first 7 days of the concrete curing process when the cement was mixed together with water and sand, an exothermic chemical reaction between cement and water took place which released energy in the form of heat. This heat raised the temperature of the concrete matrix in which the internal temperature due to cement hydration could simply rise up to 70°C (Sozen, Ichinose et al. 2014). The combination of an alkaline environment and temperature could lead to a significant increase in micro-cracks due to the degradative hydrolysis of both water-based epoxy coating and perhaps the BVC matrix. The hydrolytic degradation of polymer composites generally appeared when water molecules built up at the interface of the water-based coating and BVC surface, or between the bamboo fiber and the epoxy-resin matrix of the BVC sample, which could potentially displace some of the inorganic particles present in the microstructure of the water-based coating and BVC sample. This could consequently result in the degradation of the composite structure which would negatively affect its overall integrity and properties.
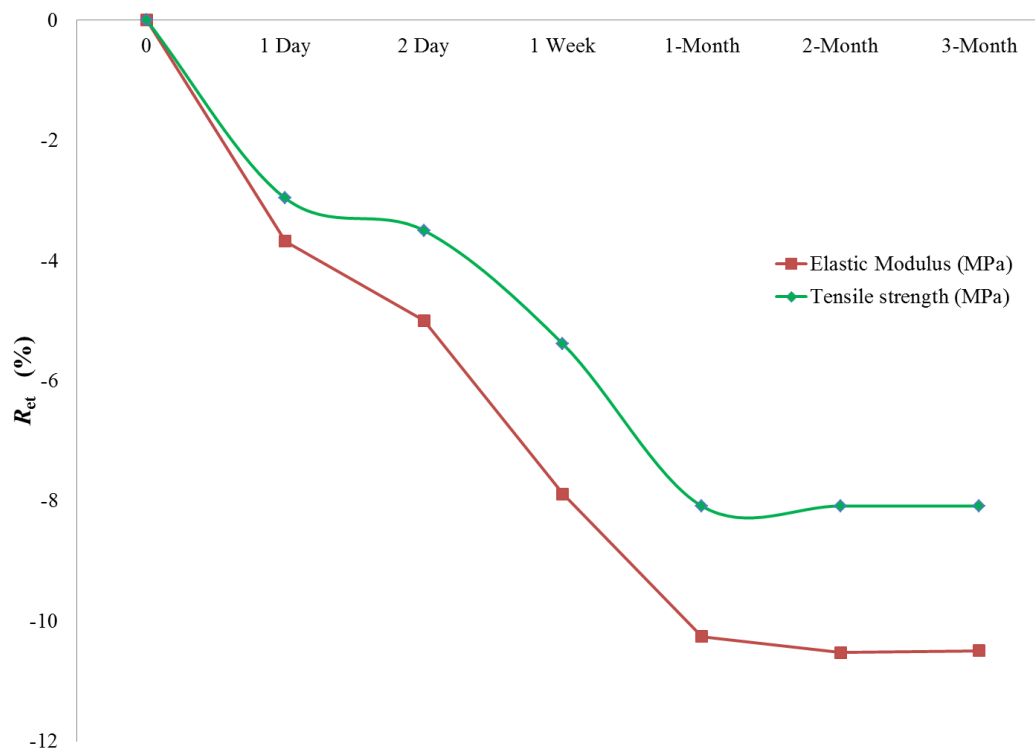
Fig. 127 Tensile capacity retention (R_{et}) for tensile strength and modulus of elasticity

Studies carried out by Somjai Kajorncheappunngam from Khon Kaen University in Thailand, together with Rakesh Gupta and Hota GangaRao from West Virginia University in the US, showed a similar degradation process and drop in the mechanical properties of GFRP composite samples exposed to an alkaline solution for up to five months (Kajorncheappunngam, Gupta et al. 2002).

Another parameter which could potentially introduce a faster degradation process at higher temperatures is the presence of micro-cracks in the water-based coating applied on the surface of the BVC samples. These micro-cracks would lead to higher water/alkaline solution uptake which follows by matrix expansion of the coating that would subsequently result in swelling of the microstructure of the coating; ultimately, the bond between the BVC samples and coating starts to deteriorate. With the presence of micro-cracks and loss of bond between the water-based coating and BVC bar, the BVC matrix would be directly exposed to the alkaline solution. Therefore the type of epoxy-resin matrix employed in the production of BVC samples plays a crucial role in protecting the bamboo fibers from being exposed and attacked by the alkaline solution and water present in the concrete matrix surrounding the BVC bar.

The results obtained in this study showed an overall reduction of less than 10% for modulus of elasticity and less than 8% for the tensile strength of the BVC bar. The results clearly showed that, unlike studies carried out by Somjai Kajorncheappunngam, Rakesh Gupta and Hota GangaRao on Glass Fiber Reinforced Polymer (GFRP) composite samples where a reduction of up to 70% in tensile strength were observed after three months' exposure to an alkaline solution, the BVC samples produced in this PhD research proved to have significantly superior performance when exposed to a similar alkaline solution for the same period of time. Furthermore, the results confirmed that the type of epoxy-resin system employed to fabricate the bamboo based composite sample (BVC bars) was fundamental in protecting the bamboo fibers from any further deteriorations due to exposure to water and alkaline solution of the concrete matrix, in comparison to previous studies on GFRP reinforcement where up to a 70% reduction of the strength was observed after exposure to alkaline solutions. To further evaluate the test samples, a Scanning Electron Micrographs (SEM) analysis was carried out through a collaboration with the Republic Polytechnic of Singapore, School of Material Science, on the samples before and after exposure to the alkaline solution. Fig. 128 shows the surface of the coated BVC sample before exposure to the alkaline solution, while Fig. 129 and Fig. 130 show the surface of the sample after one month and three months' exposure to the alkaline solution respectively. As Fig. 128 shows, the coating provided a full protection layer on top of the BVC sample's surface though some irregular patterns were observed in the SEM micrograph, but in general, the water-based epoxy coating could bond perfectly to the surface of the BVC sample. There was no uncoated surface observed in the SEM micrograph in Fig. 128. As described earlier, the bonding between the water-based coating and BVC surface could have crucial influences on the performance of the bamboo based composite sample. A poor bond between coating and the BVC bar would lead to faster degradation of the coating and potentially could result in a direct attack on the BVC sample by the alkaline environment, due to the presence of voids and cavities that could accumulate water and alkaline solutions as described earlier in this section. Fig. 129 shows some evidence of degradation of the coating after one month's exposure to the alkaline solution on the surface of the coated BVC samples. The same sample shown in Fig. 128 developed pits and cracks after one month's exposure to the alkaline solution. As explained earlier, such pits and cracks could be the result of matrix expansion of the coating as a result of water uptake and subsequent swelling of the microstructure of the water based coating applied on the surface of the BVC bar.
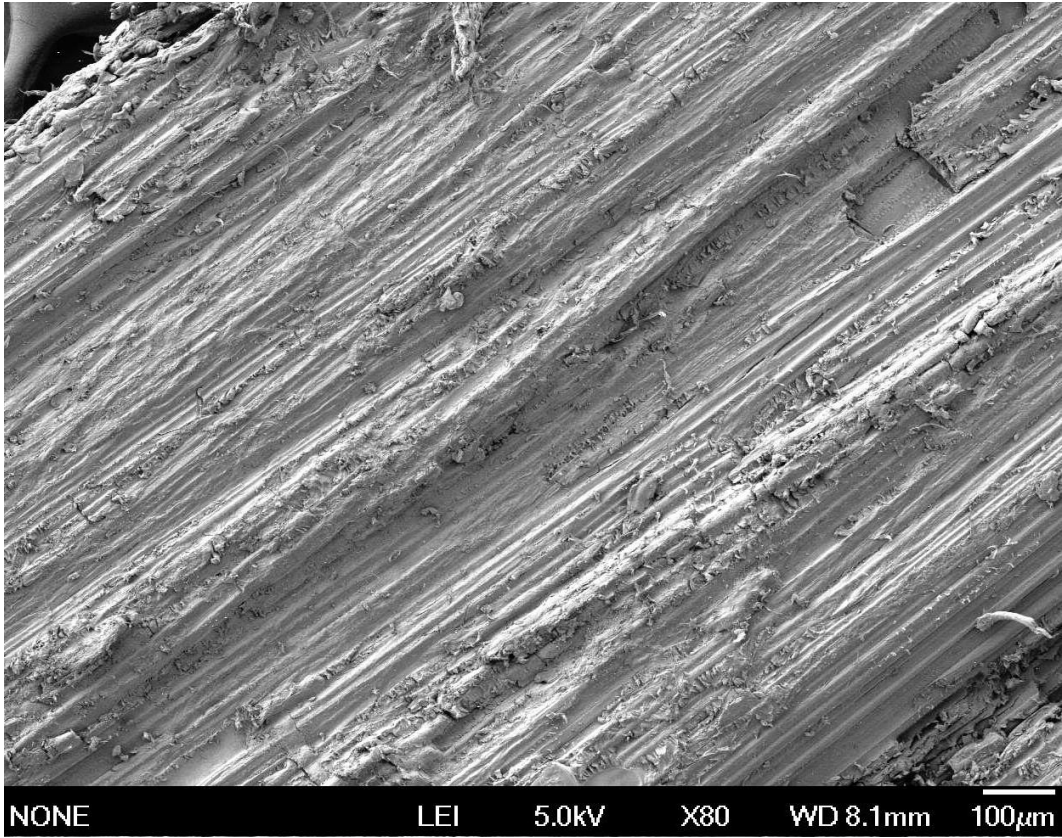
Fig. 128 SEM micrograph of surface of the coated BVC sample before exposure to alkaline solution
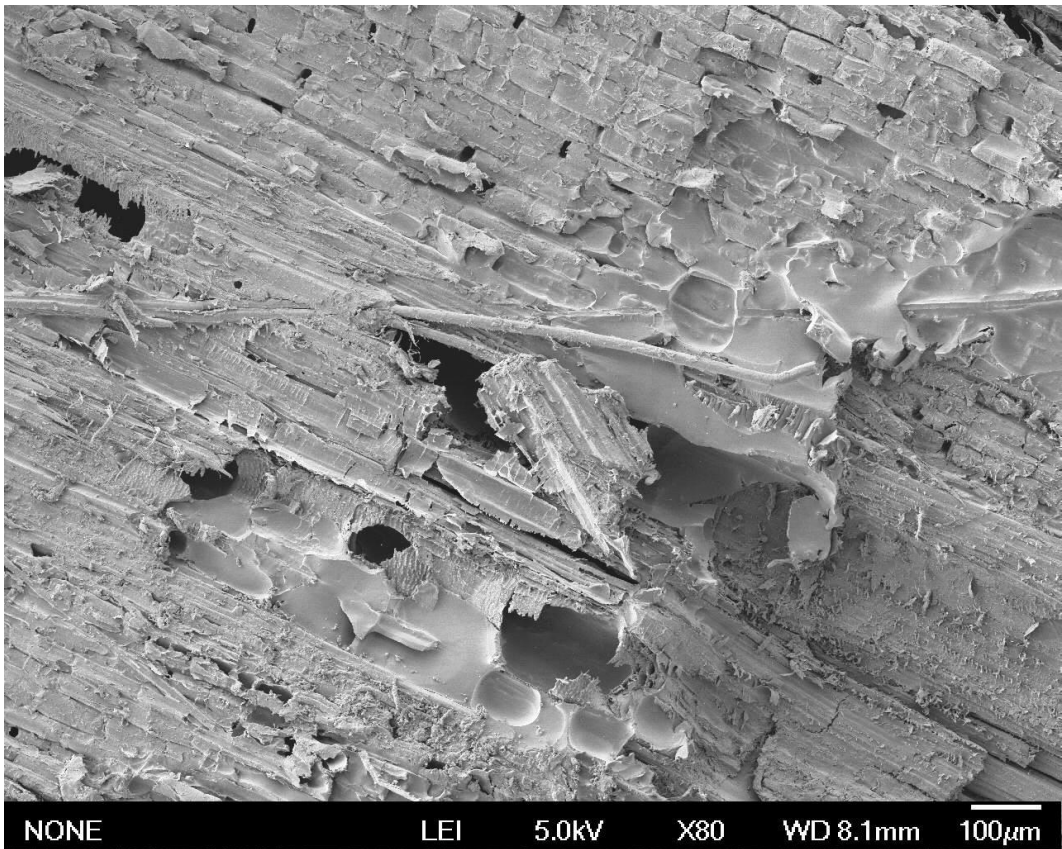
Fig. 129 SEM micrograph of surface of the coated BVC sample after one month's exposure to alkaline solution

Longer exposure time resulted in formation of larger cracks on the surface of the coating as shown in Fig. 130. The swelling of the water-based coating applied on the surface of the BVC reinforcement after three months' soaking in the alkaline solution had turned into wider and longer cracks at the microstructural section of the coating. These cracks could further promote the direct exposure of the BVC surface, through the holes and voids of the cracks, to the alkaline environment.

However, as the results in Fig. 125, Fig. 126 and Fig. 127 suggested, after a certain exposure time, the effect of water or alkaline solution on the tensile properties of BVC samples become stable. Though changes in tensile properties or water uptake behavior were observed after three months' exposure to the alkaline solution, the changes developed to a steady state without further adverse impact after only one month. Furthermore, the epoxy-resin matrix used in the production of the BVC samples had shown great benefits in protecting the natural bamboo fibers from both water uptake as well as alkaline degradation compared to typical GFRP materials investigated in previous works, as described earlier in this section.

6.5. BVC reinforced concrete beam conceptual design, experiment and evaluation

After careful investigation of the bond performance of the newly developed BVC reinforcement in concrete matrix and employing the necessary techniques to enhance the bond strength between the two materials, in the final stage of this research, a series of concrete beams reinforced with BVC materials were prepared at AFCL in Singapore. The concrete beams were prepared with BVC materials employed as longitudinal as well as shear reinforcements. Four-point bending tests were performed on the concrete beam samples to evaluate the flexural performance of the concrete beams under various loading conditions and reinforcement arrangements.

Limit State Design (LSD), also known as Load and Resistance Factor Design (LRFD), was employed as the basis for the design and calculation of the BVC reinforced concrete beams, as explained in section 3.1. The American Concrete Institute's (ACI) guide for the design and construction of structural concrete reinforced with Fiber Reinforced Polymer (FRP) bars (ACI 440.1R-15) was used as the primary guideline to the LRFD concepts during the design and evaluation of the BVC reinforced concrete beams (American Concrete Institute 2015). Comparison with steel reinforced concrete beams of similar cross sections were made in this section to further prove the technical suitability of the new type of reinforcement materials developed within this PhD thesis.

6.5.1. Concrete beam design with BVC reinforcement according to ACI 440.1R-15

There are various factors involved in the design and proportioning of concrete beams reinforced with the new type of reinforcement materials. The ACI 318 "Building Code Requirements for Structural Concrete", as briefly discussed in chapter 3, has fully covered all the necessary requirements for the application of structural concrete, including the design and construction for strength, serviceability, and durability, as well as load combinations, load factors, and strength reduction factors, and structural analysis methods and deflection limits. However, the newly developed Bamboo Veneer Composite (BVC) reinforcement system was shown to have distinct behaviors compared to conventional steel reinforcement in terms of physical and mechanical properties when used in structural concrete. The Bamboo Veneer Composite (BVC) reinforcement developed within this PhD thesis was shown to have similar mechanical behavior as typical FRP reinforcement produced with carbon fiber (CFRP) or glass fiber (GFRP), as described in detail in chapter 3.

As the results from the mechanical tests in chapter 5 showed, the newly developed BVC reinforcement had high tensile strength only in the direction of the fibers (uniaxial strength), unlike steel reinforcement which, due to its isotropic behavior, has similar properties in all directions. The anisotropic behavior of BVC materials would affect the shear strength and bond performance of the reinforcement when used as reinforcement in concrete beam. The relatively high shear strength of the BVC materials would only be available at certain directions (along the fiber), which restricts the application of the fabricated stirrups in section 5.5.2 into certain shapes and arrangements along the concrete beam. Therefore, for applications in which sufficient mechanical properties and mainly tensile properties of the reinforcement materials perpendicular to the fiber direction (main axis of the beam) are needed, diligent precautions and detailed design of the BVC materials as reinforcement should be undertaken to ensure the uniaxial BVC reinforcement is mechanically activated up to their ultimate capacities.

Furthermore, as shown in section 6.2, BVC materials similar to FRP materials exhibit an elastic behavior up to the ultimate failure point and do not yield like steel. ACI 440.1R-15 has provided the necessary design guides for the application of FRP materials as reinforcement in concrete to justify the lower ductility of the FRP (e.g. GFRP) reinforced concrete elements as compared to steel reinforced concrete members. Given the consideration of ductility by ACI 440.1R-15, this design guide has been followed closely in this PhD research to evaluate the performance of BVC reinforced concrete beams. Unfortunately, at present, no specific design considerations are available for bamboo based composite reinforcement materials and thus ACI 440.1R-15 design standard is the most relevant available standard guidelines for this PhD research.

The design guides provided by ACI 440.1R-15 are based on the concepts of equilibrium and compatibility. To design the concrete beams reinforced with BVC reinforcement in this PhD thesis, the strength design method was preferred over the working stress design approach to achieve comparable results with methods employed by other standards such as ACI 318 for steel reinforced concrete design. However due to lower modulus of elasticity of BVC reinforcement compared to steel, the serviceability limit state could control the design of the concrete members reinforced with BVC materials to prevent excessive deflections during the service life of the structure as a result of lower ductility.

The effect of water uptake and alkaline solution on the tensile properties of the BVC reinforcement was investigated in the previous section. According to Fig. 126, a drop of up to 10% in modulus of elasticity and up to 8% in tensile strength values were expected after three months' exposure to the alkaline solution with similar pH values to concrete pore solution, but at a relatively higher temperature of 60℃. As a result of exposure to various environmental conditions, a reduction in material properties for FRP reinforcement was expected, and similarly ACI 440.1R-15 had recommended applying reduction factors to the guaranteed tensile strength without the effects of long-term exposure. The application of the reduction factors ensures that the margin of safety in design of brittle FRP reinforcement for concrete application is large enough to provide enough strength to resist the applied loads. Eq. 66 from ACI 440.1R-15 recommends the tensile properties that should be used in the design of structural concrete elements reinforced with FRP materials.

$$f_{fu} = C_E f_{fu}^*　(Eq.\ 66)$$

Where:

C_E: is the reduction factor depending on the type of FRP composite, e.g. CFRP or GFRP, and

f_{fu}^*: is the guaranteed tensile strength of the FRP reinforcement.

ACI 440.1R-15 has given various reduction factors as shown in Table 42. These values are conservative estimates and no consideration was given for bamboo based composite materials.

Table 42 Environmental reduction factor as advised by ACI 440.1R-15 for material properties

Exposure condition	Fiber type	Environmental reduction factor C_E
Concrete not exposed to earth and weather	Carbon	1.0
	Glass	0.8
	Aramid	0.9
Concrete exposed to earth and weather	Carbon	0.9
	Glass	0.7
	Aramid	0.8

From the results of this PhD thesis, a reduction factor of 0.90 seems to be acceptable for environmental exposure. However, in order to have a conservative estimate and to account for other conditions such as an acidic environment not investigated in this study, a reduction

factor of 0.80, similar to that for GFRP reinforcement exposed to earth and extreme weather conditions, will be used for designing the concrete beams for laboratory conditions.

However, in ACI 440.1R-15, no reduction factor is recommended for the modulus of elasticity. It recommends only using the mean values of the modulus of elasticity or simply the average values from the laboratory tests as the design values for modulus of elasticity. In this PhD thesis, the average values obtained after exposure to alkaline solution are used as design values of modulus of elasticity of the reinforcement to have conservative estimates of the reinforced concrete beams serviceability limit states.

Beside the tensile strength and modulus of elasticity, the rupture strain also has an important influence in the design of reinforced concrete beams with BVC reinforcement. Given the brittle mode of failure observed within various FRP reinforcement, the ACI 440.1R-15 recommended employing similar reduction factors (C_E) as for the tensile strength for the rupture strain as shown in Table 42. Eq. 67 should be used to calculate the design rupture strain.

$$\varepsilon_{fu} = C_E \varepsilon_{fu}^* \quad \text{(Eq. 67)}$$

Where:

C_E: is the reduction factor as shown in Table 42, and

ε_{fu}^*: is the guaranteed rupture strain of the FRP reinforcement.

In the case of BVC reinforcement, the average guaranteed rupture strain measured during the tensile tests was 1.35%, which could be used during the design stage of the BVC reinforced concrete beams according to ACI 440.1R-15. The rupture strain has an important role in determining the serviceability limit states of design for which acceptable deflection limits of the reinforced concrete member should be controlled versus the available deflection values of the member. Large deflection or excessive cracking should be prevented during the design stage to protect the safety of the occupants of the respective buildings.

Beside the tensile properties of the longitudinal bars, the tensile strength of the FRP bars at bends should also be evaluated, especially when the shear reinforcements (stirrups) are designed for flexural concrete member. As described in chapter 5, the bent portions of the BVC stirrups had not been tested due to a lack of available testing features at AFCL, but the

straight sections were evaluated for their tensile and flexural properties. ACI 440.1R-15 clearly indicates that the tensile force developed by the bent portion of a FRP bar is generally influenced by the ratio of the bend radius to the FRP bar diameter r_b/d_b. Therefore ACI 440.1R-15 recommends using the following formulae to calculate the design tensile strength of FRP bars at a bend.

$$f_{fb} = \left(0.05 \cdot \frac{r_b}{d_b} + 0.3\right) f_{fu} \leq f_{fu} \qquad \text{(Eq. 68)}$$

Where:

f_{fb}: is the design tensile strength of the bend of FRP reinforcement (MPa),

r_b: is the radius of the bend (mm),

d_b: is the diameter of reinforcing bar (mm), and

f_{fu}: is the design tensile strength of FRP reinforcing bar according to Eq. 45 (MPa).

Eq. 66, Eq. 67 and Eq. 68 are among the essential equations used in designing concrete beams reinforced with FRP materials as reinforcement. These equations are used in this thesis to further evaluate the experimental results obtained by testing the BVC reinforced concrete beams and to assess the relevance of ACI 440.1R-15 to the application of BVC materials as reinforcement in concrete.

The flexural design philosophy for FRP reinforced concrete members is similar to what was explained in chapter 3 for the design of steel reinforced concrete members, except that for FRP reinforced members, the stress-strain relationship of FRP materials differs from steel and needs to be considered in the design process. The FRP materials and BVC materials display a linear elastic behavior up to the failure point, while steel has a unique behavior in which elastic behavior is observed up to the yield point and subsequently plastic deformation leads the material behavior. Therefore, steel reinforced concrete members are normally designed to have a tension-controlled behavior in which the steel reinforcement yields before the concrete section fails, to prevent any excessive damage to the occupants and thus increasing the overall load-bearing capacity of the member.

In the case of BVC reinforcement, similar to FRP materials, the concrete member will not display any ductile behavior as commonly seen in tension-controlled concrete elements reinforced with steel reinforcement as a result of lower ductility (stiffness) of BVC or FRP

reinforcement compared to steel reinforcement. Due to the lower modulus of elasticity of BVC reinforcement compared to steel reinforcement, significant elastic elongation is expected for the concrete beams. Therefore, either compression-controlled (concrete crushing) or tension-controlled behavior is acceptable according to ACI 440.1R-15. For the design of BVC reinforced concrete beams for this thesis, both types of failure modes would be investigated, but both strength and serviceability criteria must be thoroughly controlled to prevent excessive deformation of the BVC reinforced concrete beam.

The design concept for FRP materials application in concrete in accordance with ACI 440.1R-15, which is also employed for BVC reinforcement within this research, would lead to higher safety factors that could prevent the unexpected failure of the reinforced member comparable to ACI 318 guidelines for steel reinforced concrete members. The higher safety factors could guarantee the optimum performance of the FRP/BVC reinforced concrete members up to the ultimate allowable tensile capacity of the BVC reinforcement systems. In practical terms, the higher safety factors would translate into a reinforced concrete member with higher reserve strength comparable to a steel reinforced concrete member. This could be achieved by either employing greater quantity of the BVC reinforcement bars, or by increasing the cross-section of the concrete member. Both approaches would result in a BVC reinforced member with acceptable load-bearing capacity comparable to conventional steel reinforced concrete members. Further details are provided in the following sections.

The main assumptions of the strength design theory as explained in section 3.2.1 are valid for the calculation of the strength of the sections reinforced with FRP bars. The Koenen's theory of flexure for reinforced concrete beams (chapter 3) remains essential for the design of FRP reinforced concrete beams. In this PhD research and for BVC reinforced concrete beams, Koenen's theory of flexure could be used as a basis for the design. According to the strength design philosophy, the design flexural strength at any section of a reinforced concrete member should exceed the factored moment (applied loads) as shown in Eq. 14.

$\Phi \, Mn \geq Mu$ (Eq. 14)

The factored moment (Mu) is calculated by applying load factors to the loadings enforced on the reinforced concrete member. In this study, the factored moment can be calculated simply by using the forces applied to the concrete beam during the flexural test by the UTM machine. The nominal moment, or the flexural capacity of the FRP or BVC reinforced concrete element, can be computed by comparison between the actual reinforcement ratio of

the member under the test and the balanced reinforcement ratio. A balanced reinforcement ratio is the ratio of reinforcement in a member in which concrete crushing and reinforcement rupture happen at the same time, according to ACI 440.1R-15. The reinforcement ratio of the reinforced concrete element (in the research concrete beam) can be calculated by using Eq. 69, which is similar to the reinforcement ratio of steel reinforced concrete members.

$$\rho_f = \frac{A_f}{bd} \quad \text{(Eq. 69)}$$

Where:

A_f: is the area of FRP reinforcement (mm^2) in tension zone of the member,

b: is the width of the rectangular cross section of the beam as shown in Fig. 12 (mm), and

d: is the distance from extreme compression fiber to centroid of tension reinforcement as shown in Fig. 12 (mm).

The balanced reinforcement ratio is calculated by Eq. 70 as described below.

$$\rho_{fb} = 0.85\beta_1 \frac{f'_c}{f_{fu}} \frac{E_f \varepsilon_{cu}}{E_f \varepsilon_{cu} + f_{fu}} \quad \text{(Eq. 70)}$$

Where:

β_1: is the factor taken as 0.85 for concrete strength up to and including 28MPa, similar to Eq. 9 for steel reinforced concrete members,

f'_c: is specified compressive strength of concrete (MPa), which in this study is 20MPa,

f_{fu}: is the design tensile strength of FRP or BVC reinforcing bar according to Eq. 66 (MPa),

E_f: is the design or guaranteed modulus of elasticity of FRP or BVC defined as the average modulus of sample of test specimens, and

ε_{cu}: is the ultimate strain of concrete which is assumed to be 0.003 based on ACI design recommendations as the maximum acceptable concrete strain.

Depending on the reinforcement ratio, two modes of failure are expected for FRP or BVC reinforced concrete members: FRP rupture and concrete crushing according to ACI 440.1R-15. If the reinforcement ratio is less than the balanced reinforcement ratio, the FRP rupture occurs first, otherwise concrete crushing controls the failure mode. Fig. 131 shows the stress

and strain distribution at ultimate conditions for the concrete crushing failure mode, while Fig. 132 shows the stress block calculations for the FRP rupture mode of failure, similar to the steel reinforced concrete design philosophy described in chapter 3 of this thesis.
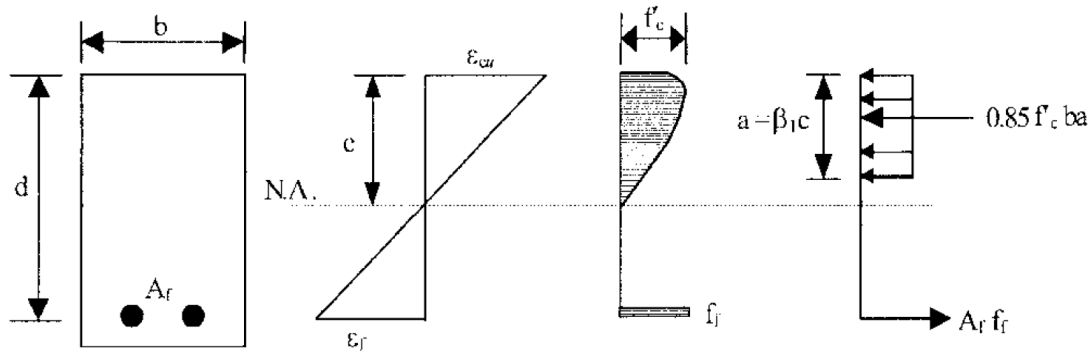
Fig. 131 Stress and strain distribution for concrete crushing mode of failure according to ACI 440.1R-15
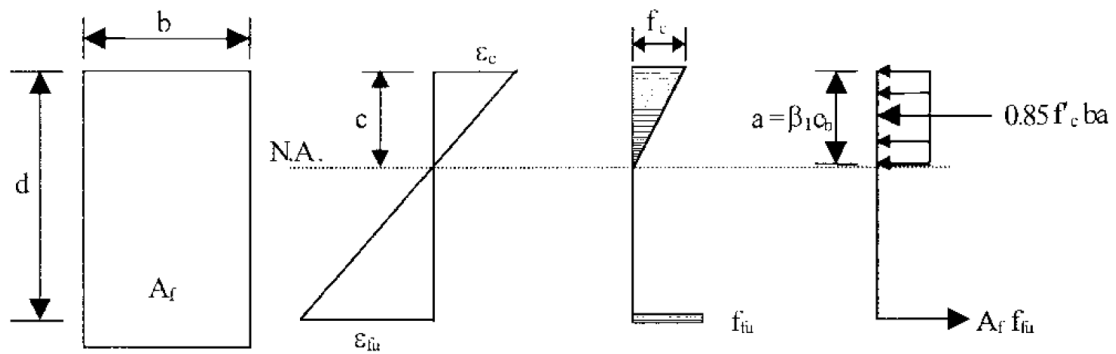
Fig. 132 Stress and strain distribution for FRP rupture mode of failure according to ACI 440.1R-15

If the concrete crushing limit state controls the failure (>) Eq. 13 as described in chapter 3, which is based on the equilibrium of the forces within, the rectangular stress block shown in Fig. 11 can be used to compute the nominal flexural strength. After replacing the parameters described in Eq. 13 with the relevant information from Fig. 131, the following formulae can be used to determine the nominal flexural strength of FRP or BVC reinforced concrete member according to ACI 440.1R-15.

$$M_n = \rho_f f_f \left[1 - 0.59 \, \frac{\rho_f f_f}{f_c'}\right] bd^2 \qquad \text{(Eq. 71)}$$

Where f_f is the stress in FRP/BVC reinforcement in tension in MPa and can be computed with the use of the following formulae based on the equilibrium of the forces in Fig. 131.

$$f_f = \left[\sqrt{\frac{(E_f \varepsilon_{cu})^2}{4} + \frac{0.85 \beta_1 f_c'}{\rho_f} E_f \varepsilon_{cu}} - 0.5 E_f \varepsilon_{cu}\right] \leq f_{fu} \qquad \text{(Eq. 72)}$$

In the case of FRP rupture mode of failure (<) as shown in Fig. 132, the nominal flexural strength can be determined by using the following formulae.

$$M_n = A_f f_{fu} \left(d - \frac{\beta_1 c}{2}\right) \qquad \text{(Eq. 73)}$$

Eq. 73 involves the unknown parameter (c), which is the depth to the neutral axis (N.A) as shown in Fig. 132. Furthermore, since the concrete compressive strain (ε_c) is also unknown when the FRP reinforcement ruptures, it is rather complex to find the value of (c), the depth to the neutral axis. Therefore ACI 440.1R-15 has recommended using a simplified and a more conservative approach for computing the nominal flexural strength by assuming a maximum concrete strain of (0.003) when the FRP reinforcement ruptures. The maximum usable concrete strain ensures that concrete crushing will not occur before any FRP rupture, which is important in the design of BVC/FRP reinforced concrete member with lower ductility compared to streel, to prevent premature failure of the concrete matrix which could pose serious damage to the building and its occupants. This value has been recommended by both ACI 318 and ACI 440.1R-15 for concrete matrix. The ultimate compressive strain is only attained when the depth to neutral axis is computed at the balanced strain condition. Hence Eq. 73 can be simplified into the following formulae.

$$M_n = A_f f_{fu} \left(d - \frac{\beta_1 c_b}{2}\right) \qquad \text{(Eq. 74)}$$

$$c_b = \left(\frac{\varepsilon_{cu}}{\varepsilon_{cu} + \varepsilon_{fu}}\right) d \qquad \text{(Eq. 75)}$$

Where ε_{fu} can be computed from Eq. 67 as explained earlier.

Another important parameter in designing any FRP/BVC reinforced concrete member is to adopt a suitable strength reduction factor (Φ) for Eq. 14. As explained earlier, BVC reinforcement and FRP reinforcement in general exhibit lower modulus of elasticity compared to steel reinforcement; therefore, to compensate for the lack of ductility of the reinforced concrete member, a conservative design approach is used whereby the member is designed with a higher reserve of strength to ensure sufficient material strength is provided to resist the applied forces. ACI 440.1R-15 has recommended following variations for computing the strength reduction factors according to the reinforcement ratio.

$$
\Phi = \begin{cases} 0.55 \; for \; \rho_f \leq \rho_{fb} \\ 0.3 + 0.25 \frac{\rho_f}{\rho_{fb}} \; for \; \rho_{fb} < \rho_f < 1.4\rho_{fb} \\ 0.65 \; for \; \rho_f \geq 1.4\rho_{fb} \end{cases} \qquad (Eq. 76)
$$

The variations shown in Eq. 76 were obtained after years of experimenting with FRP as reinforcement in different concrete applications. Therefore, obtaining similar formulae for BVC as reinforcement in concrete requires extensive research regarding the applications of BVC reinforcement in various structural concrete members, including beams, columns, and slabs; this is beyond the scope of the present thesis. This would be discussed further in chapter 8 on future works, where such relationships could be established for the newly developed BVC materials. For the design of BVC reinforced concrete members, the relationships established by Eq. 76 were used, given the conservative design approach of ACI 440.1R-15 and the similarity in behavior of the FRP materials with the BVC materials developed in this research.

To prevent sudden failure of the reinforced member due to concrete crushing, a minimum amount of reinforcement is required for the section during the design process to ensure adequate resistance are provided to the minimum tensile stresses developed as a result of external loadings. The minimum amount of reinforcement should be provided for any structural concrete member to allow for the least required resistance against the deflection and cracking. Eq. 77 can be used to determine the minimum amount of reinforcement for FRP reinforced concrete members according to ACI 440.1R-15. This equation can be used in the case of BVC reinforcement, as described earlier.

$$
A_{f,min} = \frac{0.41\sqrt{f_c'}}{f_{fu}} b_w d \geq \frac{2.3}{f_{fu}} b_w d \qquad (Eq. 77)
$$

The minimum amount of required reinforcement should be controlled in the early stage of the concrete beam design to estimate the primary size and number of reinforcement bars.

As described earlier and shown in the previous chapter, BVC reinforcement as well as FRP reinforcement have lower modulus of elasticity compared to steel reinforcement, therefore concrete members reinforced with FRP or BVC reinforcement would display relatively small stiffness after cracking. In most cases, members designed with FRP reinforcement under flexural strength theory may not necessarily satisfy the serviceability limit state of design for

deflection and cracking. The cracking is not a desirable phenomenon, not only for aesthetic reasons, but also due to long-term durability and structural integrity concerns.

The long-term presence of macro and micro cracks could lead to progressive seepage of water or acidic and alkaline solutions into the member through the voids and holes of the existing cracks. Long-term exposure to such environments could damage the structural integrity of the reinforced concrete member, especially in steel reinforced concrete members; steel corrosion is one of the primary causes of concrete deterioration and structural failure as explained in chapter 3.

In the case of BVC or FRP reinforcement, larger or wider crack widths might be permitted in the design calculations, given the non-corrosive behavior of bamboo based composite materials compared to steel reinforcement. But this suggestion should be scientifically investigated through extensive research and testing of BVC reinforced concrete members in various environmental conditions; this is beyond the time limit of this thesis. Nonetheless such a statement has already been evaluated for FRP reinforced concrete members. For instance, only aesthetic considerations would dominate the design for serviceability limit state of cracking in FRP or BVC reinforced concrete members according to ACI 440.1R-15. Therefore ACI 440.1R-15 recommends employing the following formulae to control the flexural cracks in FRP reinforced concrete elements by limiting the maximum spacing between the reinforcement in the flexural member.

$$s_{max} = 1.15 \frac{E_f w}{f_{fs} k_b} - 2.5 C_c \leq 0.92 \frac{E_f w}{f_{fs} k_b} \quad \text{(Eq. 78)}$$

Eq. 78 is based on various experiments carried out by ACI committee members since 1999 and is an experimental indirect evaluation of the allowable crack width under the flexural strength limit state. According to the research carried out by Carlos Ospina and Charles Bakis in 2007, a flexural crack control procedure in terms of maximum bar spacing, rather than a direct crack width measurement, and subsequent comparison with allowable crack width limits is to avoid all the unnecessary calculations associated with direct crack width measurements (Ospina and Bakis 2007). The evaluation is called an indirect method because the maximum spacing between the reinforcement is indirectly associated with a desirable crack width limit that the design has to adhere to that limit. Another advantage of this indirect method, besides convenient calculation, is that this method can be employed to either steel-

or FRP-reinforced concrete beams, thus allowing for a direct comparison of spacing and crack width limit between the two types of reinforcement materials.

Besides the maximum spacing of the reinforcement, the concrete cover to the reinforcement in tension should also be controlled to protect the reinforcement, mainly against durability issues such as water absorption through the cracks as explained earlier. Eq. 79, which is recommended by ACI 440.1R-15, ensures sufficient concrete cover to justify the acceptable crack width and the maximum reinforcement spacing allowed by Eq. 78.

$$d_c \leq \frac{E_f w}{2 f_{fs} \beta k_b} \quad \text{(Eq. 79)}$$

Where:

d_c: is the thickness of concrete cover measured from extreme tension face of the member to the center of reinforcement bar (mm),

C_c: is the clear concrete cover above the reinforcement,

f_{fs}: is the FRP stress at service (MPa) which can be computed by performing a cracked-elastic section analysis,

w: is the maximum crack width (mm),

β: is ratio of the distance from the neutral axis to the extreme tension fiber to the distance from neutral axis to the center of tensile reinforcement, and

k_b: is a coefficient which is attributed to the degree of bond between the FRP/BVC bar and concrete matrix. k_b is assumed to be 1.0 for bond behavior similar to uncoated steel bars, larger than 1.0 for bond behavior inferior to steel, and for FRP bars with bond behavior greater to steel, k_b is smaller than 1.0. However, ACI 440.1R-15 recommends using a conservative value of 1.40 for k_b where there is no experimental data available. In the case of BVC reinforcement where preliminary pull-out tests have shown bond strength values in the range of GFRP reinforcement and comparable to uncoated steel bars, a value of 1.0 for k_b could be assumed in the design when necessary.

Besides cracking, in serviceability limit state, the deflection of the flexural members reinforced with FRP materials need to be controlled, as with steel reinforced concrete members. ACI 440.1R-15 recommends a minimum dimension, mainly the depth and

thickness, for flexural members reinforced with FRP materials as reinforcement to limit the deflection to span ratio. The recommended minimum thickness for the design of FRP reinforced concrete members are given in Table 43 as a function of the span length of the member (L).

Table 43 Recommended minimum thickness of beams or one-way slabs from ACI 440.1R-15

| Member | Minimum thickness h | | | |
	Simply Supported	One end continuous	Both ends continuous	Cantilever
One-way slabs	L/13	L/17	L/22	L/5.5
Beams	L/10	L/12	L/16	L/4

For instance, in the case of this study for a reinforced concrete beam with a span length of 1,050mm on a simply supported fixture for loading, the minimum required depth would be 105mm to limit the deflection. The final depth would be revised based on the calculations of the stress limit in the FRP/BVC reinforcement, as well as the calculations of the actual serviceability limit state for the reinforcement spacing and deflections.

Furthermore, due to lower stiffness of FRP reinforcement compared to steel reinforcement, a direct calculation of the deflection of any flexural concrete member reinforced with FRP reinforcement is required when designing the member for the serviceability limit state of deflection. When a member deforms under applied service loads and subsequently deflects, cracking of the member occurs and the maximum service load moment (M_a) exceeds the minimum cracking moment (M_{cr}). This event results in a considerable drop in the reinforced concrete member's stiffness. Therefore, to compute the cracking moment (M_{cr}) and evaluate the flexural moment when the member has deflected and cracked, the moment of inertia of the cracked section (I_{cr}) for a cracked transformed section based on elastic analysis should be used. For a rectangular section, the gross moment of inertia when the reinforced concrete member is not cracked is calculated by Eq. 80.

$$I_g = \frac{bh^3}{12} \quad \text{(Eq. 80)}$$

Where h is the overall height (depth) of the rectangular cross section.

The cracked moment of inertia can be calculated based on Eq. 81 and Eq. 82, as described by ACI 440.1R-15 based on elastic analysis.

$$I_{cr} = \frac{bd^3}{3}k^3 + n_f A_f d^2 (1-k)^2 \quad \text{(Eq. 81)}$$

$$k = \sqrt{\left(2\rho_f n_f + \left(\rho_f n_f\right)^2\right)} - \rho_f n_f \quad \text{(Eq. 82)}$$

Where:

k: is the ratio of depth of neutral axis (N.A) to reinforcement depth,

n_f: is the ratio of modulus of elasticity of FRP bars to modulus of elasticity of concrete

However, to consider the variation in stiffness along the length of the reinforced concrete member, ACI 440.1R-15 recommends using an effective moment of inertia (I_e) to estimate the deflection of FRP reinforced concrete beams. Following the formulae proposed by ACI 440.1R-15 is used to compute I_e.

$$I_e = \frac{I_{cr}}{1 - \gamma\left(\frac{M_{cr}}{M_a}\right)^2\left[1 - \frac{I_{cr}}{I_g}\right]} \leq I_g \quad Where \; M_a \geq M_{cr} \quad \text{(Eq. 83)}$$

The factor γ accounts for the variation in stiffness along the length of the concrete member and can be computed by the following formulae. This factor was obtained after various experiments carried out with FRP reinforced concrete beams in 2009 in a study led by Carlos Ospina to investigate the most relevant approaches in carrying out the serviceability design of FRP reinforced concrete (Bischoff, Gross et al. 2009).

$$\gamma = 1.72 - 0.72\left(\frac{M_{cr}}{M_a}\right) \quad \text{(Eq. 84)}$$

The cracking moment of the member (M_{cr}) can be calculated by the following formulae as advised by ACI 440.1R-15.

$$M_{cr} = \frac{0.62\lambda\sqrt{f_c'}I_g}{y_t} \quad \text{(Eq. 85)}$$

Where:

y_t: is the distance from the centroid axis of gross section without considering the reinforcement effect to the tension face of the concrete section, and

λ: is the modification factor reflecting the reduced mechanical properties of lightweight concrete, which is equal to 1.0 for normal weight concrete and 0.75 for lightweight concrete.

Once the initial cross section of the reinforced member is estimated and the deflection check has been carried out, and the strength limit states of the BVC/FRP reinforcement in the concrete beam are controlled, the reinforced concrete member resistance to shear forces should be controlled. Stirrups need to be provided normally to prevent potential shear failure in reinforced concrete beams. Various considerations are applied for the shear design of FRP reinforced concrete members.

First of all, the modulus of elasticity of BVC and FRP materials are lower compared to steel reinforcement, especially when they are used as stirrups with bent portions. Secondly, the tensile strength of the bent portion of the FRP or BVC reinforcement is significantly lower than the straight portions, as described in detail in the previous chapter. Finally, as explained earlier, FRP and BVC materials do not show a yielding behavior like steel when they fail in tension, but rather, they exhibit a linear brittle mode of failure up to the failure point. The design of the shear reinforcement for FRP or BVC reinforced concrete beams follows the strength design theory and Eq. 16, as explained in chapter 3.

$$\Phi V_n \geq V_u \quad \text{(Eq. 16)}$$

As explained in section 3.1.1 on shear strength design for steel reinforced concrete beams, the design shear strength (ΦV_n) should be larger than the factored shear force (V_u) at any section of the reinforced concrete beam. Similar to steel reinforced concrete members, the strength reduction factor (Φ) is taken as equal to 0.75, according to the ACI design guide. As shown in Eq.17, the nominal shear resistance in a reinforced concrete beam is provided by the concrete matrix (V_c) and the shear stirrups (V_s).

$$V_n = V_c + V_s \quad \text{(Eq. 17)}$$

Furthermore, the longitudinal reinforcement in the tension zone of the concrete element can contribute to the shear resistance of concrete section through its axial stiffness, as evaluated by researchers at the Japan Society of Concrete Engineers in the 1990s and further explained in ACI 440.1R-15 (American Concrete Institute 2015). Therefore the concrete shear resistance of FRP reinforced concrete members can be computed by Eq. 65 as suggested by ACI 440.1R-15.

$$V_c = \frac{2}{5} \sqrt{f_c'} b_w (kd) \quad \text{(Eq. 86)}$$

In which (*k*) can be calculated by Eq. 82, and the (*kd*) factor accounts for the axial stiffness of the FRP reinforcement in shear strength design philosophy. The ACI 318 design method employed for computing the shear capacity of steel stirrups can also be used for FRP shear reinforcement. The shear resistance of FRP stirrups perpendicular to the axis of the reinforced concrete member can be calculated by the following formulae.

$$V_f = \frac{A_{fv} f_{fv} d}{s} \quad \text{(Eq. 87)}$$

Where:

A_{fv}: is the amount of FRP shear reinforcement within the spacing s,

f_{fv}: is the tensile strength of FRP for shear design, taken as smallest of the design tensile strength f_{fu}, strength of bent portion of FRP stirrups f_{fb}, or stress corresponding to $0.004E_f$ according to ACI 440.1R-15,

d: is the distance from the extreme compression face of the section to centroid of tension reinforcement, and,

s: is the stirrup spacing.

The ACI standard has limited the stress level of the FRP shear reinforcement to $0.004E_f$ to minimize shear cracking and to prevent the failure of the stirrups at the bent portions. The following formulae should be checked for the tensile strength of FRP stirrups for shear design.

$$f_{fv} = 0.004E_f \leq f_{fb} \quad \text{(Eq. 88)}$$

f_{fb} is the tensile strength of the bent portion of FRP stirrup which can be calculated according to Eq. 89.

$$f_{fb} = \left[0.05 \times \frac{r_b}{d_b} + 0.3\right] f_{fu} \leq f_{fu} \quad \text{(Eq. 89)}$$

Where $\frac{r_b}{d_b}$ is the ratio of the internal radius of the bent portion of the stirrup to the diameter of the FRP stirrup.

The required spacing (*s*) between the vertical stirrups along the reinforced concrete beam can be computed by following formulae.

$$\frac{A_{fv}}{s} = \frac{(V_u - \Phi V_c)}{\Phi f_{fv} d} \quad \text{(Eq. 90)}$$

From Eq. 87 and Eq. 90, an initial estimation of the number and size of the shear reinforcements can be made, but repetitive analysis is required until the final size, number and spacing of the stirrups are found. In terms of shear strain, ACI 440.1R-15 limits the maximum tensile strain of the stirrups to 0.004 to control the shear cracks and to ensure adequate bonding between concrete and shear reinforcements. To prevent any potential sudden and brittle shear failure in FRP reinforced concrete beams, a minimum amount of shear reinforcement must also be provided in the concrete section. ACI 440.1R-15 enforces the following requirement to control the minimum shear reinforcement when the factored shear force (V_u) exceeds almost half of the shear capacity of the concrete matrix ($\Phi V_c/2$).

$$A_{fv,min} = 0.35 \frac{b_w s}{f_{fv}} \quad \text{(Eq. 91)}$$

Furthermore, the ACI 440.1R-15 limits the maximum spacing of the vertical stirrups to the smaller of d/2 or 600mm, to ensure that each shear crack is caught by at least one stirrup and sufficient shear resistance is provided along the shear span of the reinforced concrete member (American Concrete Institute 2015).

The ACI 440.1R-15 standard is a relatively new design guide established less than a decade ago and still needs further investigation and evaluation, before it can be fully integrated into the design and application of FRP reinforcement or BVC reinforcement for reinforced concrete members. Therefore, for the purpose of this thesis, preliminary design and calculations of the concrete beams reinforced with BVC reinforcement have been carried out with respect to ACI 440.1R-15 as the only relevant design guide available internationally for fiber-based composite materials. In this chapter, the experimental results have been evaluated in comparison with ACI 440.1R-15 to assess the suitability and relevance of this standard for the application of the newly developed bamboo veneer composite reinforcement in concrete.

6.5.2. Experimental design and test set-up for BVC reinforced concrete beams

There were various details to be considered while preparing the reinforced concrete beams. The essential parameters investigated through this research were:

- Concrete strength

- Concrete beam cross section and span length

- Number and size of the longitudinal reinforcement

- Number, size and spacing of the stirrups

The concrete strength was chosen with respect to the most commercially available grade of concrete produced and used in the majority of countries around the world. Normal strength concrete of grade 20MPa prepared with Ordinary Portland Cement (OPC), with a mix design according to Table 34, was used for this study, which was similar to the concrete grade prepared for pull-out tests.

Only one concrete grade was chosen for this study to minimize unnecessary complex calculations that could rise from the interactions of concrete strength with BVC reinforcement. Since the main purpose of these tests was to evaluate the performance of BVC materials as reinforcement in structural concrete beams, variations in concrete strength would have made the design of the necessary samples required for evaluation rather complicated, thus it was not feasible, within the time limit and scope of this thesis, to cover the variations in concrete grade. The cross section of the concrete beam and the span length were designed in accordance with the ACI 440.1R-15, after preliminary calculations of the load-bearing capacity of the beams that could fit the available UTM testing machine at AFCL with a loading capacity of maximum 100kN. Furthermore, the cross section of the concrete beam was bound by the dimensions of the produced BVC stirrups as shown in Fig. 106. As explained in section 5.5.2, the final closed loop BVC stirrups had a dimension of 130×130mm. Therefore to accommodate the minimum concrete cover (15mm) around the stirrups as per the recommendations of ACI 440.1R-15, a concrete cross section of 160×160mm was designed and produced in this study. Fig. 133 shows the schematic view of one of the concrete beam's cross section and the cover around the BVC stirrups. The total length of the concrete beams was set to 1,300mm, which remained the maximum available length that the available UTM testing machine at AFCL could test.
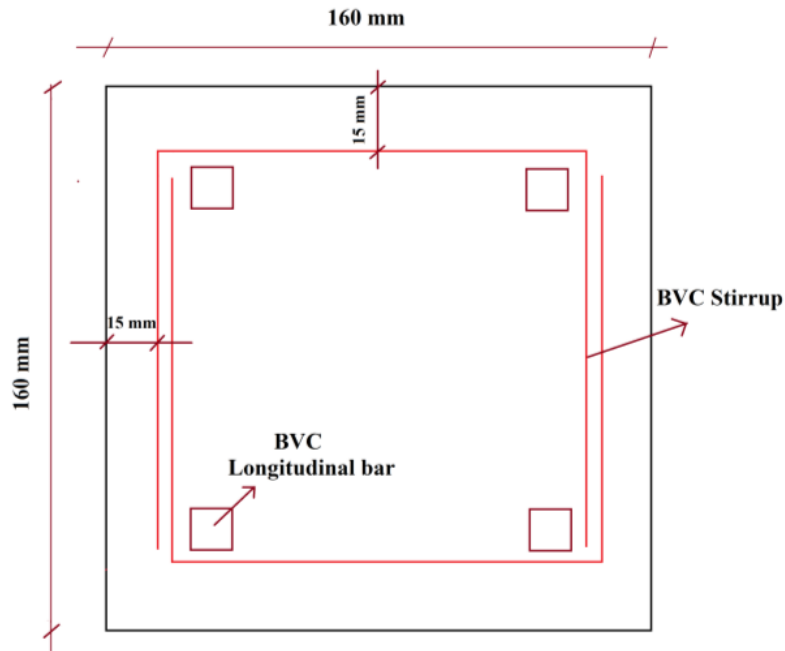
Fig. 133 A typical cross section of BVC reinforced concrete beam

The number and size of the longitudinal BVC reinforcement for this study were arranged in a way such that the loading capacity of the UTM testing machine was not exceeded. It was also ensured that the reinforcement could fit the concrete beam cross section properly, with sufficient allowance for the spacing between the longitudinal reinforcements according to ACI 440.1R-15 guidelines. To investigate the behavior of concrete beams reinforced with BVC reinforcement, various numbers of longitudinal reinforcement were employed in this section to represent different failure patterns that could be obtained when longitudinal BVC reinforcement was used in concrete.

Since all the longitudinal reinforcement in this study had similar cross-sectional dimensions of 10×10mm, therefore, to investigate the effect of the cross-sectional area of provided reinforcements in a section, the number of reinforcements were varied, so that the effective area of the reinforcements could change. Larger or smaller reinforcement cross sections could have also functioned in the same way to alter the effective area of the provided reinforcements resisting the applied stresses; but, producing various sizes of BVC reinforcement (e.g. 6×6mm or 12×12mm) would have required additional time and much more effort in the production, testing and evaluation of those samples; this was not feasible during the course of this PhD research.

310

Similar to the longitudinal reinforcement design, the BVC stirrup size was governed by the fabrication procedure explained in section 5.5. The thickness of the stirrups was 6 ± 0.20mm which was found to be the optimum thickness that the mold of the hot-press compression molding machine could produce with the highest mechanical properties. The only cross-sectional parameter that could be varied with regard to the stirrup design in this research was the width of the stirrup. The preliminary width of 15 ± 0.20mm was chosen after an initial calculation of the shear resistance of BVC stirrups, according to ACI 440.1R-15, with the necessary details explained in section 6.5.1.

Since the main objective of employing the stirrups was to prevent any potential shear failure of the BVC reinforced concrete beams and to ensure that the BVC materials used as longitudinal reinforcements were activated in tension during the flexural tests, much emphasis was placed on the spacing rather than the width and thickness of the BVC stirrups according to Eq. 90. The spacing of the stirrups would then dictate the required number of stirrups that could fit in a span length of 1,300mm.

To evaluate the performance of the simply supported BVC reinforced concrete beams, the four-point (or so-called third-point loading) flexural test set-up was chosen over the center-point flexural test set-up. Fig. 134 shows a typical shear (V) and moment (M) distribution of the applied loads (P) during the four-point flexural test.
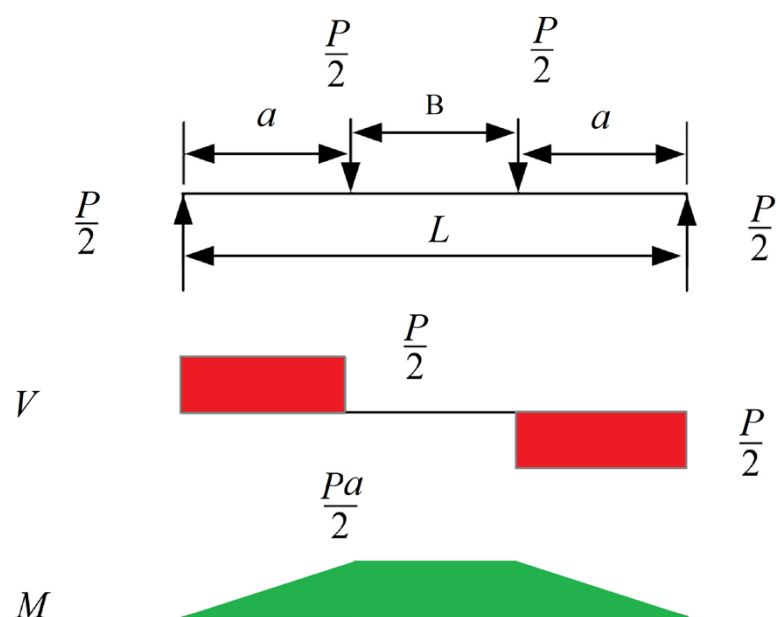
Fig. 134 *Shear (V) and bending moment (M) changes over the length of the specimen under four-point loading*
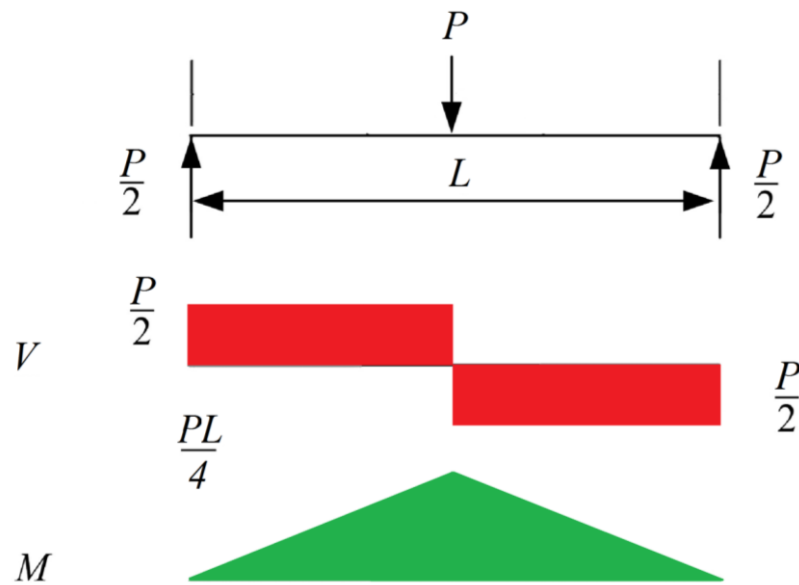
Fig. 135 *Shear (V) and bending moment (M) changes over the length of the specimen loaded centrally*

There are two specific reasons for preferring the four-point flexural test over the center-point test set-up:

- The four-point loading set-up spreads the stress distributions over a larger volume of the concrete beam sample compared to the centrally-loaded flexural test where only the area under the central load is evaluated, as shown in Fig. 135. Therefore the flexural strength obtained in the four-point flexural test would be more conclusive in indicating any potential flaws or defects present in both the concrete matrix and BVC reinforcement. In other words, in center-point loading, the concrete beam fails directly under the center of the loading which is the center of the beam. This central location might not necessarily be the weakest part of the BVC reinforced beam. But in the four-point loading test, the entire middle section of the concrete beam between the points of load introduction is uniformly loaded, and thus the concrete beam will likely fail at the weakest point in the middle section.

- The four-point loading set-up allows for a zero shear zone along the middle section (b) of the BVC reinforced concrete beam as shown in Fig. 134. The zero shear zone permits the designer to eliminate the BVC stirrups in this section, thus the BVC longitudinal reinforcement will be loaded completely in tension and flexure.

312

Therefore the calculation of the ultimate load-bearing capacity of the concrete beams becomes simplified in comparison to center-point loading in which the shear distribution is constant along the beam span and requires stirrups along the whole length of the beam. This set-up ensures that in the middle section between the points of load introduction, consistent flexural moment is distributed and no shear forces are acting on the beam cross sections; therefore it would be possible to activate the BVC longitudinal reinforcement to its ultimate tensile capacity. However, beyond this area, stirrups are required to prevent potential shear failure.

At present, no specific international standard guide for mechanical testing (e.g. flexural test) of either BVC reinforced concrete beams or FRP reinforced concrete beams exists. Therefore the general requirements from ASTM C78−16 titled "Standard Test Method for Flexural Strength of Concrete (Using Simple Beam with Third-Point Loading)" were observed during the four-point flexural tests of the BVC reinforced concrete beams in this section; however modifications and amendments were carried out to fit the samples of this study as well as the available testing facility at AFCL Singapore. For instance, ASTM C78−16 requires the concrete beam to have a test span (L) within 2% of being 3 times its depth (d) which, in the case of this study, is not feasible given the maximum loading capacity of the available UTM at AFCL and the physical constraints imposed by the test set-up at AFCL for larger concrete beams.

Therefore, in this study, all the BVC reinforced concrete beams had cross sections of 160×160mm and total length of 1,300mm while their loading span (L) was kept at 1,050mm. The longitudinal reinforcement had cross sections of 10×10mm. A total of 15 primary design concepts were developed based on three influential parameters:

- Number of longitudinal tension bars at the bottom of the beam
- Number and spacing of the stirrups outside the middle section of the beam
- Distance between the load introduction points in the middle section of the beam

Table 44 summarizes the BVC reinforced concrete beam designs prepared in this study.

Table 44 Details of the BVC reinforced beams

Beam label	Number of bottom reinforcement	Number and spacing of the stirrups at each side of beam (mm)	Distance between load introduction points (b) (mm)
B1b2	2	6 @ 70	350
B1b3	3	6 @70	350
B1b4	4	6 @70	350
B2b2	2	8 @50	350
B2b3	3	8 @50	350
B2b4	4	8 @50	350
B3b2	2	4 @ 115	350
B3b3	3	4 @ 115	350
B3b4	4	4 @ 115	350
B4b2	2	4 @ 75	600
B4b3	3	4 @ 75	600
B4b4	4	4 @ 75	600
B5b2	2	6 @ 45	600
B5b3	3	6 @ 45	600
B5b4	4	6 @ 45	600

The top reinforcements at the compression side of the beams were placed at the top corner of the BVC stirrups and were employed only to maintain the position of the stirrups along the vertical axis of the beams, and to further prevent their movement, especially during concrete casting and preparation. Therefore, only two BVC reinforcement bars were used as top compression reinforcement for all the beams tested in this study. The beams were labeled in a way that the design type (B1, B2, B3, B4, and B5) and the number of bottom reinforcements (b2, b3, and b4) could be clearly differentiated. For each of the 15 designs, 5 samples were prepared. Fig. 136 to Fig. 150 show the sketches of the BVC reinforced beam designs prepared in this thesis. All dimensions are in mm.
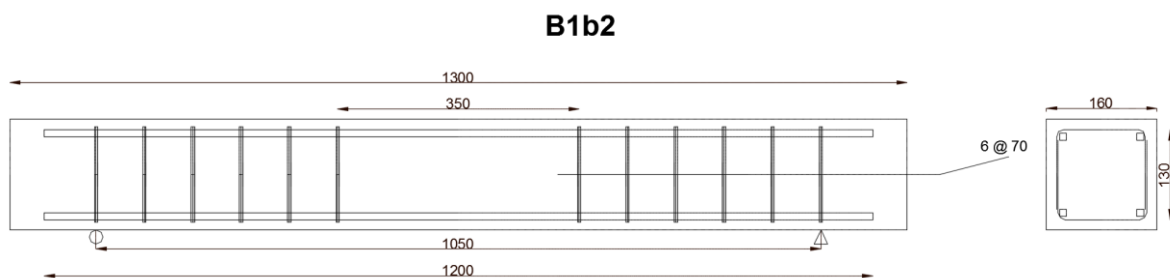
B1b2

Fig. 136 BVC reinforced concrete beam design of B1b2
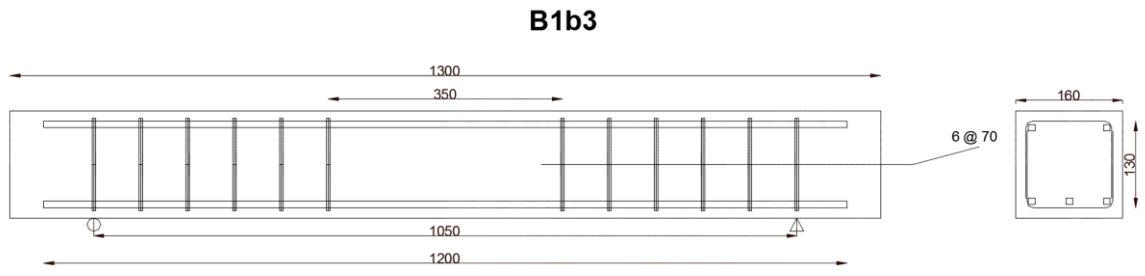
B1b3

Fig. 137 BVC reinforced concrete beam design of B1b3
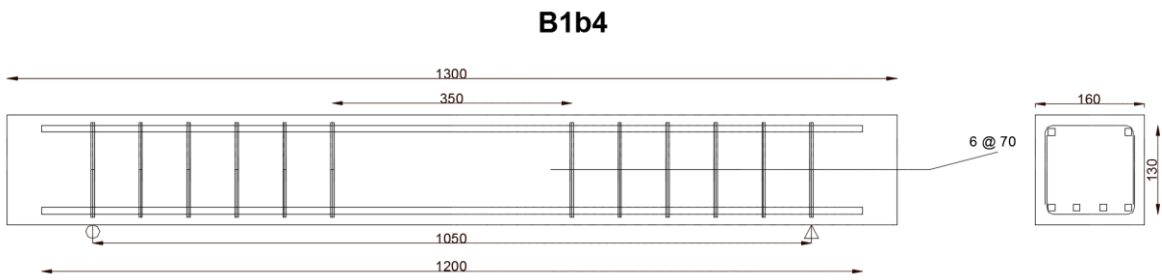
B1b4

Fig. 138 BVC reinforced concrete beam design of B1b4
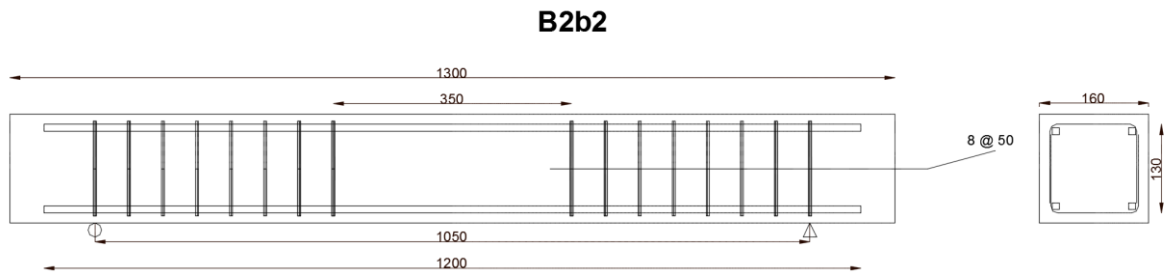
B2b2

Fig. 139 BVC reinforced concrete beam design of B2b2

315
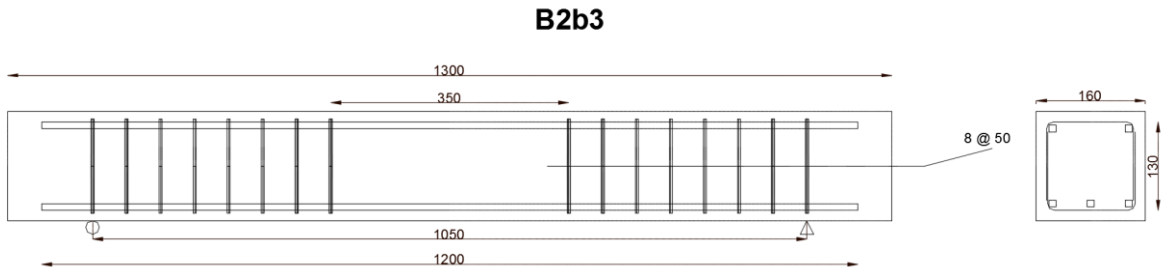
B2b3
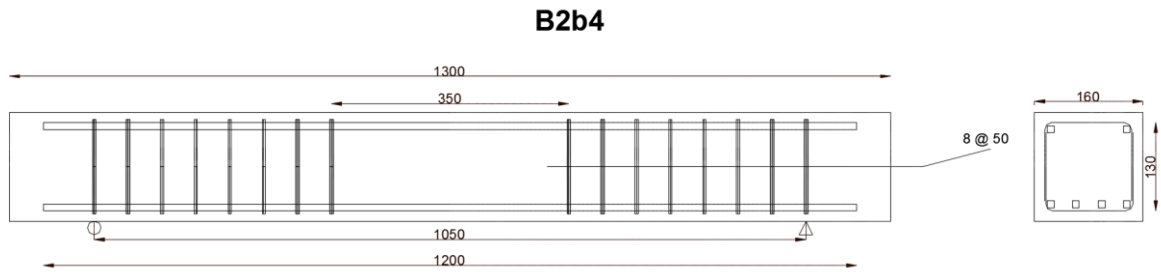
B2b4

Fig. 141 BVC reinforced concrete beam design of B2b4
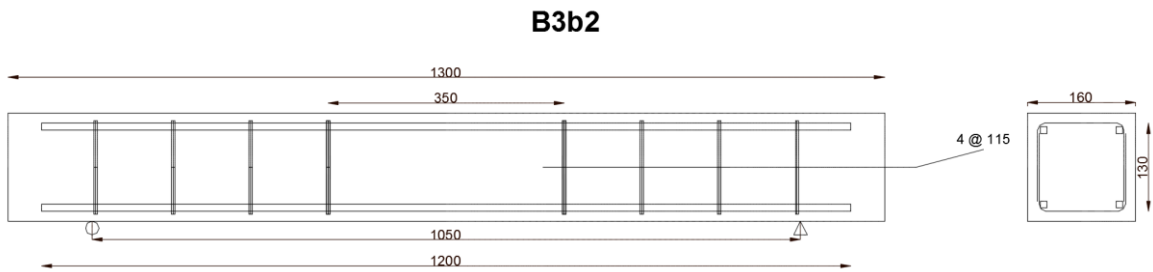
B3b2

Fig. 142 BVC reinforced concrete beam design of B3b2
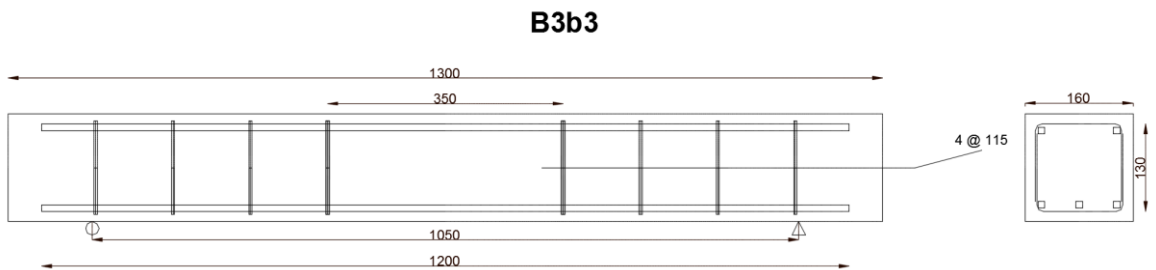
B3b3

Fig. 143 BVC reinforced concrete beam design of B3b3

316
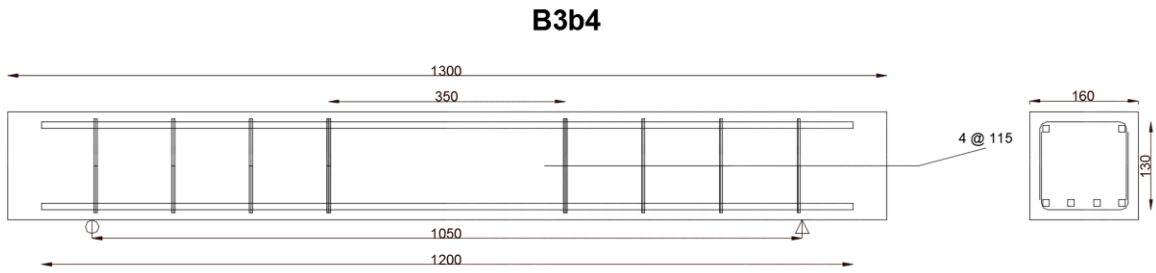
B3b4

Fig. 144 BVC reinforced concrete beam design of B3b4
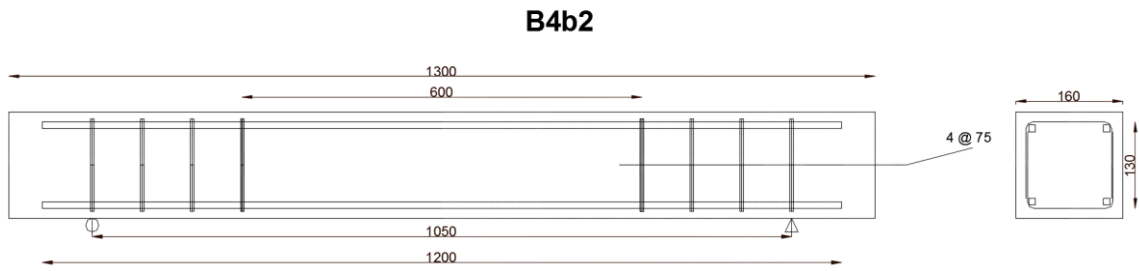
B4b2

Fig. 145 BVC reinforced concrete beam design of B4b2
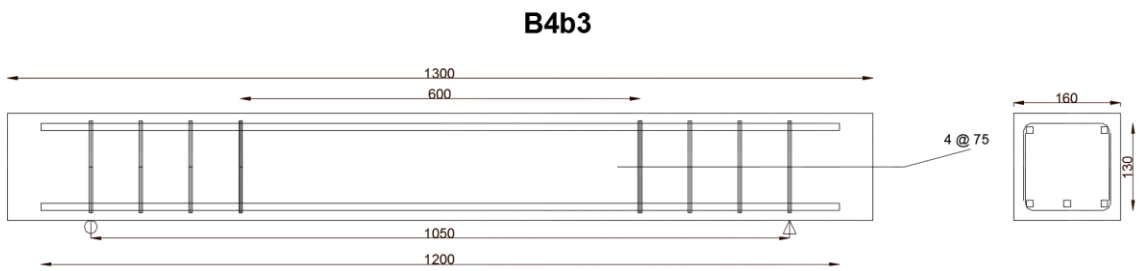
B4b3

Fig. 146 BVC reinforced concrete beam design of B4b3
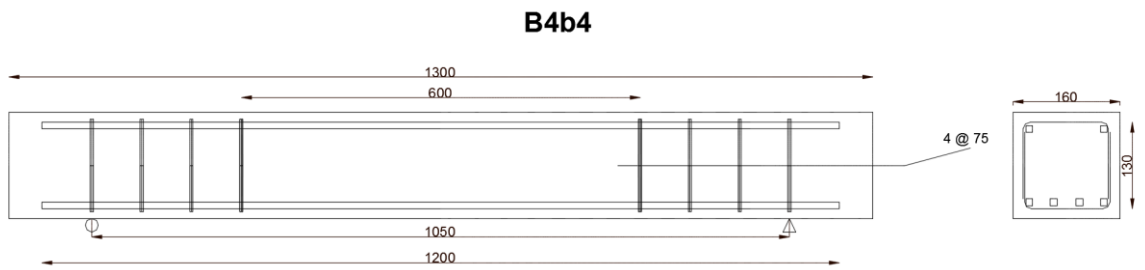
B4b4

Fig. 147 BVC reinforced concrete beam design of B4b4

317
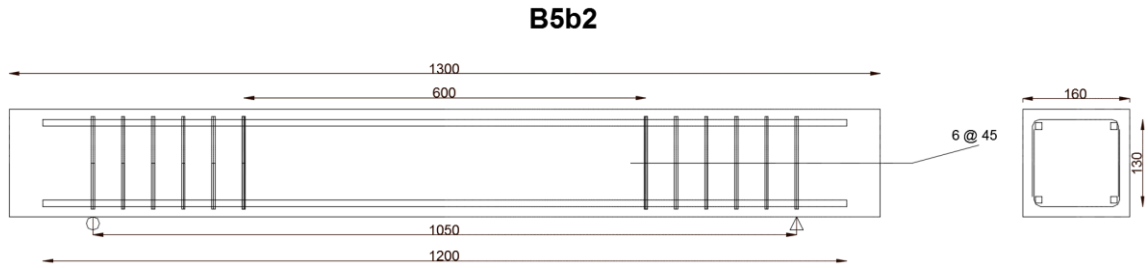
B5b2

Fig. 148 BVC reinforced concrete beam design of B5b2
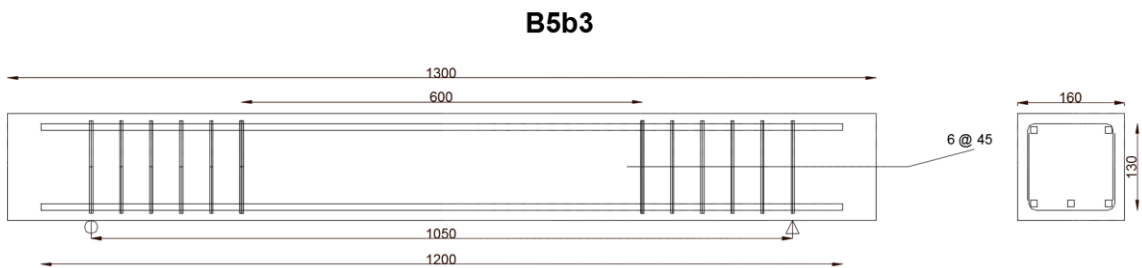
B5b3

Fig. 149 BVC reinforced concrete beam design of B5b3
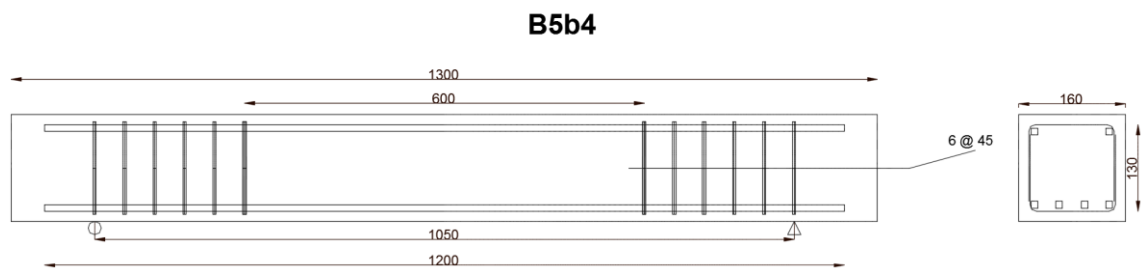
B5b4

Fig. 150 BVC reinforced concrete beam design of B5b4

Placing more than four BVC reinforcement bars at the tension face of the concrete beams was not feasible due to the lack of required spacing in between the bottom reinforcements to allow for the concrete mix, and especially the aggregates, to smoothly pass through the spacing provided between the bars. The spacing provided between the longitudinal BVC reinforcement at the cross section of the concrete beams should be larger than the aggregate size used for preparing the concrete mix. In this study, the maximum aggregate size used was 20mm, which implied that the spacing between the longitudinal BVC reinforcement needed to be at least larger than 20mm. Therefore placing more than five BVC reinforcements was not feasible.

318

As seen in Table 44, the number of BVC stirrups alternated between 4, 6 and 8 for all the designs, except in the case in which the distance between the load introduction points (B) was 600mm, which made the placement of 8 BVC stirrups at a center to center spacing of 32mm almost impossible in practical terms, due to the lack of sufficient space and gaps in between and which could not allow the concrete mix to simply flow in between the reinforcements. The distance between the load introduction points (B) was set to either 350mm or 600mm. The minimum distance of 350 was chosen to comply with the requirements of ASTM C78−16 in which the ratio of the horizontal distance between the point of application of the load and the point of application of the nearest reaction to the depth of the beam should be at least 1.0.

To further evaluate the performance of the BVC reinforcement in flexure and tension, a larger zero shear zone with a length of 600mm between the load introduction points was introduced and designed in this section, as shown in Table 40. This length allowed a better understanding of the flexural performance of the BVC reinforcement where no shear forces and thus no stirrups were present. The ASTM C78-16 was prepared mainly for normal reinforced concrete with and without steel as the main reinforcement type; therefore such recommendations taken from this standard may not necessarily be suitable for the newly developed BVC reinforcement, given the lower stiffness that it has compared to steel. Therefore it was essential to test and investigate the flexural performance of the BVC reinforced concrete beams with larger zero shear zones to establish their ultimate load-bearing capacity with the available facilities at AFCL in Singapore.

Given the length of the longitudinal BVC reinforcement produced was 1,200mm and the loading span was set to 1,050mm, thus an excess length of 75mm, as shown in Fig. 136 to Fig. 150, was provided beyond each side of the bottom supports for the anchorage of longitudinal reinforcement, and to prevent any slippage of the reinforcement ends during the flexural tests. Unlike steel reinforcement in which bending of the reinforcement ends would provide additional anchorage length at the two ends of the beam, in the case of BVC reinforcement, such techniques were not applicable due to the material characteristics of BVC reinforcement and production limits. Therefore, the additional length of 75mm beyond the bottom supports was provided on each side of the simply supported beams to minimize any potential slippage of the reinforcements during the tests, and to ensure failure of the reinforced concrete beam was controlled by either concrete crushing or BVC rupture.

The longitudinal and transverse (stirrup) BVC reinforcement were first coated with Moisture Seal water-based epoxy coating and silica sand particles, given the preliminary results obtained in sections 6.2 on the bonding behavior of water-based epoxy coated BVC bars with concrete matrix, as well as their durability performance in various conditions. Grade 20MPa concrete mix was prepared according to the mix design shown in Table 38. The top and bottom BVC reinforcements together with the BVC stirrups were tied together before pouring the concrete mix. The reinforcements were tied together with the help of steel cables ties, as explained in section 5.5.2, to form a prefabricated reinforcement system. The center to center spacing of the BVC stirrups was carefully measured to ensure that final samples would follow the design parameters shown in Table 44 as closely as possible. Fig. 151 and Fig. 152 show samples of the BVC reinforcement systems before and after coating with water-based coating.

Once the water-based coating was cured completely (after 48 hours), the concrete mix was prepared and the coated BVC reinforcement systems were placed together with the mix into the fabricated wooden molds prepared for the casting of the concrete beam. Fig. 159 and Fig 160 show the sample preparation during the casting of the concrete beam. Fig. 160 shows the final concrete beam while the BVC reinforcement systems have been embedded within the matrix. It was essential to the design of the beams to measure the distance from the edge of the BVC reinforcement to the internal side of the mold while preparing the concrete beams, to ensure that sufficient concrete cover was provided according to the design figures shown in Fig. 136 to Fig. 150.

The concrete mix placement into the wooden mold was carried out in three stages, and at each step, a hand-held concrete vibrator was used inside the wooden mold to ensure that all the voids between the concrete ingredients, including aggregates and cement particles, were minimized. Through the vibration, the entrapped air within the concrete mix was also released which ensured that the concrete mix could fully cover BVC reinforcement and bind to its surface properly.

Furthermore, to ensure that all the concrete mixes prepared for the different batches of concrete beams had similar consistency and workability, slump tests were carried out, similar to those in section 6.2 as shown in Fig. 106. For each series of beam designs shown in Table 44, at least 3 concrete cubes of dimensions 150×150×150mm were prepared for 7-day and 28-day compression tests to guarantee that the average compressive strength of 20 MPa could be achieved in all samples from the various batches.
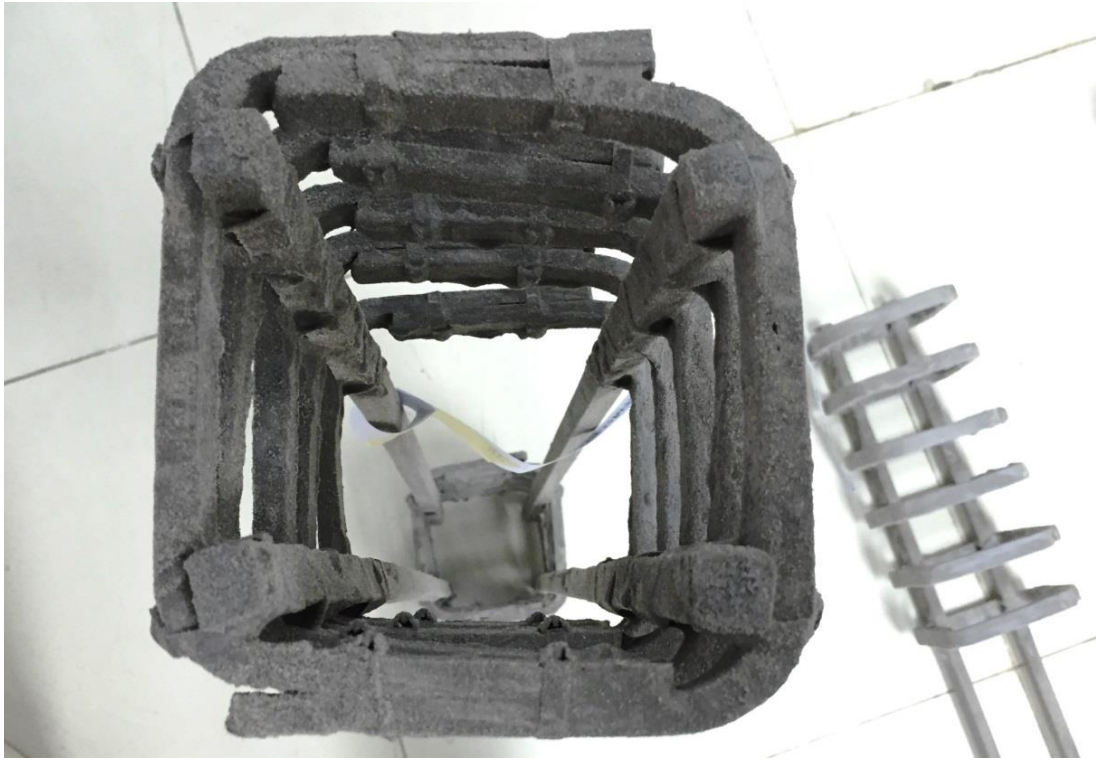
The BVC reinforced concrete beams were cured for 28 days by wrapping the prepared samples with plastic sheets (Fig. 156) to minimize the evaporation of the pore water of concrete, and further enhance the cement hydration process within the concrete matrix by providing a moist environment. The wrapped concrete beams were placed in a curing room with a temperature of 25℃ and a humidity of 65% for 28 days. Once the 28-day curing process was completed, the plastic wrap was removed and the concrete beams were prepared for the four-point flexural test at AFCL. The test set-up for four-point flexural test consisted of two metal rollers on top as the points of load introduction and two metal rollers on the bottom acting as the supports for the concrete beam. Fig. 157 shows the sketch of the flexural test set-up used in this study.
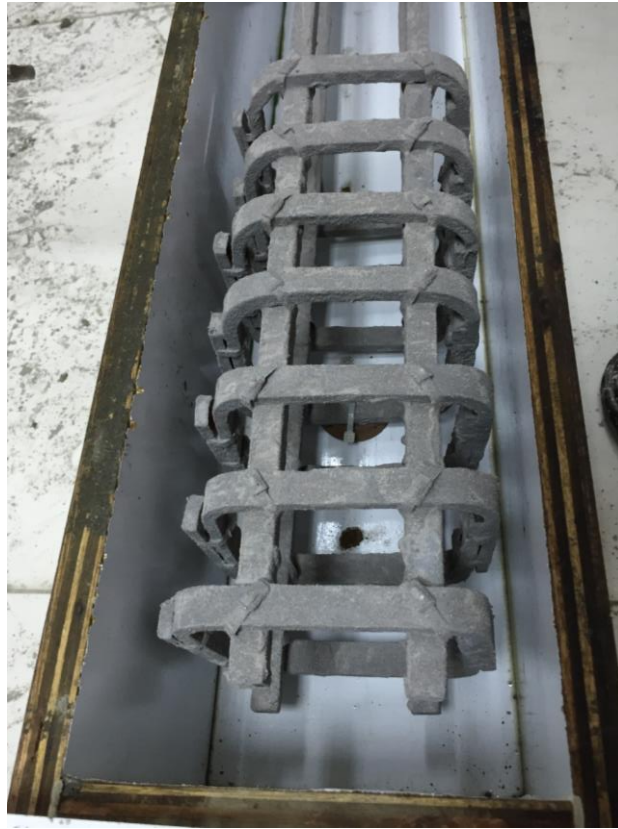
Fig. 153 Coated BVC reinforcement systems in wooden mold prepared for concrete casting

Fig. 154 Pouring concrete mix in three stages into the wooden mold

Fig. 155 Final concrete beam prepared with coated BVC reinforcement

Fig. 156 Concrete beams wrapped in plastic sheets for the curing process to be completed
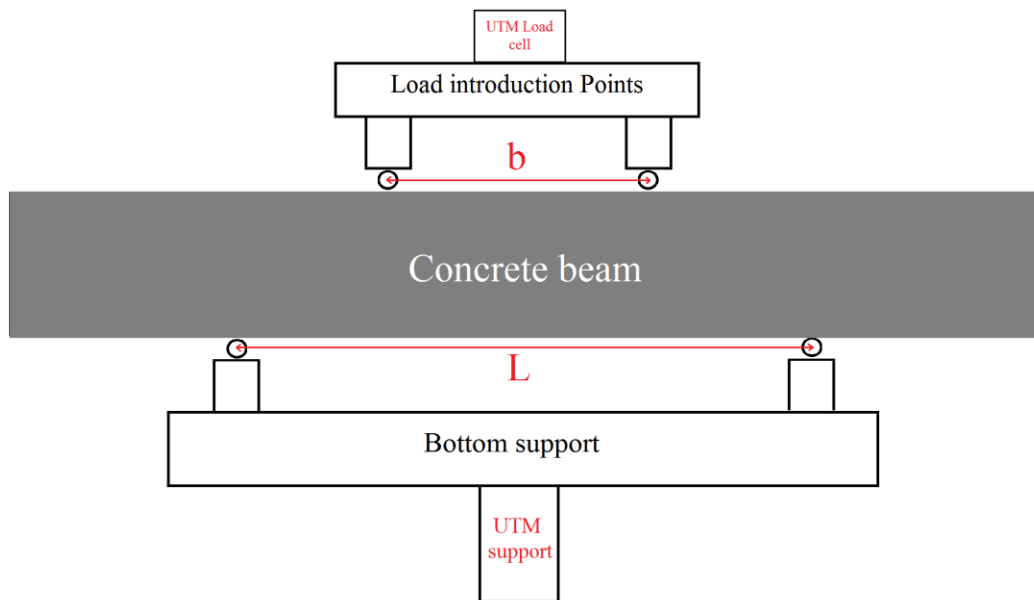
The distance between the bottom metal rollers (L) and between the top metal rollers (b) was adjusted according to the design concepts shown in Table 44. The metal rollers had a diameter of 20mm and were fixed to the bottom support through adjustable pins. The concrete beam was marked for the proposed location of the top and bottom rollers on the surface to ensure accurate positioning of the sample before the test could commence. The top loading block with the rollers was placed in contact with the top surface of the BVC reinforced concrete beam; however, due to the rough texture of the surface of the concrete beam, leaf-type feeler gages as shown in Fig. 158 were used to measure the gaps between the surface of the concrete beam and the bottom or top metal rollers. In cases in which gaps of larger than 0.10mm in depth or width were observed, a 6mm-thick layer of leather strip with a width of at least 25mm extending across the width of concrete beam was used to eliminate such gaps. This method recommended by ASTM C78-16 ensured that such gaps would be eliminated and full contact between the metal rollers and concrete surface could be established.

The loading was applied at a stroke-controlled rate of 0.50mm/min to ensure the first initial cracks could be accurately recorded. ASTM C78-16 recommended a stress-controlled loading rate, but this method was not suitable for the BVC reinforced concrete beams given the lower stiffness of BVC reinforcement compared to conventional steel reinforcement. The stroke-controlled loading rate allowed for a better control of the sample while being tested in flexure compared to stress-controlled loading rate.

The stress-controlled loading rate only captures the stress being developed in the concrete beam during the test, thus monitoring the crack formation and propagation would be more difficult compared to stroke-controlled rate which allows for a lower rate.

The BVC reinforced concrete beam was tested until final failure was observed within the beam by either concrete crushing or rupture of BVC reinforcement in the region of maximum bending moment. All the cracks developed during the tests were marked along the surface of the concrete beams and the deflection of the samples was measured by employing an extensometer at the center of the concrete beams.

For comparison purposes, three concrete beams without any reinforcements and three concrete beams reinforced with steel as longitudinal and shear reinforcements were tested in this study. ASTM grade A615-60 steel reinforcement with an average yield tensile strength of 525MPa and elastic modulus of 210,000MPa were used as the longitudinal reinforcements, and ASTM grade A615-40 steel reinforcement with an average yield tensile strength of 330MPa and elastic modulus of 210,000MPa were used as the stirrups for the three steel reinforced control beams. The steel reinforcement was purchased from a local supplier in Singapore. Fig. 159 shows the concrete beam while being tested at AFCL under the four-point flexural test set-up. As can be seen in Fig. 159, a special supporting block was designed

and manufactured for the test set-up which was able to hold the concrete beams of up to 1,300mm in length at the bottom of the UTM machine. Blocks with lengths longer than 1,300mm could not be supported by the available UTM with a loading capacity of 100kN.

The limitation imposed by the available facilities led to the concrete beam sizes as explained in this section. The load corresponding to the first crack appearing on the surface of the concrete beams was recorded for each series of concrete samples. The failure modes of each series of reinforced concrete beams were carefully investigated and comparison within the samples of each series was carried out. The load displacement curves for each concrete sample were also obtained from the deflection measurement with the help of an extensometer at the center of each concrete beam.

Fig. 159 Concrete beam under four-point flexural test set-up at AFCL Singapore

6.5.3.   Results and discussion

Experimental results

The concrete beams were tested until failure and for each test, the maximum deflection at the center of the beam, ultimate failure load, ultimate flexural capacity (MOR), load corresponding to first crack, flexural capacity at the time of first crack and failure modes

were obtained. The flexural capacity, also known as Modulus of Rupture (MOR), was obtained according to Eq. 92.

$$MOR = \frac{3P(L-b)}{2WD^2} \quad \text{(Eq. 92)}$$

Where W and D are the width and depth of concrete beam respectively, while L and b are shown in Fig. 156.

Table 45 summarizes the main results of the flexural tests carried out on various reinforced and non-reinforced concrete beams in this study. As stated earlier, for each concrete beam, 5 samples were prepared and tested; thus the results shown in Table 41 are the values obtained from the measurement of each sample in each design series. The reinforcement ratio shown in Table 45 was calculated according to Eq. 69.

As seen in Table 45, the initial cracking load (P/2), where the first crack was observed in the concrete beam, started to increase via the addition of more reinforcements at the bottom of the concrete cross section of the beam. The lowest initial cracking load was observed for non-reinforced concrete beams, followed by BVC reinforced concrete beams with two bottom reinforcement bars. The highest initial cracking load was observed with steel-reinforced concrete beams, followed by BVC reinforced concrete beams with three reinforcement bars at the tension face of the concrete cross section.

Specimens of BVC reinforced concrete beams belonging to series five (B5b2, B5b3, B5b4) had the highest average ultimate failure load compared to all the other BVC reinforced concrete beam samples. Concrete beams belonging to series three (B3b2, B3b3, B3b4) samples had the lowest average ultimate failure load. Fig. 160 displays the average initial cracking load and average ultimate failure load for the various beam series tested in this section.

The average initial cracking load of concrete beams reinforced with two BVC reinforcement bars at the bottom increased by up to 250% compared to non-reinforced concrete beams. Adding 3 and 4 BVC reinforcement bars at the tension face of concrete beam cross section resulted in an increase of up to 300% and 370% in the initial cracking load of BVC reinforced concrete samples compared to non-reinforced concrete beams.

Table 45 Summary of results obtained in four-point flexural test of concrete beam specimens

Beam Design	Specimen	Reinforcement ratio (%)	Initial cracking load (P/2) (kN)	Ultimate Failure load (P/2) (kN)	Initial cracking MOR (MPa)	Ultimate MOR (MPa)	Maximum mid-span deflection (mm)
B1b2	1		10.2	32.8	2.6	8.4	13.4
	2		11.6	32.1	3.0	8.2	12.3
	3	0.93	12.1	34.3	3.1	8.8	13.9
	4		11.3	34.8	2.9	8.9	12.7
	5		12.8	33.1	3.3	8.5	14.1
B1b3	1		12.9	38.3	3.3	9.8	12.2
	2		14.1	36.1	3.6	9.2	12.9
	3	1.40	13.5	37.7	3.5	9.7	11.8
	4		13.1	39.3	3.4	10.1	12.3
	5		14.8	37.2	3.8	9.5	13.1
B1b4	1		15.8	44.1	4.1	11.3	11.2
	2		16.3	41.3	4.2	10.6	10.8
	3	1.86	15.1	43.1	3.9	11.0	10.1
	4		15.5	44.8	4.0	11.5	11.1
	5		16.8	43.6	4.3	11.2	9.8
B2b2	1		10.3	31.9	2.6	8.2	12.1
	2		11.7	31.7	3.0	8.1	13.2
	3	0.93	12.2	32.9	3.1	8.4	12.8
	4		11.4	33.9	2.9	8.7	13.1
	5		12.9	33.2	3.3	8.5	14.7
B2b3	1		13.0	37.4	3.3	9.6	12.4
	2		14.2	36.7	3.6	9.4	12.5
	3	1.40	13.6	37.3	3.5	9.6	12.1
	4		13.2	39.9	3.4	10.2	13.0
	5		14.9	38.4	3.8	9.8	13.3
B2b4	1		15.9	44.7	4.1	11.5	11.4
	2		16.4	41.9	4.2	10.7	10.1
	3	1.86	15.2	42.2	3.9	10.8	9.7
	4		15.6	44.4	4.0	11.4	10.0
	5		16.9	44.8	4.3	11.5	9.2
B3b2	1		9.8	31.1	2.5	8.0	13.1
	2		10.5	22.1	2.7	5.7	NA
	3	0.93	10.7	30.5	2.7	7.8	12.6
	4		10.0	19.9	2.6	5.1	NA
	5		10.1	21.3	2.6	5.4	NA
B3b3	1		9.5	38.6	2.4	9.9	14.1
	2		9.1	35.8	2.3	9.2	12.7
	3	1.40	10.0	36.4	2.6	9.3	13.5
	4		10.7	19.3	2.7	4.9	NA
	5		9.9	39.8	2.5	10.2	14.9

Beam Design	Specimen	Reinforcement ratio (%)	Initial cracking load (P/2) (kN)	Ultimate Failure load (P/2) (kN)	Initial cracking MOR (MPa)	Ultimate MOR (MPa)	Maximum mid-span deflection (mm)
B3b4	1		18.9	46.4	4.8	11.9	11.4
	2		14.5	40.8	3.7	10.4	NA
	3	1.86	17.5	47.8	4.5	12.2	9.7
	4		16.8	44.3	4.3	11.3	10.0
	5		18.5	45.2	4.7	11.6	9.2
B4b2	1		9.5	34.8	1.4	5.1	14.8
	2		9.1	36.1	1.3	5.3	15.2
	3	0.93	10.2	33.7	1.5	4.9	NA
	4		8.8	31.1	1.3	4.6	NA
	5		8.2	34.4	1.2	5.0	15.5
B4b3	1		10.6	42.8	1.6	6.3	13.2
	2		11.1	41.1	1.6	6.0	12.5
	3	1.40	11.5	40.1	1.7	5.9	13.8
	4		10.3	42.2	1.5	6.2	14.1
	5		9.5	33.5	1.4	4.9	NA
B4b4	1		13.5	48.4	2.0	7.1	11.4
	2		15.2	49.3	2.2	7.2	10.1
	3	1.86	14.8	52.3	2.2	7.7	9.8
	4		13.1	46.4	1.9	6.8	11.1
	5		15.5	55.6	2.3	8.1	12.3
B5b2	1		10.1	35.2	1.5	5.2	9.8
	2		8.9	34.3	1.3	5.0	14.3
	3	0.93	9.1	35.8	1.3	5.2	15.4
	4		8.4	30.2	1.2	4.4	NA
	5		9.5	25.5	1.4	3.7	NA
B5b3	1		11.5	42.1	1.7	6.2	NA
	2		10.4	38.8	1.5	5.7	13.5
	3	1.40	12.2	43.4	1.8	6.4	12.1
	4		11.9	44.1	1.7	6.5	14.8
	5		10.1	41.7	1.5	6.1	15.6
B5b4	1		14.6	58.5	2.1	8.6	10.1
	2		16.1	62.5	2.4	9.2	12.5
	3	1.86	15.2	52.8	2.2	7.7	11.5
	4		14.9	48.6	2.2	7.1	14.3
	5		16.8	50.9	2.5	7.5	11.8
Non-reinforced	1		4.5	6.3	1.2	1.6	5.8
	2	0	4.9	6.8	1.3	1.7	6.5
	3		4.4	6.5	1.1	1.7	7.5
Steel reinforced Beam	1		22.2	57.4	5.7	14.7	2.4
	2	0.61	25.6	55.6	6.6	14.3	2.9
	3		24.3	60.1	6.2	15.4	3.1
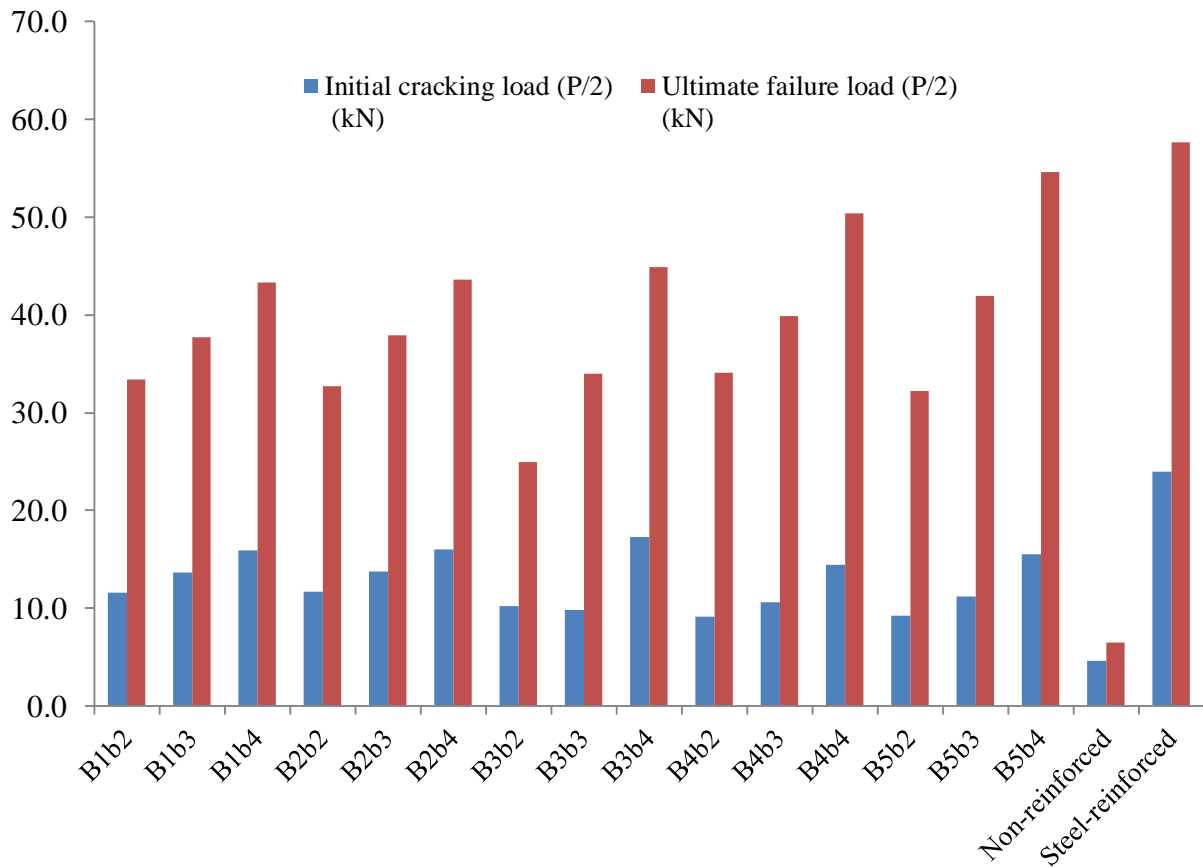
Fig. 160 Average initial cracking and ultimate failure load of various beam series

The ultimate failure load of concrete beams reinforced with 2, 3 and 4 BVC reinforcement bars at the tension face of the concrete cross section also increased by up to 5, 9 and 11 times that of the non-reinforced concrete beams respectively.

One interesting observation made during all the flexural tests carried out in this section was the influence of stirrups spacing on both initial cracking load and ultimate failure load of the beams. It was found that when the spacing between the BVC stirrups was reduced, thus improving the shear strength of the beams, both initial cracking and ultimate failure load were improved. This could be explained by the enhancement in shear span of the beam where shear failure was prevented, and therefore the BVC longitudinal reinforcement was activated up to the maximum tensile capacity. Furthermore, the number of BVC reinforcement employed at the bottom of the beams was to some extent contributing to the shear capacity of the concrete beams. This observation was made when the failure modes of the different concrete beams were investigated. Table 46 shows the failure modes corresponding to each concrete beam series. Three modes of failure were observed within various concrete beam samples: rupture of BVC longitudinal reinforcement in tension, crushing of concrete in

compression, and shear failure of the beams due to either lack of sufficient numbers of stirrups or failure of the BVC stirrups. As seen in Table 46, the shear failure mode was observed mostly in concrete beams reinforced with fewer numbers of longitudinal BVC reinforcement and with larger spacing of the BVC stirrups. In concrete beam series of B1b2 with a stirrup spacing of 70mm, two concrete beam specimens experienced shear failure, while increasing the number of longitudinal bars with similar spacing of stirrups improved the shear capacity to the point that no shear failure was observed within samples of concrete beams belonging to the B1b3 and B1b4 series.

Table 46 Failure modes of concrete beams

Beam Design	Failure Mode
B1b2	3 BVC rupture, 2 shear failure
B1b3	All BVC rupture
B1b4	1 BVC rupture, 4 concrete crushing
B2b2	All BVC rupture
B2b3	All BVC rupture
B2b4	2 BVC rupture, 3 concrete crushing
B3b2	2 BVC rupture, 3 shear failure
B3b3	3 BVC rupture, 2 shear failure
B3b4	4 concrete crushing, 1 shear failure
B4b2	3 BVC rupture, 2 shear failure
B4b3	4 BVC rupture, 1 shear failure
B4b4	4 concrete crushing, 1 BVC rupture
B5b2	3 BVC rupture, 1 shear failure
B5b3	4 BVC rupture, 1 shear failure
B5b4	3 concrete crushing, 2 BVC rupture

A similar observation was made when samples of concrete beams from the B2, B3, B4 and B5 series with 2, 3 and 4 bottom reinforcements were compared. This observation could perhaps be explained by the dowel action between the longitudinal reinforcement and the stirrup, especially when the concrete beam was fully loaded to its maximum load-bearing capacity. However, further testing and evaluation are required in this regard to reach a final conclusion which, in theory, can validate it. The highest number of shear failure modes was observed within samples of concrete beams with a spacing of 115mm between the BVC stirrups (B3b2, B3b3, B3b4). No shear failure was observed within the concrete beam samples with spacing of 50mm between the BVC stirrups. Fig. 161 shows a typical shear

failure of concrete beam sample from the B1b2 series of beams. Similar shear failure was also observed for concrete beams from the B5b2 and B5b3 samples as shown in Fig. 162.

Fig. 161 Shear failure of concrete beam from B1b2 series
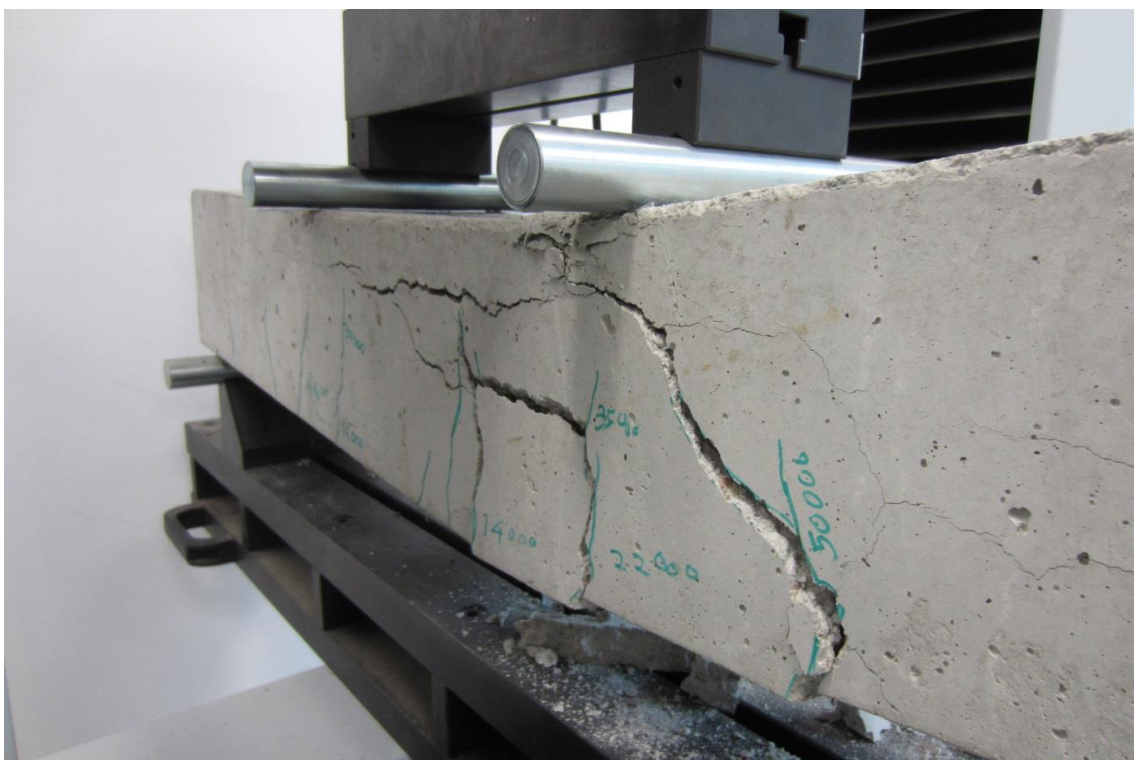
Fig. 162 Shear failure of concrete beam from B5b3 series

As can be seen in both Fig. 161 and Fig. 162, the shear failure was recognizable by its large inclined or diagonal cracks along the surface of the beams at an angle of around 45 degrees. This type of failure could be initiated due to insufficient shear strength of the beam provided by the BVC stirrups. According to ACI 44.1R-15, reducing the spacing of the stirrups has a direct impact on the shear strength of the concrete beam; therefore increasing the spacing would reduce the overall shear capacity of BVC reinforced concrete beam and could result in shear failure.

This could be explained by the shear transfer mechanism in which diagonal tension forces develop diagonal cracks in the concrete beam which could be resisted by any form of effectively anchored shear reinforcement in the form of stirrups that would intersect these diagonal cracks. Thus, in the absence of sufficient number of stirrups to stop those diagonal cracks from further propagation into the concrete beam cross section, the failure of the concrete beam is not avoidable.

The different spacing of BVC stirrups used in this study and the failure modes observed showed the importance of stirrups in preventing the shear failure and the effectiveness of newly developed BVC stirrups in enhancing the shear capacity of the concrete beams when used with appropriate spacing. It should also be noted that in the case of concrete beam samples belonging to B5b3 series, where shear failure was observed in only one specimen, the failure was not due to lack of sufficient stirrups, but was caused by the movement of the BVC stirrups.

The movement of the vertical stirrups was caused by the failure of the steel cable ties used to hold the vertical sides of the BVC stirrup. As shown in Fig. 163 and Fig. 164, the failure was initiated by the movement of the stirrups as a result of the opening of the secured vertical legs. Once the tied vertical legs detached from one another, the effectiveness of the stirrups in intersecting the inclined shear cracks became very limited. However, this phenomenon was only observed in 2 specimens belonging to B5b3 and B5b2 series. In other concrete beam series in which shear failure was observed, the steel cable ties remained intact after the test. Fig. 165 shows the fractured section of a concrete beam from the B3b2 series in which the steel cable ties were holding the stirrups even after the ultimate failure. In this case, the shear failure most likely was the result of insufficient shear capacity of the concrete beam, and not due to the disintegration of the cable ties or movement of the stirrups.

Fig. 163 Failure of the steel cable ties used to hold the vertical legs of the stirrups

Fig. 164 The opening of the steel cable ties followed by the ultimate failure of the beam

The BVC rupture failure mode is shown in Fig. 166. This mode of failure was characterized by the tensile failure of BVC reinforcement at the region of the maximum bending moment. In the majority of the samples, the first cracks were observed as vertical flexural cracks near the tension face of the concrete beams and near the consistent moment area (Fig. 135). These cracks continued to propagate towards the compression face of the concrete beam, and smaller cracks started to develop near the lower tension face of the beam until final rupture of the BVC reinforcement took place. Fig. 167 shows a close view of the failure of the BVC reinforcement in tension at the bottom face of the beam during a BVC rupture mode of failure of the concrete beams in this study. As can be seen in Fig. 167, at the space between the top load introduction rollers, no BVC stirrups were employed so as to ensure that only flexural mode of failure through rupture of longitudinal BVC reinforcement at the tension face of the beam would occur. The BVC reinforcement rupture was caused as a result of reaching the ultimate tensile capacity of the material, which can be seen in Fig. 167 where the two BVC reinforcements split along the long axis of the beam.

336
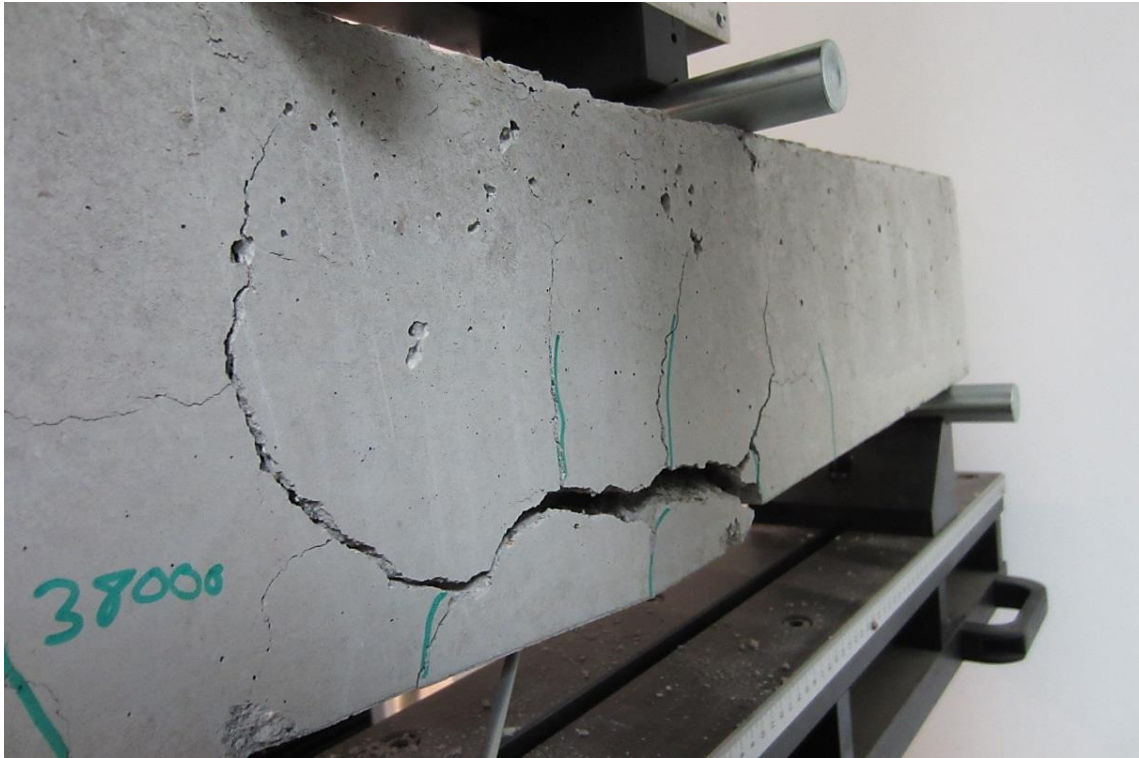
Fig. 166 BVC rupture mode of failure

Fig. 167 Tensile failure of the BVC reinforcement at the tension face of the concrete beam sample

In all the tests carried out in this section, no clear de-bonding between the coated BVC reinforcement and concrete was observed. This observation validated the earlier results

obtained during the pull-out tests in section 6.1 in which the water-based epoxy coating (Moisture Seal) showed the highest bond strength among various coatings investigated.

The concrete crushing mode of failure is shown in Fig. 168. This mode of failure was caused by the high amount of compressive stresses at the distance between the load introduction points.

Fig. 168 Concrete crushing mode of failure

A large horizontal crack developed between the two top metal rollers during the test and it further widened until the final failure occurred. Furthermore, the concrete crushing was accompanied by the tensile rupture of the BVC reinforcement at the tension face of the beam as shown in Fig. 168. All the 3 modes of failure observed in this study, including the shear failure, BVC rupture, and the crushing of the concrete beam, were brittle failure modes in comparison with steel reinforced concrete beam in which the yielding behavior of steel reinforcement allowed for a ductile failure of reinforced concrete beam which was not sudden or brittle. However, in the case of BVC materials, due to the linear elastic behavior of reinforcement, the failure modes were rather sudden and brittle.

The ACI 440.1R approach towards the design of the FRP reinforcement for structural concrete is to ensure that adequate amount of tensile reinforcement is provided in the member such that concrete crushing mode of failure occurs before BVC rupture or shear failure of the

stirrups. According to ACI 440.1R, this approach prevents the sudden and catastrophic failure of the concrete beam by allowing warning signs through concrete crushing before the final failure occurs through the rupture of the BVC reinforcement. Fig. 169 shows the load-displacement curve of a typical concrete beam failure initiated by concrete crushing and followed by the BVC rupture mode of failure of BVC reinforced concrete beam tested in this section. The force shown in Fig. 169 is the load reading obtained from UTM software (P). The critical points are marked in Fig. 169.
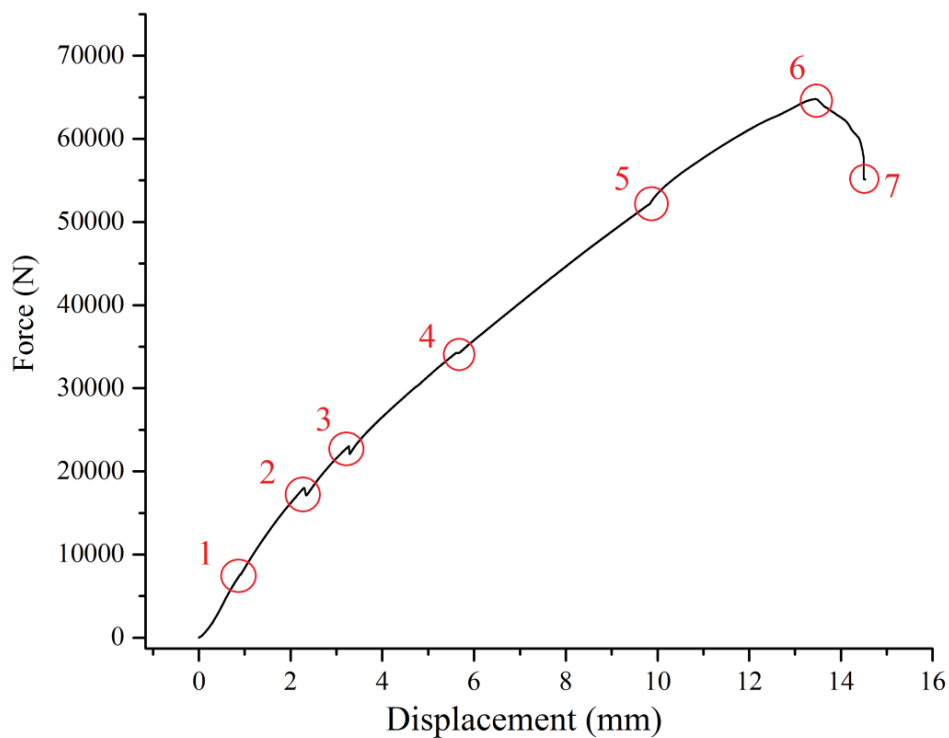
Fig. 169 Load-displacement curve for BVC reinforced concrete beam with concrete crushing mode of failure

Point 1 corresponds to the initial cracks observed within the BVC reinforced concrete beam. The loading recorded at this point is associated with the initial cracking load described in Table 45. Point 2, point 3, and point 4 correlate to the subsequent cracks, either shear or flexural cracks, which start to propagate across the tension face of the concrete beam. Point 5 corresponds to the widening process of the existing flexural cracks, followed by the crushing of the concrete at the compression face of the beam at point 6. As can be seen from point 1 to point 6, the slope of the curve is constantly reducing which indicates the decline in overall stiffness of the BVC reinforced concrete beam. Furthermore, the curve shows a linear elastic behavior between the various points highlighted in Fig. 169, until the final rupture of the BVC reinforcement occurs at point 7. Between the crushing of the concrete in compression

face of the beam and the rupture of BVC reinforcement at point 7, the BVC reinforced concrete beam has undergone further deformation before the final failure. This observation, interestingly enough, is in accordance with the design approach stated in ACI 440.1R, where the initial crushing of concrete in compression face of the beam is preferred over the BVC rupture as the mode of failure, to permit sufficient warning signs to the occupants of a concrete building reinforced with BVC or FRP reinforcement, rather than a brittle and sudden failure which is not desirable. Fig, 170 presents the load displacement curve for the BVC rupture mode of failure in which a sudden and abrupt failure occurred during the test.
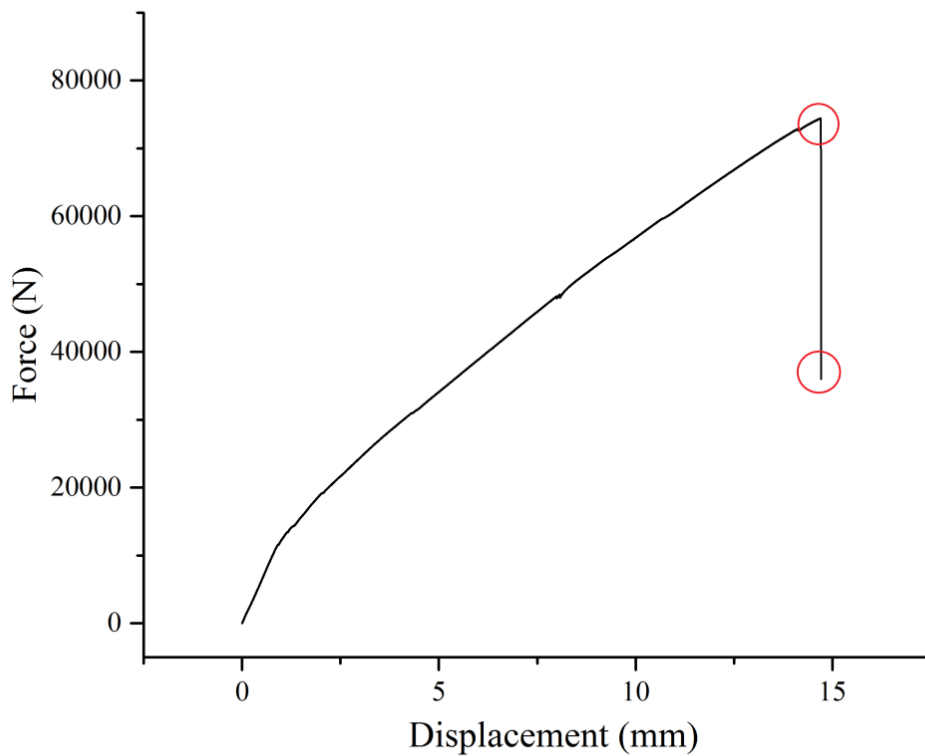
Fig. 170 Load-displacement curve for BVC reinforced concrete beam with BVC rupture mode of failure

The points highlighted in Fig. 170 show the moment when the BVC reinforced concrete beam fails due to the rupture of the BVC reinforcement at the tension face of the beam. As can be seen in Fig. 170, there was no gap between the BVC rupture and the final failure of the beam. The reinforced concrete beam was not able to deform further after the rupture of its tensile reinforcements, and thus no warning signs would be available to the occupants of concrete buildings reinforced with such BVC reinforcement which fail due to the rupture of the BVC reinforcement rather than concrete crushing.

However, in both cases, large deflections were observed during the tests and up to the ultimate failure condition. The largest deflection was observed for the B4b2 beam series for which a maximum average deflection of 15.2mm was recorded for the condition where 2 BVC reinforcements were employed at the bottom of the concrete cross section and the BVC stirrups were used at a spacing of 75mm with a loading span of 600mm. It was observed that by increasing the amount of tensile reinforcements, the mid-span deflection decreased. Fig, 171 shows the maximum mid-span deflection of the various beam series tested in this study. In almost all the beam designs, the maximum mid-span deflection of beams with 4 BVC reinforcements at the tension face of the concrete beams was the lowest among the BVC reinforced concrete beams as highlighted in Fig. 171.
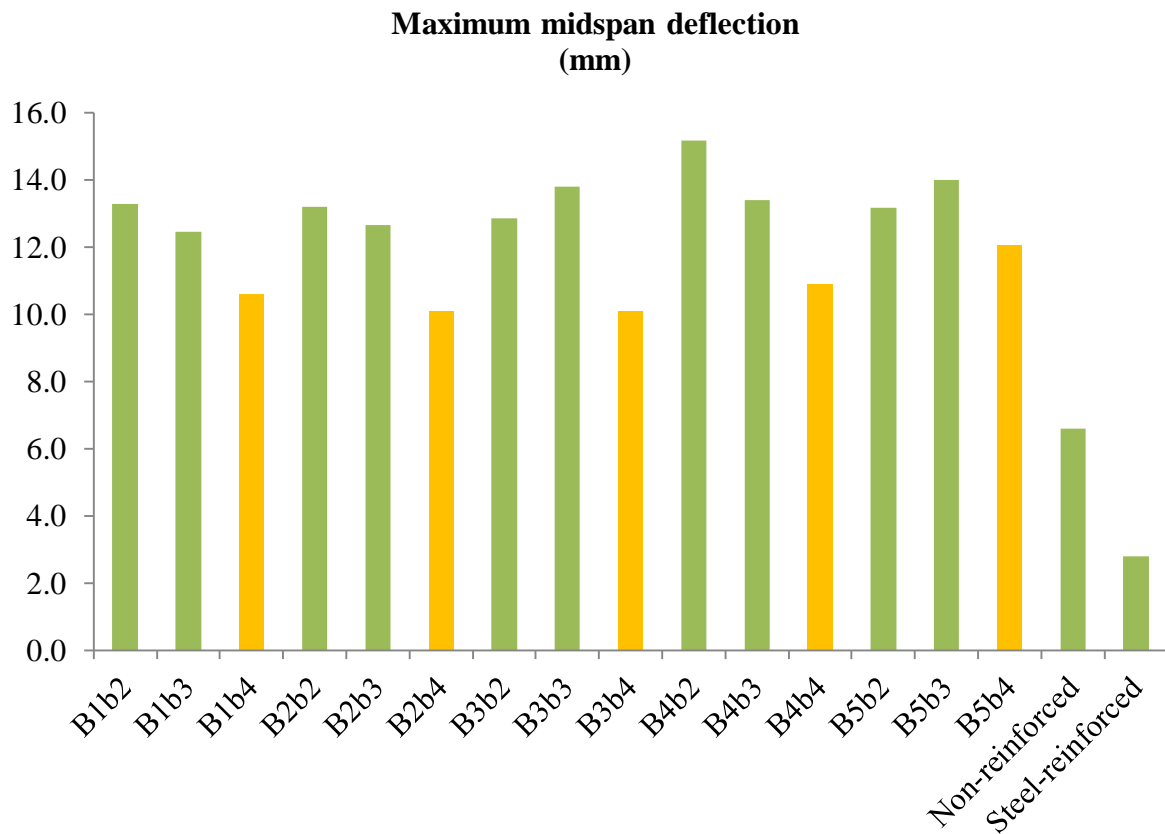
Fig. 171 Maximum mid-span deflection of various beams investigated in this study

However, the maximum mid-span deflection of the steel reinforced concrete beam specimens remained the lowest among all the beams tested in this section. Comparing the maximum average deflection of the BVC reinforced concrete beams at the ultimate failure load, larger deflections in the order of 3.6 to 5.4 times the maximum average deflection of the steel

reinforced concrete beams were observed. This could be explained by the lower stiffness of BVC reinforcement compared to steel reinforcement, as explained in section 5.4.3. As shown in Fig. 171, by increasing the number of BVC reinforcement from 2 to 3 at the bottom side of the concrete cross section while maintaining the stirrups spacing, a reduction of 9% to 28% in maximum mid-span deflection of BVC reinforced concrete beams was achieved.

The non-reinforced concrete beams' maximum mid-span deflection was compared to that of BVC reinforced concrete; it was found that the non-reinforced concrete beams had lower maximum mid-span deflection. However, the lower deflection was not caused by the stiffness characteristics of the beam, but was the result of the lower ultimate failure load obtained during the tests. Since the non-reinforced beam failed much earlier than BVC reinforced concrete beams at a lower ultimate failure load, lesser deformation was experienced during and after the test. As shown in Table 41, the ultimate failure load for non-reinforced concrete beam was only 10% of the maximum ultimate failure load observed within the concrete samples of the B5b4 beam series. Therefore, the BVC reinforcement was effective in improving the ultimate load capacity of the concrete beam, while enhancing the ductility of the beams by the addition of more reinforcement bars at the tension face of the concrete beam cross section. Nonetheless, due to lower elastic modulus, the BVC reinforced concrete beams showed higher deformations compared to steel reinforced concrete beam.

The results obtained in this section were based on the conditions defined at the beginning of the tests, including the size, number and spacing of the longitudinal and transverse (stirrups) reinforcements to accommodate the restrictions imposed by the available testing facilities at AFCL. To evaluate the results obtained in this section on the ultimate failure load and the maximum deflection as well as the mode of failure with respect to the recommendations and calculations specified in ACI 440.1R-15, a series of computations based on ACI 440.1R-15 were carried out to estimate the failure load, deflection and mode of failure. Subsequently comparisons were made with respect to the experimental results shown in Table 41, Table 46 and Fig. 169 to investigate the suitability of the ACI standard for the design and evaluation of concrete members reinforced with newly developed BVC reinforcement.

Calculations according to ACI 440.1R-15

As described earlier in section 6.5.2 and shown in Fig. 136 to Fig. 150, three main parameters were investigated in this section to evaluate their effects on the flexural and shear performance of the concrete beams reinforced with newly developed BVC reinforcement and

BVC stirrup. The three parameters were the number of longitudinal BVC reinforcement, the spacing of the BVC stirrups, and the distance between the load introduction points. In terms of flexural behavior, concrete beam samples from the B1b2, B2b2 and B3b3 series had similar theoretical cracking and ultimate failure load as well as similar maximum allowable deflection limits according to ACI 440.1R-15. Therefore, the beam series with similar flexural design calculations were grouped together according to Table 47. For each group, the design recommendations described in section 6.5.1 were closely followed and further explained in the following section.

Table 47 Beam series with similar design calculations according to ACI 440.1R-15

Group	Beam series
1	B1b2,B2b2,B3b2
2	B1b3,B2b3,B3b3
3	B1b4,B2b4,B3b4
4	B4b2,B5b2
5	B4b3,B5b3
6	B4b4,B5b4

Deign and calculation for the beams in Group 1

The beams in group 1 had two BVC bars as tension reinforcements at the bottom of the beams. Therefore the reinforcement ratio can be calculated according to Eq. 69 shown in section 6.5.1. The BVC reinforcement had a cross-section of 10×10mm and the concrete beam had a cross-section of 160×160mm. Therefore the reinforcement ratio can be calculated as follows:

$$\rho_f = \frac{A_f}{bd} = \frac{2 \times 10 \times 10}{160 \times 134} = 0.00932$$

Furthermore, the design tensile strength should be determined by Eq. 66. As mentioned in section 5.5.3, the average tensile strength (f^*_{fu}) of longitudinal BVC reinforcement was 408MPa and the average elastic modulus was 41,350MPa. These two values were used in the

following sections as the characteristic values of strength and stiffness of the longitudinal BVC reinforcement.

A strength reduction factor of 0.80 was used for Eq. 66. According to Table 42, a factor of 0.80 was the most conservative factor between all the values presented in this table; thus a conservative design value could be established as follows.

$$f_{fu} = C_E f_{fu}^* = 0.80 \times 408 = 326.4 \, MPa$$

In the next step, the reinforcement ratio of the beam should be checked versus the balanced reinforcement ratio defined by Eq. 70 to control the mode of failure.

$$\rho_{fb} = 0.85\beta_1 \frac{f_c'}{f_{fu}} \frac{E_f \varepsilon_{cu}}{E_f \varepsilon_{cu} + f_{fu}}$$

$$\rho_{fb} = 0.85 \, (0.85) \times \frac{20}{326.4} \times \frac{41350 \times 0.003}{41350 \times 0.003 + 326.4} = 0.0122$$

Given that $\rho_{fb} > \rho_f$, the reinforced concrete section is controlled by the FRP rupture limit states according to ACI 440.1R-15 which was discussed earlier in section 6.5.1. The nominal flexural strength could be found by Eq. 71. However, to compute the nominal flexural strength, the depth of Neutral Axis (N.A) shown in Fig. 130 has to be found according to Eq. 72. Furthermore, the distance from the extreme compression face of the cross-section to the centroid of the bottom reinforcement (d), as shown in Fig. 132, was calculated based on the concrete cover assumption made earlier.

$$d = 160 - 15(concrete\ cover) - 6(stirrup\ thickness\ ) - 5(center\ of\ longitudinal\ bar) = 134\ mm$$

Once d is known, the depth of N.A could be found according to Eq. 75 based on the assumptions made earlier regarding the strain of concrete and BVC reinforcement in section 6.5.1;

$$c_b = \left(\frac{\varepsilon_{cu}}{\varepsilon_{cu} + \varepsilon_{fu}}\right) d = 37\ mm, \text{ and subsequently the flexural strength is:}$$

$$M_n = A_f f_{fu} \left(d - \frac{\beta_1 c_b}{2}\right) = 2 \times 10 \times 10 \times 326.4 \left(134 - \frac{0.85 \times 37}{2}\right) \times 10^{-6} = 7.72 kN.m$$

Since $\rho_{fb} > \rho_f$, the strength reduction factor (Φ) for the group 1 beam series would be (0.55) according to Eq. 72. Therefore the design flexural strength of the member would be:

Φ M$_n$ = 0.55 (7.72) = 4.24 kN.m

Furthermore, the minimum required reinforcement area should be controlled by Eq. 77 as follows;

$$A_{f,min} = \frac{0.41\sqrt{f_c'}}{f_{fu}} b_w d \geq \frac{2.3}{f_{fu}} b_w d$$

$$A_{f,min} = \frac{0.41\sqrt{20}}{326.4} \times 160 \times 134 \geq \frac{2.3}{326.4} \times 160 \times 134$$

$$A_{f,min} = 151.1 \; mm^2$$

$$A_{f,provided} = 2 \times 10 \times 10 = 200 > 151.1 \; mm^2$$

Therefore the provided reinforcement area satisfied the minimum required reinforcement area. The nominal and design ultimate failure load can be found according to Fig. 134, where the maximum moment along the beam length would be ($\frac{Pa}{2}$) and the failure load could be computed accordingly.

$$M_n = \frac{Pa}{2} = \frac{P\,(0.35)}{2} = 7.72 \text{ kN.m} \; ;$$

$$\frac{P_n}{2} = 22.05 \text{ kN}$$

Similarly the design failure load could be calculated, which results in the following.

$$\Phi M_n = \frac{Pa}{2} = \frac{P\,(0.35)}{2} = 4.24 \text{ kN.m};$$

$$\Phi \frac{P_n}{2} = 12.12 \text{ kN}$$

In a separate section, both the design and ultimate failure loads would be compared with the results obtained from the tests carried out in this study. In the next step, the shear capacity of the beam should be controlled. As explained in section 6.5.1, the design shear strength (ΦV_n) should be larger than the factored shear force (V_u) at any section of the reinforced concrete beam. The shear capacity provided by the concrete itself can be calculated according to Eq. 86. However, before using Eq. 86, the parameter k needs to be evaluated using Eq. 82.

$$k = \sqrt{\left(2\rho_f n_f + \left(\rho_f n_f\right)^2\right)} - \rho_f n_f$$

$$n_f = \frac{E_f}{E_c} = \frac{41350}{25410} = 1.627$$

$$k = \sqrt{(2 \times 0.00932 \times 1.627 + (0.00932 \times 1.627)^2)} - 0.00932 \times 1.627 = 0.160$$

Once parameter k is found, Eq. 86 can be used to compute the concrete shear capacity as follows.

$$V_c = \frac{2}{5}\sqrt{f_c'}\,b_w(kd)$$

$$V_c = \frac{2}{5}\sqrt{20} \times 160(0.160 \times 134) = 6.14 \text{ kN, and}$$

$\Phi \text{Vc} = 0.75\,(5.63) = 4.60 \text{ kN}$

According to ACI 440.1R-15, if the applied shear forces (Vu) exceeds the $\frac{\Phi V_c}{2}$ then shear reinforcement is required. For the purpose of this study, it was assumed that the maximum shear forces applied on the beam during the test would be the ultimate design failure load ($\Phi\frac{P_n}{2}$) obtained in this section. This assumption was made in the absence of any external forces except the loading from the UTM. Furthermore, the calculations carried out based on ACI 440.1R were not meant to provide a design concept for the reinforced beam subjected to the loading applied by the UTM in the laboratory, but were performed to evaluate the shear capacity of the reinforced beam and to compare the design shear strength recommended by ACI standard with the shear capacity that was provided in reality by the beam during the test. Therefore in this section the following assumption was made:

Factored shear force (V_u) = $\Phi\frac{P_n}{2}$ = 12.12 kN

Since $V_u > \frac{\Phi V_c}{2} = 2.11$ kN, therefore shear reinforcement is required. The design tensile strength of the shear reinforcements (BVC stirrups) should be controlled by Eq. 88 and Eq. 89, and subsequently the required spacing (s) between the stirrups could be calculated using Eq. 90. The radius of the bent portion of BVC stirrups was 20mm while the thickness was 6mm. Therefore the ratio of $\frac{r_b}{d_b} = 3.33$ was used for all the BVC stirrups in this study. Eq. 89 was subsequently used to calculate the f_{fb}. The design tensile strength (f_{fu}) to be used in Eq. 89

should be calculated based on the tensile properties of BVC stirrups presented in Table 33, where a tensile strength of 371MPa and an elastic modulus of 38,101MPa were measured for the BVC stirrup samples. Thus Eq. 66 can be rewritten for the BVC stirrups as follows.

$f_{fu} = C_E f_{fu}^* = 0.80 \times 371 = 296.8$ MPa and the tensile strength of the bent portion would be calculated subsequently using Eq. 85 as follows.

$$f_{fb} = \left[0.05 \times \frac{r_b}{d_b} + 0.3\right] f_{fu} \leq f_{fu}$$

$f_{fb} = [0.05 \times 3.33 + 0.3] \times 296.8 \leq 296.8 = 138.5$ MPa

Substituting f_{fb} into Eq. 88, the design tensile strength of the BVC stirrups could be found as follows.

$f_{fv} = 0.004 E_f \leq f_{fb} = 0.004 \times 38101 \leq 138.5$ MPa $\rightarrow 152.4 \geq 138.5$ MPa,

Therefore the final value of f_{fv} would be 138.5MPa. Eq. 90 could be subsequently used to calculate the required spacing of the BVC stirrups, given the available area A_{fv} as shown below.

A_{fv}= 15 mm (width) × 6 mm (thickness) × 2 (legs) = 180 mm^2

$$\frac{A_{fv}}{s} = \frac{(V_u - \Phi V_c)}{\Phi f_{fv} d} \rightarrow \frac{180}{s} = \frac{(12.12 - 4.60)}{0.75 \times 138.5 \times 134} \rightarrow s = 333 \text{ mm}$$

Furthermore, ACI 440.1R-15 requires a minimum amount of shear reinforcements, according to Eq. 87 which can be used to calculate the maximum spacing of the stirrups permitted by this standard as explained here.

$$A_{fv,min} = 0.35 \frac{b_w s}{f_{fv}} \rightarrow s_{max} = \frac{A_{fv} \times f_{fv}}{0.35 b_w}$$

$s_{max} = \frac{180 \times 138.5}{0.35 \times 160} = 445$ mm

The ACI 440.1R-15 limits the maximum spacing of the vertical stirrups to the smaller of d/2 or 600mm, which, in the case of the beams tested in this study, $\frac{d}{2} = \frac{134}{2} = 67$mm. The required spacing (s) after calculating the three different scenarios would be 67mm for the BVC stirrups produced in this thesis, since this value was the most critical between the three

different spacing values obtained above. Therefore, by providing BVC stirrups at a spacing of not more than 67mm, no shear failure should be expected for beams in group 1.

The next step in establishing the necessary design requirements for the reinforced concrete beam would be evaluating the cracking load and the allowable deflection according to the ACI 440.1R-15 recommendations. The cracking load can be calculated based on Eq. 85 and Fig. 131. However, three parameters used in Eq. 85, including λ, I_g and y_t, need to be defined before computing the required cracking moment. I_g could be calculated using Eq. 70 as follows.

$$I_g = \frac{bh^3}{12} = \frac{160 \times 160^3}{12} = 54613333 \text{ mm}^4$$

$\lambda = 1.0$ for normal concrete

$$\gamma_t = \frac{160}{2} = 80 \text{ mm}$$

Therefore the cracking moment can be found:

$$M_{cr} = \frac{0.62\lambda\sqrt{f_c' I_g}}{y_t} = \frac{0.62 \times 1 \times \sqrt{20} \times 54613333}{80} \times 10^{-6} = 1.89 \text{ kN.m}$$

Therefore according to the statistical analysis given in Fig. 132,

$$\frac{P_{cr}}{2} \times a = M_{cr} \rightarrow \frac{P_{cr}}{2} \times 0.35 = 1.89 \rightarrow \frac{P_{cr}}{2} = 5.4 \text{ kN}$$

To compute the allowable deflection limits by ACI 440.1R-15, the applied moment (M_a) should be compared with cracking moment (M_{cr}). However, in the absence of applied moments as explained earlier with respect to the shear capacity of the beam, the design ultimate moment (ΦM_n) was used, which could result in a relatively more conservative deflection limits.

Since $M_a = \Phi M_n = 4.24$ kN.m $\geq M_{cr}$, therefore, in order to estimate the deflection limits of the reinforced concrete beam, the effective moment of inertia of the cracked section (I_e) should be used instead of the gross movement of inertia (I_g). Eq. 83 should be used to calculate the effective moment of inertia; before that, the cracked moment of inertia (I_{cr}) needs to be estimated using Eq. 81.

$$I_{cr} = \frac{bd^3}{3}k^3 + n_f A_f d^2 (1-k)^2; where \; k = 0.160, n_f = 1.627 \; and \; A_f = 200 \text{ mm}^2,$$

$$I_{cr} = \frac{160 \times 134^3}{3} \times 0.160^3 + (1.627)(200)(134)^2(1 - 0.160)^2 = 4648359 \text{ mm}^4$$

Following the calculation of I_{cr}, the parameter which accounted for the variation in stiffness along the length of the concrete member must be estimated according to Eq. 84, which subsequently could be used in Eq. 83 to estimate the effective moment of inertia (I_e).

$$\gamma = 1.72 - 0.72 \left(\frac{M_{cr}}{M_a}\right) = 1.72 - 0.72 \left(\frac{1.89}{4.24}\right) = 1.40$$

$$I_e = \frac{I_{cr}}{1 - \gamma\left(\frac{M_{cr}}{M_a}\right)^2\left[1 - \frac{I_{cr}}{I_g}\right]} = \frac{4648359}{1 - (1.40)\left(\frac{1.89}{4.24}\right)^2\left[1 - \frac{4648359}{54613333}\right]} = 6235219 \text{ mm}^4$$

Once the effective moment of inertia has been established, the following formulae could be used to estimate the deflection of a simply supported beam.

$$\Delta = \frac{5KM_aL^2}{48E_cI_e} \quad \text{(Eq. 93)}$$

Where K is a load factor corresponding to a value of 1.0 for simple beams and E_c is the concrete modulus of elasticity in compression. Substituting the values of each parameter into Eq. 93, the acceptable deflection limit of the BVC reinforced concrete beams belong to group 1 could be established.

$$\Delta = \frac{5KM_aL^2}{48E_cI_e} = \frac{5(1)(4.24)(1050)^2}{48(25410)(6235219)} \times 10^6 = 3.07 \text{ mm}$$

Therefore the maximum allowable deflection based on the design ultimate load would be 3.07mm for a BVC reinforced concrete beam with two tensile reinforcement bars.

Similar calculations were carried out in following sections for the other groups of beam series shown in Table 47.

Design and calculation for the beams in Group 2

The beams in group two had three BVC bars as the tensile reinforcements, thus the reinforcement ratio had changed but the balanced reinforcement ratio remained the same as for the beams in group one.

$$\rho_f = \frac{A_f}{bd} = \frac{3 \times 10 \times 10}{160 \times 134} = 0.0139$$

Given this, the failure of the section is therefore controlled by concrete crushing rather than tensile failure of the BVC reinforcement. The stress distribution in the concrete can be approximated by the ACI rectangular stress block shown in Fig. 130. Eq. 71 and Eq. 72 were used to estimate the nominal flexural strength of the beam.

$$f_f = \left[\sqrt{\frac{(E_f \varepsilon_{cu})^2}{4} + \frac{0.85 \beta_1 f_c'}{\rho_f} E_f \varepsilon_{cu}} - 0.5 E_f \varepsilon_{cu} \right] \leq f_{fu}$$

$$f_f = \left[\sqrt{\frac{(41350 \times 0.003)^2}{4} + \frac{0.85 \times 0.85 \times 20}{0.0139} \times 41350 \times 0.003} - 0.5 \times 41350 \times 0.003 \right] \leq 326.4$$

$$f_f = 302.4 \leq 326.4 \rightarrow f_f = 302.4 \text{ MPa}$$

Therefore the nominal flexural moment can be found below.

$$M_n = (0.0139)(302.4) \left[1 - 0.59 \frac{0.0139 \times 302.4}{20} \right] 160 \times 134^2 \times 10^{-6} = 10.58 \text{ kN.m}$$

The design flexural moment should be found by obtaining the strength reduction factor from Eq. 76 and subsequently multiplied by the nominal flexural moment, as described in the following calculations.

$$\frac{\rho_f}{\rho_{fb}} = \frac{0.0139}{0.0122} = 1.139 < 1.4 \rho_{fb} \rightarrow \varPhi = 0.3 + 0.25 \times 1.1.139 = 0.58$$

$$\varPhi M_n = 0.58 \times 10.58 = 6.19 \text{ kN.m}$$

Therefore the nominal and design ultimate failure loads could be obtained as below.

$$\text{M}_n = \frac{Pa}{2} = \frac{P(0.35)}{2} = 10.58 \text{ kN.m} ; \rightarrow \frac{P_n}{2} = 30.22 \text{ kN}$$

$$\varPhi \text{M}_n = \frac{Pa}{2} = \frac{P(0.35)}{2} = 6.19 \text{ kN.m}; \rightarrow \varPhi \frac{P_n}{2} = 17.68 \text{ kN}$$

The shear capacity provided by the concrete itself could be calculated according to Eq. 86, similar to group 1 beam series, but with a different parameter k since the reinforcement ratio had changed.

$$k = \sqrt{\left(2\rho_f n_f + (\rho_f n_f)^2 \right)} - \rho_f n_f$$

$$k = \sqrt{(2 \times 0.0139 \times 1.627 + (0.0139 \times 1.627)^2)} - 0.0139 \times 1.627 = 0.191$$

Therefore concrete shear capacity can be found below.

$$V_c = \frac{2}{5}\sqrt{f_c'}\,b_w(kd) = \frac{2}{5}\sqrt{20} \times 160\,(0.191 \times 134) = 7.32 \text{ kN, and}$$

$\Phi V_c = 0.75\,(7.32) = 5.49$ kN

To estimate the required spacing (s) of the BVC stirrups, similar assumptions were made regarding the applied shear forces on the beam where V_u was assumed to correspond to the ultimate design failure load.

Factored shear force $(V_u) = \Phi\frac{P_n}{2} = 17.68$ kN

Since $V_u > \frac{\Phi V_c}{2} = 2.75$ kN, therefore shear reinforcement is required.

However, there is no change in the design tensile strength of the BVC stirrups in which MPa, and the spacing of the BVC stirrups could be found below;

$$\frac{A_{fv}}{s} = \frac{(V_u - \Phi V_c)}{\Phi f_{fv}d} \rightarrow \frac{180}{s} = \frac{(17.68 - 5.49)}{0.75 \times 138.5 \times 134} \rightarrow s = 205 \text{ mm}$$

And the maximum spacing of the stirrups was found according to Eq. 91;

$$S_{max} = \frac{A_{fv} \times f_{fv}}{0.35b_w} = \frac{180 \times 138.5}{0.35 \times 160} = 445 \text{ mm}$$

While ACI 440.1R-15 limits the maximum spacing of vertical stirrups to the smaller of d/2 or 600mm;

$$\frac{d}{2} = \frac{134}{2} = 67 \text{ mm}$$

Therefore the required spacing (s) would be the most critical value obtained in this section, which is 67mm.

The cracking load and the maximum acceptable deflection limit could be computed, similar to how it was done for the group 1 beam series. The cracking moment (M_{cr}) did not change compared to the group 1 beam series, since the beam cross section remained the same. Therefore the cracking load ($\frac{P_{cr}}{2}$) remained at 5.4kN. It was assumed that the applied moment (M_a) corresponds to ΦM_n and since $M_a = \Phi M_n = 6.19$kN.m $\geq M_{cr}$=1.89kN, therefore the

effective moment of inertia of the cracked section (I_e) should be used, instead of the gross movement of inertia (I_g), to calculate the deflection limit. The cracked moment of inertia (I_{cr}) has to be first estimated using Eq. 81.

$$I_{cr} = \frac{bd^3}{3}k^3 + n_f A_f d^2 (1-k)^2; where\ k = 0.191, n_f = 1.627\ and\ A_f = 300\ \text{mm}^2,$$

$$I_{cr} = \frac{160 \times 134^3}{3} \times 0.191^3 + (1.627)(300)(134)^2(1-0.191)^2 = 6630239\ \text{mm}^4$$

The parameter which accounted for the variation in stiffness along the length of the concrete member could be estimated according to Eq. 84.

$$\gamma = 1.72 - 0.72\left(\frac{M_{cr}}{M_a}\right) = 1.72 - 0.72\left(\frac{1.89}{6.19}\right) = 1.50$$

The effective moment of inertia was found afterwards.

$$I_e = \frac{I_{cr}}{1-\gamma\left(\frac{M_{cr}}{M_a}\right)^2\left[1-\frac{I_{cr}}{I_g}\right]} = \frac{6630239}{1-(1.50)\left(\frac{1.89}{6.19}\right)^2\left[1-\frac{6630239}{54613333}\right]} = 7558959\ \text{mm}^4$$

Thus the deflection could be estimated according to Eq. 93.

$$\Delta = \frac{5KM_aL^2}{48E_cI_e} = \frac{5(1)(6.19)(1050)^2}{48(25410)(7558959)} \times 10^6 = 3.70\ \text{mm}$$

Design and calculation for the beams in Group 3

The main difference between the beams in group 2 and 3 is the number of tensile reinforcements. The beams in group 3 had four BVC bars as the tensile reinforcements; the reinforcement ration could be found below while the balanced reinforcement ratio remained the same as the beams in groups 1 and 2.

$$\rho_f = \frac{A_f}{bd} = \frac{4 \times 10 \times 10}{160 \times 134} = 0.0186$$

Given that $\rho_{fb} < \rho_f$, therefore the failure of the section was controlled by concrete crushing rather than tensile failure of the BVC reinforcement, similar to beams in group 2 as explained in the previous section. Therefore the ACI rectangular stress block shown in Fig. 131 could be used to estimate the stress and strain in the section. Eq. 71 and Eq. 72 should be used to evaluate the nominal flexural strength of the beams with three tensile reinforcements.

$$f_f = \left[\sqrt{\frac{\left(E_f \varepsilon_{cu}\right)^2}{4} + \frac{0.85\beta_1 f_c'}{\rho_f}} E_f \varepsilon_{cu} - 0.5 E_f \varepsilon_{cu} \right] \le f_{fu}$$

$$f_f = \left[\sqrt{\frac{(41350 \times 0.003)^2}{4} + \frac{0.85 \times 0.85 \times 20}{0.0186}} \times 41350 \times 0.003 - 0.5 \times 41350 \times 0.003 \right] \le 326.4$$

$$f_f = 225 \le 326.4 \rightarrow f_f = 255 \text{ MPa}$$

Therefore the nominal flexural moment can be found below.

$$M_n = (0.0186)(255)\left[1 - 0.59 \frac{0.0186 \times 255}{20}\right] 160 \times 134^2 \times 10^{-6} = 11.71 \text{ kN.m}$$

The design flexural moment should be found by obtaining the strength reduction factor from Eq. 76 and subsequently multiplied by the nominal flexural moment, as described in the following calculations.

$$\frac{\rho_f}{\rho_{fb}} = \frac{0.0186}{0.0122} = 1.524 > 1.4\rho_{fb} \rightarrow \Phi = 0.65$$

$$\Phi M_n = 0.65 \times 11.71 = 7.61 \text{ kN.m}$$

Therefore the nominal and design ultimate failure loads could be obtained as below.

$$M_n = \frac{Pa}{2} = \frac{P(0.35)}{2} = 11.71 \text{ kN.m} ; \rightarrow \frac{P_n}{2} = 33.46 \text{ kN}$$

$$\Phi M_n = \frac{Pa}{2} = \frac{P(0.35)}{2} = 7.61 \text{ kN.m}; \rightarrow \Phi\frac{P_n}{2} = 21.74 \text{ kN}$$

The shear capacity provided by the concrete itself could be calculated according to Eq. 86 similar to the group 2 beam series, but with a different parameter k as shown in the calculations below.

$$k = \sqrt{\left(2\rho_f n_f + \left(\rho_f n_f\right)^2\right)} - \rho_f n_f$$

$$k = \sqrt{(2 \times 0.0186 \times 1.627 + (0.0186 \times 1.627)^2)} - 0.0186 \times 1.627 = 0.217$$

Finally the concrete shear capacity was found as follows.

$$V_c = \frac{2}{5}\sqrt{f_c'}b_w(kd) = \frac{2}{5}\sqrt{20} \times 160(0.217 \times 134) = 8.32 \text{ kN, and}$$

ΦVc = 0.75 (7.32) = 6.24 kN

The required spacing (s) of the BVC stirrups was estimated by assuming that the applied shear forces on the beam (V_u) was corresponding to the ultimate design failure load.

Factored shear force (V_u) = $\Phi \frac{P_n}{2}$ = 21.74 kN

Since $V_u > \frac{\Phi V_c}{2}$ = 3.12 kN, therefore shear reinforcement was required.

However there was no change in the design tensile strength of the BVC stirrups where f_{fv} = 138.5 MPa, and the spacing of the BVC stirrups could be found below while the area of BVC stirrups was 180mm;

$$\frac{A_{fv}}{s} = \frac{(V_u - \Phi V_c)}{\Phi f_{fv} d} \rightarrow \frac{180}{s} = \frac{(21.74 - 6.24)}{0.75 \times 138.5 \times 134} \rightarrow s = 161 \text{ mm}$$

And the maximum spacing of the stirrups was found according to Eq. 91.

$$S_{max} = \frac{A_{fv} \times f_{fv}}{0.35 b_w} = \frac{180 \times 138.5}{0.35 \times 160} = 445 \text{ mm}$$

While ACI 440.1R-15 limits the maximum spacing of vertical stirrups to the smaller of d/2 or 600mm;

$$\frac{d}{2} = \frac{134}{2} = 67 \text{ mm}$$

Therefore the required spacing (s) would be the most critical values obtained in this section which is 67mm.

The cracking moment (M_{cr}) remained the same as the group 1 and 2 beam series. Thus the cracking load ($\frac{P_{cr}}{2}$) would be 5.4kN. It was assumed that the applied moment (M_a) corresponds to ΦM_n and since $M_a = \Phi M_n$ = 7.61kN.m $\geq M_{cr}$=1.89kN, therefore the effective moment of inertia of the cracked section (I_e) should be used, instead of the gross movement of inertia (I_g), to calculate the deflection limit. The cracked moment of inertia (I_{cr}) was first estimated using Eq. 81.

$$I_{cr} = \frac{bd^3}{3} k^3 + n_f A_f d^2 (1 - k)^2; where\ k = 0.217, n_f = 1.627\ and\ A_f = 400 \text{mm}^2,$$

$$I_{cr} = \frac{160 \times 134^3}{3} \times 0.217^3 + (1.627)(400)(134)^2(1 - 0.217)^2 = 847,5684 \text{mm}^4$$

354

The parameter γ which accounted for the variation in stiffness along the length of the concrete member could be estimated according to Eq. 84.

$$\gamma = 1.72 - 0.72\left(\frac{M_{cr}}{M_a}\right) = 1.72 - 0.72\left(\frac{1.89}{7.61}\right) = 1.54$$

The effective moment of inertia was found by substituting the calculated parameters into Eq. 83.

$$I_e = \frac{I_{cr}}{1 - \gamma\left(\frac{M_{cr}}{M_a}\right)^2\left[1 - \frac{I_{cr}}{I_g}\right]} = \frac{8475684}{1 - (1.54)\left(\frac{1.89}{7.61}\right)^2\left[1 - \frac{8475684}{54613333}\right]} = 9{,}215{,}179 \text{ mm}^4$$

Finally the acceptable deflection limit could be estimated according to Eq. 89.

$$\Delta = \frac{5KM_aL^2}{48E_cI_e} = \frac{5(1)(7.61)(1050)^2}{48(25410)(9215179)} \times 10^6 = 3.73 \text{ mm}$$

Design and calculation for the beams in Group 4

The main difference between the beams from group 4 and group 1 was the distance between load introduction points. All other parameters, including the beam cross section, size and number of reinforcements at the tension face of the concrete beam, remained the same. Thus the flexural moment of the beams in group 1 and group 3 was the same. Therefore the flexural moment calculated for the group 1 beam series would be used to estimate the design and nominal ultimate failure loads according to the following calculations. In this case, only parameter (a) had changed from 350mm for the group 1 to 3 beam series to 600mm for the group 4 to 6 beam series.

$$M_n = \frac{Pa}{2} = \frac{P\,(0.60)}{2} = 7.72 \text{ kN.m} \; ;$$

$$\frac{P_n}{2} = 12.87 \text{ kN}$$

Similarly the design failure load could be calculated which resulted in the following.

$$\Phi M_n = \frac{Pa}{2} = \frac{P\,(0.60)}{2} = 4.24 \text{ kN.m};$$

$$\Phi\frac{P_n}{2} = 7.06 \text{ kN}$$

The shear design of the beams would be similar to the group 1 beam series, since both groups have similar numbers of tensile reinforcements and the distance between the load

introduction points would not affect the design process. Therefore a spacing (s) of 67mm for BVC stirrups should be implemented, based on the shear design calculations for group 4 beam series. Similarly, the cracking moment calculated for group 1 would be used to estimate the cracking load of group 4 beam series.

$$\frac{P_{cr}}{2} \times a = M_{cr} \rightarrow \frac{P_{cr}}{2} \times 0.60 = 1.89 \rightarrow \frac{P_{cr}}{2} = 3.15 \text{ kN}$$

The deflection limit given by Eq. 93 would be similar to group 1 beam series since all the parameters in Eq. 83 remained the same.

$$\Delta = \frac{5 K M_a L^2}{48 E_c I_e} = 3.07 \text{ mm}$$

Design and calculation for the beams in Group 5

The beams in group 5 had three BVC bars as the tensile reinforcements, therefore the nominal and design flexural capacity would remain the same as the beams in group 2. In this case, the section is designed according to the concrete crushing mode of failure, given the higher ratio of BVC reinforcement compared to the balanced reinforcement ratio. The only difference between the group 2 and group 5 beam series was the distance between load introduction points which only affected the ultimate and design ultimate failure load as well as the cracking load. The nominal and design ultimate failure loads were found according to calculations as follows.

$$M_n = \frac{Pa}{2} = \frac{P\,(0.60)}{2} = 10.58 \text{ kN.m} \; ; \rightarrow \frac{P_n}{2} = 17.63 \text{ kN}$$

$$\Phi M_n = \frac{Pa}{2} = \frac{P\,(0.35)}{2} = 6.19 \text{ kN.m}; \rightarrow \Phi\frac{P_n}{2} = 10.31 \text{ kN}$$

The shear capacity and shear design calculation would remain the same as the group 2 beam series, therefore a spacing (s) of 67mm between the BVC stirrups is recommended for the group 5 beam series. The cracking load and the maximum acceptable deflection limit could be computed, similar to the group 4 beam series, given there were no changes in the parameters used for the calculation of both cracking load and deflection limit.

$$\frac{P_{cr}}{2} = 3.15 \text{ kN}$$

$$\Delta = \frac{5 K M_a L^2}{48 E_c I_e} = 3.70 \text{ mm}$$

The beams in group 6 had four BVC reinforcements similar to the beams from group 3; however, the distance between the load introduction points increased from 350mm to 600mm in the case of the group 6 beam series. Since both groups had similar reinforcement ratios, the failure of the concrete beam was controlled by concrete crushing rather than tensile failure of the BVC reinforcement. The nominal and design ultimate failure loads could be calculated, similar to the group 3 beam series.

$$M_n = \frac{Pa}{2} = \frac{P\,(0.60)}{2} = 11.71 \text{ kN.m} ; \rightarrow \frac{P_n}{2} = 19.51 \text{ kN}$$

$$\Phi M_n = \frac{Pa}{2} = \frac{P\,(0.60)}{2} = 7.61 \text{ kN.m}; \rightarrow \Phi\frac{P_n}{2} = 12.68 \text{ kN}$$

The spacing (s) between the BVC stirrups would remain the same as the beams from group 3, where a spacing of 67mm was recommended by ACI 440.1R-15. The cracking load would be similar to the group 5 beam series, since both groups have a similar distance of 600mm between the load introduction points and the same cross-sectional dimensions. The deflection limit would be the same as the group 3 beam series where similar parameters were used to calculate the deflection according to Eq. 93.

$$\frac{P_{cr}}{2} = 3.15 \text{ kN}$$

$$\Delta = \frac{5KM_aL^2}{48E_cI_e} = 3.73 \text{ mm}$$

Discussion

In the previous sections, the experimental results were presented, and design recommendations given in ACI 440.1R-15 for the application of FRP reinforcement in structural concrete were reviewed with respect to the properties of the newly developed BVC reinforcement. Up to now, no research has been carried out on the suitability of this relatively new standard for the application of BVC material as reinforcement for structural concrete. Therefore, comparisons between the results obtained during the tests for cracking load, failure load, maximum deflection, modes of failure and the shear performance of BVC reinforced concrete beams were made with regard to the values obtained through analysis according to ACI 440.1R-15 in this section.

Table 48 shows the comparison of the cracking loads, nominal and design ultimate failure loads as well as maximum mid-span deflection between the values measured during the test series and design values obtained according to ACI 440.1R-15 standard recommendations. The values presented for the experimental results were the average values obtained for each beam series shown in Table 45.

Table 48 Comparison between ACI 440.1R-15 design values and experimental results obtained in this study

Beam Design	ACI 440.1R	Experiment	ACI 440.1R	Experiment	Experiment	ACI 440.1R	Experiment
	Design cracking load (P/2) (kN)	Initial cracking load (P/2) (kN)	Nominal Ultimate failure load (P/2) (kN)	Design Ultimate failure load (P/2) (kN)	Ultimate failure load (P/2) (kN)	Maximum midspan deflection (mm)	Maximum midspan deflection (mm)
B1b2	5.40	11.6	22.05	12.12	33.4	3.07	13.3
B1b3	5.40	13.7	30.22	17.68	37.7	3.70	12.5
B1b4	5.40	15.9	33.46	21.74	43.3	3.73	10.6
B2b2	5.40	11.7	22.05	12.12	32.7	3.07	13.2
B2b3	5.40	13.8	30.22	17.68	37.9	3.70	12.7
B2b4	5.40	16.0	33.46	21.74	43.6	3.73	10.1
B3b2	5.40	10.2	22.05	12.12	25.0	3.07	12.9
B3b3	5.40	9.8	30.22	17.68	33.9	3.70	13.8
B3b4	5.40	17.2	33.46	21.74	44.9	3.73	10.1
B4b2	3.15	9.2	12.87	7.06	34.1	3.07	15.2
B4b3	3.15	10.6	17.63	10.31	39.9	3.70	13.4
B4b4	3.15	14.4	19.51	12.68	50.4	3.73	10.9
B5b2	3.15	9.2	12.87	7.06	32.2	3.07	13.2
B5b3	3.15	11.2	17.63	10.31	42.0	3.70	14.0
B5b4	3.15	15.5	19.51	12.68	54.7	3.73	12.0

As shown in Table 48, the BVC reinforcement showed better initial cracking load and much higher ultimate load-bearing capacity compared to the design values obtained through calculations according to ACI 440.1R-15. The estimated design cracking loads based on ACI 440.1R-15 were lower than the values obtained by testing the BVC reinforced concrete beams. The cracking loads measured during the four-point flexural test of the BVC reinforced concrete beams on average was 2 to 5 times larger than the design values of the ACI 440.1R-15 standard, confirming the superior performance of the BVC reinforcement in comparison to the estimates according to the ACI standard.

Fig. 172 shows the variations in cracking loads obtained through the tests and cracking load estimates based on ACI 440.1R-15. It was clear that the ACI design guide was conservative in the design of the BVC reinforced concrete beam in comparison to the FRP reinforcement. As shown in Table 48, the BVC reinforced concrete beams with similar load introduction points (B1b2 to B3b4) showed similar design cracking loads estimated based on the recommendations of ACI 440.1R-15.
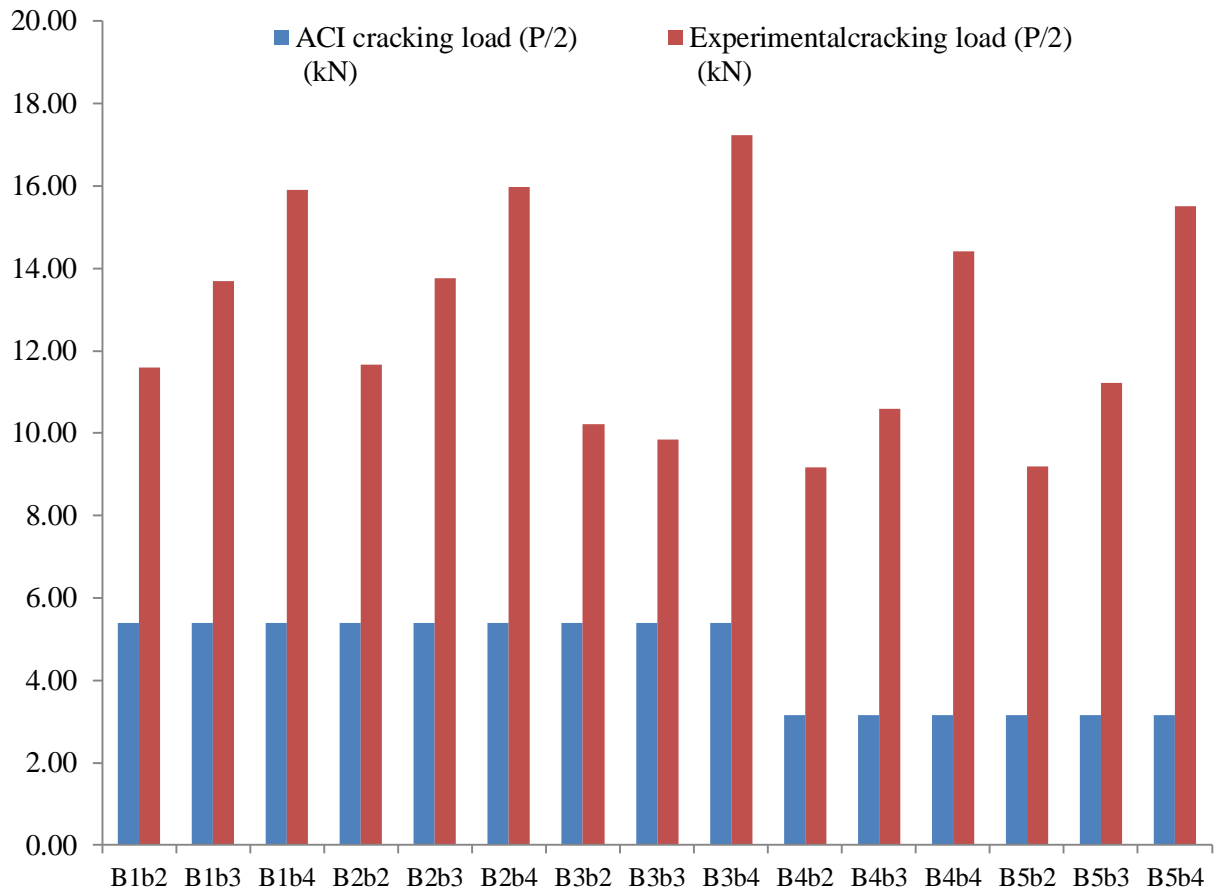
Fig. 172 Comparison of the cracking loads obtained through lab tests with the design cracking loads obtained based on ACI 440.1R-15 standard recommendations

As shown in the previous sections, the cracking moment (M_{cr}) and cracking load estimated by ACI 440.1R-15 were based purely on the cross-sectional dimensions (width and height) of the beam and concrete properties, rather than on the properties of the tensile reinforcements and stirrups employed in the section. Therefore, the contribution of the BVC reinforcement in enhancing the stiffness of the cross section of the beam was not thoroughly taken into account in the design of the reinforced concrete beams based on the ACI guidelines.

Furthermore, cracking loads obtained according to ACI standard recommendations were the acceptable cracking limits rather than the maximum available limits. These design values

indicated that the beams reinforced with FRP/BVC reinforcement should not crack beyond these limits found through the analysis. In the case of the BVC reinforced concrete beam tested in this section, the cracking loads obtained through the four-point flexural tests were relatively higher than the ACI cracking load limits. This finding could point to the importance of the safety factors and strength reduction factors in the design and evaluation of FRP/BVC reinforced concrete beams which were considered by the ACI standard.

The safety factors and strength reduction factors could allow the engineer to include unknown variations in the material's properties, including tensile and flexural strength. In the case of BVC reinforcement where a natural-based (bamboo) composite material was employed as the main load-bearing element, the safety factors and strength reduction factors should also be incorporated in the design, similar to the recommendation given in ACI 440.1R-15 for FRP reinforcement. As shown in this section, the safety margin for the cracking loads ranged from 20% to 55% for BVC reinforcement, which was in accordance with the main philosophy behind the safety factors and strength reduction factors imposed by the ACI design guide for the application of FRP reinforcement in concrete.

The results obtained by the flexural tests of BVC reinforced concrete beams proposed that new safety factors and strength reduction factors be employed for BVC reinforcement compared with FRP reinforcement, since higher values were obtained for the cracking load limits for BVC reinforced concrete beams compared to the ACI design values for FRP reinforced concrete beams. This could save construction costs by allowing the application of BVC reinforcement of smaller sizes for higher load-bearing applications. Further research in this area should be carried out to establish appropriate design guidelines for the application of newly developed BVC reinforcement in structural concrete; this will be discussed in a future work chapter in this thesis.

Fig. 173 compares the measured failure loads by the flexural tests versus nominal as well as design failure loads obtained by the analysis carried out according to the ACI 440.1R-15 standard. The ultimate failure loads increased via the addition of more reinforcements at the tension face of the concrete beam. Both experimental and the ACI results consistently validated this observation, as shown in Fig. 173. The experimental ultimate failure loads improved more by the addition of tensile reinforcements, in comparison to the design and nominal ultimate failure loads obtained according to ACI 440.1R-15 recommendations.

When the experimental failure loads were compared to the estimated nominal failure loads based on the ACI standard, a safety margin of 2 to 3 was observed. This was similar to the patterns observed for cracking loads when the measured values during the tests were 2 to 5 times higher than the calculated values of the loads according to ACI recommendations. Therefore the BVC reinforcement performed significantly better than the expected ultimate failure load limits estimated according to the ACI standard. BVC reinforced concrete beams showed higher ultimate load-bearing capacity when tested under flexural four-point tests, when the results were compared to the respective values of the ACI standard for the FRP reinforced concrete beams.

Once the strength reduction factors were employed to estimate the design ultimate failure loads, a reduction in the ultimate failure loads was observed according to the ACI recommendations. The actual failure loads measured through the four-point flexural tests ranged between 2 to 8 times the design ultimate failure loads. This showed the higher reserve of strength that BVC reinforcement had to offer in comparison to the FRP reinforcement. The BVC reinforcement showed ultimate failure loads which were higher than the estimated values based on the ACI standard.

Another important observation made was the effect of increasing the distance between the load introduction points from 350mm (for group 1 to 3 beam samples) to 600mm (for group 4 to 6 beam samples). Both the nominal and design failure loads obtained, based on the ACI standard, were largely reduced, while the experimental failure loads did not show a significant reduction via increasing the distance between the load introduction points. The reason for such behavior could be explained largely by the conservative design approach of ACI 440.1R-15. The BVC reinforcement showed higher than expected load-bearing capacity in comparison to the load bearing capacity estimated based on the design recommendations of ACI 440.1R-15. The ACI standard did not take into account the differences in material characteristics between the FRP reinforcement and BVC reinforcement.

Furthermore, when the distance between the load introductions points were increased from 350mm to 600mm, the reserve flexural capacity of the BVC reinforcement was activated, developing a balance stress transfer from the concrete matrix to the BVC reinforcement within the beam. This reserve strength could have been largely effective in maintaining the overall load-bearing capacity of the BVC reinforced concrete beams in comparison to the FRP reinforced concrete beams designed according to the ACI guidelines.
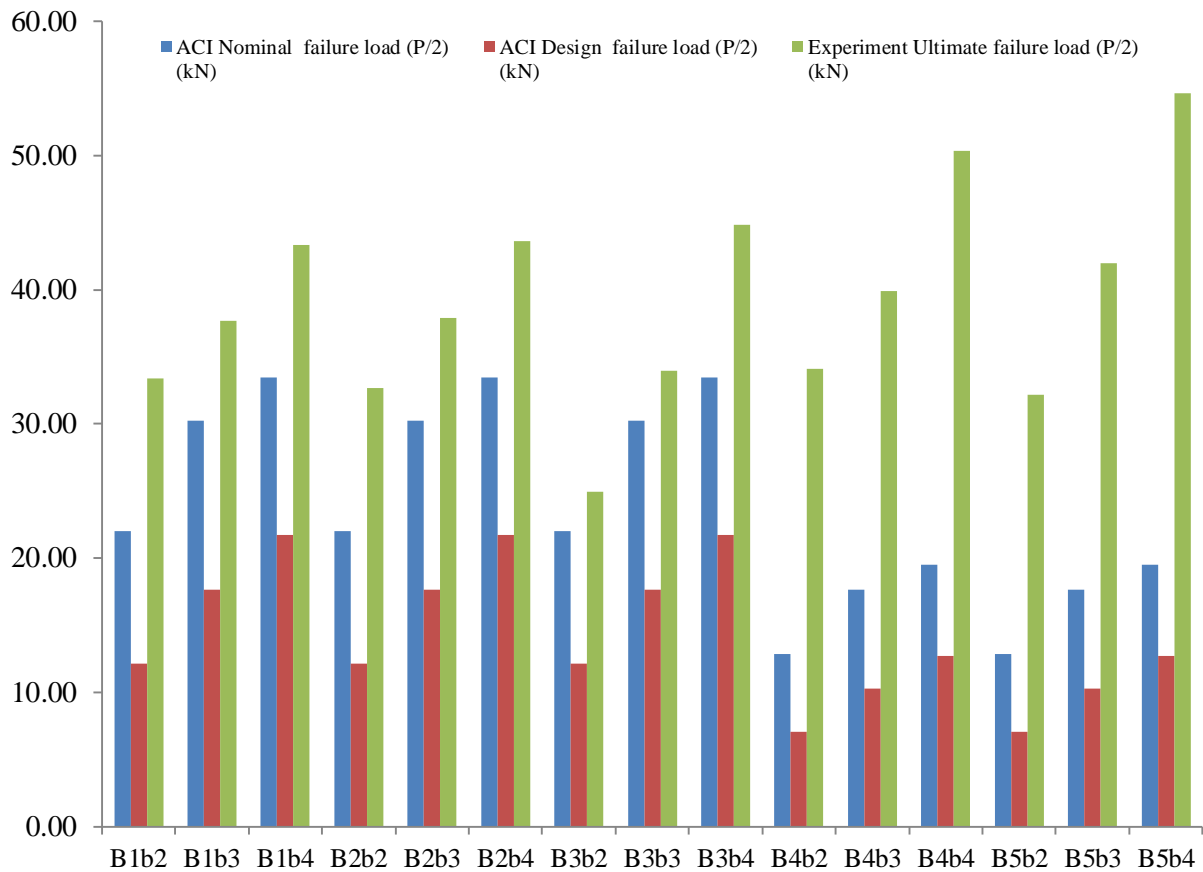
Furthermore, as explained earlier, the ACI design guide showed lower design values when it came to the ultimate flexural capacity of the reinforced concrete beams, reinforced with polymer composite materials, for safety reasons. The larger uncertainties and unknown variations that existed in the FRP or BVC materials in comparison to steel reinforcement could have led to the higher margin of safety taken into account by the ACI standard for ultimate load bearing capacity of the beams in comparison to steel reinforced concrete beams.

Steel as a metal is considered a homogenous and isotropic material with similar physical and mechanical properties in all directions and at any sections within the entire length of the reinforcement. As explained in the previous chapters, bamboo veneer composite materials produced in this study showed some slight variations in the measured mechanical properties, which were mainly the results of the variations in the properties of the natural bamboo culms employed during the production process.

Bamboo as a natural material is a non-homogenous material. It has different properties in various sections along the length and diameter of the culm, and these properties can vary between culms of the same species. Therefore, these natural variations in properties of the

raw bamboo fibers contribute to the overall fluctuations in properties of the final BVC reinforcement. Although the processing and fabrication methods developed within this study successfully reduced such variations to a large extent, some slight variations still remained after the production of the final BVC reinforcement.

Since the hypothesis of this research was to demonstrate that "it is possible to develop a new bamboo composite material that can be designed to have the necessary mechanical and physical properties and to be applied as reinforcement system in structural concrete", with respect to flexural load bearing capacity, BVC reinforcement have showed better-than-expected performance when used in concrete beams, which supported the hypothesis of the research.

In any structural design, the final goal is to build a structure with flexural or shear capacity larger than the expected loadings applied. In this respect, the ACI standard employs strength reduction factors to reduce the experimental values of the materials strength to ensure this goal can be achieved with a relatively high margin of safety, which may not necessarily be the most economical way in saving construction costs. Although the BVC reinforcement showed higher than expected overall load-bearing capacity compared to the estimation of the ACI design code, further investigation is necessary to establish design values suitable for BVC reinforced concrete beams in future.

In terms of deflection limit, the estimated values obtained by the ACI 440.1R-15 with respect to the maximum acceptable values according to serviceability limit state are shown in Fig. 174 in comparison to the maximum midspan deflection of the BVC reinforced concrete beams.
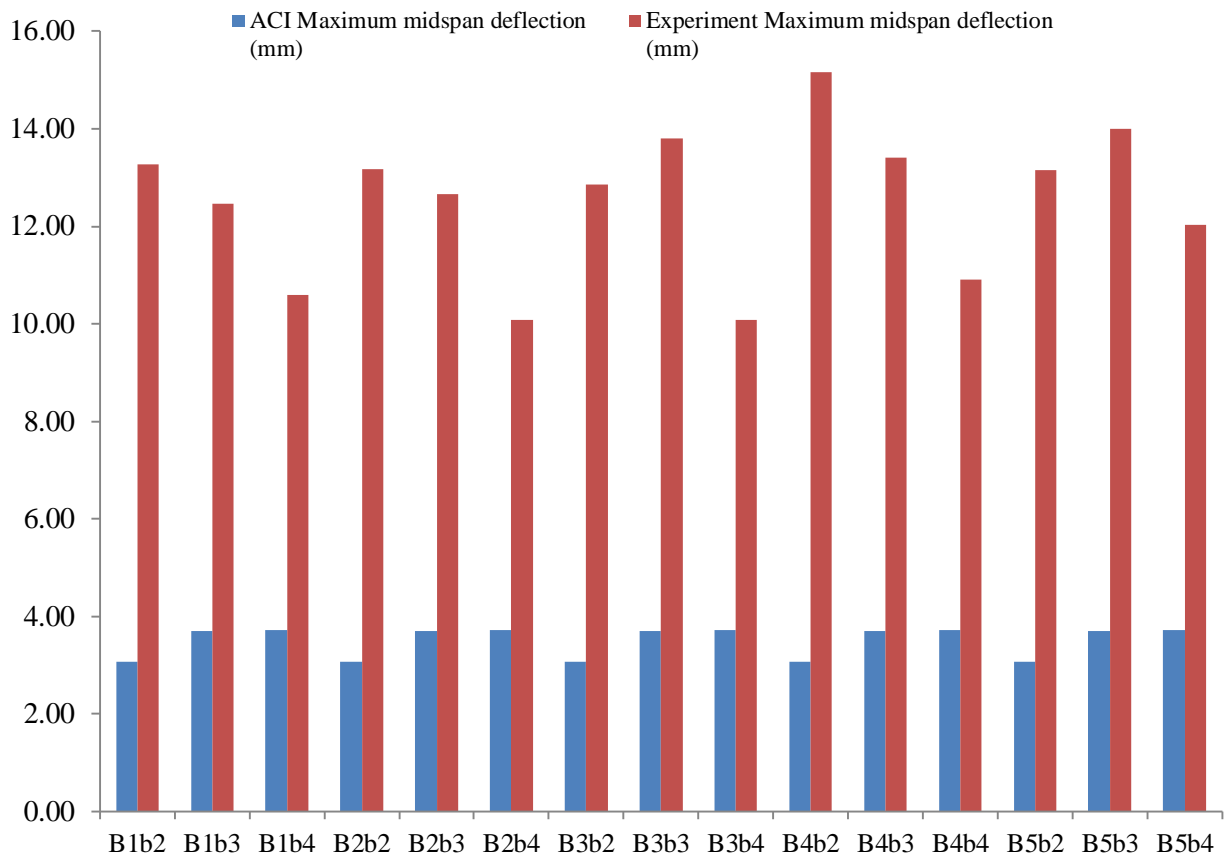
Fig. 174 demonstrates that differences existed between the deflection limits obtained through analysis according to the ACI 440.1R-15 standard and the experimental values measured during the four-point flexural tests. The deflection values measured during the tests were 2 to 5 times greater than the estimated limits obtained according to the ACI standard. The results confirmed the effect of lower elastic modulus of BVC reinforcement in comparison to steel reinforcement and some of the FRP reinforcement on the deflection behavior. Lower ductility of BVC reinforcement was the main reason for the relatively higher deflection values obtained during the flexural four-point test. The average maximum midspan deflection of BVC reinforced concrete beams could be further reduced through increasing the reinforcement ratio. Either increasing the number of reinforcement or employing larger reinforcement bars could help to enhance the deflection behavior of the BVC reinforced concrete beams. Furthermore, the concrete grade could help to further improve the ductility behavior of the BVC reinforced concrete beams.

The ACI standard ensured that excessive deflections and cracking were limited in the actual building; thus lower deflection values were obtained. Excessive deflection of the structural members within the building frame could negatively influence the structure's efficiency, especially affecting the finishes and partitions and service equipment employed within the building. Therefore, it was deemed necessary to have acceptable deflection limits that minimized such adverse effects during the life span of the building when considering the design recommendations of the ACI standard.

Similar to what was explained earlier regarding the effect of the reinforcement ratio on the deflection behavior, the ACI standard also allowed higher deflection limits for beams with higher amount of longitudinal reinforcements at the tension face of the concrete cross section as shown in Table 48 and Fig. 174. This approach considered the greater overall stiffness that could be achieved through increasing the reinforcement ratio, by employing more tensile reinforcement bars. The higher the stiffness of the concrete beam, the lower the maximum midspan deflection. Though the BVC reinforcement had a lower modulus of elasticity compared to steel reinforcement, increasing the reinforcement ratio was effective in fulfilling the ductility requirement of the BVC reinforced concrete beams. As explained earlier, the increase in reinforcement ratio resulted in higher overall stiffness of the beams and therefore smaller deflection limits were observed.

Similar methods could be used in future for BVC reinforced concrete elements in construction where certain deflection limits have to be maintained with respect to the serviceability limit state of design. The result of the deflection measurement showed the importance of the serviceability limit state compared to the ultimate load limit state of design when the BVC reinforced concrete beams were designed.

The experimental results confirmed the higher stiffness of the concrete beams which was achieved by increasing the number of tensile reinforcement (Fig. 173). When the number of tensile reinforcement increased from 2 to 4, the measured deflection values were reduced by up to 28%. The results indicated the significant effect that BVC reinforcement's ductility had in improving the overall stiffness of BVC reinforced concrete beams and in maintaining the required deflection limits.

The deflection of the reinforced concrete beam depended largely on the concrete stiffness and modulus of the tensile reinforcement as shown by Eq. 93. Since a similar concrete mix was used for all the beam samples in this study, the only influential parameter in Eq. 93 was the

effect of the tensile BVC reinforcement. In general, BVC reinforced concrete beams showed relatively higher deflection values than the steel reinforced concrete beams and in comparison to the ACI design values. The lower elastic modulus of BVC reinforcement was the main factor affecting the overall stiffness of the concrete beams, as explained earlier in this section. It was shown that by increasing the reinforcement ratio, a significant increase in the overall stiffness of the beams was observed during the experiments.

The defection limits measured through the tests or obtained by the analysis according to ACI 440.1R-15 were short-term defections which occurred immediately after casting the concrete element and/or after application of the external loads on the structure. Another important set of deflection limits are the long-term deflection limits which normally take place over a longer period of time (e.g. 5 to 20 years).

The long-term deflection is mainly the result of concrete shrinkage and creep. Creep or shrinkage behavior of concrete can be influenced by several factors, including but not limited to humidity, temperature, type and size of aggregates, and the water-to-cement ratio used to mix the concrete. Therefore investigating the long-term deflection limits would require additional test set-ups and special laboratory facilities, which are beyond the scope of this thesis. The long-term deflection evaluation will be discussed in a future work chapter.

The shear design of BVC reinforced concrete beams in this study was carried out according to the ACI 440.1R-15 standard, by considering the lower strength and stiffness of the BVC stirrups compared to the longitudinal BVC reinforcement due to fabrication constraints explained in sections 5.5.2 and 5.5.3. The shear capacity of the BVC reinforced concrete beams in this study was evaluated by the variation of the spacing (s) between the BVC stirrups, given the width, thickness and shape of the BVC stirrups were fixed during the fabrication process as explained in section 5.5.2. Table 49 shows the spacing values obtained through analysis according to ACI 440.1R-15 in comparison to spacing distances that were specified during the BVC reinforced concrete beam's preparation.

The spacing values obtained according to ACI standard were largely governed by the depth of the BVC reinforced concrete beams for all the beam series in this study ($d/2 = 67$ mm). This limit set by the ACI standard ensured that nearly all diagonal shear cracks were intercepted by at least one BVC stirrup to prevent shear failure of the beam. As explained in section 3.2, the shear cracks within a reinforced concrete beam were mainly developed into

diagonal patterns which had to be controlled by the stirrups, which if not properly designed, could result in premature failure of the reinforced concrete beam.

Table 49 Comparison of the theoretical and empirical spacing of various beam series

Beam Design	ACI 440.1R-1	Experiment
B1b2	67	70
B1b3	67	70
B1b4	67	70
B2b2	67	50
B2b3	67	50
B2b4	67	50
B3b2	67	115
B3b3	67	115
B3b4	67	115
B4b2	67	75
B4b3	67	75
B4b4	67	75
B5b2	67	45
B5b3	67	45
B5b4	67	45

The spacing values between the BVC stirrups defined by the experimental test set-up followed the ACI recommended values very closely. Only for beam samples from the B3b2, B3b3 and B3b4 series were slight deviations from ACI recommended spacing values observed. The spacing provided between the BVC stirrups for these groups of samples was 115mm, 1.7 times the ACI recommended value. This difference between the two sets of spacing values could have triggered the failure of the BVC reinforced concrete beam, due to shear forces given the insufficient shear capacity provided by the BVC stirrups. Therefore it was deemed necessary to analyze the failure modes observed during the tests versus the failure modes found through analysis using the ACI standard. The comparison could be helpful in determining the relevance of the ACI standard for designing the BVC stirrups for preventing shear failure of BVC reinforced concrete beams.

Table 50 compares the ACI failure modes with the experimental failure modes of the different beam samples tested in this section.

Table 50 Comparison of the theoretical and empirical spacing of various beam series

Beam Design	ACI 440.1R-15	Experiment
B1b2	BVC rupture	3 BVC rupture, 2 shear failure
B1b3	Concrete crushing	All BVC rupture
B1b4	Concrete crushing	1 BVC rupture, 4 concrete crushing
B2b2	BVC rupture	All BVC rupture
B2b3	Concrete crushing	All BVC rupture
B2b4	Concrete crushing	2 BVC rupture, 3 concrete crushing
B3b2	BVC rupture	3 shear failure, 2 BVC rupture
B3b3	Concrete crushing	2 shear failure, 3 BVC rupture
B3b4	Concrete crushing	4 concrete crushing, 1 shear failure
B4b2	BVC rupture	3 BVC rupture, 2 shear failure
B4b3	Concrete crushing	4 BVC rupture, 1 shear failure
B4b4	Concrete crushing	4 concrete crushing, 1 BVC rupture
B5b2	BVC rupture	4 BVC rupture, 1 shear failure
B5b3	Concrete crushing	4 BVC rupture, 1 shear failure
B5b4	Concrete crushing	3 concrete crushing, 2 BVC rupture

As explained in the design and calculations of the beams in this section, the ACI 440.1R-15 recommended two modes of failure for polymer composite reinforced structural concrete member: concrete crushing and reinforcement rupture. The shear failure was considered an undesirable failure mode for a reinforced concrete element. The shear failure would not allow the full flexural capacity of the reinforced concrete member to be safely activated, given the ultimate failure could occur due to lack of sufficient shear capacity.

During the series of tests carried out in this section on BVC reinforced concrete beams, only a few cases of shear failure modes were observed. The largest number of shear failure modes was observed in the case of beam samples from the B3b2, B3b3 and B3b4 series, in which the ACI recommended spacing between the BVC stirrups was lower than the provided spacing in the test set-up.

A total of six shear failure modes was observed for the (B3) beam series, which confirmed the theoretical design approach recommended by the ACI standard to prevent shear failure by providing the minimum required spacing of 67mm between the BVC stirrups. For the B3b4 beam series, only one shear failure mode was observed and the other beam samples failed due to concrete crushing, which followed closely the estimated failure mode based on the ACI standard.

Some of the shear failure modes observed within the samples of this study (B5b3 and B5b2) was mainly caused by the rupture and movement of the steel cable ties used to hold the legs of the BVC stirrup to the longitudinal reinforcement, rather than by insufficient shear capacity which was explained earlier in the experimental results section. The steel cable ties could have heterogeneous properties due to the presence of some imperfections during the production. Thus, properties of the ties might change from one cable tie to the other. It was not feasible to test and evaluate each and every one of them before using it to fix the BVC reinforcement system. Therefore, a few steel cable ties with lower than the estimated mechanical properties could have been employed within this study; these could have broken earlier than the others and thus resulted in the movement of the BVC reinforcement systems and led to a premature shear failure mode.

Beam samples that displayed almost similar failure modes based on the ACI analysis and experimental test setup belonged to the (B1b4, B2b2, B3b4, B4b4 and B5b2) beam series. Beam samples with only 2 BVC reinforcement bars at the tension side of the concrete beam cross section failed mainly due to the rupture of the reinforcement, while beam samples with 4 BVC tensile reinforcements had a tendency to fail due to concrete crushing at the compression side of the beam.

This result could be explained by the effect of the reinforcement ratio on the failure modes of the beam samples. Larger BVC reinforcement ratio resulted in the concrete crushing mode of failure rather than rupture of reinforcement, while lower reinforcement ratio resulted in the reinforcement rupture mode of failure. The longitudinal BVC reinforcement was also effective in enhancing the shear capacity of the BVC reinforced concrete beams. The combination of transverse and longitudinal BVC reinforcement in general showed great performance during the four-point flexural tests. As mentioned earlier, only a few shear failure modes were observed in the BVC reinforced concrete beam samples, which were mainly affected by the BVC stirrups fabrication constraints and the use of steel cable ties for their arrangement. All the other beams samples showed acceptable shear capacity based on the ACI standard, and in which no shear failure mode was observed.

The shear capacity of the BVC reinforced concrete beam played an important role in determining the ultimate failure modes. The ACI 440.1R-15 standard enforces the required spacing of the stirrups to prevent any potential shear failure of the beam, and to activate either concrete crushing or reinforcement rupture as the desirable modes of failure.

In terms of thermal expansion evaluation, as shown in section 6.3, the water-based epoxy coating and sand provided strong bonding between the BVC reinforcement and concrete, which was effective in overcoming any potential residual stresses that occurred during the temperature variations as a result of transverse thermal expansion of the BVC material. No signs of cracking due to temperature variations were observed on the surface of the concrete beams in this study. Furthermore, it was shown that as long as the concrete cover thickness was 2 times the reinforcement thickness, no significant thermal stresses developed within the reinforced concrete matrix kept at laboratory conditions, and thus no signs of tensile cracking were observed in the concrete beam samples. The results of the temperature monitoring and thermal stress development proved the feasibility and suitability of the BVC reinforcement system for reinforcing concrete elements under certain environmental conditions, though different CTE with concrete matrix was observed.

The results from the experiments carried out in this study and the analysis based on the relevant ACI standard have proved the great performance of BVC reinforcement systems for reinforcing structural concrete members, when certain combinations of shear, flexure and tension forces under certain environmental conditions are met. The tensile and flexural capacities of the newly developed BVC reinforcement are comparable to ASTM certified steel reinforcement systems as well as GFRP reinforcement, which make the BVC material a suitable alternative to steel and GFRP reinforcement systems for concrete structures in terms of mechanical capacity and technical feasibility.

The performance of the BVC reinforced concrete beams tested in this section demonstrated the superior performance of these BVC materials in which the inherent capacity was higher than the design values estimated by the relevant international standards. The reserved material capacity of BVC reinforcement was 2 to 3 times of the recommended design values estimated by the ACI design guide. This observation highlighted the feasibility of employing the newly developed BVC reinforcement systems for concrete applications in which similar loading and environmental conditions could be provided.

For instance, in Southeast Asia, in the majority of the developing countries such as Indonesia, Myanmar, Thailand, Cambodia and Vietnam, typical buildings normally have 1 to 2 stories which can be designed with simple span beams and column systems similar to what was tested in this research, with BVC materials as the main reinforcement systems for concrete beams as the main load-bearing elements of the building. Such applications will be feasible in

technical terms that have been proved by the test series carried out throughout this research. The guidelines given in ACI 440.1R can function as a preliminary guide for the design and proportioning of concrete beams reinforced with BVC reinforcement systems, before new design guides are established for BVC reinforced concrete members for future applications. Future research is therefore needed to establish the necessary design guides similar to those found in ACI 440.1R-15 for FRP materials as reinforcement. Feasibility study was done using the example of low-rise housing unit in Indonesia.

Indonesia is experiencing rapid metropolitan change, from a largely rural economy to an urban economy. As reported by the World Bank recently, there are more than 34 million Indonesians living in the slums of the suburbs of big cities such as Jakarta, Bandung and Surabaya. In Indonesia, there are 3,201 slum areas with a total size of 34,374 hectares (World Bank 2015). The Indonesian government has already considered long-term plans to improve the slum areas by 2019. In this regard, bamboo composite reinforcement can be a suitable and affordable alternative to steel reinforcement to provide affordable accommodation for Indonesia's fast-growing urban population.

According to a report published by the United Nations Human Settlements Programme in 2008, the majority of Indonesian households live in non-attached dwelling units and the total stock is more than 54 million housing units. The report further emphasizes that more than 2.5 million units need to be replaced by new housing units due to damage arising from long-term exposure to extreme environmental conditions (United Nations Human Settlements Programme 2008). More than 80% of Indonesians live in single-storey non-attached housing units and close to 40% of the housing units are less than 49m^2.

A typical single-storey housing unit in Indonesia constituting of one, two or more rooms is generally characterized as having a symmetric layout in the form of a square or rectangle plan. Furthermore, the walls are not more than 3m apart to minimize the construction of bracing or crosswall and to reduce the construction cost. Fig. 175 displays a typical plan of a single-storey unit for low-cost housing. As shown in Fig. 175, the beams have a span length of 3m. To evaluate the strength and maximum deflection of the BVC reinforced concrete beams in Fig. 175, ACI 318 recommends employing the following load combination as described in section 3.2.1 to evaluate the applied moment.

$U = 1.2DL + 1.6LL$ (Eq. 8)
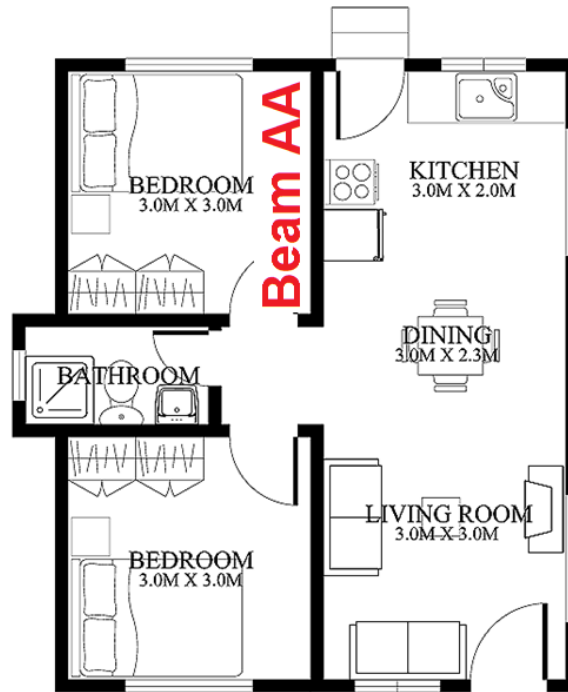
For the feasibility study in the section, only the beam with the largest imposed load is considered for the design, labeled in Fig. 175 as "beam AA" at the roof level. Typical dead loads acting on the beam at roof level consist of the self-weight of the beam and all flooring and insulation materials. The typical live load recommended by ACI 318 is between 0.90kN/m² and 2 N/m². However for a typical single-storey housing unit in Indonesia, the live load acting on the roof is normally assumed to be 0.90kN/m². According to Table 43, the recommended thickness for a simply supported beam is L/10 which in the case of beam "AA" in Fig. 175 with a span length of 3,000mm is at least 300mm. Therefore a typical cross section of 250mm (width) by 300mm (height) is assumed for the BVC reinforced beam "AA". Given the density of concrete mix used in this study is 2,362 kg/m³ according to Table 34, the distributed dead load acting on beam "AA" can then be calculated according to the following expression:

$$DL = 2362 \times 0.25 \times 0.35 \times 10 \times 10^{-3} = 2.07 \ \frac{kN}{m}$$

The distributed live load can also be found by considering the loading span of beam "AA".

$$LL = 0.90 \times 3 = 2.70 \ \frac{kN}{m}$$

Subsequently the uniform load acting on the beam "AA" can be found by using Eq. 8:

$$U = 1.2(2.07) + 1.6(2.7) = 6.80 \frac{kN}{m}$$

The minimum required reinforcement area should be controlled by Eq. 77 as follows:

$$A_{f,min} = \frac{0.41\sqrt{f_c'}}{f_{fu}} b_w d \geq \frac{2.3}{f_{fu}} b_w d$$

Where $b_w = 250$mm and

$d = 300 - 20$ (concrete cover) $- 6$ (stirrup) $- 5$ (center of reinforcement) $= 269$mm

$$A_{f,min} = \frac{0.41\sqrt{20}}{326.4} \times 250 \times 269 \geq \frac{2.3}{326.4} \times 250 \times 296$$

$$A_{f,min} = 474 \ mm^2$$

Therefore at least 5 pieces of BVC reinforcements need to be provided in the concrete beam to ensure the minimum required reinforcement criteria is satisfied:

$$A_{f,provided} = 5 \times 10 \times 10 = 500 > 474 \ mm^2$$

The reinforcement ratio can be calculated as follows:

$$\rho_f = \frac{A_f}{bd} = \frac{5 \times 10 \times 10}{250 \times 269} = 0.00743$$

As mentioned in section 5.5.3, the average tensile strength (f^*_{fu}) of longitudinal BVC reinforcement is 408MPa and the average elastic modulus is 41,350MPa. A strength reduction factor of 0.80 can be used for Eq. 66 to calculate the design tensile strength as follows:

$$f_{fu} = C_E f^*_{fu} = 0.80 \times 408 = 326.4 \ MPa$$

To evaluate if the reinforced concrete beam's failure is controlled by the FRP rupture or concrete crushing, the balanced reinforcement ratio should be compared with the provided reinforcement ratio. The balanced reinforcement ratio can be calculated by Eq. 70:

$$\rho_{fb} = 0.85\beta_1 \frac{f_c'}{f_{fu}} \frac{E_f \varepsilon_{cu}}{E_f \varepsilon_{cu} + f_{fu}}$$

$$\rho_{fb} = 0.85 \ (0.85) \times \frac{20}{326.4} \times \frac{41350 \times 0.003}{41350 \times 0.003 + 326.4} = 0.0122$$

Given that $\rho_{fb} > \rho_f$, the reinforced concrete section is controlled by the FRP rupture limit states according to ACI 440.1R-15 which have been discussed earlier in section 6.5.1 and 6.5.3. The depth of Neutral Axis (N.A) can be found according to Eq. 75 based on the assumptions made in section 6.5.1:

$c_b = \left(\frac{\varepsilon_{cu}}{\varepsilon_{cu} + \varepsilon_{fu}}\right) d = 74.1 \ mm$, and subsequently the flexural strength is:

$M_n = A_f f_{fu} \left(d - \frac{\beta_1 c_b}{2}\right) = 5 \times 10 \times 10 \times 326.4 \left(269 - \frac{0.85 \times 74.1}{2}\right) \times 10^{-6} = 38.77 kN.m$

Since $\rho_{fb} > \rho_f$, the strength reduction factor (Φ) for the group 1 beam series will be (0.55) according to Eq. 72. Therefore the design flexural strength of the member can be calculated accordingly:

Φ M$_n$ = 0.55 (38.77) = 21.32 kN.m

The maximum applied moment along the beam length for uniformly distributed load U = 6.8 kN/m can be found as follows;

$M_u = \frac{UL^2}{8} = \frac{6.8(3^2)}{8} = 7.65 \ kN.m$

Therefore according to the strength design philosophy discussed in section 6.5.1, the design flexural strength at any section of BVC reinforced beam "AA" exceeds the factored moment (applied loads) as shown in Eq. 14.

Φ M$_n \geq$ M$_u$ (Eq. 14)

The design flexural strength of beam "AA" is almost 3 times the factored moment applied, thus beam "AA" has sufficient reserve capacity to withstand the moment applied from imposed loads. Similar to flexural strength calculation, the design shear strength (ΦV$_n$) should be larger than the factored shear force (V$_u$) at any section of the BVC reinforced concrete beam as explained in section 6.5.1. To calculate the shear capacity of the concrete, the parameter k needs to be evaluated using Eq. 82.

$k = \sqrt{\left(2\rho_f n_f + \left(\rho_f n_f\right)^2\right)} - \rho_f n_f$

$n_f = \frac{E_f}{E_c} = \frac{41350}{25410} = 1.627$

$\rho_f = 0.00743$

$k = \sqrt{(2 \times 0.00743 \times 1.627 + (0.00743 \times 1.627)^2)} - 0.00743 \times 1.627 = 0.144$

Eq. 86 can then be used to compute the concrete shear capacity as follows:

$$V_c = \frac{2}{5}\sqrt{f_c'}b_w(kd)$$

$$V_c = \frac{2}{5}\sqrt{20} \times 250(0.144 \times 269) = 17.30 \text{ kN, and}$$

$\Phi Vc = 0.75 \ (17.30) = 12.90 \text{ kN}$

The maximum shear forces applied on the beam "AA" can be found by structural analysis as follows;

$$V_u = \frac{UL}{2} = \frac{6.8 \times 3}{2} = 10.20 \text{ kN}$$

Since $V_u > \frac{\Phi V_c}{2} = 6.45$ kN, therefore shear reinforcement is required. The design tensile strength of BVC stirrups has been found in section 6.5.3;

$f_{fv} = 138.5 \text{ MPa}$

The maximum spacing of the stirrups permitted by ACI 440.1R-15 can be calculated accordingly by using BVC stirrups of 15mm (width) by 6mm (thickness) as shown in section 6.5.3:

$$A_{fv,min} = 0.35\frac{b_w s}{f_{fv}} \rightarrow s_{max} = \frac{A_{fv} \times f_{fv}}{0.35 b_w}$$

$$s_{max} = \frac{180 \times 138.5}{0.35 \times 250} = 285 \text{mm}$$

Furthermore ACI 440.1R-15 limits the maximum spacing of the vertical stirrups to the smaller of d/2 or 600mm, which, in the case of the concrete beam "AA" designed in this feasibility study, $\frac{d}{2} = \frac{269}{2} = 134.5$mm

Therefore, by providing BVC stirrups at a spacing of not more than 134.5mm, no shear failure should be expected for beam "AA". The next step is to evaluate the cracking load and the allowable deflection according to the ACI 440.1R-15 recommendations. Before

computing the required cracking load and moment three parameters used in Eq. 85, including λ, I_g and y_t, need to be defined;

$$I_g = \frac{bh^3}{12} = \frac{250 \times 300^3}{12} = 562500000 \text{ mm}^4$$

$\lambda = 1.0$ for normal concrete

$$\gamma_t = \frac{300}{2} = 150 \text{ mm}$$

Therefore the cracking moment can be found subsequently:

$$M_{cr} = \frac{0.62\lambda\sqrt{f_c'}I_g}{y_t} = \frac{0.62 \times 1 \times \sqrt{20} \times 562500000}{150} \times 10^{-6} = 10.40 \text{ kN.m}$$

To compute the allowable deflection limits by ACI 440.1R-15, the applied moment (M_a) should be compared with cracking moment (M_{cr}). The applied moment (M_a) can be found by calculating the moment from dead load and live load imposed on beam "AA":

$$M_{DL} = \frac{W_{DL}L^2}{8} = \frac{2.07 \times 3^2}{8} = 2.33 \text{ kN.m}$$

$$M_{LL} = \frac{W_{LL}L^2}{8} = \frac{2.70 \times 3^2}{8} = 3.04 \text{ kN.m}$$

$$M_a = M_{DL} + M_{LL} = 5.37 \text{ kN.m}$$

Since $M_a < M_{cr}$, then the beam section is un-cracked and its moment of inertia is equal to the gross moment of inertia I_g. The following formulae can be used to estimate the maximum deflection of a simply supported beam with uniformly distributed loads:

$$\Delta = \frac{5(DL+LL)L^4}{384E_cI_g} \quad \text{(Eq. 92)}$$

$$\Delta = \frac{5(2.07+2.70) \times 3000^4}{384 \times 25410 \times 562500000} = 0.35 \text{ mm}$$

In Indonesia, the deflection limit for roof construction is set to $\frac{L}{240}$ which for the case of beam "AA" in this case study $\frac{L}{240} = 12.5$mm. Therefore the BVC reinforced concrete beam "AA" satisfies the deflection limit.

Considering that majority of housing units in Indonesia are not designed perfectly following the criteria mentioned earlier (e.g. beams with 3m span), it is beneficial to calculate the upper

span limit of beam "AA" that can satisfy both strength and serviceability limit states. For this purpose, it is assumed that the beam "AA" cross section remains the same while the number of BVC reinforcements can be adjusted to meet the limit states of design. A span length of L= 6m is assumed for the following calculations.

Assuming 5 BVC reinforcements for beam "AA", similar to the calculation carried out earlier in this section, flexural strength is found;

$$M_n = A_f f_{fu} \left(d - \frac{\beta_1 c_b}{2} \right) = 38.77 kN.m$$

$\Phi M_n = 0.55 (38.77) = 21.32$ kN.m

The dead and live loads remain the same but the factored moment increases as a result of the larger span length assumed for beam "AA". The factored moment can be found as follows:

$$M_u = \frac{UL^2}{8} = \frac{6.8(6^2)}{8} = 30.60 \ kN.m$$

The design flexural strength of the beam (ΦM_n) is lower than the applied factored moment. Two methods can be undertaken to enhance the beam's design flexural strength: increasing the reinforcement ratio or increasing the beam cross-section. Increasing the cross section of the beam adds on the construction cost given that larger concrete volume is required, thus this method of improving the design strength is not feasible especially for low-cost housing units. Assuming FRP rupture mode of failure for the beam "AA", the required area of BVC reinforcement can be found using Eq. 73.

$$M_n = A_f f_{fu} \left(d - \frac{\beta_1 c}{2} \right) = A_f \times 326.4 \left(269 - \frac{0.85 \times 74.1}{2} \right) \times 10^{-6} = \frac{30.60}{0.55}$$

$A_f = 718$ mm^2

Therefore at least 8 reinforcements need to be provided at the bottom of concrete beam in the form of two layers each consisting of 4 BVC reinforcements. To assess the mode of failure the reinforcement ratio is compared with balanced reinforcement ratio:

$$\rho_f = \frac{A_f}{bd} = \frac{8 \times 10 \times 10}{250 \times 269} = 0.0118$$

Given that $\rho_{fb} > \rho_f$, the reinforced concrete section is controlled by the FRP rupture limit states according to ACI 440.1R-15. The next step is to design the beam for shear strength

according to the spacing of the BVC stirrups. The maximum shear forces applied on the beam "AA" can be found by structural analysis as follows:

$$V_u = \frac{UL}{2} = \frac{6.8 \times 6}{2} = 20.40 \text{ kN}$$

Since $V_u > \frac{\Phi V_c}{2} = 6.45$ kN, therefore shear reinforcement is required. The maximum spacing of the stirrups permitted by ACI 440.1R-15 can be calculated subsequently:

$$S_{max} = \frac{A_{fv} \times f_{fv}}{0.35 b_w} = \frac{180 \times 138.5}{0.35 \times 250} = 250 \text{mm}$$

As ACI 440.1R-15 limits the maximum spacing of the vertical stirrups to the smaller of d/2 or 600mm, which, in the case of the concrete beam "AA" designed in this feasibility study, $\frac{d}{2} = \frac{269}{2} = 134.5$mm

Therefore, by providing BVC stirrups at a spacing of not more than 134.5mm, no shear failure should be expected for beam "AA". The deflection of the beam "AA" can be found following the steps explained earlier in this section for the span length of 6m. The applied moment (M_a) can be found by calculating the moment from dead load and live load imposed on beam "AA":

$$M_{DL} = \frac{W_{DL} L^2}{8} = \frac{2.07 \times 6^2}{8} = 9.31 \text{ kN.m}$$

$$M_{LL} = \frac{W_{LL} L^2}{8} = \frac{2.70 \times 6^2}{8} = 12.15 \text{ kN.m}$$

$$M_a = M_{DL} + M_{LL} = 21.46 \text{ kN.m}$$

Since $M_a > M_{cr} = 10.40$, then the beam section is considered cracked and to estimate the deflection limits of the reinforced concrete beam, the effective moment of inertia of the cracked section (I_e) should be used instead of the gross movement of inertia (I_g). Eq. 83 should be used to calculate the effective moment of inertia; before that, the cracked moment of inertia (I_{cr}) needs to be estimated using Eq. 81.

$$I_{cr} = \frac{bd^3}{3} k^3 + n_f A_f d^2 (1 - k)^2 \qquad \text{(Eq. 81)}$$

where the parameter k needs to be evaluated using Eq. 82 and $n_f = 1.627, \ A_f = 800 \text{ mm}^2$;

$$k = \sqrt{\left(2\rho_f n_f + \left(\rho_f n_f\right)^2\right)} - \rho_f n_f \quad \text{(Eq. 82)}$$

$$k = \sqrt{(2 \times 0.0118 \times 1.627 + (0.0118 \times 1.627)^2)} - 0.0118 \times 1.627 = 0.178$$

$$I_{cr} = \frac{250 \times 269^3}{3} \times 0.178^3 + (1.627)(800)(269)^2(1 - 0.178)^2 = 17128133340 \text{ mm}^4$$

Subsequently the effective moment of inertia (Ie) can be cacluated according to Eq. 83 and Eq. 84;

$$\gamma = 1.72 - 0.72 \left(\frac{M_{cr}}{M_a}\right) = 1.72 - 0.72 \left(\frac{10.40}{21.46}\right) = 1.37$$

$$I_e = \frac{I_{cr}}{1 - \gamma\left(\frac{M_{cr}}{M_a}\right)^2\left[1 - \frac{I_{cr}}{I_g}\right]} = \frac{17128133340}{1 - (1.37)\left(\frac{10.40}{21.46}\right)^2\left[1 - \frac{17128133340}{562500000}\right]} = 173619548 \text{ mm}^4$$

Eq. 93 could then be used to estimate the deflection of a simply supported beam with uniformly distribute load;

$$\Delta = \frac{5KM_aL^2}{48E_cI_e} = \frac{5(1)(21.46)(6000)^2}{48(25410)(173619548)} \times 10^6 = 18.2 \text{ mm}$$

Comparing the deflection with the deflection limit for roof construction which is set to $\frac{L}{240} = \frac{6000}{240} = 25$mm, beam "AA" with a span length of 6m and reinforced with 8 pieces of BVC reinforcement satisfies the limit states of serviceability and strength while retaining the overall cross section.

The example of beam "AA" in this feasibility study shows the suitability of BVC reinforcements for construction of low-cost and low-rise reinforced concrete housing units for small cities and towns in developing countries in Southeast Asia like Indonesia where housing demands have put tremendous pressure on local governments in recent years. Furthermore BVC reinforcement systems have been shown to satisfy strength and serviceability limit states through optimized design and construction of the concrete member which can effectively reduce the overall weight of the member and thus minimize the cost of constructing affordable housing units.

6.6.   Conclusions

Longitudinal and transverse (stirrups) reinforcements made of the newly developed BVC materials are suitable for use in structural concrete beams. The results of the tests carried out indicate that BVC reinforcement coated with water-based epoxy coating and sand particles develop acceptable bonding with the concrete matrix. The results of the pull-out tests suggest that water-based epoxy coating with sand particles will improve the bond mechanism through developing a better interfacial microstructure between the concrete and reinforcement, resulting in superior stress transfer from the concrete to the reinforcement systems. Furthermore, the water-based epoxy coating protects the BVC reinforcement systems from potential chemical and environmental degradation parameters over the life span of the structure. The results obtained for the water absorption and dimensional change of the BVC samples demonstrate the effect of water ingress into the concrete, and subsequently to the BVC reinforcement, can have on the properties of the BVC samples, especially in severe conditions (higher temperatures). However, it is shown that presence of the water-based epoxy coating on the surface of the BVC samples will impede the water uptake into the microscopic voids and cavities.

In this chapter, BVC samples are also subjected to an alkaline environment with similar pH level as concrete matrix. The results suggest a drop of less than 10% in the ultimate tensile properties of the BVC samples after three months' exposure to the alkaline solution. Following preliminary bonding and durability investigations, BVC reinforced concrete beams prepared with various combinations of longitudinal and shear BVC reinforcement are tested under a flexural-test set-up. ACI 440.1R-15 has also been adopted as the reference design guide in the absence of relevant international standards for the design and evaluation of BVC reinforced concrete beams. Four-point flexural tests reveal that, in terms of nominal ultimate failure load, there is a close correlation between the code and experimental values of the ultimate loads when safety factors and strength reduction factors are not employed. However, a reduction of up to 50% in the ultimate failure loads obtained by the ACI code is observed compared to the values obtained by the experiments when the recommended safety factors and strength reduction factors are employed. The deflection values obtained by the tests are greater than the design values recommended by the ACI standard. Furthermore, comparisons between the failure modes estimated by the ACI 440.1R-15 with the actual modes of failure observed during the tests reveal some discrepancies. The conservative design approach of the ACI 440.1R-15 ensures that premature failure of the reinforced concrete beam can be

prevented by providing the required spacing between the stirrups to prevent a sudden and undesirable shear failure mode. Overall, this chapter shows that for the majority of BVC reinforced concrete beams tested in this study, differences between the code and experimental values are found. The ACI 440.1R-15 standard for the design and calculation of the FRP reinforced concrete beam can function as a primary conservative design guide for the design and evaluation of BVC reinforced concrete beams. However, considering the differences that exist between the properties of BVC and FRP materials, not all the recommendations given by the ACI standard are appropriate for the design of BVC reinforced concrete beams. Therefore, further investigations are needed on the design and evaluation of BVC reinforced concrete beams to develop the design recommendations suitable for BVC materials for a range of future uses in structural engineering.

7. Conclusions and limitations

The following conclusions are drawn based on the results of this thesis. Subsequently, limitations of this study are also described with respect to the results obtained, and leads to suggestions for overcoming these limitations for future work scopes.

7.1. Conclusions

The hypothesis of this research is "to develop a new bamboo composite material that can be designed to have the necessary mechanical and physical properties and to be applied as reinforcement system in structural concrete". Therefore, this thesis contains proposals for processes and methods for development and evaluation of a new class of composite materials containing natural bamboo fibers, as well as a study of a new reinforcement system for structural-concrete elements. Steel reinforcement production requires higher energy compared to the energy needed to make the newly developed bamboo composite materials. Steel needs to be processed in an electric arc furnace with temperatures up to 1500℃, while in bamboo-composite production, a maximum temperature of 100℃ is sufficient.

More importantly, steel comes from a non-renewable source, while bamboo is a renewable natural resource which grows fast enough to provide a sufficient supply of raw materials for structural engineering applications. Furthermore, steel production is responsible for significant levels of greenhouse gas emissions, while bamboo removes carbon from the atmosphere and plays a significant role in mitigating the negative impacts of climate change. In terms of long-term performance, steel suffers from corrosion (oxidation) which affects many steel-reinforced concrete elements. Bamboo composite materials do not corrode, thus creating significant potential savings in corrosion-related costs of repair and retrofitting of reinforced concrete members.

Steel is a product of the developed world; most countries in the developing world in Asia, Africa and the Americas have little or no access to steel for construction purposes. Unlike steel, bamboo can be found in almost every developing country in large quantities. In terms of technical properties, bamboo has many advantages, including tensile strength. The tensile strength of the fiber bundles of some bamboo species is similar to or higher than common steel reinforcement. The availability of bamboo resources in developing countries, where steel reinforcement is imported at high costs, provides unique opportunities for the local industry to create new value chains within the country through the fabrication of bamboo composite materials.

So far, no scientific studies have been carried out on evaluating the physical and mechanical properties of bamboo composite materials for reinforcing structural concrete members. Therefore, this thesis provides descriptions of new production methods which have not been previously investigated for the development of a new class of composite materials based on natural bamboo fibers. Systematic investigations carried out through the course of this study have developed such composite bamboo materials and evaluated their performance as reinforcement elements for structural concrete.

The potential of bamboo as a natural material for the production of high-performance composite material to be used ultimately as reinforcement in concrete applications has been demonstrated. The research has tackled several aspects related to the use of natural bamboo for composite reinforcement.

To test the hypothesis of this thesis and achieve the goals of this research, the results have been divided into three parts: raw bamboo selection and evaluation of the physical and mechanical properties, bamboo composite reinforcement fabrication and investigation of properties, and use of bamboo composite reinforcement in structural concrete beams. The conclusions made for each of the three parts of this study are described in the following sections.

7.1.1. Raw bamboo selection and evaluation of physical and mechanical properties

Dendrocalamus asper, known locally as *Petung* bamboo, from Indonesia is chosen for the purpose of this study after careful investigation. The Moisture Content (MC), Specific Density (SD), Compressive Strength (CS) along the fiber direction, Tensile Strength (TS) along the fiber direction, modulus of Elasticity in tension (E_t), flexural strength or Modulus of Rupture (MOR) and modulus of Elasticity in flexure (E_f) of samples from *Petung* bamboo culms with diameters in the range of 80mm to 150mm, wall thicknesses of 6mm to 20mm and heights in the range of 20m to 30m are thoroughly investigated. The correlations between the culm diameter and wall thickness with physical and mechanical properties are studied through statistical analyses by means of the two-tailed t-test.

The highest average tensile strength and modulus of elasticity of the bamboo samples of *Dendrocalamus asper* are 323MPa and 28,230MPa respectively. In terms of flexural properties measured in this study, the highest average MOR and modules of elasticity in flexure are found to be 205MPa and 12,851MPa respectively. The maximum compressive strength measured for bamboo samples of *Dendrocalamus asper* in this study is 66MPa.

The statistical analysis of the results shows that there are moderate to strong correlations between the mechanical properties measured during this study and the culm geometrical parameters, including diameter and wall thickness as well as the SD. MC does not show a significant dependence on the mechanical properties, except in the case of MOR in which a relatively moderate correlation is observed. Several mathematical models and equations are suggested for estimating the mechanical properties of bamboo *Dendrocalamus asper* by only measuring the culm diameter and wall thickness, which could provide useful preliminary information on the quality of the selected bamboo species without the need for highly equipped laboratories.

The models are useful tools for the on-site estimation of the properties of bamboo culms for selecting the culms with desirable characteristics suitable for the production of the bamboo composite materials with the required range of mechanical properties without the need for primary access to laboratory facilities. So far, no such models are presented for bamboo *Dendrocalamus asper* for the estimation of its properties without the need for destructive techniques.

If the fibers did not have the required capacity (a tensile strength comparable to steel reinforcement), the final composite matrix would not be able to transfer forces higher than the expected capacity of the fibers. In simple terms, the bamboo fiber alone should have sufficient load-bearing capacity which then could be used within the composite matrix to resist the external forces applied on the final composite element. The results of physical and mechanical evaluations confirm the suitability of the bamboo fibers for composite fabrication in supporting the hypothesis of this research.

7.1.2. Bamboo composite materials fabrication and investigation of properties

Two methods for processing the raw bamboo culms are investigated: stranding and veneering. Through these two techniques, the bamboo culms are processed into bamboo strips and bamboo layers of various lengths and thicknesses. The results show the higher mechanical properties that Bamboo Veneer Composite (BVC) materials display in comparison to Bamboo Strand Composite (BSC) samples. Therefore, BVC materials are most appropriate for reinforcement production.

The hand layup processing technique is employed to produce the composite samples which allows for better quality control of the production process. The method consists of different steps: impregnating the required bamboo veneer with the epoxy-resin matrix, subsequently

aligning them along the fiber direction, and finally assembling layer by layer on top of each other to form a uni-directional composite sample. Pressing the epoxy impregnated perforated bamboo veneer layers pre-treated by 1wt% NaOH solution at a temperature of 100℃ and a pressure of 20MPa for 30/30 minutes of curing/post-curing time followed by second post-curing step at a temperature of 55℃ for 48 hours lead to the highest mechanical properties for the BVC samples. These specifications are attainable in developing countries with little advanced training.

The high mechanical properties of the BVC samples are the result of enhanced specific surface area of the bamboo veneer layers which have been achieved through creating linear groves along the fiber direction, improving the interaction between fiber bundles and the epoxy matrix. The presence of such grooves and perforations leads to enhanced penetration of the epoxy matrix into the bamboo veneer layers through the applied pressure by the hot-press compression molding machine, thus creating a stronger interface between the bamboo fiber bundles and epoxy matrix.

The surface roughness of veneer layers is improved not only by incorporating the linear cracks/perforations along the fiber direction, but also by employing thinner veneer sections. The microstructural analysis of the BVC samples under the microscope affirmed the improved surface roughness of the bamboo veneer layers, which results in higher interfacial strength between the epoxy-resin matrix and bamboo veneer fiber bundles of the BVC samples. Therefore, as a result of better interfacial strength of the BVC samples, the stress transfer between the epoxy-resin matrix and the bamboo fiber bundles is largely enhanced, which ultimately contributes to the higher mechanical properties of the BVC samples in comparison to the BSC samples.

The excellent properties of the BVC samples are also attributed to the fabrication techniques employed during the production process, including the fabrication parameters and the combination of the temperature, pressure and curing time. The veneer layers offer many benefits in comparison to bamboo strands. The veneer layers can be produced in larger widths and lengths, and in various thicknesses, while bamboo strands dimensions are limited by the properties of the available processing machine. Therefore, during the fabrication of the uniaxial bamboo composite boards, maintaining the alignment of the fiber bundles of the veneer layers along the fiber direction is relatively easy in comparison to strands in which shorter width and thicker cross sections do not allow for an easy alignment of the uniaxially

positioned fiber bundles. Maintaining the fiber direction during the production phase of the bamboo composite boards is crucial for achieving a unidirectional high-performance composite sample.

Two techniques are employed to enhance the tensile properties of the BVC boards: alkaline treatment of the veneer layers before composite fabrication, and the optimum combination of the hot-press compression-molding machine parameters, including temperature, pressure and pressing/curing time. The alkaline pre-treatment of the bamboo veneer layers is effective in enhancing the mechanical properties of BVC samples through improving the interfacial bond strength between the bamboo fibers and epoxy matrix. Furthermore, the combination of temperature, pressure and pressing/curing time has a direct impact on the mechanical properties of the BVC samples. The higher the pressure, the better the penetration of the epoxy matrix into the veneer fiber bundles. A high enough temperature can reduce the time required for the curing of the epoxy matrix system, but too high a temperature can destroy the bamboo fibers. Therefore, an optimum combination of these parameters is necessary for the production of high-strength BVC materials with minimum negative impact on microstructure.

Two series of reinforcement designs are presented: one for longitudinal reinforcement which resists the axial and flexural loads, and one for transverse reinforcement to resist the shear forces. The ultimate tensile strength of longitudinal BVC reinforcement is found to be comparable to ASTM A615 grade 60 steel with a minimum tensile strength of 420MPa, while the BVC stirrup shows an average tensile strength comparable to ASTM A615 grade 40 steel reinforcing bar with a minimum tensile strength of 280MPa. These values are recommended by many international building codes as the minimum acceptable strength limits for reinforcement materials used for reinforcing structural concrete members. Therefore, BVC reinforcement has the necessary technical qualifications to be used as reinforcement systems for structural concrete elements.

The average Coefficient of Thermal Expansion (CTE) of BVC reinforcement along the fiber direction dominantly controlled by the bamboo fibers is comparable to the linear CTE values of concrete, while the transverse CTE ranges from 4 to 5 times the CTE values of concrete as it is largely affected by the high thermal expansion coefficient of the epoxy resin. The similar CTE values of concrete and BVC reinforcement in longitudinal direction allows both the BVC reinforcement and concrete to expand similarly, which ensures sufficient bond between concrete and BVC reinforcement is provided when the two materials undergo thermal cycles.

This results in successful application of BVC reinforcement systems, in which a strong bond between the two different materials could be established without being negatively influenced by temperature fluctuations and thermal expansion. The difference between the transverse CTE of BVC reinforcement and the concrete matrix has been thoroughly investigated by, firstly, monitoring the temperature variations between the internal and external surface of the concrete matrix and, secondly, by evaluating the thermal stresses developed as a result of the difference in CTE values through visual and analytical models. More details are provided in the next section.

7.1.3. Use of bamboo composite reinforcement in structural-concrete beams

The concrete beams reinforced with BVC reinforcement systems are prepared only after evaluating the bond strength between the BVC reinforcement and concrete matrix through a series of pull-out tests. The bond strength between the concrete matrix and BVC reinforcement is improved by employing a water-based epoxy coating and sand particles. The coating and the sand particles enhance the interfacial microstructure at the concrete-BVC reinforcement interface. A perfect bond between the concrete and BVC reinforcement ensures smooth stress transfer between the two materials. Two modes of failure are observed during the pull-out tests: one is associated with the rupture of the BVC bar, and the other failure mode is related to the bond failure of the BVC bar embedded in the concrete matrix.

In general, the addition of coating to the surface of BVC reinforcement used for concrete beams is proved to be effective, firstly, by protecting the BVC reinforcement against potential chemical degradation in alkaline environments of concrete and, secondly, by maintaining the required bonding strength with the concrete matrix necessary for stress transfer between the concrete matrix and the reinforcement systems.

The BVC reinforced concrete beams and cylinders samples have also been monitored for temperature variations to evaluate the effect of transverse thermal expansion on concrete matrix and BVC reinforcement. No significant temperature difference was recorded for the concrete pull-out samples after 7 days of curing. The maximum temperature difference observed during this study is 28°C. The longitudinal CTE of BVC reinforcement and concrete are similar and thus the longitudinal thermal stresses developed within the concrete cylinders at the interface between the BVC bar and concrete is not significant.

The difference in transverse CTE of BVC reinforcement and concrete can result in thermal stresses within the concrete matrix around the reinforcement element. The concrete cover is

effective in minimizing the temperature variations between the internal and external surface of the concrete matrix. A concrete cover thickness of 2 times the reinforcement thickness in this study results in no concrete cracking due to temperature variations and thermal expansion. The concrete cover prevents high tensile stresses developed due to the thermal expansion, by creating a thermal layer around the reinforcement element. This cover also mitigates the onset of radial cracking in concrete matrix when the temperature rises by providing a larger space for the differential movement of the BVC reinforcement. When the concrete matrix expands, the pores and cavities within the concrete cover around the BVC reinforcement provide necessary space for the expansion of the reinforcement without developing tensile cracks as a result of the internal pressure developed by the expansion. No signs of tensile cracking due to temperature variations are observed within the concrete beams and cylinders. This confirms the effectiveness of the concrete cover thickness as well as the water-based coating and sand in mitigating the transverse thermal expansion of BVC reinforcement.

The bonding between the water-based epoxy coated BVC reinforcement and concrete plays an important role in mitigating the effect of transverse thermal expansion of BVC reinforcement. If the bonding between the two materials is weak, the transverse thermal expansion can further degrade the bonding mechanism, and subsequently can affect the overall load-bearing capacity of reinforced-concrete beams. Therefore, maintaining a strong bond between BVC reinforcement by selecting the appropriate type of coating has huge benefits for the long-term efficiency and performance of the BVC reinforced concrete beams based on the results obtained in this thesis.

The possibility of radial cracking within the concrete matrix has also been investigated through an analytical approach in which the tangential stresses developed due to thermal expansion of the BVC reinforcement in concrete is estimated using the temperature difference measured between the internal and external faces of the concrete samples. The results from the analytical model show that the maximum tangential stress of 5.27MPa is marginally higher than the measured tensile strength of concrete matrix (6.2MPa). The analytical method thus indicates that internal radial cracks can occur due to the transverse thermal expansion of the BVC reinforcement. However, as indicated above, no significant tangential (thermal) cracking is observed. This discrepancy is most likely due to inaccurate assumptions involved in the use of the analytical model and which requires further investigation.

The residual stresses developed at the interface of the concrete and reinforcement caused by expansion and retraction of the BVC reinforcement do not show a significant effect on the bonding mechanism. Pull-out tests involving BVC reinforcement coated with water-based epoxy coating and sand particles have indicated a near perfect bond between BVC reinforcement and concrete. The bond strength is thus sufficient to prevent tensile cracking that may affect the bonding mechanism.

In terms of durability-related properties, the coated BVC samples have been subjected to normal and high temperature water solutions as well as alkaline solutions with pH levels similar to the concrete matrix for up to 3 months. The coated BVC samples do not show a significant water uptake behavior, with the highest absorption value of less than 0.55% observed after three months of exposure. This shows that BVC reinforcement resists water absorption, especially when used in concrete elements subjected to cycles of wet and dry weather conditions. The coating applied has further created protective layers around the BVC reinforcement to prevent water uptake. Unlike natural bamboo elements used in concrete as reinforcement bars, BVC reinforcement does not have the problem of swelling and expansion which may ultimately affect the bond between the concrete matrix and reinforcement. Therefore, with regard to the hypothesis of the research, the results of the water uptake tests support the fact that newly developed BVC reinforcement system can be used in structural concrete elements, given its superior performance when exposed to water solutions of varying temperatures.

The mechanical properties of the BVC samples exposed to alkaline solution for up to three months are evaluated by measuring the ultimate tensile properties. In general, no significant reduction in tensile strength is observed after the 3 months' exposure to alkaline solutions at different temperatures. Slight reductions of less than 10% for modulus of elasticity and less than 8% for the tensile strength of the coated BVC reinforcement are observed after one month's exposure to the alkaline solution. No further reduction in tensile properties is observed after 2 and 3 months' exposure.

The slight reduction in the tensile properties is associated with the properties of the water based coating applied on the surface of BVC samples. The Scanning Electron Microscopy (SEM) analysis of the samples has further supported the results obtained from the tensile tests. Some cracks and cavities are observed on the surface of the coated BVC samples after one month's exposure to the alkaline solution; this can be explained by frequent swelling and

shrinking of the water-based coating of BVC samples. Therefore, the presence of suitable coating on the surface of the BVC reinforcement can prevent the onset of matrix degradation of the coated reinforcement in concrete in the long term. The epoxy matrix of the BVC reinforcement itself performed extremely well in creating a water-resistant membrane around the bamboo fibers to prevent matrix degradation when exposed to water and alkaline environments, in comparison to natural bamboo fibers in which excessive swelling and fiber degradation are observed after exposure to alkaline solution of concrete matrix. The presence of the water-based coating can further improve the long-term durability performance of the BVC reinforcement in similar conditions as what have been tested in this study.

In the absence of a detailed standard guide relevant for the design and calculation of newly developed BVC reinforced concrete beams for this study, the ACI 440.1R-15 standard is followed closely and treated as the primary guide. The standard has been prepared for the use of fiber reinforced polymer (FRP) reinforcement in concrete members. It is used to compare the results of the flexural tests of the BVC reinforced concrete beams with the recommended design values given for FRP reinforcement in concrete.

The initial cracking loads observed within the BVC reinforced concrete beams are higher than the estimated loads based on the ACI 440.1R-15 recommendations for the first crack in the FRP reinforced concrete beams. This better-than-expected performance of the BVC reinforcement is attributed to the novel production methods for BVC materials developed within this study. The high mechanical capacity of the bamboo fibers remains intact while the physical and mechanical properties of the final composite are enhanced. This result supports the aims of this research since it demonstrates the fabrication of a new class of natural fiber based composite material with the necessary physical and mechanical properties for use as reinforcement in structural concrete elements.

Similarly, the ultimate failure loads measured during the tests are also improved by increasing the number of BVC reinforcement elements. The real failure loads measured through four-point flexural tests ranged from 2 to 8 times the design ultimate failure loads based on the ACI standard. This shows the higher reserve of strength that BVC reinforcement has to offer in comparison with FRP reinforcement. This reserve strength is effective in maintaining the overall load-bearing capacity of the BVC reinforced concrete beams in comparison to the FRP reinforced concrete beams designed according to the ACI guidelines.

The BVC reinforced concrete beams showed improved stiffness, higher ultimate failure loads as well as higher shear capacity compared to non-reinforced concrete beams, while the ultimate failure loads are comparable to that of reinforced concrete beams with ASTM graded steel reinforcement bars. In terms of deflection values measured during the tests, BVC reinforced concrete display higher values than the steel-reinforced concrete beams, though lower deflection values are obtained when the reinforcement ratio increases. Furthermore, given the significantly lower costs of BVC reinforcement compared to steel, the addition of reinforcement to improve the ductility and reduce the deflection will not have a significant effect on overall building costs. This is a huge advantage of newly developed BVC reinforcement compared to steel and common FRP reinforcement, such as GFRP and CFRP, as the cost of raw materials can dominate the number and arrangement of reinforcement bars selected during the design.

In terms of thermal expansion, no significant thermally induced tensile cracks are observed within the concrete beams and cylinders reinforced with BVC reinforcement though the transverse CTE values of concrete and reinforcement are different.

The primary aim of this research is supported by demonstrating the suitability of the newly developed bamboo composite material to be used as a new type of reinforcement element for reinforcing typical structural-concrete members. The results of the test series carried out in this study demonstrated that the performance of the BVC reinforced-concrete beams was more than sufficient. The newly developed BVC reinforcement system has much potential for low-cost and low-rise concrete infrastructure for which similar loading and environmental conditions are found. A typical two-story building in which simply supported concrete beams form the main load-bearing elements of the structure can be the starting point for the application of BVC reinforcement in developing countries around Singapore, where the research is carried out and abundant local resources of natural bamboo forests can be found. For the majority of the construction projects in countries such as Myanmar, Indonesia, Thailand and Vietnam, where steel reinforcement is currently being used, the newly developed BVC reinforcement system provides an alternative reinforcing material which can be produced locally at much lower costs compared with steel. This allows many developing countries, located within the tropical zone and with abundant bamboo resources, to reduce steel imports and thus reduce their dependence on developed countries for construction materials.

7.1.4. Summary of main conclusions

The main conclusions of the thesis can be summarized as follows:

- Bamboo *Dendrocalamus asper* offers high mechanical properties, including tensile strength which are comparable to some of the available ASTM graded steel reinforcement materials.

- The results of the physical and mechanical evaluations confirm the suitability of the bamboo fibers for composite fabrication in supporting the hypothesis of this research.

- Mathematical models and equations are proposed for estimating the mechanical properties of bamboo *Dendrocalamus asper* by only measuring the culm diameter and wall thickness; these are useful tools for on-site estimation of the properties of bamboo culms for selecting the culms with desirable characteristics suitable for composite production.

- Application of natural bamboo as reinforcement in concrete elements has been proven as not successful due to problems of environmental degradation when used in concrete matrix.

- Bamboo-composite reinforcement does not have the problem of swelling, expansion and environmental degradation.

- The processing methods and fabrication technology developed in this thesis show that it is possible to protect the natural bamboo fibers and their inherent tensile strength while enhancing their durability-related properties for the use in concrete elements.

- Bamboo Veneer Composite (BVC) materials are most appropriate for reinforcement production due to higher mechanical properties that they display compared to Bamboo Strand Composite (BSC) materials.

- Alkaline treatment of the veneer layers before composite fabrication leads to an increase in the surface roughness of the fiber bundles and thus an increase in the average tensile properties of BVC materials is observed.

- The optimum combination of temperature, pressure and pressing time during the hot-press compression molding process is crucial in achieving the production of the high-performance bamboo-composite material.

- The ultimate tensile strength of the longitudinal BVC reinforcement is found to be comparable to ASTM A615 grade 60 with a minimum average tensile strength of 420MPa.

- A perfect bond between the concrete and BVC reinforcement has been achieved by employing water-based epoxy coating and sand particles on the surface of the reinforcement.

- Concrete cover thickness of two times the reinforcement thickness and a strong bond between the water-based epoxy coated BVC reinforcement and concrete are sufficient in preventing any concrete cracking due to temperature variations and transverse thermal expansion.

- The application of an analytical model to predict the onset of radial tensile cracking that may be caused by transverse thermal expansion of BVC materials is useful if the required concrete cover is not available.

- The BVC reinforcement performed extremely well in creating a water-resistant membrane around the bamboo fibers to prevent matrix degradation when exposed to water and alkaline environments in comparison to natural bamboo fibers.

- The BVC reinforced concrete beams show improved stiffness, higher ultimate failure loads as well as higher shear capacity compared to non-reinforced concrete beams, while the ultimate failure loads are comparable to that of reinforced concrete beams with ASTM graded steel reinforcement bars.

- The results of the concrete beam test series carried out in this study demonstrate more than sufficient performance of the BVC reinforced concrete beams, which can be utilized for low-cost and low-rise concrete infrastructure with similar loading and environmental conditions.

7.2.   Limitations

The limitations of the present study are discussed below for each of the three main activities carried out in this work.

7.2.1. Raw bamboo selection and evaluation of physical and mechanical properties

Although there are over 1,200 species of bamboo globally, only a limited number of species is available for the purpose of bamboo composite material fabrication. Furthermore, the list of species suitable for composite manufacturing has been further narrowed down in this study to only 4 species found in countries around Singapore. Among the 4 species, comprising *Dendrocalamus asper*, *Phyllostachys edulis*, *Oxytenanthera abyssinica* and *Guadua angustifolia,* only **Dendrocalamus asper** is selected for composite production in this research. This selection is solely made because *Dendrocalamus asper* is one of the most

widely available bamboo species in Southeast Asia. Furthermore, the shipment of the bamboo culms from Indonesia to the research lab in Singapore is straightforward and inexpensive.

Physical and mechanical properties of the raw bamboo sections have been investigated according to available international standards for wood and timber, due to a lack of recognized scientific standard for evaluating bamboo samples. Therefore, not all recommendations given by the available ASTM standards are suitable for bamboo samples due to microstructural differences between bamboo and wood. Therefore, measurement of the properties and evaluation of the results obtained by the relevant wood standards affects the values of the physical and mechanical properties of the bamboo samples in this research.

The bamboo culms of *Dendrocalamus asper* are categorized into seven classes of diameters and wall thicknesses before their physical and mechanical properties are measured. The reason for such classification is to mitigate the need to evaluate every single bamboo section before processing into veneer layers. Therefore, for the production of the final BVC reinforcement in this study, the average mechanical properties of the seven classes of bamboo *Dendrocalamus asper* are used. Testing each and every single veneer layer used for the fabrication of the BVC reinforcement is not feasible, and therefore it is unlikely that all the veneer layers prepared for composite production have exactly the same mechanical properties.

The statistical models presented for the estimation of the mechanical properties of raw bamboo culms with respect to their geometry have limitations with respect to the samples tested in this study. While the models can safely be used for the bamboo samples of *Dendrocalamus asper* obtained from Indonesia for the purpose of this study, they may not be suitable for all bamboo samples of *Dendrocalamus asper*. Although the models developed within this study may not fit perfectly for other bamboo species, they provide a preliminary estimation of the mechanical properties without the need for laboratory investigation, especially at the bamboo plantation sites where testing facilities are not available.

7.2.2. Bamboo composite materials fabrication and investigation of properties

The main limitation of the composite fabrication in this study is the size of the steel mold that is available for the hot-press compression-molding machine. The maximum length of the hot-press compression molding machine is 1,800mm. Longer steel molds for the hot-press machine can permit the production of larger pieces of bamboo composite boards. Such production may reveal the presence of a size effect.

In the case of the veneer production, the maximum length of bamboo sections that can be processed with the available peeling machine is limited to 90cm. Therefore, all the bamboo culms have to be cut into 90cm sections before the veneer can be produced. The length of the bamboo veneer used for the production of the composite samples is therefore limited to less than 80cm after taking into account the excess of the veneers cut from the two ends of the peeling machine's rotating supports. This length has affected the production method of the BVC samples through the overlaying and overlapping techniques.

The peeling machine employed for this study is designed such that it cannot process bamboo sections with existing cracks along the full length of the section. The high contact pressure applied on the surface of the culm through peeling process results in the widening of the existing cracks which then leads to the splitting the section of bamboo into pieces before the peeling process can be completed. Aside from the effect of existing cracks on the efficiency of the peeling process, the natural off-axis deformations along the length of the bamboo sections, as shown in Fig. 65, have also reduced the overall efficiency of the peeling process. The minimum thickness of the veneer layers that can be obtained during the peeling process of bamboo culms is 0.40mm, which cannot be further reduced due to limitations imposed by the design of the available peeling machine. Therefore, design of the peeling machine, including the rotating parts, the blade and the position of the blade, can be further enhanced to achieve higher efficiency during the peeling process.

In terms of composite fabrication, in this study, only 4 types of epoxy adhesive systems are investigated together with the bamboo strands and bamboo veneer layers as discussed in section 5.3.1. The selection, which has been carried out together with the industrial partner Rehau and their chemists, are meant to provide a suitable set of epoxy systems based on the criteria discussed in section 5.3.1. Additives which can be used together with the selected epoxy systems to enhance the mechanical properties of the final composite samples have not been evaluated. The enhancement in the properties of the final BVC materials are carried out only by optimizing the hot-press compression molding machine's parameters, including temperature, pressure and pressing time, together with pretreatment of veneer layers with an alkaline solution.

The production of the BVC stirrups in this study has been limited by the size of the U-shape steel molds. The thickness of the stirrups as well as the length of the side legs are all designed in a way that sufficient pressure can be maintained during the production process and highest

mechanical properties can be achieved for all sections of BVC stirrup, including the side legs and bottom sections. As explained in section 5.5, a lack of adequate side pressure results in insufficient penetration of the epoxy system through the veneer layers on the two sides of the U-shape steel mold of the BVC stirrups. Therefore, BVC stirrups with lower qualities than the longitudinal reinforcements are produced, which have affected the performance of the BVC reinforced concrete beams in this study.

Due to the limitation imposed by the size of the U-shape mold, the size of the available BVC stirrups has restricted the final size of the BVC reinforced concrete beams cross sections to 160×160mm. The constraints imposed by the available hot-press compression molding machine and the molds at AFCL have restricted the application of the BVC reinforcement systems to certain shapes.

The final BVC stirrups produced in this study have been prepared in closed loop shape, as shown in Fig. 100, to accommodate the longitudinal BVC reinforcement at each corner of the concrete beam cross section. To prepare the closed loop stirrups, the two wide-angled single stirrups shown in Fig. 99 are bent slightly such that the two legs of the BVC stirrups can stay parallel. Subsequently, steel cable ties are used to hold the parallel legs together. This method of forming the closed loop stirrups creates stress concentrations at the bent sections of the stirrups which may be a source of bond failure between concrete matrix and BVC reinforcement systems.

Though no sign of failure at the bent portion of the stirrups has been observed during the concrete beam tests throughout this study, the long-term evaluation and testing of BVC reinforced concrete beams with BVC stirrups need to be carried out to investigate the bent sections of the BVC stirrups. Furthermore, the bent portions of the BVC stirrups cannot be tested for their mechanical properties in this study due to the limitations of the available testing facilities. The properties of the BVC stirrups are obtained by testing the flat sections and the properties of the bent portions are subsequently estimated through employing strength reduction factors.

7.2.3. Use of bamboo composite reinforcement in structural-concrete beams

The BVC reinforcement systems are employed as the longitudinal reinforcement and stirrups to reinforce concrete beams of specific cross section and length. The bonding mechanism between the BVC reinforcement and concrete has been investigated through a series of pull out tests with concrete cylinders only of grade 20MPa.

The bonding mechanism has been investigated through laboratory tests at a temperature of 23°C and a relative humidity of 65%, with a maximum absolute temperature variation measured between the inside and outside of the samples of 28°C. However, the effect of higher temperature variations (above 28°C) on the bonding performance of BVC reinforcement to concrete and on the transverse thermal expansion have not been investigated due to a lack of testing facilities. Furthermore, there was insufficient time for the execution of tests for the direct evaluation of the transverse thermal expansion and bonding performance.

The effect of different concrete cover thickness around the reinforcement on mitigating the transverse thermal stresses have been investigated using only two types of cover thickness, due to the limited time available for preparing and testing concrete samples.

The BVC reinforcement systems produced throughout this study have a square cross-section of 10×10mm for longitudinal reinforcement and 6×15mm for BVC stirrups, as explained in section 5.5. Unlike the typical reinforcement systems available in the market including steel, GFRP and CFRP where round bars with and without ribs on the surface are found, the BVC reinforcement developed in this study are prepared by using flat or U-shape steel molds. Therefore, the BVC reinforcement shape is limited to rectangular cross sections only.

The selection of the flat steel mold for the production of the longitudinal BVC reinforcement and the choice of the U-shaped steel mold for the fabrication of the BVC stirrups have been made considering the technical feasibility of handling the raw bamboo fiber bundles. Steel elements can be melted into various forms, while bamboo veneer layers or strands can only be produced into certain dimensions by using the right type of mold for the hot-press machine. The available hot-press compression molding machine can only apply the pressure from the bottom hydraulic cylinders and no side pressure is available during the pressing process of the veneer layers. Therefore, production of round cross sections for the BVC reinforcement is not possible, due to the lack of sufficient pressure which can allow for the penetration of the epoxy-resin system into the layers of perforated veneer sheets placed into a round steel mold.

Therefore, only flat steel molds are employed, which can perfectly distribute a homogenous pressure along the full length of the hot-press compression machine. Production of BVC reinforcement systems with various cross sections requires careful design of the necessary steel molds, which can only be accomplished through extensive studies with an advanced hot-press compression molding machine. It should be emphasized here that, in general, the BVC

397

reinforcement systems with rectangular cross section tested in this study display good performance in comparison to steel reinforcement systems as well as with FRP-reinforcement design values based on the ACI standard.

The preliminary durability tests of the BVC reinforcement are carried out during a three-month period due to the time limit available for this thesis. The conditions chosen for the durability tests during this study are based on the relevant ASTM standard and are designed for the short-term investigation of the water uptake and alkaline resistance of the BVC materials.

Another assumption made during this study is the concrete strength of 20MPa to simplify the process of evaluation of the BVC reinforced-concrete-beam performance. Concrete strength of higher than 20MPa can further enhance the bonding strength with BVC reinforcement by creating higher frictional forces and developing a better mechanical interlocking mechanism with the reinforcement embedded in concrete.

The limitations imposed by the fabrication process of the BVC stirrups have led to the fixed size of the concrete beam cross section. Furthermore, the length of the concrete beams is also restricted to 1,300mm due to the maximum capacity of the UTM machine at AFCL. Due to the predefined concrete beams cross section and length, variations in spacing between the longitudinal BVC reinforcement and BVC stirrup for evaluating the performance of larger BVC reinforced concrete beams are not possible.

The spacing between the longitudinal BVC reinforcements or between BVC stirrups can only be varied according to the values specified in section 6.5.1. These values correspond to the maximum aggregate size used for concrete casting. Furthermore, the maximum spacing between the stirrups is also restricted to the length of the concrete beams. The distance between the load introduction points are also limited to certain values, due to the fixed length of the beams and the maximum capacity of the UTM machine for testing the BVC reinforced concrete beams.

The results of the concrete beam tests in this study are compared to ACI 440.1R-15 as it remains the most relevant international standard for the application of the newly developed BVC reinforcement systems for concrete members. The ACI 440.1R-15 has been developed to cater for the design and application of FRP reinforcement systems for structural concrete member, but not for the newly developed BVC reinforced concrete members. Due to the

similarity in mechanical behavior of BVC materials and typical FRP reinforcement produced with carbon fiber (CFRP) or glass fiber (GFRP), this standard is chosen as the primary basis for comparison.

As the results of the experiments have suggested, there are a few discrepancies between the recommendations given by ACI 440.1R-15 and the results of the tests. This can be explained by the conservative approach of design undertaken by the ACI 440.1R-15 and general differences between BVC materials as nature based fiber composite materials in comparison to synthetic based fiber composite materials such as GFRP. Further research seems necessary to establish similar safety factors and strength reduction factors for BVC reinforcement, similar to the recommendations of the ACI 440.1R-15 for FRP reinforcement systems.

8. Future work

This chapter presents the potential studies that can be carried out in future, based on the limitations of the present study discussed in the previous section. There are several areas that could be further investigated with respect to the three main subjects of this work. The future work for each of these subjects is described in the following sections.

8.1. Raw bamboo selection and evaluation of the properties

In this study, bamboo *Dendrocalamus asper* from Indonesia was selected for the composite production due to its easy accessibility and relatively high mechanical properties. Therefore, future work should be done on investigating, firstly, the physical and mechanical properties of other bamboo *Dendrocalamus asper* species found in other regions in Southeast Asia besides Indonesia and, secondly, on other bamboo species, besides *Dendrocalamus asper*, to test their suitability for composite fabrication. Evaluating the suitability of bamboo species of *Guadua angustifolia* from Latin America, for example, could be carried out, given its high mechanical properties and wide availability in the Latin America.

As mentioned in section 7.2.1, the measurement of the mechanical properties of each and every single veneer layer was not feasible during this study, due to the extensive time required for such investigations. Therefore, a future study should focus on developing a standard method to evaluate and estimate the properties of every veneer layer before composite fabrication to ensure of the quality of the veneer layers. Though such investigations require extensive studies and detailed test series, it could provide the manufacturers of BVC materials with a reliable tool to inspect the veneer layers during the bamboo processing and before using the layers for the fabrication of composite materials.

Future work could be carried out on further development of the statistical models for estimation of the mechanical properties of raw bamboo culms with respect to their geometry. Other bamboo species could be used to evaluate the fitness of the models and its suitability for preliminary investigation of the properties of bamboo culms without the need for laboratory tests. Therefore, to be able to use the suggested models for a variety of bamboo species, studies need to carried out on bamboo species from around the world through detailed laboratory tests to validate the mathematical models and make adjustments to adopt the models to various bamboo species. Such mathematical models would provide local farmers and manufacturers of bamboo composite materials useful tools for preliminary

evaluation of the bamboo species on site, to help in the selection of suitable culms with the required physical and mechanical properties without the need for sophisticated facilities.

8.2.   Bamboo composite materials fabrication and investigation of properties

The design of the hot-press compression molding machine could be further investigated through a future study on the size of the hot-press as well as the pressure transfer from not only the bottom hydraulic cylinders, but also through providing side mechanisms for pressure application which could be helpful for the production of BVC stirrups with various thicknesses and widths. This study needs to be carried out through careful studies of the pressure and heat transfer within the steel mold of the press and through collaboration with respective machine manufacturers.

Beside the hot-press size limitations, the peeling machine employed for the veneer production has the limitation that it could only process bamboo sections with the maximum length of 90cm, as explained in section 7.2.2. Therefore, future work should be carried out on developing a peeling machine capable of processing bamboo sections with various lengths which could produce veneer layers of different widths and lengths. Such peeling machine would allow the bamboo composite manufacturer to produce BVC reinforcement without the need for overlaying and overlapping, thus the properties of the final BVC reinforcement could further be enhanced when the overlaying of the veneer layers are minimized as much as possible. Furthermore, as mentioned in section 7.2.2, the minimum thickness of the veneer layers that could be produced with the available veneer machine was only 0.40mm, therefore further studies need to be carried out on the effect of thinner veneer layers on the properties of the BVC material. This could only be achieved through modifications of the available peeling machine or by the designing and fabrication of a new peeling machine.

The type of the epoxy-resin system used for the production of the BVC reinforcement in this study was chosen together with industry partner Rehau; all of them were petroleum-based systems with some bio-based contents. Therefore, future studies should be carried out on the development of a 100% bio-based epoxy resin systems suitable for production of bamboo composite materials with properties comparable to the BVC materials developed within this thesis. The bio-based epoxy resin, together with the natural bamboo fiber bundles, could pave the way for the development of 100% bio-based composite materials for applications in building and construction sector, which could reduce the dependence on petroleum and other non-renewable resources. Furthermore, such bio-based composite products would address the

future demand for affordable, high-performance and sustainable building materials for developing countries around the world.

8.3.   Use of bamboo composite reinforcement in structural-concrete beams

The concrete grades should be further investigated in future work to evaluate the effect of various concrete strengths on the performance of pull-out samples as well as the ultimate flexural strength, cracking patterns and maximum deflection limits of BVC reinforced concrete beams. The concrete grade of 20MPa was used in this study for preliminary investigations, therefore it is necessary to prepare the pull-put samples as well the concrete beams with various concrete grades. Concrete with higher compressive strength could improve the bonding mechanism between the concrete matrix and BVC reinforcement, as well as minimize the negative impact of radial cracking developed as a result of transverse thermal expansion of the BVC reinforcement embedded in concrete.

The effect of higher temperature variations on the thermal expansion of the BVC reinforcement in concrete, and subsequently on the bonding mechanism of reinforcement with the surrounding concrete matrix, should be further investigated through a series of pull-out tests carried out at various temperatures, simulating hot and cold weather conditions. The thermal strains developed due to temperature variations should be monitored, and correlations with strain development due to radial cracking within the concrete matrix should be established to determine the onset of cracking at particular ambient temperatures. Results could be used to establish necessary safety factors and strength reduction factors based on the thermal stress and strain for the design and application of BVC reinforcement in different concrete applications.

As mentioned in section 7.2.3, regarding the shape of the BVC cross section, a future study could be carried out on round cross sections in addition to the square shapes used in this study. Such studies would require the design of a new type of steel mold that produces the round cross sections for which sufficient pressure for penetration of the epoxy matrix could be provided by the hot-press machine. The hot-press compression molding machine would have to be re-designed, as explained earlier in section 8.2, to be able to employ uniform pressure on all sides of the steel mold for the production of the round BVC reinforcement. Furthermore, variations in the BVC reinforcement's cross sections and dimensions would allow the application of longer and larger reinforcement into concrete beams, which would then require a UTM machine with a higher loading capacity for the flexural test. Therefore

large-scale tests of the concrete beams reinforced with BVC reinforcement could be the subject of a future study. Such large-scale tests could provide insights on the performance of the newly developed BVC reinforcement at full scale of typical one- or two-story buildings.

Durability aspects should be further investigated by exposing the BVC reinforcement to freeze-thaw cycles and acidic solutions such as acidic rains found in certain climates. Longer exposure times (longer than three months) to various environmental conditions could be evaluated through tests which measure both the physical and mechanical properties of the BVC materials, before and after exposure to such conditions.

Finally, the design recommendations of ACI 440.1R-15 should be thoroughly validated with lab-scale and large-scale testing of the BVC reinforced concrete beams. As shown in section 6.6, the two examples for feasibility study of using BVC reinforcement system for low-cost and low-rise housing unit in Indonesia have shown that the design of the building according to recommendations of ACI 440.1R-15 depends much on the properties of BVC reinforcement materials. Fabrication methods used for development of BVC materials can have various impacts on the properties of the material, including the ultimate stress and strain limits which are used mainly in the design of the reinforced concrete member.

A pilot study should be designed to evaluate, on a small scale, the feasibility of the fabrication and subsequently implementation of BVC reinforcement system for construction of low-rise housing units in several small towns in Indonesia. The pilot study should consider the setting up of a company first in Singapore, where AFCL is located, and then in Indonesia, where the fabrication of the BVC materials can take place through the employment of local people from the small towns where the housing units are to be constructed. The local people need to be trained on and taught the various aspects of fabrication and processing of the BVC materials. The Singapore team should regularly update and advise the Indonesian team of the latest research results in the laboratory that should be implemented for the fabrication of the BVC materials in the factory and on site for the implementation phase, where BVC reinforcements will be used for constructing the housing units. Furthermore quality control techniques need to be effectively implemented, especially when low-skilled workers are being employed in Indonesia to ensure the quality of the BVC materials produced. The pilot study will allow for further reviews of the flexural design, shear design and deflection limits according to ACI 440.1R-15 to provide designers with appropriate design guides and

applicable values that could be used with the BVC reinforcement of varying physical and mechanical properties.

References

(2016). "China's steel sector hit by losses."   Retrieved 01.04.2016, 2016, from http://www.ft.com/cms/s/0/338b4394-c8aa-11e5-be0b-b7ece4e953a0.html#ixzz48Dy96RI0.

(FTC), U. F. T. C. (2015). "Federal Trade Commission Definition for Aramid Fiber." from www.ftc.gov.

(IEA), I. E. A. (2007). Tracking Industrial Energy Efficiency and CO2 Emissions, Organisation for Economic Co-operation and Development.

(UNDP), U. N. P. D. (2015). World population prospects, United Nations.

Abdalla, H. (2006). "Concrete cover requirements for FRP reinforced members in hot climates." Composite structures **73**(1): 61-69.

Abdel-Magid, B., S. Ziaee, K. Gass and M. Schneider (2005). "The combined effects of load, moisture and temperature on the properties of E-glass/epoxy composites." Composite Structures **71**(3): 320-326.

Adams, R., A. Collins, D. Cooper, M. Wingfield-Digby, A. Watts-Farmer, A. Laurence, K. Patel, M. Stevens and R. Watkins (2014). "Recycling of Reinforced Plastics." Applied Composite Materials: 1-22.

Adewuyi, A. P., A. A. Otukoya, O. A. Olaniyi and O. S. Olafusi (2015). "Comparative Studies of Steel, Bamboo and Rattan as Reinforcing Bars in Concrete: Tensile and Flexural Characteristics." Open Journal of Civil Engineering **5**(02): 228.

Agarwal, A., B. Nanda and D. Maity (2014). "Experimental investigation on chemically treated bamboo reinforced concrete beams and columns." Construction and Building Materials **71**: 610-617.

Ahmed, E. A., A. K. El-Sayed, E. El-Salakawy and B. Benmokrane (2009). "Bend strength of FRP stirrups: Comparison and evaluation of testing methods." Journal of composites for construction **14**(1): 3-10.

Albert, R. E. (1994). "Carcinogen risk assessment in the US Environmental Protection Agency." Critical reviews in toxicology **24**(1): 75-85.

Almusallam, A. A. (2001). "Effect of degree of corrosion on the properties of reinforcing steel bars." Construction and Building Materials **15**(8): 361-368.

Alvin, K. and R. Murphy (1988). "Variation in fibre and parenchyma wall thickness in culms of the bamboo Sinobambusa tootsik." IAWA J **9**(4): 353-361.

Ambrose, J. E. and P. Tripeny (2007). Simplified Design of Concrete Structures, Wiley.

American Concrete Institute (2008). Building Code Requirements for Structural Concrete (ACI 318-08) and Commentary, American Concrete Institute.

American Concrete Institute (2015). ACI 440.1R-15 Guide for the Design and Construction of Structural Concrete Reinforced with Fiber-Reinforced Polymer Bars, ACI Committee 440.

Angelakos, D., E. C. Bentz and M. P. Collins (2001). "Effect of concrete strength and minimum stirrups on shear strength of large members." Structural Journal **98**(3): 291-300.

ASTM International (2011). Standard Test Method for Splitting Tensile Strength of Cylindrical Concrete Specimens. ASTM C496-11. West Conshohocken, PA, ASTM International,.

ASTM International (2011). Standard Test Methods for Structural Panels in Flexure. ASTM D3043-00(2011). West Conshohocken, PA, ASTM International.

ASTM International (2012). ASTM D7705 / D7705M-12, Standard Test Method for Alkali Resistance of Fiber Reinforced Polymer (FRP) Matrix Composite Bars used in Concrete Construction. West Conshohocken, PA, ASTM International.

ASTM International (2014). Standard Test Method for Moisture Absorption Properties and Equilibrium Conditioning of Polymer Matrix Composite Materials. ASTM D5229 / D5229M-14. West Conshohocken, PA,, ASTM International,.

ASTM International (2014). Standard Test Method for Static Modulus of Elasticity and Poisson's Ratio of Concrete in Compression. West Conshohocken, PA, ASTM International,.

ASTM International (2014). Standard Test Method for Tensile Properties of Polymer Matrix Composite Materials. ASTM D3039 / D3039M-14. West Conshohocken, PA, ASTM International.

ASTM International (2014). Standard Test Methods for Density and Specific Gravity (Relative Density) of Wood and Wood-Based Materials. ASTM D2395-14e1. West Conshohocken, PA, ASTM International.

ASTM International (2014). Standard Test Methods for Small Clear Specimens of Timber. ASTM D143-14. West Conshohocken, PA, ASTM International.

ASTM International (2015). Standard Test Method for Flexural Properties of Polymer Matrix Composite Materials. ASTM D7264 / D7264M-15. West Conshohocken, PA, ASTM International.

ASTM International (2015). Standard Test Method for Slump of Hydraulic-Cement Concrete. ASTM C143 / C143M-15a. West Conshohocken, PA, ASTM International.

ASTM International (2015). Standard Test Methods for Direct Moisture Content Measurements of Wood and Wood-Base Materials. ASTM D4442-15. West Conshohocken, PA, ASTM International

ASTM International (2016). Standard Test Method for Compressive Strength of Cylindrical Concrete Specimens. . ASTM C39/C39M. West Conshohocken, PA, ASTM International.

Baena, M., L. Torres, A. Turon and C. Barris (2009). "Experimental study of bond behaviour between concrete and FRP bars using a pull-out test." Composites Part B: Engineering **40**(8): 784-797.

Bakirdere, S., S. Orenay and M. Korkmaz (2010). "Effect of boron on human health." The Open Mineral Processing Journal **3**(1).

Balaguru, P., A. Nanni and J. Giancaspro (2008). Frp composites for reinforced and prestressed concrete structures: A guide to fundamentals and design for repair and retrofit, CRC Press.

Bellezze, T., M. Malavolta, A. Quaranta, N. Ruffini and G. Roventi (2006). "Corrosion behaviour in concrete of three differently galvanized steel bars." Cement and Concrete Composites **28**(3): 246-255.

Ben-Zhi, Z., F. Mao-Yi, X. Jin-Zhong, Y. Xiao-Sheng and L. Zheng-Cai (2005). "Ecological functions of bamboo forest: research and application." Journal of Forestry Research **16**(2): 143-147.

Bentur, A., N. Berke and S. Diamond (1997). Steel Corrosion in Concrete: Fundamentals and civil engineering practice, Taylor & Francis.

Berg, A. C., L. C. Bank, M. G. Oliva and J. S. Russell (2006). "Construction and cost analysis of an FRP reinforced concrete bridge deck." Construction and Building Materials **20**(8): 515-526.

Berndsen, R., R. Klitzke, D. Batista, E. do Nascimento and F. Ostapiv (2013). "Compressive strength and flexure of Moso bamboo (Phyllostachys pubescens)." Floresta **43**(3): 485-494.

Bertolini, L., B. Elsener, P. Pedeferri, E. Redaelli and R. B. Polder (2013). Corrosion of steel in concrete: prevention, diagnosis, repair, John Wiley & Sons.

Biagiotti, J., D. Puglia and J. M. Kenny (2004). "A review on natural fibre-based composites-part I: structure, processing and properties of vegetable fibres." Journal of Natural Fibers **1**(2): 37-68.

Bischoff, P., S. Gross and C. Ospina (2009). "The story behind proposed changes to ACI 440 deflection requirements for FRP-reinforced concrete." Special Publication **264**: 53-76.

Bledzki, A. and J. Gassan (1999). "Composites reinforced with cellulose based fibres." Progress in polymer science **24**(2): 221-274.

Bostik. (2015). "Technical Data Sheet Moisture Seal Bostik." 2016, from http://www.bostik.com.au/construction-trade-products-catalogue-sheet-28565-moisture_seal-m-0-g-0.html.

Brena, S. F., M. A. Benouaich, M. E. Kreger and S. L. Wood (2005). "Fatigue tests of reinforced concrete beams strengthened using carbon fiber-reinforced polymer composites." ACI structural journal **102**(2).

Brennan, E. M. (1993). "Urban land and housing issues facing the Third World."

Brik, V. B. (1997). Basalt fiber composite reinforcement for concrete.

Brink, F. E. and P. J. Rush (1966). Bamboo Reinforced Concrete Construction. Port Hueneme, California Defense Technical Information Center.

Broomfield, J. P. (2002). Corrosion of steel in concrete: understanding, investigation and repair, CRC Press.

Brown, L. R. (1984). "The global loss of topsoil." Journal of Soil and Water Conservation **39**(3): 162-165.

Buchan, P. and J. Chen (2007). "Blast resistance of FRP composites and polymer strengthened concrete and masonry structures–A state-of-the-art review." Composites Part B: Engineering **38**(5): 509-522.

Burgoyne, C. and I. Balafas (2007). Why is FRP not a financial success.

Bystriakova, N. and V. Kapos (2006). "Bamboo diversity: the need for a Red List review." Biodiversity **6**(4): 12-16.

Célino, A., S. Fréour, F. Jacquemin and P. Casari (2013). "The hygroscopic behavior of plant fibers: A review." Frontiers in chemistry **1**.

Ceroni, F., E. Cosenza, M. Gaetano and M. Pecce (2006). "Durability issues of FRP rebars in reinforced concrete members." Cement and concrete composites **28**(10): 857-868.

Cervenka, A., D. Bannister and R. Young (1998). "Moisture absorption and interfacial failure in aramid/epoxy composites." Composites Part A: Applied Science and Manufacturing **29**(9): 1137-1144.

Chaallal, O. and B. Benmokrane (1993). "Pullout and bond of glass-fibre rods embedded in concrete and cement grout." Materials and structures **26**(3): 167-175.

Chen, H., M. Miao and X. Ding (2009). "Influence of moisture absorption on the interfacial strength of bamboo/vinyl ester composites." COMPOS PART A APPL S **40**(12): 2013-2019.

Chen, J. and J. Teng (2003). "Shear capacity of fiber-reinforced polymer-strengthened reinforced concrete beams: Fiber reinforced polymer rupture." Journal of Structural Engineering **129**(5): 615-625.

Chen, W. F. and E. M. Lui (2005). Principles of Structural Design, CRC Press.

Chen, Y., J. F. Davalos, I. Ray and H.-Y. Kim (2007). "Accelerated aging tests for evaluations of durability performance of FRP reinforcing bars for concrete structures." Composite Structures **78**(1): 101-111.

Cheng, A., R. Huang, J. Wu and C. Chen (2005). "Effect of rebar coating on corrosion resistance and bond strength of reinforced concrete." Construction and Building Materials **19**(5): 404-412.

Chow, H.-k. (1914). Bamboo as a Material for Reinforcing Concrete, Massachusetts Institute of Technology, Department of Naval Architecture and Marine Engineering.

Cleuren, H. and A. Henkemans (2003). "Development of the bamboo sector in Ecuador: harnessing the potential of Guadua angustifolia." Journal of Bamboo and Rattan **2**(2): 179-188.

Clifford, M., K. Simmons and P. Shipway (2012). An Introduction to Mechanical Engineering, CRC Press.

Clifton, J. R., H. Beeghly and R. G. Mathey (1974). "Nonmetallic coatings for concrete reinforcing bars."

Collins, P. (2004). Concrete: The Vision of a New Architecture, McGill-Queen's University Press.

Colombo, C., L. Vergani and M. Burman (2012). "Static and fatigue characterisation of new basalt fibre reinforced composites." Composite structures **94**(3): 1165-1174.

Composite Technical Services. (2012). "ExaPhen Technical Data sheet ", 2016, from http://ctsusa.us/wordpress/?page_id=56.

Conren Limited. (2015). "Technical Data Sheet EnamelCoat Conren." 2016, from http://www.conren.com/products/enamelcoat/.

Conren Limited. (2015). "Truegrip Technical Data Sheet ", 2016, from http://www.conren.com/products/truegrip-bt/.

Cook, D., R. Pama and R. Singh (1978). "The behaviour of bamboo-reinforced concrete columns subjected to eccentric loads." Magazine of concrete Research **30**(104): 145-151.

Correal, D., J. Francisco and C. Arbeláez (2010). "Influence of age and height position on Colombian Guadua angustifolia bamboo mechanical properties." Maderas. Ciencia y tecnología **12**(2): 105-113.

Cox, H. (1952). "The elasticity and strength of paper and other fibrous materials." British journal of applied physics **3**(3): 72.

Crawford, J. E., L. J. Malvar, B. W. Dunn and D. J. Gee (1996). Retrofit of reinforced concrete columns using composite wraps to resist blast effects, DTIC Document.

Czigány, T. (2004). Basalt fiber reinforced hybrid polymer composites. Materials Science Forum, Trans Tech Publ.

Dajun, W. and S. Shao-Jin (1987). Bamboos of China. London, Helm.

Defoirdt, N., S. Biswas, L. De Vriese, J. Van Acker, Q. Ahsan, L. Gorbatikh, A. Van Vuure and I. Verpoest (2010). "Assessment of the tensile properties of coir, bamboo and jute fibre." Composites Part A: applied science and manufacturing **41**(5): 588-595.

Demers, M., D. Hebert, P. Labossiere and K. Neale (1996). "The strengthening of structural concrete with an aramid woven fibre/epoxy resin composite." Proceedigns of the advanced composite materials in bridges and structures. Montreal: Canadian Society for Civil Engineering: 435-442.

Desayi, P. and S. Krishnan (1964). "Equation for the stress-strain curve of concrete." Journal of the American Concrete Institute **61**(3): 345-350.

Deshpande, A. P., M. Bhaskar Rao and C. Lakshmana Rao (2000). "Extraction of bamboo fibers and their use as reinforcement in polymeric composites." Journal of applied polymer science **76**(1): 83-92.

Edwards, M. (2016). "The housing crisis: too difficult or a great opportunity?" Soundings **62**(62): 23-42.

Ehsani, M. R. and H. Saadatmanesh (1997). "Fiber composites: an economical alternative for retrofitting earthquake-damaged precast-concrete walls." Earthquake Spectra **13**(2): 225-241.

El-Salakawy, E., B. Benmokrane, A. El-Ragaby and D. Nadeau (2005). "Field investigation on the first bridge deck slab reinforced with glass FRP bars constructed in Canada." Journal of Composites for Construction **9**(6): 470-479.

Embaye, K. (2000). "The Indigenous Bamboo Forests of Ethiopia: An Overview." AMBIO: A Journal of the Human Environment **29**(8): 518-521.

Embaye, K. (2003). Ecological aspects and resource management of bamboo forests in Ethiopia.

Entropyresins (2012). Technical Data Sheet SUPER SAP® 100/1000 System. C. E. R. Inc. U.S.

Entropyresins (2012). Technical Data Sheet; SUPER SAP® CPM Epoxy System. E. R. Inc.

Entropyresins (2013). Technical Data Sheet; SUPER SAP® INF Epoxy System. Entropyresins. USA, ENtropyresins.

Erdogdu, S. and T. W. Bremner (1993). "Field and laboratory testing of epoxy-coated reinforcing bars in concrete." Transportation Research Circular(403).

F. Ramirez, A. M. J. F. C. M. E. (2011). BAMBOO-GUADUA ANGUSTIFOLIA KUNT FIBERS FOR GREEN COMPOSITES. Jeju Island, Korea.

Fanshawe, D. (1972). "The bamboo, Oxytenanthera abyssinica—Its ecology, silviculture and utilization." Kirkia 8(2): 157-166.

Farrell, S. (2015). Anglo American to slash workforce by 85,000 amid commodity slump. The guardian. United Kingdom, The guardian. 2016.

Faruk, O., A. K. Bledzki, H.-P. Fink and M. Sain (2012). "Biocomposites reinforced with natural fibers: 2000–2010." Progress in Polymer Science 37(11): 1552-1596.

Faruk, O., A. K. Bledzki, H. P. Fink and M. Sain (2014). "Progress Report on Natural Fiber Reinforced Composites." Macromol Mater Eng 299(1): 9-26.

Febrianto, F., W. Hidayat, E. S. Bakar, G.-J. Kwon, J.-H. Kwon, S.-I. Hong and N.-H. Kim (2012). "Properties of oriented strand board made from Betung bamboo (Dendrocalamus asper (Schultes. f) Backer ex Heyne)." Wood Sci Technol 46(1-3): 53-62.

Food and Agriculture Organization of the United Nations (2003). Application of Natural Fibre Composites in the Development of Rural Societies. USA, United Nations.

Fu, J. (2001). "Chinese moso bamboo: its importance." Bamboo 22(5): 5-7.

Fu, S.-Y., B. Lauke, E. Mäder, C.-Y. Yue and X. Hu (2000). "Tensile properties of short-glass-fiber-and short-carbon-fiber-reinforced polypropylene composites." Composites Part A: Applied science and manufacturing 31(10): 1117-1125.

Galati, N., A. Nanni, L. R. Dharani, F. Focacci and M. A. Aiello (2006). "Thermal effects on bond between FRP rebars and concrete." Composites Part A: Applied Science and Manufacturing 37(8): 1223-1230.

Gentry, T. R. and M. Husain (1999). "Thermal compatibility of concrete and composite reinforcements." Journal of Composites for Construction 3(2): 82-86.

Geymayer, H. G. and F. B. Cox (1970). Bamboo reinforced concrete, US Army Engineer Waterways Experiment Station.

Ghavami, K. (1995). "Ultimate load behaviour of bamboo-reinforced lightweight concrete beams." Cement and concrete composites 17(4): 281-288.

Ghavami, K. (2005). "Bamboo as reinforcement in structural concrete elements." Cement and Concrete Composites 27(6): 637-649.

Glass, G. and N. Buenfeld (2000). "Chloride-induced corrosion of steel in concrete." Progress in Structural Engineering and Materials 2(4): 448-458.

Glasser, W. G. and S. Sarkanen (1989). Lignin, properties and materials, Washington, DC (USA); American Chemical Society.

Glenn, H. E. (1950). Bamboo Reinforcement in Portland Cement Concrete, Engineering Experiment Station.

Gori, R. (1999). "Evaluating performance of RC beams using turn-of-the-century theories." Journal of performance of constructed facilities 13(2): 67-75.

Gössel, P. and G. Leuthäuser (2001). Architecture in the Twentieth Century, Taschen.

Guta, D. D. (2012). "Assessment of biomass fuel resource potential and utilization in Ethiopia: sourcing strategies for renewable energies." International Journal of Renewable Energy Research (IJRER) 2(1): 131-139.

Gylfason, T. (2001). "Natural resources, education, and economic development." European economic review 45(4): 847-859.

Harrison, M. (2005). "Science and the British empire." Isis 96(1): 56-63.

Hartsuijker, C. and J. W. Welleman (2007). Engineering Mechanics: Volume 1: Equilibrium, Springer.

Hebel, D. E., M. H. Wisniewska and F. Heisel (2014). Building from Waste: Recovered Materials in Architecture and Construction, Birkhäuser.

Heisel, F. (2015). "FCL Magazine special issue, Constructing Alternatives, Research Projects 2012-2015."

Hensher, D. A. (2013). Fiber-reinforced-plastic (FRP) reinforcement for concrete structures: properties and applications, Elsevier.

Hidalgo-Lopez, O. (2003). Bamboo The Gift of The GODS. Bogotá, Colombia, D'VINNI LTDA.

Hognestad, E., N. W. Hanson and D. McHenry (1955). Concrete stress distribution in ultimate strength design. ACI Journal Proceedings, ACI.

Holbery, J. and D. Houston (2006). "Natural-fiber-reinforced polymer composites in automotive applications." Jom 58(11): 80-86.

Hughes, B. P. (1976). Limit state theory for reinforced concrete design.

Huntsman International LLC (2011). ARALDITE® AW 106 Resin and Hardener HV 953U MULTI-PURPOSE EPOXY ADHESIVE. H. I. LLC. U.S.

International Monetary Fund (2015). World Economic Outlook Database, International Monetary Fund.

Ishihara, K., T. Obara, Y. Sato, T. Ueda and Y. Kakuta (1997). Evaluation of ultimate strength of FRP rods at bent-up portion. Proc., 3rd Int. Symp. on Nonmetallic (FRP) Reinforcement for Concrete Structures, Sapporo Japan.

Jain, A. K. (1993). Reinforced Concrete: Limit State Design, Nem Chand.

Jain, S., U. Jindal and R. Kumar (1993). "Development and fracture mechanism of the bamboo/polyester resin composite." Journal of materials science letters 12(8): 558-560.

Javadian, A., M. Wielopolski, I. F. Smith and D. E. Hebel (2016). "Bond-behavior study of newly developed bamboo-composite reinforcement in concrete." CONSTR BUILD MATER 122: 110-117.

Jiang, Z., H. Wang, G. Tian and Y. Yu (2012). "Sensitivity of several selected mechanical properties of Moso bamboo to moisture content change under the fibre saturation point." BioResources 7(4): 5048-5058.

John, M. J. and R. D. Anandjiwala (2008). "Recent developments in chemical modification and characterization of natural fiber-reinforced composites." Polymer composites 29(2): 187-207.

Kajorncheappunngam, S., R. K. Gupta and H. V. GangaRao (2002). "Effect of aging environment on degradation of glass-reinforced epoxy." Journal of composites for construction 6(1): 61-69.

Kamthai, S. and P. Puthson (2005). "The Physical Properties, Fiber Morphology and Chemical Compositions of Sweet Bamboo (Dendrocalamus asper Backer)." Kasetsart J.(Nat. Sci.) 7(1): 581-587.

Kankam, J., M. Ben-George and S. Perry (1988). "Bamboo-reinforced concrete beams subjected to third-point loading." Structural Journal 85(1): 61-67.

Kankam, J. and S. Perry (1989). "Variability of the Bond Strength Between Bamboo and Concrete." Materials Journal 86(6): 615-618.

Kelemwork, S. (2009). "Effects of some anatomical characteristics of Ethiopian lowland bamboo (Oxytenanthera abyssinica) on physical and mechanical properties." Journal of Bamboo and Rattan 8(3/4): 161-174.

Kent, D. C. and R. Park (1971). "Flexural members with confined concrete." Journal of the Structural Division 97(7): 1969-1990.

Khalil, H. A., I. Bhat, M. Jawaid, A. Zaidon, D. Hermawan and Y. Hadi (2012). "Bamboo fibre reinforced biocomposites: A review." Materials & Design 42: 353-368.

Khan, I. (2014). "Bamboo Sticks as a substitute of Steel Reinforcement in Slab." International Journal of Engineering and Management Research **4**(2): 123-126.

Khare, L. (2005). Performance evaluation of bamboo reinforced concrete beams. MASTER OF SCIENCE IN CIVIL ENGINEERING, University of Texas Arlington.

Khosrow, G. (1995). "Ultimate load behaviour of bamboo-reinforced lightweight concrete beams." Cement and Concrete Composites **17**(4): 281-288.

Kirby, R. S. and P. G. Laurson (1932). The early years of modern civil engineering, Yale University Press.

Kitula, A. (2006). "The environmental and socio-economic impacts of mining on local livelihoods in Tanzania: A case study of Geita District." Journal of cleaner production **14**(3): 405-414.

Kliger, R., C. Christian, R. Haghani, R. Rempling and J. P. Quinchía (2012). FRP APPLICATIONS IN LOW-DISTURBANCE, SUSTAINABLE URBAN INFRASTRUCTURE. Proceedings of 1st International Conference on Civil Engineering Infrastructure Based on Polymer Composites.

Kobayashi, K. and K. Takewaka (1984). "Experimental studies on epoxy coated reinforcing steel for corrosion protection." International Journal of Cement Composites and Lightweight Concrete **6**(2): 99-116.

Kocaoz, S., V. Samaranayake and A. Nanni (2005). "Tensile characterization of glass FRP bars." Composites Part B: Engineering **36**(2): 127-134.

Kodur, V. and L. A. Bisby (2005). "Evaluation of fire endurance of concrete slabs reinforced with fiber-reinforced polymer bars." Journal of structural engineering **131**(1): 34-43.

Kong, F. K. and R. H. Evans (2013). Reinforced and Prestressed Concrete, Springer US.

Kotsovos, M. D. and M. Pavlovic (1999). Ultimate Limit-state Design of Concrete Structures: A New Approach, Thomas Telford.

Krishna, R. N. (2007). Reinforced Concrete Design: Principles And Practice, New Age International (P) Limited.

Kumar, S. and M. M. Prasad (2003). Performance of bamboo reinforced flexural members.

Kurrer, K. E. and E. Ramm (2012). The History of the Theory of Structures: From Arch Analysis to Computational Mechanics, Wiley.

Kushwaha, P. K. and R. Kumar (2009). "The studies on performance of epoxy and polyester-based composites reinforced with bamboo and glass fibers." Journal of Reinforced Plastics and Composites.

Langmead, D. and C. Garnaut (2001). Encyclopedia of Architectural and Engineering Feats, ABC-CLIO.

Latif, M. A. (1993). "Effects of age and height of three bamboo species on their machining properties." Journal of Tropical Forest Science: 528-535.

Lee, H.-S., T. Noguchi and F. Tomosawa (2002). "Evaluation of the bond properties between concrete and reinforcement as a function of the degree of reinforcement corrosion." Cement and Concrete research **32**(8): 1313-1318.

Lee, J.-Y., T.-Y. Kim, T.-J. Kim, C.-K. Yi, J.-S. Park, Y.-C. You and Y.-H. Park (2008). "Interfacial bond strength of glass fiber reinforced polymer bars in high-strength concrete." Composites Part B: Engineering **39**(2): 258-270.

Lee, S.-K., P. D. Krauss and J. Wiss (2004). Long-term performance of Epoxy-coated reinforcing steel in heavy salt-contaminated concrete, Federal Highway Administration, Turner-Fairbank Highway Research Center.

Leelatanon, S., S. Srivaro and N. Matan (2010). "Compressive strength and ductility of short concrete columns reinforced by bamboo." Sonklanakarin Journal of Science and Technology **32**(4): 419.

Li, W. and J. Xu (2009). "Mechanical properties of basalt fiber reinforced geopolymeric concrete under impact loading." Materials Science and Engineering: A **505**(1): 178-186.

Li, X., T. Shupe, G. Peter, C. Hse and T. Eberhardt (2007). "Chemical changes with maturation of the bamboo species Phyllostachys pubescens." Journal of Tropical Forest Science **19**(1): 6-12.

Li, X., L. G. Tabil and S. Panigrahi (2007). "Chemical treatments of natural fiber for use in natural fiber-reinforced composites: a review." Journal of Polymers and the Environment **15**(1): 25-33.

Liang, H., L. Dong, H. Tanikawa, N. Zhang, Z. Gao and X. Luo (2016). "Feasibility of a new-generation nighttime light data for estimating in-use steel stock of buildings and civil engineering infrastructures." Resources, Conservation and Recycling.

Liese and Jackson (1985). Bamboos biology, silvics, properties, utilization. Eschborn, Germany, Deutsche Gesellschaft für Technische Zusammenarbeit (GTZ).

Liese, W. (1985). Anatomy and properties of bamboo. International Bamboo Workshop, Hangzhou. China.

Liese, W. (1998). The anatomy of bamboo culms. Boston, USA, BRILL.

Liese, W., A. Kumar, I. Rao and C. Sastry (2002). The two bamboos of Ethiopia. Bamboo for sustainable development. Proceedings of the Vth International Bamboo Congress and the VIth International Bamboo Workshop, San José, Costa Rica, 2-6 November 1998., VSP BV.

Liese, W. and G. Weiner (1996). "Ageing of bamboo culms. A review." Wood Science and Technology **30**(2): 77-89.

Lima Jr, H. C., F. L. Willrich, N. P. Barbosa, M. A. Rosa and B. S. Cunha (2008). "Durability analysis of bamboo as concrete reinforcement." Materials and Structures/Materiaux et Constructions **41**(5): 981-989.

Lobovikov, M., S. Paudel, M. Piazza, H. Ren and J. Wu. (2009). "bamboo species worldwide." from http://www.fao.org/index_en.htm.

Londoño, X., G. C. Camayo, N. M. Riaño and Y. López (2002). "Characterization of the anatomy of Guadua angustifolia (Poaceae: Bambusoideae) culms." Bamboo Science and Culture **16**(1): 18-31.

Macias, A. and C. Andrade (1987). "Corrosion of galvanized steel reinforcements in alkaline solutions: Part 1: Electrochemical results." British Corrosion Journal **22**(2): 113-118.

Madhukar, M. S. and L. T. Drzal (1991). "Fiber-matrix adhesion and its effect on composite mechanical properties: II. Longitudinal (0) and transverse (90) tensile and flexure behavior of graphite/epoxy composites." Journal of Composite Materials **25**(8): 958-991.

Mahzuz, H., M. Ahmed, M. Ashrafuzzaman, R. Karim and R. Ahmed (2011). "Performance evaluation of bamboo with morter and concrete." Journal of Engineering and Technology Research **3**(12): 342-350.

Malanit, P., M. Barbu and A. Frühwald (2009). "Mechanical properties of sweet bamboo Dendrocalamus asper." Journal of Bamboo and Rattan **8**(3/4): 151-160.

Malanit, P., M. C. Barbu and A. Frühwald (2011). "Physical and mechanical properties of oriented strand lumber made from an Asian bamboo (Dendrocalamus asper Backer)." EUR J Wood Wood Prod **69**(1): 27-36.

Mallick, P. K. (2007). Fiber-reinforced composites: materials, manufacturing, and design, CRC press.

Malvar, L. J., J. E. Crawford and K. B. Morrill (2007). "Use of composites to resist blast." Journal of Composites for Construction **11**(6): 601-610.

Mander, J., M. Priestley and R. Park (1988). "Observed stress-strain behavior of confined concrete." Journal of structural engineering **114**(8): 1827-1849.

Manning, D. G. (1996). "Corrosion performance of epoxy-coated reinforcing steel: North American experience." Construction and Building Materials **10**(5): 349-365.

Masmoudi, R., A. Zaidi and P. Gérard (2005). "Transverse thermal expansion of FRP bars embedded in concrete." Journal of Composites for Construction **9**(5): 377-387.

Matos, B. and J. COREA (2010). "Concrete beams reinforced with GFRP bars: structural response of hyperstatic beams in service and at failure." COMPOSITE STRUCTURES **1**: 1200-1210.

Mattock, A. H., L. B. Kriz and E. Hognestad (1961). Rectangular concrete stress distribution in ultimate strength design. ACI Journal Proceedings, ACI.

Matuana, L. M., R. T. Woodhams, J. J. Balatinecz and C. B. Park (1998). "Influence of interfacial interactions on the properties of PVC/cellulosic fiber composites." Polymer composites **19**(4): 446-455.

McCormac, J. C. and R. H. Brown (2013). Design of Reinforced Concrete, 9th Edition, Wiley Global Education.

McMullen, P. (1984). "Fibre/resin composites for aircraft primary structures: a short history, 1936–1984." Composites **15**(3): 222-230.

Meier, U. (1992). "Carbon fiber-reinforced polymers: modern materials in bridge engineering." Structural Engineering International **2**(1): 7-12.

Mekuriaw, Y., U. Mengistu and A. Getachew (2011). "Role of indigenous Bamboo species (Yushania alpina and Oxytenanthera abyssinica) as ruminant feed in northwestern Ethiopia." Livestock research for rural development **23**(9).

Meng, L. J. Y. Y. Y. and Z. Yan (2007). "Experimental Research on the Mechanical Behavior of Chopped Basalt Fiber Reinforced Concrete [J]." Industrial Construction **6**(002).

Meyer, C. (2004). "Concrete materials and sustainable development in the USA." Structural engineering international **14**(3): 203-207.

Montemor, M., A. Cabral, M. Zheludkevich and M. Ferreira (2006). "The corrosion resistance of hot dip galvanized steel pretreated with Bis-functional silanes modified with microsilica." Surface and Coatings Technology **200**(9): 2875-2885.

Murphy, R. and K. Alvin (1992). "Variation in fibre wall structure in bamboo." IAWA J **13**(4): 403-410.

Nanni, A. (1993). "Properties of FRP reinforcements for concrete."

Nataraja, M., N. Dhang and A. Gupta (1999). "Stress–strain curves for steel-fiber reinforced concrete under compression." Cement and concrete composites **21**(5): 383-390.

National Precast Concrete Association (2015). Epoxy Coated bars, National Precast Concrete Association.

Nervi, P. L. (1956). Structures, F.W. Dodge Corp.

Newby, F. (2001). Early reinforced concrete, Ashgate.

Newlon, H. (1976). A Selection of historic American papers on concrete, 1876-1926, American Concrete Institute.

Nogueira, P., C. Ramirez, A. Torres, M. Abad, J. Cano, J. Lopez, I. López-Bueno and L. Barral (2001). "Effect of water sorption on the structure and mechanical properties of an epoxy resin system." Journal of Applied Polymer Science **80**(1): 71-80.

Nystrom, H. E., S. E. Watkins, A. Nanni and S. Murray (2003). "Financial viability of fiber-reinforced polymer (FRP) bridges." Journal of Management in Engineering **19**(1): 2-8.

Obataya, E., P. Kitin and H. Yamauchi (2007). "Bending characteristics of bamboo (Phyllostachys pubescens) with respect to its fiber–foam composite structure." Wood science and technology **41**(5): 385-400.

Offer, A. (1993). "The British empire, 1870-1914: a waste of money?1." The Economic History Review **46**(2): 215-238.

Okubo, K., T. Fujii and Y. Yamamoto (2004). "Development of bamboo-based polymer composites and their mechanical properties." COMPOS PART A APPL S **35**(3): 377-383.

Osorio, L., E. Trujillo, A. Van Vuure and I. Verpoest (2011). "Morphological aspects and mechanical properties of single bamboo fibres and flexural characterization of bamboo/epoxy composites." Journal of Reinforced Plastics and Composites: 0731684410397683.

Ospina, C. E. and C. E. Bakis (2007). Indirect flexural crack control of concrete beams and one-way slabs reinforced with FRP bars.

Ozbakkaloglu, T. and M. Saatcioglu (2004). "Rectangular stress block for high-strength concrete." ACI Structural Journal 101(4): 475-483.

Oztekin, E., S. Pul and M. Husem (2003). "Determination of rectangular stress block parameters for high performance concrete." Engineering structures 25(3): 371-376.

Palmieri, A., S. Matthys and M. Tierens (2009). Basalt fibers: Mechanical properties and applications for concrete structures. International conference on Concrete Solutions, CRC Press/Balkema.

Panar, M., P. Avakian, R. Blume, K. Gardner, T. Gierke and H. Yang (1983). "Morphology of poly (p-phenylene terephthalamide) fibers." Journal of Polymer Science: Polymer Physics Edition 21(10): 1955-1969.

Papanicolaou, G., T. V. Kosmidou, A. Vatalis and C. Delides (2006). "Water absorption mechanism and some anomalous effects on the mechanical and viscoelastic behavior of an epoxy system." Journal of applied polymer science 99(4): 1328-1339.

PaulinMary, B. B. and D. D. Tensing (2013). "State of The Art Report on Bamboo Reinforcement." International Journal of Engineering Research and Applications (IJERA) Vol 3: 683-686.

Pawar, S. (2014). "Bamboo in Construction Technology." Research India Publications 4(4): 347-352.

Pendhari, S. S., T. Kant and Y. M. Desai (2008). "Application of polymer composites in civil construction: A general review." Composite structures 84(2): 114-124.

Pérez, J., J. Munoz-Dorado, T. de la Rubia and J. Martinez (2002). "Biodegradation and biological treatments of cellulose, hemicellulose and lignin: an overview." International Microbiology 5(2): 53-63.

Phong, N. T., T. Fujii, B. Chuong and K. Okubo (2012). "Study on how to effectively extract bamboo fibers from raw bamboo and wastewater treatment." Journal of Materials Science Research 1(1): 144.

Pickering, S. (2006). "Recycling technologies for thermoset composite materials—current status." Composites Part A: Applied Science and Manufacturing 37(8): 1206-1215.

Popescu, G. H., E. Nica, E. Nicolăescu and G. Lăzăroiu (2016). "China's steel industry as a driving force for economic growth and international competitiveness." Metalurgija 55(1): 123-126.

Popovics, S. (1970). "A review of stress-strain relationships for concrete." ACI Journal 67(3): 243-248.

Poursaee, A. and C. Hansson (2009). "Potential pitfalls in assessing chloride-induced corrosion of steel in concrete." Cement and Concrete Research 39(5): 391-400.

Prasad, A. R. and K. M. Rao (2011). "Mechanical properties of natural fibre reinforced polyester composites: Jowar, sisal and bamboo." Materials & Design 32(8): 4658-4663.

Puglia, D., J. Biagiotti and J. Kenny (2005). "A review on natural fibre-based composites—Part II: Application of natural reinforcements in composite materials for automotive industry." Journal of Natural Fibers 1(3): 23-65.

Punmia, B. C., A. K. Jain, A. K. Jain, A. K. Jain and A. K. Jain (2007). Limit State Design of Reinforced Concrete, Laxmi Publications.

Quagliarini, E., F. Monni, S. Lenci and F. Bondioli (2012). "Tensile characterization of basalt fiber rods and ropes: A first contribution." Construction and Building Materials 34: 372-380.

Rahman, M., M. Rashid, M. Hossain, M. Hasan and M. Hasan (2011). "Performance evaluation of bamboo reinforced concrete beam." International Journal of Engineering & Technology **11**(4): 142-146.

Rajulu, A. V., S. A. Baksh, G. R. Reddy and K. N. Chary (1998). "Chemical resistance and tensile properties of short bamboo fiber reinforced epoxy composites." Journal of Reinforced plastics and composites **17**(17): 1507-1511.

Ransome, E. L. (1884). Building construction, Google Patents.

Rao, K. M. M. and K. M. Rao (2007). "Extraction and tensile properties of natural fibers: Vakka, date and bamboo." Composite structures **77**(3): 288-295.

Rasheeduzzafar, S. Al-Saadoun and A. Al-Gahtani (1992). "Corrosion cracking in relation to bar diameter, cover, and concrete quality." Journal of Materials in Civil Engineering **4**(4): 327-342.

Ray, A. K., S. K. Das, S. Mondal and P. Ramachandrarao (2004). "Microstructural characterization of bamboo." J MATER SCI **39**(3): 1055-1060.

Ray, A. K., S. Mondal, S. K. Das and P. Ramachandrarao (2005). "Bamboo—a functionally graded composite-correlation between microstructure and mechanical strength." Journal of materials science **40**(19): 5249-5253.

Reis, J. and A. Ferreira (2003). "Fracture behavior of glass fiber reinforced polymer concrete." Polymer testing **22**(2): 149-153.

Renard, O. and P. L. GRET (2009). "Creating sustainable jobs and incomes to reduce poverty: lessons from bamboo supply chain development project in North West Vietnam." VOLUME 2 Bamboo for Thailand and Southeast Asia: 35.

Riaño, N., X. Londoño, Y. López and J. Gómez (2002). "Plant growth and biomass distribution on Guadua angustifolia Kunth in relation to ageing in the Valle del Cauca–Colombia." The Journal of the American Bamboo Society **1**(16): 43-51.

Rohit, K. and S. Dixit (2016). "A Review-Future Aspect of Natural Fiber Reinforced Composite." Polymers from Renewable Resources **7**(2): 43.

Rusch, H. (1960). Researches toward a general flexural theory for structural concrete. ACI Journal Proceedings, ACI.

Sabnani, C., M. Latkar and U. Sharma (2013). "Can bamboo replace steel as reinforcement in concrete, for the key structural elements in a low cost house, designed for the urban poor?" International Journal of Chemical, Environmental & Biological Sciences (IJCEBS) Vol **1**: 257-262.

Sagüés, A. A., J. B. Lee, X. Chang, H. Pickering, E. Nystrom, W. Carpenter, S. Kranc, T. Simmons, B. Boucher and S. Hierholzer (1994). "Corrosion of epoxy coated rebar in Florida bridges." University of South Florida. Final Report to Florida DOT WPI(0510603).

Salau, M. A., I. Adegbite and E. E. Ikponmwosa (2012). "Characteristic strength of concrete column reinforced with bamboo strips." Journal of Sustainable Development **5**(1): 133.

Saraswathy, V. and H. W. Song (2005). "Performance of galvanized and stainless steel rebars in concrete under macrocell corrosion conditions." Materials and Corrosion **56**(10): 685-691.

Sarsam, K. F. and J. M. Al-Musawi (1992). "Shear design of high-and normal strength concrete beams with web reinforcement." ACI Structural Journal **89**: 658-658.

Scurlock, J., D. Dayton and B. Hames (2000). "Bamboo: An overlooked biomass resource?" Biomass and bioenergy **19**(4): 229-244.

Sen, T. and H. J. Reddy (2011). "Application of sisal, bamboo, coir and jute natural composites in structural upgradation." International Journal of Innovation, Management and Technology **2**(3): 186.

Sethia, A. and V. Baradiya "Experimental Investigation on Behavior of Bamboo Reinforced Concrete Member."

Shao, Z.-P., C.-H. Fang, S.-X. Huang and G.-L. Tian (2010). "Tensile properties of Moso bamboo (Phyllostachys pubescens) and its components with respect to its fiber-reinforced composite structure." Wood science and technology **44**(4): 655-666.

Shin, F., X.-J. Xian, W.-P. Zheng and M. Yipp (1989). "Analyses of the mechanical properties and microstructure of bamboo-epoxy composites." Journal of Materials Science **24**(10): 3483-3490.

Sim, J. and C. Park (2005). "Characteristics of basalt fiber as a strengthening material for concrete structures." Composites Part B: Engineering **36**(6): 504-512.

Singer, C. J. and T. I. Williams (1954). A History of Technology, Clarendon Press.

Singha, K. (2012). "A short review on basalt fiber." International Journal of Textile Science **1**(4): 19-28.

Sinha, S. N. (1996). Handbook of Reinforced Concrete Design, Tata McGraw-Hill.

Sistonen, E., A. Cwirzen and J. Puttonen (2008). "Corrosion mechanism of hot-dip galvanised reinforcement bar in cracked concrete." Corrosion Science **50**(12): 3416-3428.

Slater, J. E. (1983). Corrosion of Metals in Association with Concrete: A Manual Sponsored by ASTM Subcommittee G01. 14 on Corrosion of Reinforcing Steel, and Metal Properties Council, ASTM International.

Slaton, A. E. (2003). Reinforced Concrete and the Modernization of American Building, 1900-1930, Johns Hopkins University Press.

Smith, L., R. Kessler and R. G. Powers (1993). "Corrosion of epoxy-coated rebar in a marine environment." Transportation Research Circular(403).

Soles, C. L. and A. F. Yee (2000). "A discussion of the molecular mechanisms of moisture transport in epoxy resins." Journal of Polymer Science Part B: Polymer Physics **38**(5): 792-802.

Sonter, L. J., D. J. Barrett, B. S. Soares-Filho and C. J. Moran (2014). "Global demand for steel drives extensive land-use change in Brazil's Iron Quadrangle." Global Environmental Change **26**: 63-72.

Sozen, M. A., T. Ichinose and S. Pujol (2014). Principles of Reinforced Concrete Design, CRC Press.

Stephanie, L. K., R. S. Wayne and W. M. Paul (1962). Process of making wholly aromatic polyamides, Google Patents.

Strong, A. B. (2008). Fundamentals of Composites Manufacturing: Materials, Methods and Applications, Society of Manufacturing Engineers.

Suprapti, S. (2010). "Decay resistance of five Indonesian bamboo species against fungi." Journal of Tropical Forest Science: 287-294.

Surjokusumo, S. and N. Nugroho (1995). A study on Dendrocalamus asper as concrete reinforcement. Proceedings of the Vth International Bamboo Workshop and the IV International Bamboo Congress. Indonesia.

Sutherland, R. J. M., D. Humm and M. Chrimes (2001). Historic Concrete: Background to Appraisal, Thomas Telford.

Swamy, R. and H. Stavrides (1979). Influence of fiber reinforcement on restrained shrinkage and cracking. Journal Proceedings.

Tan, Z. and C. Hansson (2008). "Effect of surface condition on the initial corrosion of galvanized reinforcing steel embedded in concrete." Corrosion Science **50**(9): 2512-2522.

Tang, X., J. D. Whitcomb, Y. Li and H.-J. Sue (2005). "Micromechanics modeling of moisture diffusion in woven composites." Composites Science and Technology **65**(6): 817-826.

Terai, M. and K. Minami (2011). "Fracture behavior and mechanical properties of bamboo reinforced concrete members." Procedia Engineering **10**: 2967-2972.

Terai, M. and K. Minami (2012). Research and Development on Bamboo Reinforced Concrete Structure. Proceedings of 15th World Conference on Earthquake Engineering, Lisbon (Portugal), proceedings (USB).

The International Organization for Standardization (ISO) (2004). Bamboo -- Determination of physical and mechanical properties -- Part 1: Requirements, ISO22157-1:2004. Switzerland.

Thompson, N. G., D. J. Dunmire and M. Yunovich (2005). "Corrosion Costs and Maintenance Strategies--A Civil/Industrial and Government Partnership." Materials performance 44(9): 16-21.

Thompson, N. G., M. Yunovich and D. Dunmire (2007). "Cost of corrosion and corrosion maintenance strategies." Corrosion Reviews 25(3-4): 247-262.

Thompson, W. S. (1938). "The effect of housing upon population growth." The Milbank Memorial Fund Quarterly 16(4): 359-368.

Thwe, M. M. and K. Liao (2002). "Effects of environmental aging on the mechanical properties of bamboo–glass fiber reinforced polymer matrix hybrid composites." Composites Part A: Applied Science and Manufacturing 33(1): 43-52.

Tompos, E. J. and R. J. Frosch (2002). "Stirrup Effectiveness on Concrete Shear Strength." ACI Structural Journal.

Toutanji, H. A. and M. Saafi (2000). "Flexural behavior of concrete beams reinforced with glass fiber-reinforced polymer (GFRP) bars." ACI structural journal 97(5).

Tripler, A. B. and E. L. White (1966). "Methods for reducing corrosion of reinforcing steel." NCHRP Report(20).

United Nations Human Settlements Programme (2008). Housing Finance Mechanisms in Indonesia. Nairobi, United Nations Human Settlements Programme.

United States International Trade commisson, I. (1986). Certain Aramid Fibers, Investigation No.337-TA-194, DIANE Publishing.

Valadez-Gonzalez, A., J. Cervantes-Uc, R. Olayo and P. Herrera-Franco (1999). "Effect of fiber surface treatment on the fiber–matrix bond strength of natural fiber reinforced composites." Composites Part B: Engineering 30(3): 309-320.

Van de Velde, K., P. Kiekens and L. Van Langenhove (2003). Basalt fibres as reinforcement for composites. Proceedings of 10th international conference on composites/nano engineering, University of New Orleans, New Orleans, LA, USA.

Van Der Lugt, P., A. Van den Dobbelsteen and R. Abrahams (2003). "Bamboo as a building material alternative for Western Europe? A study of the environmental performance, costs and bottlenecks of the use of bamboo (products) in Western Europe." Journal of Bamboo and Rattan 2(3): 205-223.

Van Gemert, D., K. Brosens and N. Triconsult (2002). Non-Metallic Reinforcements for Concrete Construction. Proceedings of International Congress: Challenges of Concrete Construction, Seminar.

Varghese, P. C. (2008). Limit state design of reinforced concrete PHI Learning.

Venkatesan, P., N. Palaniswamy and K. Rajagopal (2006). "Corrosion performance of coated reinforcing bars embedded in concrete and exposed to natural marine environment." Progress in Organic Coatings 56(1): 8-12.

Verpoest, I. and G. S. Springer (1988). "Moisture absorption characteristics of aramid-epoxy composites." Journal of reinforced plastics and composites 7(1): 2-22.

Virmani, Y. P. and G. G. Clemena (1998). Corrosion Protection-Concrete Bridges.

Vrentas, J. and J. Duda (1977). "Diffusion in polymer—solvent systems. I. Reexamination of the free-volume theory." Journal of Polymer Science: Polymer Physics Edition 15(3): 403-416.

Vyazovkin, S. and N. Sbirrazzuoli (1996). "Mechanism and kinetics of epoxy-amine cure studied by differential scanning calorimetry." Macromolecules **29**(6): 1867-1873.

Wallenberger, F. T. and N. E. Weston (2004). Natural Fibers, Plastics and Composites, Springer.

Wambeke, B. W. and C. K. Shield (2006). "Development length of glass fiber-reinforced polymer bars in concrete." ACI structural journal **103**(1).

Wambua, P., J. Ivens and I. Verpoest (2003). "Natural fibres: can they replace glass in fibre reinforced plastics?" composites science and technology **63**(9): 1259-1264.

Wang, P., S. Shah and A. Naaman (1978). "Stress-Strain Curves of Normal and Lightweight Concrete• 1n Compression." ACI JOURNAL.

Wang, X., T. Keplinger, N. Gierlinger and I. Burgert (2014). "Plant material features responsible for bamboo's excellent mechanical performance: a comparison of tensile properties of bamboo and spruce at the tissue, fibre and cell wall levels." Annals of botany **114**(8): 1627-1635.

Wang, X., H. Ren, B. Zhang, B. Fei and I. Burgert (2011). "Cell wall structure and formation of maturing fibres of moso bamboo (Phyllostachys pubescens) increase buckling resistance." Journal of the Royal Society Interface: rsif20110462.

Widjaja, E. A. and H. Bogoriense (1998). "Bamboo genetic resources in Indonesia." Bamboo and rattan genetic resources in certain Asian countries: 63.

Wielopolski, M., N. Aigner, D. Griebel, D. Hebel and T. Zimmerman (2016). Grüner Stahl — Hochfeste Naturfaserverbundwerkstoffe für strukturelle Anwendungen in der Industrie. Projekt abschlussbericht KTI-Commission for Technology and Innovation. Bern, Switzerland, ETH Zurich, Empa Dubendorf. **1**.

Wilfong, R. and J. Zimmerman (1977). Strength and durability characteristics of Kevlar aramid fiber. Journal of Applied Polymer Science: Applied Poymer Symposium.

Wilkinson, W. B. (1911). Construction of Fire-proof Buildings, &c: Letters Patent to William Boutland Wilkinson ... for the Invention of "improvements in the Construction of Fire-proof Dwellings, Warehouses, and Other Buildings, Or Parts of the Same.". Great Britain, Patent Office.

Williams, A. (2003). Design of Reinforced Concrete Structures, 2nd Edition, Dearborn Trade Pub.

Witik, R. A., R. Teuscher, V. Michaud, C. Ludwig and J.-A. E. Månson (2013). "Carbon fibre reinforced composite waste: an environmental assessment of recycling, energy recovery and landfilling." Composites Part A: Applied Science and Manufacturing **49**: 89-99.

Wong, K., S. Zahi, K. Low and C. Lim (2010). "Fracture characterisation of short bamboo fibre reinforced polyester composites." Materials & Design **31**(9): 4147-4154.

Wooldridge, M. (2012). Booming bamboo: The next super-material? , BBC News.

World Bank (2015). Global Macroeconomic Performance and Outlook: Prospects for Growth. Global Monitoring Report 2015/2016: Development Goals in an Era of Demographic Change**:** 117-134.

World Bank (2015). World Bank; Population growth (annual %). United Stated, The World Bank. **2016**.

World Bank (2016). World Bank Report; Country and Lending Group, The World Bank Group.

World Steel Association (2015). World Steel in Figures, World Steel Association

Yamaguchi, M., K. Murakami and K. Takeda (2013). Flexural performance of bamboo-reinforced-concrete beams using bamboo as main Rebars and Stirrups. Third International Conference on Sustainable and Technologies.

Yeomans, S. (2004). Galvanized steel reinforcement in concrete, Elsevier.

Yoon, S., K. Wang, W. J. Weiss and S. P. Shah (2000). "Interaction between loading, corrosion, and serviceability of reinforced concrete." Materials Journal **97**(6): 637-644.

Young, R., D. Lu, R. Day, W. Knoff and H. Davis (1992). "Relationship between structure and mechanical properties for aramid fibres." Journal of materials science **27**(20): 5431-5440.

Yu, H., Z. Jiang, C. Hse and T. Shupe (2008). "Selected physical and mechanical properties of moso bamboo (Phyllostachys pubescens)." Journal of Tropical Forest Science: 258-263.

Yu, X. (2008). Bamboo: structure and culture, Universität Duisburg-Essen, Fakultät für Geisteswissenschaften» Institut für Kunst und Kunstwissenschaft.

Zervas, T., J. McMullan and B. Williams (1996). "Developments in iron and steel making." International journal of energy research **20**(1): 69-91.

Zhang, Z. and C.-T. T. Hsu (2005). "Shear strengthening of reinforced concrete beams using carbon-fiber-reinforced polymer laminates." Journal of Composites for Construction **9**(2): 158-169.

Zhou, A., D. Huang, H. Li and Y. Su (2012). "Hybrid approach to determine the mechanical parameters of fibers and matrixes of bamboo." Construction and Building Materials **35**(0): 191-196.

Zou, L., H. Jin, W.-Y. Lu and X. Li (2009). "Nanoscale structural and mechanical characterization of the cell wall of bamboo fibers." Mater Sci Eng C Mater Biol Appl **29**(4): 1375-1379.

Curriculum Vitae

Personal Particulars

Name   Alireza Javadian

Email   Javadian@arch.ethz.ch

Address   1 Create Way, Create Tower, #06-01, Singapore-ETH Centre, Singapore 138602

Education qualifications

PhD

Name of University	ETH Zurich	Year	Sep 2012-March 2017
Major	*Architecture and Construction*	*GPA*	*NA*

MBA

Name of University	Anglia Ruskin University, Cambridge UK (ARU)	Year	2011-2012
Major	*Business Administration and Marketing*	*GPA*	*Merit*

MSc

Name of University	National University of Singapore (NUS)	Year	2009-2011
Major	*Structures and Mechanics*	*GPA*	*3.75 out of 5*

MEng

Name of University	Nanyang Technological University (NTU) Singapore	Year	2007-2009
Major	*Structures and Materials*	*GPA*	*4.88 out of 5*

BSc

Name of University	University of Tehran (UT), IRAN	Year	2003-2007
Major	*Civil Engineering (Hons)*	*GPA*	*4.39 out of 5*

Work experience

2012-present   **Researcher and PhD candidate,** ETH Singapore SEC Ltd.
http://www.hebel.arch.ethz.ch/
2011-2012   **Structural Engineer,** Beca Carter Hollings and Ferner (SEA) Ltd.
http://www.beca.com/
2009-2010   **Project Engineer,** National University of Singapore
http://www.eng.nus.edu.sg/ero/
2007-2009   **Research Assistant,** Nanyang Technological University
http://www.cee.ntu.edu.sg/Pages/Home.aspx

Scholarships and awards

A*STAR SG50 Challenge Award (2015), <u>Distinguished</u> award for "Singapore Challenge: The Science of Future Cities", Singapore, for works on developing natural fiber composite materials for future housing development plans in the ASEAN region
http://www.science50.com.sg/

Zumtobel Group Award (2014), together with the team of Chair of Architecture and Construction Prof. Dirk Hebel, Zumtobel Group and Aedes Architecture, Berlin
http://www.zumtobel-group-award.com/en/857.htm

Engineering for Development (E4D) Scholarship Grant (2013), Sawiris Foundation for Social Development and ETH Global for 150,000 CHF; to pursue a PhD degree from ETH Zurich for developing sustainable and affordable construction material from bamboo for housing and infrastructure for developing countries
https://www.ethz.ch/en/the-eth-zurich/global/funding-opportunities/research-for-development/sawiris-scholarships/e4d-doctoral-scholarships.html

SMART Innovation Grant (2013), together with the team of Chair of Architecture and Construction Prof. Dirk Hebel, Singapore-MIT Alliance for Research and Technology Innovation Centre in Singapore; 200,000 SGD
http://smart.mit.edu/innovation-centre/innovation-grant.html

A*STAR Graduate Scholarship Grant (2007), Singapore Agency for Science Technology and Research; to pursue Master of Engineering at Nanyang Technological University Singapore; 50,000 SGD
http://www.a-star.edu.sg/astar/index.do

Publications, Conferences and Media

Javadian, A., Wielopolski, M., Smith, I.F. and Hebel, D.E., 2016. Bond-behavior study of newly developed bamboo-composite reinforcement in concrete. *Construction and Building Materials*, *122*, pp.110-117.

Hebel, D.E., Heisel, F., **Javadian, A.**, Wielopolski, M., Lee, S., Muller, P. and Schlesier, K., 2016. Engineering bamboo-a green economic alternative, Part 1 Professorship of Architecture and Construction Dirk E. Hebel. *A+ U-ARCHITECTURE AND URBANISM*, (548), pp.162-167.

Kwiecień, A., Hebel, D.E., Wielopolski, M., **Javadian, A.** and Heisel, F., 2015. Bamboo fibre reinforced polymers as highly flexible reinforcement of masonry structures in seismic areas.

Javadian, A., Heisel, F., Schlesier, K., Wielopolski, M. and Hebel, D., 2015. Green Steel.

Cardno, C.A. et al., 2014. Bamboo Reinforcement Could Help Developing Cities. *Civil Engineering*, Online Magazine.

Hebel, D.E., **Javadian, A.**, Heisel, F., Schlesier, K., Griebel, D. and Wielopolski, M., 2014. Process-controlled optimization of the tensile strength of bamboo fiber composites for structural applications. *Composites Part B: Engineering*, *67*, pp.125-131.

Hebel, D.E., **Javadian, A.**, Wielopolski, M., Schlesier, K., Heisel, F. and Griebel, D., Process-Controlled Tensile Properties of Newly Developed Bamboo Composite Materials. In *Symposium Bio-Based Composites* (Vol. 1).

Hebel, D.E., **Javadian, A.**, Wielopolski, M., Schlesier, K., Heisel, F., Bamboo Reinforcement - A Carbon Alternative to Steel. In *What role can renewable materials play in sustainable construction?* World Sustainable Building Conference, 29 October 2014. Barcelona.

Yong, C. et al., 2014. A bamboo composite that's as strong as steel, Singapore Premium News & Headlines. *The Business Times*.

Hebel, D., Heisel, F., **Javadian, A.**, Wielopolski, M. and Schlesier, K., 2013. Constructing bamboo.

Hebel, D.E., Heisel, F. & **Javadian, A.**, 2013. Bambus statt Stahl. *TEC21*, Betonexperimente(35/2013), pp.36–40.

Hebel, D.E., Heisel, F. & **Javadian, A.**, 2013. Bamboo: the new super fiber. *Construction Ahead. Constructing Alternatives part II*, 23/2013, pp.54–57.

Hebel, D.E., Heisel, F. & **Javadian, A.**, 2013. Engineering Bamboo: Composite fiber materials as an alternative reinforcement in structural concrete applications. *FCL Magazine*, 1(1/2013), pp.46–59.

Hebel, D.E., Heisel, F. & **Javadian, A.**, 2013. Engineering Bamboo - The new composite reinforcement. In *Proceedings of the Annual International Conference on Architecture and Civil Engineering (ACE 2013)*. ACE 2013, 1st Annual International Conference on Architecture and Civil Engineering, 18 March 2013. Singapore: GSTF, pp. 94–100.

Hebel, D.E., Heisel, F. & **Javadian, A.**, 2013. Bamboo Composite Reinforcements in Structural Concrete Applications. In *Book of Abstracts and Proceedings International Conference on Advances in Cement and Concrete Technology in Africa*. ACCTA 2013, Advances in Cement and Concrete Technology in Africa, 28 January 2013. Johannisburg: BAM Federal Institute for Materials Research and Testing Germany, p. 177.

Hebel, D.E., **Javadian, A.**, Wielopolski, M., Schlesier, K., Heisel, F.; 2013. Bambusbeton. In *Material Revolution 2: Neue nachhaltige und multifunktionale Materialien für Design und Architektur*. Basel: Birkhäuser Verlag GmbH, p. 115.

Hebel, D.E. et al., 2013. Local Alternatives: replacing steel with bamboo. In N. Janson, A. Ruby, & I. Ruby, eds. *The Economy of Sustainable Construction*. Berlin: Ruby Press, pp. 44–55.

Hebel, D.E. et al., 2013. Process-Controlled Tensile Properties of Newly Developed Bamboo Composite Materials. In *Symposium Bio-Based Composites*. 1. CompositesWeek@Leuven and TexComp-11, 17 September 2013. Leuven, Belgium: KU Leuven.

Javadian, A., 2013. *Composite bamboo and its application as reinforcement in structural concrete*. Research Proposal. Zurich, Switzerland: ETH Zurich.

Alireza, J., Susanto, T. and Hooi, T.T., 2008. High temperature effect on flexural strength of steel-fibre concrete. *HIGH TEMPERATURE*, *500*, p.22.

Patent

Dirk E. Hebel, Mateusz Wielopolski, Dragan Griebel, Felix Heisel and **Alireza Javadian** (2016); "Bamboo fiber-reinforced composite material, Use thereof and methods for producing a Bamboo fiber-reinforced composite material". State Intellectual property office of the People's Republic of China, PCT1502681-filed.